DEVELOPMENT AND CHARACTERIZATION OF BIODEGRADABLE MICROSPHERES CONTAINING SELECTED ANTIMYCOBACTERIALS

by

DAVID F BAIN

A thesis submitted in partial fulfilment of the requirements of The Robert Gordon University for the degree of Doctor of Philosophy

November 1998

Acknowledgements

The help and advice provided by Drs D.L. Munday and P. J. Cox is gratefully acknowledged.

I am indebted to Dr A. Smith for his unfailing advice, encouragement and critical comment. I am most grateful also to Knoll Pharmaceuticals and specifically Professor K. Khan for generous financial support throughout this work.

I shall be forever grateful to Linda for her love, encouragement and understanding throughout this work, and Omar for his friendship.

Finally I should like to acknowledge my father, who's courage and determination to fight debilitating illness has always been a great source of inspiration, and my mother for her love and patience.

Abstract

Prolonged therapy required to effectively treat mycobacterial infection frequently results in severe dose-limiting side-effects and drug resistance due to patient non-compliance with protracted dosage regimens. Biodegradable poly-α-hydroxy acid microspheres and microcapsules containing rifampicin (RIF) and isoniazid (INH) respectively have been prepared with the intention of providing high sustained site-specific concentrations to overcome some of the shortcomings of existing oral treatments. Due to the high dose, hydrophilicity and instability of both drugs, formulation strategies to attain high drug loading and methodologies to characterize *in vitro* drug release during ongoing decomposition were required. Stability indicating HPLC assays to quantify drug release have been developed, validated and applied to monitor drug release based on cumulative quantification of drug and degradates. A mathematical correction for serial decompositions associated with RIF was made based on the terminal pseudo equilibrium observed during stability studies. An isocratic HPLC assay was prospectively developed for the quantification of both drugs and their major metabolites in biological samples. Further preformulation studies confirmed the absence of significant polymorphs for both drugs when recrystallized from solvents later used in formulation development. Furthermore, thermal analysis revealed only modest interaction between the drugs and Resomer®. The high and moderate water solubilities of INH (145 $mgmL^{-1}$) and RIF (1 $mgmL^{-1}$) determined the selection of spray-drying (SD) and emulsion solvent evaporation (ESE) for RIF, whereas preparation of INH microcapsules relied solely on the former technique. Examination of the effects of varying RIF:polymer ratio, phase volumes and continuum presaturation with selected poly(L-lactide) and poly(D,L-lactide-co-glycolide) (PDLGA) Resomer® identified optimum conditions to maximize drug loading during a comparison of aqueous ESE with spray-drying with a range of nine further amorphous Resomer® polymers. Although yields were generally higher with ESE (85-90 %), SD (45-75 %) was considered a superior preparation technique on the basis of the rapid production of microspheres of high and predictable drug loading (100 % of that attempted), with monodisperse granulometry and superior morphology. Release profiles were typically asymptotic characterized by a rapid 'burst' of release followed by a slow release of residual entrapped RIF, irrespective of the preparative technique or polymer used. Poor yields (7.2 %) when SD low molecular weight (MW) PDLGA (8 kD) were greatly enhanced (74.8 %) by reduction in drying temperature and substitution of chloroform:dichloromethane (CFM:DCM) (1:1) cosolvent with DCM. These conditions were adopted as the optimum parameters for further studies of blends of low (2 kD, R104) and moderate (11 kD, R202H) MW poly(D,L-lactide) (PDLLA); materials which demonstrated excellent sprayability and dramatically modulated the release of drug when combined compared to their use alone. Drug release showed a remarkable dependence on blend, dramatic acceleration being observed between 44 and 48 %w/w R104. Release over this range showed a marked dependence on medium temperature and led to the proposal of an autohydration mechanism linked to the hydrophilicity and glass transition (T_g) of the blend which accounted for the sigmoidal profiles observed. First order dependence of release allowed calculation of Arrhenius derived activation energies of drug release in glassy anhydrous and rubbery plastic matrices of 630 and 320 J mol^{-1}. Hydration and thermal studies supported the postulated diffusion mechanism, whereas granulometric and morphological examinations demonstrated that erosion did not contribute significantly. The criticality of matrix composition was further highlighted when interchange with nominally identical polymer, R202H, shifted the critical composition to 30 %w/w R104. Moreover, this observation contested the batch-to-batch reproducibility of commercial polymer. Substitution of DCM with halothane (HAL) and acetone (ACT) had a profound influence on the properties of compositionally identical (R104:R202H, 30:70) microspheres, particularly release kinetics. This was attributed to the more rapid drying kinetics with the poor solvent, ACT, and the generation of a porous matrix. Consequently,

drug was largely released during the 'burst' phase. Superior solvents, HAL and DCM resulted in enhanced matrix coherence at the expense of considerable residual solvent burdens (6 - 12.5 %), which allowed extensive matrix relaxation as solvent was lost with first order kinetics. This ageing process was followed by the development of an endotherm associated with the T_g as the matrix stabilized with a resultant increase in the induction period and a general retardation of drug release. Extension of the concept of blending R104 as release 'initiator' to a range of MW PDLGA of 50:50 and 75:25 comonomer ratio as release 'modulator' was of limited success generating release profiles reminiscent of each polymer when used alone. The magnitude of the 'burst' correlated to the precipitation kinetics of the predominant complementary PDLGA polymer as determined by cloud-point titration. Due to the more hydrophilic nature of the copolymers, at the critical concentration uncontrolled hydration resulted in a single rapid release phase. Spray-dried biodegradable INH microcapsules were prepared by a two stage process whereby SD cores of drug or in combination with biodegradable albumin or casein were subsequently coated with PDLGA by SD. The highly crystalline, aggregated and irregular morphology of SD drug resulted in poor coating efficiency and a rapid release of encapsulated drug. Protein microspheres of superior sphericity allowed more effective coating and hence slower INH release. It is concluded that SD has excellent industrial potential for the preparation of biodegradable poly-α-hydroxy acid microspheres for high dose drugs to be delivered directly to their site of action, e.g., intra-pulmonary. Indeed, the granulometry of these particles and, in particular, the hydrophilic character of blends of PDLLA described have considerable potential for the sustained delivery of drugs in the low volumes of fluid that prevails in the lung. These formulations might offset some of the limitations of current oral antimycobacterial therapy.

1. Introduction

Earliest examples of polymers for parenteral administration included silicone rubber and polyethylene. The major disadvantage of these inert polymers implants was their non-biodegradability, which necessitated surgical removal of the implants after drug exhaustion (Jalil & Nixon, 1990f). The development of biodegradable polymers was initially heralded as a major advance in medicine due to their potential as bioerodible and biocompatible sutures, the removal of which would no longer require surgery (Lewis, 1990). Biodegradable polymers may be defined as synthetic or natural polymers which degrade *in vivo* either enzymatically or non-enzymatically to produce biocompatible or non-toxic by-products, which themselves can be eliminated via normal physiological processes (Jalil & Nixon, 1990f). Since their inception, biodegradable materials have found use in dentistry and orthopaedics (Wood, 1980), but have been more extensively investigated as pharmaceutical excipients in the field of drug delivery (Lewis, 1990; Brannon-Peppas, 1995). A plethora of natural (Magee et al., 1993) and synthetic polymers (Whateley, 1992) to achieve prolonged or site-specific delivery of drugs have been reported. However, the thermoplastic (co)polymers based on lactic (PLA) and glycolic acid (PGA) are the most extensively employed: poly(L-lactic acid) (PLLA), poly(DL-lactic acid) (PDLLA) and poly(DL-lactic-co-glycolic acid) (PDLGA) being representative examples. Notwithstanding their biocompatibility and biodegradability, their utility is derived from the versatility and their popularity from their approval for use in formulation by the Food and Drug Administration of the USA (Tice & Cowsar, 1984). Their commercial availability further accounts for the proliferation of published work in the last decade describing their use in drug delivery systems (DDS).

1.1 Poly-α-hydroxy acids

1.1.1 Synthesis

The low molecular weight (MW) products of direct condensation of poly-α-hydroxy acid monomers were traditionally considered unsuitable for biomedical application because of their poor mechanical strength and rapid degradation (Wu, 1995). MW of 10 kD have been reported for PDLGA with the use of antimony oxide and temperatures of 120 °C, whereas efficient removal of water is the rate-limiting step at higher temperatures required for the reaction in the absence of catalyst. Because of these practical difficulties, intermediate to high MW homo- and copolymers of lactic acid and glycolic acid — chemical structures of which are shown in Figure 1.1 —are synthesized by ring-opening

melt condensation of the cyclic dimers, dilactide and diglycolide. The significant advantage of this procedure is that no dehydration step is required and that the cyclized monomers and linear polymer can be readily purified (Wu, 1995). Synthesis typically involves heating (130 - 200 °C) reactant dimers under vacuum (0.1 mmHg) in the presence of catalyst (and chain control agent) (Kulkarni et al., 1966, 1971; Deasy et al., 1989). Optically active PLA can be derived from L (+) and D (-) isomers of lactic acid, which upon polycondensation of the corresponding diester, give rise to optically active polymers of opposite birefringence to that of the starting isomer (Boehringer Ingleheim, 1992). In contrast, the polymerization of optically inactive D,L-racemate yields optically inactive PDLLA. The potential range can be further multiplied where glycolide is incorporated. Furthermore, the wide range of synthetic conditions described has produced polymers of variable MW distribution, composition and polymeric sequencing, parameters shown to be sensitive to the reaction conditions (Gilding & Reed, 1979; Rak et al., 1985; Gohel et al., 1996).

polyglycolide polylactide

Figure 1.1 *Chemical structures of polyglycolide and polylactide homopolymers.*

In a study of the synthesis of PLLGA and PDLGA, Gilding & Reed (1979) demonstrated that glycolide was preferentially incorporated at low conversions, with accelerated polymerization of lactide as glycolide was depleted. Consequently, block glycolide copolymers separated by lactide units were generated initially. Changes in the initial reactant monomeric ratio altered the preferential polymerisation mechanism and thus the polymeric product, whereby MW increased, whereas polydispersity fell, with increased glycolide content. Deasy et al. (1989) observed similar trends, albeit not as pronounced. These differences may be attributed to the different reaction temperatures in both studies, as glycolide incorporation is favoured at higher temperatures, whereby Deasy et al. (1989) used reaction temperatures 20 °C below those of Gilding & Reed (1979). Higher

MW polymers are generally produced at lower temperatures (Avgoustakis & Nixon, 1991) and with longer synthetic times (Deasy et al., 1989). Rak et al. (1985) favoured a two-step process of 4 h at 180 °C followed by 2 h at 200 °C to maximize PDLLA chain length. Initiation of a greater number of chain reactions was assigned to the reduction in MW observed as catalyst, stannous octoate, levels increased (Deasy et al., 1989). There is additional controversy in relation to the preferred catalyst employed. Tetraphenyl tin has been favoured by some on the basis of ease of handling (Kulkarni et al., 1966) and catalytic efficiency (Gohel et al., 1996). Schindler et al. (1977), however, favoured catalysts free of carbon metal bonds, such as stannous octoate or chloride. What is known, however, is that residual catalyst can render PDLLA biologically incompatible, efficient removal being a prerequisite of their biocompatibility (Asano et al., 1990) and long-term stability (Jamshidi et al., 1988).

The sensitivity of final polymer characteristics, i.e., comonomer sequence, MW, polydispersity to the many synthetic variables has confounded interpretation and elucidation of the optimum conditions for their preparation. Furthermore, the fact that these characteristics determine material behaviour, it follows that small changes in the synthetic protocol can have a profound effect on the final performance of formulations on which they are based (Deasy et al., 1989). This situation has been alleviated in the last decade by the widespread commercial availability of adequately characterized reproducible polymers, e.g., Resomer®. Some of the pertinent characteristics for drug delivery of these materials are now considered.

1.1.2 Physical, Chemical and Biological Properties

1.1.2.1 Solubility

Polymer solubility is a critical factor to the preparation of poly-α-hydroxy acid-based formulations as most manufacturing methodologies rely on solubilization and hence mobilization of the polymer phase in an effort to homogenize the drug throughout the excipient matrix. Stereochemical factors influence crystallinity, which, in turn, determines the solubility of poly-α-hydroxy acids in organic solvents. In general, solubility decreases as chain length (Jalil & Nixon, 1990b; Bodmeier et al, 1989) and glycolide content increases (Mehta et al., 1996). For comparable MW, PDLLA has greatest solubility in common organic solvents including acetone (ACT), tetrahydrofuran and most chlorinated solvents (Boehringer Ingelheim, 1992). PDLGA, however, has limited solubility in

chloroform (CFM), whereas PLLA solubilizes in chloroform, dichloromethane (DCM) and benzene often only after heating at 50 - 60 °C. PGA solubility is limited to fluorinated solvents, such as hexafluoro-propan-2-ol, the prohibitive expense of which is one factor which has limited its investigation as a pharmaceutical excipient (Sato et al., 1988; Whateley, 1992).

1.1.2.2 Crystallinity, Hydrophilicity and Thermal behaviour

Comonomer composition and ratio, chain linearity and copolymer MW are principal determinants of polymer crystallinity, thermal character and water uptake, all of which are inextricably linked (Lewis, 1990). Hydrophilicity is the key parameter, since all biodegradable devices are in intimate contact with an aqueous environment and biodegradation occurs through hydrolysis (Wood, 1980). Therefore, any factor which affects water uptake will have a huge bearing on biodegradation. In addition, crystallinity is also critical, as it not only affects water uptake and thus biodegradation, but also drug diffusion, the latter occurring predominantly through the amorphous regions of the polymeric matrix (Peterlin, 1983).

X-ray analysis of PLLA and PDLLA disclosed the crystalline and amorphous nature of these respective polymers (Kulkarni et al., 1971). Gilding & Reed (1979) studied the thermal behaviour of a range of homo- and copolymers. PLLA, PGA and PLLGA containing greater than 90 % lactide showed recrystallization exotherms, subsequent to glass transition (T_g), and prior to melting endotherms. X-ray analysis revealed that the crystalline region of PLLGA lay outwith proportions of glycolide < 25 % and > 67 %. Substitution with the D,L-lactide isomer extended the amorphous region for the copolymer from 0 - 70 %. Crystallinities of homopolymers were 46 - 52 % and 37 % for PGA and PLLA, respectively, whilst PDLLA was amorphous. The amorphous character of the latter material arises through the disruptive effect of asymmetric methyl carbon on the relatively long and aligned stereoregular chains (Wood, 1980). Gilding & Reed, (1979) showed equilibrium water uptake correlated well with polymeric crystallinity, with the exception that PGA was more hydrophilic than PLLA, due to stereoactive methyl substituent on the backbone of the latter rendering the polymer hydrophobic. For copolymers, however, water content increased with hydrophilicity to 20 - 30 %w/w in the amorphous region, then fell again corresponding to the onset of crystallinity. Similar recrystallization behaviour of quench-cooled samples was due to a stress-relaxation phenomena (Kalb & Pennings, 1980). Polymer MW *per se* does not particularly affect the permeability of

polymers unless oligomers are present. In contrast, polydispersity can modify crystallinity, T_g and mechanical strength, and thus change degradation characteristics of a given drug / polymer system (Reed & Gilding, 1981) due to preferential degradation and dissolution of the amorphous domains.

The magnitude of T_g temperature also has implications for mechanical properties and also drug diffusivity (Pitt et al., 1979). Kalb & Pennings (1980) studied the diffusion parameters of a series of steroids in crystalline poly-ε-caprolactone, PDLLA and copolymers thereof. The thousand-fold reduction in diffusivity of progesterone in PDLLA relative to poly-ε-caprolactone was at odds with their respective polymer crystallinities. However, the increase in free volume, molecular mobility and hence permeability of poly-ε-caprolactone in excess of its glass transition of -65 °C, compared with 57 °C for PDLLA accounted for these differences. Water frequently acts as a potent plasticizer for amorphous solids (Hancock & Zografi, 1994) and poly-α-hydroxy acids are no exception (Omelczuk & McGinity, 1992). Siemann (1985) observed approximately 12 °C reductions in PDLLA T_g upon hydration which the author cautioned might have a profound effect on thermomechanical and diffusive properties of implanted drug-polymer composites. Elsewhere, differential hydration behaviour of poly-α-hydroxy acids in the glassy and rubbery states has precluded the use of Arrhenius derived activation energies for the prediction of the long-term stability of these materials from data derived at elevated temperatures (Schellhorn & Buchholz, 1996).

1.1.2.3 Biocompatibility

Biocompatibility refers to the ability of a material to perform with an appropriate host response: histo- and pathologic damage, immunogenicity, carcinogenicity and thrombogenicity representing indications of lack of compatibility (Vert et al., 1992). Biocompatibility of excipient polymers is generally an essential prerequisite for their use in drug delivery applications intended for compartmental implantation. Herrman et al. (1970) represents one of the earliest studies of biocompatibility where PGA sutures showed a minimal inflammatory response, when compared with absorbable cat-gut materials. However, Kulkarni et al. (1971) later described a progression of cellular events characterized by accumulation of polymorphonuclear leukocytes; infiltration of foreign body giant cells, then finally, dense fibrotic tissue growth following implantation of films and powders of PDLLA. Yamaguchi & Anderson (1993) observed a similar mitotic sequence which could be correlated to the granulometry of the studied microspheres and

their sequential phagocytosis. This phagocytic response has been effectively suppressed by precoating PDLLA with hydrophilic bovine serum albumin (Tabata & Ikada, 1988). Moderate and comparable tissue responses following chemoembolization of PDLGA microspheres have been related to release of hydro-soluble oligomers, which, in turn, was related to polymer MW and comonomer ratio (Splenlehauer et al., 1989).

Presence of medicament can have a variable effect on polymer-tissue response. Steroid incorporation was thought to pharmacologically alter the intra-articular intolerance of PDLLA (Ratcliffe et al., 1984). Elsewhere, encapsulation of drug loaded PDLLA microspheres have been shown to reduce clarithromycin-induced tissue irritation (Gupta et al., 1993), whereby I.M. administration of PDLLA microspheres revealed only minor swelling persisting for 12 - 24 h, whereas bulk drug caused dogs to limp for 2 - 3 d. Visscher et al. (1988) observed a comparable tissue response following I.M. implantation of PDLGA ergot and placebo microcapsules. Others workers found no destructive or inflammatory changes in vessel walls with PDLGA microspheres upon chemoembolization (Grandfils et al., 1992). Further, blank PDLGA microspheres implanted in rats brains were biocompatible and degraded totally within two months (Langer, 1991).

There are, however, conflicting data on the biocompatibility of poly-α-hydroxy acids raising questions of their candidature for certain applications. Comparative studies of the biodegradation of crystalline PLLA and the same material processed to eliminate crystallinity revealed differential behaviour *in vivo* (Pistner et al., 1993). Crystalline material remained intact producing a minimal cellular response over the 116 week study period. In contrast, degradation of amorphous material produced surface roughening in the first week, which evolved to sizeable lacunae after 50 weeks. Thereafter, connective tissue deformed the remaining mass. Elsewhere, poly-α-hydroxy acids have induced intra-articular (Ratcliffe et al., 1984) and acute pulmonary inflammatory reactions (Armstrong et al., 1991; 1992; 1996). In the latter studies, significant incidence of haemorrhage and neutrophil proliferation in groups treated with blank and fluorescein microspheres, compared with saline control, indicated pulmonary incompatibility of poly-lactic acid. However, intra-pulmonary steroid delivery has been cited as the therapeutic basis for preparation of PDLLA-hydrocortisone microspheres (Giunchedi et al., 1995).

1.1.2.4 Biodegradability

1.1.2.4.1 Polymer factors

In general chemical terms, degradation occurs via random hydrolytic cleavage of accessible ester bonds, and subsequent solubilization of oligomeric fractions below a critical level (15 kD) with accompanied weight loss (Schindler et al., 1977; Wang et al., 1990; Shah et al., 1992); so-called homogeneous degradation. Mechanisms of degradation have evolved and been refined. Chu & Campbell (1982) suggested a mechanism initiated on the surface, growing inwards based on the appearance of surface cracks on polyglycolic acid sutures. However, the model of Heller (1980) supported the bulk mechanism, whereby hydrolysis proceeded uniformly throughout the polymer mass, and was for some time universally accepted.

Early investigations of the dependence of degradation rate on monomeric ratio erroneously attributed variations in relative rates to selective metabolic pathways of PLA and PGA (Miller et al., 1977). The significance of crystallinity through its dependence on copolymer ratio upon polymer degradation rate was recognized by Reed & Gilding (1981). Thus, a two-stage mechanism of semi-crystalline polymer degradation has been proposed by Chu (1985); initiated in the amorphous regions whilst terminating in adjoining crystalline domains. Freed from restricted motion, accelerated degradation of previously less dense crystalline regions occurred subsequent to preferential degradation of accessible amorphous zones. Preferential hydrolytic attack of glycolide bonds has resulted in analogous crystallization of lactide enriched zones (Li et al., 1990). Thus, variation in comonomer ratio, and, an attendant change in crystallinity and hydrophilicity, modulates the contribution of each stage to polymer degradation and thus modifies the composite rate and pattern of degradation. The relationship between copolymer composition and degradation of Miller et al. (1977), mirrored that of composition and crystallinity of Gilding & Reed (1979). These features confer considerable versatility on PDLGA as a material of variable degradation and thus release character in the design of delivery systems. Asano et al. (1990) stated that crystallinity, biodegradability and hydrophilicity of the copolymer can be freely controlled by altering monomeric co-ratio. In the same study, optimal biodegradability in the amorphous region occurred at a copolymer ratio of 70 % glycolic acid, in accord with the maximal hydrophilicity observed by Gilding & Reed (1979).

A further geometry-dependent heterogeneous mechanism has recently gained popularity, whereby entrapped oligomeric fractions promotes internal acidosis and autocatalytic degradation (Vert, et al., 1991; Witschi & Doelker, 1998), but in a size dependent manner (Flandroy et al., 1997). This mechanism has a particularly pronounced effect on degradation where a fraction of oligomers have been purposely incorporated (Park, 1994; Reich & Bernickel, 1998).

Within a polymer class, MW is another factor available to modulate degradation and release character. Degradation increases due to the higher content of autocatalytic COOH end-groups as MW decreases. Asano et al. (1989) observed the time for 100 % *in vivo* degradation of PDLGA (70:30) acid increased linearly with number average MW (M_n). Total degradation times of 10 weeks and 20 weeks were observed for copolymers of M_n = 1.6 and 3.3 kD respectively. Further examination of poly-D,L-lactic acid and poly-D,L-lactide in the M_n range 1.4 to 16.9 kD revealed two *in vivo* degradation patterns for these amorphous polymers. Below M_n 1.6 kD, a parabolic degradation profile emerged, characterized by a rapid degradation. Those above 2 kD, in contrast, exhibited an sigmoidal profile consequent of an initial lag phase before the onset of the acceleratory and terminal phases. During this lag period, water uptake and hydrophilicity concomitantly increase as the polymer fragmented, exposing alkoxylic and carboxylic groups (Hutchison & Furr, 1990). The duration of the lag or induction period was proportional to M_n above the critical level. Schindler et al. (1977) identified a threshold intrinsic viscosity of 0.5 dL g^{-1} for PDLLA, corresponding to a MW of 15 kD, below which dramatic weight loss occurred. Copolymer degradation has also been correlated with T_g (Avgoustakis & Nixon (1991), whereby the latter increased in parallel with MW and lactide content (Jamshidi et al., 1988).

1.1.2.4.2 Environmental factors

Since biodegradable systems are intended for use in physiological systems, a number of studies have examined the effect of biochemical factors on polymer degradation, i.e., pH, ionic strength, enzymatic activity of the degradation environment. The effects of pH and ionic strength have been extensively examined by Makino et al. (1985; 1986a,b). The rate of hydrolytic deesterification and polymer mass loss was most rapid at pH 9.6 and slowest at pH 5.0 (Makino et al., 1986a). The effect of pH appeared to change the mechanism of degradation based on polydispersity and lactic acid generation measurements (Makino et al., 1986b). At high pH, random chain scission was apparent,

in contrast to an 'unzipping' mechanism at lower pH values (Makino et al., 1985). In contrast, Belbella et al. (1996) have proposed a random scission at low pH and sequential cleavage from the chain ends in alkaline medium. The complex effect of pH and rejection of the simple acid-base hydrolysis mechanism was first identified by Chu and coworkers. Chu (1981a) observed a 20% retention of PGA suture strength after 21 d at pH 5.25 and 7.44, whereas no traces of sutures were evident at pH 10.09 after the same time. The variation in degradation rate was explained on the basis of the 'cage-effect', a process, specific to low pH, where reactive species can recombine following acid hydrolysis. Removal of the acidic products of polymer degradation by disodium hydrogen orthophosphate and a potential catalytic effect of buffer salts explained the increased degradation rate in buffered media (Chu, 1981b). Degradate removal by buffer salts was the proposed mechanism by which increases in buffer concentration caused parallel increases in degradation rate (Makino et al., 1986a) of PLLA microcapsules. Conflicting behaviour is probably a consequence of complex anionic and cationic specific catalytic effects reported recently for PDLLA/PDLGA films (Reich & Bernickel, 1998).

1.1.2.4.3 Physiological factors

Brady et al. (1973) demonstrated the bioresorptivity of ^{14}C-labelled PDLLA implanted blocks. They found 36.8 % of original radioactivity was lost from the implant after 168 d. However, only 7.7 % of the cumulative loss could be reconciled as radioactivity in faeces, urine and tissues, that unaccounted fraction being lost as expired CO_2.

The role of enzymes in poly-α-hydroxy acid degradation is unclear. Herrman et al. (1970) suggested an enzymatic contribution in favour of the phagocytic mechanism to the resorption of PGA acid sutures. However, phagocytosis contributes significantly to microsphere resorption of diameter < 2 μm (Tabata & Ikada, 1988). Under non-standardized conditions, Williams & Mort (1977) observed selective activity of a series of 15 enzymes on PGA sutures. Differences were probably a reflection of the substrate specificity of enzymes studied. Makino et al. (1985) demonstrated increased levels of carboxylic esterase increased degradation of PDLLA due to an effect confined initially to the material surface. The coherence of surface was considered to restrict the penetration of the large enzyme (96 kD). According to Splenlehauer et al. (1989) *in vivo* administration of poly-α-hydroxy acids accelerated their degradation by a factor of two, highlighting the failure of *in vitro* studies to mimic the biological conditions.

1.2 Drug delivery systems based on poly-α-hydroxy acids

The potential to readily alter polymer physicochemistry confers significant versatility on the poly-α-hydroxy acids. This is best highlighted by the volume of articles which describe the preparation and characterization of biodegradable delivery systems of a multitude of designs: implants (Yolles et al, 1975; Wise et al., 1978; Phillips & Gresser, 1984; Bodmeier & Chen, 1988; Scmitt et al., 1993; Deasy et al., 1993; Kader & Jalil, 1998a,b); fibres (Eenink et al., 1987); microparticles (Smith & Hunneyball, 1986); nanoparticles (Le Ray et al., 1994; Belbella at el., 1996); beads (Schwope et al., 1975); pellets (Bodmeier & Chen, 1989); rods (Wise et al., 1976); and, the most extensively examined, microspheres. The diversity of reported microencapsulation techniques is further testament to their versatility, allowing the formulator considerable flexibility in the design and fabrication of these systems. A suitable technique must achieve suitable drug loading, drug stability and release kinetics (Iwata & McGinity, 1992), the selection of which, will principally depend on the solubility of the polymer and drug to be incorporated (Jalil & Nixon, 1990f), the intended use and duration of therapy (Lewis, 1990). Although, emulsion solvent extraction (Sato et al., 1988; Arshady, 1991; Pavanetto et al., 1992); phase separation (Vidmar et al., 1984, 1985; Ruiz et al., 1989; Owusu-Ababio & Rogers, 1996); solvent partition (Leelarasamee et al., 1986; 1988a,b); interfacial deposition (Makino et al., 1985); and, *in* situ polymerization (Speiser & Hijsnsbroek, 1979) have been reported, microencapsulation based on solvent evaporation has been the most comprehensively examined, i.e., emulsion-solvent-evaporation (ESE) and spray-drying.

1.2.1 Emulsion-solvent-evaporation

In general terms, microsphere preparation by the ESE process involves three stages. The drug to be encapsulated is dissolved (or dispersed) in a suitable water-immiscible and volatile organic solvent. This solution (or suspension) is then dispersed in a hydrophilic phase containing emulsifier or viscosity enhancer to form stable microdroplets. Microsphere formation is induced by solvent evaporation by application of heat and/or vacuum which causes a phase separation process in which the polymer solution is converted into precipitated, solid microspheres (Grandfils et al., 1992). Although conceptually simple, the final physical characteristics of the product are a complex interplay between the disperse phase (i.e. drug, polymer and solvent), emulsifier, continuum and process specific factors (Watts et al., 1990). A multitude of configurations have been described, modifications often being made to compensate for unfavourable drug physicochemistry and thus to maximize loading efficiency.

1.2.1.1 Disperse phase

1.2.1.1.1 Drug

Using aqueous emulsion techniques, high encapsulation efficiencies can only be attained if 1) the drug is successfully retained within the polymeric matrix or 2), partitioning of the drug from the disperse phase is suppressed. Drug physicochemistry and drug loading, which themselves are inextricably linked, have a dramatic influence on the characteristics of the microspheres thus formed. Therefore, aqueous emulsification procedures are more amenable to drugs with low aqueous solubility. Fong et al. (1986) cited a solubility criterion of ≤ 0.023 gL^{-1} for efficient encapsulation. Accordingly, nifedipine, which complies with this solubility specification (0.010 gL^{-1}), gave encapsulation efficiencies of 80 - 100 % within the attempted range of 23 - 7.4 %w/w, respectively (Sansdrap & Möes, 1993). Conversely, water soluble drugs such as theophylline, salicylic acid and caffeine could not be entrapped due to complete migration into the aqueous phase (Bodmeier & McGinity, 1987c), whereas highly efficient encapsulation of lipophilic steroids (Beck et al., 1979; Zhifang et al., 1993), diazepam (Bodmeier & McGinity, 1987c), and hydrocortisone (Cavalier et al., 1986) have been described. In relation to solubility, incorporation efficiencies of a series of bases have been shown to be directly related to their octanol-water partition coefficients (Cha & Pitt, 1989). The relative coincidence of the values for thioridazine of 82 % (Maulding et al., 1987) and 88.8 % (Fong et al., 1986) prepared according to different protocols, highlights the relative insignificance of processing parameters, and, the criticality of inherent drug properties to successful drug entrapment at the extremes of aqueous solubility.

Efficiency of encapsulation has repeatedly been shown to be a function of attempted loading, the former generally decreasing as the latter increases (Splenlehauer et al., 1988; Polard et al., 1996; Celebi et al., 1996). This trend is theoretically reversed in the situation where sufficient drug transfer from the internal phase to attain saturation solubility of a poorly soluble drug in the continuum occurs. Here a lower mass of drug dispersed should result in reduced encapsulation efficiency, and *vice versa*. In support of this, Jalil & Nixon (1990d,e) found encapsulation efficiencies in PDLLA of 90.9 % and 72.6 % when attempting core loadings of 66.6 %w/w and 20 %w/w, respectively. Comparable observations were made by others (Cavalier et al., 1986; Ramtoola et al., 1991). Parabolic dependence of encapsulation efficiency has been reported for cisplatin (Splenlehauer et al., 1986a) and nifedipine (Sandrap & Möes, 1993), presumably due to continuum saturation being attained at intermediate attempted loadings.

1.2.1.1.2 Solvent

For efficient drug encapsulation the ideal characteristics of the polymer solvent include an ability to dissolve both drug and polymer; immiscibility with the continuum; lower boiling point than the continuum and low toxicity (Watts et al., 1990). Bodmeier & McGinity (1986; 1988b) in studies evaluating solvent selection, identified that a degree of water miscibility was required to ensure the preparation of smooth spherical spheres. The water-immiscible solvent, DCM, which also possesses measurable water solubility, achieved highest drug loading at 23 %w/w of an attempted 30 %w/w. However, CFM, which has a water solubility of 0.8 %w/w, and benzene, produced microspheres of minimal quinidine sulphate content. The authors also reported that ACT and dimethysulphoxide when used alone did not emulsify but produced large polymer agglomerates. However, inclusion of 30 %v/v ACT in DCM did form discrete microspheres (Bodmeier & McGinity, 1988a), of improved loading. These observations were explained on the basis of diffusion of solvent from the disperse phase and subsequent evaporation at the air/water interface (Bodmeier & McGinity, 1988b). An optimum rate of evaporation, and thus co-solvent ratio should theoretically exist for every ESE procedure. The optimum should induce phase separation rapidly, but in a controlled manner to achieve satisfactory densification and avoid interfacial perturbation leading to agglomerates.

Chlorinated solvents are generally considered hazardous to the environment and undesirable for manufacturing processes. Accordingly, their complete substitution for methyl (Wakiyama et al., 1981) and ethyl acetate (Wakiyama et al., 1981; Chern et al., 1996) and methyl ethyl ketone (MEK) (Sah et al.,1995) or partial substitution with water miscible ACT (Grandfils et al., 1992; Cowsar, 1985; Coombes et al., 1994) and methanol (Polard et al., 1996) has been described on both toxicological and technological grounds. Conversely, Splenlehauer et al. (1986b) included water-immiscible cyclohexane to reduce solvent residue. This was ascribed to increased porosity due to the sequential evaporation of DCM followed by the pockets of cyclohexane. Others have incubated microspheres in a polymer non-solvent, heptane, to extract residual DCM (Leelarasamee et al., 1988b).

1.2.1.1.3 Polymer

The granulometric, yield, loading and morphological characteristics can all be affected by the MW of the polymer (Jalil & Nixon, 1990b,c); its stereochemistry and concentration;

disperse volume; as well as core drug characteristics. Dispersion of greater volumes of a fixed disperse composition dramatically decreased quinidine sulphate content (Bodmeier & McGinity, 1986). Continuum-solvent saturation and thus reduced rates of polymer precipitation which promoted drug diffusion outwards, explained this trend. Optimal disperse viscosities corresponding to 7.16 %w/w, that inhibited internal crystal movement and therefore maintained spherical integrity and drug payload, were identified for cisplatin microspheres (Splenlehauer et al., 1986b). In the same study, microsphere size and size distribution increased in line with disperse viscosity. In contrast, successful microsphere formation was reported from a homogenous solution in the range 1.7 to 10 %w/v polymer, where a linear inverse dependence of mean diameter on disperse volume in the range 20 to 60 mL was observed (Sansdrap & Möes, 1993). However, the report contained no process yield or morphological data on the particles thus formed. Grandfils et al. (1992) concluded that disperse phase modification was the best parameter to achieve chemobolic particles with a narrow size range and perfect sphericity.

Microsphere properties are more dependent on polymer stereochemistry than MW. Morphology, density and phenobarbitone content of PDLLA microspheres were independent of polymer MW, although mean diameter increased within the range 5.2 to 20.5 kD (Jalil & Nixon, 1990d). Despite viscosity differences, the amorphous character of this polymer group efficiently encapsulated phenobarbitone crystals, inhibiting crystal diffusion, and thus accounted for comparable polymer performance. In contrast, PLLA of 61.3 and 43.2 kD produced large porous particles, porosity and size increasing with respect to MW and core loading. Conversely, low MW PLLA (2.4 kD) polymers yielded microspheres with uniform, smooth morphology when prepared at low drug content. Increasing core loading met with surface deterioration, porosity and a greater propensity to aggregate. Particle size showed a complex parabolic behaviour with respect to core loading reaching a minimum at a drug:polymer (D:P) ratio of unity (Jalil & Nixon, 1990b). These observations were assigned to faster polymer deposition as polymer solubility decreased in the disperse with increases in MW and crystallinity.

1.2.1.2 Emulsifier

Judicious selection of aqueous emulsifier should produce a stable emulsion which upon solvent evaporation yields small, uniform and discrete particles which deaggregate with minimal agitation (Arshady, 1991). Hydrophilic colloids are most frequently employed such as gelatin (Wakiyama et al., 1981; 1982a,b); polyvinyl alcohol (PVA) (Zhifang et

al.,1993; Le Corre et al., 1994b; Sah et al., 1995; Chern et al., 1996); and, methylcellulose (Benita et al., 1984; Cavalier et al., 1986; Maulding et al., 1987). PVA is most frequently used, generally alone (Beck et al., 1979; Maulding et al., 1986), or, alternatively, with viscosity enhancers, e.g., methylcellulose (Splenlehauer et al., 1986a, Bissery et al., 1984). Others have used anionic surfactants, e.g., sodium lauryl sulphate (Suzuki & Price, 1985); polyoxyethylene sorbitan mono-oleate (Bodmeier & McGinity, 1986); sodium oleate (Fong et al., 1986) and hydroxymethylcellulose (Sansdrap & Möes, 1993). Bodmeier & McGinity (1987b) have, however, prepared satisfactory yields of microspheres at pH 12 without emulsifier. The authors considered electrostatic repulsion of deprotonated polymer COO^- end-groups at high pH maintained emulsion stability.

The choice of emulsifying agent has a significant influence on particle size of microspheres. Microsphere aggregation may be avoided by increasing the viscosity grade of PVA used (Splenlehauer et al., 1986a). This effect was considered to be due to the longer polymeric chains of a higher grade emulsifying agent, and enhanced steric repulsion of droplets within the more viscous aqueous phase. Successful preparation of microspheres using PVA at concentrations as low as 0.01 % (Le Corre et al., 1994b) and at levels as high as 10 % (Boisdron-Celle et al., 1995) can be found. These low levels were presumably sufficient because disperse phase volume was small, i.e., 5 mL. Benita et al. (1984), found that microsphere size increased as the PVA concentration increased due to an increase in the viscosity of the aqueous phase in the range 0.27 to 5.0 %w/v, while further increases from 5 - 10 % have been shown to reduce particle size from 100 to 20 μm by others (Boisdron-Celle et al., 1995). However, other workers found no correlation of PVA concentration with particle size between the range 0.5 and 0.1 %w/v (Celebi et al., 1996). The variety of results reported are a result of the non-standardized conditions under which these observations were made. Singh et al. (1996) have demonstrated that compliance of residual PVA limits is best achieved by using minimal volumes and concentrations of emulsifier during preparation, which, in turn, minimizes the need for tedious successive microsphere washings.

Production of large coarse particles indicated emulsion instability using 1 %w/v gelatin solution due to viscosity limitations (Wakiyama et al., 1981) which were eliminated at 2 %. Inclusion of dibasic sodium phosphate further disrupted the viscosity of 1 % gelatin producing a blend of spherical and non-spherical particles. The inclusion of baffles in the emulsion vessel can significantly alter fluid dynamics resulting in reduced microsphere

particle diameter (Crossan & Whateley, 1994), polydispersity and increased yield (Bodmeier & McGinity, 1987a).

Emulsifier has been identified as the cause of crystal deposition at the microsphere-continuum interface. Consequently, interrupted solvent evaporation strategies have been developed, in which the original continuum is replaced in-process with emulsifier-free medium (Beck et al., 1979; Benita et al., 1984). Benita et al. (1984) considered an optimum time for continuum exchange existed, before which, immature particles could agglomerate due to matrix plasticity conferred by residual solvent. Bissery et al. (1984) used a two-stage protocol whereby initial emulsification was performed in 0.25 %w/v PVA, followed by dilution in 1 %w/v methylcellulose. Aggregation noted was probably consequent of the low polymer (2 %w/v) and primary emulsifier concentrations.

1.2.1.3 Continuum

Strategies intended to minimize drug partitioning from microdroplets during hardening have comprised continuum modification in terms of volume (Sansdrap & Möes, 1993), pH (Bodmeier & McGinity, 1987a,b,) and composition (Jalil & Nixon, 1989; 1990a-h). Such modifications are not always, however, without detriment to other microsphere characteristics.

Continuum volume affects the rate and extent of disperse solvent partitioning which was identified by Bodmeier & McGinity (1986) as a critical determinant of drug loading efficiency. Increasing the volume of continuum from 1.0 to 1.8 L resulted in a increased quinidine loading in the range 18.9 to 25.0 %w/w. Owing to the small disperse:continuum phase ratio, solvent extraction, not evaporation was the predominant phase separation mechanism. Larger continuum volumes, however, were also associated with an increase in particle size which has been shown also to increase drug loading (Zhifang et al., 1993; Sánchez et al., 1993; Boisdron-Celle et al., 1995). On the contrary, insignificant granulometric changes were evident elsewhere upon a five-fold increase in continuum volume (Sansdrap & Möes, 1993).

Bodmeier & McGinity (1987a,b) showed pH manipulation of the continuum to high values, suppressed ionization of the base quinidine sulphate, thus minimizing drug partition from the dispersed droplets. For an attempted drug loading of 30 %w/w, negligible drug levels were attained at acidic pH, whereas 23.6 %w/w loading was observed at pH 13. Surface

layer peeling and the exposure of a porous substructure occurred at extreme pH, but were absent at pH < 10, with minimal effect on drug loading. Higher osmotic pressures generated by quinidine sulphate, which promoted surface degradation, explained the superior morphology seen with microspheres prepared with free base. In a further study (Bodmeier & McGinity, 1987b), rapid pH change between 12 and 7 (and vice versa) had no effect on drug loading beyond two minutes. This time was considered optimal, allowing the use of short exposure times thus protecting the polymer coat without compromising loading. The authors postulated that sufficient solvent rapidly diffused into the large continuum volume (1.4 L) creating a coherent membrane, thus hindering further drug partitioning. In the same report, a 'partition method' was devised, whereby saturated solutions of quinidine sulphate at pH 8 (high drug solubility) were prepared, into which drug free polymeric solutions were dispersed. A linear relationship between the quantity of drug dissolved and final loading was observed. These observations verified the ideas of rapid solvent-drug exchange and that ultimate loading was a function of the total drug in the system. Comparable improvements in microsphere loading of morphine (Polard et al., 1996) and local anaesthetic (Wakiyama et al., 1981; Le Corre et al., 1994b) have been attained on the basis of the pH-partition principle.

On the one hand, presaturation of the continuum with incipient drug has been repeatedly demonstrated to improve loading efficiency: tetracaine (Wakiyama et al., 1981), phenobarbitone (Jalil & Nixon, 1989), cisplatin (Splenlehauer et al., 1986a,b; 1988), quinidine (Bodmeier & McGinity, 1987c) and diazepam (Pavanetto et al., 1994a); on the other hand, microspheres with substantial embedded surface crystals are associated with continuum presaturation (Jalil & Nixon, 1989). Others have successfully attempted to prevent drug partition by equalization of disperse:continuum osmotic potential by addition of salts to the continuum (Joly et al., 1994; Esposito et al., 1997).

A number of anhydrous encapsulation procedures have been described in an attempt to improve the inherent limitations of encapsulation of hydrophilic substances using the aqueous ESE procedure. Tsai et al. (1986) pioneered a non-aqueous o/o' ESE technique, whereby a solution of mitomycin-C and PLLA was dispersed in light liquid paraffin (LLP) containing, as emulsion stabilizer, Span 65. Subsequent evaporation of acetonitrile at 55 °C resulted in the precipitation of polymer and drug as coherent, spherical microparticles with a particle average size of 95 μm. Jalil & Nixon (1989; 1990a-e,g,h;) have extensively investigated this technique using phenobarbitone as core reference. The authors have

reported that both encapsulation efficiency and microsphere yield improved significantly using the o/o^{l}, opposed to a conventional aqueous emulsion procedure (Jalil & Nixon, 1989). Poor solubility of phenobarbitone in LLP relative to aqueous media explained this observation. However, microspheres produced by the o/o^{l} were large and irregular in shape compared with those prepared using the o/w procedure and required large volumes of organic solvent to remove residual oil and emulsifier. High speed homogenization has recently generated particles of substantially smaller granulometry (Atkins et al., 1998). Aqueous substitution for silicone oil increased encapsulation efficiency of cisplatin from 10 to 80 % of an unspecified attempted loading (Wada et al., 1988b). Other workers have investigated glycerin-water combinations (Gupta et al., 1993) and glycerin alone (Pavanetto et al., 1994a) as alternative continuous phases.

1.2.1.4 Process

The effect of continuum viscosity is a function of the manufacturing technique and the manner by which viscosity modification arise. Jalil & Nixon (1990e) attributed reduced particle size at elevated temperatures to a reduction in continuum and disperse viscosity which facilitated dispersion. However, the same cause, but opposite effect was described by Wakiyama et al., (1981), whereby processing at 40 °C, using 1 %w/v gelatin, produced larger microspheres than those obtained at room temperature under vacuum due to droplet coalescence. Higher viscosity of 1 %w/v Na alginate, compared to 1% w/v gelatin, produced smaller microspheres under equivalent conditions. It has also been reported that increasing levels of gelatin produced progressively smaller microspheres (Wakiyama et al., 1981; Juni et al., 1985a).

Generally, increased stirring rates are associated with a decrease in mean particle size and distribution breadth (Benita et al., 1984, Splenlehauer et al., 1986a; Sánchez et al., 1993; Zhifang et al., 1993; Sansdrap & Möes, 1993). With these changes, encapsulation efficiencies typically decrease in parallel with an increase in particle specific area (Splenlehauer et al., 1986a). Exceptions to these trends do however exist. For example, despite a 30-fold reduction in mean microsphere size to 1 μm at 3000 rpm compared with 1000 rpm, Sánchez et al. (1993) assigned the invariant and high encapsulation efficiency to the affinity of cyclosporin A for the disperse phase. Conti et al. (1995a) observed an anomalous increase in particle size as the rate of high speed homogenization increased at 0.5 %w/v PVA level, but size was invariant above 2 %w/v PVA.

A study of the effect of temperature of evaporation concluded that the observed reduction in microcapsule size with increased temperature of solvent evaporation was due to viscosity reduction of both the disperse and continuous phases (Jalil & Nixon, 1990e). Rapid phase separation, induced by excessive temperatures, accounted for the disrupted surface of microcapsules prepared at 85 °C. Furthermore, morphologically smooth microcapules were prepared from amorphous PDLLA, independent of polymer MW, in contrast to the highly porous and textured products of semi-crystalline PLLA. Evaporation of acetonitrile at temperatures above the T_g temperature of PDLLA probably facilitated the film-forming character of the polymer (Jalil & Nixon, 1990e). Amorphous PLLA matrices can be readily formed by more rapid solvent evaporation induced by application of vacuum to the emulsion during microsphere hardening (Izumikawa et al., 1991).

Overall, the extensive and occasionally contradictory results from ESE highlight the need for empirical studies because of the complex interaction between the drug substance and the polymer matrix, as well as the manufacturing technology.

1.2.2 Spray-drying

The aforementioned preparative techniques are often time-consuming and dependent on many variables. Ideally, microsphere preparation should be simple, reproducible, rapid (Takada et al., 1995) and easy to scale-up (Bodmeier & Chen, 1988); criteria which are arguably best satisfied by spray-drying. Most research laboratories use the same apparatus; the Mini-spray Büchi 190/1 (Bitz & Doelker, 1995; Bodmeier & Chen, 1988; Bruhn & Müller, 1991; Castelli et al., 1994; Clarke et al., 1998; Conte et al., 1994a,b; Conti et al., 1991, 1994, 1997; Genta et al., 1991, 1994; Giunchedi et al., 1994a,b, 1995, 1998; Gupta et al., 1993; Mathiowitz et al., 1992; Pavanetto et al., 1992; 1994a,b; Rafler & Jobmann, 1994; Volland et al., 1994; Wagenaar & Müller, 1994), a schematic of which is shown in Figure 1.2. The codissolved or suspended feed (A) is fed at a controlled rate (B) through the nozzle (C). Flow rate — which controls the characteristics of the microdroplet aerosol (D) — and aspiration (F) — which draws the air through the glassware assembly — when balanced, ensure efficient separation of product from the drying air at the level of the cyclone (G). This, in turn, promotes deposition of product in the collector (I). Whereas the inlet temperature is preset, the temperature of air detected by the thermocouple (H) is a function of the inlet temperature, flow rate, and the drying load. The latter factor is determined by the heat capacity of the liquid being processed and the feed rate of same.

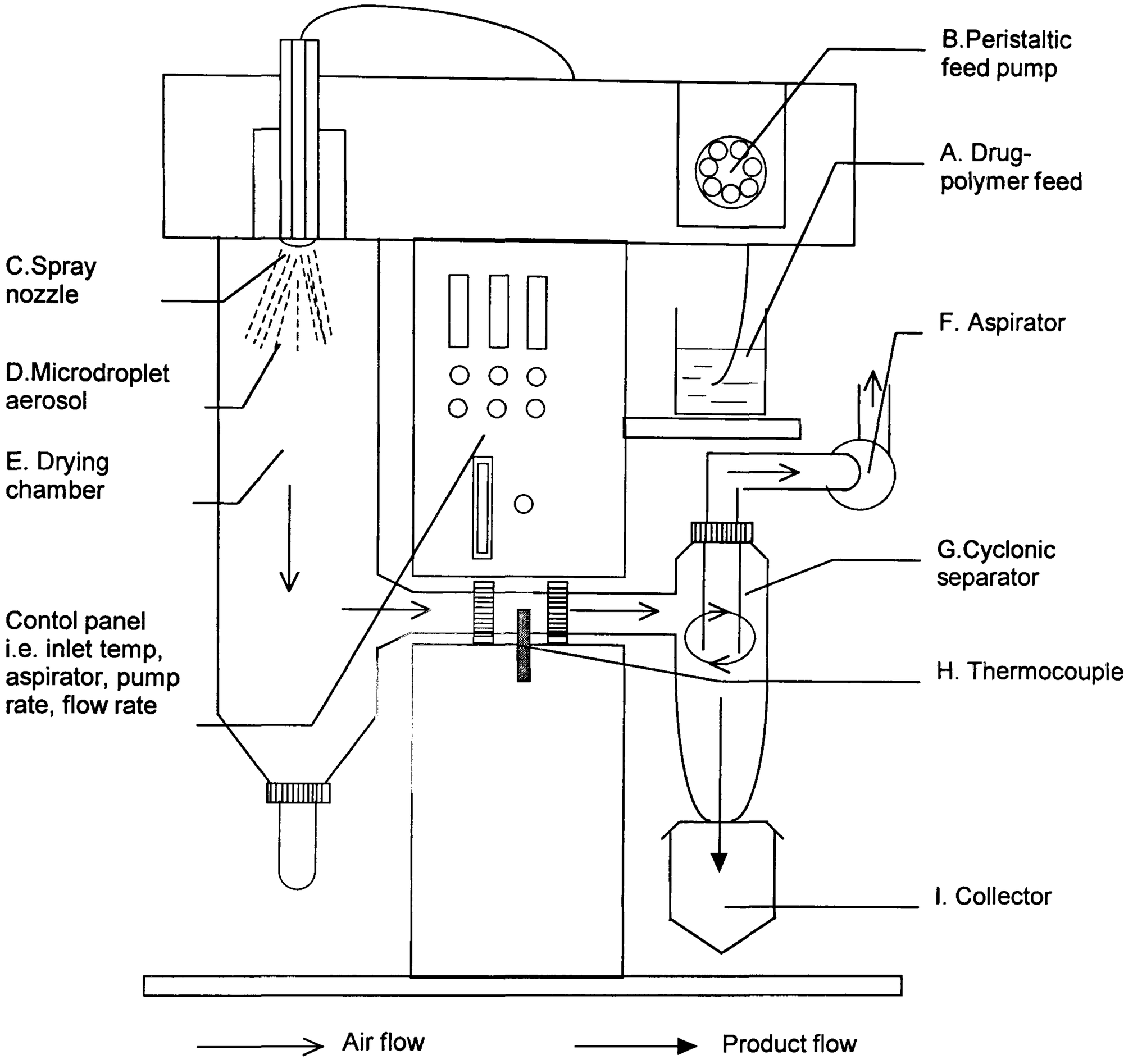

Figure 1.2 *Schematic of the two-fluid nozzle co-current Büchi® Minispray 191 spray-drier. Arrows indicate the idealized directions of both air and product flow*

1.2.2.1 Drug

Unlike other microencapsulation strategies, efficient encapsulation can be achieved with little dependence on the solubility of the drug or polymer using spray-drying (Bruhn & Müller, 1991). The earliest report of spray-dried biodegradable particles described the preparation of antimalarial PDLGA (25:75) microspheres (Wise et al., 1976). Encapsulation of 2,4-diamino-6-(2-naphthylsulphonyl)-quinazoline at levels of 16.7 % and 33.3 %w/w drug produced finely divided particles of < 125 μm although no other physical characteristics were presented. Presumably, the unusual cosolution of 1,1,1,3,3,3-

hexafluoro-2-propanol and benzene was employed to promote polymer solubility, although no rationale was specified. Bodmeier & Chen (1988) illustrated the effects of drug characteristics on spray-dried microsphere formation. Drug was either dissolved (progesterone) or suspended (theophylline) in PDLLA prior to spray-drying. The polymorphic form of progesterone varied with spray conditions, whereby entrapment within PDLLA promoted formation of the β-form. Although morphology was not discussed, retarded dissolution indicated that theophylline was in part encapsulated; dissolution rate increasing with respect drug payload. In the same study, caffeine produced rod-like particles indicative of a drug-polymer incompatibility.

Considering all the drug and the polymer are sprayed and no drug can be lost to the continuum as it is hot air (Bodmeier & Chen, 1988), encapsulation efficiencies of < 100 % have quite surprisingly been reported (Pavanetto et al., 1993; 1994a). For vitamin D_3, this effect was drug load dependent which the authors stated erroneously was analogous to partitioning observed in emulsion technology (Pavanetto et al., 1993). Stereospecific PLLA achieved highest loadings, whereas, racemic polymers of low and medium M_n produced lower but comparable drug levels. Again no explanation was offered, although polymer dependent drug decomposition is inferred owing to the instability of vitamin D_3. In general, actual and theoretical loadings have shown good correspondence (Conti et al., 1994; Wagenaar & Müller, 1994).

1.2.2.2 Polymer

Polymer MW is a critical factor to successful microsphere formation using the Büchi 190/1 equipment (Bodmeier & Chen, 1988; Pavanetto et al., 1993; Rafler & Jobmann, 1994). Bodmeier & Chen (1988) encountered the problem of fibre formation owing to insufficient forces to break the liquid into droplets, consistent with the fibrous recrystallization behaviour observed for PLLA by Kalb & Pennings (1980). Filament formation was strongly dependent on the stereochemistry of the polymer used and to a lesser degree its viscosity. Higher solution viscosity of PLLA, when compared with optically inactive PDLLA, arose as a result of the chain-stiffening effect of isotactically arranged methyl groups. Accordingly, the optimal MW range and the concentration at which PLLA inclines towards fibre formation are both lower than for PDLLA of equivalent MW. Solvent choice appeared to have no influence on fibre formation (Rafler & Jobmann, 1994). Pavanetto et al. (1993) identified optimal concentrations and polymer MW in the ranges 0.5 - 2.5 %w/v and 16 - 209 kD, respectively; which where highly stereospecific.

Another important determinant of particle morphology is D:P ratio (Conte et al., 1994b; Pavanetto et al., 1993). Pavanetto et al. (1993) did not comment on the morphological consequences of increasing vitamin D_3 payload from 5 - 30 % (an increase in D:P ratio of 1:19 to 1:3.33. Conte et al. (1994b), however, described a smooth spherical product at D:P ratio of 1:2, whereas a deterioration in sphericity coincided with the onset of agglomeration at a D:P ratio of 2:1. For polyanhydrides, spray-drying had the effect of reducing or eliminating polymer crystallinity which, in turn, affected morphology. Crystalline polymers, such as poly (sebacic anhydride) gave microspheres with a porous and crenelated surface. In contrast, copolymers of carboxyphenoxypropane and sebacic acid which possess low crystallinity, yielded microspheres with a smooth exterior (Mathiowitz et al., 1992).

In a general sense, PDLLA appears to produce superior morphologies (Pavanetto et al, 1993; Wagenaar & Müller, 1994) compared with both PLLA and PDLGA. Small craters (Wagenaar & Müller, 1994), surface concavities (Gupta et al., 1993) particle collapse (Thoma et al., 1992) have more frequently been described with the latter two polymer types. These observations can only partially be explained on the basis of crystallinity (see 1.1.2.2). In addition, PDLLA is solubilized under moderate conditions, that may favour solubilization and thus entrapment of drugs over a broader solubility range. The superior film-forming character of PDLLA compared with PLLA might also be influential (Arshady, 1991)

1.2.2.3 Solvent

Pavanetto et al. (1993) obtained superior morphology with a 1:1 cosolvent of DCM:CFM, when DCM, CFM and 1,2 dichloro-ethylene and mixtures thereof were compared. However, comparable morphologies have been attained using DCM alone using PDLLA of equivalent MW at elevated inlet temperatures (60 compared with 51 °C) and feed rates (800 compared with 225 mLh^{-1}) (Wagenaar & Müller, 1994). Others have advocated the complete or partial substitution of ACT on toxicological grounds, which did not seem to adversely affect particle morphology in their studies (Rafler & Jobmann, 1994).

1.2.2.4 Process

Limited systematic assessment of the influence of process parameters have been reported using diazepam and PDLLA as model drug and polymer, respectively (Conte et al., 1994a). At a fixed D:P ratio of 3:7, whilst 3 %w/w total solid gave good microsphere

morphology, 1.25 % gave incomplete microspheres, whereas 5 % promoted agglomeration. A temperature increase from 44 to 63 °C dramatically reduced particle size. The effect of feed rate, however, appeared complex and dependent on inlet temperature. Overall, at higher temperatures, increased feed rate reduced particle size, while the effect on particle size distribution was reversed at lower temperatures. No explanation for these observations was offered by the authors.

A major advantage of spray-drying is the short preparation times (Pavanetto et al., 1992; Takada et al., 1995). Pavanetto et al. (1992) estimated a four-fold increase in production rate when compared with traditional emulsion methods. Comparison of spray-drying with w/o/w gave profound decreases in preparation time for 10 g batches; 3 min compared with 24 h, respectively (Takada et al., 1995).

Yields as low as 30 % (Giunchedi et al., 1998; Pavanetto et al., 1993) are not uncommon, and as high as 60 % (Conti et al., 1994; Wagenaar & Müller, 1994) have been reported. Bodmeier & Chen (1988) identified polymer T_g, and residual solvent as potential determinants of yield. An optimum spray-air flow pattern, which minimizes particle-wall collision and restricts product loss via the exhaust, was thought to exist (Bodmeier & Chen, 1988). Indeed, polymer MW and concentration had little influence on the yield of vitamin D_3, highlighting the criticality of process parameters (Pavanetto et al., 1993). Yield does, however, appear to be more strongly influenced by the character of the feed; 10 - 40 % for emulsions (Takada et al., 1995); 50 % for solutions (Conti et al., 1994b) being representative. When clarification using spray-drying of solvent-evaporated microspheres was employed very low yields were reported, although no data were presented (Gupta et al., 1993). No explanation was offered by the authors, but factors such as the small particle size produced by microfluidization of immature microspheres which could more easily be exhausted; low solid content of the feed (2 - 6 x 10^{-3} gmL^{-1}); and, low temperature of recovery whereby residual moisture would promote glassware adherence, undoubtedly made a contribution. Takada et al., (1995) demonstrated a double nozzle method whereby formed particles were coated with mannitol in-process. This modification was reported to greatly improve yield by minimizing particle-glassware adherence.

Particle size distribution, morphology and particle formation are a function of different process and material factors: polymer used, i.e., concentration, stereochemistry, MW (Pavanetto et al., 1993; Bodmeier & Chen, 1988) and its solubility; apparatus design

(Wise, 1976); and, the proportion and nature of drug (Rafler & Jobmann, 1994). Generally, particle size distributions reported are typically in the range 1 - 10 μm and with little variation. Different designs have yielded smaller particles of range 0.5 - 2.0 μm (Wang et al., 1990) and considerably larger particles (Wise et al., 1976), although no detail of the atomization principle for the latter two was given. At low concentrations, spray-dried PDLLA piroxicam microspheres exhibited a constant mean volume diameter of 5 μm, whereas increasing D90% values, was ascribed to fibre formation at polymer concentrations exceeding 2 % (Wagenaar & Müller, 1994). Rafler & Jobmann, (1994) observed small increases in size and distribution of drug-loaded when compared with blank microspheres, corresponding to a greater solid content of the feed. Generally, particle size will increase with respect to polymer concentration in the feed and polymer MW (Pavanetto et al., 1993) but not necessarily with a linear dependence (Wagenaar & Müller, 1994).

There is evidently a complex interplay between process-specific (e.g. inlet temperature, air flow rate, aspiration) and feed specific (e.g. drug, polymer concentration, solvent choice) variables which influence particle morphology and, in turn, release kinetics. A detailed account of the factors influencing release from poly-α-hydroxy polyesters is presented later. Here, process factors, and their inter-relationships with polymer feed will be reviewed. Rafler & Jobmann (1994) stated with a constant feed, different release profiles utilizing spray-drying parameters could only be achieved to a limited extent, probably owing to their minimal effect on particle granulometry. Conte et al. (1994a) compared the release of particles collected from the cyclone and product collector. For each batch, particles from the collector released drug faster than those from the cyclone, in agreement with their smaller diameter. However, when different batches from the same location were compared, those collected from the cyclone with smaller diameters released diazepam more slowly. The authors concluded only that process parameters had an influence. Possible reasons for this behaviour might have been a surface curing in the hotter region of the cyclone. Curing of microparticles has been previously described as a means of retarding drug release (Zhou & Chang, 1988).

Spray-drying with poly-α-hydroxy acids has been used elsewhere for product recovery (Gupta et al., 1993; Wichert & Rohdewald, 1990), excipient preparation (Avgoustakis & Nixon, 1993a,b) and more recently, spray-coating (Lee et al., 1997). Wichert & Rohdewald (1990) compared a solvent evaporation-extraction procedure with a 'melting-

method' for the preparation of vinpocetine-loaded PDLLA microspheres. This novel method involved emulsification of a pre-molten blend of drug and polymer in an aqueous continuum, in which polvinylpyrrolidone (PVP) had been dissolved to prevent agglomeration. Spray-drying of the hot emulsion (50 - 95 °C) resulted in discrete microparticles with a porous microinterior embedded in PVP. Particle morphology was dependent on MW of the polymer and preparative technique. Spray-dried particles of polymer, MW 2 kD, were smooth and regular, whereas those of polymer, MW 16 kD, were rod-like and more irregular in size. Irregular particles were probably a result of the high viscosity of the polymer-drug melt which required higher temperatures and the inclusion of plasticizer polyethylene glycol (PEG) to facilitate emulsification. Sam et al. (1994) have reported a related spray desolvation technique which also avoids the use of toxic chlorinated solvents.

Finally, notwithstanding the fact size distribution manipulation is restricted (using the Büchi apparatus) and limitations of the feed exist, it can be concluded that spray-drying has considerable potential in microencapsulation. Advantages include general applicability, concerning both the drugs (heat sensitive and heat resistant materials can be used) and polymers (hydrophilic and hydrophobic); one-stage continuous operation; and, its adaptability on an industrial scale.

1.3 Characterization of biodegradable microspheres

Characterization techniques should be appropriately selected so as to adequately examine desired characteristics, particularly those sensitive to manufacturing variables whose constancy is critical to the preparation of a reproducible and effective product. Characterization should allow an understanding and eventual prediction of the system's behaviour (Hausberger & DeLuca, 1995). Techniques selected should also consider the reliability of the measurements made, ease of measurement and availability.

1.3.1 Microscopy

The utility of light microscopy is generally limited to subjective assessment of microsphere shape, general granulometry and presence of aggregates (Jalil & Nixon, 1989), although modern image analysis allows rapid objective measurement of the same attributes. Scanning electron microscopy (SEM) affords high magnification and definition images for direct visualization of microsphere morphology and topography (Watts et al., 1990) and correlation with other characteristics such as drug release profile (Wakiyama et al., 1981),

surface area and bulk density (Hausberger & DeLuca, 1995). Surface continuity, pores, pitting and surface crystals can be readily assessed after microsphere preparation, during degradation (Jalil & Nixon, 1990c) and long-term storage (Jalil & Nixon, 1990h). Sample drying is crucial, as cursory misinterpretation of disintegrated microspheres as a result of polymer degradation was later found to be due to internal volatilization of residual moisture which fractured particles not adequately dried before coating (Bodmeier & McGinity, 1988a). Freeze fracture SEM of microspheres (Jalil & Nixon, 1990d; Wagenaar & Müller, 1994; Esposito et al., 1997) allows characterization of internal architecture. Sophisticated microscopic techniques, such as atomic force microscopy and image analysis have recently been applied to the characterization of adsorbed emulsifier (Boury et al., 1997).

1.3.2 Particle size

The size of the microsphere and particle size distribution of the encapsulated product are important parameters to control in microparticle delivery systems to ensure syringeability (Beck et al.,1985) and efficient organ targeting, particularly for products intended for chemoembolization (Grandfils et al., 1992; Flandroy et al., 1997) and intrapulmonary delivery (Armstrong et al., 1994, 1995; Guiziou et al., 1996). Therefore, methodologies to reproducibly manufacture uniform microspheres in specified ranges, and others to check compliance, are required (Iwata & McGinity, 1992).

1.3.3 Drug characterization

Microparticles are differentiated by morphology and architecture, i.e., how the drug is deposited. This generally gives two distinct structures, microspheres and microcapsules with subdivisions of the latter according to Figure 1.3. With reference to Figure 1.3, microcapsule classically defines a microparticle in which a central core is surrounded by a rate-limiting membrane (A), whereas microspheres comprise an homogeneous blend of both drug, polymer and other ingredients (B). When the microparticle contains several distinct drug domains it is a matter of semantics if that particle is to be defined as a multinuclear microcapsule (C) or a heterogeneous microsphere (D). What can be stated with some certainty is that the physical character of the embedded drug and the polymer can have a profound effect on, in particular, drug release kinetics. Two complementary techniques have enjoyed most extensive use to elucidate the dispersed state of entrapped drug, differential scanning calorimetry (DSC) and X-ray powder diffraction (XRD).

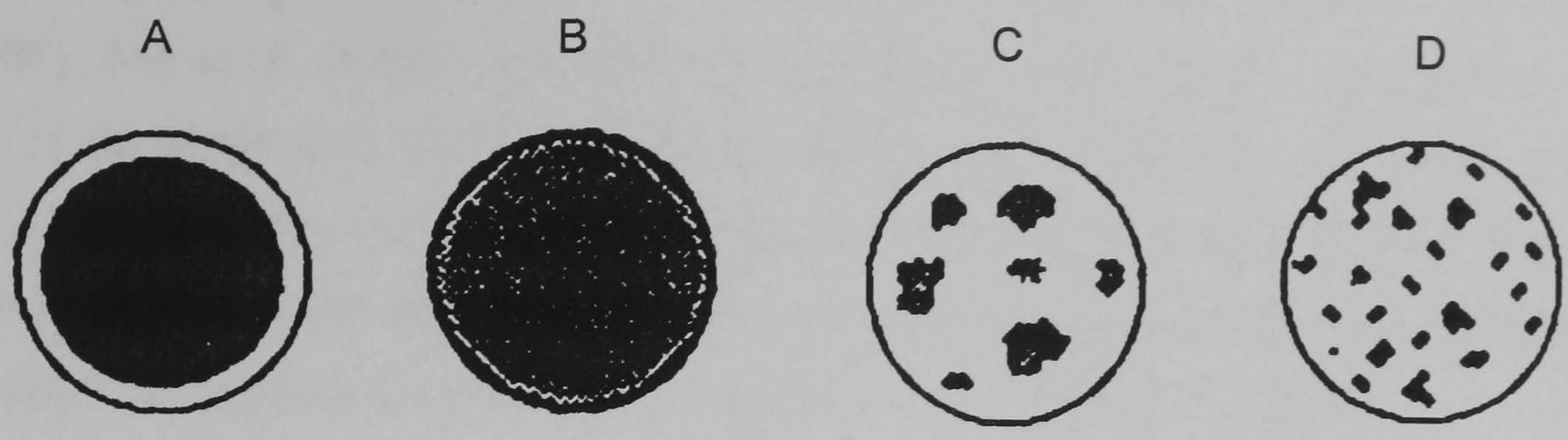

Figure 1.3 *Structures of classes of microproducts*

1.3.3.1 Differential scanning calorimetry

The final form of an incorporated drug will be affected by factors such as relative drug and polymer solubility in the organic medium; rate of solvent evaporation; drug-polymer interactivity, e.g., solid solution and initial D:P ratio. Simplistically, where drug loading is low, precipitation thereof will occur only after polymer viscosity is so high as to impede crystallization. Conversely, at high drug loadings drug precipitation will occur in a more fluid polymer phase which permits significant molecular orientation, nucleation and subsequent crystallization (Dubernet, 1995). Jalil & Nixon (1990e) identified a monolithic distribution of core crystalline phenobarbitone in PDLLA from the appearance of sharp endotherms corresponding to drug. Depressions in polymer T_g temperature after microsphere preparation signalled a degree of drug-polymer solid solution. In contrast, that progesterone could not be detected at 31.7 %w/w in PDLLA was suggestive of solid solution. However, annealing studies established a molecular distribution with little mutual miscibility (Benoît et al., 1986). Bodmeier & McGinity (1987c) observed a metastable distribution of quinidine and quinidine sulphate in PDLLA which yielded recrystallization exotherms during the heating cycle. Rapid solvent partitioning during preparation which hindered matrix stabilization accounted for these effects. Castelli et al., (1994) used DSC to indirectly characterize tolmetin release from PDLLA microspheres by measuring the thermal behaviour of a receptor lipid membrane whose response to drug had been previously calibrated.

1.3.3.2 X-ray powder diffraction

XRD is generally used to confirm the presence of crystalline drug (Cavalier et al., 1986) or polymer (Izumikawa et al., 1991; Richey & Harris, 1995) detected by DSC, but XRD might be considered more sensitive as evidenced by the fact dehydro-iso-androsterone

crystals were detected by this technique to which DSC was oblivious (Ramtoola et al., 1991). Aso et al. (1992) used XRD to illustrate that the long-term stability of amorphous PLLA matrices was compromised by storage above their T_g temperature and under conditions of high relative humidity. Recrystallization of matrix polymer was shown to generally accelerate drug release, although these changes might have been equally due to polymer degradation rather than a redistribution of drug and polymer.

1.3.4 Spectroscopy

A plethora of spectroscopic methodologies have been utilized to study drugs and polymer prior to (Avgoustakis & Nixon, 1991) and following their fabrication as microspheres. Ultraviolet absorption (UV) is generally employed to quantify loading efficiency and drug release kinetics due to the rapid and reliable nature of these measurements (Jalil & Nixon, 1989; 1990a-e,g,h). Mauduit et al. (1993a) used FTIR to verify polymer acid end-group neutralization with basic, gentamycin, during release studies. Conversely, the absence of molecular interaction between drug and PLLA was confirmed by FTIR (El-Baseir et al., 1997). The chain intimacy of amorphous and crystalline matrices has also been compared with FTIR (Izumikawa et al., 1991). Nuclear magnetic resonance (NMR), which relies on separate chemical shifts produced by carbons in specific molecular environments has been employed to examine sequence distribution or 'blockiness' of PDLGA copolymers (Avgoustakis & Nixon, 1991; Bendix, 1990). Recently, the utility of electron paramagnetic (EPR) and magnetic resonance imaging (MRI) for the assessment of PDLGA microviscosity and erosive changes during *in vivo* implantation have been demonstrated. These techniques allow real-time assessment of biodegradation without sequential sacrifice of study animals (Mäder et al., 1995).

1.3.5 Surface analysis

Surface area may affect drug release, biodegradability and product flowability. Gas adsorption (BET) gives more reliable measurements of surface area than air permeatry, as the former can efficiently measure small and tortuous surface discontinuities which can commonly feature on microspherical delivery systems. Hausberger & DeLuca (1995) have demonstrated that use of krypton in favour of nitrogen enhanced analytical sensitivity allowing accurate determinations on 50 mg of sample, whereas 500 mg is generally considered the minimum required when the latter adsorbent is employed.

1.3.6 Gel permeation chromatography

Although relatively crude measurements of MW can be made based on viscometry (Rak et al., 1985; Cha & Pitt, 1989), gel permeation chromatography (GPC) based on the size exclusion principle allows efficient separation of molecules based on chain length. Accordingly, MW distribution and associated statistical indices, number-average (M_n) and weight-average MW (M_w) and polydispersity can be readily calculated; the latter being a measure of distribution breadth (Hausberger & DeLuca, 1995). GPC has therefore been employed to assess the effect of factors considered to alter polymer MW distribution. Thus, polymer batch reproducibility (Boehringer Ingelheim, 1992); polymer degradation during microencapsulation (Witschi & Doelker, 1998); the effect of γ-sterilization (Splenlehauer et al., 1988; Hausberger et al., 1995); *in vitro* (Wang et al., 1991; Sandrap & Möes, 1997) and *in vivo* degradation (Flandroy et al., 1997; Takada et al., 1997) have been examined. The technique has also distinguished between heterogeneous and homogeneous polymer degradation mechanisms (Witschi & Doelker, 1998).

1.3.7 Assessment of *in vitro* drug release

The release of entrapped drug from biodegradable microspheres is governed by an interplay of many factors, some specific to the formulation, i.e., polymer properties; process conditions; matrix morphology; drug physicochemistry, others related to the environment and conditions of the *in vitro* testing, i.e., pH, ionic strength, mechanism of agitation. Drug release may be diffusion or degradation controlled. More often, release will be a function of both mechanisms, the relative contribution of each being dependent on the factors mentioned above.

Dissolution testing can be considered the definitive *in vitro* characteristic in determining the *in vivo* potential of a prototype formulation; as a useful determinant of microsphere quality; and, as an indicator of batch-to-batch reproducibility (Cowsar et al., 1985). As no official recommendations for the examination of drug release from microspherical formulations currently exist, a range of methodologies have been described, varying considerably in geometry, hydrodynamics and composition of the test environment. These variables, in addition to those specific to the formulation, confound comparison of the reported literature. The USP paddle dissolution apparatus (Jalil & Nixon, 1990c,d,g; Suzuki & Price, 1985), 'shaken-flask' (Wakiyama et al., 1982a), 'rotating bottle' (Leelarasamee et al., 1986; Bodmeier & McGinity 1987a; Conti et al., 1991, 1994; Pavanetto et al., 1992, 1994a) have all been described.

More recently, in attempts to mimic *in vivo* drug release conditions (Sansdrap & Moës, 1997), no difference was found in release of water insoluble nifedipine below and in excess of the 'sink' threshold. This 'sink' convention has implications for the quantity and nature of media employed, these factors being primarily dependent on the solubility character of the drug. Generally, drug release from microspherical systems has been examined using isotonic phosphate buffer at physiological pH (Wakiyama et al., 1982a,b). However to solubilize drug, release accelerant, ethanol (Cowsar et al.,1985; Pavanetto, 1993), has been added to the release medium to obtain 'meaningful' results in shorter periods of time. Additionally, the proposed use of high (Cowsar et al., 1985) and low (Gupta et al., 1993) pH to accelerate polymer hydrolysis, has obvious potential to interfere with the release mechanism. Indeed, release of levonorgesterol in proportion to media ethanolic content from reservoir fibres suggested a pore-diffusion mechanism was operative, which was degradation controlled in the absence of alcohol (Eenink et al., 1987). Dissolution testing under stressed conditions has advantages in expediting formulation development, although interpretation of results is clearly restricted to comparison, rather than extrapolation to their potential *in vivo* performance.

Surfactants are added to dissolution media principally to deaggregate particles, though their potential to reduce microsphere-medium interfacial tension has also contributed to enhanced drug liberation (Leelarasamee, 1986, 1988a; Wagenaar & Müller, 1994). Surfactants, in spite of their positive attributes, are not always without problem. Maulding et al. (1986) considered a complex formation between thioridazine and polyethylene oxide monostearate was responsible for apparent decrease in drug concentration in the dissolution medium at 2 weeks. Elsewhere, use of hypertonic release medium has been shown to restrict water penetration, increasing the lag phase before drug release in linear relation to ionic strength (Bodmeier & McGinity, 1988a).

Factors affecting drug release from biodegradable systems are complex and interactive, and compound the difficulty in predicting release from these devices. Nonetheless, a variety of primary factors have been identified and evaluated in order to achieve a better understanding of drug release from these preparations.

A number of generalized release profiles have been observed, the shape of which can be assigned to sequential release phenomena, their duration being dependent largely on drug loading and drug and polymer physicochemistry. Biphasic release profiles are

typified by water soluble drug release from insoluble matrices (Tsai et al., 1986; Suzuki & Price, 1985). The initial release is by dissolution and diffusion of drug from peripheral regions of the microsphere, whereas secondary release occurs via drug diffusion through the microsphere matrix from less accessible regions. Where the second process is complete before degradation of polymer below a critical level where erosion proceeds, drug release will be independent of the latter. However, a triphasic release mechanism has been repeatedly described (Bodmeier & McGinity, 1988b; Sandrap & Möes, 1993; Asano et al., 1989, 1990, 1991; Hora et al., 1990; Sanders et al., 1985) yielding a characteristic sigmoidal release profile. The three distinct phases have been differentiated and interpreted in a variety of ways by different authors depending on the properties of entrapped drug. Bodmeier & McGinity (1987c) assessed release of quinidine base and sulphate salt on the basis of a biphasic diffusional mechanism, comprising an initial lag period, a period of rapid drug release and finally, a slow terminal phase. The initial lag represented a period of water imbibition, thus plasticizing the polymer. Thereafter, rapid drug release corresponded to leaching and diffusion of the drug through pores in the hydrated matrix, terminating in matrix diffusion of remaining drug from more inaccessible regions. The mechanisms by which triphasic profile arise is highly dependent on drug MW. For drug diffusion to occur, a limited solubility in the polymer at least is required. Unlike low MW drugs, in the absence of specific chemical interaction, polypeptides will either be insoluble in or incompatible with polyesters due to distinct structural dissimilarities (Lewis, 1990). Therefore, triphasic release of peptide have been interpreted, in contrast to Bodmeier & McGinity (1987b), by a mechanism involving significant matrix erosion and degradation. Initial immediate and rapid release was attributed to desorption of poorly encapsulated peptide from the periphery of the matrix (Hora et al, 1990). The relative contributions of erosion and diffusion were a function of protein loading. Little drug release occurred during the lag phase of polymer hydrolysis until the oligomers had reached a critical MW, when the implant became sufficiently hydrated, and solubilization of oligomers heralded erosion and concomitant peptide release. In contrast, biphasic release of the peptide, cyclosporin A, was attributed to a typical 'burst' initially and a subsequent linear release in parallel with polymer erosion as measured by GPC. Compensatory mechanisms of polymer erosion which increased matrix porosity, balanced against a thickening diffusion barrier as drug was depleted from outer regions may account for these differences (Sánchez et al., 1993).

Wakiyama et al. (1981,1982b) studied the release rates of a series of local anaesthetics from PDLLA. From SEM studies, after an initial period of diffusion-control, accelerated release of butamben corresponding to matrix disintegration was shown to predominate. Release rate increased with core loadings, which, in turn, increased disintegration rate (Wakiyama et al., 1981). In contrast, drug release independent of drug loading in the range 6.5 to 22.8 %w/w has been reported for the hydrophobic drug, nifedipine (Sandsrap & Möes, 1993). In a further study (Wakiyama et al., 1982b), release rate decreased as anaesthetic solubility in the dissolution medium decreased and as PDLLA MW increased in the range 9.1 to 25 kD. The authors considered osmotic pressure generated by high loadings of water soluble drugs, accounted for the increased disintegration of microspheres at high tetracaine levels. They did not, however, consider base-induced hydrolysis of the matrix by the drug as has been observed elsewhere (Maulding et al., 1986; Cha & Pitt, 1989). In analogy, thioridazine was shown to substantially increase polymer degradation during both microsphere preparation and *in vitro* release studies (Maulding et al., 1986).

Physicochemistry of the drug determines its solubility in the dissolution medium, but also that in the polymer, which, in turn, affects its distribution within the matrix. The microstructure of the matrix, i.e., the size of the drug particle in relation to microsphere size, porosity etc. has a substantial influence on the release mechanism. Crystalline dispersions (Splenlehauer et al., 1986b), molecular dispersions (Le Corre et al., 1996; Benoît et al., 1984) and solid solution (Jalil & Nixon, 1990e) are the three primary dispersive states of drug within microspheres. Theoretical, where the drug is dispersed at the molecular level in the polymer, release should be strictly controlled by the erosion rate of the matrix. Benoît et al. (1984) described release according to first-order kinetics for progesterone microspheres containing 68 %w/w drug, part of which existed as a discrete crystalline phase. In contrast, molecularly dispersed progesterone arose at lower loadings of 23 %w/w, release of which followed a square root of time relationship. Le Corre et al. (1996) described complex release behaviour inconsistent with the aqueous solubility characteristics of four anaesthetic drugs from PDLLA and PDLGA microspheres. Thermal analysis explained the significant burst, i.e., 45 % 30 min^{-1} of lipophilic etidocaine from PDLLA where it was present as a particulate dispersion. It was also observed that lipophilic etidocaine and bupivocaine paradoxically released faster with increasing PDLGA MW, whereas hydrophilic mepivocaine and lidocaine followed the opposite trend consistent with polymer hydrophilicity. This was attributed to increasing matrix porosity as

polymer precipitation rate increased with MW which significantly increased the rate of release of lipophilic drugs in particulate dispersion, but had lesser influence on hydrophilic drugs in molecular dispersion. A 'channelling threshold' has been coined to describe drug loadings, above which the matrix acts more as a scaffold than a barrier (Splenlehauer et al., 1986b). In this situation, loadings are at a critical level to form a contiguous network, whereby all drug crystals are in intimate contact with neighbouring domains. This results in a rapid drug release via dissolution, pore formation and drug diffusion.

Contrary to the diffusivity and hydrophilicity patterns of crystalline and amorphous polymers, morphological factors and the crystalline state of phenobarbitone accounted for its more rapid release from semi-crystalline PLLA when compared with PDLLA (Jalil & Nixon, 1990c,d,g). For PDLLA, increased polymer MW reduced both dynamic lag-time and steady-state release rate, whereas with PLLA the opposite trend was unexpectedly observed. This latter effect was ascribed to the earlier precipitation of high, compared to low, MW PLLA, resulting in ineffective coating of precipitated drug crystals with the latter polymer. When compared with native drug dissolution, encapsulation of phenobarbitone in high MW PLLA paradoxically accelerated drug dissolution due to the small crystallite size and high microcapsule porosity.

In general, drug release rate increases in inverse relation to particle diameter by virtue of an increased specific area. Suzuki & Price (1985) reported that the time for 50 % release was linearly related to particle diameter. Sansdrap & Möes (1993) found approximately zero-order release from nifedipine-bearing particles of 12 μm in diameter, whereas sigmoidal profiles reminiscent of Bodmeier & McGinity's (1987b,c) studies were recorded at diameters of 83 μm. The lag period (150 h) comprised the time required for deep water penetration, microsphere hydration and drug diffusion, all of which occurred simultaneously with 12 μm particles.

Processing parameters of the aqueous solvent evaporation procedure can significantly affect drug release via an alteration of drug-matrix deposition kinetics. Izumikawa et al. (1991) studied the effects of solvent removal rate in the preparation of progesterone loaded microspheres. Amorphous drug-matrix microspheres prepared under reduced pressure, released progesterone slower than those prepared under ambient conditions, irrespective of drug loading. Microspheres prepared at atmospheric pressure, in contrast, deposited crystalline drug within a crystalline PLLA matrix accounting for the rapid

leaching of drug during *in vitro* testing. Smith & Hunneyball (1986) demonstrated that microspheres of comparable sizes, 1 - 10μm, released prednisolone rapidly compared with microparticles prepared by grinding a heat-fused mass. In spite of their smooth exterior, solvent evaporated particles had a porous microstructure, whereas the dense amorphous structure of the microparticles impeded drug release more effectively (Smith & Hunneyball, 1986). Use of elevated disperse polymer concentrations has retarded drug release by impeding crystal migration to the microsphere periphery. At lower polymer concentrations, centrifugal forces within individual droplets supposedly promoted movement of dense drug crystals outwards (Splenlehauer et al., 1986b). Post-preparation curing by heat (Zhou & Chang, 1988) and solvent (Bodmeier & Chen, 1989) has conferred a more efficient sustained release character upon pre-formed particles.

The inherent properties of the polymer that affect drug release are those that also affect the degree of polymer hydrophilicity and crystallinity, namely polymer MW and copolymer ratio (Asano et al., 1989). The effect of polymer MW has been repeatedly evaluated (Suzuki & Price, 1985; Bodmeier & Chen, 1989; Jalil & Nixon, 1990h). Suzuki & Price (1985) reported that an increase in microsphere polymer MW resulted in a significant increase in the initial lag during *in vitro* drug release. The relationship between polymer MW and drug release is considered to be dependent on the T_g of the polymer (Jalil & Nixon, 1990g). Zhou & Chang (1988) suggested a 'critical range' of MW which significantly altered drug release rate. Operating in the MW range 12.5 to 16.7 kD, superimposable release of prostaglandin was observed up to 14.8 kD, whereas release from polymer MW 16.7 kD was considerably reduced. In contrast, Juni et al. (1985) reported little dependence of bleomycin release on polymer MW, perhaps as those studied lay outwith the 'critical range'.

Drug release from lactic/glycolic acid copolymers has been shown to be dependent on comonomer ratio of the polymer (Sanders et al., 1984; 1985; 1986; Heya et al., 1991). Sanders et al. (1984; 1986) reported that the copolymer ratio exerted a significant influence on the release of narfelin from PDLGA. The total duration of release correlated closely with the percent of hydrophobic lactide present in the polymer and the rate of polymer hydrolysis. A number of workers have altered the drug release properties of PDLLA by blending high with low MW polymers (Bodmeier et al., 1989b; Nozawa et al., 1991; Asano et al., 1991). Bodmeier et al. (1989b) reported that the rate of caffeine and salicylic acid release from PDLLA solvent-cast films increased, as the relative proportion

of low MW PDLLA in the formulation was increased. The faster drug release from polydisperse blends was attributed to a reduction in the T_g temperature of the film and a corresponding improvement in polymer hydrophilicity. In contrast, *in vitro* quinidine release decreased as the fraction of low MW PDLLA increased which was attributed to ionic interaction of basic and acidic functions on the drug and polymer, respectively.

1.4 Sustained delivery of antimycobacterials

In parallel with the AIDS pandemic, the century long decline in the incidence of tuberculosis (TB) dramatically reversed in 1985 (Sepkowitz, 1995; Huebner & Castro, 1995). This epidemiological pattern can be seen world-wide causing serious socio-economic stress particularly in developing countries (Chaulet, 1987). In 1993, the World Health Organisation (WHO) declared TB a 'global emergency'; the first ever declaration of its kind. Nearly three million people died from TB in 1995, surpassing the worst epidemic previously recorded in 1900, when an estimated 2.1 million people died (Press report, WHO/22). Current prospective estimates of the resurgence consider that the yearly death toll will climb to 4 million by the year 2005 (Press report, WHO/23).

In the presence of drug sensitive organisms, current first line treatments for TB are effective in 99 % of cases (Medfile, 1993). However, recommended combinations of drugs are complex requiring typically oral administration of two or more drugs for up to 18 months (Tuberculosis chemotherapy centre, 1970). Compliance is notoriously poor (Kilpatrick,1987), particularly in developing countries where there are logistical difficulties in ensuring continuity of supply (Shearer, 1994). Against this background, a more alarming trend is the emergence of multi-drug resistant strains of TB (MDR-TB), attributable amongst other factors to the failure of patients to adhere to prescribed regimes (Huebner and Castro, 1995). Major outbreaks of MDR-TB have resulted in clusters of death, particularly in institutional settings such as hospitals, shelters and prisons (Waxman et al., 1995). In the developed world it has been estimated that one third of all TB cases are resistant to at least one anti-tubercular, and approximately 20% have organisms resistant to both of the most efficacious agents, isoniazid (INH) and rifampicin (RIF). These statistics are even more pronounced in the developing world (Sawert, 1996). The consequences of resistance to both of these agents is severe, especially in those co-infected with the HIV virus where fatality rates of up to 89% are reported (Shearer, 1994). Furthermore, MDR-TB necessitates the use of less effective,

more toxic second-line agents which are several times more expensive than first line agents.

MDR-TB is thought to arise through two main mechanisms: primary drug resistance arises through infection with organisms already resistant to antimycobacterial agents; and, secondary drug resistance, where infection with an originally sensitive strain develops through poorly conceived or complied with therapy (Shimao, 1987). The latter has classically been the most common mechanism by which resistant organisms have developed. It follows, by reducing the incidence of secondary resistance, by ensuring compliance, the latent pool of primary resistant organisms should be reduced.

The concept of patient non-compliance is not new. As early as 1958, Fox identified the necessity of strict adherence to effect a cure, using TB as his model (Fox, 1958). Directly observed programs are undoubtedly the most effective way of ensuring patient compliance where the administration of each dose is supervised (Fox, 1993a,b; Weis et al., 1994). Since daily supervision of chemotherapy is not always practical, attempts have been made to determine whether intermittent administration would give satisfactory cure rates. Operationally, even twice-weekly intermittent therapy created many problems in rural and semi-rural areas, particularly in developing countries (Tuberculosis Chemotherapy Centre, 1970). In the absence of new drugs, procedures or devices which afford a reduction in dosage frequency and assure effective plasma drug levels should greatly facilitate tuberculosis treatments all over the world.

1.4.1 Isoniazid

Over the last decade the group led by Gangadharam and Wise have extensively studied the feasibility of ensuring patient compliance by delivery of isoniazid (INH) in biodegradable PLLGA matrices (Gangadharam et al., 1989, 1991; 1993; 1994; Gangadharam & Kailasam, 1993; Hsu et al., 1994, 1996; Kailasam et al. 1994a,b). Implants were originally manufactured by solvent casting of an INH dispersion in a PLLGA (90:10) matrix as irretrievable films (Gangadharam et al., 1989, 1991). The extrusion of this same blend has since afforded a retrievable rod device, 2 mm in diameter, which can be readily removed by the clinician in the event of toxicity (Gangadharam et al., 1993, 1994; Hsu et al., 1994). A single dose of INH (25 mg kg^{-1}) achieved sustained levels of the drug for 6 weeks in animal lung and liver homogenates, comparable to daily oral dosing. The tissue homogenates showed high antimycobacterial

activity against *Mycobacterium tuberculosis in vitro* and in macrophages. Higher doses (75 mg kg^{-1}) delivered in the same matrix have shown impressive survival rates of 93 % after 30 d when challenged to a virulent *M. tuberculosis* strain. In the same study, mortality rate was equal to that of survival in the saline group at 93 %.

Gangadharam et al. (1993) examined the morphological changes in INH-PLLGA rods under *in vitro*, simulated *in vivo* conditions and in animals. Polarization microscopy revealed three distinct drug domains of 50 - 200 μm, 5 - 50 μm and < 5 μm, the latter abundant two of which did not readily leach from the implant and thus accounted largely for the approximately zero-order release after the initial 'burst' had subsided. The polymer recrystallized, swelled 10 fold and became filled with voids after 4 weeks *in vivo* incubation. The folded topography of the implant was not accounted for, but may have arisen due to preferential degradation of the amorphous regions of this semi-crystalline polymer which created internal stresses during implantation. Hsu et al. have recently studied the mathematical treatment of the *in vitro* release of INH from implants (Hsu et al., 1994;1996) and polymeric foams (Hsu et al., 1996). Confirmation of a pore diffusion mechanism was established by the fitting of fractional release data as a function of time to the Roseman-Higuchi model. The main processing parameter affecting drug release was extrusion pressure, drug loading and rod diameter having a minimal effect. Higher extrusion pressures were considered to result in a less porous matrix thus reducing the contribution of pore diffusion. Drug receptor foams have been prepared by lyophilizing a frozen solution of polymer PLLGA (85:15) in glacial acetic acid. During incubation of these foams in a concentrated solution of INH, successive cycles of evacuation and repressurization ensured effective solution penetration to the core of the foam. These were again lyophilized, micronized and subsequently extruded. The distribution of drug along polymer grain boundaries for dry-mixed implants, compared with the more homogeneous distribution throughout the foams, accounted for the lower diffusion coefficients of the latter formulations derived from the Roseman-Higuchi model (Hsu et al., 1996).

The same implant has been successfully transferred to other antimycobacterial drugs, pyrazinamide (Gangadharam & Kailasam, 1993) and clofazimine (Kailasam et al., 1994b). The group have ambitiously suggested that an entire tuberculosis chemotherapy regimen, consisting of INH, RIF, and pyrazinamide (PYZ) could be conceivably delivered in a single or a small number of doses. This laudable aim, if achievable, would contribute

significantly to controlling the serious threat of patient non-compliance to the effective treatment of tuberculosis.

1.4.2 Rifampicin

Micron sized drug delivery systems based on proteinaceous microspheres, liposomes and multiple emulsion technology have been recently considered to passively target RIF to tuberculosis cavities of the lung. By maximizing RIF concentrations at the affected site, it has been reasoned that development of resistance (Pande et al., 1991) and hence clinical failure would be reduced, whilst undesirable effects to other organs, particularly hepatotoxicity (Mandell & Sande, 1985), would be avoided. Iseri et al. (1989) inferred satisfactory localization of RIF loaded albumin microspheres following *in vitro* characterization based on previous scintographic assessment of similarly prepared streptomycin bearing systems of the same group (Gürkan et al., 1986). In a sequel report, the *in vivo* distribution of ^{99m}Tc-labelled albumin and gelatin microspheres revealed significant concentration of these formulations in the lung when injected via a peripheral vein (Iseri et al., 1991). Pande et al., (1991) recovered 63 % of administered microspherical RIF after 3 h, 30 % persisting at 24 h. Jain & Vyas (1995) similarly found 65 % localization of liposomal-based drug in the lungs by controlling niosome size. Improved therapeutic efficacy and toxicity profile of INH and RIF have been observed for INH and RIF encapsulated in lung-specific stealth liposomes challenged to experimental *M. tuberculosis* infection in mice (Deol et al., 1997). Nakhare & Vyas (1995a) successfully stabilized RIF containing multiple w/o/w emulsions for prolonged delivery via an unspecified route. Furthermore, no reference was made to the effective loading (nor chemical stability of entrapped RIF), but that attempted was particularly low at 0.025 %w/v. Multiple emulsion stabilization of the internal phase was later demonstrated by formation of interfacial complex films between macromolecules in the internal aqueous phase and non-ionic surfactant in the oil phase (Nakhare & Vyas, 1995b).

1.5 Purpose of the present work

The formulation of antibiotics in lactide/glycolide is hindered by three main factors: large daily doses are often required; many antibiotics are relatively unstable; and, most are water soluble (Lewis, 1990). Consequently, long-acting antibiotic formulations based on poly-α-hydroxy acids have previously been fabricated by anhydrous techniques such as phase separation (Vidmar et al., 1984 (oxytetracycline); Owusu-Ababio & Rogers, 1996 (cephalexin); Yu et al., 1998 (ciprofloxacin)) and o/o[1] ESE (Atkins et al., 1998 (vancomycin)). Although aqueous ESE procedures have been additionally described (Martinez et al., 1997 (ciprofloxacin); Esposito et al., 1997 (tetracycline)), recourse to more involved techniques such as w/o/w have been required to achieve even modest drug loadings (Menegatti et al., 1995; Esposito et al., 1997).

It was the purpose of this work to investigate the microencapsulation of the antimycobacterials, RIF and INH in biodegradable poly-α-hydroxy acids by more amenable techniques based on solvent evaporation. These drugs were specifically selected due to their high dose, moderate to high water solubility and chemical instability; properties which have hampered efficient encapsulation and subsequent characterization of long-acting microspherical forms. Furthermore, these formulations were designed with the intention of delivery via alternative routes to address some of the short-comings of existing oral therapies, e.g., patient non-compliance and systemic side effects.

2. Analytical Method Development

2.1 Introduction

One of the most important tasks for the preformulation scientist is the development of analytical procedures which allow the accurate determination of drug in a number of different media and contexts. Direct UV absorption measurements — in the absence of matrix chromophoric interferents or significant drug instability — are generally favoured due to the rapid and reliable nature of these measurements. However, where other UV absorbing species are present, or significant drug decomposition is a feature of the drug(s) under study with the solvents or procedures used, techniques which specifically separate and quantify the species of interest are required. High-performance-liquid-chromatography (HPLC) is now generally considered the technique of choice for such assays due to its separation selectivity and versatility in terms of analyte detection.

The inherent instability of RIF and INH necessitates techniques of accurately determining not only the parent drugs but also the putative decomposition products, i.e., stability-indicating assays. These should allow the accurate determination of drug release from biodegradable systems, as well as the assessment of any deleterious effects of the processes and solvents used in the preparation of these systems. Associated with the development of biodegradable microspheres is the high analytical burden of multiple samples which require replicate measurements, demanding assay procedures which are not only robust, and, by definition, reproducible, but are also rapid allowing efficient throughput of samples without compromising analytical accuracy. Therefore, in the absence of suitable established assays, it was necessary to develop methodology which satisfied these criteria. Furthermore, the fact that heat denaturation of albumin-bearing microspheres and prolonged release studies were anticipated as part of the formulation development work in this study, it was also considered necessary to develop suitable HPLC methods to quantify the effects of such operations.

Following development of satisfactory chromatographic separations, it is generally accepted that the reliability of analytical procedures can only be assured when the attributes of the methodology have been scrutinized under the conditions of the procedures intended use. These data comprise what is known as assay validation, which,

for stability-indicating procedures, should describe fairly rigorous testing of the analytical accuracy, specificity and reproducibility of the technique.

As INH and RIF are often administered together, the validity of a technique for their simultaneous determination is axiomatic. In addition, combination assays have several operational and pragmatic advantages when compared with individual determinations of the species of interest. These include time efficiencies, increased sample throughput, reduced capital costs in terms of not having dedicated equipment for individual assays, notwithstanding the economic and environmental implications of reduced solvent consumption. For *in vivo* assessment of the formulations suggested as future work in this thesis, a chromatographic separation of RIF, INH and their principal metabolites was additionally developed.

2.2 Experimental procedures

2.2.1 Materials

All materials used in the experimental work contained in this thesis are tabulated in Appendix 1. No further reference is made to these hereafter.

2.2.2 Chromatographic procedures

The modular liquid chromatograph comprised a Jasco (Tokyo, Japan) PU-980 isocratic chromatography pump and a UV-975 variable wavelength UV/VIS detector. Chromatograms were recorded either on a BBC Servegor chart recorder (Belmont Instruments, Glasgow) or a Shimadzu SPD-M6A UV photodiode array (PDA) detector in conjunction with its associated software package (Tokyo, Japan). The latter equipment allowed the spectral properties of eluted analytes to be additionally examined. Quantification of detector response was performed at 240 nm (RIF) or 263 nm (INH) and measured as heights or integrated areas using a Hewlett Packard (Avondale. PA, USA) HP 3395 integrator. A Rheodyne 7125 injection valve (Cotati, CA, USA) fitted with a 20 µl fixed volume loop was used for sample introduction by direct injection. The column-switching (CS) configuration was utilized in the backflush mode. A Shimadzu (Tokyo, Japan) LC-5A isocratic pump was used to load a 50 x 2 mm precolumn packed with 10 µm ODS-Hypersil. CS was facilitated using a Rheodyne 7120 switching valve as seen in Scheme 2.1. For CS procedures, a 400 µl fixed volume sample loop was used.

All columns used were slurry-packed in the laboratory — using propan-2-ol, hexane and methanol serially — at a pressure of 55 MPa using a Stanstead (Essex, UK) pneumatic pump. The analytical column used for the RIF and INH stability indicating HPLC assays were 100 x 4.6 mm i.d and 200 x 4.6 mm respectively, both packed with 3 μm octadecylsilyl-modified silica (ODS-Hypersil). A 30 x 4.6 mm i.d. in-line guard column was similarly packed. Development of an assay capable of simultaneously separating INH, RIF and their principal metabolites involved use of a number of reverse stationary phases in a variety of column dimensions.

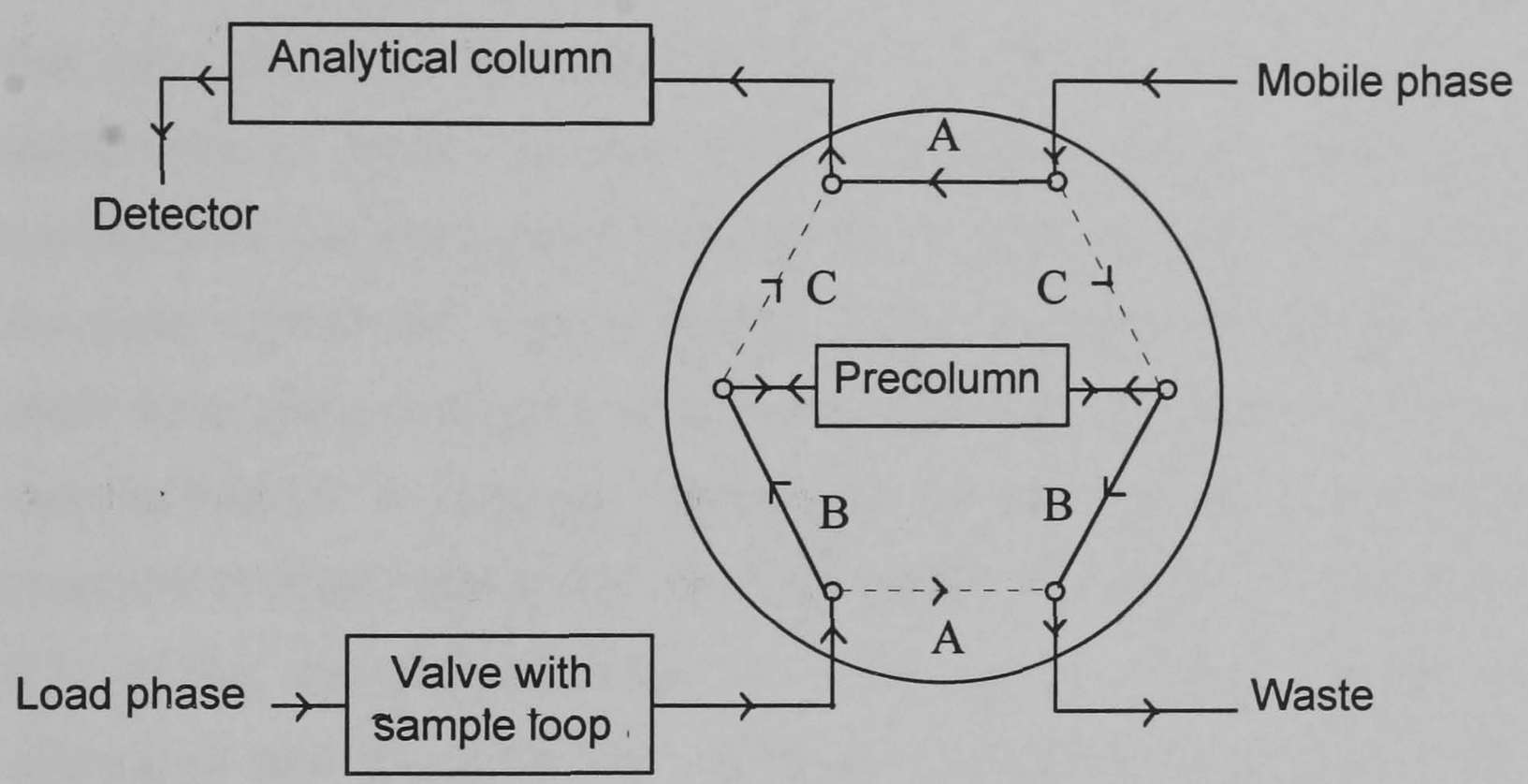

Scheme 2.1 *Schematic of switching valve configuration*

The column-switching configuration and solvent flow patterns can be seen in Scheme 2.1. Chromatographic conditions for CS were as follows:

1. the precolumn and analytical columns were conditioned with load and analytical phases respectively for two minutes (position A);
2. HPLC water was used to load the samples from the injection loop, at a rate of 1.0 mL min^{-1} to the precolumn for 1.5 min (position B). The analytes were retained at the top of the precolumn while the sample solvent and poorly retained medium adjuvants were eluted to waste, and;

3. the valve was then switched, directing the analytical phase (as above) through, and eluting the retained analytes from the precolumn for separation on the analytical column (position C).

2.2.3 Assay validation

2.2.3.1 Linearity

Linearity of detector response was established by preparing solutions of RIF and related products from DMSO standard at eight levels between 0.5 - 50 and 0.05 - 50 μgmL^{-1} for DI and CS, respectively. DMSO was chosen for preparation of standard solutions as it has been shown to maintain RIF stability (Karlson & Ulrich, 1969) unlike methanol and acetonitrile in which RIF has limited stability (Graham, 1979). These concentrations represented the anticipated concentration range of dissolution samples paying regard to the need to maintain 'sink' conditions. The resultant peak areas of triplicate injections at each level were averaged, and linear regression of these values versus concentration was performed. In analogy, calibration standards of INH and related degradates were prepared in Sørensens buffer modified (SBM) containing 0.1 %w/v Tween® 80 (pH = 7.4 ± 0.1) in the approximate range 1 - 150 μgmL^{-1}. The increased concentrations when compared with those for RIF, reflected the greater solubility of INH and the reduced sensitivity demands with respect to the need to maintain 'sink' conditions. Limited interim validation for linearity in aqueous medium of the combination assay of RIF, INH and associated analytes was performed. Individual analytes were chromatographed at 5 levels over the range 200 - 2000 $ngmL^{-1}$.

2.2.3.2 Reproducibility

Within-day precision was established by repeat injections of each analyte at an approximate concentration of 1μgmL^{-1} for RIF and associated analytes, whereas a concentration of 5 μgmL^{-1} was used for INH and isonicotinic acid (INA). In contrast, between-day precision was demonstrated by the constancy of the calibration statistics for each analyte, determined on 5 successive days.

2.2.3.3 Specificity

Assay specificity was established based on peak geometry and correspondence of peak position with that of reference standards where these were available irrespective of the

HPLC procedure. In addition, peak purity index was also computed by comparison of the absorbance ratio at two wavelengths of the up-slope, apex and down-slope of each peak using PDA detection for both RIF and INH stability-indicating procedures.

2.2.3.4 Accuracy

Accuracy of the CS configuration was established in the presence of parent drug and decomposition products by a standard addition method by spiking dissolution samples at concentrations of 1, 5 and 20 μgmL^{-1} for RIF and RSV only. Corresponding standards for INH and INA were at levels of 5, 20, and 50 μgmL^{-1}.

2.3 Results and Discussion

2.3.1 Stability indicating HPLC assay for rifampicin

Since the decomposition products of RIF have similar absorption spectra as seen in Figure 2.1, or are biologically active, their presence interferes in spectrophotometric and microbiological assay techniques, necessitating recourse to HPLC for quantitative assessment of RIF stability (Graham, 1979). Chemical structures of RIF and its degradates are shown in Figure 2.2. Two major antimicrobial decomposition products exist, namely, 3-formyl rifamycin SV (RSV) and rifampicin quinone (RQU) (Seydel, 1970). Hydrolysis of the 4-methylamino piperazine moeity in acidic medium results in RSV, whereas RQU is formed in alkaline medium in the presence of oxygen (Seydel, 1970). Conversely, 25-desacetylrifampicin (DAR) is reportedly formed in alkaline medium in the absence of oxygen (Gallo & Radaelli, 1976). 25-desacetyl-21-acetylrifampicin (25-21) and 25-desacetyl-23-acetylrifampicin (25-23) are formed sequentially from DAR, and, unlike other identified decomposition products, have negligible antimicrobial activity (Maggi et al., 1968).

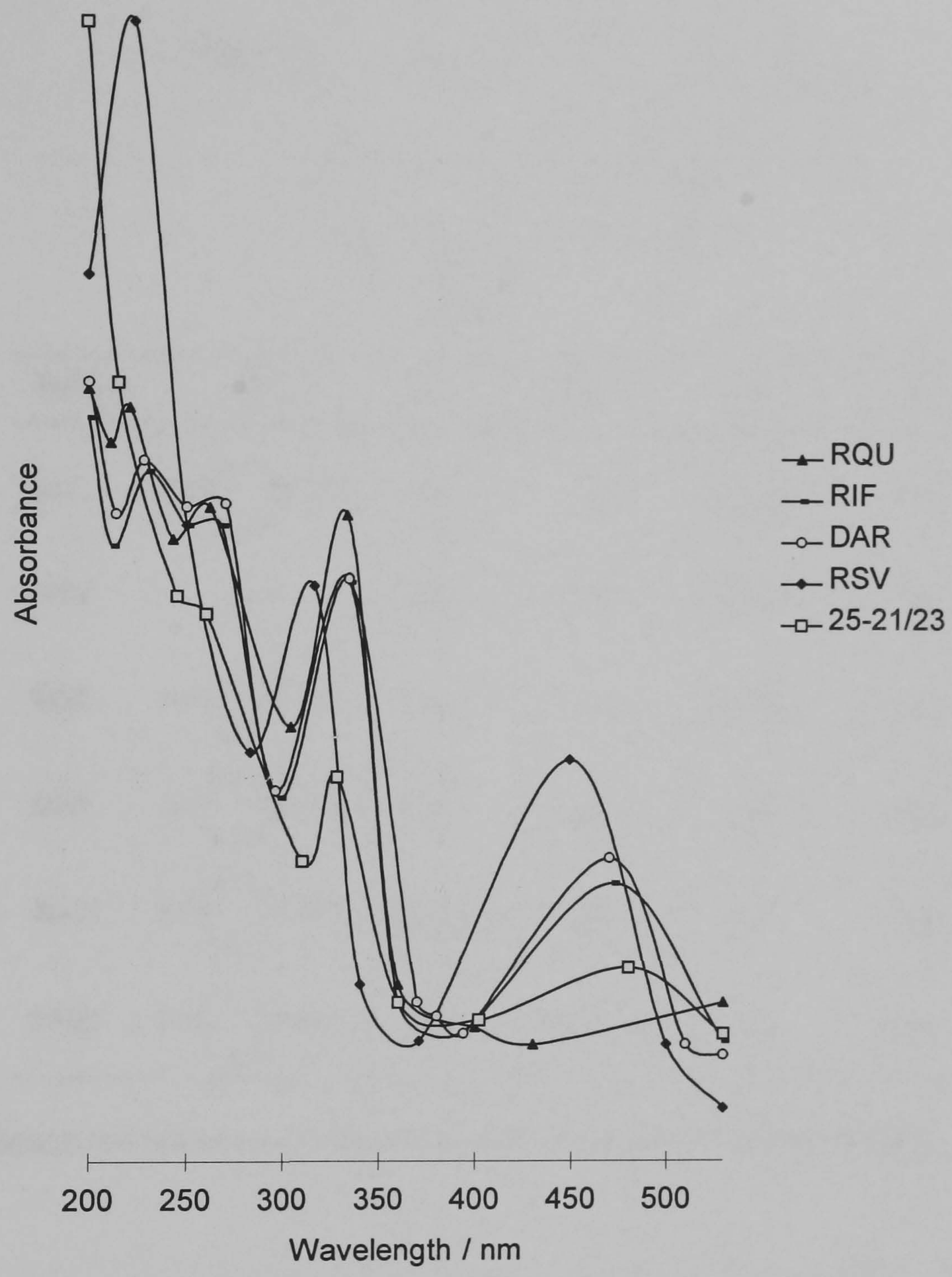

Figure 2.1 *Normalised UV spectra with respect to concentration of rifampicin and its decomposition products. Legend indicates the abbreviated analyte.*

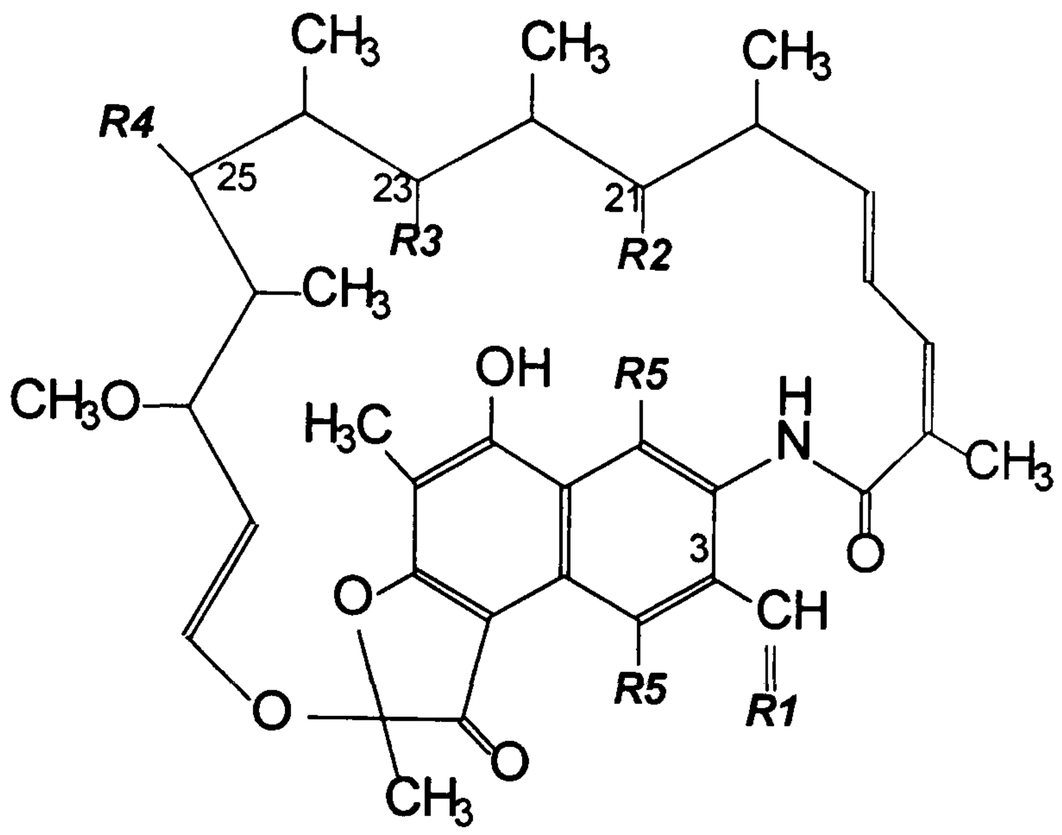

Analyte	*R1*	*R2*	*R3*	*R4*	*R5*
RIF	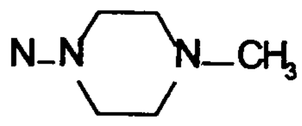	OH	OH	CH_3COO	OH
RSV	O	OH	OH	CH_3COO	OH
RQU	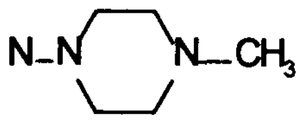	OH	OH	CH_3COO	=O
DAR	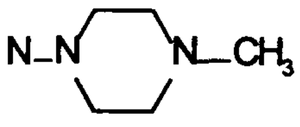	OH	OH	OH	OH
25-21	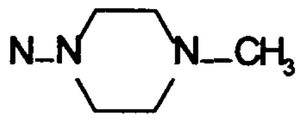	CH_3COO	OH	OH	OH
25-23	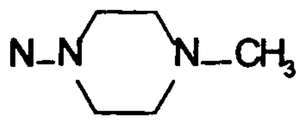	OH	CH_3COO	OH	OH

Figure 2.2 *Structural features of rifampicin and its decomposition products*

Despite the well reported stability problems associated with RIF (Seydel, 1970; Graham, 1979; Gharbo et al., 1989; Prankerd et al., 1992; Nahata et al., 1994; Jindal et al., 1995; Krukenberg et al., 1996;) few stability-indicating procedures have been described. HPLC has been used to analyse the stability of RIF in suspension formulations, although the reports lack analytical detail (Nahata et al., 1994; Jindal et al., 1995). Krukenberg et al. (1996) described a further stability-indicating HPLC method to examine the stability of extemporaneously prepared RIF suspensions. Graham (1979) developed a reverse-phase HPLC procedure capable of separating and quantifying RIF and its decomposition products in bulk formulations. Both the latter reports described chromatography having a relatively high analysis time of 18 min and both used a complex tertiary mobile phase. For

routine stability analysis, short analysis times which allow high sample throughput with a concurrent reduction in solvent consumption are advantageous. The ability to determine inactive degradates of RIF, as well as those with antimicrobial activity, provides additional information which has hitherto not been reported.

2.3.1.1 Method development

Protracted analysis times are a general feature of published RIF stability-indicating methods. Graham (1979) previously reported the need for gradient elution to produce efficient separation and to elute RQU in a reasonable time using ODS stationary phase packing, presumably due to differences in analyte hydrophobicities when compared with parent RIF and other degradation products. The chromatographic separation described here was based on a bioassay of RIF and its two main metabolites, DAR and RSV (Ratti et al., 1981). This procedure achieved adequate resolution of these three analytes on ODS with a mobile phase of acetonitrile - 50 mmol L^{-1} aqueous phosphate buffer (37 - 63) adjusted to pH 4.5.

In Figure 2.3 the effect of mobile phase pH on analyte column capacity factor is presented. With the exception of RQU, marked decreases in capacity factors and thus retention as pH increased, were generally observed around pH 4.5 - 5.5. This was attributed to changes in the ionization character of the C_1 and C_4 para-hydroxy array seen in Figure 2.2, thus explaining the alternative ionization behaviour of RQU, in which this feature is absent.

These data corroborate the existence of a third dissociation constant proposed by Prankerd et al. (1992) at pH 5.93 for RIF but contest its assignment to the N-methylpiperazine nitrogen, absent from RSV, yet present in RQU. Nonetheless, above pH 4.5 - 5.5 the charge associated with hydroxyl deprotonation reduced overall analyte hydrophobicities and therefore retention. At pH 2.0 the reduced retention of all analytes except RSV corroborates the pK_a assignment of Prankerd et al. (1992) to the piperazine nitrogens common to all other analytes except RSV. Based on this behaviour, the selection of a mobile phase pH of 4.5 by Ratti et al. (1981) would be expected to greatly reduce assay ruggedness, analyte retention being particularly sensitive to small variation in pH around this value.

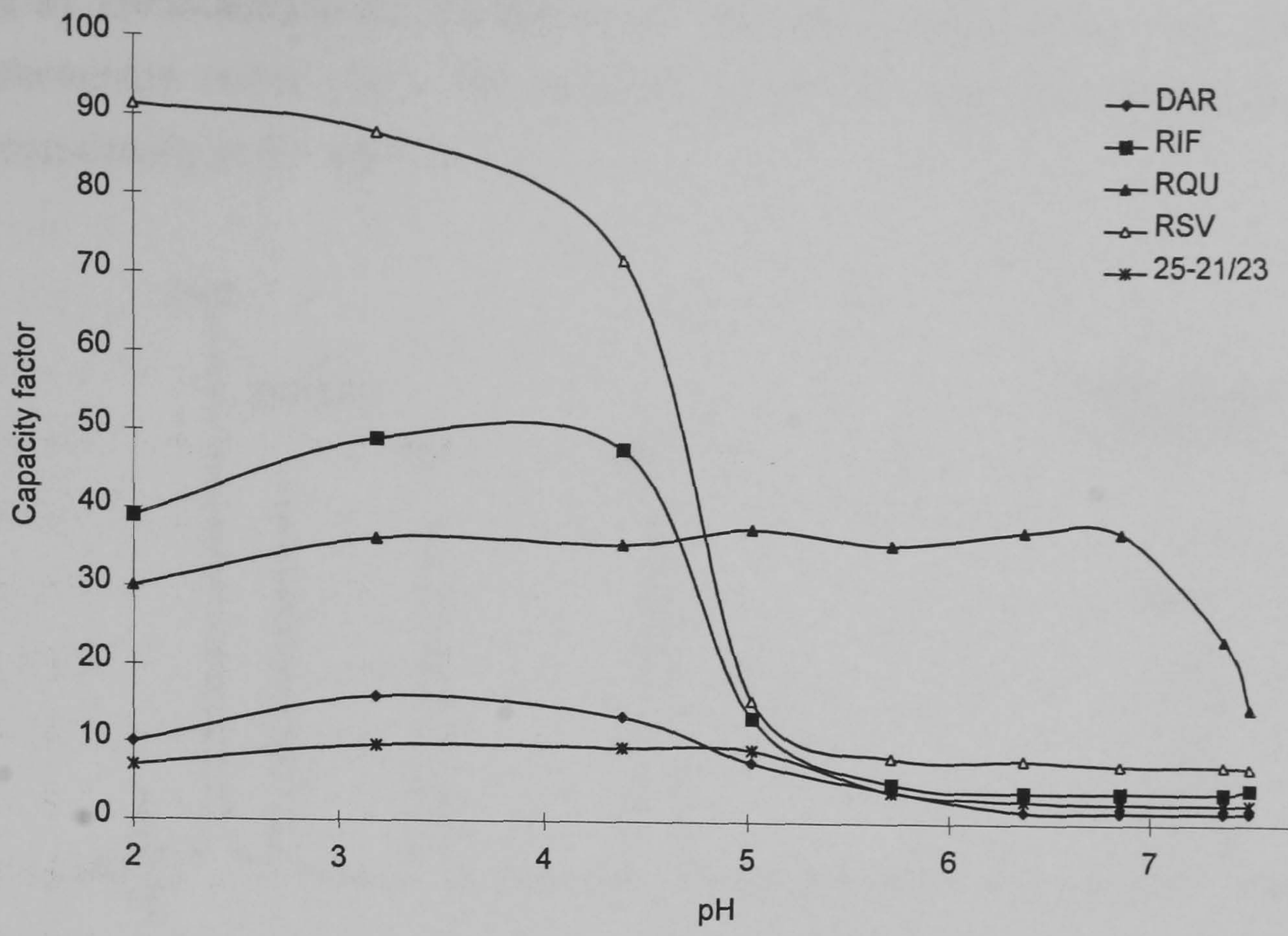

Figure 2.3 *Variation of column capacity factor for rifampicin and its degradates as a function of mobile phase pH. Chromatographic conditions: mobile phase, acetonitrile - 50 mmol L^{-1} aqueous phosphate buffer (36 - 64); flow rate of 1.0 mL min^{-1} through a 100 x 4.6 mm i.d. column packed with 3 μm octadecylsilyl-modified silica. Detection at 240 nm. Legend indicates abbreviated analyte.*

The hydrophobicity conferred on RQU by its quinone =O groups has resulted in the use of less hydrophobic stationary phases, octasilyl-modified silica, to reduce analyte retention (Graham, 1979). However, increases in pH beyond 7.0 resulted in sufficient ionization of the remaining naptholic hydroxy group of RQU to adequately reduce retention and achieve acceptable analysis times. The mobile phase flow rate was additionally increased to 1.4 mL min^{-1}, to further shorten analysis run time without affecting analyte resolution.

Elevated mobile phase pH is known to have a potentially deleterious effect on column performance through hydrolysis of the bonded ODS (R.B. Taylor, personal communication). Representative chromatograms in Figure 2.4 show that the use of pH 7.5 and an in-line guard column resulted in adequate resolution whilst maintaining acceptable analysis times. Constancy of retention times and integrated areas for all analytes throughout the present work demonstrated the in-line guard column ensured analytical column longevity. The optimal analytical phase for both direct injection (DI) and

(CS) chromatographic configurations comprised acetonitrile - 50 mmol L^{-1} aqueous phosphate buffer (36 - 64) adjusted to pH 7.5 with orthophosphoric acid delivered isocratically at 1.4 mL min^{-1}.

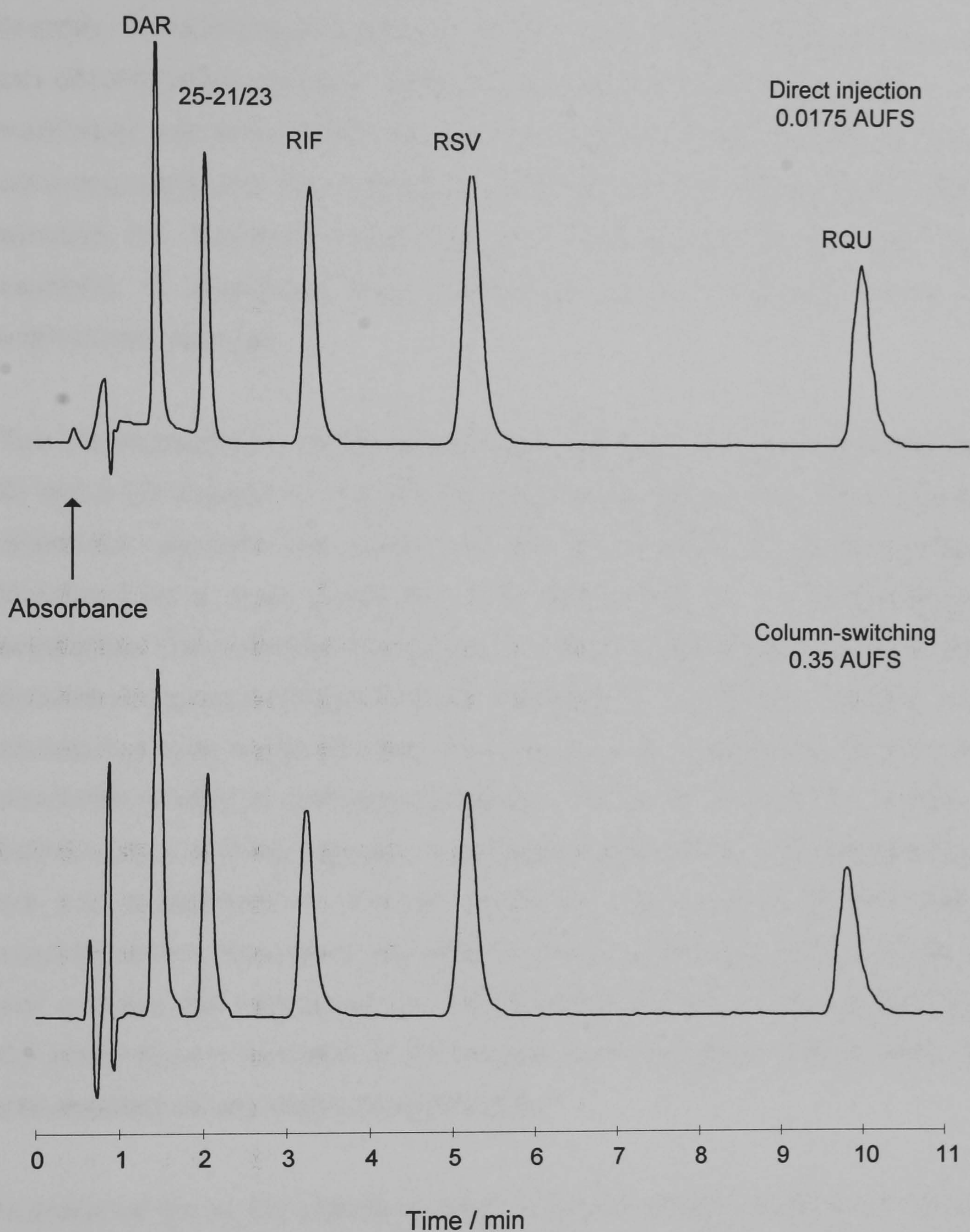

Figure 2.4 *Normalised representative chromatograms of rifampicin and its decomposition products for each chromatographic configuration. Chromatographic conditions: mobile phase, acetonitrile-50 mmol L^{-1} aqueous phosphate buffer (36-64) adjusted to pH 7.5; flow rate of 1.4 mL min^{-1} through a 100 x 4.6 mm i.d. column packed with 3μm octadecylsilyl-modified silica. Detection at 240 nm.*

Peaks were assigned by correspondence of position when compared with reference standard. It is noteworthy that 25-21 and 25-23 could not be resolved, using the described analytical phase. Attempts to resolve these by manipulation of pH and solvent strength were largely unsuccessful or had an unfavourable effect on the retention of other analytes. Nonetheless, no other published method has considered the presence of these two decomposition products, which, significantly, are biologically inactive. In addition, an equilibrium has been shown to exist between 25-21 and 25-23 with acetyl migration occurring readily in solution between positions 21 and 23 (Maggi et al., 1968). Therefore, although the described method cannot quantitate these compounds individually, the capability of quantifying these collectively would be of significance due to their antimicrobial inactivity.

Two chromatographic configurations were examined using the developed mobile phase; DI and a CS procedure. The determination of low dose potent drugs (Bell & Ip, 1993) in dissolution samples has utilized CS as a technique to preconcentrate the active ingredient on a small precolumn, with backflushing on to the analytical column for separation. This technique has particular utility for determination of released drug during dissolution testing particularly where demands on analytical sensitivity are high. Such situations prevail where the drug is of low aqueous solubility; is of low dose (given that dissolution testing is normally performed in 900 mL of aqueous buffer); or, has low intrinsic UV-absorbing capacity. In addition, batch sizes for microspherical formulations are not uncommonly in milligram amounts. This, coupled to the need for several characterization techniques with replicate measurement, e.g., drug content, DSC, particle size analysis and microscopy for a single batch of product, favours techniques such as CS which allow a reduction in the sample required without compromising the precision and accuracy of any measurements made.

In analytical terms, the loading of hydrophobic analyte with water on to hydrophobic ODS phase should ensure its tenacious retention as a plug of analyte at the top of the precolumn. Where this analyte behaviour prevails, efficient sample clean-up whilst preventing band-broadening effects, which ultimately reduce analytical sensitivity and column efficiency, should result. Band-broadening occurs as a result of the analyte being introduced to the analytical column during valve switching as a diffuse band rather than a concentrated plug. In Figure 2.5, where the effect of precolumn loading time on peak height for RIF and RSV is presented, peak depression associated with band-broadening

was observed consistent with analyte migration and diffusion in the precolumn with elevated loading times. Therefore a compromise between adequate sample clean-up and minimal band-broadening must be attained. Absence of interfering peaks from dissolution medium adjuvants, and satisfactory peak heights seen in Figure 2.4 showed these competing factors were optimally satisfied at loading times of 1.5 min.

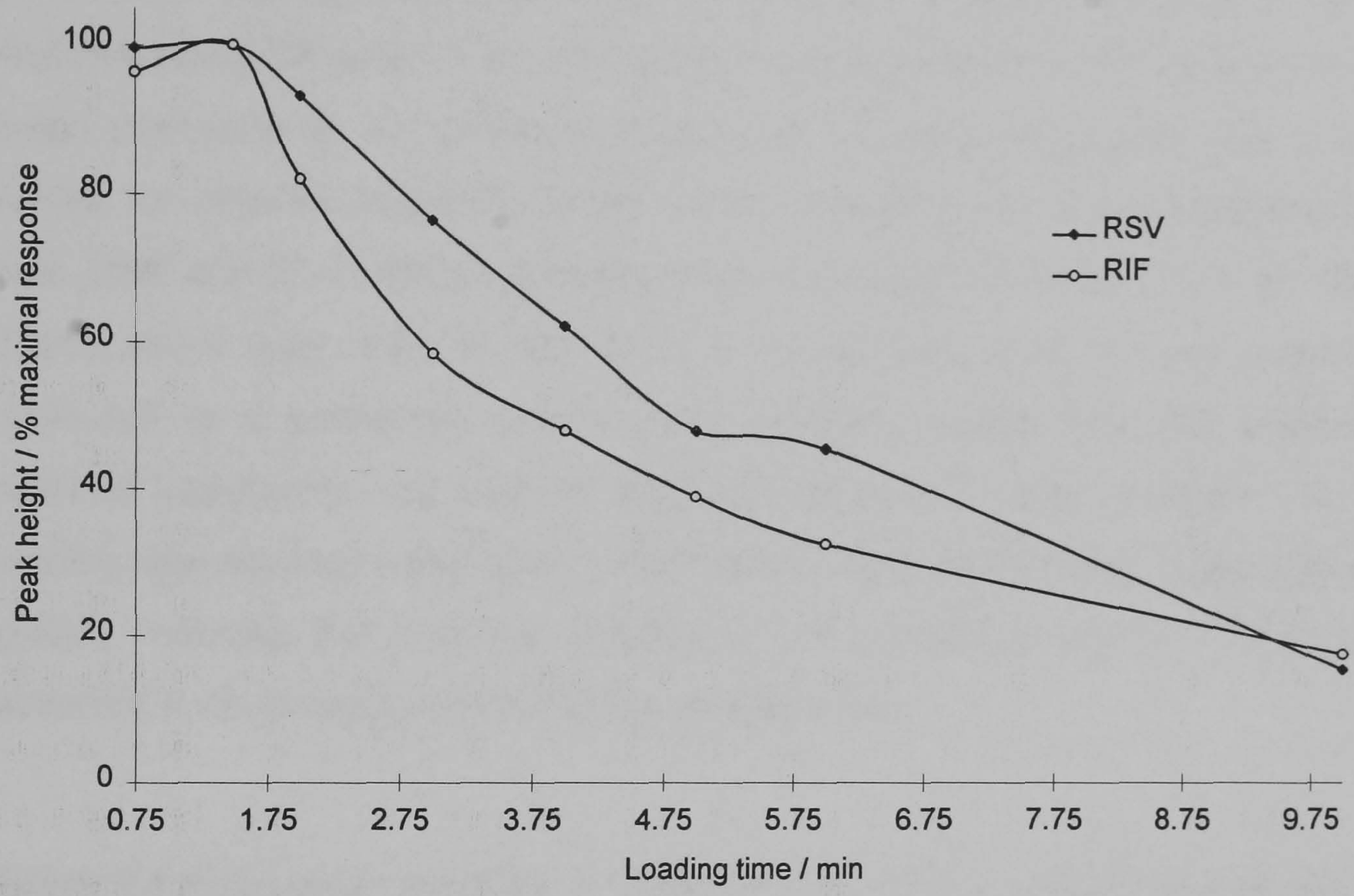

Figure 2.5 *Effect of precolumn loading time on the peak height response for rifampicin and 3-formyl rifamycin SV. Chromatographic conditions: loading phase, water isocratically delivered at 1.0 mL min^{-1} through a 50 x 4.6 mm i.d. column packed with 10 μm octadecylsilyl-modified silica. Other conditions as per Figure 2.4. Legend indicates abbreviated analyte.*

2.3.1.2 Assay validation

The results in this section are presented as a comparison of the two chromatographic configurations studied. As the assay was principally developed with a view to monitoring release of RIF from prolonged-release biodegradable polymeric devices, dissolution medium was initially used as diluent for validation of both chromatographic configurations. However, a broad peak appeared at 25 min using DI which was absent when Tween® 80 was not included in the diluent. No evidence of this peak was noted when precolumn

loading times ≥ 1.5 min were employed, thus highlighting the sample clean-up utility of CS. As no discernible differences in chromatographic characteristics were detected for RIF and its degradates in the presence or absence of Tween® 80, validation data for direct injection was obtained without the addition of Tween® 80.

The slope consistency of the standard graphs was checked on 5 successive days which yielded the regression statistics seen in Table 2.1. Whereas, the RSD of the slope for all analytes using CS was < 1 %, the corresponding statistics for DI were more variable. The mean intercepts for all calibration lines using CS were not greater than ± 0.95 % of the values for detector response at the 100 % analyte level. The corresponding values for both DAR and 25-21/25-23 exceeded the recommended limits of ± 2 % (Braggio et al., 1996) which were 3.56 % and 4.23 % respectively when DI was employed. This is attributed to a protracted solvent front probably arising from the addition of weakly retained protectants and medium adjuvants as can be seen in Figure 2.4. With CS the loading step allowed washing of these weakly retained additives during preconcentration, greatly reducing the amounts passing to the analytical column. This explains their absence in chromatograms using this configuration.

Table 2.1 *Regression statistics for calibration of detector response with rifampicin based analytes using direct injection and column switching, n = 5.*

Analyte	***Direct injection***		***Column switching***	
	Mean slope (RSD)	***Mean r^2 (RSD)***	***Mean slope (RSD)***	***Mean r^2 (RSD)***
DAR	3.008×10^5 (1.84)	0.997 (0.13)	5.755×10^6 (0.99)	0.998 (0.13)
25-21/23	2.195×10^5 (1.98)	0.998 (0.18)	4.403×10^6 (0.85)	0.999 (0.10)
RIF	3.188×10^5 (1.59)	0.998 (0.15)	5.906×10^6 (0.98)	0.999 (0.03)
RSV	3.332×10^5 (1.51)	0.999 (0.09)	6.404×10^6 (0.28)	0.999 (0.01)
RQU	2.628×10^5 (1.65)	0.992 (1.30)	5.423×10^6 (0.72)	0.998 (0.12)

CS yielded superior reproducibility for all analytes, with a RSD of 0.25 - 0.65 % compared with 1.75 - 3.56 % for DI. Ordinarily, a 2 % difference between replicate injections would be acceptable for HPLC (Bell & Ip, 1993). Clearly DI was inadequate at lower drug concentrations. Large variations for DAR (RSD = 3.56 %) and 25-21/25-23 (RSD = 2.48 %) were attributed to variable solvent front effects. Day-to-day precision was established by the low RSD values for the calibration statistics listed in Table 2.1.

Specificity was evident from the accuracy data obtained below and also from the chromatogram shown in Figure 2.4. Further to this peak purity was examined for RIF and RSV during dissolution runs using PDA detection. Peak homogeneity was established by measuring the UV spectra on the up-slope, apex and down-slope of each peak for RIF and RSV during release studies. Values of peak purity index were computed to be > 0.99 for RIF and RSV throughout.

Using the standard addition method, linear regression of the areas obtained versus concentration added yielded straight lines for RIF (r^2 = 0.997) and RSV (r^2 = 0.998) parallel to calibration lines using aqueous standards of the same concentrations. The intercepts on the area axis corresponded well to the initially determined RIF and RSV areas for pre-spiked dissolution samples (P > 0.01).

In addition to the above data, limit of quantification for each analyte studied in the RIF stability-indicating procedure was determined, the results of which can be seen in Table 2.2.

Table 2.2 *Limits of quantification for rifampicin and its decomposition products.*

Chromatographic configuration	***Sample volume / µl***	***Limit of Quantification / ngmL^{-1}***				
		DAR	***25-21/23***	***RIF***	***RSV***	***RQU***
Direct injection	***20***	215	275	250	260	400
Column switching	***400***	20	36	25	24	39

CS allowed the application of a large volume of sample to the precolumn, where the analytes were preconcentrated before separation and determination. Increases in analytical sensitivity were accordingly quantitative with the mass of analyte applied to the precolumn, whereby a 20-fold increase in detector response was recorded using CS in proportion to the increase in injection volume when compared with direct injection (P > 0.01). Band-broadening effects associated with prolonged precolumn loading stages with column switching were not discernible from comparisons of chromatograms using each configuration shown in Figure 2.4. It follows, therefore, the limits of quantification could be reduced further by sequential application of injections to the precolumn. However, for the

purposes of the current work, single application of a 400 µl loopful resulted in adequate sensitivity.

2.3.2 Stability indicating HPLC assay for isoniazid

Despite the fact that the instability of INH has been described in a number of contexts: including aqueous solution (Lewin & Hirsch, 1954; Pawelczyk et al., 1969); sugar media (Hald, 1969; Rao et al., 1971; Jain & Madan, 1974); determination of carcinogenic hydrazine residue (Butterfield et al., 1981; Matsui et al., 1978, 1983; Lovering et al., 1982); and, in biological matrices for therapeutic drug monitoring (Hutchings et al., 1983a,b, 1988); no HPLC stability-indicating procedure has been described in the English-speaking literature. Hutchings et al. (1983a, 1988) used HPLC to demonstrate the protective action on INH and its principle metabolite, acetylisoniazid, of storage at -70 °C and 4 °C for plasma and saliva samples, respectively. Instability, prevented by such treatment, may have led to erroneous assumptions of non-compliance or over-dosage in samples not so treated. Adulterant isoniazid-derived hydrazine has been detected by TLC (Matsui et al., 1977), GLC (Matsui et al., 1983) and normal phase HPLC (Butterfield et al., 1981; Lovering et al., 1983). Several reports have investigated the condensation of isoniazid with reducing sugars, glucose and fructose to form the corresponding isonicotinoyl hydrazones (Hald, 1969; Rao et al., 1971; Jain & Madan, 1974) using a variety of titrimetric and fluorimetric methodologies; specificity of which relied on the free amine moeity of the parent drug. Only two early studies of the aqueous stability of INH are reported (Lewin & Hirsch, 1954; Pawelczyk et al., 1969). These described insensitive colorimetric and non-specific microbiological methodologies in the earlier report, whereas the latter exploited an involved separation by TLC followed by polarographic analysis of the INH eluate.

In aqueous solution, INH readily undergoes hydrolysis to yield isonicotinic acid (INA); isonicotinamide (IAD), diisonicotinoylhydrazine (DIN) and hydrazine (Lewin & Hirsch, 1954). Whereas in anaerobic conditions the hydrolysis of INH follows pseudo first-order kinetics, the decomposition in O_2 is more complicated and the definitive products thereof have not been identified (Pawelczyk et al., 1969), although isonicotinamide (IAD) and isonicotinic acid N-oxide (INN) are potential candidates. Figure 2.6 illustrates the chemical structures of these products.

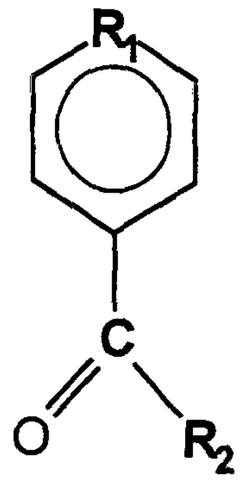

Analyte	R1	R2
INH	N	NH—NH$_2$
INA	N	OH
INN	N→O	OH
IAD	N	NH_2
DIN	N	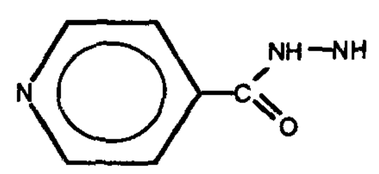

Figure 2.6 *Structural features of isoniazid and its decomposition products*

Degradation has been shown to be sensitive to the presence of free cupric or manganous ions, whereby drug destruction has been shown to be prevented by a number of substances with the common capacity of binding such ions, e.g., EDTA and certain polybasic organic acids, e.g., citrate. Furthermore, addition of dilute hydrogen peroxide greatly increased INH deterioration. Thus, oxidation catalysed by certain metal ions appears to be a significant degradative route to unprotected INH. Elimination of the effects of these insults, however, confers significant stability on the drug (Lewin & Hirsch, 1954).

2.3.2.1 Method development

The chromatographic separation was based on the parent drug, INH and its predominant hydrolytic decomposition product INA. Two other potential degradates, IAD and INN were additionally examined. The basis of the separation was performed on octadodecyl-

modified silica (ODS). Available log P_o values for INH, IAD, INA were -0.70, -0.37, -0.57, respectively (Hansch et al., 1995). Values for INN and DIN could not be sourced. These values indicate the hydrophilic nature of these analytes which were anticipated to have low retention on hydrophobic stationary phases such as ODS. Thus, adequate retention and resolution were achieved by the use of a long column packed with 3 μm particles to maximize column efficiency. In Figure 2.7 the profile of column capacity factor as a function of pH can be seen at an organic modifier level of 20 %v/v methanol.

The retention behaviour of the analytes was consistent with their ionic character between pH 2.0 - 4.0 whereby protonation of the basic terminal primary hydrazide NH_2 reduced the lipophilicity and thus retention of both INH and IAD with reduced pH. Conversely, enhanced retention of INA and INN was attributed to protonation of the carboxylic acid moeity common to these compounds as pH decreased, rendering them more hydrophobic. The anomalous behaviour above this range could not be ascribed to the ionization constants and was a consequence of the low and variable t_o values which affected the determination of column capacity factor.

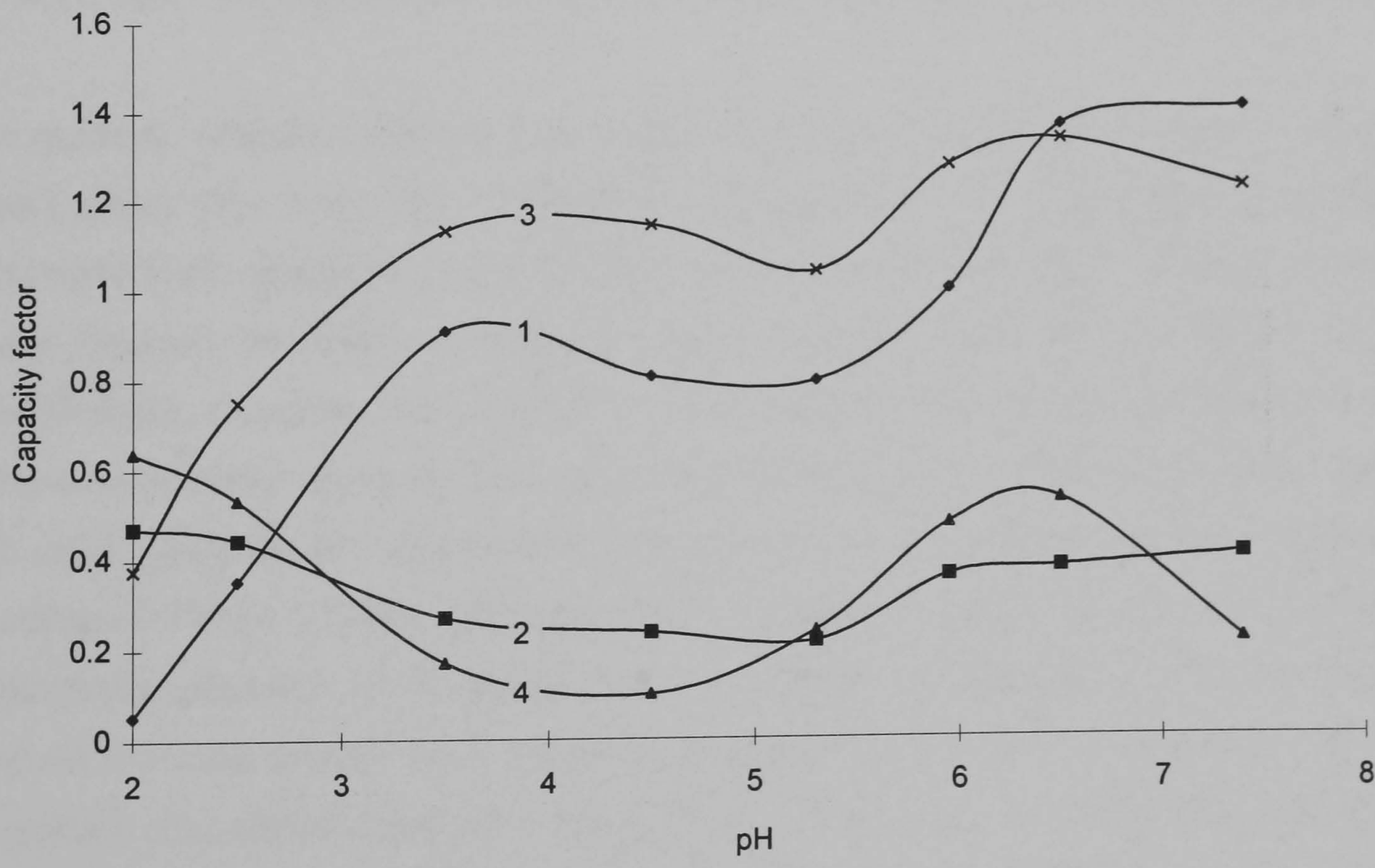

Figure 2.7 *Variation of column capacity factor as a function of pH for: 1) INH; 2) INA; 3) IAD, and; 4) INN. Chromatographic conditions: mobile phase methanol - 20 mmol L^{-1} aqueous phosphate buffer (20 - 80) at a flow rate of 1.4 mL min^{-1} through a 200 x 4.6 mm i.d. column packed with 3 μm ODS-Hypersil. Detection at 263 nm.*

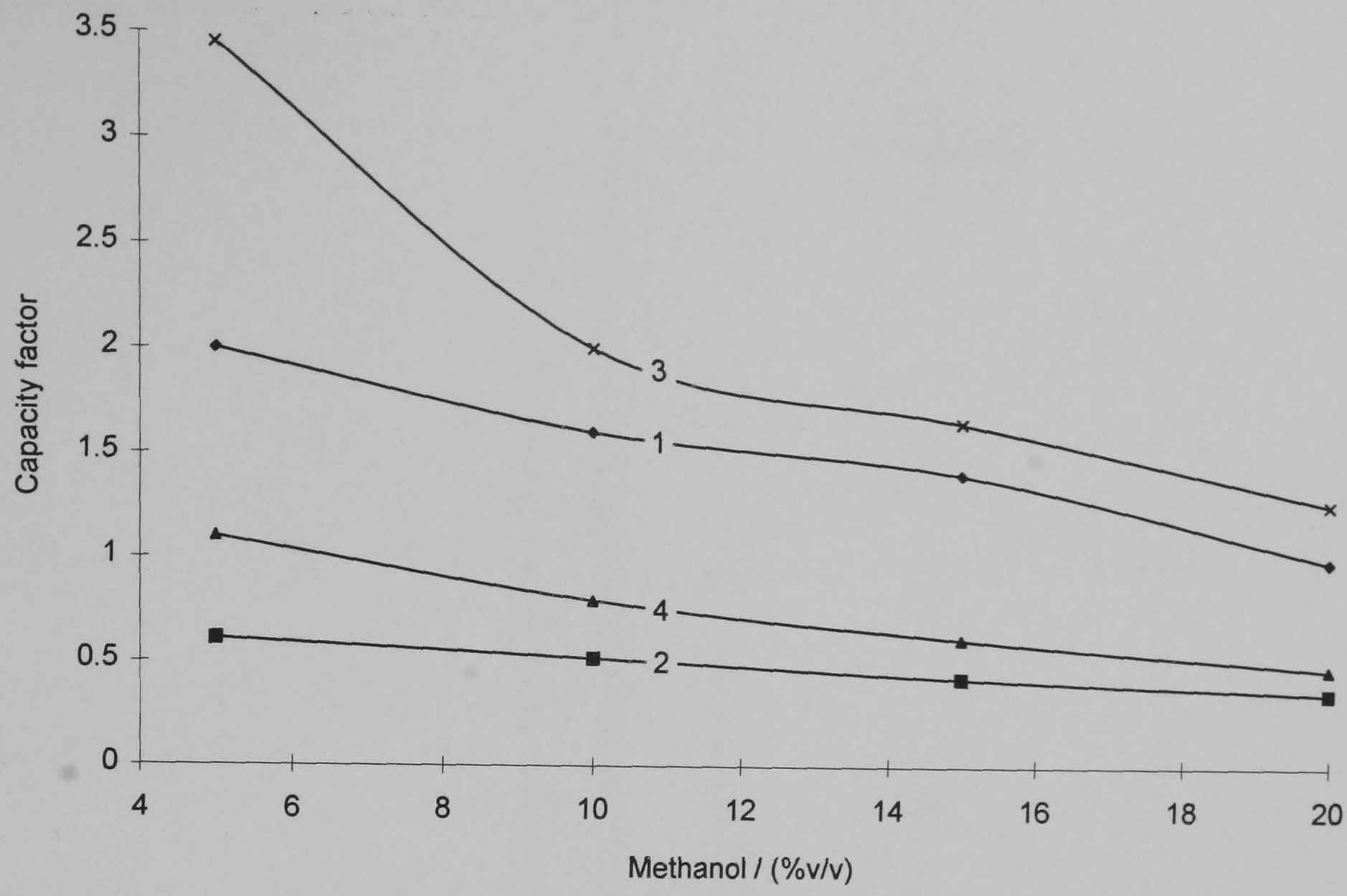

Figure 2.8 *Variation of column capacity factor as a function of organic modifier concentration: INH (1); INA (2); IAD (3); and, INN (4). Chromatographic conditions: mobile phase methanol - 20 mmol L^{-1} aqueous phosphate buffer pH 6.0 at a flow rate of 1.4 mL min^{-1} through a 200 x 4.6 mm i.d. column packed with 3 μm ODS-Hypersil.*

In general, retention was poor as indicated by the low capacity factors for all analytes, particularly INA and INN. In order to achieve adequate separation of analytes and increase their retention a pH of 6.0 was selected whilst the organic modifier concentration was reduced, the effect of which on column capacity factor can be seen in Figure 2.8. Additionally, selection of a pH at which INA eluted before INH was anticipated to increase the overall mass sensitivity for this principal degradation product which would be present in most analyses at considerably lower levels than the abundant INH. Based on the profiles in Figure 2.8, the chromatographic separation seen in Figure 2.9, which achieved adequate resolution of all analytes and a satisfactory distance of the chromatographic peaks from the solvent front, utilized a mobile phase comprising methanol - 20 mmol L^{-1} aqueous phosphate buffer (5 - 95) at pH 6.0. The assay based on this solvent system was thereafter validated according to section 2.3.2.2. At a flow rate of 1.4 mL min^{-1}, this solvent was pumped through a 200 x 4.6 mm i.d. column packed as above with 3 μm ODS-Hypersil.

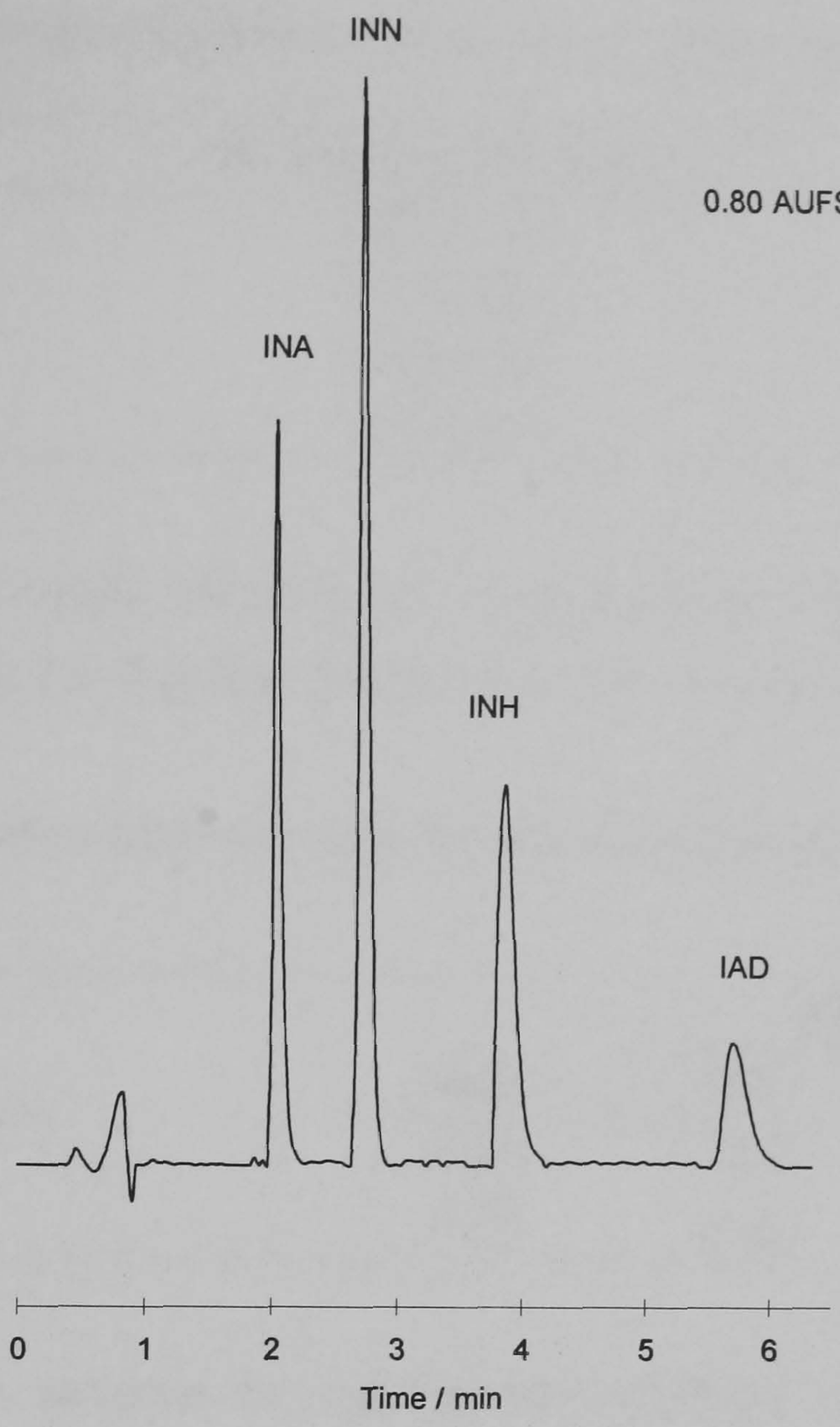

Figure 2.9 *Normalized representative chromatograms with respect concentration of isoniazid and its decomposition products. Chromatographic conditions: mobile phase, methanol - 20 mmol L^{-1} aqueous phosphate buffer (5 - 95) adjusted to pH 6.0; flow rate of 1.4 mL min^{-1} through a 200 x 4.6 mm i.d. column packed with 3 μm octadecylsilyl-modified silica. Detection at 263 nm. Labels indicate abbreviated analyte.*

2.3.2.2 Assay validation

The constancy of regression statistics was assessed on four consecutive days, regression statistics of which feature in Table 2.3. Compliance with the recommended limit of variation of the slope cited by Braggio et al. (1996) of ± 2.0 % was confirmed indicating the absence of solvent front persistence as discussed in section 2.3.1.2. The mean intercepts were less than ± 0.95 % relative to the magnitude of the corresponding detector response at the 100 % analyte level.

Table 2.3 *Between day regression statistics for isoniazid derived analytes n = 4*

Analyte	***Mean slope x 10^{-5} (RSD)***	***Mean r^2 (RSD)***
INH	1.031 (1.35)	0.999 (0.103)
INA	1.173 (1.94)	0.997 (0.125)
IAD	0.482 (0.78)	0.999 (0.054)
INN	1.963 (1.89)	0.999 (0.070)

The variability of repeat injections at an approximate analyte level of 10 μgmL^{-1} are presented in Table 2.4. Between day precision was established as per section 2.3.1

Table 2.4 *Normalized precision data for INH and degradates at a concentration of 10 μgmL^{-1}, n = 5*

	Analyte			
Attribute	***INH***	***INA***	***IAD***	***INN***
Peak area x 10^{-6}	1.002	1.178	0.479	1.928
RSD / %	0.16	0.45	0.29	0.42

Linear regression statistics for the standard additions of 5, 20 and 50 μgmL^{-1} to dissolution samples from albumin based formulations (section 9.3) yielded parallel straight lines for both INH ($r^2 = 0.989$) and INA ($r^2 = 0.970$) to that of the corresponding regression derived from aqueous standards of the same concentration. The intercepts on the area axis equated to INH and INA concentrations in pre-spiked dissolution samples ($P > 0.05$).

Specificity of the procedure was confirmed as per section 2.2.3.3 based on accuracy data, peak purity index and peak position with respect to standard solutions. Peak purity indices for INH and INA were > 0.99 and > 0.98 respectively. The interfering peak in the RIF assay (section 2.3.1), considered to emanate from Tween®, was not apparent during validation. The longer column used for INH compared with RIF would have had greater on-column diffusive effects, which apparently eliminated the baseline perturbence associated with this peak.

2.3.3 Combination HPLC assay for rifampicin and isoniazid

Determination of biological INH and RIF levels has, historically, been of great interest due to the interactions of their metabolism which frequently culminates in hepatotoxicity (Lecaillon et al., 1978; Ratti et al., 1981; Guillaumont et al., 1982; Oldfield et al., 1986; Woo et al., 1987; Lau et al., 1996). Metabolic variability between patients due to liver degradation of INH into inactive AcINH by an acetyltransferase whose activity is genetically determined, allied to powerful induction of RIF on liver metabolism, complicates dose prediction (Guillaumont et al., 1982). Numerous HPLC assays for the determination of INH (Hutchings et al., 1983) and RIF (Lecaillon et al., 1978; Ratti et al., 1981; Oldfield et al., 1986; Lau et al., 1996) in biological matrices have been reported. However, few combination assays for anti-tubercular drugs have been developed, presumably due to the chromatographic challenge of efficiently separating INH, PYZ and RIF, drugs of dramatically different hydrophobicities. Consequently, those which are described invariably involve gradient elution to achieve acceptable analysis times (Woo et al., 1987). Guillaumont et al. (1982) developed a method in which RIF and INH, and their main metabolites, DAR and AcINH, respectively, could be differentially extracted from a single plasma sample. Separation and determination thereafter was performed on the same stationary phase, ODS, but using different mobile phases. Separation of INH and RIF and some of the latter's degradation products for formulation evaluation (Shah et al., 1992) and dissolution monitoring (Gharbo et al., 1989; Jindal et al., 1994) are amongst few other combination assays described. The assay described below (section 2.3.3.1) was developed in a speculative manner, and, although not utilized in the work described hereafter, should prove invaluable pending full validation during assessment of *in vivo* performance suggested as part of further work in this thesis.

2.3.3.1 Method development

The developed HPLC procedure for simultaneous separation of RIF, INH and their predominant metabolites in man, DAR, RSV and AcINH respectively was indirectly based on a earlier chromatographic method for INH and PYZ (Gaitonde & Pathak, 1990). The oxidation product of RIF, RQU, was also prospectively considered to account for the probable deterioration of RIF during extraction procedures of analytes from biological matrices. Gaitonde & Pathak (1990) reported a rapid, sensitive and precise method for the estimation of INH and PYZ in plasma and urine. However, the authors used RIF as internal standard, a particularly illogical choice given that RIF invariably features in

treatment regimes for tuberculosis and would therefore be present as an interferent in biological samples requiring analysis. Indeed, the recoveries of > 99 % quoted for both analytes, INH and PYZ, irrespective of the biological medium, questioned the need for its inclusion. Moreover, the authors failed to identify the potential utility of a procedure purported to separate the three principle anti-tubercular drugs in clinical use.

The stationary phase utilized by Gaitonde & Pathak was a mixed-phase ODS-cyano (CN) (phase proportions unspecified). Attempts to source in the UK the Excaliber® ODS-cyano (CN) column described in that work were unsuccessful. Therefore, the current work examined a mixed-phase ODS and CN of arbitrary composition ODS : CN (1:1). A pH of 2.0 was chosen to develop the chromatographic separation as all analytes at this pH, were either protonated bases, e.g., RIF, DAR, RQU, and INH or uncharged moeties, e.g., RSV. AcINH was also considered protonated at this pH due to the available hydrazide NH_2 moeity on this molecule. Consequently, the separation strategy of Taylor et al. (1984) was adopted which involves addition of an hydrophobic ion-pairing agent to the mobile phase to manipulate retention of both charged and uncharged analytes. This has proved a powerful technique allowing the separation of analytes of widely different hydrophobicities and ionic character (Taylor et al., 1984). In Figure 2.10 the effect of hydrophobic sodium dodecyl sulphate (SDS) addition to the mobile phase on analyte retention can be seen on both mixed phase ODS-CN phase and ODS to elucidate the contribution that CN made to the overall separation.

The chromatographic response of the analytes to SDS can be generally interpreted as follows. Initially there is an increased retention for protonated species, e.g., RIF, RQU, DAR, INH and AcINH as the adsorbed charged pairing ion, SDS, electrostatically attracts these ions to the stationary phase surface, where they subsequently desolvate and are retained. The amount of SDS adsorbed on the stationary phase surface increased upon further addition of SDS, thus reducing the available surface for analyte desolvation. The retention of all charged analytes therefore reaches a maximum, after which point, retention decreased. As an uncharged solute, RSV showed a typical profile of reduced retention in parallel with the reduced availability of stationary phase surface for desolvation as SDS concentration increased.

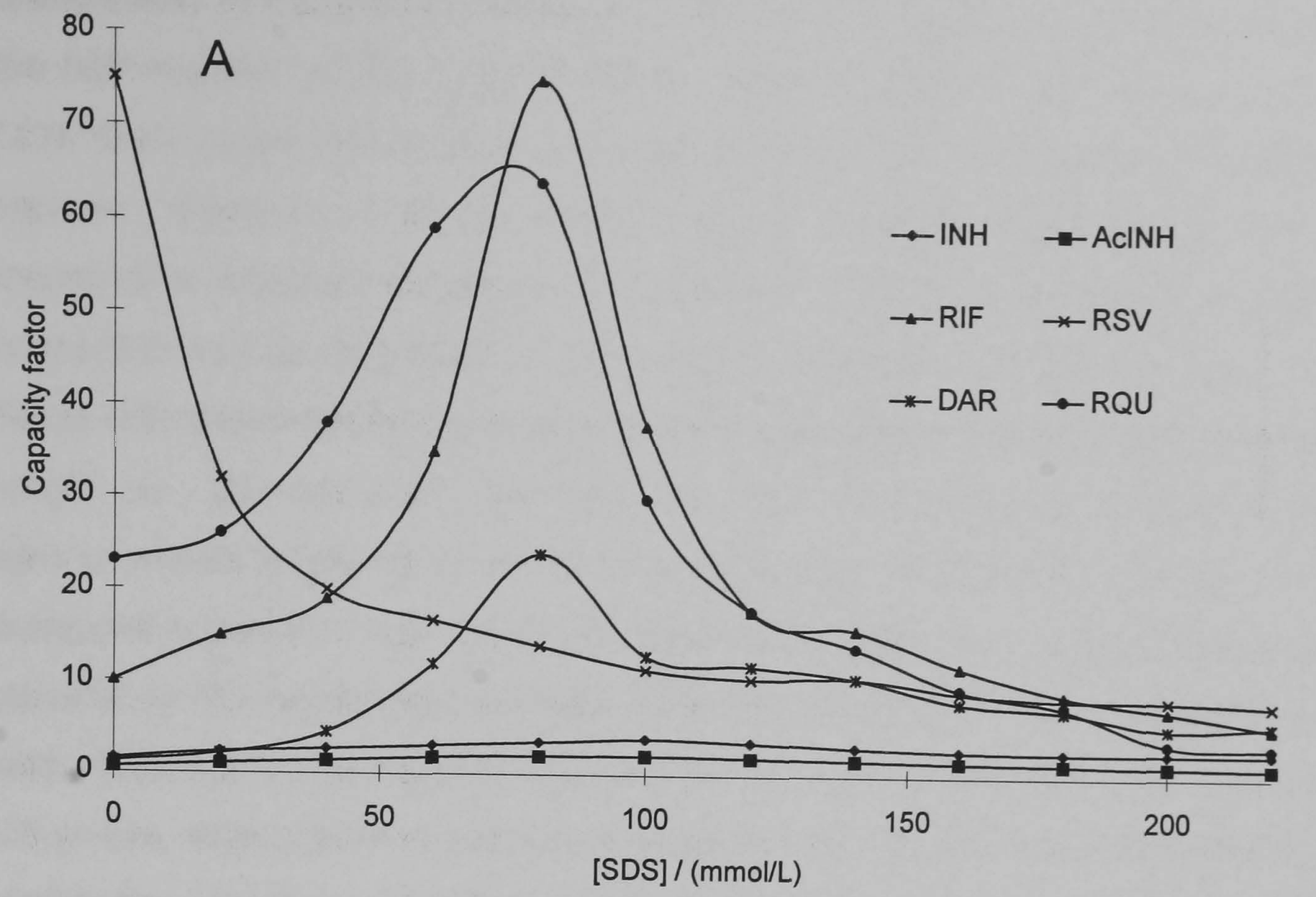

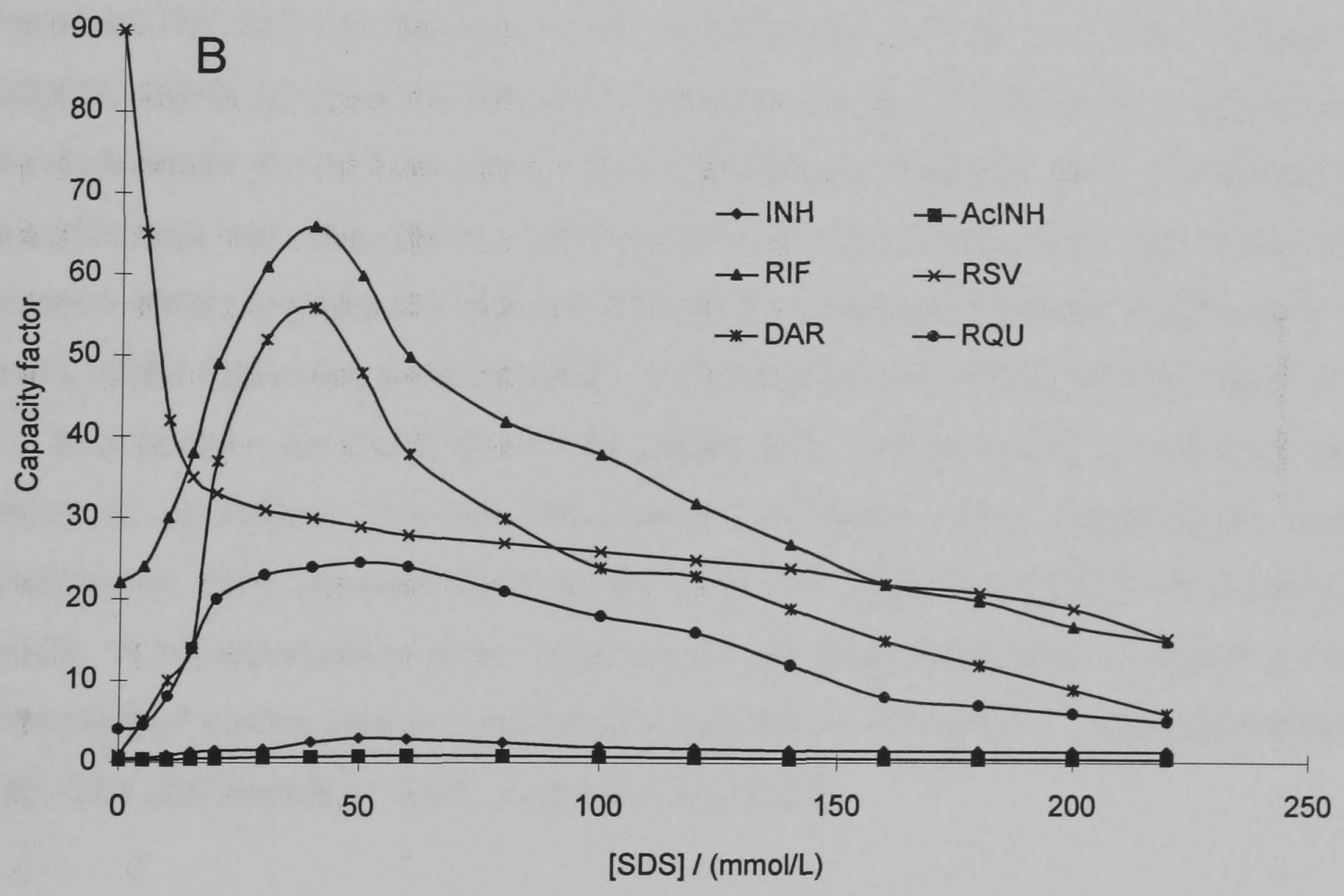

Figure 2.10 *Variation of column capacity factor for rifampicin, isoniazid and related compounds with various concentrations of sodium dodecyl sulphate (SDS) in the mobile phase. Chromatographic conditions: mobile phase, acetonitrile - 10 mmol L^{-1} aqueous phosphate buffer (50 - 50) adjusted to pH 2.0; flow rate of 1.4 mL min^{-1} through: A, a 200 x 4.6 mm i.d. column packed with 5 μm CN-ODS (50:50); and, B, a 150 x 4.6 mm i.d. column packed with 3 μm ODS. Detection at 240 nm. Legend indicates abbreviated analyte.*

Comparison of the plots in Figure 2.10 revealed a number of important observations. At the high organic modifier concentrations used, INH and AcINH were poorly retained on ODS alone as anticipated from the data in section 2.3.2.1. Therefore, SDS was added to improve retention of these weakly-retained species. Nonetheless, the small, but measurable parabolic behaviour as a function of SDS concentration revealed that ionic interaction was contributing to the retention mechanism of these analytes. Inclusion of 50 %w/w CN phase further enhanced retention disproportionately to the increase in column length, i.e., 200 compared with 150 mm, thus illustrating a contribution of this material also to overall retention of INH and its metabolite. Additionally, the use of CN ensured adequate separation from the solvent front of the most poorly retained analyte, AcINH. In general, all RIF associated analytes were less retained on the mixed-phase column. This was attributed to poorer adsorption efficiency of the SDS on the less hydrophobic ODS-CN phase, although the adsorption isotherms were not however measured to support this postulation. Further evidence for this was the up-shift in peak position of maximum retention for such analytes on the mixed-phase column. It was reasoned that the approximately two-fold reduction in retention times of RIF derived analytes at a SDS concentration of 200 mmol L^{-1} on ODS-CN compared with exclusively ODS was operationally advantageous. Therefore, these data support the use of the mixed-phase column which achieved adequate resolution of weakly retained AcINH from the solvent front, whilst maintaining acceptable analysis times. An SDS concentration of 200 mmol L^{-1} was chosen for the final mobile phase which represented the optimal separation in terms of resolution, sample throughput and finally, assay ruggedness; whereby small changes in SDS concentration would have little effect on analyte retention at such high levels. A representative chromatogram of the final separation is shown in Figure 2.11. The optimal mobile phase comprised acetonitrile - 10 mmol L^{-1} aqueous phosphate buffer (50 - 50), 200 mmol L^{-1} SDS, adjusted to pH 2.5.

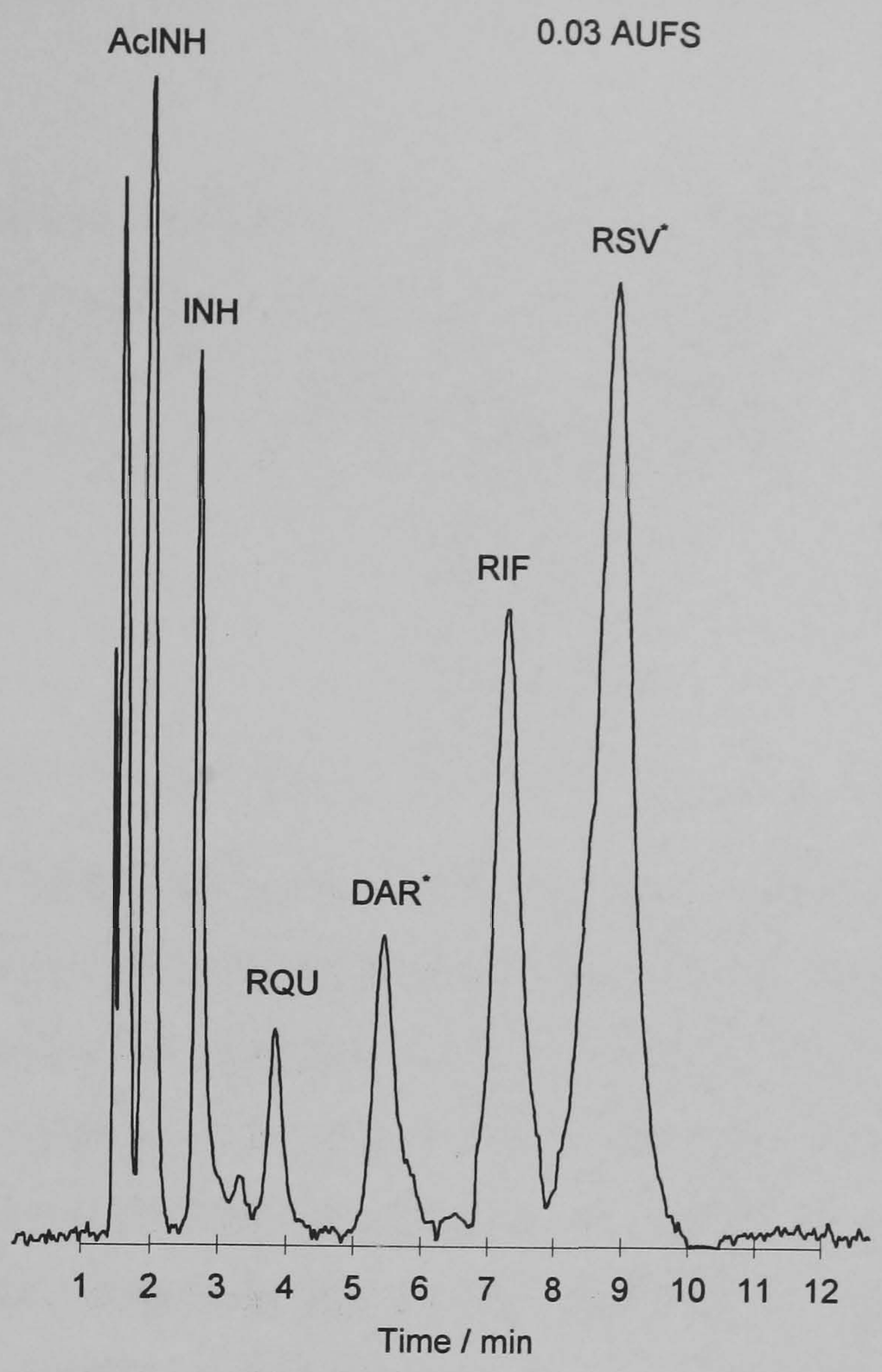

Figure 2.11 *Representative chromatogram of: rifampicin, isoniazid and related compounds. Chromatographic conditions: mobile phase, acetonitrile - 10 mmol L^{-1} aqueous phosphate buffer (50 - 50), 200 mmol L^{-1} SDS, adjusted to pH 2.5; flow rate of 1.4 mL min^{-1} through a 200 x 4.6 mm i.d. column packed with 5μm ODS-CN (50:50). Detection at 240 nm. Labels indicate abbreviated analyte.*

2.3.3.2 Assay validation

Preliminary validation of detector linearity yielded the regression statistics presented in Table 2.5. Variation in the gradient of the slope generally complied with the limits specified by Braggio et al. (1996), with the exception of INH. Correlation coefficients of the concentration-response plots established linearity for all analytes when injected individually. Whereas, the mean intercepts fell within ± 0.95 % limit relative to the magnitude of the detector response at the 100 % level, corresponding values for both INH (-2.15 %) and RSV (-2.36 %) did not comply when a mixed standard containing all analytes was analysed. In addition, the slope of the calibration lines fell to 0.795 and 2.205 for INH and RSV respectively. These data indicate a reduced detector response

than that anticipated. Furthermore, an additional peak appeared on these chromatograms at 3.25 min.

Table 2.5 *Regression statistics for calibration of detector response for rifampicin, isoniazid and related analytes, detection at 240 nm, n=3.*

Analyte	***Mean slope x 10^{-5} (RSD)***	***Mean r^2 (RSD)***
AcINH	0.786 (1.98)	0.977 (2.35)
INH	0.845 (2.15)	0.985 (1.98)
DAR	2.885 (1.28)	0.973 (1.95)
RIF	2.963 (1.89)	0.980 (1.23)
RSV	2.475 (0.94)	0.972 (2.01)

Jindal et al. (1994) earlier speculated that complex formation between INH and RSV may occur in solution in dynamic equilibrium with the starting analytes. They did not, however, elaborate on the potential mechanism of the reaction which it is proposed here occurs according to the scheme in Figure 2.12. Subsequent to hydrolysis of RIF to RSV, condensation following nucleophilic attack by the electonegative hydrazide NH_2 yields the corresponding imine. The reduction in the gradients of the calibration lines for both analytes is approximately quantitative at 5 - 10 % complete although this reaction requires rigorous characterization to assess the error it may confer on quantitative measurements of these analytes where they co-exist in biological samples.

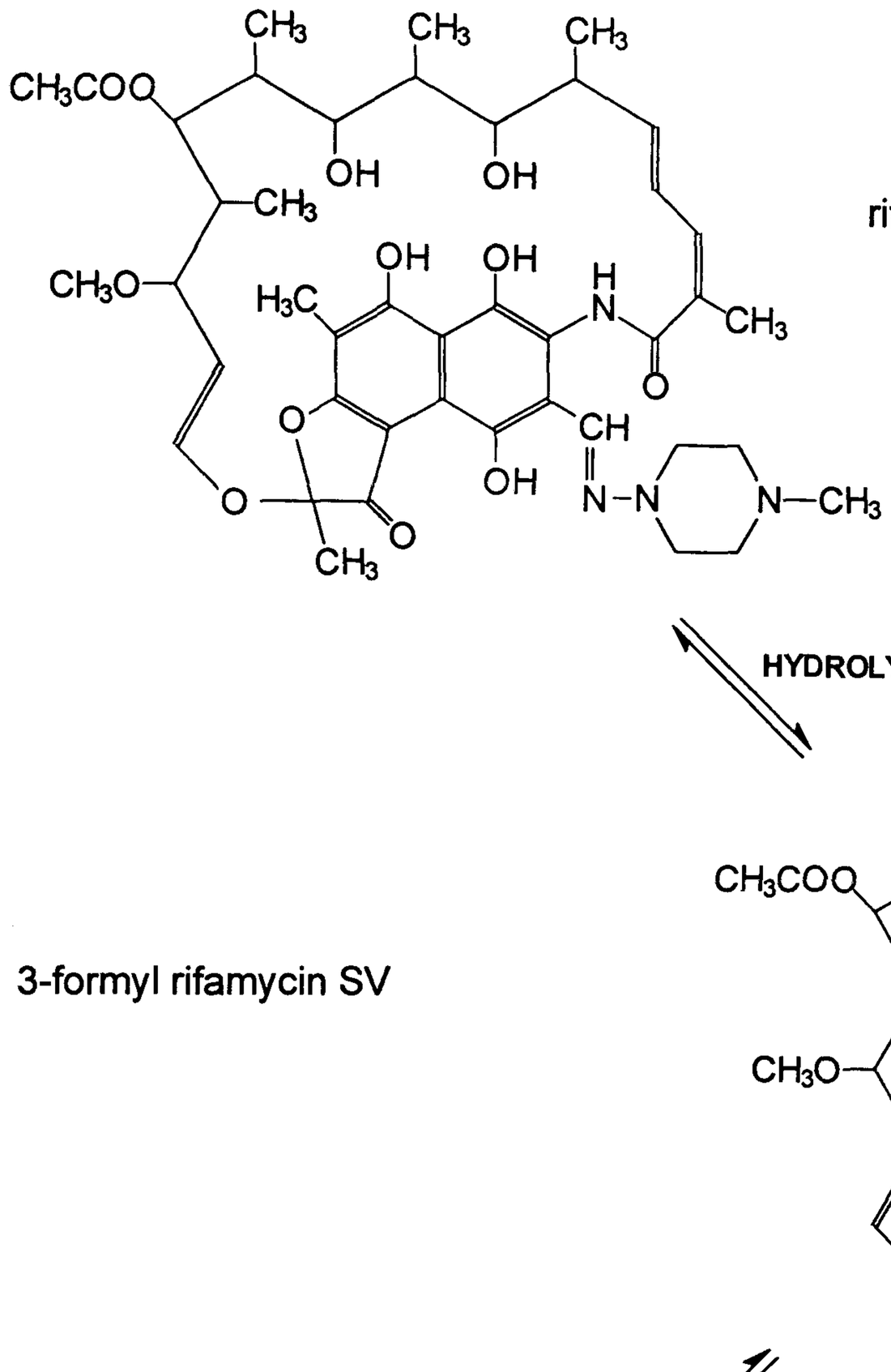

Figure 2.12 *Proposed mechanism of reaction between 3-formyl rifamycin SV and isoniazid in aqueous solution*

2.4 Conclusion

Stability-indicating assays for both INH and RIF and their predominant degradation products have been developed and suitably validated in the context of their predominant prospective use, i.e., monitoring drug release and formulation stability assessment. The use of these separations to quantify drug release from long-acting biodegradable formulations is described in the following chapter. From validation data both stability-indicating assays were concluded to be linear, precise and specific, hence conforming to the basic requirements for stability-indicating procedures (Taylor et al., 1994). Further attributes of the procedure for RIF was the use of a binary analytical phase which increases assay robustness and, most significantly, a reduced analysis time compared with procedures previously described (Graham,1979; Krukenberg et al., 1996; Jindal et al., 1995). The assay for INH used a mobile phase with a small organic modifier concentration which was considered advantageous on economic and environmental grounds.

A rapid isocratic separation for INH and RIF and their main metabolites as well as RQU was developed which obviated the use of gradient elution to achieve acceptable analysis times. The technique used ion-pairing methodology on a mixed-phase column, which, pending suitable validation and the development of extraction procedures, represents a significant improvement on previously reported work. This separation would form the basis of the quantitative determination of both drugs from *in vivo* release studies proposed in this thesis as part of further work. This method, however, requires further rigorous validation in biological media. In particular, the apparent complex formation between INH and RSV requires further investigation to elucidate its mechanism of formation and the extent of reaction before the assay may be reliably applied to the determination of levels of these analytes in biological samples.

3. Preformulation

3.1 Introduction

Preformulation encompasses techniques and studies to determine those physical and chemical properties of the particular drug substance which may affect development and performance of an efficacious dosage form. This information is essential for rational and efficient dosage form design and largely dictates the formulation strategies employed. Moreover, these preliminary data allow the formulator to anticipate problems which may preclude certain approaches, whilst exploiting inherent drug properties which favour others. Preformulation studies must be performed in the context of the overall therapeutic, and thus, formulation objective. These entail selective investigations to assess the prospective processability of the drug substance itself, and, its manufacturability when mixed and compounded with other ingredients. In short, preformulation should provide the investigator with a sound working knowledge of the drug to expedite formulation development.

In spite of having identical therapeutic indications, in Figures 2.3 and 2.7 respectively, it was shown that RIF and INH have very different chemical structures, and hence physicochemistry. Initial preformulation studies were based on solubility, spectral and crystalline properties, considered key properties for the preparation and subsequent characterization of biodegradable microspheres. These were supplemented with analytical and degradation data in response to formulation development difficulties as these were encountered.

3.2 Experimental procedures

3.2.1 Ultraviolet spectroscopy

Ultraviolet (UV) spectra were recorded in the λ range 200 - 600 nm. After obtaining UV spectra, calibration standards over the approximate concentration range 0.5 - 50 μgmL^{-1} were prepared in a range of aqueous and non-aqueous solvents and absorbance measured at their respective wavelengths of maximum absorbance, λ_{max}. From linear regression of absorbance on concentration, specific absorbance coefficients, $A^{1\%}_{1cm}$, were computed and the regression statistics recorded.

3.2.2 Crystallinity and polymorphism

3.2.2.1 Preparation of crystals

Supersaturated solutions of drug were prepared by adding excess drug to various solvents of a spectrum of polarity: water ($\varepsilon_{20\,°C}$ = 80); acetonitrile ($\varepsilon_{20\,°C}$ = 38.8); methanol ($\varepsilon_{20\,°C}$ = 33); ethanol ($\varepsilon_{20\,°C}$ = 25); acetone ($\varepsilon_{20\,°C}$ = 21); butanol ($\varepsilon_{20\,°C}$ = 17.1); dichloromethane ($\varepsilon_{20\,°C}$ = 9.08); and, chloroform ($\varepsilon_{20\,°C}$ = 4.806); which were incubated at 37 ± 0.5 °C in sealed vials. Supersaturated solution was clarified from undissolved drug. Nucleation was then induced by cooling the solution either slowly (at room temperature) or quickly by quenching in ice. The crystals thus formed were stored under vacuum at 24 ± 2.0 °C over silica gel prior to characterization. The habit of recrystallized drug was assessed microscopically.

3.2.2.2 Differential scanning calorimetry

Melting points and enthalpies of fusion for recrystallized products were assessed by differential scanning calorimetry (DSC 7, Perkin-Elmer, Connecticut, USA) as part of investigations of crystal polymorphism. Samples (5 - 7 mg) were scanned at a heating rate of 20 °C min^{-1} in a N_2 atmosphere. DSC scans were recorded with the associated computer controlled software. Instrument calibration was performed on the melting endotherms of indium and zinc standards.

3.2.2.3 Infrared spectroscopy

Subsequent to vibrational milling (Model CE95, Retsch, Germany), and drying at 100 ± 5 °C for 24 h, potassium bromide was used to prepare drug embedded discs for infrared spectral analysis. Discs containing 5 %w/w drug were pressed at 8 tonnes for 15 min under vacuum. Infrared (IR) spectra obtained (Perkin-Elmer model 186, Perkin-Elmer, USA) were examined and characteristic peaks assigned.

3.2.2.4 Intrinsic dissolution rate

Flat-faced discs of drug as supplied and crystalline products weighing 200 ± 5 mg and of diameter 11 mm were compressed at 10 tonnes for a dwell time of 5 min using a single punch Manesty F3 tablet press (Manesty Machines Ltd., Liverpool, England). High compaction pressures were used to ensure minimal tablet porosity. Single tablets were secured centrally to the base of a USP dissolution basket with molten hard paraffin wax. After complete submersion, excess wax was removed from the exposed aspect of the

tablet to provide a defined area (0.950 cm^2) from which dissolution could occur. The basket was attached to the stirring shaft rotating at 100 ± 1.0 rpm and submerged in 1 L of distilled water maintained at 37 ± 0.1 °C. Dissolved RIF and INH were determined by UV absorption at 270 and 263 nm, respectively. The amount of RIF or INH dissolved per unit surface area was plotted against time. The slope of the initial portion of each profile was expressed as a function of the surface area exposed to compute an intrinsic dissolution rate, C_o (mg cm^{-2} min^{-1}). Triplicate determinations of C_o were performed on each batch of recrystallized product.

3.2.3 Solubility studies

3.2.3.1 Saturation solubility

Saturation solubilities of both RIF and INH were examined by addition of a variety of aqueous and non-aqueous solvents to an excess of powdered drug in vials. After an equilibration period of 8 h, dissolved drug was determined by HPLC. For aqueous based solvent systems, equilibration time was limited to 1 h as a result of concomitant hydrolytic reactions which interfered with saturation solubility determination. Additionally, a number of temperatures were examined for selected solvents. Where decomposition exceeded 10 % of saturation solubility the result was disregarded and repeat determinations performed.

3.2.3.2 pH-solubility profile

The solubility of INH at various pH values was determined as follows. Under constant stirring, excess drug was added to a dilute acidic medium (0.1 mol L^{-1}) in a double jacketed beaker plumbed to a circulating water bath maintained at 37 ± 0.5 °C. This mixture was allowed to equilibrate for 2 h. Thereafter, samples (5 mL) were removed by syringe through an attached Acrodisc (Gelman, UK) syringe filter of pore diameter 0.45 μm. The samples were diluted where appropriate and the concentration of INH in the resultant solution was determined by the HPLC procedure detailed in section 2.3.2. Fresh INH suspension was prepared after the pH was successively increased by controlled addition of 0.01 mol L^{-1} NaOH. The solubilities of INH were plotted against pH.

The above procedure for INH was followed with the following modification for RIF. Due to the significant oxidative and hydrolytic decompositions, equilibration times were arbitrarily reduced to 1 h in sealed vials under agitation at 1 Hz. This step sought to minimize

degradate interference through 'salting-in' or '-out' effects. To excess drug, degassed 'universal' citric-phosphate buffer (0.01 mol L^{-1}) in the pH range 2.2 - 7.5 was added to fill the vials thus minimizing headspace and the available O_2. Dissolved drug after dilution was determined by HPLC as described in section 2.3.1 and then plotted against pH. The arbitrary 10 % decomposition limit was applied throughout.

3.2.4 Drug-polymer interactions

Subsequent to gently grinding in a mortar with a pestle and sieving (aperture size 100 μm), individual physical mixes of INH and RIF with a range of Resomer® polymers (1:1) were prepared in small vials with vigorous shaking. Samples (5 - 15 mg) for RIF containing mixes were scanned according to the following programme: 1) from 25 - 210 °C at 10 °C min^{-1}; 2) cooled to 25 °C at 30 °C min^{-1} and; 3) repeat of 1). Samples containing INH were subject to the same program with the exception that the maximum scan temperature was 185 °C. Individual polymers as supplied were similarly scanned.

3.2.5 Stability

3.2.5.1 Rifampicin

The time course of RIF instability was studied in isotonic Sørensens buffer (modified) (SBM) (Dawson et al., 1962) of pH 7.4 ± 0.1 at 37 ± 0.5 °C. Individual stock solutions of RIF, RSV and RQU (1 $mgmL^{-1}$) were freshly prepared in dimethylsulphoxide (DMSO). At time zero, amounts of stock solution of each compound yielded nine individual solutions, at three concentrations between 3 - 50 μgmL^{-1} for each compound when added to 100 mL buffer prewarmed in a Grant SS40-2 (Cambridge, UK) thermostated bath. The protective effect of various antioxidants was evaluated. Sampling frequency was determined by interim analysis of the degradation kinetics. Samples, withdrawn by syringe, were analysed by HPLC as described in section 2.3.1. Undecomposed RIF and RSV were plotted against time and the kinetics of degradation examined with the aid of an iterative curve-fitting programme (CurveExpert version 1.3, Daniel Hyams, 112B Crossgate St, Starkville, MS, 39759).

3.2.5.2 Isoniazid

The kinetics of INH decomposition were investigated in Sørensens phosphate buffer (modified) (SBM), pH 5.8 (approx. 0.07 mol L^{-1}). and pH 7.4 (approx. 0.10 mol L^{-1}); McIlvaines citric-acetate buffer, pH 5.88 (approx. 0.28 mol L^{-1}) and pH 7.4 (approx. 0.37 mol L^{-1}), and; Walpoles acetate buffer, pH 5.8 (approx. 0.07 mol L^{-1}) (Dawson et al.,

1962). An aqueous standard solution of INH was freshly prepared for each buffer system, which, upon dilution in 100 mL of buffer solution yielded a concentration of 20 ± 5 μgmL^{-1}. Actual pH ranges were all ± 0.1 pH unit of that cited and remained so throughout the 30 d period of the study. Samples were withdrawn from sealed flasks by syringe and analyte concentration was determined by HPLC (see section 2.3.2). The kinetics of degradation were computed as described above.

3.3 Results and Discussion

3.3.1 Ultraviolet spectroscopy

UV spectra of INH and RIF in aqueous solution are shown in Figure 3.1. The range of solvents were chosen to speculatively represent those to be used in subsequent microencapsulation procedures and other operations. Of particular interest were the λ_{max} values, which represented the optimum λ of measurement to achieve maximum sensitivity where direct UV quantitative methods were used. Summaries of the absorption characteristics of INH and RIF are provided in Tables 3.1 and 3.2 respectively.

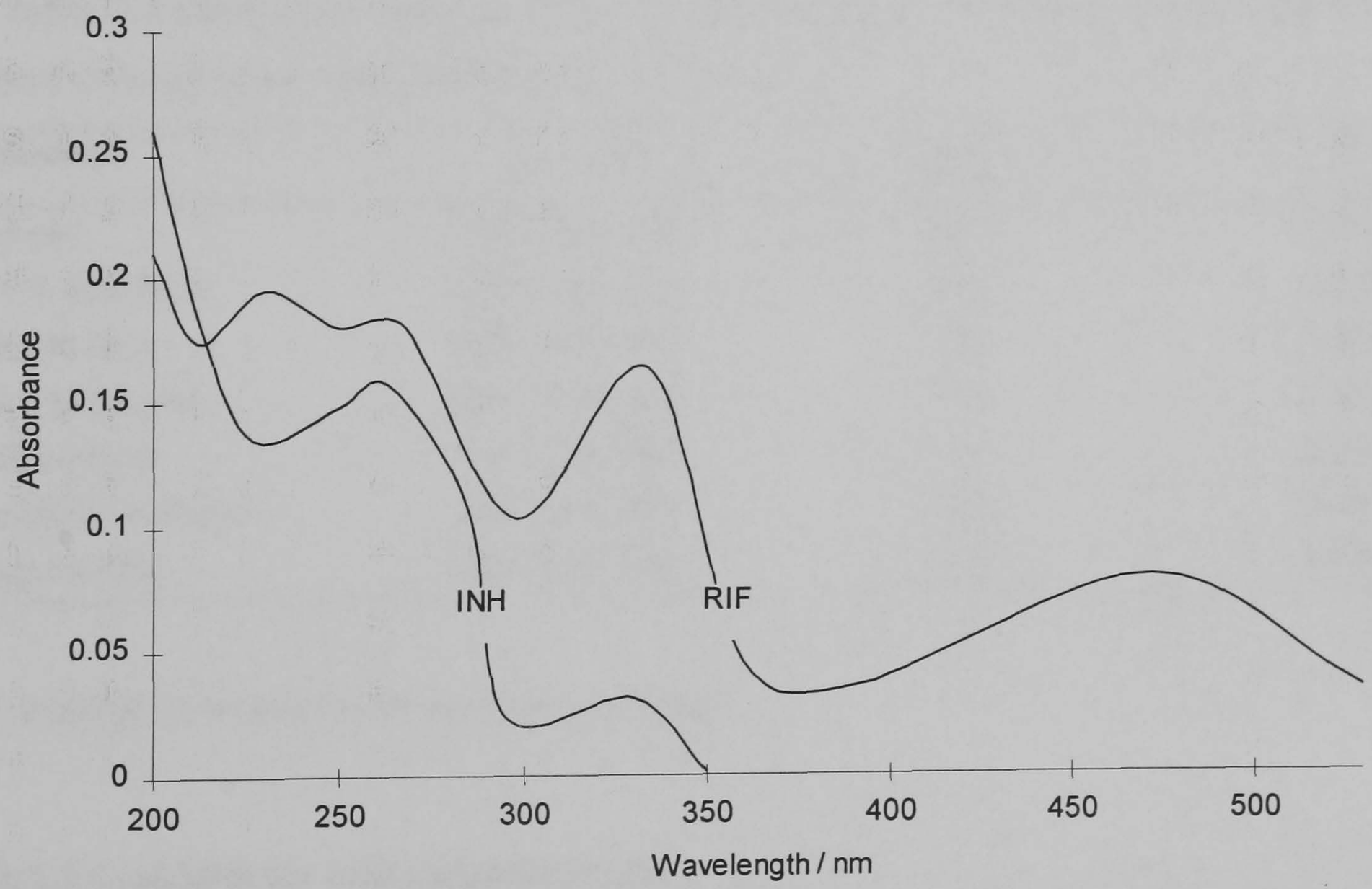

Figure 3.1 *Ultraviolet spectra of rifampicin and isoniazid in water at 24 ± 2.0 °C*

For INH, the spectral changes under basic conditions were attributed to rapid hydrolytic decomposition of INH to INA as described by Lewin & Hirsch (1954). Thus, after 5 h the

peak at 272 shifted to 256 nm, whilst that at 325 nm largely disappeared. Consequently, to minimize errors in the determination of spectral statistics from alkaline solutions, absorbance measurements were recorded immediately after solution preparation.

Table 3.1 *Ultraviolet spectral attributes and statistics of isoniazid in a range of aqueous and non-aqueous media at 24 ± 2.0 °C, n = 2.*

Solvent	λ_{max} / ***nm***	$A^{1\%}_{1cm}$	r^2
water	261	305	0.999
1 % w/w PVA	262	298	0.998
0.01 M HCl	213, 265*	417	0.999
0.01 M Na OH	272*, 295, 325	298	0.999
chloroform	259	286	0.979
dichloromethane	258	259	0.985
acetonitrile	260	262	0.987

* wavelength of measurement for Beer-Lambert regression

Table 3.2 *Ultra-violet spectral attributes and statistics of rifampicin in a range of aqueous and non-aqueous media at 24 ± 2.0 °C, n = 2.*

Solvent	λ_{max} / ***nm***	$A^{1\%}_{1cm}$	r^2
water	235*, 338, 470	403	0.979
1 % w/w PVA	235*, 337, 478	398	0.983
0.1 M HCl	235*, 335, 465	410	0.999
0.1 M Na OH	245*, 335, 458	416	0.999
chloroform	245*, 298, 390	380	0.995
dichloromethane	245*, 295, 390	394	0.999
acetonitrile	244*, 295, 390	398	0.998

* wavelength of measurement for Beer-Lambert regression

3.3.2 Crystallinity and polymorphism

The crystalline form of the drug can affect both the production and biological behaviour of the finished form (Florence and Attwood, 1988), through its influence on flow, matrix architecture and surface area-dependent dissolution (Bodmeier & Chen, 1988). In addition, during preformulation investigations it is of vital importance that sufficient care is taken to determine polymorphic tendencies of, in particular, poorly soluble drugs. It is well

documented that polymorphic forms of the same drug may exhibit significantly different dissolution behaviour resulting in significant variation in therapeutic response when administered orally (Florence & Attwood, 1988). It follows these manifestations may also alter the release behaviour of the polymorphic candidate when applied to fabrication processes involving different solvents and temperatures where these have been shown to promote their formation, e.g., microencapsulation (Benoît et al., 1986). Of more fundamental interest is the geometry of the crystalline population, referred to as crystal habit. Geometrical factors are potentially more influential in micronized systems, particularly where drug constitutes an appreciable volume of the overall solid.

3.3.2.1 Crystal habit

Irrespective of the solvent from which the drugs were recrystallized, INH yielded needle- and RIF plate-shaped crystals, respectively. Qualitatively, corresponding products prepared at 0 °C were smaller in mean size compared with those at 24 ± 2.0 °C due to greater supersaturation and more extensive nucleation under quenched conditions. Bodmeier & Chen (1988) encountered problems with crystal habit during microencapsulation studies of caffeine. The authors assigned the needle morphology of encapsulated drug to ingredient incompatibility when spray-dried with PDLLA. Moreover, such crystal habit created a crystalline network of drug contiguous with the surface which contributed to the rapid release of drug. Accordingly, similar difficulties were anticipated during microencapsulation of INH described later in this thesis.

3.3.2.2 Differential scanning calorimetry

The quantitative determination of endothermic, e.g., fusion, sublimation and exothermic events, e.g., crystallization and degradation have many applications in preformulation studies, including determination of purity, solvation, degradation and excipient compatibility. In addition, detection of polymorphism is another useful utility for which DSC has been specifically applied in these studies.

Polymorphic species have different molecular arrangements in the solid state, such that they behave as different chemical entities exhibiting variable physicochemical properties, e.g., solubility, density, crystal habit, optical, melting points and heats of fusion (Wells, 1986); the latter two properties explaining the widespread application of DSC as a suitable tool for the investigation of their prevalence under the conditions of drug formulation, manufacture and use.

Typical DSC scans for each substance are shown in Figure 3.2, whereas thermal data are summarized in Table 3.3.

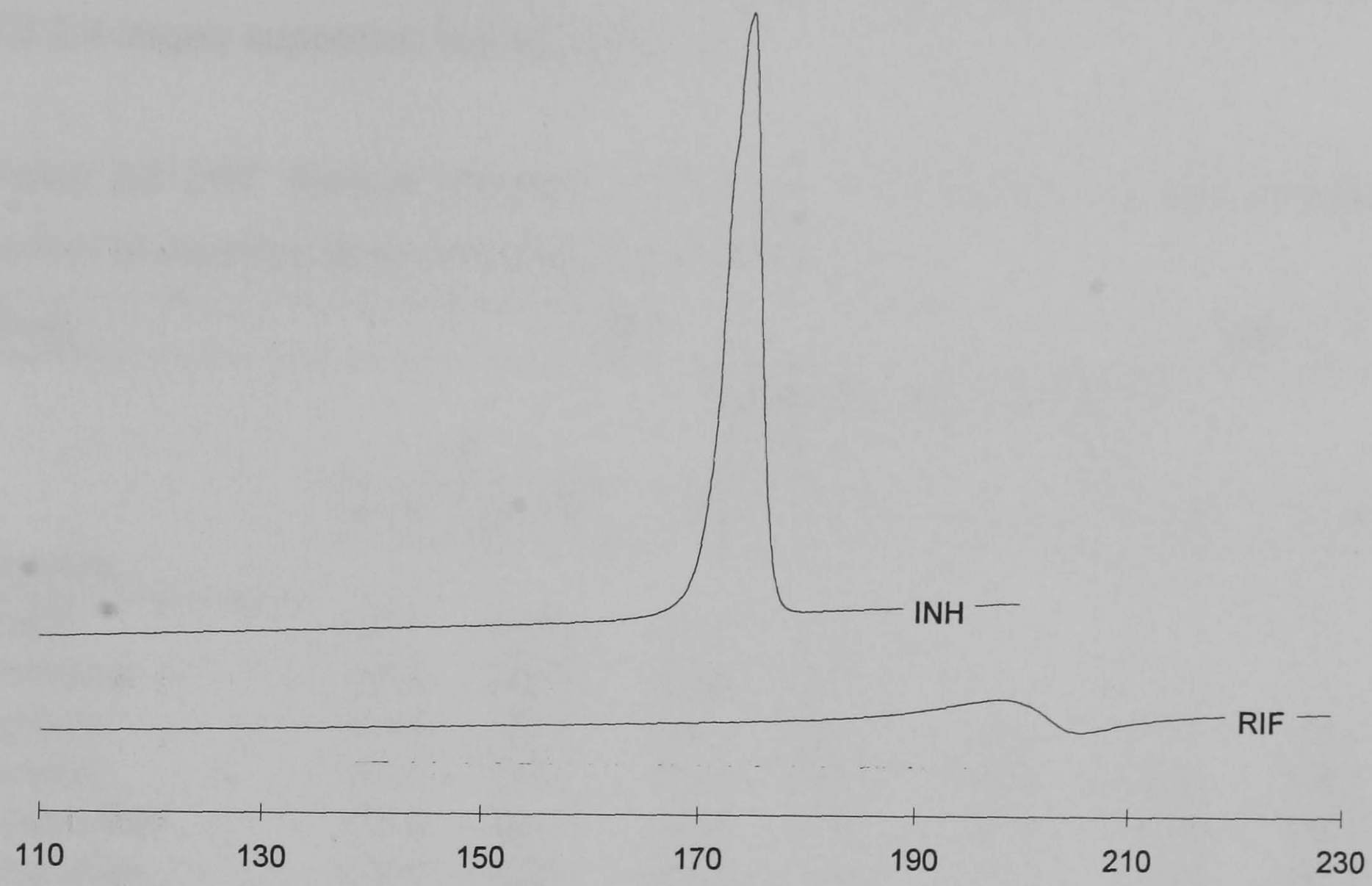

Figure 3.2 *DSC scans of isoniazid (INH) and rifampicin (RIF) as supplied*

The single sharp endotherm at approximately 175 °C for INH was typical of the melting characteristics of a highly ordered crystalline substance. The small variation in the melting point and ΔH values tabulated in Table 3.3 suggested the absence of significant polymorphic forms of this drug. In contrast, RIF as supplied showed a more diffuse melting endotherm at 197.9 °C ($\Delta H = 14.05\ Jg^{-1}$) followed by an exothermic event at 205.6 °C ($\Delta H = -9.44\ Jg^{-1}$) which may be due to either recrystalization or decomposition. Subsequent to these events, exothermic baseline noise was considered to indicate dramatic decomposition of RIF at ≅ 240 °C. Polymorphism has not been reported for RIF. However, DSC scans of precipitated crystals of RIF consistently exhibited a peak position 5 - 15 °C below that of drug supplied. The crystalline structure of a penta-hydrate form of RIF has been solved (Gadret et al., 1975), which, by inference, cannot preclude the potential for a range of pseudopolymorphs. This might have accounted for the variation in peak position observed. The variation in the enthalpy values for RIF precipitates was attributed to low enthalpies for these events allied to the difficulty in discerning where the switch from melting endo- and recrystallization exotherms occurred. Based on these data,

the assessment of polymorphism for RIF was unclear. Nonetheless, it was reasoned that the variation in heats of fusion for the recrystallized products would not translate to significant variations in dissolution rate. The intrinsic dissolution data presented in section 3.3.2.4 largely supported this statement.

Table 3.3 *DSC thermal statistics of rifampicin and isoniazid crystals prepared from a variety of aqueous and non-aqueous solvents (n=1)*

Drug	***INH***				***RIF***			
	Preparative conditions / °C							
	0		***25***		***0***		***25***	
	T_m / °C	ΔH / Jg^{-1}	T_m / °C	ΔH / Jg^{-1}	T_m / °C	ΔH / Jg^{-1}	T_m / °C	ΔH / Jg^{-1}
Solvent								
water	173.7	247.8	172.2	246.4	*	*	*	*
methanol	173.8	285.8	173.5	222.8	*	*	*	*
ethanol	174.8	202.7	172.1	264.0	185.1	14.12	182.1	16.13
butanol	172.9	219.7	173.1	245.4	185.8	14.02	188.2	15.13
acetonitrile	173.2	238.1	174.3	267.1	183.5	15.46	186.1	14.23
chloroform	173.4	222.4	172.5	240.1	185.1	12.45	189.4	13.45
dichloromethane	175.1	236.1	175.1	224.6	184.4	13.67	187.4	14.13
acetone	172.1	285.6	173.3	241.8	184.4	18.79	184.4	15.25

* no data available due to insufficient solubility and the prohibitively large quantities of expensive rifampicin required to yield sufficient crystalline product for characterization

3.3.2.3 Infrared spectroscopy

Characteristic peaks for both INH and RIF are listed in Tables 3.4 and 3.5, respectively.

Table 3.4 *Characteristic infrared vibrations for isoniazid (KBr disc)*

Wave number / cm^{-1}	***Assignment***
3300 - 3100	bonded N-H and C-H
1670	C=O
1560	amide (NH bend)
1640	NH_2 deformation

IR data may also be used to tacitly demonstrate the presence of polymorphs, where, for instance, crystallization of these forms involves significant hydrogen bonding between adjacent lattice molecules or entrapped solvent in the case of pseudopolymorphs. No significant difference in the IR spectra were observed in these studies irrespective of the solvent or crystallization conditions for both INH and RIF, casting doubt on the existence of pseudopolymorphs, of particularly, RIF.

Table 3.5 *Characteristic infrared vibrations for rifampicin (KBr disc)*

Wave number / cm^{-1}	***Assignment***
3300 -2300	broad NH and OH bonded
1715	CH_3CO
1640	CO
1620	amide I (carbonyl stretch)
1570	C=C
1540 and 1520	amide II (amide NH bend)
1255, 1040 and 1020	C-O-C acetyl (CO stretch)

3.3.2.4 Intrinsic dissolution rate

Intrinsic solubility data (C_o) for prepared RIF and INH crystals are presented in Table 3.6. Average values (RSD) were 8.12 (14.7) and 7.83 (9.76) $mgcm^{-2}$ min^{-1} for INH crystals prepared at 0 and 25 °C respectively, whereas corresponding statistics for RIF were 3.94 x 10^{-2} (12.5) and 3.51 x 10^{-2} (14.3) $mgcm^{-2}$ min^{-1}. Values derived from crystals prepared at 0 °C were, on average, greater than those at 25 °C, although there was no significant difference between preparative conditions for INH nor for RIF ($P > 0.05$). Greater C_o for crystals grown at 0 °C were probably due to the finer granulometry of these products compared with those prepared at 24 ± 2.0 °C.

The subtle differences in intrinsic solubility data for INH shown were attributed to a variety of experimental factors, although it is recognized that without accurate X-ray diffraction data no firm conclusions can be drawn nor can the absence of polymorphs be unequivocally stated. These factors include variation in compression pressure and dwell time, particle size and shape (which may effect compression behaviour and powder consolidation), and the presence of lattice-bound solvent. The relative non-reproducibility of the C_o results represented by the relative standard deviation values (RSD), support these ideas. Nonetheless, comparison of the C_o results for INH and RIF demonstrated an approximately 150 - 200 fold difference in solubility of the former compared to the latter. In general terms, the correspondence of this factor for saturation solubility data presented in section 3.3.4.2 validated the C_o results.

Table 3.6 *Intrinsic dissolution statistics for isoniazid and rifampicin crystals prepared in a variety of aqueous and non-aqueous solvents (n=3)*

Drug	**INH**				**RIF**			
	Preparative conditions / °C							
	0		**25**		**0**		**25**	
Solvent	C_o / mg cm^{-2} min^{-1}	RSD / %	C_o / mg cm^{-2} min^{-1}	RSD / %	C_o / mg cm^{-2} min^{-1} ($x 10^2$)	RSD / %	C_o / mg cm^{-2} min^{-1} ($x 10^2$)	RSD / %
water	8.21	5.6	7.44	8.2	*	*	*	*
methanol	7.28	15.1	8.35	12.5	*	*	*	*
ethanol	6.83	4.5	7.92	7.2	4.56	26.4	2.87	21.5
butanol	8.35	7.4	7.16	6.3	3.54	8.6	4.13	25.6
acetonitrile	7.33	8.1	8.26	11.3	3.46	19.2	3.75	11.2
chloroform	8.52	4.5	9.26	4.7	3.51	16.2	3.15	17.1
dichloromethane	8.81	6.7	7.12	8.8	4.23	17.9	3.67	8.7
acetone	6.62	8.6	7.14	3.2	4.35	23.5	2.95	16.5

* no data available due to insufficient solubility and the prohibitively large quantities of expensive rifampicin required to yield sufficient crystalline product for characterization

For RIF, C_o statistics were more variable compared to INH, rendering interpretation particularly difficult. The non-reproducibility of the results had arisen due to experimental variation rather than true differences between different batches of crystals. In addition to the factors listed for INH, this variation was accounted for by the difficulties and consequent inaccuracies in determination of low concentrations of RIF by direct UV measurement and the inherent elasticity of RIF, which hindered the compression of discs of smooth and unbroken morphology which did not 'cap'. The data for RIF were therefore inconclusive, against a background of IR data suggesting the absence of true polymorphic forms, whereas interpretation of DSC results was less clear. Polymorphism, however, has not been reported for this drug (Gadret et al., 1975).

3.3.3 Drug-polymer interactions

As a rapid screen, thermal analysis can be exploited to investigate and predict physicochemical interactions between ingredients which might affect the production of a stable and efficacious form with consistent biopharmaceutical performance (Wells, 1986). These studies allow ingredient substitution for alternative compatible materials where the interaction is likely to be significant during formulation manufacture, administration or use.

In a chemical sense, under anhydrous conditions, poly-α-hydroxy acids are generally stable in the solid state when in intimate contact with a drug substance. However, when

hydrated, hydrogen-bonding (Bodmeier & Chen, 1989; Mauduit et al., 1993a) and polymer degradation catalysis (Ramtoola et al., 1992; Maulding et al., 1986) have been observed with selected basic drugs. Of greater concern are physical interactions between encapsulate and encapsulant, e.g., solid solution, eutectic formation. Dependent on drug loading and their extent, such interactions determine the ultimate physical form of the drug in the polymer upon microencapsulation, or, conversely, account for variation in the thermomechanical properties of the polymer in the presence of drug (Dubernet, 1995).

In this study, all samples were double scanned: the first scan indicated the existence of chemical or physical interaction upon intimate contact during the heating cycle; the second temperature gradient was recorded to provide an indication of the effect of quench cooling, which although performed in the absence of solvents, correlated to the precipitation kinetics of codissolved materials during microsphere formation using techniques where rapid solid deposition occurs, e.g., spray-drying.

Due to the amorphous nature of the Resomer® materials investigated, they possessed a T_g with no melting endotherm. Affected by heating rate and polymer history, T_g represents a change in heat capacity of a polymer due to specific changes at this point in polymeric molecular motion. Thus, below the T_g the polymer atoms and chains undergo low amplitude vibratory motion rendering the material brittle and inelastic. This is referred to as the 'glassy' state. Above the T_g, the so-called 'rubbery' state prevails, in which the polymer chains undergo translational, rotational and diffusional movement (Ford & Timmins, 1989; Kerc & Srcic, 1995) resulting in an increase in polymer free volume (Hausberger & DeLuca, 1995). Related to a stress-relaxation phenomenon, an endothermic peak may overly the T_g, the magnitude of which is largely related to polymer nature, storage time and conditions, and the thermal history of the sample (Serajuddin et al., 1986; Dubernet, 1995).

3.3.3.1 Rifampicin

For RIF, with the exception of R104, the first scan revealed no significant interaction between drug and polymer, whereby both the T_g and melting-recrystallization events of polymer and the drug respectively were evident as seen in Figure 3.3. The absence of the T_g of R104 was attributed to the fact that the T_g for such low MW material was outwith the studied temperature range (manufacturer quotes a broad range of 5 - 25 °C).

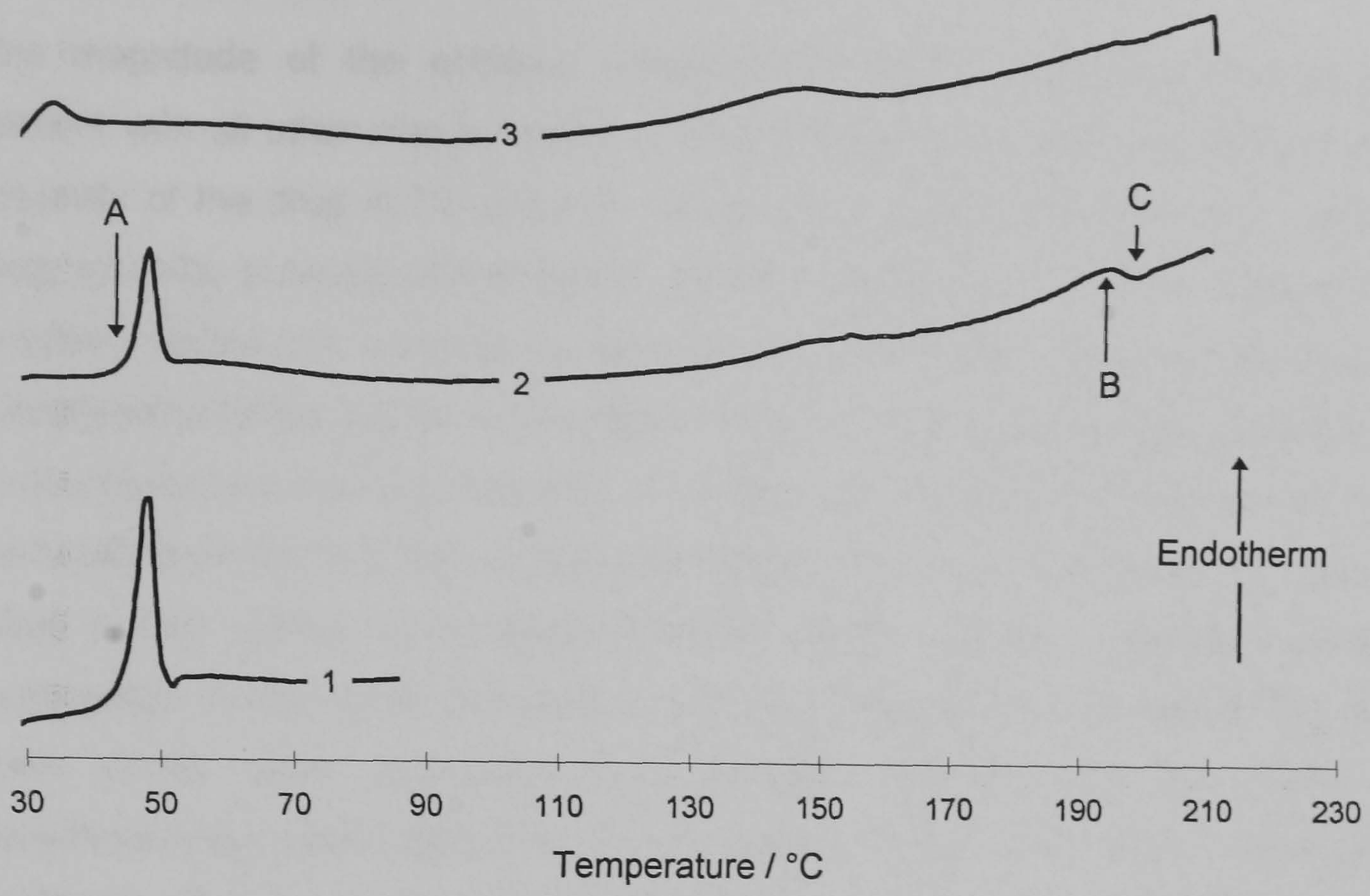

Figure 3.3 *First heat DSC scans of: 1) RG502 as supplied; 2) physical mix of RG502 : RIF (1:1) and; 3) physical mix of R104 : RIF (1:1) at 10 °Cmin^{-1}. Key: A, glass transition; B, RIF melting endotherm; and, C, RIF recrystallization exotherm.*

Table 3.7 *First heat DSC statistics for physical mixtures of rifampicin and Resomer® (1:1) (n=2). Enthalpies expressed per unit weight total sample.*

Resomer®	Anomalous endotherm			Melting endotherm			Recrystallization exotherm		
	onset / °C	peak / °C	area / J g^{-1}	onset / °C	peak / °C	area / J g^{-1}	onset / °C	peak / °C	area / J g^{-1}
RG502	44.9	47.5	2.76	188.8	193.5	0.92	196.3	198.5	0.66
RG503	51.5	53.9	2.78	188.3	193.8	1.91	198.0	200.7	1.08
RG503H	52.2	54.8	2.64	187.8	194.0	1.93	198.0	200.4	1.28
RG504	52.3	55.1	3.31	187.9	194.1	2.73	197.9	200.4	1.57
RG506	54.2	57.0	2.44	189.2	194.8	2.08	198.4	200.8	1.62
RG752	50.9	53.8	2.87	189.2	193.2	0.81	197.1	198.8	0.53
RG755	55.7	58.3	3.37	187.6	193.9	2.35	197.5	200.5	2.30
R202H	53.6	56.5	3.65	189.1	189.9	0.27	198.7	201.0	0.18

no thermal events recorded for R104

The solubilization of RIF within the rubbery R104 matrix at a temperature corresponding to, or below that of the melting point of RIF, accounted for the absence of a melting endotherm for the drug. Bodmeier et al. (1989) similarly noted an increased solubility of quinidine, a drug of comparable aqueous solubility (1 in 2000; Merck Index, 1976) to that

of RIF (1 in 1000), as the proportion of low MW R104 incorporated to high MW PDLLA (120 kD) solvent-cast films, increased.

The magnitude of the enthalpy differential between melting-recrystallization events, present with all other mixes, relative to their theoretical values, provided an index of the solubility of the drug in the polymer. Caution is recommended with such deductions as drug solubility is being determined at elevated temperatures by this method rather than ambient, where the solubility is likely to be considerably different (Dubernet, 1995). Interpretation of the results in this respect was confounded by variable enthalpy values as a consequence of sample demixing. This effect was particularly problematic in the present work with high MW RG755, RG504 and RG506. The large particle size of these materials allied to their ductile nature which hindered efficient grinding, resulted in drug-polymer segregation in the small vial used to prepare these mixes. Consequently, appreciable RSD values were associated with enthalpy measurements for these samples. Notwithstanding these difficulties, some general trends were derived from the data in Table 3.7. Melting enthalpy values increased with MW of polymer irrespective of polymer class, i.e., RG50X, RG75X and R series indicative of reduced drug miscibility. Additionally, for material of comparable MW, the solubility of RIF increased in parallel with the substitution of more hydrophilic glycolic units with D/L-lactic units. Thus, based on melting energy requirements, RIF solubility was in descending order: R202H (11 kD); $\Delta H = 0.27\ Jg^{-1}$ > RG752 (20 kD); $\Delta H = 0.81\ Jg^{-1}$ > RG502 (15.5 kD); $\Delta H = 0.92\ Jg^{-1}$.

The thermal characteristics of the second heat scan were quite different from that of the corresponding initial scan, although several common features were present. These included the disappearance of the melting-recrystallization for RIF and the reduced peak area for the endotherm associated with the polymer T_g in addition to an up-scale shift of same. The former effect was attributed to the greater solubility of RIF after solubilization, due to its deposition as micronized domains during quenching. These domains provided considerably greater exposed surface area which facilitated solubilization of drug in polymer during the second heating. Rapid solidification during cooling impeded the mobility of drug molecules in the increasingly viscous polymer, leading to extensive nucleation and the production of numerous small crystalline domains in the matrix. Therefore, unlike the original drug particles in the physical mix, these interposing domains were sufficiently small to have an additional effect at the molecular level, whereby enhanced chain stiffness was created and maintained in the polymer chains. This so-

called 'filler-effect' (Dubernet, 1995) is presumably attributable to the low heat transfer coefficient of these domains compared with neighbouring polymer chains. This results in diminished translational movement of molecules. Consequently, during the second scan a resultant elevation of the T_g was observed, most notably for R104 where, contrary to the first scan, an on-scale T_g event was observed at 41.5 °C.

3.3.3.2 Isoniazid

The first scan thermal statistics of the INH - Resomer® mixes are summarized in Table 3.8.

Table 3.8 *First heat DSC statistics for physical mixtures of isoniazid and Resomer® (1:1) (n=2) Enthalpies expressed per unit weight total sample.*

Resomer®	***Anomalous endotherm***			***Melting endotherm***		
	onset / °C	***peak / °C***	***enthalpy / Jg^{-1}***	***onset / °C***	***peak / °C***	***enthalpy / Jg^{-1}***
RG502	45.7	48.2	1.93	166.0	169.9	78.5
RG503	52.4	54.6	2.41	166.3	170.3	68.0
RG503H	53.9	55.9	1.62	164.9	169.8	78.6
RG504	53.6	55.9	1.86	167.5	170.7	90.5
RG506	54.0	56.6	1.87	165.9	170.0	92.0
RG752	51.7	54.3	2.28	169.7	173.0	70.2
RG755	56.2	58.4	1.59	170.1	172.8	74.0
R104	*	*	*	158.4	168.1	61.9
R202H	54.0	56.8	3.29	168.4	173.0	68.6

* no thermal events recorded

The results indicated that no significant interaction was evident based on the fact that all peaks were reconciled with those from individual scans. Whereas normalized enthalpy values of polymer relaxation corresponded generally well with those from polymer alone, enthalpies of fusion for INH were consistently lower than that anticipated, i.e., $\Delta H = 123$ Jg^{-1}. Enthalpy depression may have arisen due to the interaction of the drug with its polymeric environment. Consequently, the measured value has a component for the enthalpy of mixing of the molten INH in the rubbery polymer as well as solubilization of a fraction of INH which confounds the comparison of experimental and theoretical heats of melting (Theeuwes et al., 1974). This postulation is supported by the fact that irrespective of the polymer, T_g depression during the second scan was indicative of partial, if not complete, solid solution. The solvency of each polymer followed a similar pattern to that for RIF, whereby the % theoretical melting enthalpy values increased as MW increased and as glycolic units were introduced, indicative of reduced INH solubility at the melting

point of the drug. The corresponding values in ascending order were: R202H (11 kD), ΔH = 55.7 % < RG752 (20 kD), ΔH = 57.0 % < RG502 (15.5 kD), ΔH = 63.8 %.

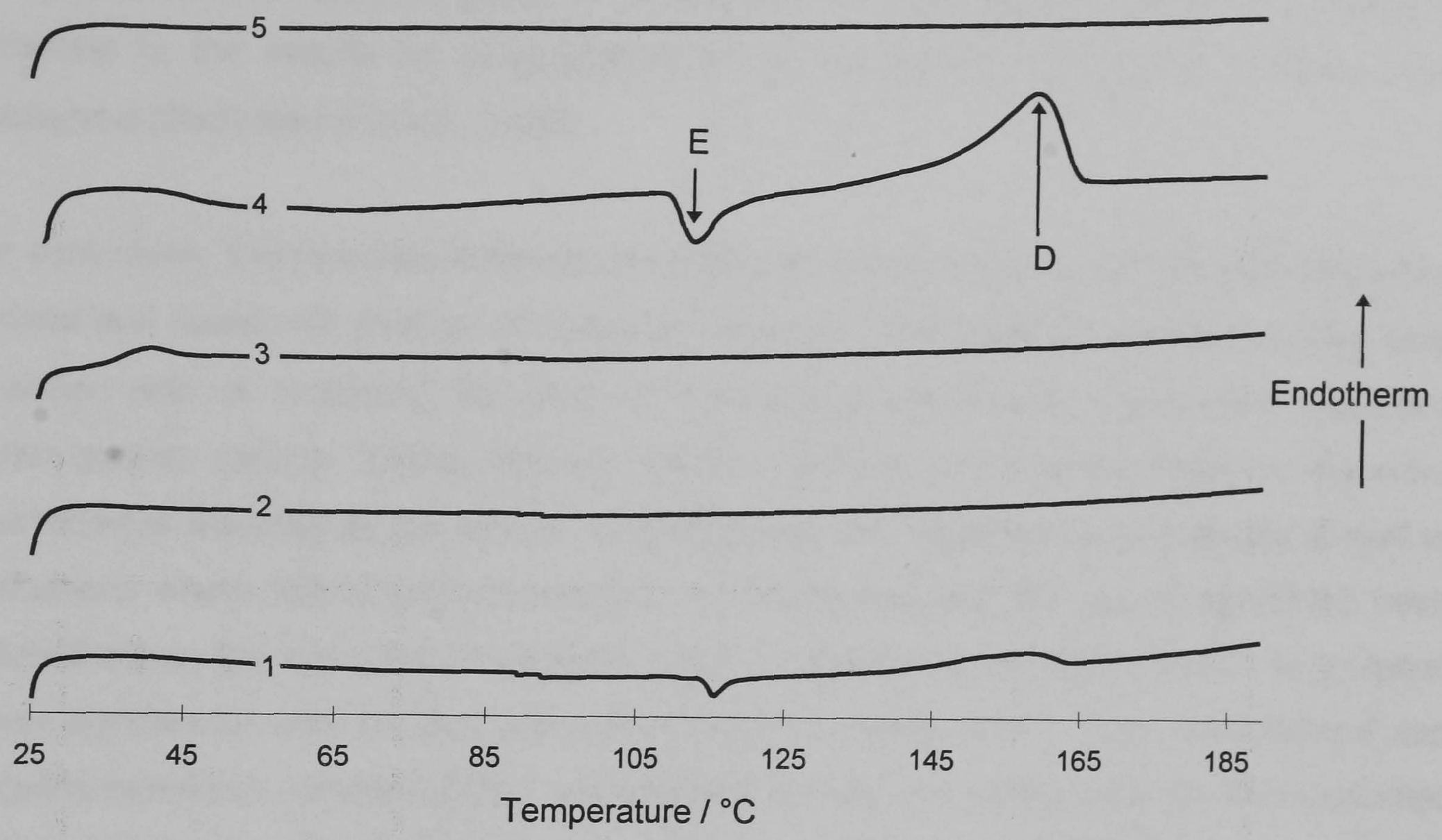

Figure 3.4 *Second heat DSC scans of physical mixes of: 1) RG755 : INH (1:1); 2) RG752 : INH (1:1); 3) RG502 : INH (1:1); 4) R202H : INH (1:1) and; 5) R104 : INH (1:1) at 10 °C* min^{-1}*. Key: as before, D, melting endotherm of INH, and E, recrystallization exotherm of INH.*

The emergence of recrystallization and melting events seen in Figure 3.4 indicated a fraction of INH existed as a molecular dispersion in addition to that as solid solution for R202H and RG755. Quench cooling (30 °Cmin^{-1}) inhibits nucleation and subsequent crystallite growth as the polymer viscosity approaches infinity below the T_g (Dubernet, 1995). Upon heating, molecular mobility increases and crystal growth occurs accounting for the exotherm at 115 °C and the associated melting endotherm at 158 °C for both R202H and RG755 as seen in Figure 3.4.

The down-shift in the melting endotherm for INH is consistent with that observed for both RIF and INH during the first run, and that of clonazepam reported elsewhere (Benelli et al., 1998). The propensity for recrystallization is a complex function of the interaction of the molecules with their polymeric environment, molecular mobility and matrix viscosity. In

general, such events correspond to limited solubility of drug in the fluid matrix, supporting the conclusions for the first scan. Furthermore, the ratios of melting endotherm: recrystallization exotherm were similar for both R202H and RG755 at 3.61 and 3.65 respectively, suggestive of the same crystalline form. The coincidence of event temperatures lent further support to the absence of polymorphism in these matrices in contrast to the results for progesterone in PDLLA where both α and β forms were observed (Bodmeier & Chen, 1988)

In conclusion, thermal data indicated the variation in the behaviour of RIF and INH when mixed and fused with a range of Resomer® polymers. INH appears to exist in partial solid solution with all materials, whereas RIF remains predominantly molecularly dispersed after quench cooling. These data are however artificial in the sense these events were recorded at elevated temperatures. Consequently, their significance is probably limited to situations where fabrication technologies are associated with the use of significant heat. Nonetheless, the operative procedures used to prepare microspheres from raw polymer may significantly alter the arrangement of polymer chains, and, in turn, their thermal and ageing behaviour, rendering DSC an excellent technique to check polymer characteristics after microsphere formation (Dubernet, 1995) in addition to elucidation of the dispersive state of drug within polymeric matrices (Bodmeier & McGinity, 1987c; El-Baseir et al., 1997; Benoît et al., 1986).

3.3.4 Solubility studies

3.3.4.1 Saturation solubility studies

Determined saturation solubilities of both RIF and INH in a variety of aqueous and non-aqueous solvents are tabulated below in Table 3.9.

These data highlight the dramatic difference in the solubility of RIF and INH, a primary factor which determines the strategies employed to encapsulate drugs in biodegradable materials (Whateley, 1992). In general, INH solubility increased with solvent polarity, whereas with RIF, the opposite trend was observed. Fong et al. (1986) cited an aqueous solubility criterion of $\leq 0.023\ gL^{-1}$ for efficient encapsulation. On this basis, neither drug, particularly INH, would be effectively encapsulated by aqueous ESE.

Table 3.9 *Saturation solubility characteristics of rifampicin and isoniazid as supplied in various aqueous and non-aqueous solvents (n=3).*

Drug		**INH**		**RIF**	
Solvent	**Temperature / °C**	**Solubility / mg mL^{-1}**	**RSD / %**	**Solubility / mg mL^{-1}**	**RSD / %**
water	25	145	1.2	0.93	9.4
water	37	245	0.9	1.72	7.5
water	50	316	0.5	2.93	3.1
ethanol	25	25.2	1.3	8.91	5.0
dichloromethane	25	1.95	1.3	216	6.5
dichloromethane	37	9.62	6.2	388	9.6
chloroform	25	6.53	4.3	349	4.6
chloroform	50	12.3	1.2	930	10.2
1 % w/w PVA	25	89.1	3.5	1.41	1.5
1 % w/w PVA	37	190	2.1	2.32	2.6
1 % w/w PVA	50	311	1.3	6.15	4.6
methanol	25	42.8	1.4	*	*
butanol	25	3.81	2.6	*	*
n-hexane	25	*[2]	4.3	*	*
ethyl acetate	25	3.21	7.2	181	2.3
acetonitrile	25	2.91	9.3	*	*
acetonitrile	50	13.4	6.3	*	*
halothane	25	*	*	76.9	2.2

* not determined

*[2] practically insoluble (British Pharmacopoeia, 1988)

3.3.4.2 pH solubility profile

Encapsulation efficiency is, with few exceptions, an attribute of the microsphere production process which is omnipresent in reports which describe microsphere characterization (Hausberger & DeLuca, 1995). This is due to the ease by which this characteristic can be readily determined; its inter-relationship with other microproduct features (morphology, drug release); its implications on dose volume; and, its utility as a ready marker of the repeatability of the overall process. The problem suffered by the aqueous ESE process of low encapsulation efficiency due to premature partitioning of soluble or moderately water soluble drugs prior to deposition of a coherent polymer microsphere crust is well documented (Bodmeier & McGinity, 1987a-c).

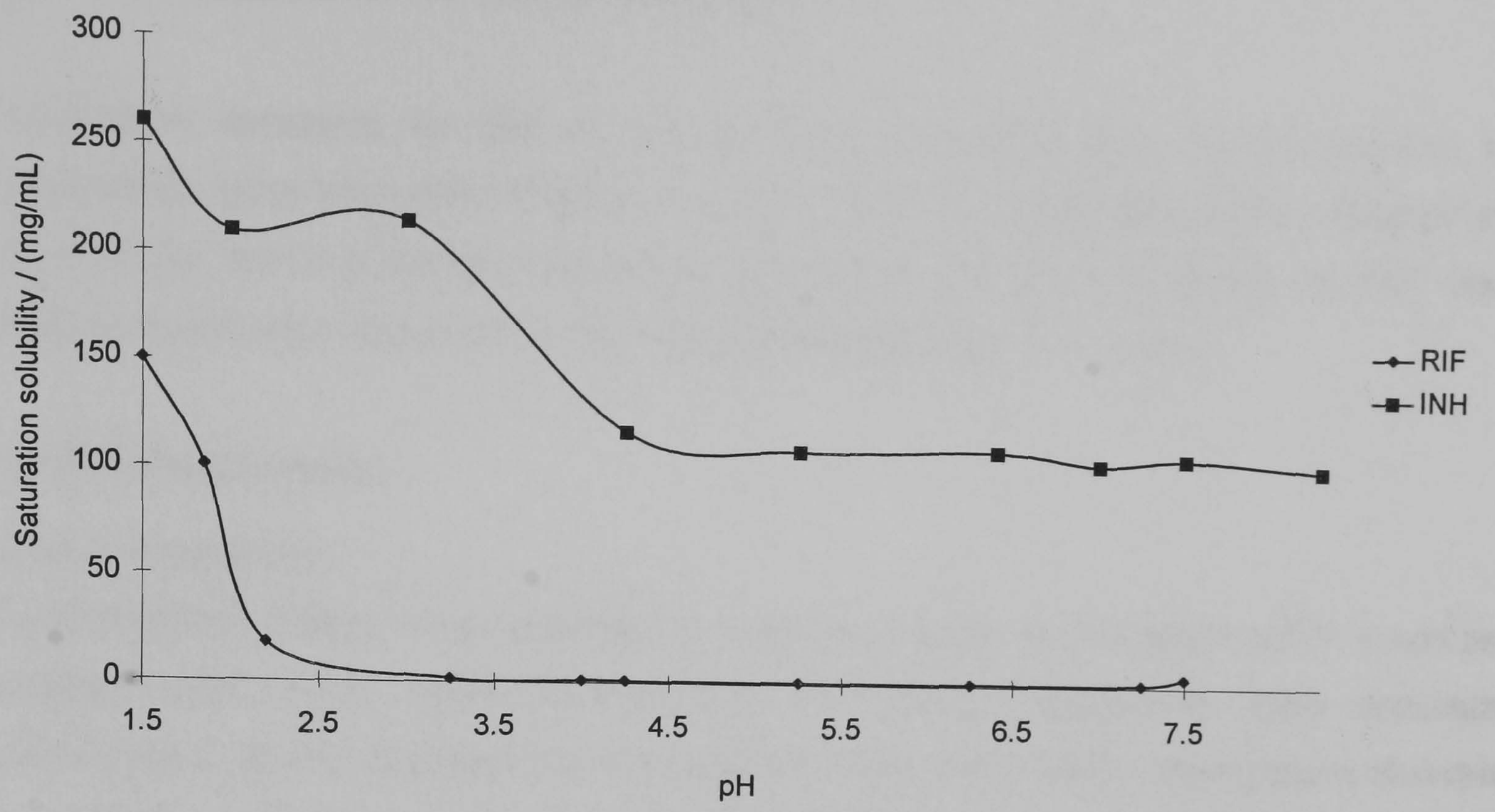

Figure 3.5 *pH-solubility profiles for rifampicin and isoniazid at 24 ± 2.0 °C*

The pH solubility profiles of INH and RIF are presented in Figure 3.5. For amphoteric compounds, such as RIF, aqueous solubility increases markedly at pH values below and above the pK_a values for the drug of 1.7 and 7.9 respectively. These respective dissociation constants have been, in the opinion of Prankerd et al. (1992), wrongly assigned to the C_1, C_4 and C_8 of the phenolic hydroxy groups (pK_a = 1.7), and the piperazine nitrogen (pK_a = 7.9), respectively. Prankerd et al. (1992) argued that the value for the piperazine nitrogen accounted for the acidic group, consistent with other azomethines, e.g., diazepam, whilst the value at 7.9 was accordingly associated with the aforementioned hydroxy array. This group also hypothesized a third dissociation constant for the N-methylpiperazine, N-CH_3, at 5.93, to which the potentiometric titration method previously used would have been oblivious (Maggi et al, 1966). However, in contrast to the chromatographic behaviour in section 2.3.1, the pH - solubility profile studies did not corroborate the existence of a third dissociation constant. During saturation solubility studies, the pH of prospective continuous phase for aqueous ESE, 1 %w/v solution of PVA, was 5.3. It has been proposed (Zhifang et al, 1993) and demonstrated (Bodmeier & McGinity, 1987a-c) that buffering of the aqueous continuum to a pH of low drug solubility can minimize drug partitioning and thus maximize encapsulation efficiency. Therefore, whereas buffered PVA solutions at pH < 1.5, or, > 8.0 were anticipated to greatly

decrease RIF encapsulation efficiency, unbuffered PVA provided a medium which minimized extraction of RIF during encapsulation.

Protonation constants for INH of 2.0 and 3.6 for the hydrazide N and pyridine N respectively have been cited (Rekker & Nauta, 1964). A further dissociation constant of 10.8 for the terminal primary amine has also been measured. In analogy to RIF, this pattern of ionization is consistent with the pH-solubility data for this drug.

3.3.5 Stability studies

3.3.5.1 Rifampicin

Decomposition studies were performed to examine whether the oxidation of RIF could be avoided, and, if so, would quantification of identified degradates allow accurate determination of RIF released over prolonged periods. Preliminary investigations showed iso-ascorbic acid (IAA) had the greatest activity in preventing oxidation of RIF to RQU.; $t_{½\ IAA}$ = 69.3 h compared with $t_{½\ control}$ = 2.45 h. Sodium metabisulphite showed intermediary activity; $t_{½}$ = 4.85 h. Addition of RQU stock solutions to SBM containing IAA caused a rapid reduction of the quinone to RIF. At an IAA concentration of 0.01 %w/v, after initial reduction of RQU to RIF, a peak corresponding to RQU appeared after 4 d, indicating lack of antioxidant protection with the introduction of air during each sampling operation. No such peak was evident when 0.1 %w/v IAA was used. Therefore, having stabilized RIF to oxidation, decomposition studies focused on the hydrolysis of RIF to RSV at an IAA level of 0.1 %w/v. The consecutive transformation of RSV to other unidentified products was also examined.

Reversible addition of water across the azomethine bond of RIF to form a transient carbinolamine, which then rearranges, is the proposed mechanism of hydrolysis (Prankerd et al., 1992) yielding RSV and UV transparent 1-amino-4-methyl-piperazine (AMP) as shown in Scheme 3.1

$$RIF + H_2O \longleftrightarrow RSV + AMP$$

Scheme 3.1 *Hydrolysis of RIF to RSV*

Table 3.10 *Initial (α) and terminal (β) rate constants for hydrolysis as a function of RIF and RSV concentration in Sørensens modified buffer, pH = 7.4 ± 0.2 and 37 ± 0.5 °C, n=3*

Analyte	Initial Conc / μgmL^{-1}	$\alpha \times 10^3$ / h^{-1}	RSD / %	$\beta \times 10^4$ / h^{-1}	RSD / %	r^2
RIF	35	6.535	2.789	2.860	2.015	0.999
	14	5.702	2.025	2.885	4.522	0.997
	3.5	4.181	1.985	2.551	5.582	0.999
RSV	35	-	-	3.092*	4.068	0.993
	14	-	-	2.777*	1.714	0.995
	3.5	-	-	2.649*	4.068	0.997

* *kinetic constants arising from secondary decompositions*

Using a feathering technique, the rate constants for the initial, α, and terminal, β, phases of RIF decomposition seen in Figure 3.6 are reported in Table 3.10 according to the biexponential expression 3.1 shown below:

$$[RIF] = Ae^{-\alpha t} + Be^{-\beta t} \qquad \textbf{(Equation 3.1)}$$

where A and B are constants, α and β are the pseudo first-order rate constants associated with the initial and terminal phases of RIF decomposition. First-order kinetic constants for RSV decomposition, when studied alone, are in Table 3.11.

Table 3.11 *Kinetic constants for deterioration of RSV in Sørensens modified buffer, pH 7.4 ± 0.2 and 37 ± 0.5 °C (n=3)*

Analyte	Initial Conc / μgmL^{-1}	$\beta \times 10^4$ / h^{-1}	RSD / %	r^2
RSV	50	2.739	2.310	0.999
	20	2.611	3.832	0.998
	5	2.689	5.132	0.987

Examination of the kinetics of other azomethine containing compounds has yielded similar biexponential patterns, indicative of an equilibrium decomposition process (Prankerd & Stella, 1989). The biexponential pattern can be explained by a rapid pseudo first-order hydrolysis of RIF to RSV until equilibrium is attained, followed by a slow parallel deterioration in concentration of both RIF and RSV as shown in Figure 3.6.

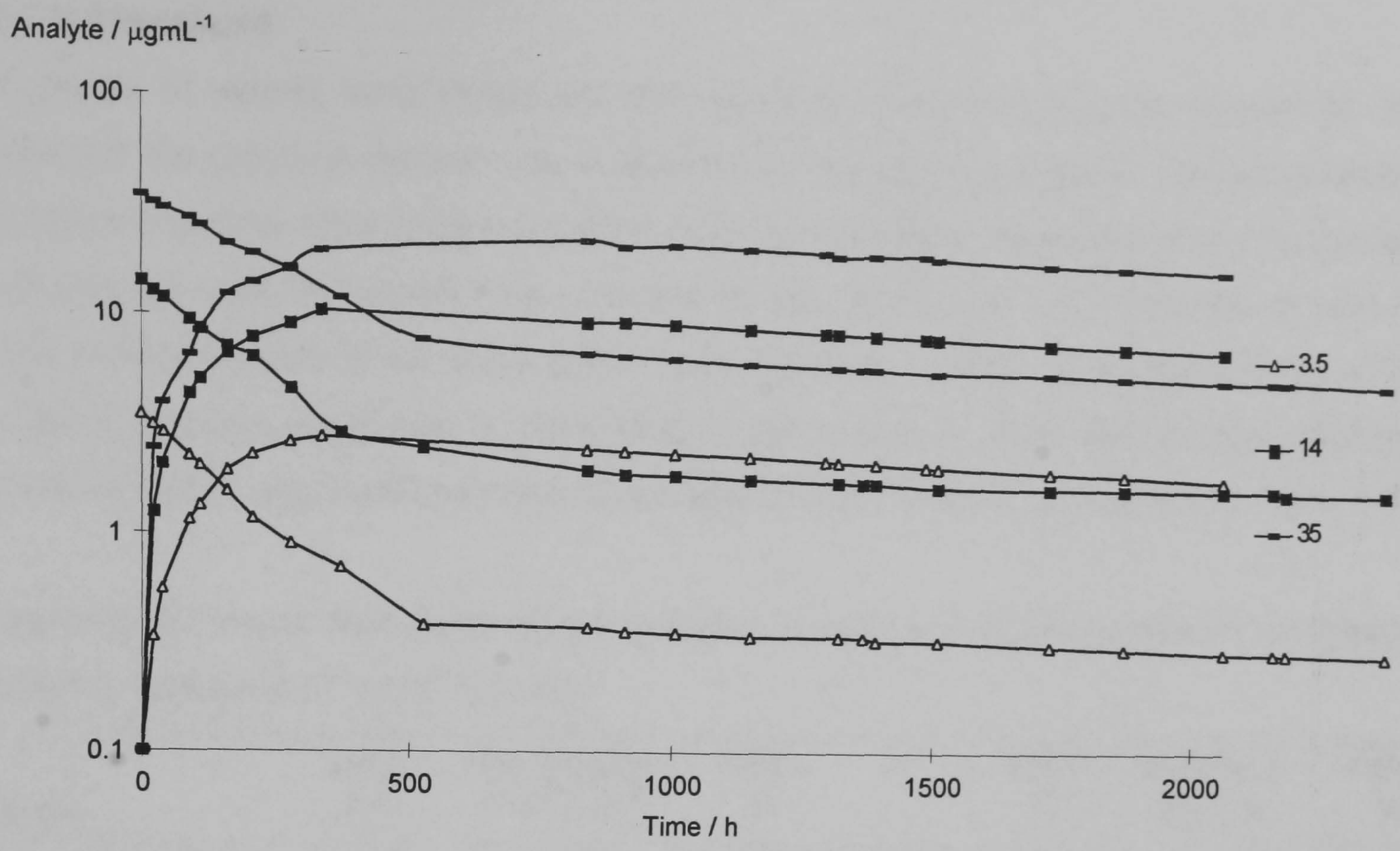

Figure 3.6 *Semi-logarithmic plots of the time-dependent decrease in rifampicin and increase in 3-formylrifamycin SV as a function of initial rifampicin concentration in Sørensens modified buffer at pH 7.4 ± 0.2 and 37 ± 0.5 °C, (concentration in key in units of μgmΓ[1]) (n=3)*

The terminal phase is a consequence of serial decomposition of RIF, RSV or both. These secondary reactions are assumed to be first-order based on the linearity of the terminal phase with semi-logarithmic treatment. This pattern was reported previously by Prankerd et al. (1992) for RIF decomposition at acidic pH which these authors attributed to parallel secondary reactions of both RIF and RSV. Chromatograms for starting solutions after equilibrium was attained showed a coincidence of peaks corresponding to these unidentified secondary products. Interestingly, all peaks appeared in both chromatograms suggesting (assuming the absence of a highly retained species associated with the secondary decomposition of RIF) all secondary decomposition products emanated from RSV. Further support for this was the absence of peaks corresponding to DAR and 25-21/23, the putative products of RIF decomposition under the conditions of the study. The nature of the secondary degradates is unknown, although the desacetylated equivalent of RSV would seem a plausible product (Seydel, 1970). Finally, in Table 3.11, the concurrence of the rate constants for RSV deterioration, when studied alone, and those for the terminal phase of RIF decomposition listed in Table 3.10, further corroborates this hypothesis.

3.3.5.2 Isoniazid

A variety of reports have described both oxidative and hydrolytic sensitivities for INH, although the products thereof, are, in general, poorly defined. However, where anaerobic conditions prevail, isonicotinic acid (INA) is the predominant degradate of INH in aqueous solution, its rate of formation is reported to be sensitive to both the nature and the concentration of the buffer salt used (Pawelczyk et al., 1969). Thus, the stability of INH under anaerobic conditions in hermetically sealed vessels filled with various degassed buffer solutions was examined, the kinetic statistics of which are presented in Table 3.12.

Table 3.12 *Pseudo first order kinetic statistics of isoniazid decomposition in a variety of buffer solutions at 37 ± 0.5 °C (n=4)*

Buffer	***pH ± 0.2***	***rate constant x 10^4 / (h^{-1})***	***RSD / %***	***r^2***	***RSD / %***	***half-life x 10^{-3} / h***	***RSD / %***
Walpoles acetate	5.8	3.481	6.70	0.981	1.75	1.996	7.00
McIlvaines	5.8	4.873	3.72	0.989	0.83	1.424	3.65
	7.4	3.136	6.65	0.985	0.96	0.231	6.64
Sørensens	5.8	5.326	6.48	0.991	0.83	1.308	6.29
	7.4	4.111	6.12	0.989	0.41	0.169	6.14

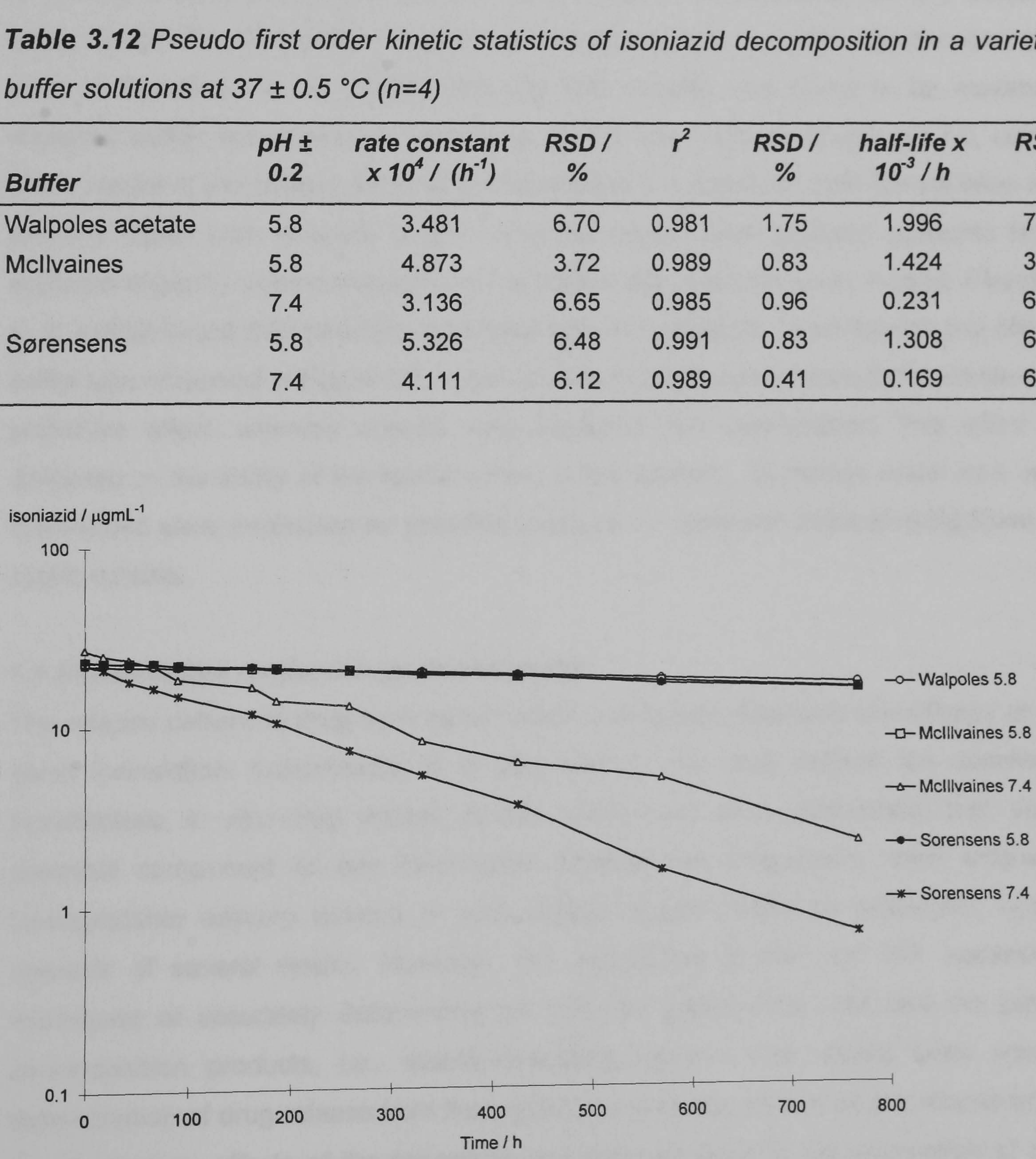

Figure 3.7 *Semi-logarithmic plots of the hydrolytic decomposition of isoniazid in various buffer system at 37 ± 0.5 °C, n=4. Legend indicates buffer system and pH ± 0.2.*

Hydrolytic decomposition arises through cleavage of the hydrazine side-chain to yield isonicotinic acid and hydrazine. During the decomposition study, the chromatographic peak area decrease for INH showed semi-logarithmic dependence on time as seen in Figure 3.7, corroborating the pseudo first-order kinetics observed by other workers (Pawelczyk et al., 1969). Meantime, a peak with capacity factor corresponding to that of INA appeared on the chromatograms. The identity of this substance was tentatively confirmed by PDA detection as INA. In general terms, these data are consistent with the observations of Lewin & Hirsch (1954) and Pawelczyk et al. (1969) where INH was shown to be maximally stable around pH 5.0 - 6.0, instability increasing above and below this value, i.e, pH 7.4. The effect of buffer salt however is only in partial corroboration of the work of Pawelczyk et al. (1969), whereby INH stability was found to be maximal in Walpoles buffer, but of reduced stability at pH 5.0 when compared with pH 7.0, contrary to the results in the present study at pH 5.8 and pH 7.4. However, both the variation in pH and the higher ionic strength at pH 7.4 in the current work probably accounts for the apparent disparity upon comparison of the results with previous work. Indeed, Pawelczyk et al. (1969) found INH instability increased with ionic strength. In contrast to the effect of buffer type observed in Figure 3.7, Lewin & Hirsch (1954) demonstrated that citrate had a protective effect, whereas acetate salts hastened INH deterioration. This effect was attributed to the ability of the former anion, unlike acetate, to chelate metal ions, which themselves were implicated as potential catalysts, in particular divalent manganese and cupric cations.

3.3.6 Dissolution methodology development

The release pattern of drug from carrier matrix will largely determine the efficacy of any given formulation. Correlations of *in vitro* and *in vivo* drug release are uncommon. Nonetheless, *in vitro* drug release studies, when used as a comparative tool, are an essential component of any formulation development programme. With long-acting biodegradable delivery devices *in vitro* release studies might be prolonged; typically upwards of several weeks. Moreover, the instabilities of INH and RIF necessitates techniques of accurately determining not only the parent drug, but also the putative decomposition products, i.e., stability-indicating assays. This should allow accurate determination of drug release from biodegradable systems, as well as the assessment of any deleterious effects of the processes and solvents used in the preparation of these systems.

When monitoring drug release from biodegradable formulations, a number of approaches can be adopted. Either the amount of drug released into the dissolution medium can be measured, or, alternatively, the amount remaining in the formulation. The former may involve recovery by clarification and replacing the total volume under study to ensure the 'sink' status of the medium. The latter procedure, utilized by Bissery et al. (1984) to indirectly determine the release of CCNU (1-(2-chloroethyl)-3-cyclohexyl-nitrosourea) from PLLA microspheres, requires tedious preparation of multiple vessels corresponding to each sampling interval. Ordinarily, therefore, aliquots are taken and the volume sampled replaced with fresh medium which is – from a throughput, accuracy and repeatability point of view – preferred.

3.3.6.1 Rifampicin

The instability of RIF has resulted in errors in determining release rate from conventional tablet and capsule formulations (Gharbo et al., 1989; Shah et al., 1992; Jindal et al., 1994). Preliminary release studies of RIF from biodegradable microspheres using direct UV spectrophotometry showed a rapid 'burst'; a characteristic of these systems. Initially, released RIF was observed to transform rapidly from an orange RIF solution to its purple quinone, RQU. This decomposition was accounted for by exploiting the approximate 'isobestic' point seen in Figure 2.1 for RIF and its decomposition products at 270 nm. However, subsequent absorbance measurements showed an exponential decay in magnitude with decomposition of RQU to a poorly absorbing or UV transparent product. Therefore, stability of RIF was investigated to identify the decomposition products and their kinetics of formation. From preliminary investigations, the rate of formation of RQU was found to be a function of the headspace and thus the amount of available O_2 in the vessels used. Therefore, a controlled investigation of the kinetics of RIF decomposition in sealed vessels was performed, the results of which are presented in section 3.3.5.1. These vessels were fitted with rubber bungs which allowed the withdrawal of samples with minimal introduction of air throughout the study.

The terminal decomposition phase shown in Figure 3.6 precluded the simple cumulative quantification of RIF and RSV as a technique to monitor overall RIF release from long-acting biodegradable systems. In this situation the apparent amount released may decrease where the rate of secondary deterioration exceeds the rate of RIF appearance in the dissolution medium. Hence, a mathematical correction for the amounts lost to secondary reactions was required to accurately monitor RIF release. Using the calculated

values of the terminal phase rate constants, equation 3.2 was applied to account for the secondary decomposition of RIF and RSV occurring between each sampling interval:

$$L = \frac{(X_{t1} + X_{t2})}{2} e^{-\beta_{term} t} \qquad \textbf{(Equation 3.2)}$$

where L is the amount of RIF-derived analyte lost between each time interval t. X_{t1} and X_{t2} are the total amounts of RIF released calculated from peak areas of RIF and RSV at time t_1 and t_2 respectively, whereas β_{term} is the terminal rate constant describing the parallel loss of RIF and RSV. The validity of this approach was based on the parallelism of the terminal phases for RIF and RSV secondary decomposition and the respective rate constants independence of concentration.

Dissolution profiles for rifampicin release from PLLA microspheres are presented in Figure 3.8. The accuracy of this approach is a function of the time interval between samples; accuracy theoretically improving with more frequent sampling. However, given the slow rate of the secondary decomposition phase, daily intervals were considered adequate.

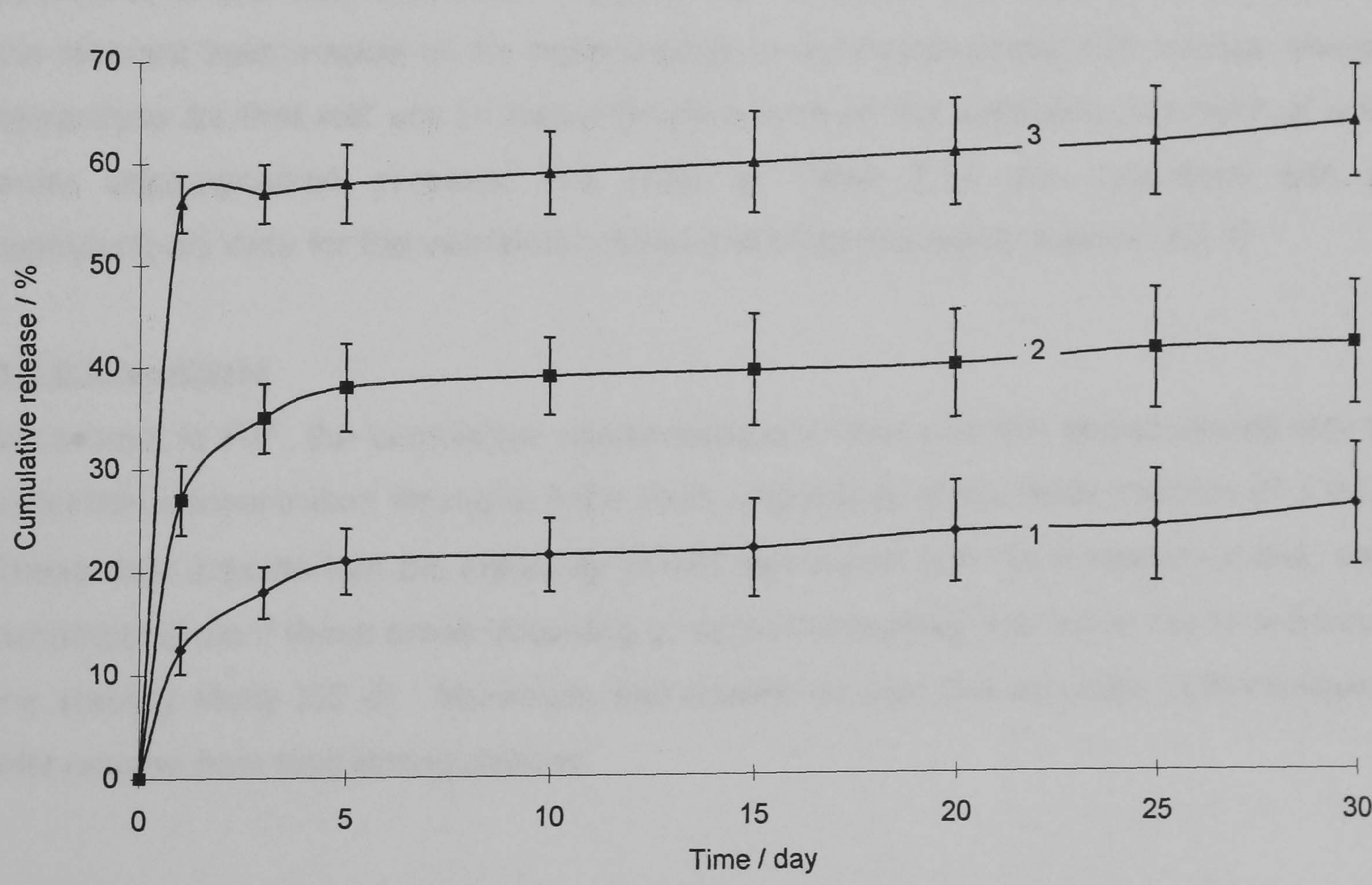

Figure 3.8 *Release profiles of rifampicin from Resomer®L204 poly(L-lactide) (MW= 78 kD) microspheres prepared by aqueous emulsion solvent evaporation at drug:polymer ratios of: 1) 0.2:1.0; 2) 0.5:1.0, and; 3) 1.0:1.0 at 37°C in Sørensens buffer modified at 37 ± 0.5 °C and pH =7.4 ± 0.1 (n=3).*

The method was further validated by the measurement, at different time periods during dissolution, of the amount of RIF remaining in recovered microspheres. This calculation accounted for the mass of sample initially added; original microsphere drug loading; and the cumulative amount released at the corresponding time point. Validation data are presented in Table 3.13.

Table 3.13 *Validation statistics of the rifampicin dissolution methodology based on reconciliation of total loaded rifampicin from microspheres prepared with Resomer®L204 by emulsion-solvent-evaporation at various drug:polymer (D:P) ratios at 37 ± 0.5 °C in Sørensens buffer modified pH =7.4 ± 0.2 (n=3).*

D:P ratio	***Loading / (%w/w)***	***Differential between residual microsphere loading and amount released / % (RSD) after time / h***		
		1	**10**	**30**
0.2:1.0	9.81	1.62 (5.62)	-1.51 (6.71)	-2.51(7.52)
0.5:1.0	18.8	1.53 (2.35)	-2.56 (6.85)	-2.54 (6.52)
1.0:1.0	23.1	1.41 (2.65)	-1.15 (7.81)	-3.51(4.52)

The differential between that released and the residual RIF in the microspheres was positive after one day, but became negative at five days. This trend was consistent with the inherent inaccuracies of the methodology to determine overall RIF release whereby corrections for that lost are an overestimate based on the arithmetic mid-point of a first order decomposition process. The RSD in Table 3.13 are consistent with the reproducibility data for the validated column-switching procedure (section 2.3.1)

3.3.6.2 Isoniazid

In contrast to RIF, the cumulative concentrations of INH and INA corresponded with the initial INH concentration throughout the study regardless of the study medium ($P > 0.05$). These data indicate that the instability of INH terminated with the formation of INA, serial decompositions if these arose occurring at an immeasurable rate within the time-frame of the stability study (32 d). Moreover, this feature allowed the accurate determination of INH release from long-acting devices.

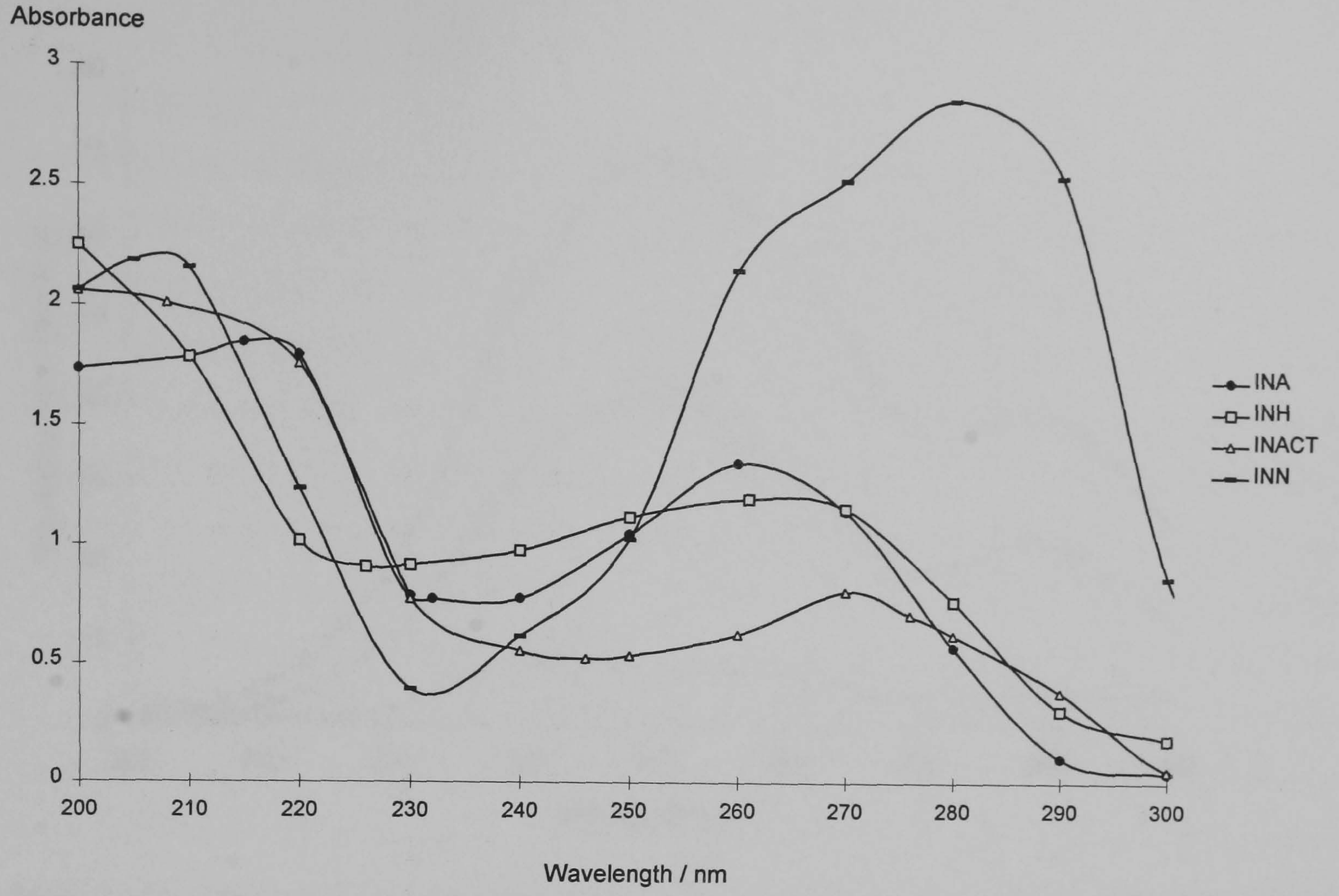

Figure 3.9 *Normalised UV spectra with respect to concentration of isoniazid (INH) and its potential degradates: isonicotonic acid (INA); isonicotinamide (INACT) and; isonicotonic acid N-oxide (INN) in distilled water at 24 ± 2.0 °C at a theoretical concentration of 0.004 %w/v. Legend indicates abbreviated analyte.*

Reports of long-acting PDLGA preparations describe a variety of analytical methodologies to monitor the release of INH. These include spectrophotometry following condensation derivitization with vanillin (Pattisapu et al., 1993; Gangadharam at al., 1994) to form an amide (Fieser & Fieser, 1957); direct spectrophotometry (Hsu et al., 1994; 1996); and, HPLC for bioanalysis of serum and urine INH and AcINH levels (Gangadharam at al., 1991; Kailasam et al., 1994). Significantly, none of these reports made mention of the instability of INH at physiological pH. Instability may have introduced errors, invalidating the mathematical analysis of INH release described in the report of Hsu et al. (1994) where direct UV spectrophotometry at 262 nm was the detection method. The potential for errors of ultimately 10 % in magnitude during the 50 d study is apparent from Figure 3.9 where comparison is made of the UV spectra for INH and INA at 262 nm.

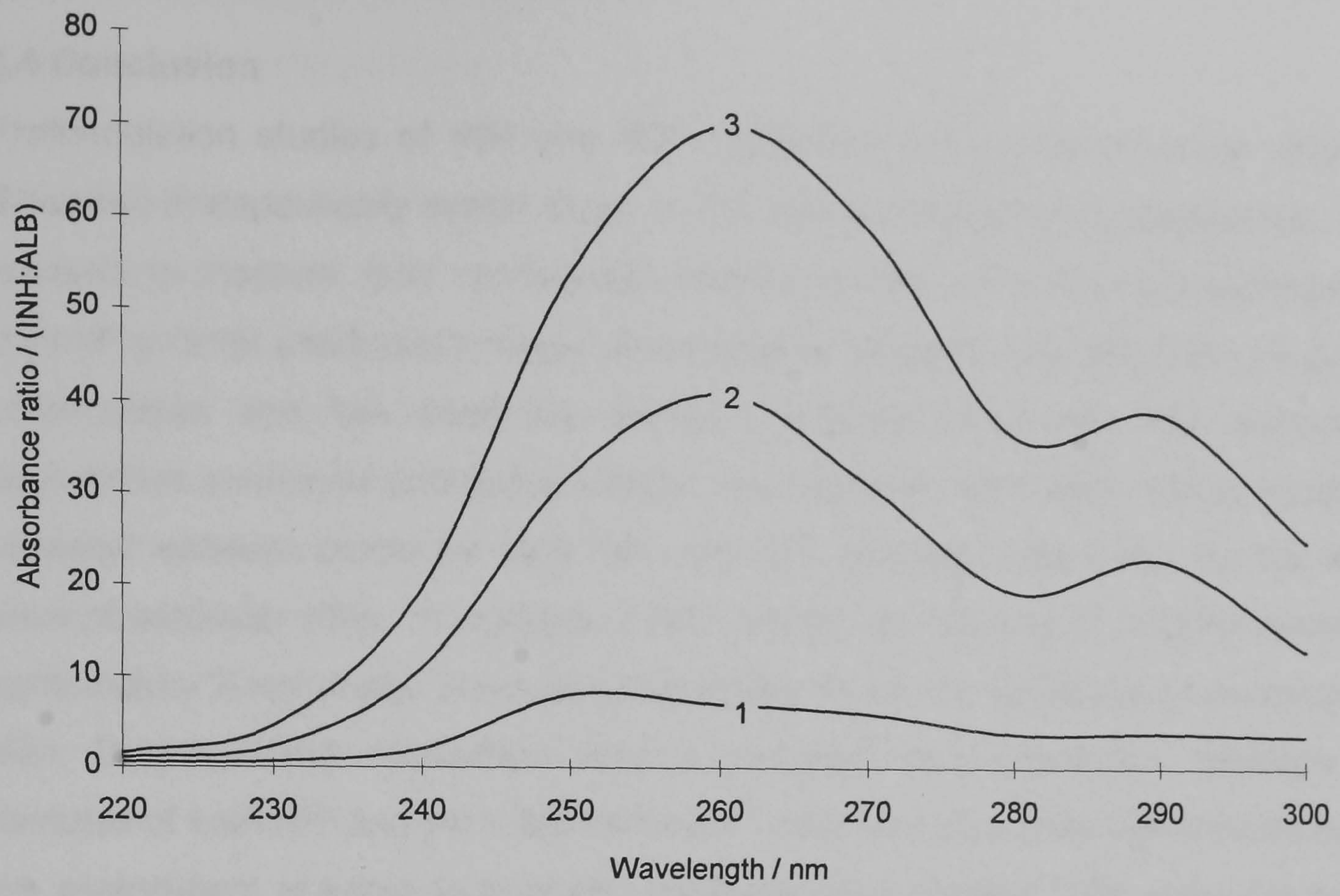

Figure 3.10 *Absorbance ratios for isoniazid and albumin (I:A) at an isoniazid:albumin concentration ratios of: 1) 1:10; 2) 1:2 and; 3) 1:1 in water at 24 ± 2.0 °C*

An alternative approach would be to exploit the isobestic point for INH and INA at 228 or 253 nm as seen in Figure 3.9. Formulations described later in this work which contained interferents, such as weakly UV absorbing or refractive excipients, e.g., albumin limited this direct approach. The data in Figure 3.10 indicates the presence of albumin would introduce spectophotometric inaccuracies into calculations of drug release based on these measurements. Based on these ratios at 228 nm, the errors introduced from direct UV measurement were 20 % and 181 % at I:A ratios of 1:1 and 1:10 respectively, whereas at the alternative isobestic point of 253 nm, these errors were reduced to approximately 1.5 and 10 % for the corresponding ratios. However, such errors were considered unacceptable necessitating recourse to HPLC for the determination of drug released.

3.4 Conclusion

Preformulation studies of INH and RIF highlighted the physicochemical differences of these two therapeutically similar drugs. In the context of the microencapsulation studies in proceeding chapters, their contrasting solubility profiles were of utmost significance. This overriding factor precluded a single encapsulation procedure by which the drugs could be coformulated and has been the principle property influencing the techniques and approaches examined during formulation development. Ultraviolet spectroscopic studies revealed isobestic points for both INH and RIF, although only those for the latter drug were of particular utility. In contrast to RIF, where the absence of polymorphism requires confirmatory X-ray study, there was little evidence for the existence of polymorphism for INH. Drug-excipient interaction studies revealed little interaction between physical mixtures of both RIF and INH with Resomer®. Repeat scans after quench-cooling allowed the assessment of interactivity at the molecular level. Overall, INH appeared to be more soluble in Resomer®, as evidenced by polymer plasticization, whereas general T_g elevation with RIF indicated little polymer-drug solid solution. Finally, stability studies allowed strategies for monitoring the release of both drugs from long-acting formulations to be devised. The method developed for INH relied on the cumulative quantification of parent and the predominant hydrolytic degradate, INA, whereas that for RIF took account of the biexponential decomposition of RIF to RSV, exploiting the terminal pseudo equilibrium under the prospective conditions of the release studies in so doing.

4. Characterization of biodegradable poly-α-hydroxy acid-rifampicin microspheres prepared by the aqueous emulsification-solvent-evaporation technique

4.1 Introduction

In parallel with the AIDS pandemic, tuberculosis is re-emerging as a global health problem (Huebner & Castro, 1995). Current oral treatments are prolonged and complex requiring strict adherence to effect a cure (British National Formulary, 1995). Compliance is notoriously poor, particularly in developing countries where there are logistical difficulties in ensuring continuity of supply, leading to treatment failure, or worse still, the development of resistant strains of *M. tuberculosis* (Fox, 1958). Therefore, operational arrangements or devices which facilitate compliance should significantly aid tuberculosis control programmes world-wide.

Few reports of RIF micronized systems exist in the literature (Pande et al., 1991; Nakhare et al., 1995). Neither of these papers reported the effective loading of RIF. Prodigious research effort to achieve high drug loadings in the biodegradable poly-α-hydroxy acid-based microspheres has been made (Bodmeier & McGinity, 1987a-c). When administered orally, relatively high doses of RIF are required to maintain effective blood levels (Shearer, 1994). In the context of injectable devices, and in particular for low potency drugs such as antibiotics (Martinez et al., 1997), high loadings should allow a reduction in dosage volume. This, in turn, aids administration, alleviates discomfort associated with injection, and/or, allows a larger dose to be administered thus reducing dose frequency.

The work in this chapter sought to investigate the utility of poly-α-hydroxy acids as a sustained release material for RIF microspheres prepared by aqueous emulsification-solvent-evaporation (ESE). To this end, the effects of: varying drug:polymer (D:P) ratio; continuous and disperse phase volumes; and, presaturation of the continuum prior to dispersion of a RIF-polymer cosolution have been examined. The effect of process parameter modification with respect to microsphere loading, morphology, size and RIF release was examined.

4.2 Experimental procedures

4.2.1 Microsphere preparation

Table 4.1 *Experimental conditions for the granulometric optimization of rifampicin-bearing microspheres prepared by aqueous emulsification-solvent-evaporation ($n \geq 2$)*

Batch		Process variables	
PLLA	***PDLGA***	***Stirring / rpm***	***PVA / %w/v***
1	2	600	1
3	4	700	1
5	6	850	1
7	8	1000	1
9	10	1100	1
11	12	1000	0.1
13	14	1000	0.5
15	16	1000	2

Other process parameters were maintained constant at: disperse volume, 20 mL; continuum volume, 150 mL; and, D:P ratio (0.2:1.0).

Table 4.2 *Experimental conditions for the drug loading optimization of rifampicin-bearing microspheres prepared by aqueous emulsification-solvent-evaporation ($n \geq 2$)*

Batch		Dispersed RIF/ g	Phase volumes / mL		RIF saturated continuum
PLLA	***PDLGA****		***Disperse***	***Continuum***	
7	8	0.2	20	150	no
17	18	0.2	20	150	yes
19	20	0.5	20	150	no
21	22	0.5	20	150	yes
23	24	1	20	150	no
25	26	1	20	150	yes
27	28	0.5	10	150	no
29	30	0.5	15	150	no
31	32	0.5	30	150	no
33	34	0.5	20	75	no
35	36	0.5	20	100	no
37	38	0.5	20	125	no

*Whereas PLLA microspheres were prepared with chloroform as the disperse solvent, dichloromethane was employed for PDLGA microspheres

Cosolutions of PDLGA (RG506) or PLLA (L204) and RIF were prepared in DCM or CFM respectively. Volumes equivalent to 1 g of polymer were dispersed in a continuum of 1 %w/v PVA in a tall-form beaker (equilibrated just below the boiling point of the respective organic solvent: 37 ± 2.0 °C for DCM; and, 53 ± 2.0 °C for CFM). Immediately prior to addition of the disperse phase, the magnetic stirrer was calibrated in a darkened room with a transistor stroboflash model 12090 stroboscopic lamp (Dawe Instruments, UK).

Stirring was maintained (1000 ± 50 rpm) for 4 h to allow adequate hardening of the microspheres. Subsequent to recovery by filtration (Wattman, UK), microspheres were washed *in situ* with deionized water (500 mL) and dried in a desiccator under vacuum for ≥ 168 h prior to characterization. Process parameters for particle size and drug loading optimization are detailed in Tables 4.1 and 4.2, respectively. All batches were prepared at least in duplicate.

4.2.2 Drug loading

Microspheres (10 ± 2.0 mg) were dissolved in 10 mL of acetonitrile. The solution thus formed was diluted to 50 mL with double distilled water and the precipitated polymer removed from a 2 mL aliquot by centrifugation at 13 500 rpm for 4 min (Micro Centaur, MSE, UK). The resulting supernatant was analysed by HPLC as described in section 2.3.1. Each batch was analysed in triplicate. The weight contribution of RIF to the overall microsphere mass was expressed in units of %w/w total material. In addition, the percentage of dispersed drug encapsulated was computed from the ratio of actual to theoretical drug loading, i.e., encapsulation efficiency .

4.2.3 Microsphere yield

After washing and drying, the recovered product was weighed and expressed as a percentage of the total solid material dispersed in the continuum.

4.2.4 Particle size analysis

Microspheres, 30 ± 6 mg, were incorporated to a paste with a few drops of dispersant (Coulter Electronics Ltd., Luton, UK), and deaggregated in 50 mL distilled water with aid of 3 min ultrasonification (Decon, UK). The mean volume diameters (μm) of the different batches were determined by Coulter Multisizer (Coulter Electronics Ltd., Luton, UK) equipped with either a 140 μm or 200 μm aperture diameter tube. Each batch was examined at least in duplicate, the result for each replicate being the average of three withdrawals.

4.2.5 Scanning electron microscopy

Photomicrographs were captured for morphological examination of the microspheres. Samples were mounted on copper stubs and sputter-coated with gold-palladium (Polaron model SC7640) and scanned using a Cambridge Stereoscan model S90B electron microscope (Cambridge instruments, UK).

4.2.6 *In vitro* drug release

Microspheres, 10 ± 2.0 mg, to which was added 100 mL Sørensens buffer containing 0.1 %w/v IAA preheated to 37 ± 0.5 °C, were shaken horizontally at 1.5 Hz in hermetically sealed bottles. Samples were withdrawn via hypodermic syringe. An identical volume was replaced through the attached syringe filter to return entrapped microspheres and to maintain dissolution volume. Drug released was determined by an HPLC method which accounted for released drug lost to secondary decompositions during release studies described in section 3.3.6.1. Dissolution profiles of percentage cumulative RIF release versus time were then plotted. Each batch was studied in triplicate. This methodology is hereafter described as method A.

4.3. Results and Discussion

That countless reports of the preparation and characterization of biodegradable drug-loaded microspheres by ESE have appeared in the literature, is testament to the conceptual simplicity of the technique and its amenability to most laboratories. Despite its simplicity, the characteristics of the product are affected by many, often interacting variables such as: drug solubility; type and concentration of emulsifier; polymer composition; viscosity; phase ratios of the emulsion system; rates of solvent transfer; and, component interactions (Bodmeier & McGinity, 1988b; Li et al., 1995). Models of microsphere formation based on phase separation were devised by Bodmeier & McGinity (1986; 1987a,b). Four major diffusional processes were considered important, namely, drug, organic solvent and oligomer out, and non-solvent in. The direction and magnitude of solvent – non-solvent transfer dictates the rate at which the microglobule surface concentration reaches a critical concentration when phase separation and simultaneous microsphere formation occur, which, in turn, determines drug loading and other microsphere properties. Given the complexity of the encapsulation process, it was therefore considered necessary to examine selected parameters in an effort to maximize previously unexamined RIF loading in the polymers selected.

4.3.1 Influence of emulsifier and stirring rate

Particle size and distribution were considered useful indices of the reproducibility of the ESE process. Moreover, for preparations intended for injection subcutaneously a target range of 10 - 90 μm for comfort of administration has been suggested (Beck et al., 1985; Jalil & Nixon, 1990a). Both dispersing agent and stirring rate are of primary importance in the emulsification step, the latter providing the energy, whilst the surfactant decreases the

interfacial tension between phases thus stabilizing dispersed droplets (Arshady, 1991). Under otherwise standard conditions, the effect of these two parameters was initially examined, the granulometric results of which are shown in Table 4.3.

Table 4.3 *Granulometric statistics (volume) of microspheres prepared by emulsification-solvent-evaporation at various stirring rates and emulsifier concentration, n ≥ 6. Preparative conditions according to Table 4.1.*

	PLLA			***PDLGA***	
Batch	***mean diameter / μm***	***RSD / %***	***Batch***	***mean diameter / μm***	***RSD / %***
1	93.2	30.2	2	46.0	25.6
3	72.2	24.6	4	30.5	20.5
5	60.3	10.2	6	26.7	3.21
7	38.5	16.5	8	21.7	20.5
9	34.5	10.2	10	19.8	5.28
11	123	11.5	12	45.1	2.25
13	42.5	8.9	14	21.8	8.95
15	34.2	11.1	16	18.9	10.0

Mean particle diameter decreased with stirrer speed which is consistent with the results of others using comparable preparative conditions (Benita et al., 1984; Jalil & Nixon, 1990b; Zhifang et al., 1993; Sansdrap & Moës, 1993; Sánchez et al., 1993; Nakhare & Vyas, 1995). Linear regression of mean diameter on stirring rate yielded correlation coefficients of r^2= 0.973 and 0.8218 for PLLA and PDLGA, respectively. Deviations from linearity were attributed to aggregation of dispersed globules at low shear rates, with a resultant positive skew in the particle size distribution as observed by others (Conti et al., 1995a). For PLLA, at 600 rpm (#1), broad particle size distributions resulted (10 - 150 μm), whereas at faster agitation rates of 1000 rpm (#7), microspheres with narrower size distributions (19 - 60 μm) were obtained. Therefore, stirring speed has an effect on both microsphere size and also their distribution, whereby as the stirring rate is increased, the microspheres become smaller and the size distribution narrower. Accordingly, an optimal stirring rate of 1000 rpm was selected, as above this value, excess bubbles and foaming were generated in the emulsion. The consistently larger mean diameters for PLLA were accountable to the greater MW and the chain stiffening action of stereospecific and -tactic CH_3 side-chain. These effects were partially offset by the viscosity-reducing action of processing at higher temperatures with PLLA compared with PDLGA.

PVA is the most commonly employed emulsifier in ESE procedures for biodegradable polymers (Wada et al., 1988a,b; Zhifang et al., 1993 Conti et al., 1995; Boisdron-Celle et al., 1995). Granulometric data in Table 4.3 shows that beyond 0.5 %w/v PVA, higher concentrations of PVA had little bearing on the mean microsphere size. However, it was observed that for very low concentrations of emulsifier, spherical microspheres were obtained, but with a notably larger mean diameter than for higher concentrations. Moreover, a considerable number of aggregates were formed during manufacture, which necessitated their removal (via sieving, mesh # 100) prior to particle size analysis. In order to eliminate these aggregates, the minimum PVA concentration used was set at 1 %w/v, which also corresponded to the concentration which gave the narrowest particle size distribution. For example, particle size for PDLGA-prepared microspheres varied between 5 - 45 μm at 1 %w/v (#8), which widened to 10 - 125 μm at 0.1 %w/v (#12), and to 8 - 57 μm at 2 %w/v (#16). Therefore, in the interest of product reproducibility, 1 %w/v was the preferred concentration.

Overall, particle size distributions complied with the recommended range for subcutaneous administration. However, although within-batch variation in mean diameter was small (typically 1 - 3 % RSD), between batch RSDs for identical conditions were often in excess of 15 %. These data highlight the importance of the initial emulsification step to the final microsphere characteristics. The temperature of the continuum was considered of particular importance. Small variations around the boiling point of the disperse solvent can dramatically alter the diffusion rate of solvent, and hence the rate of ongoing viscosity changes of the microdroplets. Measures adopted in chapter 5 to restrict such variation included more stringent control of the disperse addition rate and adoption of an in-water drying modification (Bodmeier & McGinity, 1987a,b,c) whereby evaporation proceeds at ambient temperature without the application of heat. Indeed, because the solubility of DCM in water is reduced at elevated temperatures (2.5 %v/v at 15 °C compared with 0.88 %v/v at 45 °C (Horvath, 1982)), whilst potentially improving drug loading due to accelerated solvent diffusion initially, such modification might have exacerbated the between batch non-reproducibility. However, data in chapter 5 illustrate that modifications improved granulometry overall. The inclusion of baffles in the emulsion vessel, shown to improve particle size reproducibility (Bodmeier & McGinity, 1987a), and reduce particle size and polydispersity (Crossan & Whateley, 1994) was not, however, investigated.

4.3.2 Production attributes

Mean microsphere yield was consistently greater than 70 %, yield generally increasing with encapsulation efficiency as a smaller fraction of dispersed RIF was lost to the continuum. Accordingly, yields were generally greater for microspheres prepared from PDLGA compared with those from PLLA commensurate with their enhanced drug loading. The encapsulation efficiency demonstrated a similar trend. Batch #18 prepared from PDLGA showed a paradoxical encapsulation efficiency of 120 %. This was attributed to the partitioning of dissolved drug from the continuum to the disperse prior to microsphere hardening which significantly retarded drug diffusion thereafter. By comparison, the maintenance of microglobule fluidity for longer periods when CFM was used as the solvent with the corresponding PLLA product (#17), accounted for the net outward diffusion of drug with this batch.

4.3.3 Loading

In a therapeutic context, notwithstanding patient acceptability, there exists a theoretical physiological limit to the quantity of microspheres which can be effectively administered in a single dose. Furthermore, high solid concentrations of microsphere suspensions might affect the syringeability of such forms. Hence, the practical utility of long-acting injectable formulations containing high dose drugs, such as RIF, necessitates that the drug should constitute a significant proportion of the overall formulation volume. Modification of phase volume (Sansdrap & Moës, 1993; Bodmeier & McGinity, 1986, 1987a,b; Le Corre et al., 1994), D:P ratio (Wakiyama et al., 1981, 1982b; Jalil & Nixon, 1989; Ramtoola et al., 1991); continuum pH (Bodmeier & McGinity, 1986a; 1987a,b; Le Corre et al., 1994; Polard et al., 1996) and presaturation of the continuum (Splenlehauer et al., 1988; Jalil & Nixon, 1989a; Zhifang et al., 1993) represent the principle strategies which have been previously adopted to attain high core loading of microspheres prepared by various techniques based on the ESE principle. Accordingly, selected parameters were varied to assess their influence on principally drug loading and other related microsphere characteristics. The pH of a 1 %w/v PVA solution was 5.3 which itself represented a value of minimum RIF solubility according to Figure 3.8. Therefore, unbuffered continuum was employed throughout these investigations.

4.3.3.1 Disperse volume

Table 4.4 shows the effect of change of disperse volume on drug loading. Drug loading was inversely related to initial disperse volume, irrespective of the polymer used. This can be explained by considering the viscosity of the initial polymer solution. As the disperse volume decreases, there is a concomitant increase in disperse volume viscosity. Consequently, solutions become more difficult to disperse explaining the corresponding increase in mean particle size from 44 ± 2.5 μm to 80 ± 5.4 μm and from 28 ± 2.3 μm to 58 ± 3.8 μm for PLLA and PDLGA respectively as disperse volume decreased from 30 to 10 mL. It is noteworthy that PLLA solutions were noticeably more viscous than PDLGA solutions of identical concentration at 24 ± 2.0 °C. Associated with the increase in mean microsphere size, is a reduction in the specific surface area of the product. Therefore, because of the low mass transfer surface area and high mass transfer resistance associated with an increase in viscosity, the amount of drug lost to the continuum decreased. This resulted in higher loading as disperse volume decreased.

Table 4.4 *Production attributes of microspheres prepared by emulsification-solvent-evaporation under various experimental conditions (n ≥ 2). Preparative conditions according to Table 4.1 and 4.2.*

PLLA				*PDLGA*			
Batch	***Yield / %[a]***	***Loading / %w/w[c]***	***EE / %***	***Batch***	***Yield / %[b]***	***Loading / %w/w[d]***	***EE / %***
7	88.1	7.59	51.5	8	95.2	13.89	95.3
17	90.2	12.99	83.9	18	96.3	18.12	120.7
19	89.2	13.89	50.7	20	94.2	25.89	86.7
21	92.1	14.30	51.9	22	96.5	26.12	87.4
23	78.3	21.00	42.0	24	87.5	34.11	68.2
25	74.3	19.92	39.8	26	88.2	35.12	70.2
27	74.2	20.48	61.4	28	89.2	31.60	94.8
29	88.1	17.60	52.8	30	94.5	28.39	85.2
31	86.2	12.80	38.4	32	92.5	22.82	68.5
33	85.2	16.13	48.8	34	93.2	27.59	82.8
35	90.1	15.05	45.2	36	94.2	25.89	77.7
37	87.6	14.65	44.0	38	92.1	25.79	77.4

[a] RSD ≤ 12.3, [b] RSD ≤ 10.2, [c] RSD ≤ 8.9, [d] RSD ≤ 10.1

The loading differences noted between PLLA and PDLGA, whereby loading was consistently higher for PDLGA batches, are contrary to the ideas proposed above based on differences in microsphere size, whereby a reduction in particle size should reduce

drug loading. These differences can be attributed to the nature of the organic solvent in which the drug and polymer were dissolved. DCM was chosen for PDLGA because of the solubility problems of this polymer in CFM (Bendix, 1991). CFM was initially chosen as the organic solvent for PLLA instead of DCM because of the increased solubility of RIF in CFM of 930 ± 25 $mgmL^{-1}$ (50 °C) compared with 388 ± 15 $mgmL^{-1}$ for DCM (37 °C). By maximizing RIF solubility in the disperse phase, this was considered to minimize partitioning, and therefore loss of RIF from the formed microspheres to the continuum. The results, however, do not support this rationale for reasons outlined below.

Preformulation studies gave solubilities of 2.4 ± 0.11 %v/v (25 °C) and 0.75 ± 0.18 %v/v (25 °C) for DCM and CFM in 1 %w/v PVA, respectively. With the ESE procedure, the organic solvent must first partition into the continuum, from where it then evaporates at the surface of the emulsion. The rate at which solvent partitions into the continuum will be a function of organic solvent solubility in the continuum; environmental temperature; and, the viscosities of the disperse and continuum phases. This, in turn, will determine the resistance to mass transfer of the drug out of the disperse phase and ultimately the final drug loading. During solvent evaporation, DCM diffuses more rapidly than CFM into the continuum leaving more drug in the polymer matrix. As the volume of disperse phase reduced, then the period before polymer phase separation occurs decreased and hence a smaller proportion of dispersed drug is lost to the continuum and drug loading accordingly increased.

4.3.3.2 Temperature of evaporation

The complex effect of evaporation temperature differences on overall loading could not be adequately assessed. The greater viscosity of PLLA solutions noted at 24 ± 2.0 °C would be, in part, offset at higher processing temperatures when compared with PDLGA. Moreover, solubility of RIF in 1 %w/v PVA is known to increase approximately two-fold at 55 °C, compared with 39 °C, to 6.00 ± 0.18 $mgmL^{-1}$. This would undoubtedly favour loss of dispersed RIF to the continuum, although overall, partition coefficients should have remained constant as similar changes were observed regards drug solubility in the disperse media.

4.3.3.3 Continuum volume

The effect of change of continuum volume on drug loading is shown in Table 4.4. Partitioning of drug from the disperse phase into the continuum, with a consequent

reduction in drug loading, is a common problem associated with the ESE procedure. By reduction of the continuum volume it was presumed that less drug would partition out of the central disperse phase as less drug would be accommodated by a reduced volume of liquid, and hence result in an increase in drug loading. From Table 4.4 it can be seen that only modest increases in drug loading were achieved with a two-fold reduction in continuous volume. These differences were paralleled by a modest increase in particle size, which, for reasons outlined above, could equally explain the results. Furthermore, a reduction in continuum volume might well impede organic solvent evaporation, thus negating any favourable effect.

4.3.3.4 Drug:Polymer (D:P) ratio

Table 4.4 shows that absolute loading actually increased with an increase in D:P ratio. In contrast, however, the loading efficiency decreased. This was expected as at higher D:P ratios, on one hand, more drug is available for entrapment, while on the other, higher drug concentrations initially set up greater concentration gradients across the liquid interphase so a larger proportion of the drug is lost to the continuum.

By saturating the continuum with RIF, the concentration gradient is minimized, or even reversed. However as the D:P ratio increased, the amount of undissolved drug filtered with the microspheres accordingly increased. Associated with this undissolved drug was a reduction in product yield from 95.3 ± 5.4 % to 87.5 ± 6.5 % at D:P ratios of 0.2:1.0 and 1.0:1.0 for PDLGA respectively. These values were approximately 5 to 10 % lower for the corresponding batches prepared with PLLA. At even higher D:P ratios loading paradoxically decreased (data not shown). As loading increases, it follows that drug constitutes a larger proportion of the overall microsphere volume. The probability of drug existing at the surface therefore increases. Unlike PDLGA, no obvious differences were observed with PLLA microspheres at different D:P ratios. However, Figure 4.1 shows electron micrographs of PDLGA-based microspheres at different D:P ratios and those prepared from saturated and non-saturated continuum. At low D:P ratios (A), PDLGA microspheres with a continuous surface were prepared. However, at higher D:P ratios surface roughness and large pores were evident (B), the morphology worsening in the presence of a presaturated continuum (C). Other workers have reported that presaturation had the effect of promoting crystal growth (Jalil & Nixon, 1989a) not dissimilar to the 'pockets' of RIF evident here. In comparison, in Figure 4.3 (D), PLLA microspheres showed a continuous surface, albeit 'dimpled', even at high D:P ratios.

These differences can be attributed to the higher processing temperature used with PLLA which facilitated the film-forming character of the polymer, whereby the softening temperature of PLLA was exceeded but not for PDLGA. Higher loadings for PDLGA would also increase the probability of surface defects in accordance with the concept proposed above.

4.3.4 *In vitro* drug release

The rate and profile of drug release are the definitive parameters which determines the overall efficacy of a DDS. From Figure 4.2, the principle factors affecting release are the nature of the polymer and the D:P ratio. Drug release was characterized by a biphasic profile constituting an initial 'burst' of release followed by a very slow terminal phase over the time-scale of the release study. Rapid release of surface bound or loosely associated drug in the superficial areas of the microspheres, subsequent to very slow release by diffusion through a dehydrated polymer network typically results in the essentially asymptotic profiles of release observed. The magnitude of the asymptote is a function of the proportion of drug at the surface and the depth of microporosity. On the basis of an homogeneous dispersion of drug throughout the matrix, these values were found to be directly related to drug loading. Release from PDLGA during the terminal phase was found to be slightly faster than from the corresponding PLLA microspheres, in accordance with the increased degradation rate of this family of polymers as the co-monomer ratio approaches unity. The degree of crystallinity conferred on PLLA by the stereotactic CH_3 sidechain renders the polymer hydrophobic when compared with the amorphous nature of PDLGA. However, the high MW of the examined PDLGA renders this material essentially hydrophobic.

Surface observation can be useful in assigning reasons to a particular pattern of release of a drug from biodegradable polymers. Initial release behaviour is a function of the nature of the microsphere surface, such as smoothness, porosity and continuity. In Figure 4.1 (B) & (C) the increased number, depth and diameter of pores observed, aggravated the 'burst' of release, however in (A), the absence of such defects and the correspondingly lower 'burst' substantiates this reasoning.

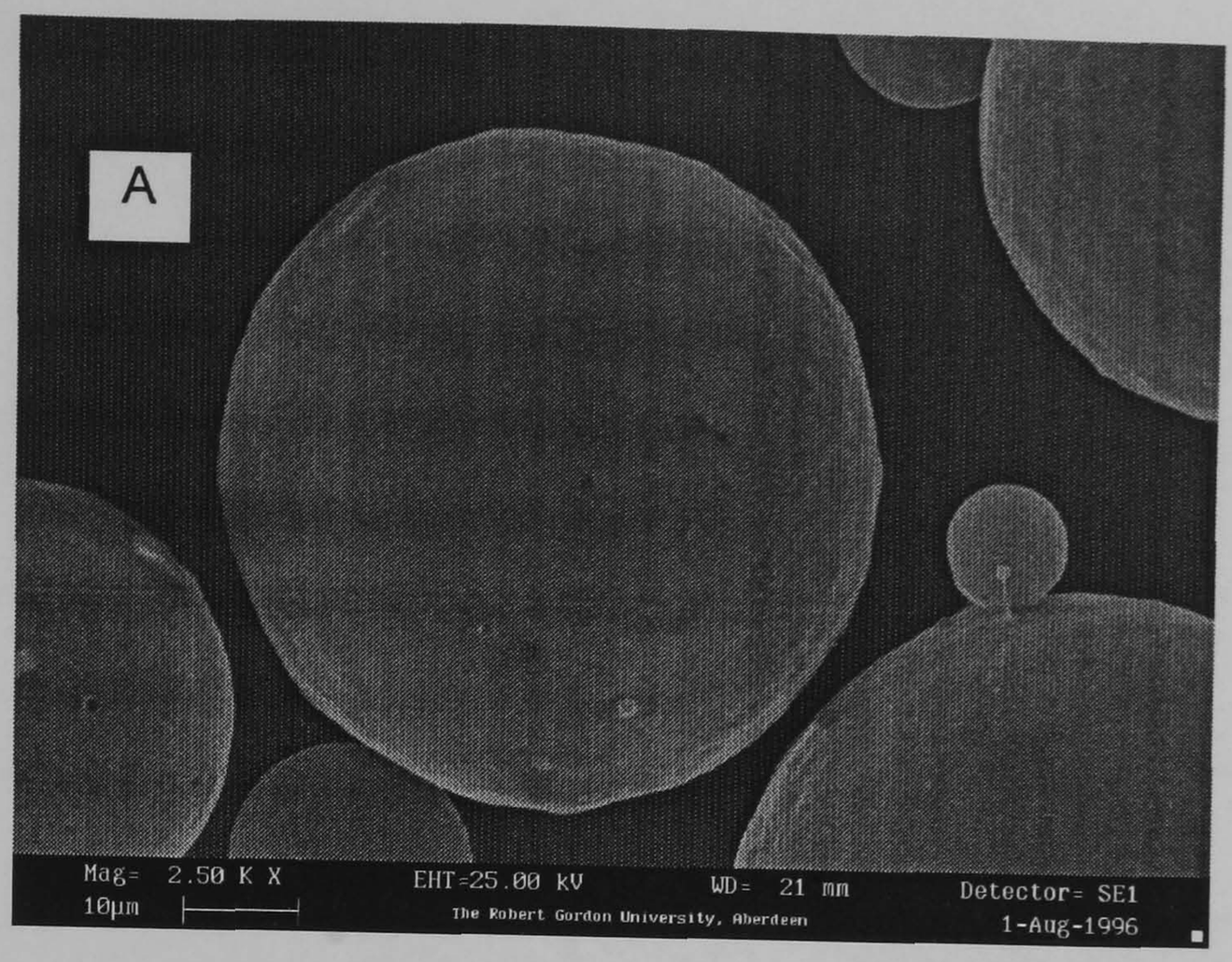

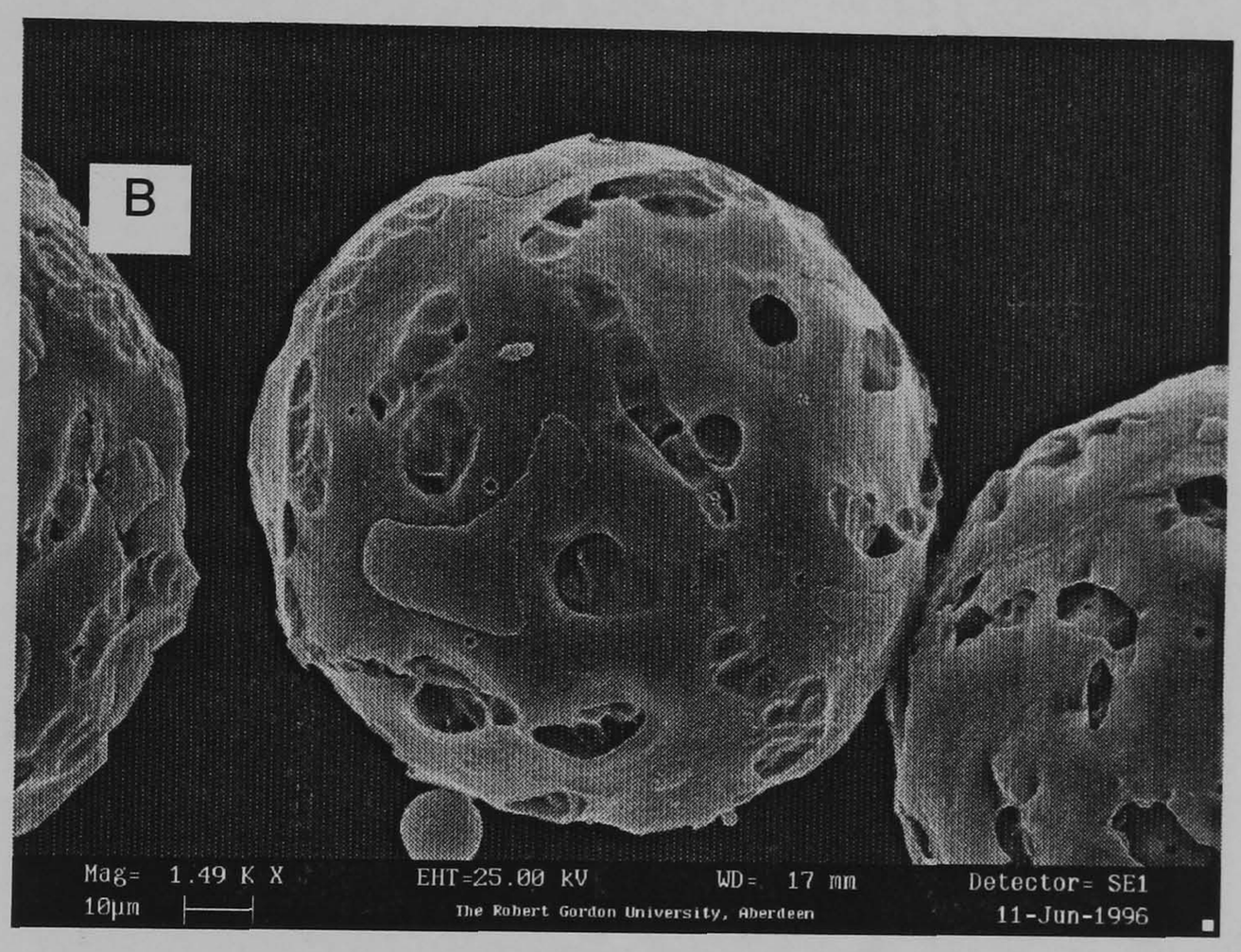

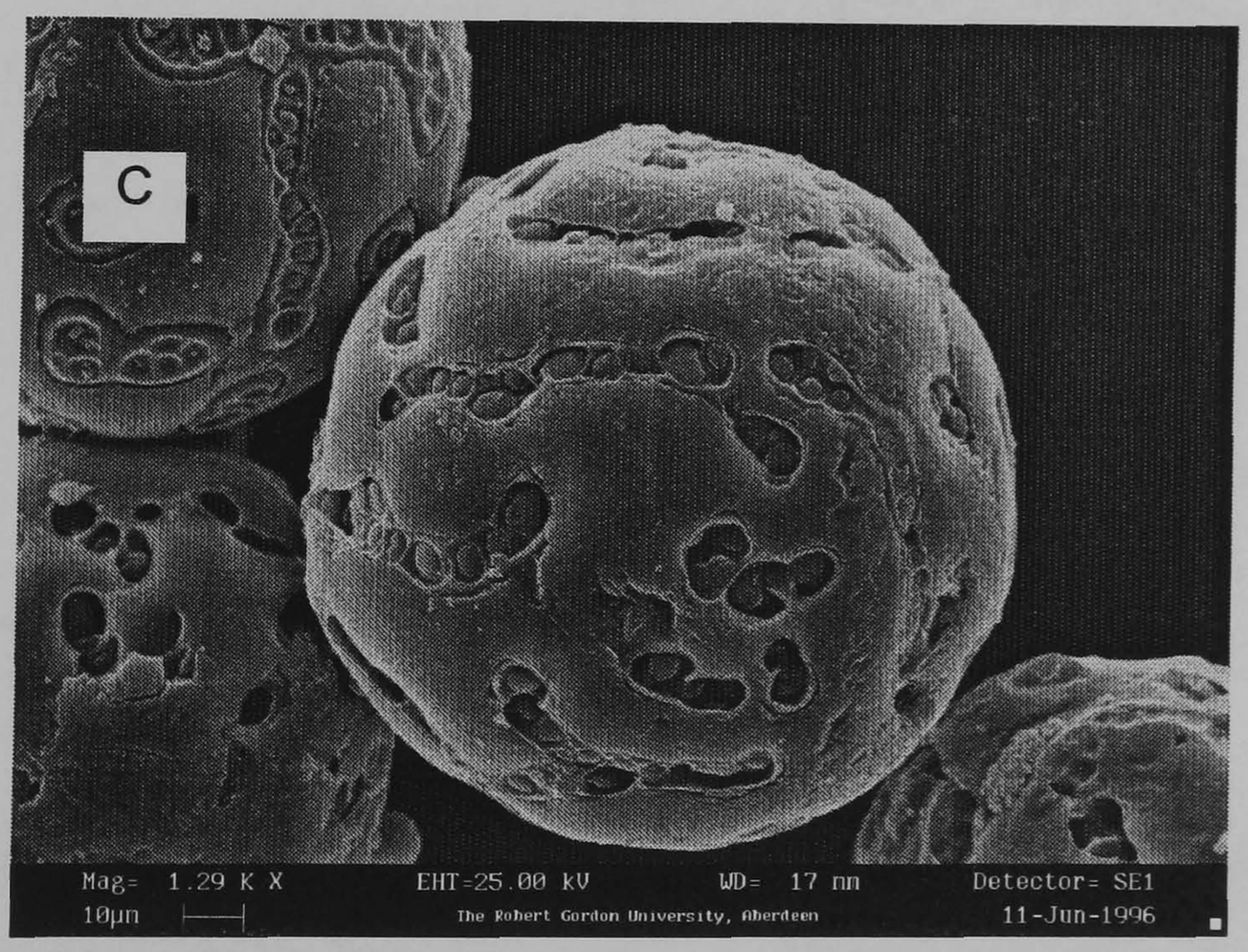

Figure 4.1 *Photomicrographs of PDLGA microspheres prepared at a drug:polymer ratio of: A, 0.2:1.0 (#8) (Mag^n, 2.5 k); B, 1.0:1.0 (unsaturated continuum) (#24) (Mag^n, 1.49 k); C, 1.0:1.0 (saturated continuum) (#26) (Mag^n, 1.29 k).*

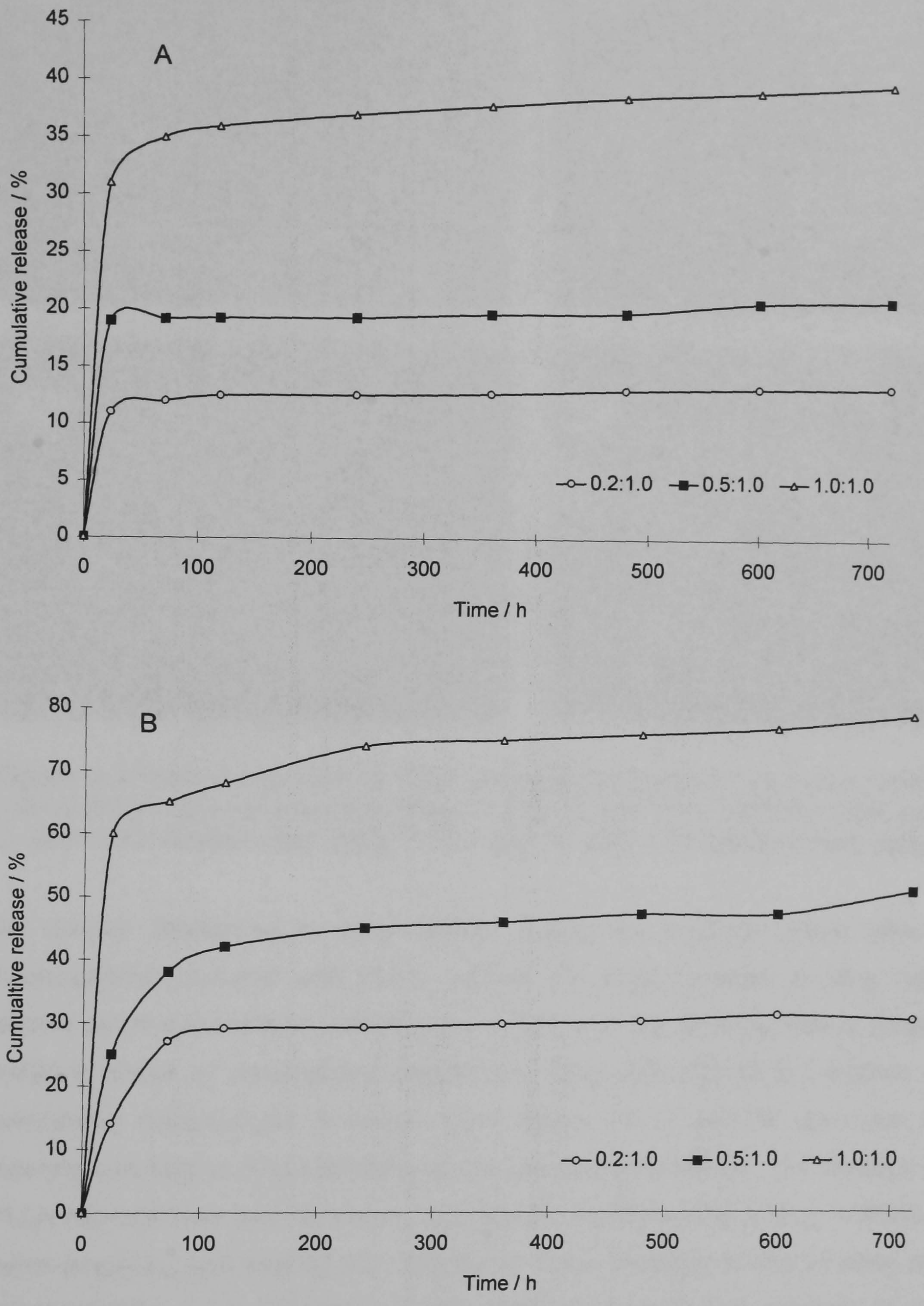

Figure 4.2 *In vitro release profiles of rifampicin from microspheres prepared by emulsification-solvent-evaporation at various drug:polymer (D:P) ratios from: A, PDLGA (68 kD); and, B, PLLA (78 kD) using method A at 37 ± 0.5 °C. Legend indicates the D:P ratio of the disperse phase. ($n \geq 3$, RSD ≤ 6.6)*

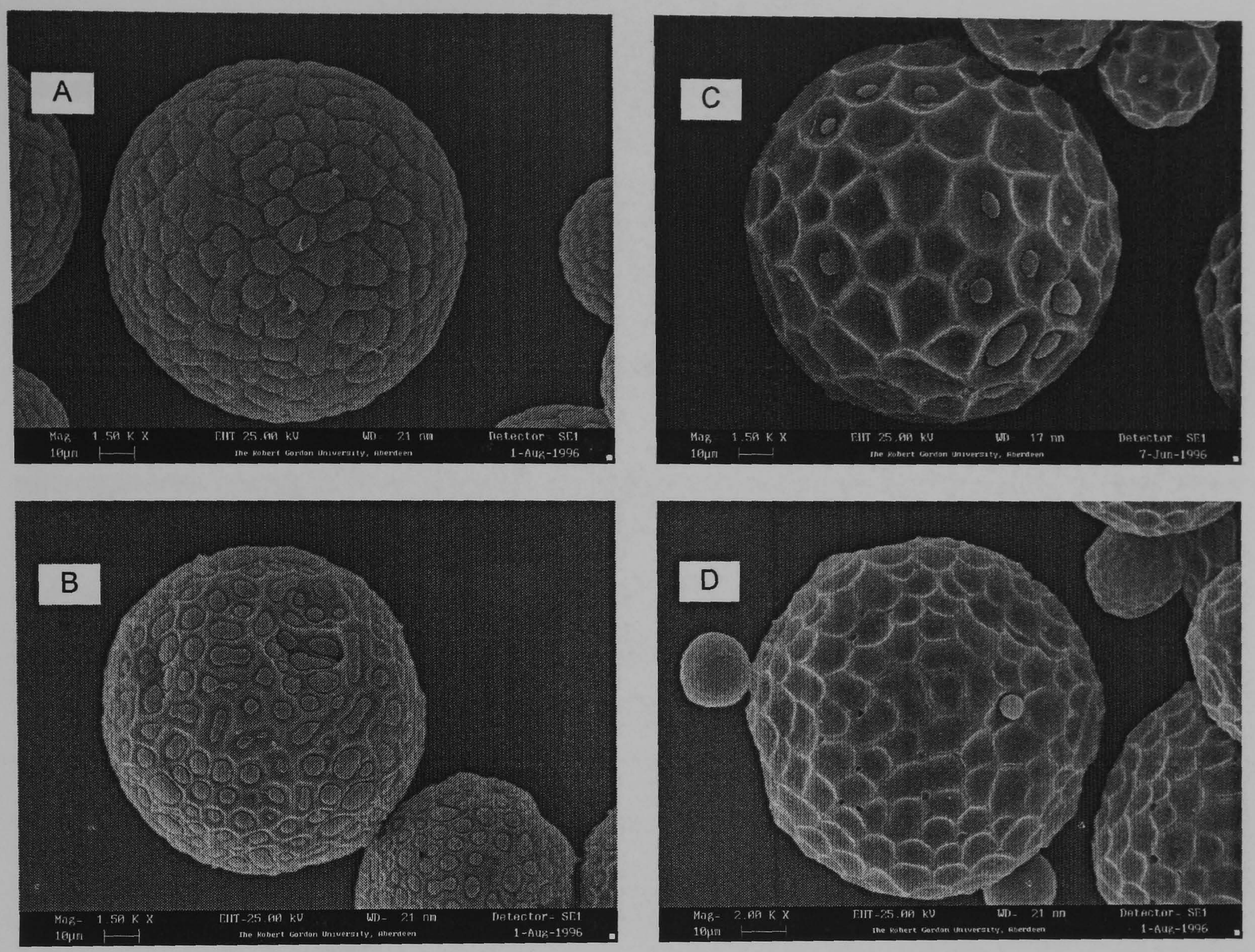

Figure 4.3 *Photomicrographs of PLLA microspheres prepared at a drug:polymer ratio of 1.0:1.0 (#23) : A, before washing (Mag^n 1.5 k); B, after 0.5 L distilled water (Mag^n 1.5 k); C, after 1.0 L distilled water (Mag^n 1.5 k); and, D, after 1.5 L distilled water (Mag^n 2.0 k).*

No distinct differences in drug release during the terminal phase were seen for microspheres prepared with PLLA, despite the large variation in drug loading. The differences in initial release with increasing D:P ratio can be explained by considering the washing phase of microsphere preparation. Drug adhering to the surface cannot be considered encapsulated. However, from Figure 4.3, it can be seen that insufficient washing can lead to drug persisting on the microsphere surface. The dimpled surface on PLLA microspheres was considered to facilitate the harbouring of drug in these loci. Each batch prepared was washed with 500 mL of water. However it can be seen from Figure 4.3 more than 1 L is required to adequately remove all drug residue. At higher D:P, increasing amounts of undissolved drug were noted in the continuum during microsphere filtration. It follows that increasing amounts would be harboured in the dimples on the surface of the microsphere. These observations would explain the differences in 'burst' release in the absence of any surface differences, and the subsequent parallelism of the dissolution profiles by the very slow degradation rate of the studied PLLA. Moreover, the

determined loadings may therefore be inaccurate, as an increasing proportion of measured drug as D:P increases may be adsorbed or otherwise physically attached, not encapsulated.

Finally, the differences in release profile for microspheres prepared from unsaturated and saturated continuum can be seen in Figure 4.4. Few differences are of note, with the exception of the initial 'burst' which was generally higher in those preparations prepared with a saturated continuum. Interestingly, at a D:P ratio of 1.0:1.0 with PLLA, microspheres prepared from a saturated continuum (#25) had a lower drug loading when compared with those prepared without continuum presaturation (#23) as shown in Table 4.4. At lower D:P ratios, increased loading with saturation of the continuum followed the general trends of greater 'burst' and overall release rate.

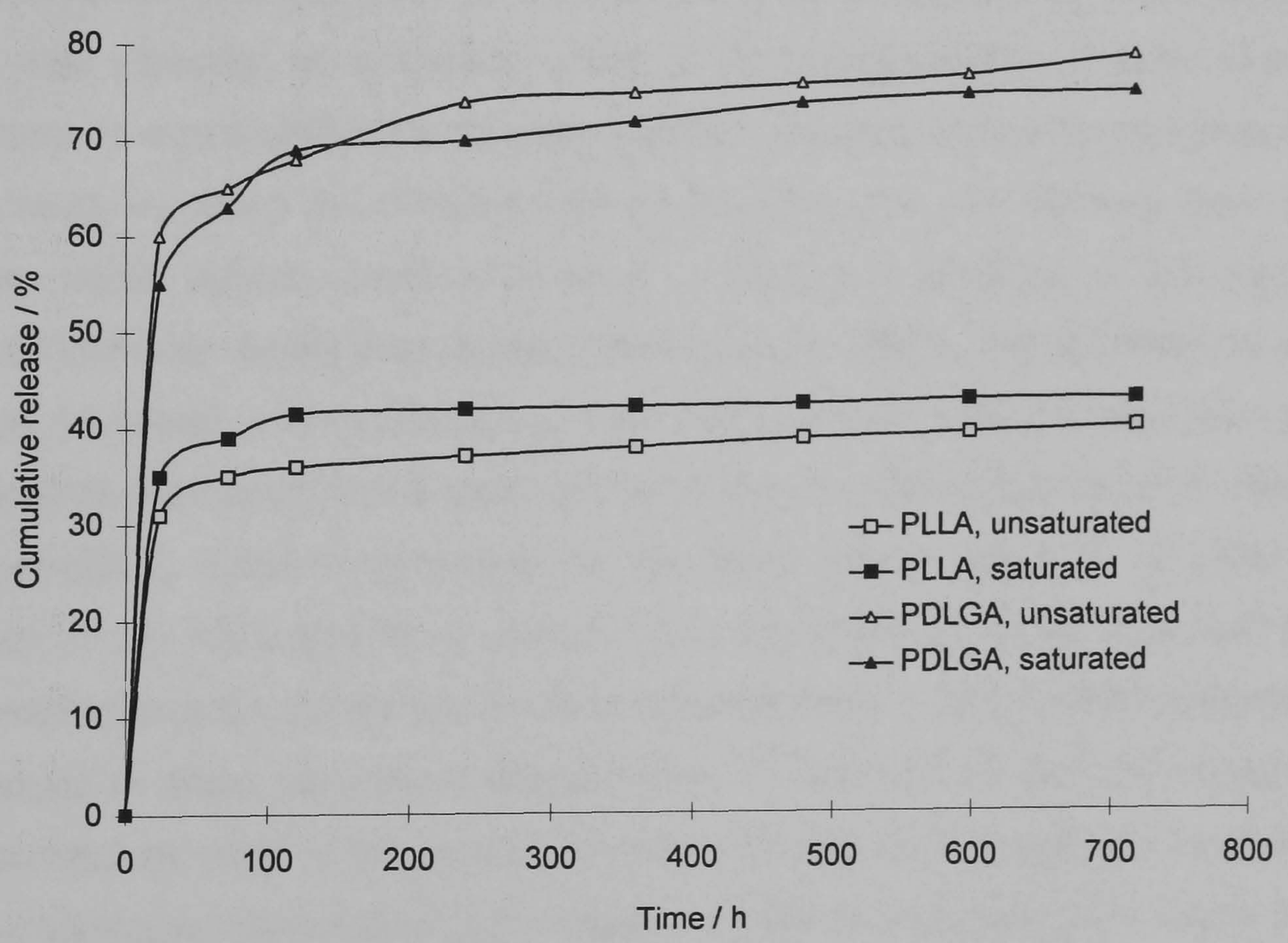

Figure 4.4 *In vitro release profiles of rifampicin from microspheres prepared by emulsification-solvent-evaporation at a drug:polymer (D:P) ratio of 1.0:1.0 using method A at 37 ± 0.5 °C. Legend indicates the polymer used, and whether rifampicin was (saturated) or not (unsaturated) added to the continuum prior to emulsification of the disperse phase. ($n \geq 3$, $RSD \leq 3.4$)*

4.4 Conclusion

The results show that the successful encapsulation of RIF into biodegradable PLLA and PDLGA microspheres is favoured by low disperse volumes, with continuum volume having a lesser influence. Loading has also been shown to be a function of D:P ratio and the organic solvent used, DCM being favoured. Further work would include studies of the encapsulation of the degradation product of RIF, RSV, which itself is not orally bioavailable, but has been shown to be pharmacologically equieffective to RIF during *in vitro* microbiological testing (Gallo & Radaelli, 1968). The rationale would be to take advantage of its significantly lower water solubility, i.e., 0.005 $mgmL^{-1}$ (Seydel, 1970) in an effort to further enhance drug loading. The asymptotic profiles of drug release irrespective of polymer represented unfavourable profiles for the intended application. Accordingly, the fabrication of microspheres based on more hydrophilic combinations of poly-α-hydroxy acids to modulate RIF release described in chapters 6, 7 and 8 requires investigation. Preliminary studies have been undertaken using albumin as emulsifier, where satisfactory microspheres were prepared of approximately 20 %w/w drug loading. Albumin was selected as emulsifier owing to its biocompatibility (Bazile et al., 1992). Furthermore, it is postulated that post-preparation recovery of the microspheres by spray-drying should lay down an effective coat of albumin upon the existing layer of protein molecules which adsorb (Verrecchia et al., 1993) and denature at the microsphere-continuum interface during preparation (Landry et al., 1997). The examination of various techniques to denature this coating, e.g., heat and chemical, and the separation of the RIF microcapsules from spray-dried coating should also constitute further work. Microsieving should provide a suitable technique for the latter stage. However, to allow effective separation of the two populations, particle size would require to be optimized to ensure the microspheres were sufficiently small to allow effective coating, whilst being sufficiently large enough to allow population differentiation. Preliminary studies with image analysis have indicated its utility in the expedient determination of the agitation requirements to achieve a particular prospective granulometry based on measurements made during the emulsification stage. This technique also offers excellent potential for real-time investigations of the microsphere formation mechanism under different experimental conditions, and should be additionally considered as further work.

5. Characterization of biodegradable rifampicin microspheres prepared by spray-drying

5.1 Introduction

In chapter 4, modification of phase volumes allied to continuum presaturation using an emulsification-solvent-evaporation (ESE) technique, achieved 30 %w/w drug loading for RIF-bearing PDLGA microspheres. Despite high loadings, these formulations generally showed a characteristic (Smith & Hunneyball, 1986; Ike et al., 1992; Polard et al., 1996) and intolerable 'burst' of drug release during the early stages, followed by a very slow release of residual entrapped RIF. In recent years, as an alternative to ESE as a preparative technique, spray-drying has emerged as a convenient method for the production of large quantities of biodegradable microspheres as a one-step process from a polymeric solution in which drug has been suspended — as solid particles (Bodmeier & Chen, 1988; Mathiowitz et al., 1992; Benelli et al., 1998) or emulsified droplets (Bitz & Doelker, 1995; Bittner et al., 1998) — or codissolved (Conte et al., 1994a; Wagenaar & Müller, 1994; Pavanetto et al., 1993). Consequently, in contrast to ESE prepared microspheres, respective production and characteristics of which are time-consuming and dependent on many variables, comparatively fast throughput of a product with high and predictable drug loading and reproducible product character can be readily attained (Giunchedi & Conte, 1995). The ease of scale-up and the techniques potential as a continuous process are further evidence of its industrial applicability. Indeed, Parlodel® LAR (Sandoz, Switzerland), which is one of only a few commercialized injectable microsphere formulations currently available (Benita, 1996), originates from spray-drying technology.

A number of workers have compared the attributes of spray-dried biodegradable microspheres with other preparative techniques including: aqueous ESE (Pavanetto et al., 1994a; Conti et al., 1994; Benelli et al., 1998); glycerin ESE (Conti et al., 1991; Pavanetto et al., 1992; Benelli et al., 1998); solvent extraction (Conti et al., 1991; Pavanetto et al., 1992); o/o[1] ESE (Benelli et al., 1998); w/o/w ESE (Giunchedi et al., 1998); and, ASES (Bitz & Doelker, 1995; 1996). Pavanetto et al. (1991, 1992) prepared spray-dried particles of superior sphericity, narrower size distribution, higher encapsulation efficiency — from which vitamin D_3 was released in a more controlled manner — than equivalent products prepared by ESE. Spray-dried hydrocortisone acetate-PDLLA microspheres demonstrated a two-fold increase in encapsulation

efficiency allied to a more controlled release when compared with those of equivalent diameter from ESE (Giunchedi et al., 1998). During a further comparison of ESE with spray-drying, Conti et al. (1994) observed approximately equivalent yields and particle granulometry for both techniques. The absence of surface-attached tolmetin with the latter technique, compared with the former, yielded a reduced 'burst', despite drug loading being higher with spray-dried products. Comparison of theoretical and actual specific surface areas for ESE and spray-dried diazepam-PDLLA microspheres highlighted the porous nature of those prepared by ESE with otherwise equivalent characteristics in terms of drug loading and release (Pavanetto et al., 1994a). Benelli et al. (1998) recently reported that extensive partitioning and subsequent recrystallization of suspended clonazepam particles resulted in ESE-prepared microspheres with substantial adsorbed, but little entrapped, drug (despite modification of both the volumes and natures of the individual phases). In contrast, spray-drying achieved efficient encapsulation of similarly dispersed particles due to the rapid rate of microsphere formation. Significantly, this appears to be the only report of the use of the Resomer®-H series for microencapsulation by spray-drying.

In view of these encouraging results, the purpose of the work described in this chapter was to compare the characteristics of microspheres prepared by the ESE technique optimized with respect to RIF loading in chapter 4, with highly loaded RIF products prepared by spray-drying. These investigations allowed the selection of a preparative procedure for further investigation based on the overall features of the products from, and the attributes of, each technique. A range of amorphous biodegradable Resomer® polymers was examined to identify individual materials providing satisfactory release profiles which warranted further investigation.

5.2 Experimental procedures

5.2.1 Microsphere preparation

5.2.1.1 Emulsification-solvent-evaporation

Microspheres were prepared by the procedure described in section 4.2.1 with the exception that evaporation was performed at ambient (24 ± 2.0 °C), not elevated (37 ± 1.0 °C), temperature. Processing parameters were maintained constant at: continuum, 150 mL of 1 %w/w PVA; disperse phase, 20 mL; D:P (0.5:1.0) (3 g total solid). The

disperse was added to the continuum at a rate of 0.66 mLs^{-1} under constant stirring at 1000 ± 50 rpm. Each batch was prepared in either duplicate or triplicate.

5.2.1.2 Spray-drying

A cosolution similar to that of the disperse phase above was diluted appropriately to 100 mL to yield a 3 %w/w solution (20 %w/w RIF) in a CFM:DCM (50:50) cosolvent. Process parameters were: inlet = 50 °C; outlet = 43 °C; feed = 3.5 $mLmin^{-1}$; flow = 600 NLh^{-1}; and, aspiration = 100 %. Spray-dried microspheres based on RG502, R202H and R104 were additionally examined at RIF loading of 11.1 %w/w (D:P = 0.125:1.0, 2.25 %w/v) 20 %w/w (D:P = 0.250:1.0, 2.50 %w/v) and 27.3 %w/w (D:P = 0.375:1.0, 2.75 %w/v). The effects of altering aspiration, inlet temperature and feed solvent were examined in an effort to improve microsphere yield for those based on RG502H. Microspheres were stored at 24 ± 2.0 °C *in vacuo* for ≥ 168 h prior to characterization. Each batch was prepared in either duplicate or triplicate.

5.2.2 Cloud-point titration

Polymer solubilities in DCM and DCM:CFM (50:50) cosolvent were indirectly determined by methanol (MeOH) cloud-point titration as described by Hausberger & DeLuca (1995). Polymer, 125 ± 5 mg, was dissolved and titrated against MeOH. The cloud-point was determined as the minimum volume of MeOH that resulted in a sustained turbidity.

5.2.3 Microsphere characterization

5.2.3.1 Yield

Whereas microsphere yield from aqueous ESE was determined by the procedure in section 4.2.3, the following procedure was followed to determine the proportion of material retrieved after spray-drying. With reference to Figure 1.2, powder was recovered by meticulously scraping all material from the collector (I) and the down-facing aspect of the cyclone (G) – collector interface. These materials were pooled and stored under vacuum at 24 ± 2.0 °C for ≥ 168 h before characterization.

5.2.3.2 Drug loading

Drug loading and encapsulation efficiency were determined by the method detailed in section 4.2.2.

5.2.3.3 Particle size analysis

Microspheres prepared by ESE were sized according to section 4.2.4, whereas the following modifications were made to that procedure for the corresponding spray-dried products. Microspheres (20 ± 5.0 mg) were prepared into a paste with two drops of dispersant (Coulter Electronics, Luton, UK) to which was added 50 mL of filtered saline. Deaggregation was facilitated by ultrasonification using an Sonicator XL ultrasonic probe (Heat Systems, N.Y., USA). Following validation of the deaggregation method, analyses were performed by Coulter Multisizer (Coulter Electronics Ltd., Luton, UK) fitted with a 70 μm orifice tube under constant stirring. Mean diameter and other granulometric statistics were thereafter determined on a population and volume basis by analysis of the % undersize particle size distribution using an iterative curve-fitting programme (CurveExpert version 1.3, Daniel Hyams, 112B Crossgate St, Starkville, MS, 39759). Selected samples were also examined by Laser diffraction for comparison purposes (Helos, Sympatec, Germany). Statistics, d_{25}, d_{50} , d_{75}, were selected as indices of distribution dispersity.

5.2.3.4 *In vitro* drug release

Drug release was examined by method A described in section 4.2.6. Additionally, initial RIF release was examined by the USP paddle (type II) apparatus (Sotax AT7, Basel, Switzerland); which is hereafter referred to as method B. Thus, microspheres, 50 ± 5.0 mg, were immersed in 500 mL of medium maintained at 37 ± 0.1 °C and agitated at 100 ± 1 rpm. Samples were withdrawn automatically over 3 h and assayed spectrophotometrically at 330 nm, i.e., the isobestic point of RIF and its major quinone degradation product at the analytical pH.

5.2.3.5 Scanning electron microscopy

Images were captured according to section 4.2.5.

5.2.3.6 Differential scanning calorimetry

A computer-associated Perkin Elmer Pyris 1 differential scanning calorimeter (Connecticut, USA) was used to characterize the thermal behaviour of microspheres and establish the dispersed state of entrapped RIF. Microspheres, 3 - 6 mg, were analysed under a stream of N_2. Instrument calibration was established by using the melting endotherms of indium and zinc standards. The heating programme was as follows: 1) 25 to 200 °C at 10 °Cmin^{-1} (first run); 2) 200 to 25 at 30 °Cmin^{-1}; 3) isothermal for 4 min at 25 °C, and; 4) repeat of 1 (second run).

5.3 Results and Discussion

The industrializability of any DDS preparative process is based on factors such as 'process efficiency', i.e., the ratio of product output to time and financial input, and process sophistication, which, in turn, determines the extent to which the process can be repeated and scaled-up without affecting the properties so carefully designed into the system at the development stage. One further determinant is the proportion of overall material processed that results in product with the intended characteristics. The relative expense of commercially available poly-α-hydroxy acids gives added significance to this latter factor, i.e., product yield.

5.3.1 Yield

The factors which determine product yield are the solubility of the polymer and drug in the organic solvent (and aqueous phase with ESE), whereas the mechanisms by which material is lost from the microspheres is a function of the microsphere formation principle for each technique. The yield with ESE is determined by the ability of the process to prevent aggregation of the microspheres and on the solubility of the polymer in the extraction and washing media. The characteristics of aerosol drying, which, in turn, determines the aerodynamic and impaction behaviour of the particles within the glassware, are known to affect yield with spray-drying (Masters, 1992).

Production attributes are presented in Table 5.1. With the exception of RG752, yields were consistently higher for ESE compared with spray-drying due to the factors discussed below. With ESE, yield decreased with RIF loading as drug was lost to partitioning, although that lost could not be quantitatively reconciled with the overall yield due to inherent material losses during recovery and washing procedures. This was particularly true of RG752 (#17), where an average yield of 54.7 % indicated significant loss of polymer in addition to drug during microsphere formation. By comparison, RG502H (#7) had a comparable yield to other batches — and a similar RIF payload to #17 — in spite of the fact that RG502H has a lower MW (8 compared with 20 kD) which would be presumably more liable to chain leaching during emulsification than RG752 (Bodmeier et al., 1989; Le Corre et al., 1994b). Alternatively, this apparent anomaly may be attributable to greater loss of material during microsphere recovery as the particle size decreases. However, on this basis, R104 (#3) was expected to show the poorest yield.

Table 5.1 *Production attributes of microspheres prepared by emulsification-solvent-evaporation (ESE) and spray-drying from a range of Resomer® materials (RSD in parenthesis) (n ≥ 2)*

	ESE				Spray-drying			
	Batch	**Yield / %**	**Loading / %w/w**	**EE [a] / %**	**Batch**	**Yield / %**	**Loading / %w/w**	**EE [a] / %**
R202H	1	86.0 (3.2)	27.0 (5.4)	81.8	2	52.0 (5.4)	32.4 (0.6)	98.2
R104	3	80.7 (5.8)	29.4 (6.2)	89.1	4	48.8 (1.4)	32.2 (1.0)	97.6
RG502	5	76.3 (6.3)	12.5 (3.2)	30.6	6	56.2 (22.2)	32.2 (1.2)	97.6
RG502H	7	81.0 (4.6)	16.1 (5.2)	33.9	8	44.2 (2.6)	32.8 (1.3)	99.4
RG503	9	78.0 (1.2)	21.3 (7.1)	64.5	10	69.6 (4.0)	32.7 (1.4)	99.0
RG503H	11	78.0 (0.1)	23.7 (8.5)	71.8	12	58.8 (18.8)	33.9 (1.2)	102.7
RG504	13	84.3 (11.7)	20.8 (5.2)	63.0	14	63.3 (4.7)	33.2 (0.8)	100.6
RG506	15	-	-	-	16	71.3 (1.9)	34.1 (0.8)	103.3
RG752	17	54.7 (8.6)	10.1 (3.7)	30.6	18	65.8 (7.5)	33.1 (1.0)	100.3
RG755	19	72.3 (3.2)	16.8 (7.8)	50.9	20	68.3 (0.6)	32.9 (0.0)	99.7

[a] encapsulation efficiency

For spray-dried microspheres, adherence of partially dried microparticles to the glassware walls (see Figure 1.2) and/or their discharge through the cyclone (G) exhaust will result in a reduction in product yield. Thus, a spray-heat-air pattern should be established which minimizes these effects and ensures maximal deposition of the dried material in the product collection chamber (I). The optimum conditions are a function of factors such as: residual solvent, and thermal behaviour of the product, which themselves are interrelated to the parameters of processing: drying temperature; aspiration and feed rate; choice of solvent; and, volumetric air flow. Given the multitude of interacting factors which might affect yield, optimal parameters for individual feeds are difficult to predict. However, from observations made in this work, a number of general rules have been established. Inlet air flow and temperature should have sufficient drying capacity to ensure efficient desiccation of the sprayed microdroplets. Conversely, the drying temperature should be below that of T_g of the polymer, or, more correctly, that of the drug-polymer composite, so as to prevent sticking of tacky material to the glassware.

Under otherwise identical conditions, variation in production yield shown in Table 5.1 was ultimately attributable to differences in polymer physicochemistry. Important factors are the T_g and the solubility character of the polymer, the latter of which influences the

residual solvent content of the polymer, which itself alters the former through a plasticizing action. Absolute solubility determinations of poly-α-hydroxy acids are inherently difficult due to gel formation at high polymer (40 - 60 %w/w) concentration. Indirect measurements of the solvation power of organic solvents can be made based on cloud-point titration (Hausberger & DeLuca, 1995; Mehta et al., 1996) and viscosity determinations (Stevens, 1990). Methanolic cloud-point volumes for individual polymers are shown in Table 5.2.

Table 5.2 *Methanolic cloud-point for selected Resomer® polymers, n =2.*

	Methanol / mL								
Polymer	***R202H***	***R104***	***RG502***	***RG502H***	***RG503***	***RG503H***	***RG504***	***RG752***	***RG755***
Solvent									
DCM	18.84	> 30	4.05	3.95	3.20	3.17	2.95	6.20	4.68
DCM:CFM	17.39	> 30	1.88	1.75	1.43	1.24	0.80	5.98	4.35

In general terms, for the same class of polymer, as the T_g reduced and the solubility of the polymer in the feed medium increased with a reduction in MW as shown in Table 5.2, the yield fell. Reduced yield was also attributable to increased levels of solvent residue, which plasticized the polymer and further reduced its T_g. Upon impact with the hot glassware walls, the resultant surface tackiness promoted microsphere adherence and consequently a lower proportion of material reached the product collector. The reduced yields observed with PDLLA compared with PDLGA were therefore accountable to the considerably greater solubility of PDLLA in the cosolvent used. Solubility of PDLGA copolymers were considerably greater in DCM compared with DCM:CFM, but likewise decreased as both MW and glycolide content increased. Furthermore, dependent on the molar ratio of monomeric units, materials of comparable MW possessing terminal free carboxylic end-groups were of lower solubility than their end-capped equivalents. Thus, from indirect measurements of polymer solubility based also on methanolic 'cloud-point', Mehta et al. (1996) found the solubility of PDLGA (50:50) was essentially independent of MW, whereas PDLGA (75:25) demonstrated a significant inverse dependence below 15 kD. The results in Table 5.2 show this trend extends beyond the narrow range studied by these workers.

Product porosity should also influence yield through its dependency on polymer deposition rate during drying as discussed in detail in chapter 7. Briefly, rapid solvent

evaporation rates associated with spray-drying typically result in a product of high porosity (Wagenaar & Müller, 1994; Rafler & Jobmann, 1994). Scanning electron microscopy revealed dimpled but otherwise smooth surfaces for all products, absent of 'blow-holes' and overt surface porosity. More controlled rates of polymer deposition that prevail as polymer solubility increases with a reduction in MW, allow greater microglobule contraction and polymer consolidation. This should conceivably result in a product of reduced porosity. Associated with an increase in product density is a commensurate increase in product yield as fewer particles are exhausted from the apparatus. The results however contradict this pattern, whereby increased polymer solubility reduced product yield, e.g., R202H and R104. These data suggest that the effect of residual solvent is more influential than that of product porosity in the context of the drying parameters used. Alternatively, increases in MW, which result in higher precipitation rates should more rapidly form a dried crust at the surface of the particle during drying. This crust then acts to impede further solvent transfer which results in high levels of solvent residue. However, during the short sojourn involved in the transformation of spray microglobules to solid microparticles, this residual DCM (1.325 gcm^{-3}) and CFM (1.48 gcm^{-3}), which is predominantly concentrated deep in the particle, will maintain the density of the product diffusing hours to days later, after which time the product has been harvested. Furthermore, the surface of the products would be essentially 'dry' and would not, therefore, readily adhere to the glassware. Conversely, with lower MW materials, particularly PDLLA, more controlled deposition and consolidation result in retention of greater loads of plasticizing organic solvent for longer periods in the surface layer. The probability that upon collision with walls of the drying chamber the polymeric matrix would be sufficiently tacky to remain attached is greatly increased. These theoretical considerations of polymer-dependent plasticizing organic load were not however confirmed (the DSC investigations were performed after loss of solvent during extensive storage). Residual solvent appears to have a far from simple effect depending on its position of entrapment: surface residue can reduce yield by promoting glassware adherence; or, conversely, solvent located in the microsphere core might minimize density-dependent loss through the exhaust.

5.3.2 Drug loading

As a result of enhanced polymer solubility and consequently delayed microsphere solidification with ESE, drug loading generally decreased with MW decrease within a polymer class. Additionally, as shown in Table 5.3, the associated increase in specific

surface area and decrease in diffusional pathlength as mean particle diameter decreased with polymer MW, facilitated the diffusion of RIF during preparation from premature microspheres. Differential behaviour between polymers of approximately equal MW, i.e., RG752 (10 kD); RG502 (15.5 kD); and, R202H (11 kD), illustrated that MW did not exclusively dictate drug loading. In terms of monomer composition, drug loading was minimal with 75:25 (D,L:G), increasing at ratios of unity and further still with PDLLA. Indeed, the lowest MW polymer studied, R104, which should have theoretically showed the lowest drug loading by virtue of its superior solvent solubility and smallest mean diameter, demonstrated the highest loading of all the materials examined.

Theoretically, drug loading of microspheres prepared by spray-drying should be identical to the weight percentage of drug in the homogeneous component solution sprayed providing drying parameters, solvents or additives used do not promote drug decomposition as air is the theoretical continuous phase to which drug cannot be lost. In spite of this, a continuum of encapsulation efficiencies have been reported from 99 % for tolmetin (Wagenaar & Müller, 1994), through 60 - 80 % for diazepam (Pavanetto et al., 1993b) to as low as 14 % for vitamin D_3 (Pavanetto et al., 1991; 1992). RIF is an unstable compound, degrading in air to its quinone derivative (Maggi, 1966). Instability in some organic solvents has also been reported (Graham, 1979). Under the mild conditions used to spray-dry the feed and the short contact time with CFM:DCM, no detectable decomposition occurred. Therefore, encapsulation efficiencies determined were quantitative ($P > 0.05$), corresponding to 97.6 - 103.3 % of that initially added regardless of the polymer used. This variation coincided with the precision and recovery data of the chromatographic technique employed. Moreover, this feature allowed the preparation of microspheres of predictable and reproducible drug loading. The poor encapsulation efficiency in reported work (Wagenaar & Müller, 1994; Pavanetto et al., 1991; 1992) remains unexplained, but may have arisen due to decomposition of encapsulant or inaccuracies in the analytical methodology.

5.3.3 Particle size analysis

Owing to the small particle size of spray-dried microspheres and their associated high surface energy, samples for analysis required fairly aggressive dispersion to ensure effective deaggregation and hence reliability of results. Accordingly, the effects of: various concentrations of dispersant, Tween® 80; sonification time; and, sonification intensity

were investigated, the granulometric statistics for batch #4 subjected to such treatment are shown in Table 5.3.

Table 5.3 *Effect of dispersion treatment on the granulometric (volumetric) characteristics of batch #4 determined by Coulter Multisizer ®*

		Sonification / min								
		1			***3***			***5***		
	diameter / μm	d_{25}	d_{50}	d_{75}	d_{25}	d_{50}	d_{75}	d_{25}	d_{50}	d_{75}
Power	***Tween® 80 / %w/v***									
2	0	8.40	10.4	12.3	6.42	9.48	11.1	6.05	8.75	9.9
	0.01	4.89	6.75	9.56	4.39	5.45	8.15	4.08	5.15	7.80
	0.1	3.72	4.68	7.50	3.38	4.40	7.60	2.89	3.92	6.50
3	0	8.50	10.1	12.2	5.81	7.02	9.85	4.62	5.26	5.99
	0.01	2.75	3.45	6.08	2.69	3.89	5.95	2.75	3.51	5.81
	0.1	2.70	4.45	7.40	2.64	3.59	6.06	2.70	3.51	5.65
4	0	3.95	5.70	7.75	3.15	5.40	6.27	2.95	5.15	5.80
	0.01	2.63	3.90	5.50	2.60	3.58	5.40	2.41	3.71	5.48
	0.1	2.40	3.68	5.50	2.40	3.59	5.35	2.38	3.61	5.45

d_{25} d_{25} d_{25}, represent the 25, 50 and 75 % undersize quartiles

Particle size was found to decrease as: the wetting action of Tween® 80 increased with increased surfactant concentration; and, the energy delivered increased with time and power of ultrasonification. Intense forces delivered by the ultrasonic probe, conventionally used to homogenize biological media, have obvious potential to rupture the microspheres. It was therefore prudent to utilize the minimum intensity and duration of dispersion to obviate negative skew of the size distribution. Accordingly, power 4 delivered for 1 min in a medium containing 0.1 %w/w Tween® 80 was selected as the optimal conditions for thorough dispersion without particle break-up. The constancy of diameter indices with treatment time seen in Table 5.3 validated this selection. Furthermore, dispersion medium was surrounded by an ice jacket to minimize drug dissolution and microsphere distortion by the heat generated during operation. Using this protocol, granulometric statistics for each preparation are shown in Table 5.4. Corresponding statistics determined by laser diffraction are shown in Table 5.5. The higher mean diameters with the Coulter electrical zone technique compared with laser diffraction reflected the differences in the two diameters presented and the counting principles of each technique.

Table 5.4 *Ganulometric statistics (volume) of microspheres prepared by emulsification-solvent-evaporation (ESE) (RSD ≤ 18.03) and spray-drying (RSD ≤ 10.8) from a range of Resomer® materials determined by Coulter Multisizer®*

		Mean particle diameter / μm						
		ESE				**Spray-drying**		
	Batch	**d_{25}**	**d_{50}**	**d_{75}**	**Batch**	**d_{25}**	**d_{50}**	**d_{75}**
R202H	1	18.2	33.8	40.2	2	4.46	4.37	6.14
R104	3	12.1	18.6	28.5	4	2.99	3.37	5.68
RG502	5	19.2	28.2	38.2	6	4.18	5.64	8.60
RG502H	7	17.9	27.8	38.4	8	4.21	5.82	8.62
RG503	9	35.1	44.4	49.8	10	3.49	4.38	5.92
RG503H	11	33.2	45.2	50.2	12	4.24	6.18	9.32
RG504	13	37.4	48.3	53.5	14	3.57	4.46	5.85
RG506	15	-	-	-	16	3.82	4.75	6.39
RG752	17	13.9	16.4	23.4	18	4.18	5.68	8.45
RG755	19	38.1	50.2	61..3	20	3.89	5.11	7.79

Table 5.5 *Ganulometric statistics (population) of microspheres prepared by emulsification-solvent-evaporation (ESE) (RSD ≤ 15.12) and spray-drying (RSD ≤ 9.2) from a range of Resomer® materials determined by laser diffraction*

		Mean particle diameter / μm						
		ESE				**Spray-drying**		
	Batch	**d_{25}**	**d_{50}**	**d_{75}**	**Batch**	**d_{25}**	**d_{50}**	**d_{75}**
R202H	1	26.7	33.9	43.5	2	2.02	4.13	7.22
R104	3	14.9	21.1	30.4	4	2.04	4.04	7.03
RG502	5	18.5	38.7	48.0	6	2.03	3.94	6.63
RG502H	7	19.5	29.6	40.3	8	1.66	3.19	5.66
RG503	9	28.0	41.7	53.5	10	2.11	3.99	6.65
RG503H	11	36.0	44.4	54.5	12	2.10	4.10	6.85
RG504	13	47.5	60.1	66.5	14	2.36	4.62	7.77
RG506	15	-	-	-	16	2.39	4.44	7.39
RG752	17	17.6	26.7	35.5	18	1.78	3.40	5.56
RG755	19	42.5	51.3	65	20	2.39	4.71	7.98

In general terms, the mean diameter, d_{50}, was several fold larger for microspheres prepared by ESE when compared with those derived from spray-drying. The exponential dependence of solution viscosity with %w/v polymer demonstrated by Armstrong et al. (1994), accentuated MW dependent viscosity changes. Accordingly, under constant agitation (1000 ± 50 rpm), mean diameter increased with MW for each class of polymer, as disperse viscosity, and hence resistance to shear, increased. Previous comparisons of the techniques yielded similarly distributed ESE-prepared tolmetin-PDLLA (Conti et al.,

1994), diazepam-PDLLA (Pavanetto et al., 1994a), vitamin D_3-PDLLA microspheres (Pavanetto et al., 1992) when compared with spray-drying. These results were attributable simply to the more energetic emulsification of the disperse afforded by the Ultraturrax equipment used in published reports when compared with the limited dispersion capacity of the magnetic bar used here.

Particle size distributions of spray-dried microspheres are characteristically monodisperse, polymer concentration and MW being primary determinants of mean particle size (Pavanetto et al., 1993; 1994a). Where polymer concentration in the starting solution is maintained constant, the spray globule size increases with polymer MW (Pavanetto et al., 1992) due to enhanced intermolecular forces between polymer chains (Bodmeier & Chen, 1988), until a limiting MW is reached, where threads, not microspheres result due to insufficient force to break up the stream of feed solution. Discrete microspheres were observed by SEM confirming that this critical MW was not exceeded in the present work. Owing to the use of relatively dilute solutions (2 %w/w polymer), granulometric statistics for spray-dried microspheres demonstrated only a general qualitative dependence on polymer MW (size increasing as solution viscosity, microdroplet volume and final porosity increased with polymer MW). This feature, however, had the advantage that particles of comparable granulometry could be readily prepared from materials of contrasting chemistry and MW. Conversely, these data equally illustrate the relative inflexibility of the Minispray® 191 apparatus in terms of preparation of particles of widely different size distribution, in comparison to ESE where process changes can achieve several decade shifts in mean diameter.

5.3.4 Scanning electron microscopy

The morphology of microspheres prepared by ESE were consistently inferior than respective batches prepared by spray-drying as illustrated by selected photomicrographs shown in Figures 5.1. The only exception was for R104, where monodisperse smooth spheres were prepared by ESE, largely free of associated particulate debris. Surface flaws included crenulation, surface pockets and pitting, whereas ill-formed spheroidal, disc-shaped and broken microspheres were apparent on a population basis. These features became more prevalent as MW increased within a class of polymers, with the exception of microsphere breakage which became more frequent as MW decreased. The solidification point, at which polymer precipitation commences, occurs later as the MW of the polymer decreased. Furthermore, the associated persistence of matrix plasticity

permitted more extensive and controlled contraction of the microdroplets as MW reduced prior to surface hardening which thereafter resisted further consolidation. In analogy to spray-dried microspheres, the diffusion of residual solvent occurred with a partial collapse of the hardened surface to produce the crenulated morphology. The within batch spectrum of surface features seen in Figure 5.1 (C) was attributed to the controlled addition of disperse to initially solvent free continuum. This created a range of DCM transfer rates amongst microglobules as the continuum rapidly saturated and equilibrium was achieved.

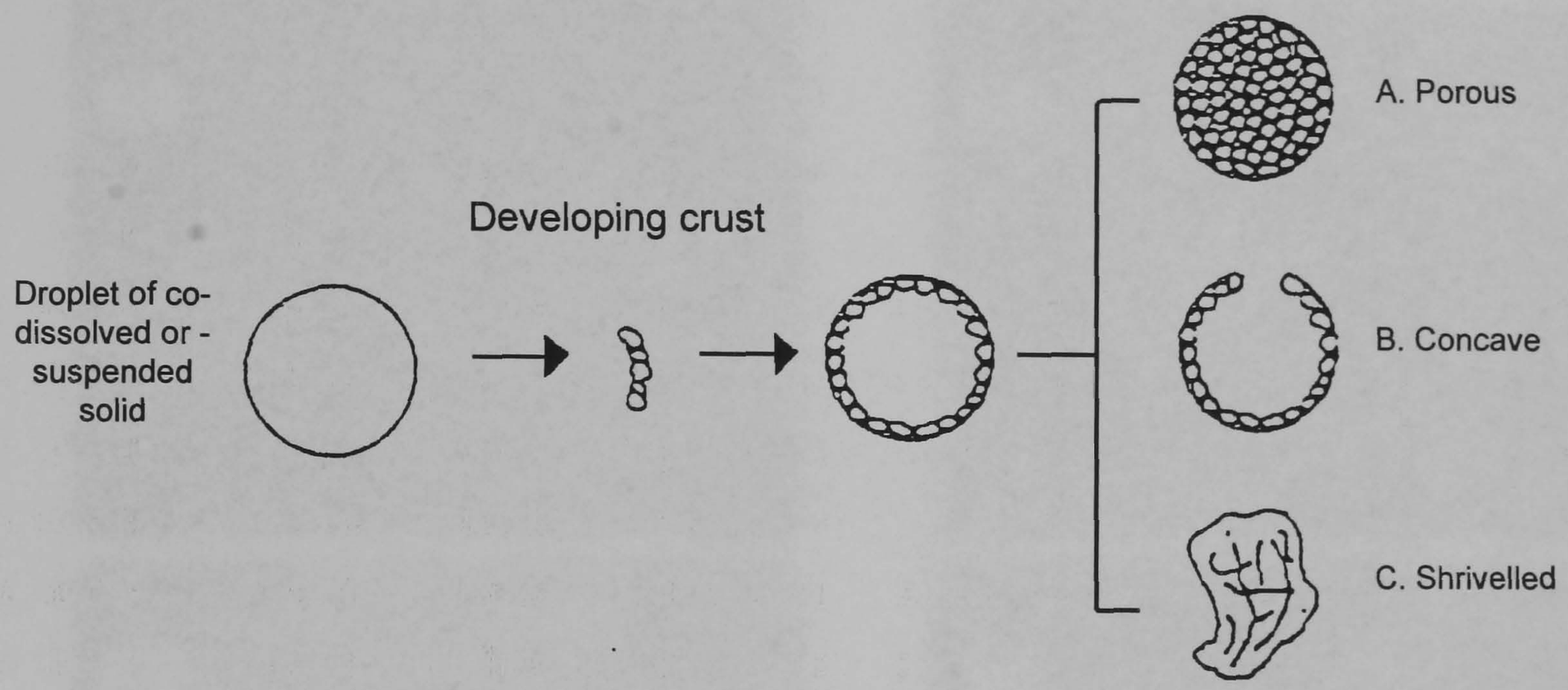

Figure 5.2 *Schematic of particle formation during spray-drying*

Figure 5.2 shows a generalized particle formation mechanism proposed by Kawashima et al. (1972), based on the physicochemistry of spray-dried salicylate-binder microgranules and observations of the morphological changes of the droplets as a result of the drying process. During drying, rapid evaporation of solvent from the droplet surface results in crust formation once the surface concentration reaches saturation point. Where the crust is sufficiently permeable (A) to allow passage of core solvent no change in appearance occurs during subsequent drying. On the contrary, low porosity films impede mass transfer, resulting in the formation of craters or holes as vapour expands and inflates and/or fractures the particles (B). Alternatively, more pliable, albeit impermeable crusts may yield a dimpled / shrivelled surface (C). Particle architecture is therefore a function of the vaporization characteristics of the solvent and its interaction with polymeric and other dissolved components, e.g., solubility of the microdroplet.

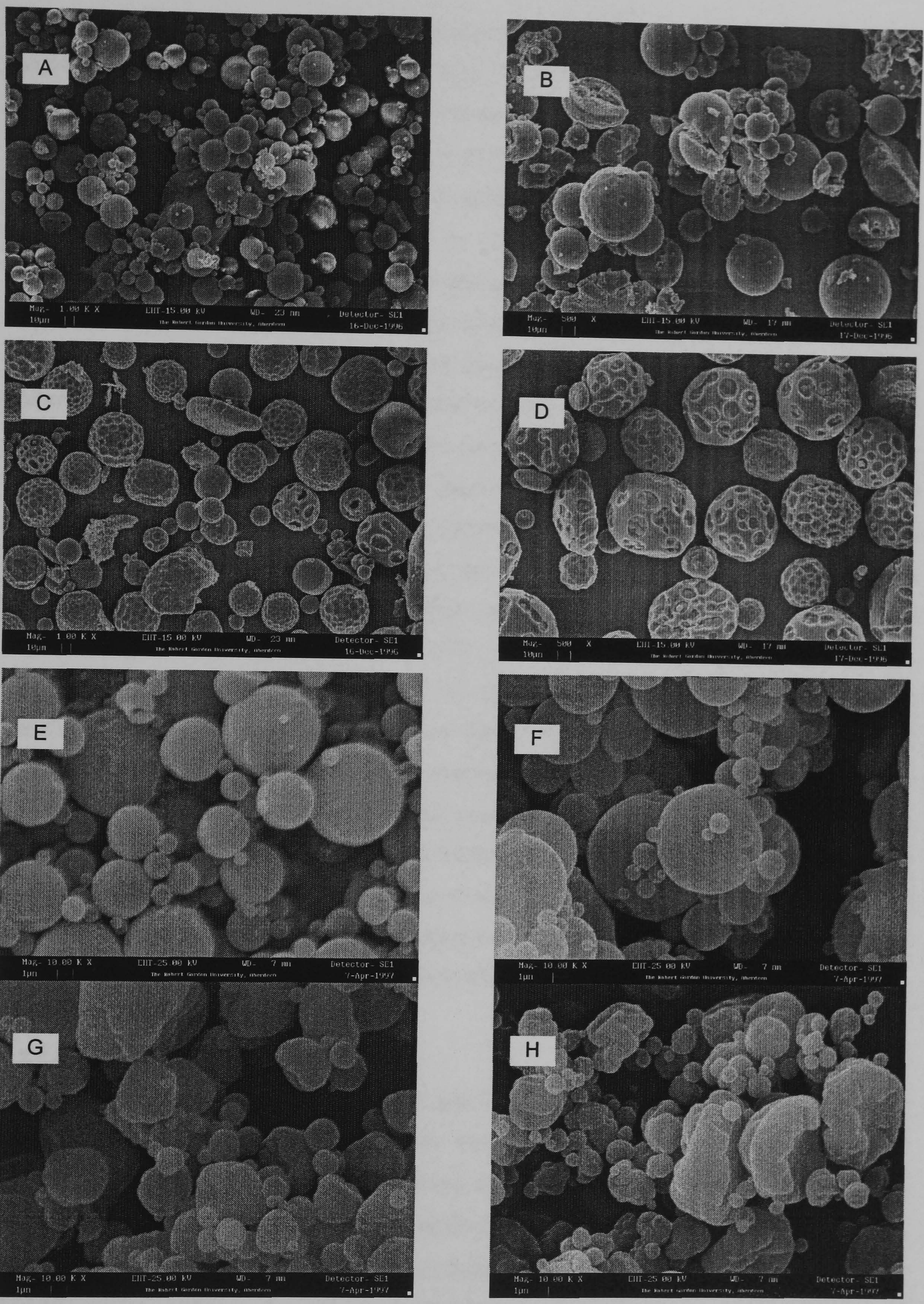

Figure 5.1 *Photomicrographs of microspheres prepared by emulsification-solvent-evaporation from: A, R104 (#3); B, RG502H (#7); C, RG503H (#11); and D, RG503 (#9) (all Mag^n x0.5 k);. and by spray-drying from: E, R202H (#2); F, R104 (#4); G, RG502 (#6); and H, RG504 (#14). (all Mag^n x10 k).*

The variable morphology of the spray-dried particles was ascribed to MW and associated solubility differences between the polymers studied, which, in turn, affected the kinetics of microdroplet drying and consolidation. The poor solubility of PDLGA (monomer ratio 50:50) has been attributed to the existence of blocks of consecutive glycolide units which confer a degree of crystallinity on the material (Bendix, 1990) with consequently very poor solubility in common solvents (Deasy et al. 1989), particularly CFM. Therefore, during drying a crust rapidly forms at the surface of microspheres prepared from PDLGA. Subsequent loss of deep-seated solvent causes core contraction and surface collapse, leading to a partial destruction of sphericity as deep folds are formed at the microsphere surface. These features generally became increasingly apparent as polymer solubility decreased with MW and glycolide ratio increase as seen in Figure 5.1. On the contrary, PDLLA, for which CFM is considered a good solvent, yielded microspheres of smooth spherical morphology for both low (R104, #4) and moderate MW (R202H, #2) polymer as shown in Figure 5.1 (E,F); due to more controlled consolidation associated with its enhanced solubility. Pavanetto et al. (1993) examined a range of MW PDLLA, PDLGA and PLLA materials spray-dried from CFM, CFM:DCM (50:50) and dichloroethane. Despite similar surface distortion with PDLGA prepared microspheres, the authors concluded that CFM:DCM cosolvent was the most convenient in terms of yield of production (35 - 45 %) and microsphere morphology as detected by optical microscopy. On the basis of this, and subsequent reports using this system (Pavanetto et al., 1993, Conti et al., 1994), this cosolvent was accordingly selected for preliminary spray-drying work in this thesis. The work of Pavanetto et al. (1993) did not, however, examine DCM alone which has been subsequently identified as a universally superior solvent for spray-dried poly-α-hydroxy acids during the work in this chapter.

5.3.5 Differential scanning calorimetry

The dispersed character of entrapped RIF and its effect on the thermal properties of each individual polymer were examined by DSC. The thermal indices for the first run and that after quench cooling to remove any thermal history are shown in Tables 5.6 and 5.7, respectively. The first DSC scans were typified by an endotherm which overlaid the T_g prior to broad and shallow endo- and exotherms between 140 - 190 °C. These latter events, shown in Figure 5.3 (A), were assigned to the melting and recrystallization of largely molecularly dispersed RIF; their diffuse character being a function of the finely divided state of these domains. In the absence of confounding variables such as drug loading, polymer deposition rates, residual solvent load and drug-polymer interaction, the

T_g should exhibit a MW dependence. However, the position and magnitude of the anomalous endotherm is a function of the degree of disorder conferred on the matrix during fabrication; the dispersed nature of entrapped drug; and, the extent of relaxation recovery that occurs on storage. The extent of the latter ageing process is also a function of the residual solvent load as discussed in chapters 6 and 7 of this thesis. Accordingly, faster deposition rates associated with spray-drying generated greater matrix disorder and hence higher temperatures were required to free restricted chain motion. The greater 'filler' effect with higher drug loadings made an additional contribution to this up-scale shift with spray-drying. By comparison of respective batches with comparable drug loads prepared by ESE and spray-drying (#1 & #2; #3 & #4), the influence of the former factor cannot be underestimated.

Table 5.6 *First heat DSC statistics for rifampicin-loaded microspheres prepared with a range of Resomer® materials by emulsion-solvent-evaporation and spray-drying*

	ESE				Spray-drying			
Resomer®	**Batch #**	**Onset / °C**	**Peak / °C**	**Area / Jg^{-1}**	**Batch #**	**Onset / °C**	**Peak / °C**	**Area / Jg^{-1}**
R202H	1	56.0	57.9	11.5	2	65.2	67.7	3.28
R104	3	47.8	49.8	7.37	4	63.8	66.5	7.76
RG502	5	47.8	49.8	7.32	6	50.5	53.1	6.40
RG502H	7	53.2	55.8	4.77	8	58.1	61.4	5.71
RG503	9	57.4	59.0	10.6	10	55.9	57.7	7.02
RG503H	11	56.0	57.8	7.82	12	56.8	59.2	5.51
RG504	13	55.8	57.7	7.88	14	57.0	58.7	6.00
RG506	15	-	-	-	16	56.2	58.0	6.33
RG752	17	56.7	58.0	10.0	18	58.3	59.6	6.11
RG755	19	59.8	61.2	7.62	20	61.1	62.7	5.96

The area of the endotherm associated with the T_g was shown to increase as the MW of the polymer decreased due to the enhanced mobility of shorter chains and, as drug loading decreased due to a reduced chain stiffening effect of fewer interposing drug molecules. The actual position of the T_g showed a pattern consistent with drug loading and the factors detailed above. Apparently anomalous behaviour with low MW material, R104 (2 kD), which registered a T_g at 49.8 °C, when compared with higher MW RG502 (15 kD) was adequately explained on the basis of drug loading and polymer structure. Analogous patterns were exhibited by lower MW RG503H and RG502H and higher MW RG503 and RG502, although it is acknowledged their lower MW may have facilitated stress-relaxation associated elevations of T_g.

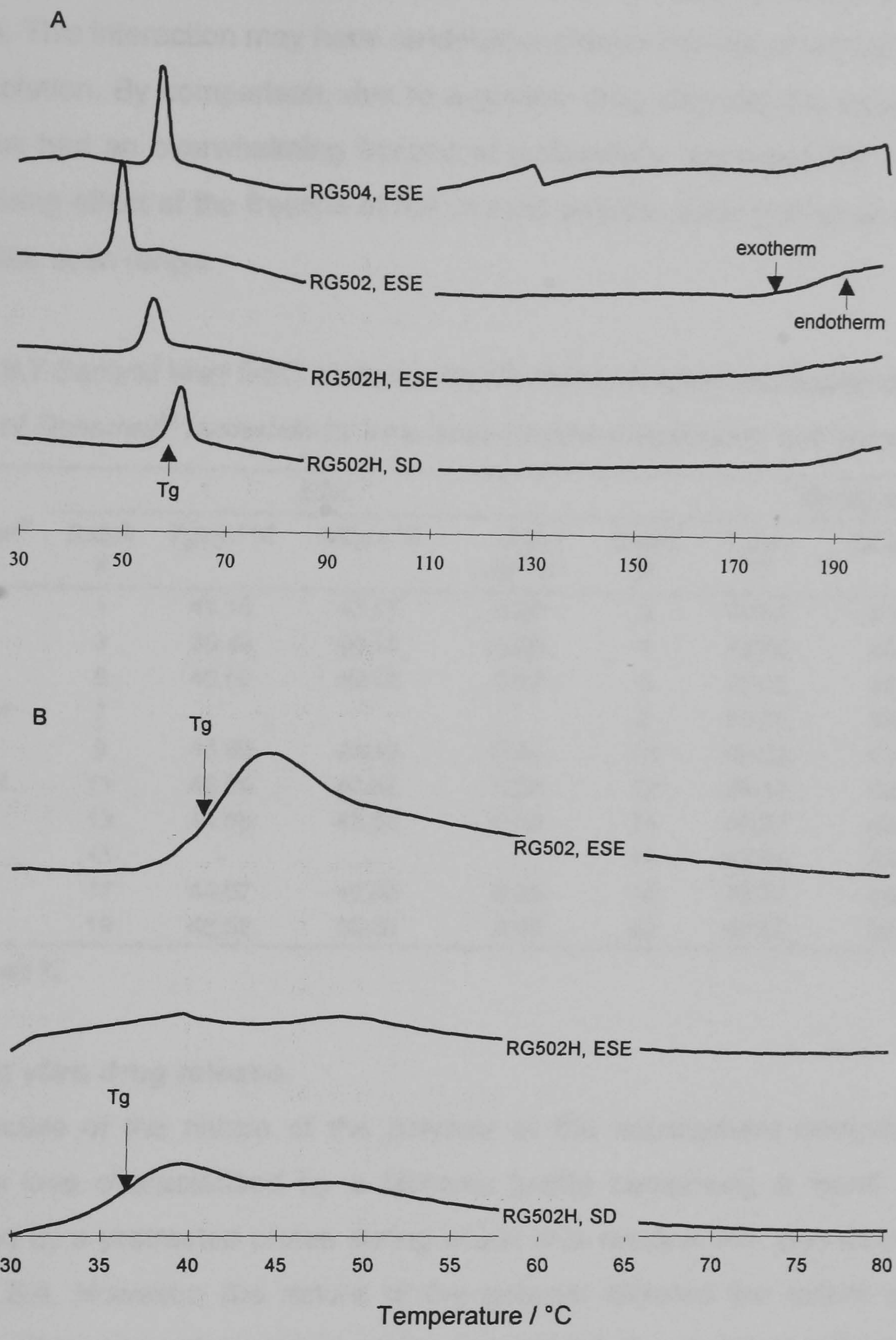

Figure 5.3 *First (A) and second (B) DSC scans of selected batches of microspheres prepared by emulsification-solvent-evaporation (ESE) and spray-drying (SD). Legend indicates polymer used, abbreviated preparative technique.*

Subsequent to quench cooling, the statistics for the second run, whilst being independent of the fabrication process, are, however, influenced by the melt-quench process in so far as it appears to alter the balance of RIF which exists molecularly dispersed and that which is in solid solution. In Figure 5.3 (B), the absence of an on-scale T_g with ESE prepared RG502H compared with RG502 microspheres was considered due to an

enhanced polymer interaction with RIF due to an increased density of free COOH end-groups. This interaction may have rendered a greater fraction of loaded RIF in plasticizing solid solution. By comparison, due to a greater drug payload, the respective spray-dried particles had an overwhelming fraction of molecularly dispersed RIF which negated the plasticizing effect of the fraction of RIF in solid solution such that an on-scale T_g persisted within the scan range.

Table 5.7 *Second heat DSC statistics for rifampicin-loaded microspheres prepared from a range of Resomer® materials by emulsion-solvent-evaporation and spray-drying*

	ESE				Spray-drying			
Resomer®	**Batch #**	**T_g(o) / °C**	**½Cp / °C**	**ΔCp / Jg^{-1}*C**	**Batch #**	**T_g(o) / °C**	**½Cp / °C**	**ΔCp / Jg^{-1}*°C**
R202H	1	41.15	43.17	0.26	2	48.81	51.55	0.35
R104	3	39.43	40.76	0.26	4	42.02	44.78	0.20
RG502	5	40.00	40.76	0.37	6	37.05	39.26	0.30
RG502H	7	*	*	*	8	33.78	34.44	0.12
RG503	9	43.90	45.33	0.47	10	40.23	41.22	0.21
RG503H	11	42.04	43.62	0.22	12	39.18	40.86	0.26
RG504	13	44.68	45.98	0.30	14	42.27	42.70	0.23
RG506	15	-	-	-	16	42.84	44.05	0.27
RG752	17	44.67	46.00	0.38	18	43.78	44.98	0.24
RG755	19	48.52	50.30	0.38	20	49.52	50.27	0.25

*no on-scale T_g

5.3.6 *In vitro* drug release

Irrespective of the nature of the polymer or the microsphere fabrication process, RIF release was characterized by a biphasic profile comprising a 'burst' of drug release, followed by a protracted phase during which time residual RIF was liberated as shown in Figure 5.4. However, the nature of the polymer dictated the extent and rate of these phases. A number of general trends were identified consistent with polymer MW, drug loading and particle granulometry. Microspheres prepared from relatively hydrophilic RG502 (#5 & #6), RG502H (#7 & #8) and R104 (#3 & #4) demonstrated a substantial 'burst' (50 - 100 %) within 24 h, prior to a relatively slow release thereafter. With the exception of RG752 (#17) and RG502 (#6) prepared by ESE and spray-drying respectively, all other products seldom achieved greater than 30 % drug release during the 14 d study period of examination using method A. Whereas the magnitude of the 'burst' from comparably loaded spray-dried products showed greater correspondence with polymer MW and hydrophilicity, deviations from this pattern for ESE were attributed to variation in drug loading, whereby 'burst' increased with drug loading. Consistent with

their greater mean diameter and diffusional pathlength, respective microspheres prepared by ESE demonstrated a generally slower release and reduced 'burst' when compared with the corresponding product prepared by spray-drying. The porous matrix of #17 with RG752 accounted for deviation from this trend.

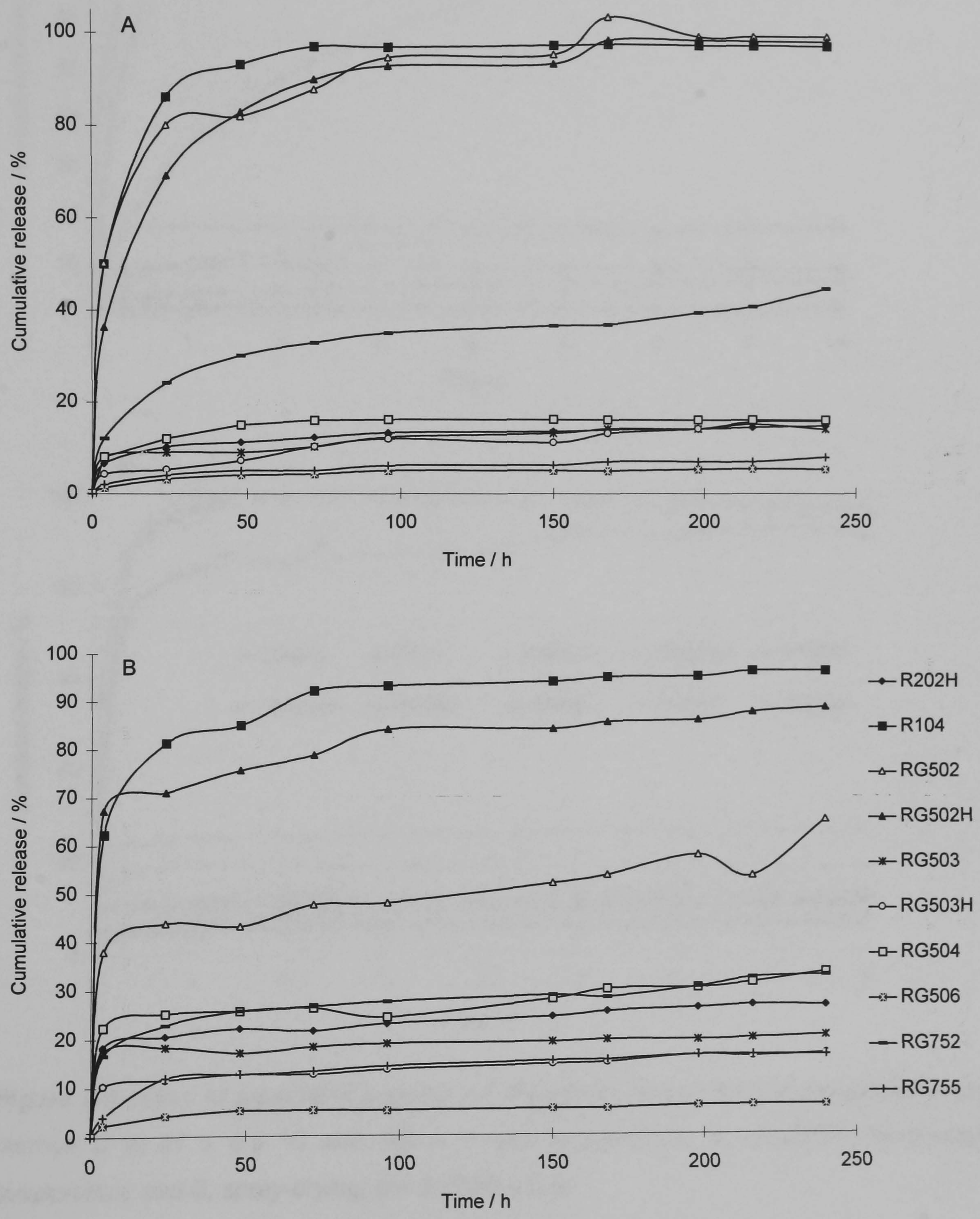

Figure 5.4 *Effect of fabricating polymer on rifampicin release from microspheres using method A prepared by: A, emulsification-solvent-evaporation; and B, spray-drying, n = 3 (RSD ≤ 3.5)*

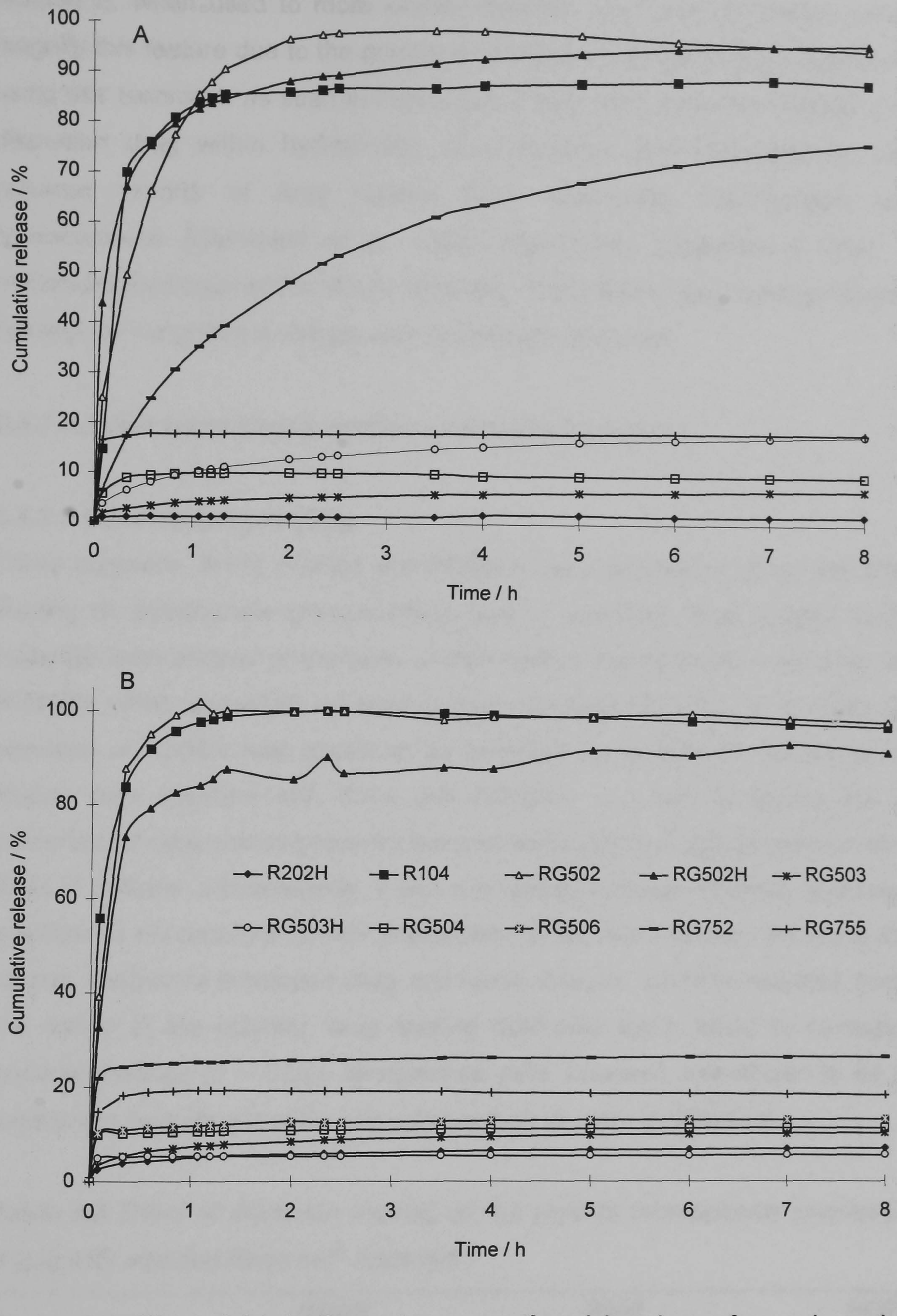

Figure 5.5 *Effect of fabricating polymer on rifampicin release from microspheres using method B at 37 ± 0.5 °C and 100 ± 1 rpm prepared by: A, emulsification-solvent-evaporation; and B, spray-drying, n = 3 (RSD ≤ 3.5)*

Method B, when used to more closely examine the 'burst' of release, only served to magnify this feature due to the greater microsphere surface area exposed to the medium using this technique as seen in Figure 5.5. These data typify the release of molecularly dispersed drug within hydrophobic poly-α-hydroxy acid microspheres, corroborating previous reports of drug release from spray-dried microspheres loaded with hydrocortisone (Giunchedi et al., 1995), theophylline (Bodmeier & Chen, 1988) and naftidrofurylhydrogenoxalat (Bruhn & Müller, 1991) where drug loading dependent 'burst' followed by insignificant release was consistently observed.

5.3.7 Further spray-drying studies on selected polymers

5.3.7.1 Effect of drug loading

Three polymers, R104, R202H and RG502H were selected to study the effect of drug loading on microsphere characteristics, and, in particular, drug release kinetics. These materials were chosen on the basis of their relative hydrophilicity in the case of R104 and RG502H which permitted substantial drug release within the 14 d study period. The selection of R202H was based on its excellent sprayability as evidenced by SEM, a feature also apparent with R104 and RG502H. In order to reduce the 'burst', the proportion of drug was sequentially reduced whilst polymer concentration in the feed was fixed at 2 %w/w. Consequently, it was anticipated because relatively more polymer was available to encapsulate the RIF codissolved in the feed solution, the accessibility of the release medium to entrapped drug, and hence release, would be reduced. Irrespective of the nature of the polymer, drug loading itself was again found to correspond to the nominal loadings ($P > 0.05$). Microsphere yield, however, was shown to be particularly sensitive to both drug loading and polymer type as seen in Table 5.8.

Table 5.8 *Effect of rifampicin loading on the yield of microspheres prepared by spray-drying with selected Resomer® materials.*

	R202H		R104		RG502H	
Loading / %w/w	**Batch**	**Yield / %**	**Batch**	**Yield / %**	**Batch**	**Yield / %**
11.1	21	58.6	24	21.7	27	4.4
20	22	84.0	25	70.0	28	7.2
27.3	23	68.4	26	42.2	29	42.5
33	2	52.0	4	48.8	8	44.2

Two general drying effects were considered to account for the parabolic dependence of microsphere yield on drug loading. On the one hand, T_g temperature increased with drug loading due to the 'filler' effect of interposing drug domains, the magnitude of which increased as the volume contribution of RIF increased. Accordingly, the probability that microspheres adhere to the hot glassware elements in the event of collision was inversely proportional to drug loading. On the other, the aerodynamic balance which promotes particle deposition in the product collector was progressively disrupted as the solid content of the feed increased. Theoretically, there exists a critical mass and density at each instrument flow rate and aspiration which allows efficient product-air separation in the cyclone and the onward descent of particles into the collector. Interpretation is therefore further complicated by changes in solid content and solubility differences of the feed which alter the mass and density of the microspheres prepared. Nonetheless, by comparison with R104 and R202H, the former effect appeared to predominate with microspheres prepared with RG502H over the studied loading range. These data highlight some of the potential scale-up issues of spray-drying despite its otherwise excellent industrial potential as a preparative technique.

Drug release profiles of these products are presented in Figure 5.6. Contrary to that anticipated, release rate actually decreased as drug loading increased. This was attributed to T_g elevation and increased matrix hydrophobicity as drug payload increased, both of which retarded water penetration and subsequent RIF release by diffusion from these relatively hydrophilic matrices. The influence of drug loading became more apparent as the hydrophilicities of the materials decreased in rank order R104 > RG502H > R202H. The influence of T_g on drug release from similar systems is discussed in detail in chapter 6.

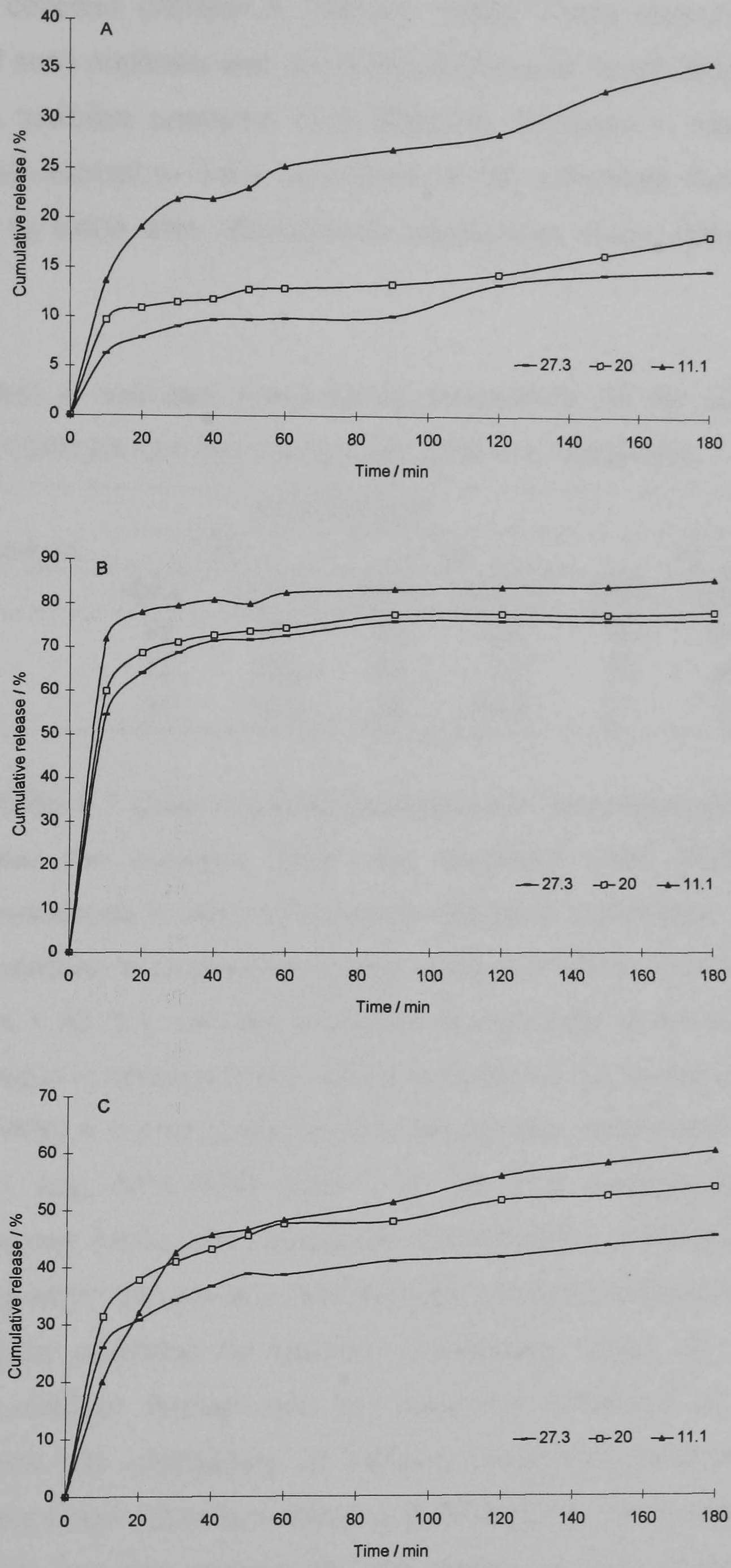

Figure 5.6 *Effect of drug loading on the release of rifampicin using method B (at 37 ± 0.1 °C and 100 ± 1 rpm) from spray-dried microspheres prepared with: A, R202H; B, R104; and C, RG502H. Legend indicates the drug loading in units of %w/w, n = 3 (RSD ≤ 3.2)*

5.3.7.2 Effect of processing parameters

Particularly low yields when spray-drying low MW materials has been attributed to heating effects in the collector (Witschi & Doelker, 1998). These authors concluded that the spray-drying of such materials was generally problematic. In an effort to improve the yield of spray-dried samples prepared from RG502H, variation in inlet temperature, feed (co)solvent and aspiration were examined at an otherwise fixed feed composition corresponding to batch #28. Microsphere yields from these studies are presented in Table 5.7.

Table 5.7 *Effect of selected spray-drying parameters on the yield of microspheres prepared from RG502H (2.5 %w/v total solid, 20% w/w rifampicin)*

		CFM:DCM (1:1)				***DCM***			
	Inlet / °C	***60***		***50***		***50***		***40***	
Aspiration / %		***Batch***	***Yield / %***	***Batch***	***Yield / %***	***Batch***	***Yield / %***	***Batch***	***Yield / %***
100		28	7.2	32	8.0	35	62.8	38	74.8
75		30	16.0	33	7.2	36	40.0	39	42.4
50		31	17.6	34	16.8	37	6.4	40	33.2

The results in Table 5.7 show that yield increased with decreased aspiration for the mixed solvent, whereas the opposite trend was observed when DCM was used alone. Furthermore, reductions in inlet temperature resulted in generally a reduced yield with CFM:DCM, in contrast to consistently higher yields with DCM. Under identical processing conditions (inlet = 50 °C), with the exception of aspiration at 50 %, yield was improved several fold. This is in contrast to the results in section 7.3.2 where comparable yields (40 - 60 %w/w) of PDLLA microspheres were obtained with: DCM (inlet = 40 °C); CFM:DCM (inlet = 50 °C); and, CFM:DCM (inlet = 40 °C). This anomaly was attributed to the solubility differences found with cloud-point investigations of PDLGA and PDLLA in the studied solvents which can result in architectural, solvent residue and thermal differences between products prepared by identical processing, which, in turn, alter both the aerodynamic behaviour through and the impaction behaviour of the material to the glassware. Given the interactivity of various processing parameters and a lack of knowledge of the exact solubility behaviour of RG502H in the studied solvents, it proved difficult to assign concrete reasons for the pattern of yield observed. That said, the following possible explanations are advanced.

Assuming ideal behaviour, the heat requirements to evaporate DCM and CFM:DCM are approximately equal. Therefore, the rate of solvent evaporation increases with drying temperature resulting in a more porous microsphere matrix. As aspiration is then increased, a higher proportion of material of low specific weight is exhausted from the apparatus. The differential behaviour between solvents at inlet = 50 °C could be assigned to solubility differences between the feed solvents. The poor solubility of PDLGA (monomer ratio 50:50) compared with PDLLA was discussed above. Therefore, the inclusion of CFM in the feed solvent created greater matrix porosity due to faster polymer deposition during drying. Accordingly, the fraction lost via the exhaust again increased with an increase in the vacuum applied. Additionally, regulation of aspirator performance also serves to alter the volume of heated drying air within the apparatus and in turn the energy available for evaporation. It follows, as aspiration is reduced, evaporation occurs in a more controlled fashion to yield a more coherent product which is less readily exhausted. Moreover, the theoretical value of critical specific density required to overcome the aspirating vacuum and ensure deposition in the collector is reduced, and so the proportion of material deposited increased. Conversely, due to the comparatively greater solubility of PDLGA in DCM alone, during drying a more coherent matrix is deposited. In contrast to those prepared from a proportion of CFM, an increased vacuum is therefore required to draw this material of higher specific weight through the apparatus, thus accounting for the increased yield as the vacuum increased. Additionally, further reductions in inlet temperature resulted in enhanced microsphere densification and conceivably higher solvent residual which itself increased microsphere apparent density and further promoted product yield. Furthermore, that the solubility of PDLLA is approximately equal in DCM and CFM accounts for the differential behaviour between PDLGA here and the yield data for PDLLA based microspheres in chapter 7.

Collected product (and that exhausted from the apparatus) require further fundamental investigation, i.e., pycnometric, granulometric and thermal to establish the architectural changes associated with varying drying parameters to establish their effect on particle impaction and aerodynamic properties. Preliminary investigations of this type for PDLLA are accordingly described in chapter 7. In view of the interactivity of process and material-related factors, such tedious empirical investigations appear necessary to define the drying conditions providing optimum yield. Preliminary studies of polymer solubility based on cloud-point titration and a knowledge of the vaporization characteristics of the solvent used, however, provide a considered starting point for such investigations. In general, use

of good polymer solvents and a compromise drying temperature in terms of solvent residue and particle coherence appear to promote the formation of relatively dense particles with acceptable yields.

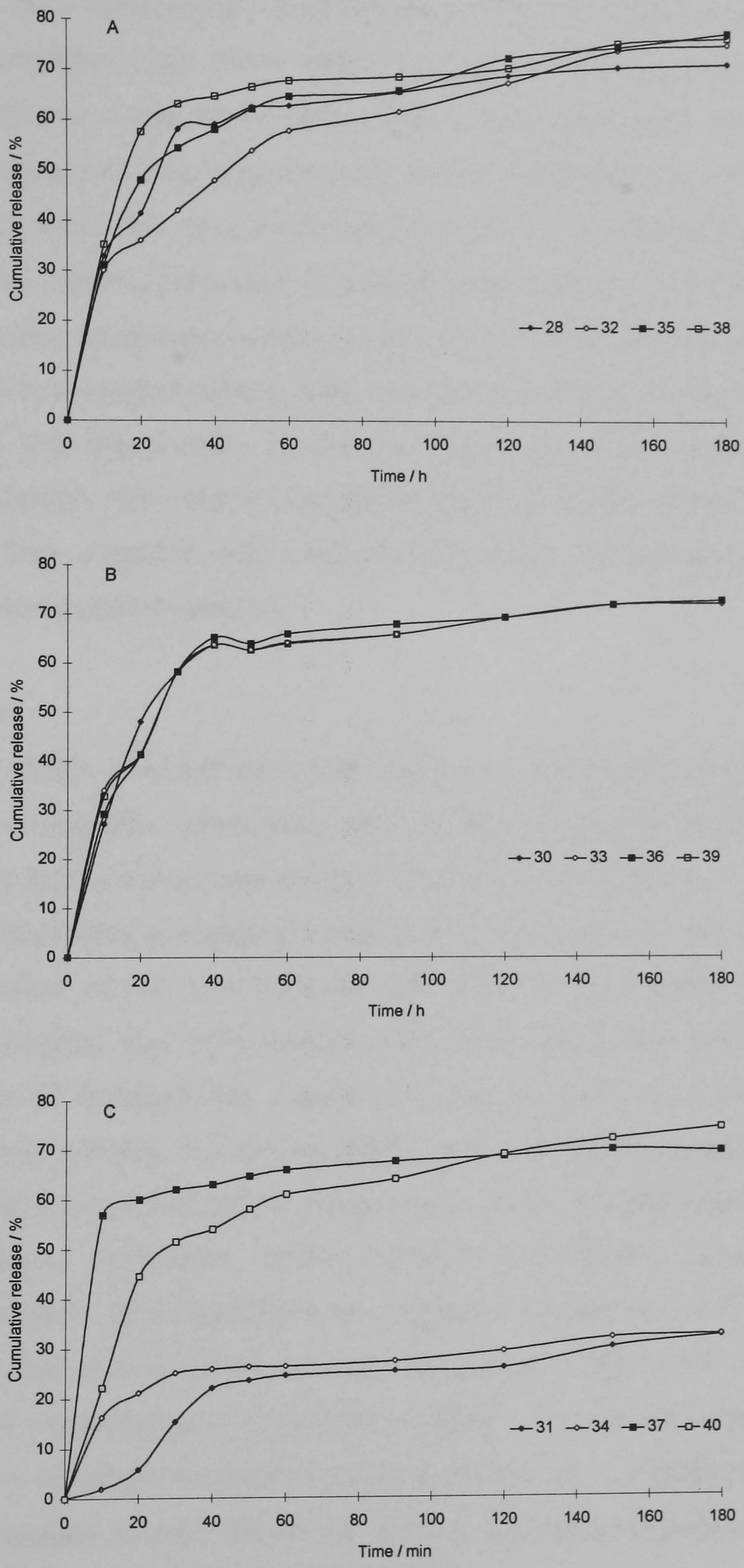

Figure 5.7 *Effect of selected spray-drying parameters on the release of rifampicin using method B at 37 ± 0.1 °C and 100 ± 1 rpm from microspheres prepared from batches, #28, 30-40 (RSD ≤ 7.25, n=3). Legend indicates batch #.*

The effect of spray-drying parameters on drug release profiles is shown in Figure 5.7. In contrast to microsphere yield, the release of RIF was generally insensitive to variation in drying parameters with the exception of batch #31 and #34 prepared at inlet = 60 and 50 °C respectively from cosolvent at an aspiration of 50 %. Contrary to the considerations of microsphere formation rate, these highly porous products paradoxically showed the slowest drug release. However, reasons for poor yield considered why material was lost from the apparatus, not why the proportion which constituted the yield was deposited in the collector. On this basis, it is considered that due to the theoretically high porosity of #31 and #34, the cyclone selectively deposited large particles which possessed sufficient critical mass to overcome the aspirating vacuum. The much reduced specific surface area associated with such large particles might have accounted for this apparent anomaly. It is acknowledged that these ideas require verification by granulometric and pycnometric investigation. Overall, the relative insensitivity of drug release from these products was attributable to their relatively high hydrophilicity which overshadowed otherwise subtle variation in microsphere architecture.

5.4 Conclusion

In contrast to ESE, microspheres with high and predictable loadings, reproducible granulometry, acceptable morphology and of high production yields could be readily produced using spray-drying regardless of the physicochemistry of the poly-α-hydroxy acid used. Furthermore, comparable quantities of product can be prepared by spray-drying in a fraction of the time required with ESE. Other workers have reported that microsphere formation was not possible using ESE when high proportions of low MW PDLLA were to be incorporated, presumably due to leaching of the polymer into the aqueous continuum during the emulsification and evaporation stages (Bodmeier et al., 1989). By avoiding the use of water, spray-drying allows the preparation of microspheres containing relatively hydrophilic R104, RG502H and RG502. Limited examination of processing conditions identified DCM as a superior solvent to the CFM:DCM cosolvent conventionally used due to the superior solvent power of the single solvent as identified from cloud-point measurements of polymer solubility. Use of low inlet temperatures and high aspiration — to offset reductions in drier performance — attained high yields with low MW RG502H, despite its high affinity for organic solvent and its low T_g, features which generally limit the proportion of recovered material.

In analogy to ESE, spray-dried biodegradable microspheres exhibited considerable 'burst' release particularly at high drug loadings (Conti et al., 1994), due to their small particle size. Contrary to diffusion theory, increased drug loading paradoxically decreased drug release rate from selected spray-dried hydrophilic systems due to a 'water-proofing' effect. Use of slowly degrading polymers resulted in a reduced 'burst' but with a protracted terminal release phase. Accordingly, in the following chapter, the utility of blending hydrophilic low MW with moderate MW PDLLA is examined to modulate both the 'burst' and protracted phases of RIF release.

Overall, based on the favourable attributes of the technique, spray-drying has been selected for the remaining work in this thesis. Moreover, a limited but systematic study of selected parameters has established both conditions and materials, i.e., polymers and solvents suitable for further investigation of RIF encapsulation within the context of the current work.

6. Modulation of rifampicin release from spray-dried microspheres: combinations of low and moderate molecular weight poly(DL-lactide)

6.1 Introduction

In chapter 5, as an alternative to ESE as a preparative technique, spray-drying was demonstrated to be a convenient method for the production of large quantities of biodegradable microspheres as a one-step process from a polymeric solution in which RIF was co-dissolved. Additionally, comparatively fast throughput of a product with high and predictable drug loading and reproducible product character could be achieved. In analogy to ESE, spray-dried biodegradable PDLLA microspheres exhibited a considerable 'burst' release (Bruhn & Müller, 1991) particularly at high drug loadings (Conti et al., 1994) due to the small particle size, large surface area and short diffusional pathlength of these systems as shown in chapter 5. Use of slowly degrading polymers resulted in a reduced 'burst', e.g., RG504 and RG755 but with a protracted terminal release phase.

The permeability of these polymers has been increased by incorporating channelling agents, such as polyethylene glycol (PEG) and polyvinyl pyrrolidone (Lalla and Sapna, 1993). Wichert & Rohdewald (1990) improved the processability of high MW PDLLA by addition of plasticizing PEG to facilitate emulsification of solvent-free disperse phases. Juni et al. (1985b) accelerated the release of bleomycin by inclusion of fatty acid esters to the microsphere matrix. Pluronic™ surfactants have also been investigated as a means to control the initial 'burst' of protein and to modify its long-term release profile (Park et al., 1991). Alternatively, incorporation of protein, bovine serum albumin (BSA), to hydrophobic PLLA has modulated theophylline release by leaching from hydrophilic channels thus formed from directly compressed pellets (Kader & Jalil, 1998a). Release of propranolol HCl and quinidine SO_4 from similarly prepared PLLA composites has been accelerated by addition of PDLLA oligomers and salt (NaCl), whereas reduced release rate was observed from pellets subjected to a post-preparation DCM dipping treatment (Bodmeier & Chen, 1989). Deasy et al. (1993) attained suitable drug release rates from an implant formed from a series of compressed mini-matrices, whereby faster degrading PDLGA adjacent spacers increased the surface area and therefore release rate from active compacts threaded along a single filament. Differential degradation, dependent upon spacer composition, allowed considerable flexibility and a progressive increase in delivery rate of anabolic steroid in response to the increased pharmacological need of the thriving

steers. The use of a terpolymer, poly(D,L-lactide-co-glycolide-D-glucose) has accelerated the release of bromocriptine from spray-dried microspheres by offering preformed break points in the polymer backbone (Kissel et al, 1991).

An alternative approach, whereby the release of RIF, as a model drug, could be modulated, is by varying the proportions of low and moderate MW PDLLA. This technique, which avoids the use of potentially toxic release-controlling excipients, has previously been applied to the release of relatively small organic molecules from films (Bodmeier et al., 1989), o/w solvent-evaporated microspheres (Bodmeier et al., 1989; Le Corre et al., 1994b) and microparticles (Mauduit et al., 1993b). Elkheshen (1996) examined the ternary effects of mixing low and high MW PDLLA and moderate MW PDLGA on microsphere properties prepared by o/o^{l} ESE using a simplex lattice design and surface response methodology based on triangular diagrams. Surface responses illustrated a range of antagonistic and synergistic interactions for microsphere characteristics (e.g., yield, loading, particle size, 'burst' effect) illustrating the interaction between material and process factors. Nonetheless, within the parameters of the study, good correlation of experimental responses and those predicted from model equations was demonstrated. Incorporation of fractions of PDLLA significantly sustained the release of ciprofloxacin from phase separated microcapsules due to the amorphous film-forming character conferred upon the otherwise crystalline PLLA coacervate (Yu et al., 1998). Other reports describe the manipulation of release of therapeutic peptide from implantable polydisperse PDLLA rods prepared by 'melt-pressing' blends of PDLLA of M_n, 1.4 and 11.5 kD (Asano et al, 1991). *In vivo* degradation of rods, MW depletion and pharmacological response all decelerated or decreased in intensity as the proportion of component higher MW PDLLA increased. These trends were paralleled by a progressive shift in the degradation profile from parabolic to sigmoidal. Flandroy et al. (1997) moderated the chemoembolic duration of microspheres prepared with Resomer® R206 (Grandfils et al., 1992) by accelerating the degradation of modified microspheres by incorporation of R104.

Despite the technological advantages of the technique, the approach of blending hydrophobic moderate MW biodegradable material with hydrophilic low MW material to modulate drug release has hitherto not been examined using spray-drying as an alternative to conventional biodegradable DDS preparative methods. The work described in this chapter sought to exploit the favourable features of spray-drying as a preparation

technique, whilst assessing the utility of blending % weight ratios of rapidly and moderately degrading PDLLA on modulation of *in vitro* drug release from these systems.

6.2 Experimental procedures

6.2.1 Microsphere preparation

Microspheres containing 20 %w/w RIF were prepared by spray-drying a solution of drug and polymer in DCM (3 %w/v total solid) through a 0.7 mm nozzle of a Mini Büchi model 191 spray-drier (Flawil, Switzerland): inlet temp., 40 °C; outlet temp., 35 °C; flow rate, 600 NLh^{-1} ; aspiration, 100 %; and, feed rate, 3.5 $mLmin^{-1}$. Microspheres were prepared with blends of R104 and R202H in the weight proportions 0:100,10:90, 20:80, 40:60, 44:56, 48:52, 52:48, 56:44. 60:40, 80:20, 90:10, 100:0 respectively. Under identical conditions, spray-dried RIF and blank microspheres at weight proportions 48:52, 44:56 and 40:60 were also examined. Further studies with new batches of polymer required that optimal proportions of polymer were re-established using weight proportions 40:60, 36:64, 32:68, 31:69, 30:70, 29:71, 28:72, 24:76, 20:80 (R104:R202H). Additionally, the effect of drug loading was examined at 1, 3, 5, 10, 20 and 50 %w/w total weight at polymer weight proportions, R104:R202H, 44:56 and 40:60. All prepared materials were vacuum desiccated at ambient temperature for at least 168 h before examination, unless otherwise stated.

6.2.2 Microsphere characterization

Microsphere characterization was performed as previously described in sections 4.2 and 5.2. with the following modifications. SEM was used for morphological examination of the microspheres after, in addition to before, release studies. Particle size distributions for selected batches were alternatively determined by manual measurement of the diameter of $\geq$ 100 individual particles from SEM photomicrographs.

The thermal behaviour of microspheres during, and after release studies, was additionally examined. Release studies were performed using method B at 33, 35, 39 °C in addition to 37 ± 0.1 °C. First and zero order and power law kinetic models were fitted to 10 - $\leq$ 80 % cumulative release using an iterative curve-fitting programme (CurveExpert version 1.3). Activation energies of drug release were thereafter determined by plotting the logarithm of the first order rate constants against the reciprocal of temperature (K) assuming classical Arrhenius kinetics.

Hydration investigations were performed during concurrent release studies. Samples of microspheres from method B were recovered at predetermined intervals for further thermal and gravimetric investigation. Dissolution medium was passed through a 0.2 μm filter under vacuum (Edwards, Crawley, UK) to recover suspended microsphere residue, then washed with 200 mL of distilled water. Filtration was continued for 20 s after medium had been clarified to remove extra-microspherical surface and interstitial medium. The sample was immediately scraped off the preweighed filter, transferred to a tared glass slide and uniformly spread across the surface of same. Samples were reweighed after 48 h storage *in vacuo* at 24 ± 2.0 °C to determine dried weight and hence the moisture content. Thermal analyses were also performed on hydrated samples. In addition the effect of annealing conditions on thermal behaviour of selected samples at 37 °C was examined.

6.3 Results and Discussion

6.3.1 Microsphere characterization

6.3.1.1 Microsphere morphology and granulometry

Microsphere characteristics are summarized in Table 6.1. Discrete spherical particles with ostensibly smooth morphology as seen in Figure 6.1 were observed from photomicrographs of products irrespective of the polymer used. Particle size distributions were typical of the technique (Pavanetto et al., 1992), being narrow and monodisperse regardless of the polymer blend used. A general increase in mean microsphere diameter within the narrow range from 2.11 to 2.98 μm was observed as the proportion of more viscous PDLLA, R202H, increased from 10 to 90 %w/w total polymer (Table 6.1). The unimodality of particle size distribution was further illustrated by the fact that at all weight proportions studied, more than 95 % of particles were < 10μm. These results were consistent with the factors discussed in section 5.3.3which affect particle size distribution of products prepared by spray-drying.

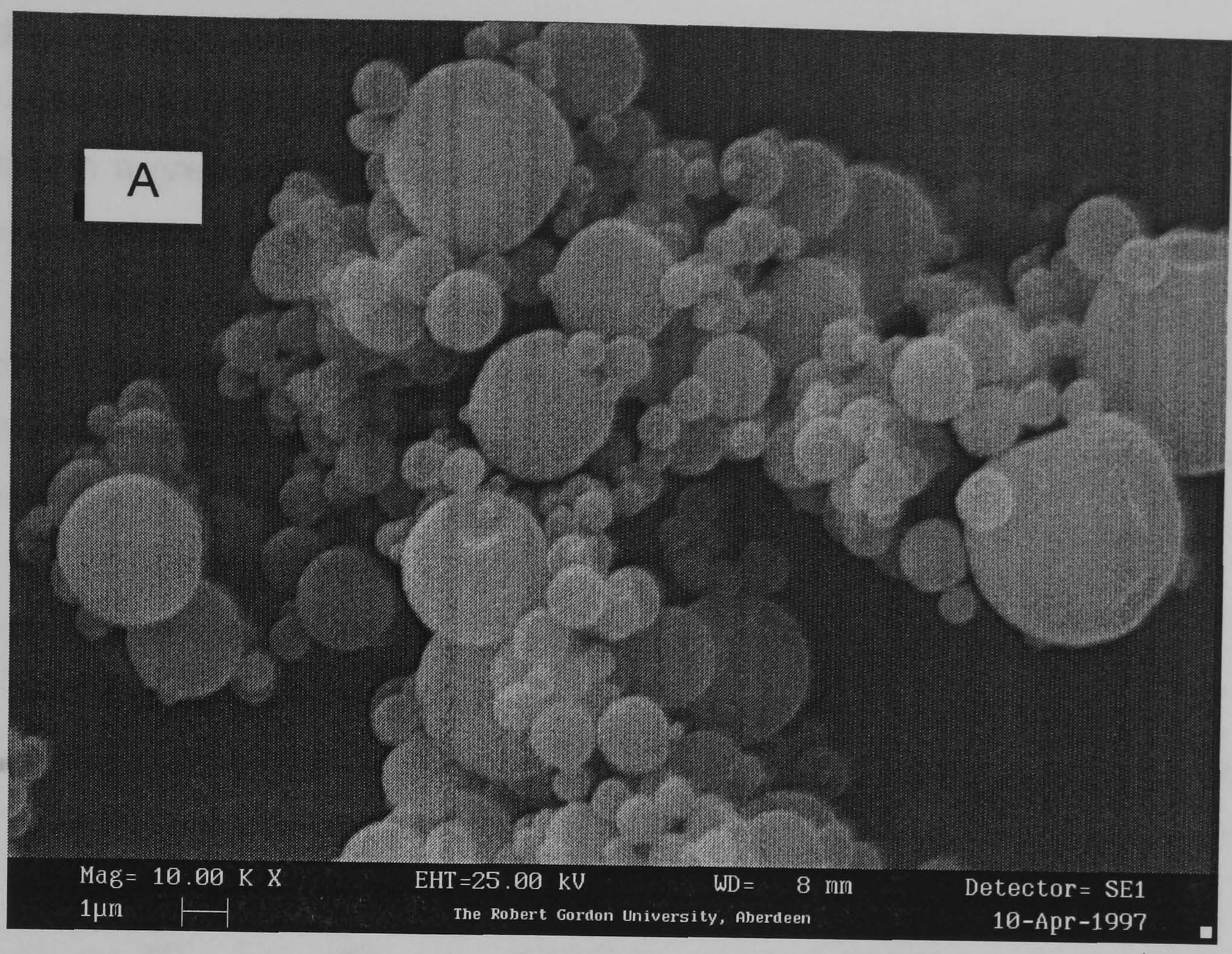

Figure 6.1 *Scanning electron micrographs of spray-dried microspheres containing 20 %w/w rifampicin prepared at weight proportions of Resomer® R104:R202H of A) 90:10 and B) 10:90 (3 %w/v total solid)(mag^n x 10^4).*

An additional factor affecting microsphere size is the deposition kinetics of the polymer blend. Low MW polymers have a greater solubility in DCM and hence during microsphere preparation a greater fraction of the solvent must be removed before solidification and microsphere formation occurs. Consequently, the greater the fraction of low MW PDLLA used, the higher the polymer concentration in the microdroplet at the point of polymer precipitation and the greater the density (and lower the porosity) of the matrix. Assuming identical microdroplet volume at the point of generation, particle size should accordingly decrease in parallel with overall polymer composite MW.

Table 6.1 *Summary of microsphere characteristics, n=3*

Batch	Polymer composition		Yield / % (RSD)	d_{50} / μm (RSD)	Endothermic peak / °C
	R104	R202H			
1	100	0	55.8 (6.4)	2.01 (3.4)	54.1
2	90	10	63.3 (2.2)	2.11 (5.5)	55.3
3	80	20	63.4 (0.1)	2.39 (1.3)	55.3
4	60	40	69.9 (9.5)	3.14 (3.9)	57.2
5	56	44	65.0 (6.5)	2.45 (5.1)	57.9
6	52	48	67.1 (6.5)	2.65 (2.6)	58.1
7	48	52	67.2 (1.5)	2.61 (4.2)	58.2
8	44	56	65.1 (2.1)	2.73 (0.8)	58.0
9	40	60	73.3 (3.2)	2.77 (4.7)	58.0
10	20	80	73.8 (4.2)	2.69 (1.4)	58.2
11	10	90	80.7 (2.3)	2.98 (0.7)	58.7
12	0	100	75.5 (9.3)	3.23 (2.3)	59.3
13	48*	52*	51.2 (3.9)	3.01 (2.3)	42.5
14	48*	56*	46.2 (5.3)	3.12 (6.3)	39.4
15	40*	60*	50.3 (5.4)	3.42 (3.5)	34.9

* blank microspheres

6.3.1.2 Microsphere yield

Yields of production progressively increased overall within the range 55.8 - 80.7 % of the total dissolved solid (1.5g) as the fraction of R202H increased as can be seen in Table 6.1. These data correlated semi-quantitatively with the slight and progressive increase in softening onset from 54.1 to 59.3 °C as the fraction of R202H increased. Under identical process conditions, yield of production decreases as a function of physicochemical factors of the drug - polymer composite, such as softening onset and the affinity of the polymer for the feed solvent increase. Consequently, these two factors culminate in a reduced product yield as the fraction of low MW PDLLA increases attributable to a greater fraction of the total product adhering to the hot glassware walls. Nonetheless, use of a reduced inlet temperature and low boiling point solvents, such as DCM, resulted in comparatively high product yields compared with previous reports where higher boiling

point solvents, such as CFM (Bodmeier & Chen, 1988), or cosolvents of this with DCM (Pavanetto et al., 1992; 1993) were employed. Finally, thread production due to insufficient force at the spray nozzle can further contribute to poor product yield. However, air flow rates of, or above, 600 NLh^{-1} overcame the intermolecular polymer interactions responsible for this phenomenon (Bodmeier & Chen, 1988) resulting in efficient spray and subsequent microsphere formation at a polymer concentration of 2.4 %w/w irrespective of polymer composition.

6.3.1.3 Drug loading

As in chapter 5 where individual polymers were used, drug loading was found to be quantitative with the proportion of RIF initially dissolved in the feed ($P > 0.05$).

6.3.1.4 *In vitro* drug release

Studies of a range of poly-α-hydroxy acids in chapter 5 identified two racemic PDLLA materials, R104 and R202H, which upon combination might modulate the release of drug from each when used alone, i.e., addition of low MW R104 would accelerate the release of RIF from moderate MW R202H and vice versa. In comparison to PDLLA of similar MW, the Resomer® H series are more hydrophilic, possessing free carboxylic acid end-groups which are not end-capped via esterification with alcohols. Consequently, water uptake, associated deesterification, erosion and drug release are all more rapid when compared with their end-capped equivalents (Mehta et al., 1996; Rothen-Weinhold et al., 1997).

Preliminary examination of release kinetics of RIF from microspheres prepared with relatively large compositional changes showed a dramatic shift in release profile between 40 and 60 %w/w R104 as seen in Figure 6.2. The gradual effect of increased release rate with increased low MW polymer as anticipated and reported elsewhere for films (Mauduit et al., 1993c) and solvent-evaporated microspheres (Bodmeier & Chen, 1989), was not however realized. Clearly, properties of the polymers and their interaction with their environment were contributing to the release profile at a finite polymer composition. Zhou & Chang (1988) proposed a critical MW existed, around which the release pattern of drug varied significantly. They did not, however, elaborate on the physicochemical factor(s) affecting this value.

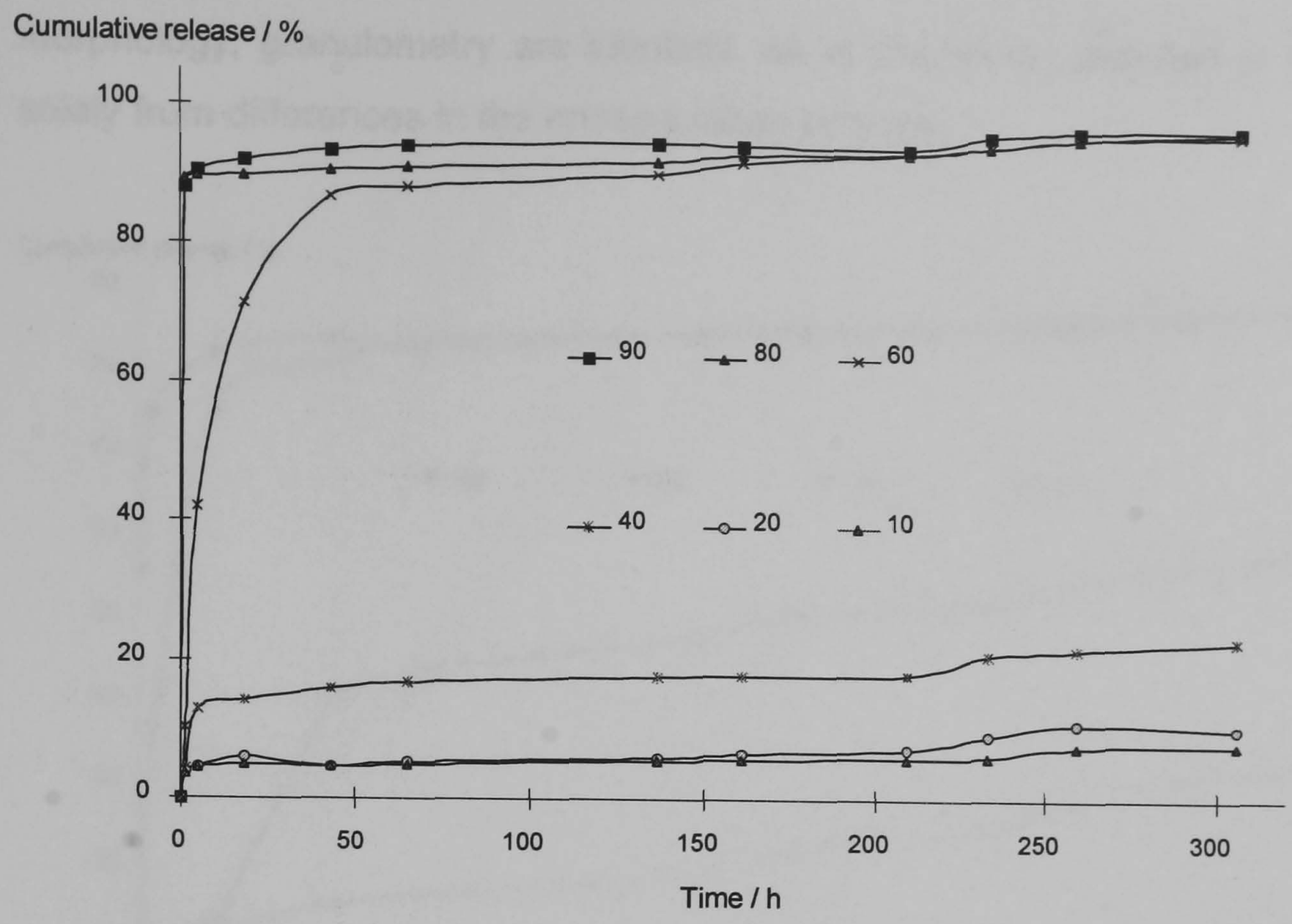

Figure 6.2 *In vitro release profiles from microspheres containing 20 %w/w rifampicin at wide matrix compositional intervals using method A at 37 ± 0.5 °C, n = 3. (legend indicates the matrix composition expressed as %w/w Resomer® R104) (standard deviation ≤ 5.0)*

Figure 6.3 represents the release profiles of RIF between the range of polymer composition of 40 - 60 %w/w R104. The general trend of increased release rate was observed, consistent with polymer composition. However, disproportionate differences were evident between 44 and 48 %w/w R104. In general terms, PDLLA polymers release entrapped drugs by a mechanism initially dependent upon diffusion of drug bound to, or near, the superficial areas of the microsphere surface. Subsequent to this initial phase, dissolution and erosion of oligomeric fractions generated by hydrolytic chain scission is the predominant mechanism which facilitates drug release. During this phase, an increase in pore volume within the matrix leads to the formation of aqueous channels. The inclusion of low MW R104 might serve to propogate pore genesis via leaching of low MW material to the release medium (Bodmeier et al., 1989; Fukuzaki et al., 1989; Le Corre et al., 1994a). The relative extent of these phases are determined by the nature of the entrapped drug (solubility, MW, drug loading and physical form) and the coating polymer (polymer MW and MW distribution, copolymer ratio, sequential distribution of comonomers and crystallinity). Where drug loading and microsphere characteristics, e.g.,

morphology, granulometry are identical, as in this study, changes in release rate arise solely from differences in the encapsulating polymer.

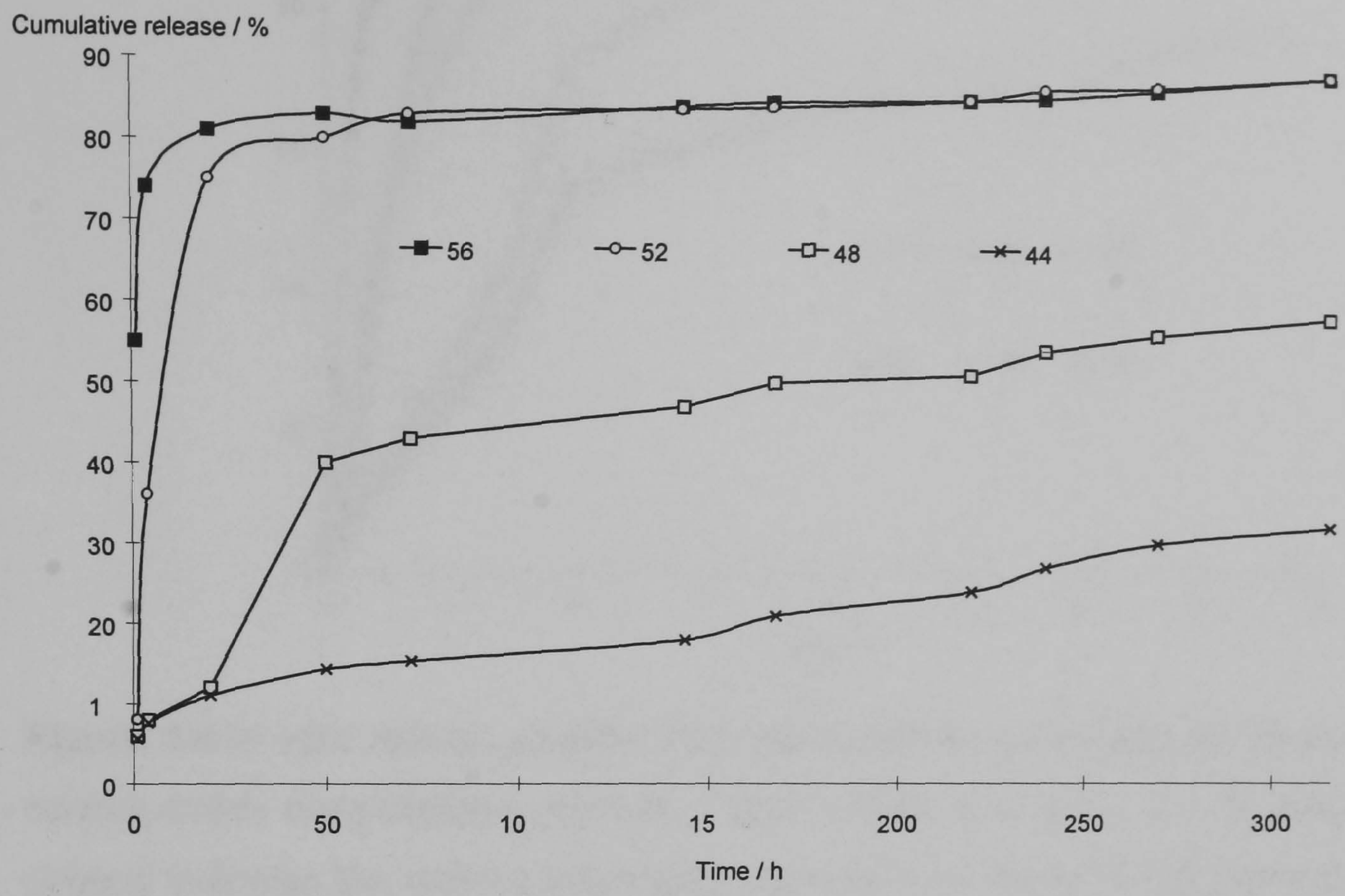

Figure 6.3 *In vitro release profiles from microspheres containing 20 %w/w rifampicin at narrow matrix compositional intervals using method A at 37 ± 0.5 °C, n = 3. (legend indicates the matrix composition expressed as %w/w Resomer® R104) (standard deviation ≤ 5.9).*

The marked difference in dissolution rate which are apparent in Figure 6.4 when method B (USP II paddle) was used was attributed to the considerably greater and three dimensional agitation afforded by the paddle method when compared to method A (shaking bath). In method A, the microspheres aggregated at the base of the vessel as opposed to remaining suspended and individualized in method B. Under the aggregated conditions which prevail in method A, the available surface area from which drug can be liberated via diffusion is markedly reduced, whereas the stationary diffusion boundary associated with the diffusion surface is greatly enhanced. These factors culminate in a multi-fold reduction in drug release rate.

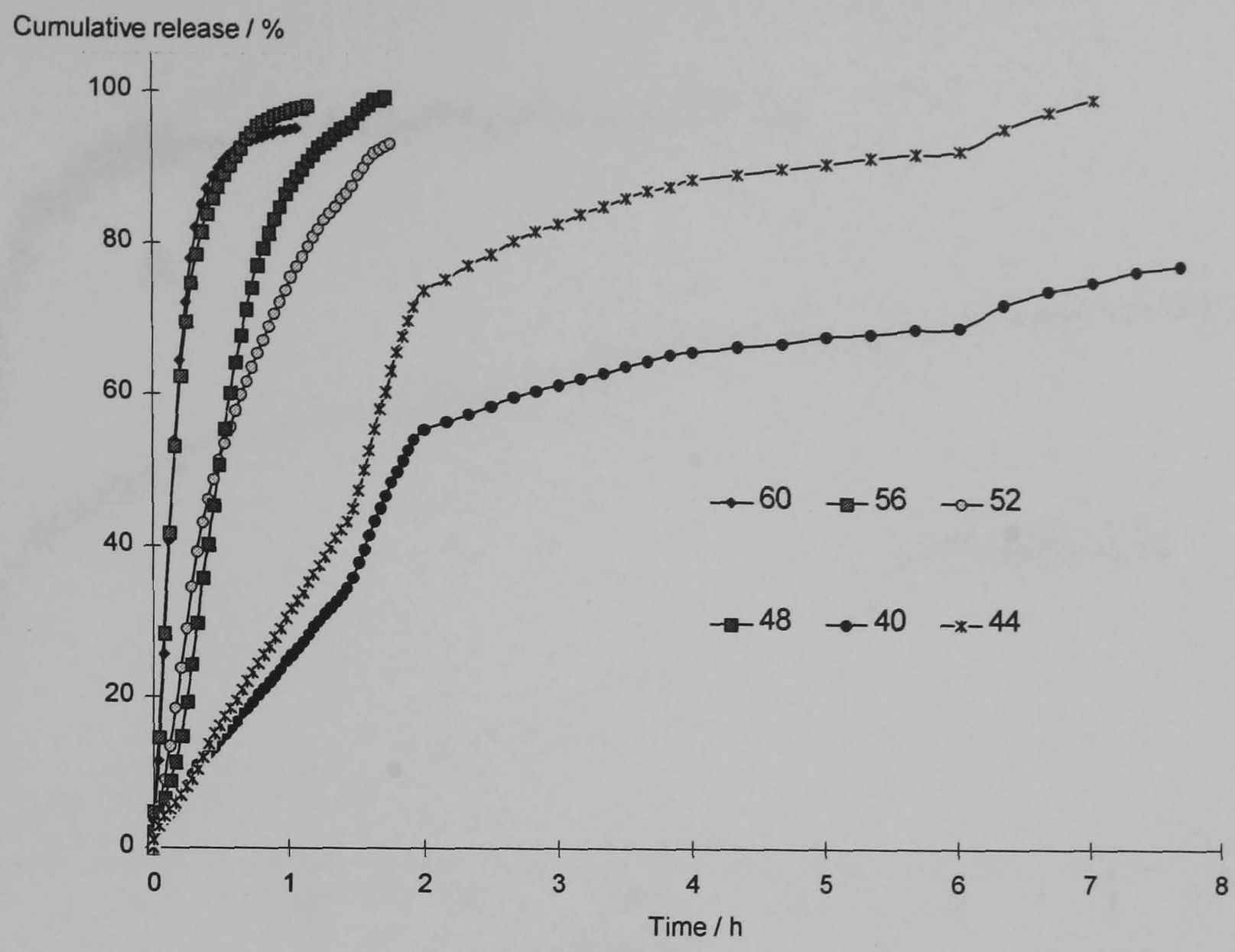

Figure 6.4 *In vitro release profiles from microspheres containing 20 %w/w rifampicin at narrow matrix compositional intervals using method B at 37 ± 0.1 °C and 100 ± 1 rpm (legend indicates the matrix composition expressed as %w/w R104) (standard deviation ≤ 2.0).*

Studies of the release at different stirring rates shown in Figure 6.5 supported this, whereby insufficient agitation at reduced stirring rates resulted in a plug of aggregated microspheres, which, after settling to the base of the dissolution vessel, showed a very slow release of residual drug. The dependence of drug release profile on dissolution methodology has been reported elsewhere, albeit not as pronounced (Conti et al., 1995b). A further contribution to the dramatic differences in release rate for the two methods may have arisen due to slight variability in temperature control. The more stringent control with method B, i.e., ± 0.1 °C compared with method A, i.e., ± 0.5 °C, may have considerably influenced the release profile due to the temperature dependent release observed in Figure 6.6. Overall, these data highlight the need for careful consideration of experimental variables when studying the *in vitro* release of drugs from long acting DDS. Moreover, wide variation in these data invalidates extrapolation of such results to their prospective *in vivo* performance.

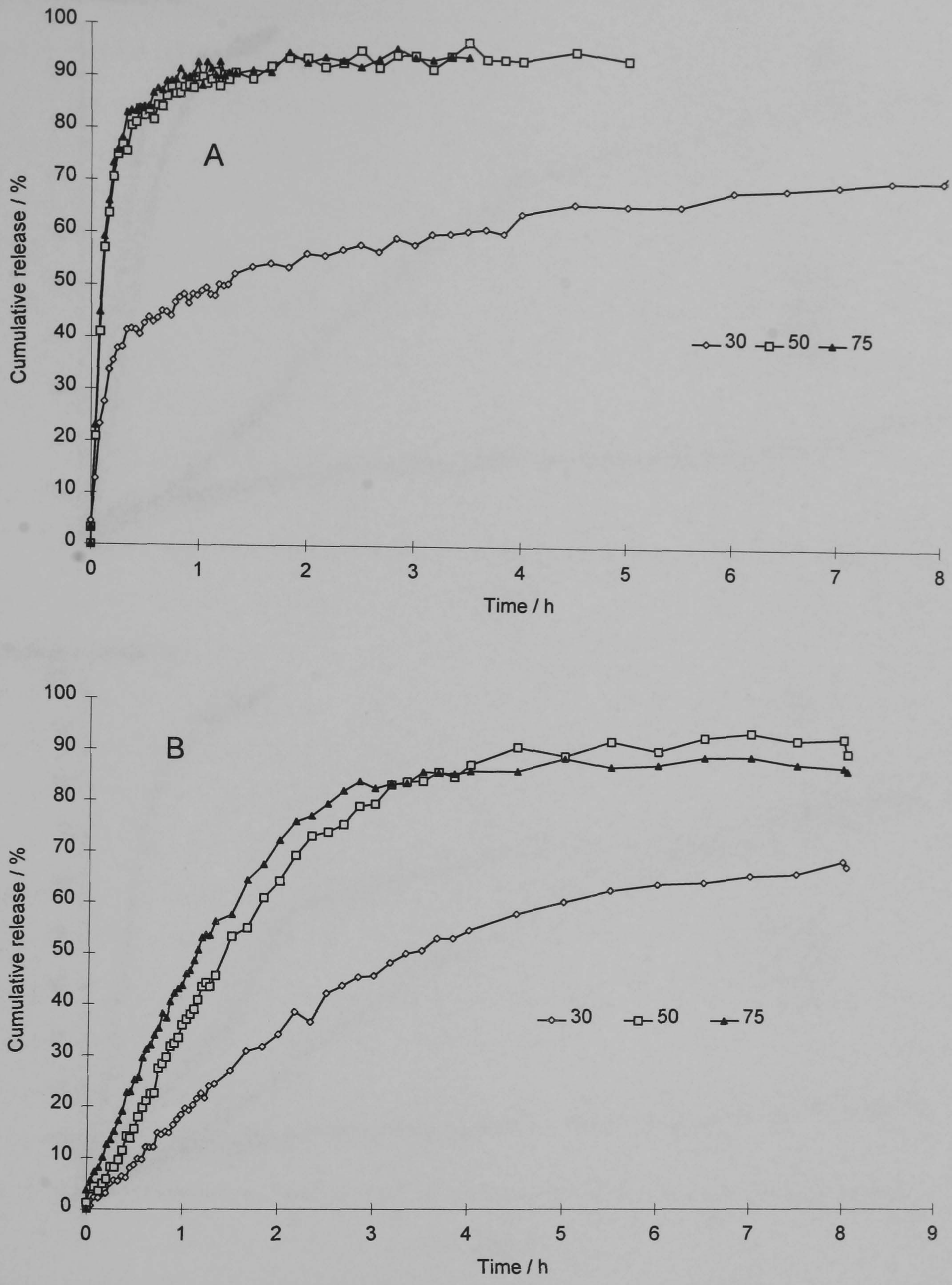

Figure 6.5 *In vitro release profiles from microspheres containing 60% (A) and 48% (B) R104 illustrating the effect of stirring rate on drug release using method B at 37 ± 0.1 °C, n = 3 (legend indicates the stirring rate expressed as rpm) (standard deviation ≤ 3.4).*

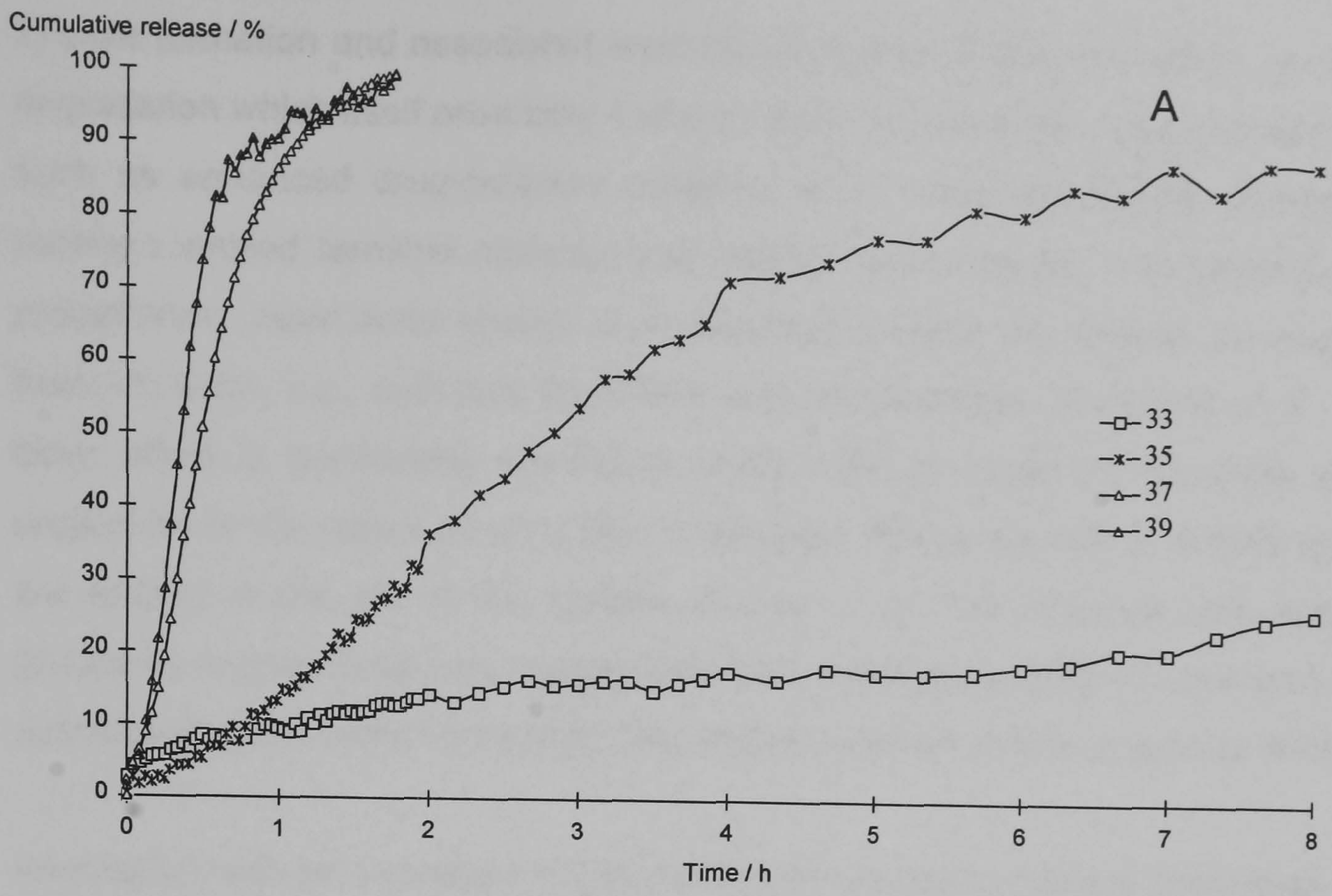

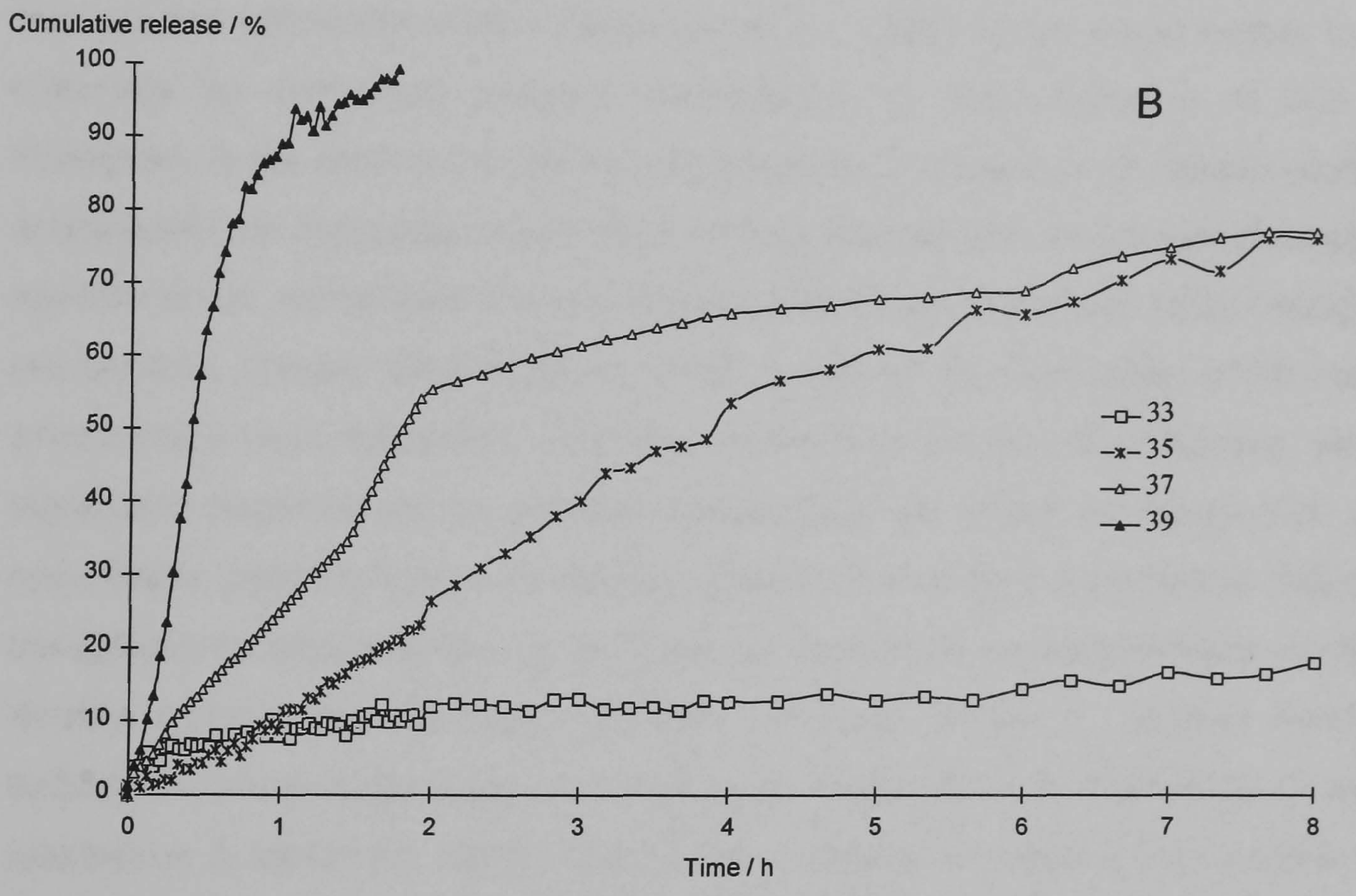

Figure 6.6 *In vitro release profiles from microspheres containing: A, 48 %w/w: and, B, 44 %w/w R104 illustrating the temperature dependent release observed using method B at 100 ± 1 rpm, n = 3 (legend indicates the temperature of release medium ± 0.1 °C) (standard deviation ≤ 2.0)*

A number of competing factors are influential to the release of drug by diffusion from matrices prepared with a fraction of PDLLA oligomers (Bodmeier et al., 1989; Le Corre et al., 1994b). On one hand, faster drug release may be attributed to: 1) the reduction of T_g;

2) pore formation and associated leaching of oligomers from the matrix, and; 3) polymer degradation which itself promotes 1 and 2 above. On the other, drug-polymer interactions, such as enhanced drug-polymer solubility, and, more significantly, charge interaction between ionized terminal carboxyl and tertiary amine groups, and consequent complex precipitation, have been shown to significantly impede the release of drugs with such basic moieties, e.g., quinidine from films and microspheres (Bodmeier et al., 1989). This latter effect is particularly significant where PDLLA oligomers comprise a substantial proportion of the matrix volume due to the high charge density of COOH groups, which are ionized at the pH of the release studies (7.4). The effective end-capping of such groups by counter drug ions complicates the anticipated pattern of increased release rate associated with a more hydrophilic, and hence hydrated matrix of greater diffusivity.

Associated with an increased matrix density of ionizable carboxyl endgroups is a greater free volume within the matrix (Bodmeier et al., 1989) which would further improve drug diffusivity by increasing polymer permeability as the proportion of low MW R104 increased. In the absence of confounding factors, a continuum of release profile would be anticipated with a gradual acceleration of drug release with an increased matrix fraction of low MW R104, rather than the pronounced differences noted with small changes in matrix composition. Clearly other factor(s) which governed the interaction of the matrix with its environment were influential. That the mechanism and the drug release rate showed a significant dependence on polymer composition as shown in Figure 6.4, and also a remarkable dependence on temperature as illustrated by the profiles in Figure 6.6, were considered to implicate the T_g as a pivotal parameter in determination of drug release kinetics owing to its influence on matrix diffusivity. At the T_g, intrinsic matrix energy is sufficient to move large segments of polymer chains (20 - 50 consecutive carbon atoms) (Omelczuk & McGinity, 1992). Such motion requires increased free volume and is thus associated with a change in the polymer's expansion coefficient. These molecular changes greatly facilitate mass transfer by diffusion. Correlation of drug release and the matrix T_g *per se* was not, however, established. The results were attributable to principally a reduction in the T_g of the microspheres upon incubation, the magnitude of which was inextricably linked to the inherent hydrophilicity of the polymer blend, which increased as the proportion of R104 increased.

In general terms, as water ingresses, matrix plasticization occurs, and the thermal character of the polymer changes as the matrix softens. Once the softening temperature

of the matrix bulk decreases below the temperature of the release medium, water uptake accelerates, thus promoting drug release. Accordingly, at a critical polymer composition, the inherent hydrophilicity of the matrix is such that the water uptake, and thus matrix plasticization, reduces the T_g to a value which approximates to the temperature of the dissolution medium. Where medium and T_g temperatures equate, water uptake increases, matrix softening propagates and drug release occurs at a controlled rate as the diffusive properties of the matrix slowly change under the influence of ingressing water. Outwith this range, release is either uncontrollably fast — where inherent hydrophilicity overshadows the influence of T_g —or unacceptably slow — where insufficient depression of T_g arises due to matrix hydrophobicity. In the latter case, the critical MW or polydispersity at which matrix hydrophilicity represents correspondence of the T_g and medium temperatures, occurs subsequent to ongoing matrix deesterification. The sigmoidal patterns of release comprising induction and acceleratory phases observed by Bodmeier & McGinity (1987a-c; 1988a) and Ramtoola et al. (1992) with quinidine and fluphenazine respectively, were consistent with the mechanism of release described herein and the central importance of an evolving polymer T_g. The autocatalytic degradation mechanism (whereby propagation of active sites by COOH generation and catalysis), described in particular by Ramtoola et al. (1992), did not consider the role of matrix T_g, but that increased diffusivity was associated with enhanced microsphere permeability, not enhanced molecular mobility of the polymer chains. That said, it is recognized that the degradation rate should be substantially accelerated as the matrix enters the rubbery hydrated state where chain motion is freed and hydrolytic accessibility is enhanced by the concomitant increase in free volume.

In the context of the proposed role of matrix T_g, as dissolution medium temperature is elevated, the smaller the differential between the T_g of the plasticized matrix and the medium temperature. Therefore, for each matrix composition there exists a narrow range of temperatures at which drug release rate shows a significant rise. At 37 °C, matrices comprised of ≥ 48 %w/w R104 represented a composition above the critical value, leading to single rapid release phase. In Figure 6.6 by elevating the temperature at which release was studied, approximately superimposable profiles of drug release are observed for matrices with higher R202H content. This further highlights the interplay of dissolution medium temperature and polymer composition on drug release.

6.3.1.5 Thermal analysis

DSC thermograms in Figure 6.7 represented a monodisperse matrix characterized by a single T_g temperature indicative of an homogeneous dispersion of drug and polymeric fractions throughout the matrix. Spray-drying of RIF resulted in an apparent destruction of the crystallinity evident with unprocessed drug. This was corroborated by the fact no crystalline melting endotherm or recrystallization exotherm for RIF were noted with drug-loaded microspheres. The endothermic peak which overlaid the T_g of the polymeric matrix was attributed to internal stresses created during the rapid evaporation of the solvent during micro-droplet drying. This pattern is comparable to that observed with biodegradable microspheres prepared using an aqueous ESE technique. In contrast, however, Bodmeier et al. (1989) observed a greater reduction of the T_g temperature with solvent cast films compared to microspheres thus prepared which they attributed to leaching of low MW polymeric fractions to the aqueous continuum with the latter technique. It appeared that the T_g position is influenced by the microsphere formation mechanism, which Bodmeier et al. (1989) cited as being rapid, a feature which according to these workers accounted for the high drug loading and minimum partitioning of the drug outwith the disperse phase. However, under these microsphere formation conditions it would seem unlikely that low MW polymer would be leached in preference to drug. The results of Bodmeier et al. (1989) were more likely attributable to higher residual organic solvent burdens in films when compared to microspheres of identical composition. A further endothermic event persisted beyond the main endotherm, which can be seen as a tail on this main peak. Limited thermal gravimetric analysis excluded residual solvent as the cause. Hot stage microscopy showed a dramatic colour change from the characteristic orange of RIF to yellow suggesting solubilization of the drug within the rubbery matrix.

Figure 6.7 shows the thermograms of microspheres before and during release studies (method A, 7 d) for microspheres composed of 44 and 48 %w/w R104. Distinct changes in matrix microstructure were evident after 7 d incubation characterized by a broadening of the endothermic peak and its downshift to transitions of lower temperature. Initially, this reduced onset, particularly at 48 %w/w R104, was considered attributable to oligomeric fractions generated by the hydrolysis of the component polymers. However, the degree of hydration, which plays a key role in drug release from these systems, results in a diverse population of microsphere residue and thus accounts for the broad endotherm observed. Significantly, although this broad endotherm persisted with combinations containing 44

%w/w R104, superimposed upon this was the original endothermic peak indicating partial preservation of matrix integrity thus further accounting for the slower release from this combination.

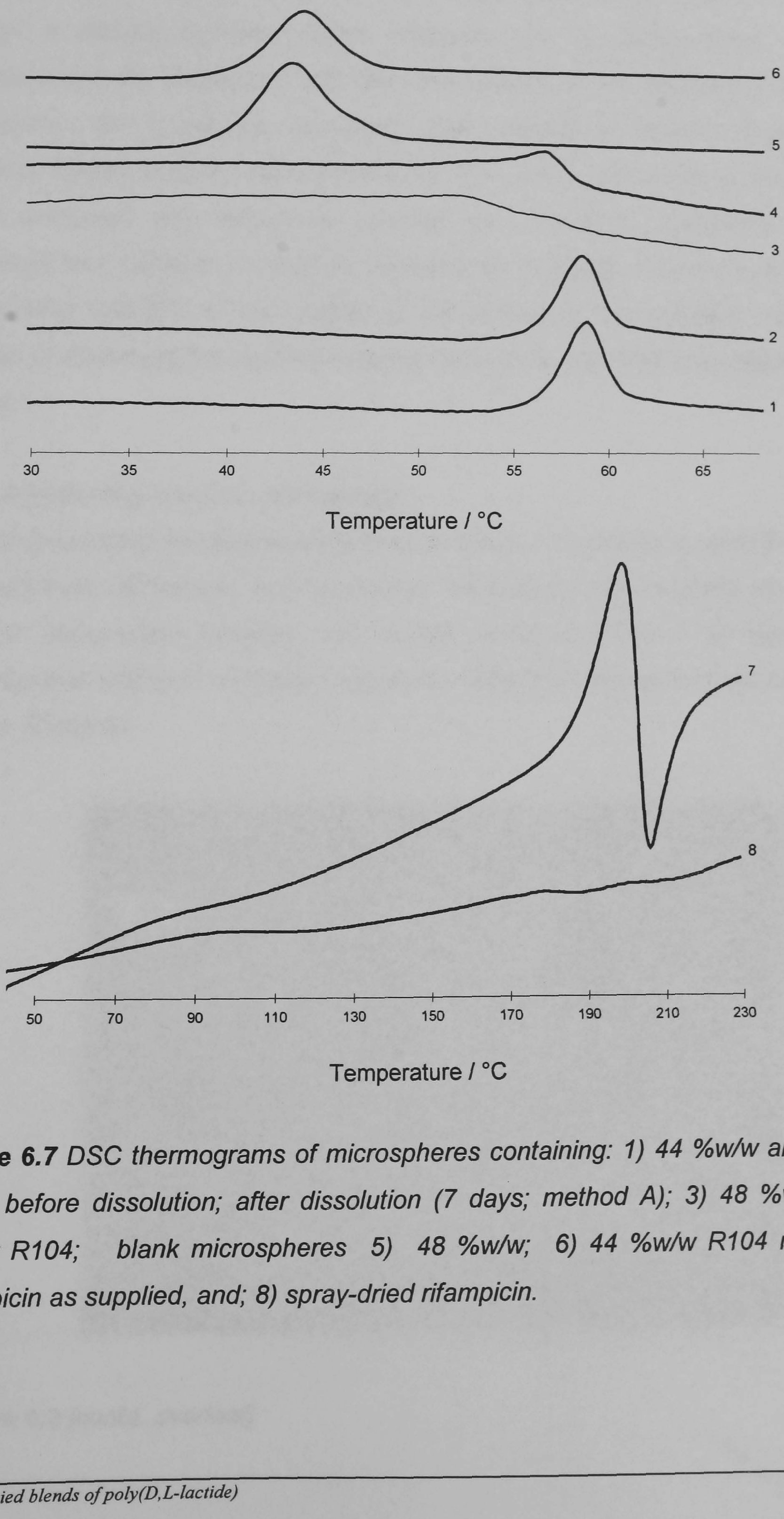

Figure 6.7 *DSC thermograms of microspheres containing: 1) 44 %w/w and 2) 48 %w/w R104 before dissolution; after dissolution (7 days; method A); 3) 48 %w/w and 4) 44 %w/w R104; blank microspheres 5) 48 %w/w; 6) 44 %w/w R104 respectively; 7) rifampicin as supplied, and; 8) spray-dried rifampicin.*

Furthermore, the position of the endotherm is shifted up-scale by increased residue of interposing drug molecules at higher drug loadings which are thought to maintain polymer chain stiffness within the matrix. This was confirmed by the thermograms of the corresponding blank microspheres which exhibited a markedly reduced T_g temperature. Therefore, the downshift of this endotherm supports the fractional loss of RIF by diffusion through a partially hydrated matrix. However, the T_g temperature of the samples assessed did not correspond with the temperature of the dissolution medium. During desiccation, the T_g partially recovered upon removal of aqueous plasticizer. Indeed, Siemann (1985) recorded reductions of 18 °C in the T_g temperature of hydrated PDLLA when compared with anhydrous polymer, i.e., conditions conducive to significantly enhanced drug diffusion. In order to establish the interplay of matrix hydrophilicity and T_g of hydrated matrices in the context of the proposed autohydration mechanism, DSC studies of recovered microsphere residue from release studies are described later in this chapter.

6.3.1.6 Scanning electron microscopy

Scanning electron micrographs presented in Figure 6.8 partially support these arguments. No significant differences in microsphere morphology were evident around the critical polymer composition whereas, only at high levels of R104, > 80 %w/w, were overt microsphere softening and fusion observed, whilst the original microsphere outline could still be discerned.

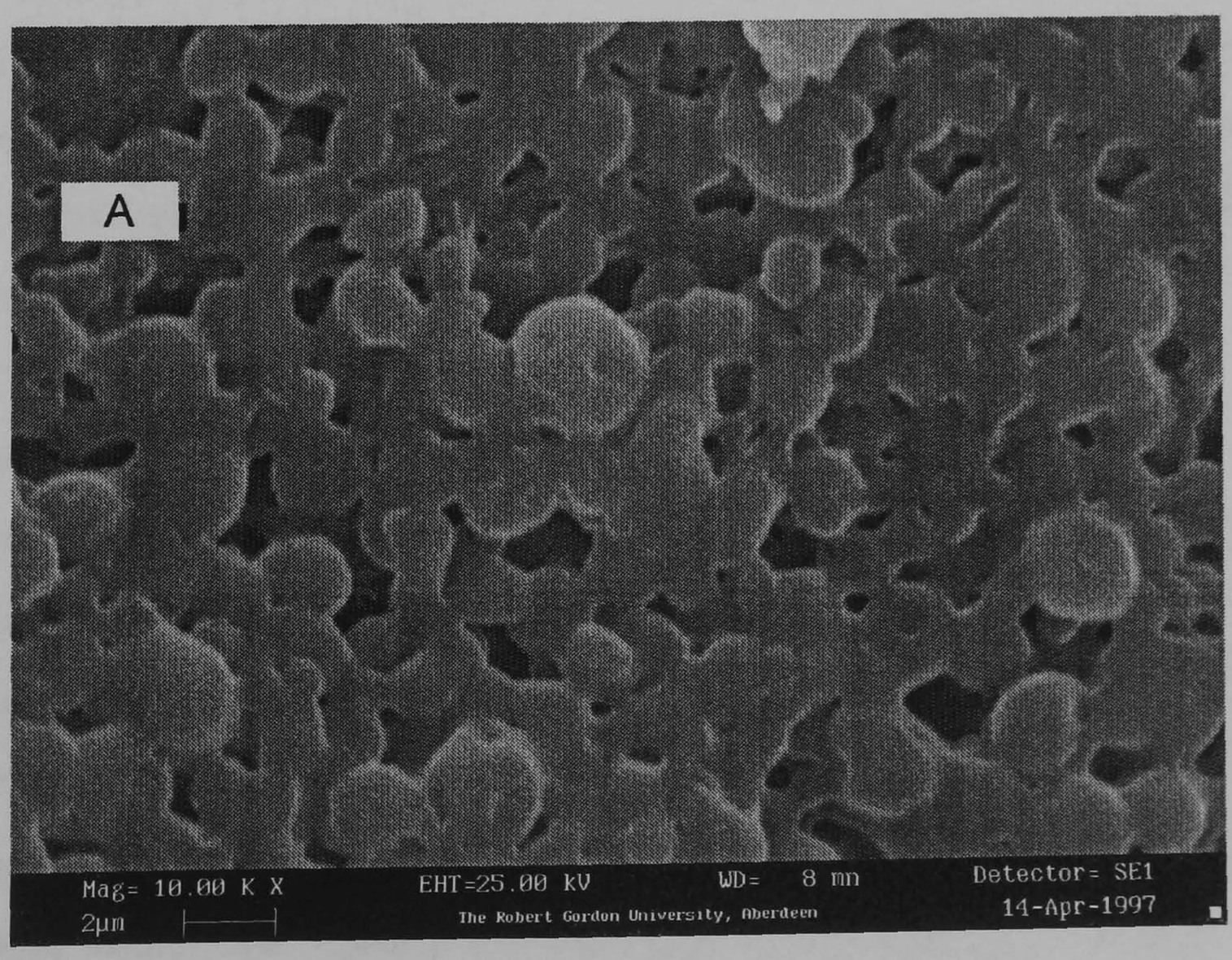

***Figure 6.8** [contd. overleaf]*

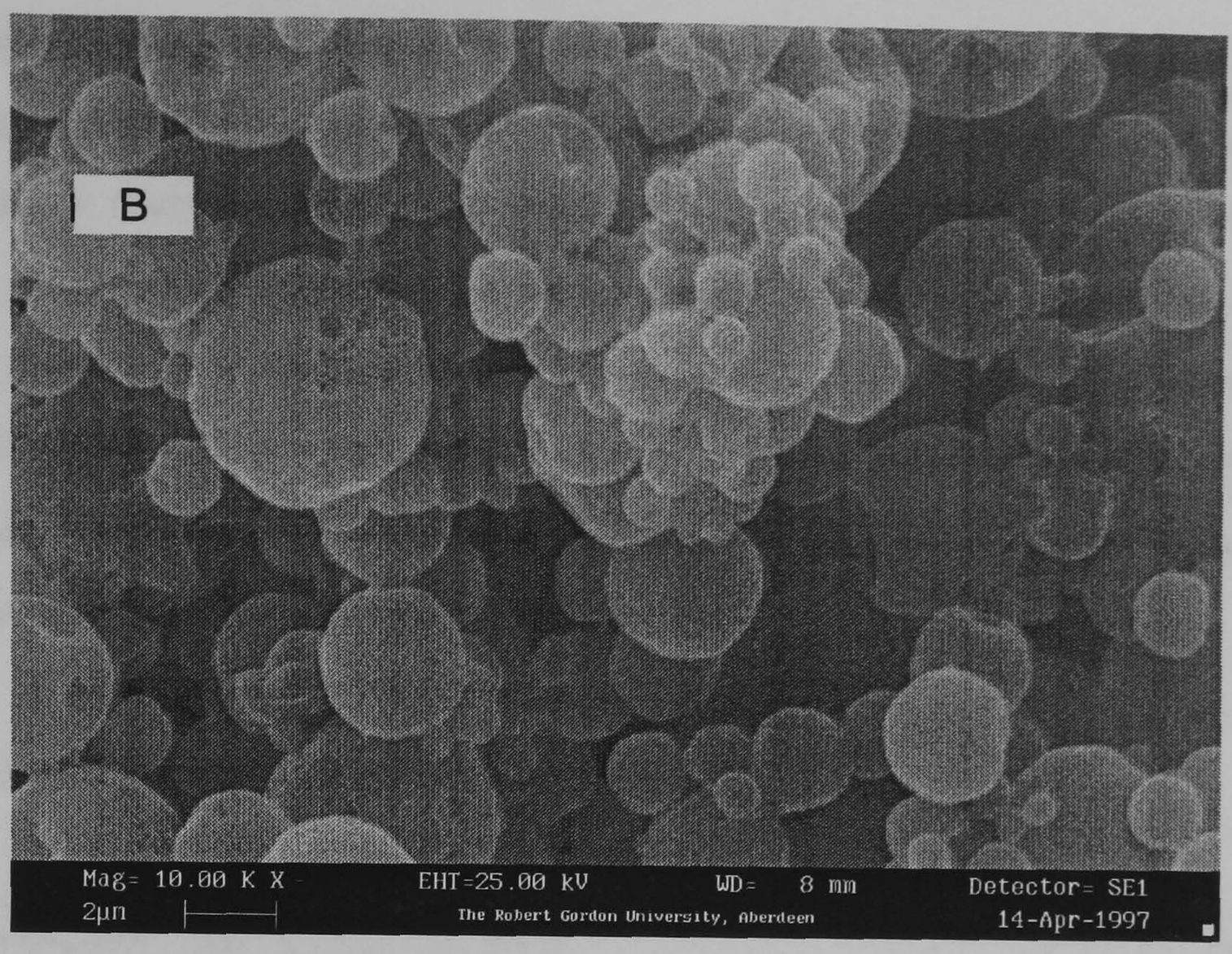

Figure 6.8 *Scanning electron micrographs of spray-dried microspheres remaining after dissolution for 7 d using method A at 37 ± 0.1 °C prepared at weight proportions of R104:R202H of A) 90:10 and B) 44:56 (magnification x 10^4).*

6.3.2 Further studies of PDLLA blends

In order to confirm criticality of composite T_g and, assess the relative importance of erosion and diffusion to overall drug release, complementary gravimetric, hydration and erosion studies, in parallel with thermal and drug release investigations were performed. In addition, due to the apparent sensitivity of drug release to matrix composition, separate batches of R104 and R202H were re-examined to: 1) to investigate the robustness of this approach to the regulation of drug release; and, 2) to ensure an adequate mass of microspheres for comprehensive characterization. The effect of drug loading on microsphere characteristics of reprepared blends was also examined. Production attributes of these microspheres are listed in Table 6.2.

6.3.2.1 Effect of drug loading on microsphere characteristics

Thermograms in Figure 6.9 illustrate the progressive elevation of T_g as drug loading increased (as tabulated in Appendix 2), consistent with the deposition of insoluble drug throughout the matrix. Owing to an increase in microsphere T_g temperature and a reduced affinity of the matrix for DCM, yield of production generally increased with drug loading. Drug particles uniformly dispersed throughout the matrix served to enhance chain stiffness; molecular rigidity increasing with volume and number of interposing particles. Prior to thermal comparison, peak area normalization with respect sample size

and also polymer proportion was performed. Irrespective of this treatment, the energy of the anomalous endotherm decreased with increased drug loading, indicative of reduced stress-relaxation due to restricted chain motion imposed by elevated levels of drug. Batches of matrix composition 44:56 (R104:R202H) (#16 - 21) behaved similarly. Attempts to linearly (r^2 = 0.894) and logarithmically (r^2 = 0.921) equate drug loading for #22 - 27 with T_g displacement (and the endothermic area, r^2 < 0.900) were, however, unsuccessful. The lack of linearity was partially attributable to the fact that a fraction of RIF was considered to exist in solid solution.

Table 6.2 *Microsphere composition and yields of production*

Batch	Matrix composition			Yield / % total solid		
	Polymer / %w/w total polymer					
	R104	R202H	RIF / %w/w	Collector	Cyclone	Total
16	44	56	1	42.7	22.0	64.7
17	44	56	3	41.3	22.0	63.3
18	44	56	5	46.7	21.3	68.0
19	44	56	10	32.7	28.0	60.7
20	44	56	20	40.0	29.3	69.3
21	44	56	50	47.3	31.3	78.7
22	40	60	1	45.0	18.0	63.0
23	40	60	3	42.0	21.7	63.7
24	40	60	5	32.7	37.7	70.3
25	40	60	10	21.3	41.3	62.7
26	40	60	20	25.3	42.7	68.0
27	40	60	50	42.0	31.7	73.7
28	40 [a]	60	20	16.7	56.7	73.3
29	40	60	20	16.7	60.7	77.3
30	36	64	20	38.7	42.0	80.7
31	32	68	20	27.0	37.0	64.0
32	31	69	20	35.7	40.7	76.3
33	30	70	20	42.3	46.0	88.3
34	29	71	20	21.7	60.7	82.3
35	28	72	20	40.5	31.0	71.5
36	24	76	20	33.5	39.5	73
37	20	80	20	37.0	30.5	67.5

[a] prepared with original batch of polymer

The effect of annealing samples at 37 °C for various times was investigated to examine the microspheres response when subjected to the simulated heat of the release study, the data for which are shown in Appendix 3. Generally, as duration of annealing increased, all thermal indices moved up-scale due to the loss of plasticizing residual

solvent. It was therefore concluded that the influence of heat alone did not significantly alter the character of the matrix, nor did it account for the pattern of release observed. The results did, however, indirectly confirm the mutual interaction of microsphere hydration and thermal behaviour.

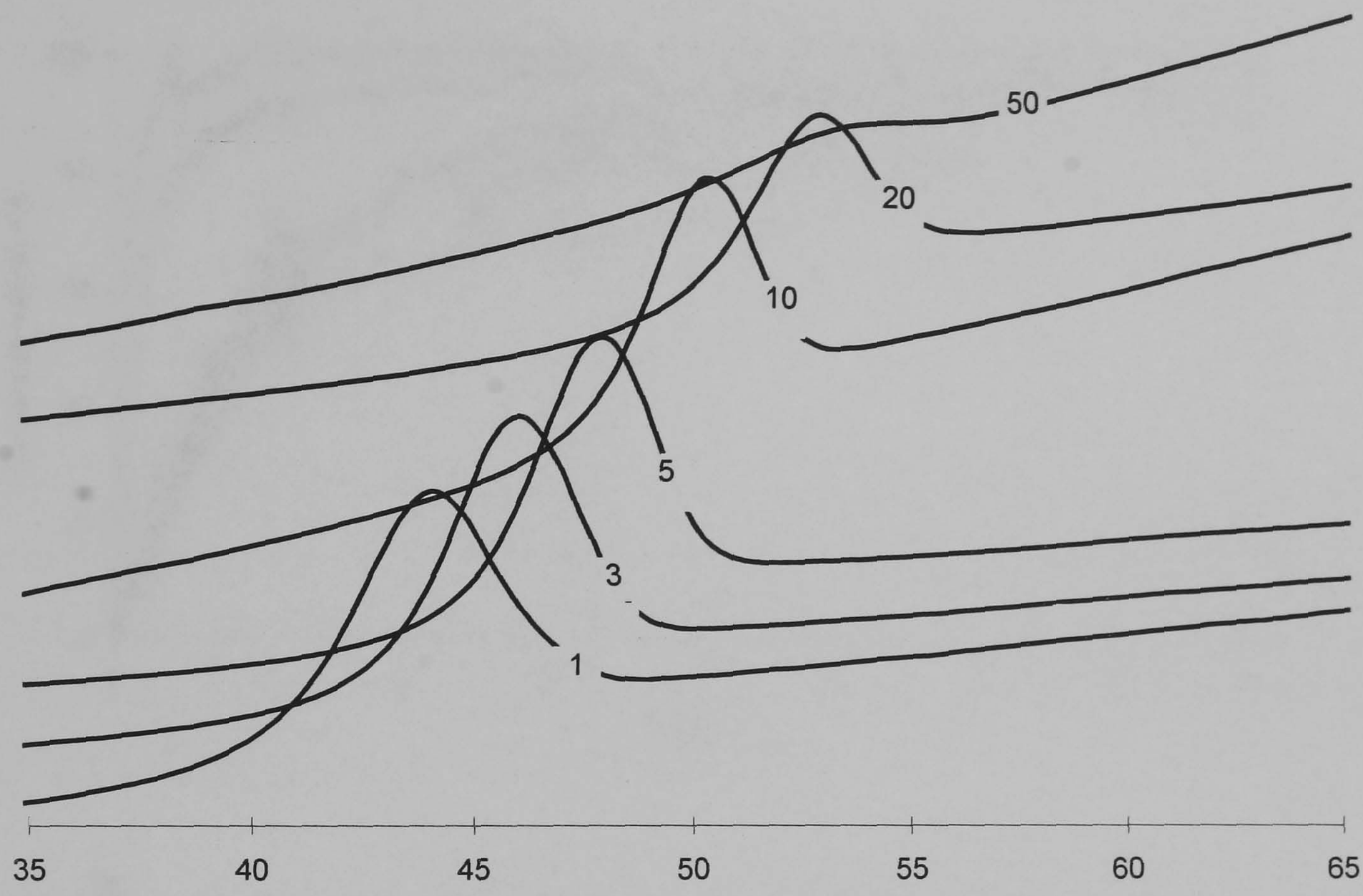

Figure 6.9 *Normalized DSC thermograms of microspheres with a matrix polymer composition of 40:60 (R104:R202H). Labels indicate rifampicin loading in units of %w/w.*

The corresponding release profiles of batches prepared from 44 %w/w (#16 - 21) and 40 %w/w R104 (#22 - 27) are shown in Figure 6.10. Release rate was faster, as anticipated from microspheres of equivalent drug loading, as the level of R104 increased. Release rate also increased as the drug loading increased, commensurate with a relative reduction in the amount of available encapsulating polymer and the propensity of the matrix to a pore leaching, rather than a matrix diffusion release mechanism. Moreover, release rates as defined by first order rate constants were faster — #21, 1.804 h^{-1} (r^2 = 0.978); #28, 1.974 h^{-1} (r^2 = 0.982) — when compared with that obtained from the original batch of polymers — #8, 0.699 h^{-1} (r^2 = 0.937); #9, 0.198 h^{-1} (r^2 = 0.912) — at nominally identical composition. These data highlight the necessity for extremely stringent polymer specification, e.g., MW, polydispersity and comonomer distribution to ensure between batch reproducibility of product performance of microspheres prepared in this manner. Apparent sensitivity of release character to change in polymer batch was attributed to

either an actual difference in polymer character, lack of standard pre-characterization storage conditions, i.e., time, temperature and vacuum which affected residual solvent; or a combination of both (see section 7.3.7).

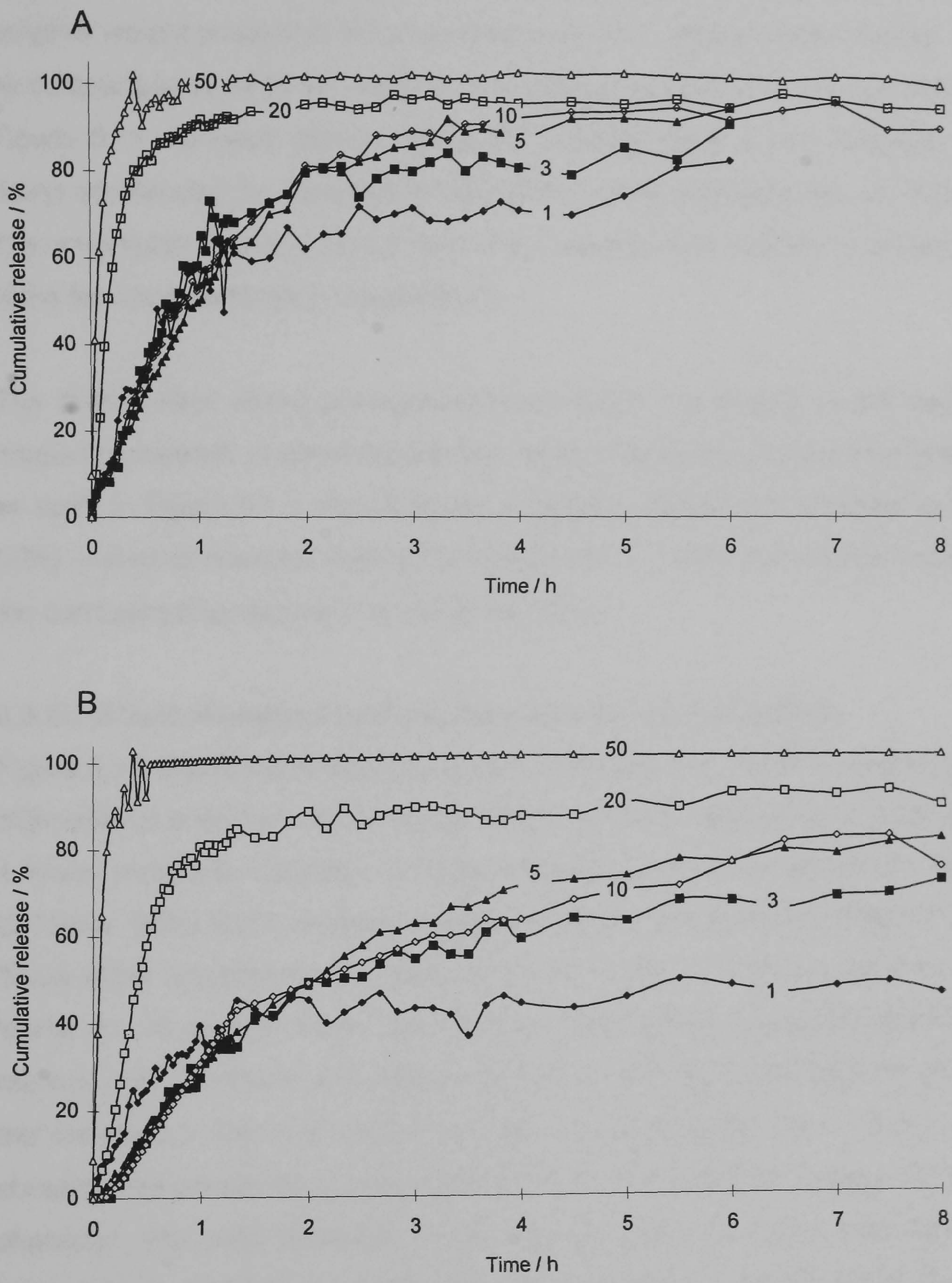

Figure 6.10 *Effect of drug loading on release profiles using method B of rifampicin at a stirring rate of 100 ± 1 rpm and 37 ± 0.1 °C from microspheres with a matrix polymer composition of: A, 44:56 (R104:R202H); and, B, 40:60 (R104:R202H). Labels indicate the rifampicin loading in units of %w/w. (n=3, standard deviation ≤ 2.5)*

6.3.2.2 Effect of polymer batch on microsphere characteristics

Microspheres were reprepared with blends of two batches of R104 with the second batch of R202H. Combinations of the original batch of R202H were not examined due to the non-availability of this material. With the re-examined batches of microspheres, the critical polymer weight proportion for drug release at 37 °C was between 28 and 32 %w/w R104, by comparison to 44 to 48 %w/w for the original batches of R104 and R202H as shown in Figure 6.11. Release kinetics generally corresponded to that originally observed, rate being accelerated by elevated temperature and by the proportion of R104 incorporated. Thermographic analysis of the recovered microsphere residue is shown in Figure 6.12 (data for which features in Appendix 4).

The deterioration of the pre-dissolution endotherm increased as the temperature of the medium increased, commensurate with more extensive hydration and hence drug release as seen in Figure 6.11. Nonetheless, a sizeable endotherm persisted at 28 %w/w R104 (#34) —even at elevated medium temperatures — which was always greater in area than the corresponding sample from 32 %w/w (#29).

6.3.2.3 Effect of storage time on microsphere characteristics

Figure 6.11 shows some disparity in the release data for batches prepared with a 1 %w/w differential around the critical range, when compared with products originally prepared at 4 %w/w variations. Contrary to that expected, microspheres prepared with 31 (#32) and 28 %w/w (#35) R104 released drug more rapidly than those prepared at 32 (#32) and 29 %w/w (#34) respectively. Products prepared within 12 h of one another, i.e., 32 and 24 %w/w, 31, 30 and 29 %w/w, did indeed comply with the expected kinetic pattern of drug release. (NB, 28 %w/w was reprepared within 24 h of characterization and not subject to the standard ≥ 168 h *in vacuo* storage). As all samples were stored under otherwise standardized conditions, it was apparent that the duration of storage affected the release character. This was attributed to an ongoing ageing process associated with residual solvent load. Batches containing 31 (#32), 30 (#33) and 29 (#34) %w/w R104 were therefore freshly prepared and examined at intervals thereafter on the basis of solvent residue, thermal and drug release behaviour The latter thermal and drug release data feature in Appendices 5 and 6, respectively. Comparable solvent loads of 56.45, 55.23 and 62.23 x 10^3 ppm were recorded after *in vacuo* drying to constant weight (for 100 d) for batches #32, #33 and #34 respectively. Thermal analyses shown in Figure 6.13 traced the rapid development of a significant endotherm associated with the T_g, representing the

attainment of a more stable microsphere matrix as demonstrated by the progressive retardation of RIF release shown in Figure 6.14.

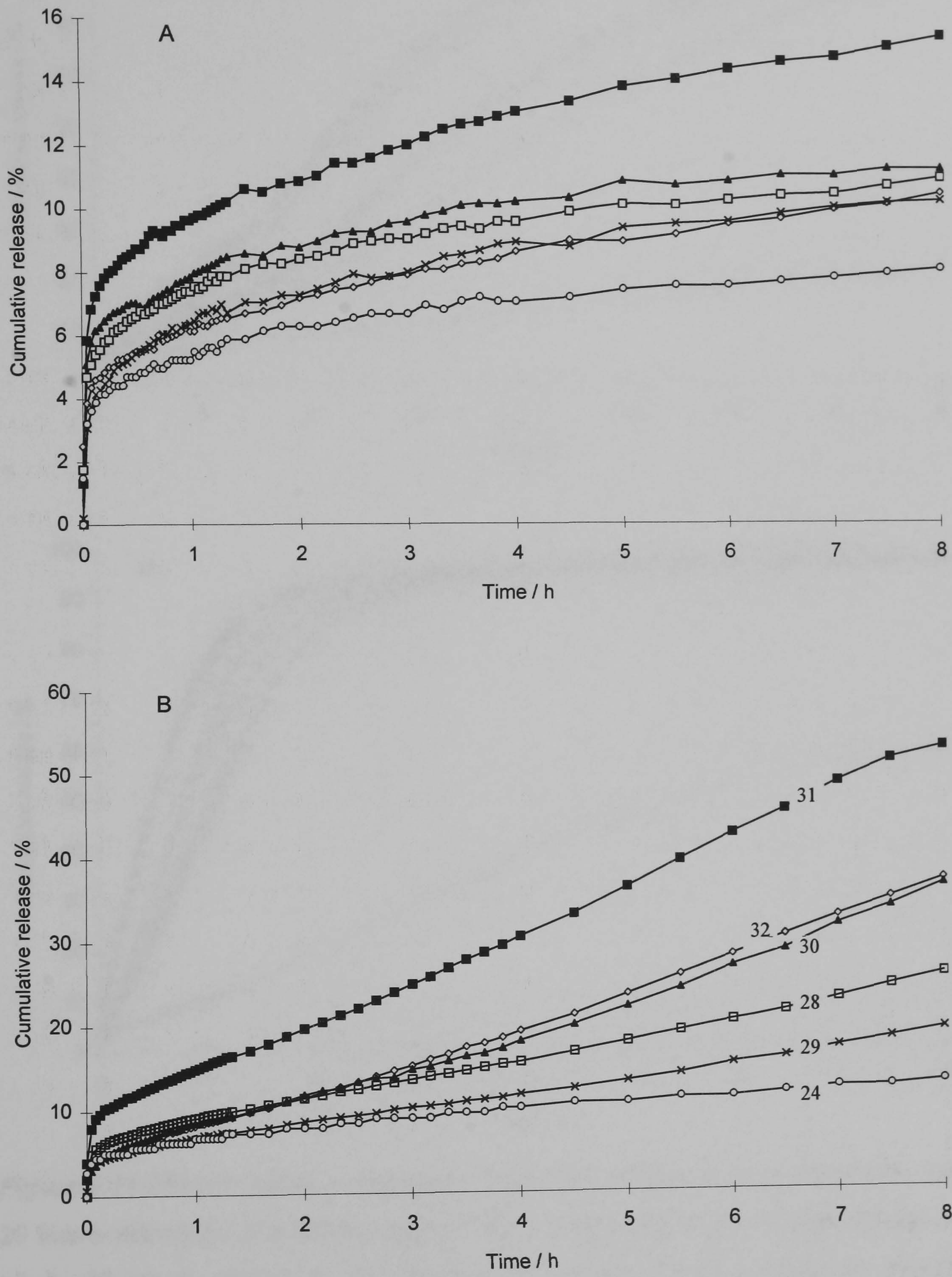

Figure 6.11 *[contd. overleaf]*

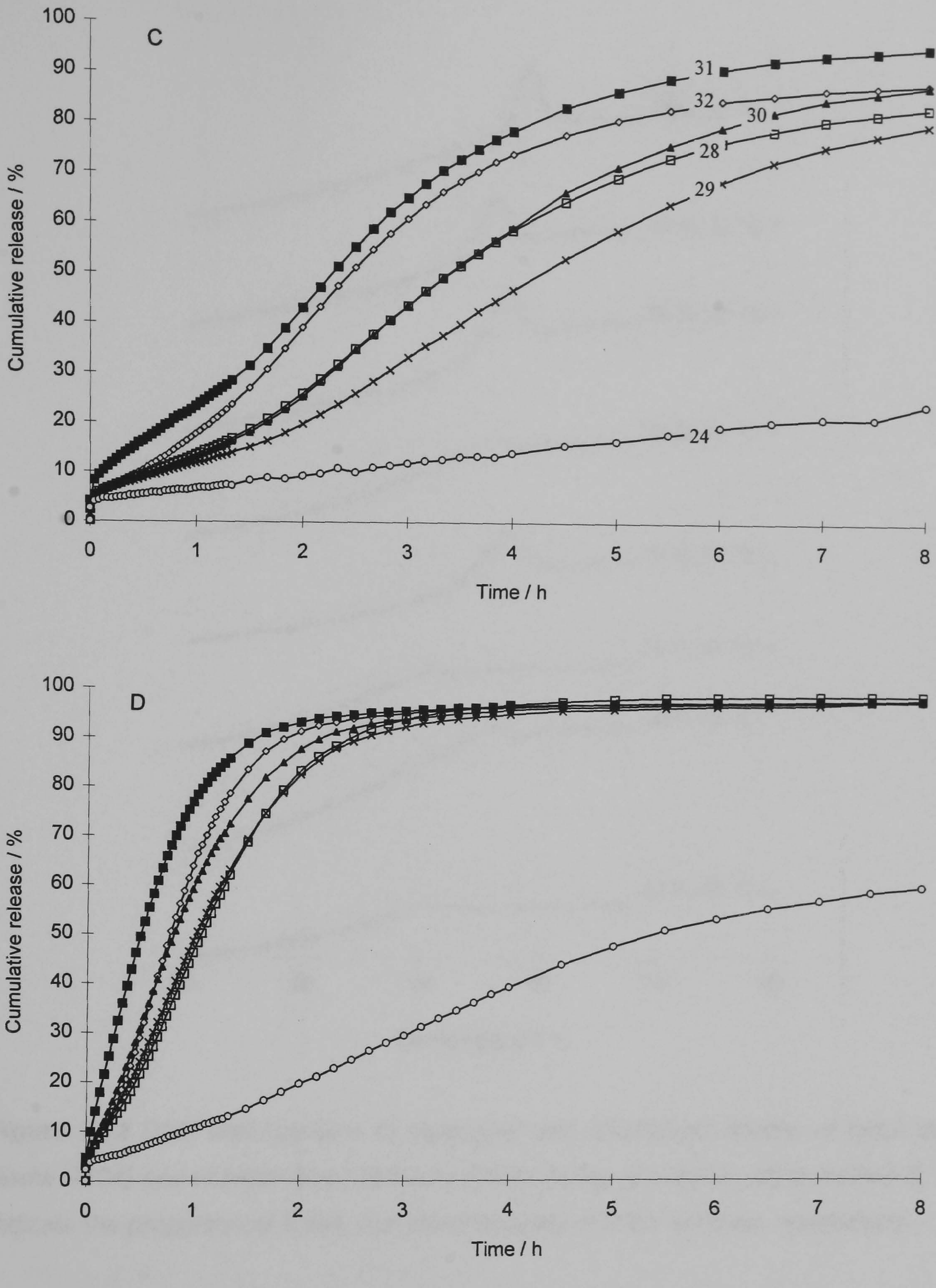

Figure 6.11 *Effect of matrix composition on release profiles from microspheres containing 20 %w/w rifampicin at a stirring rate of 100 ± 1 rpm and medium temperatures ± 0.1 °C of: A, 33 °C; B, 35 °C; C, 37 °C; and, D, 39 °C. Labels indicate the proportion of Resomer® R104 as %w/w total polymer, n = 3 (standard deviation ≤ 2.3)*

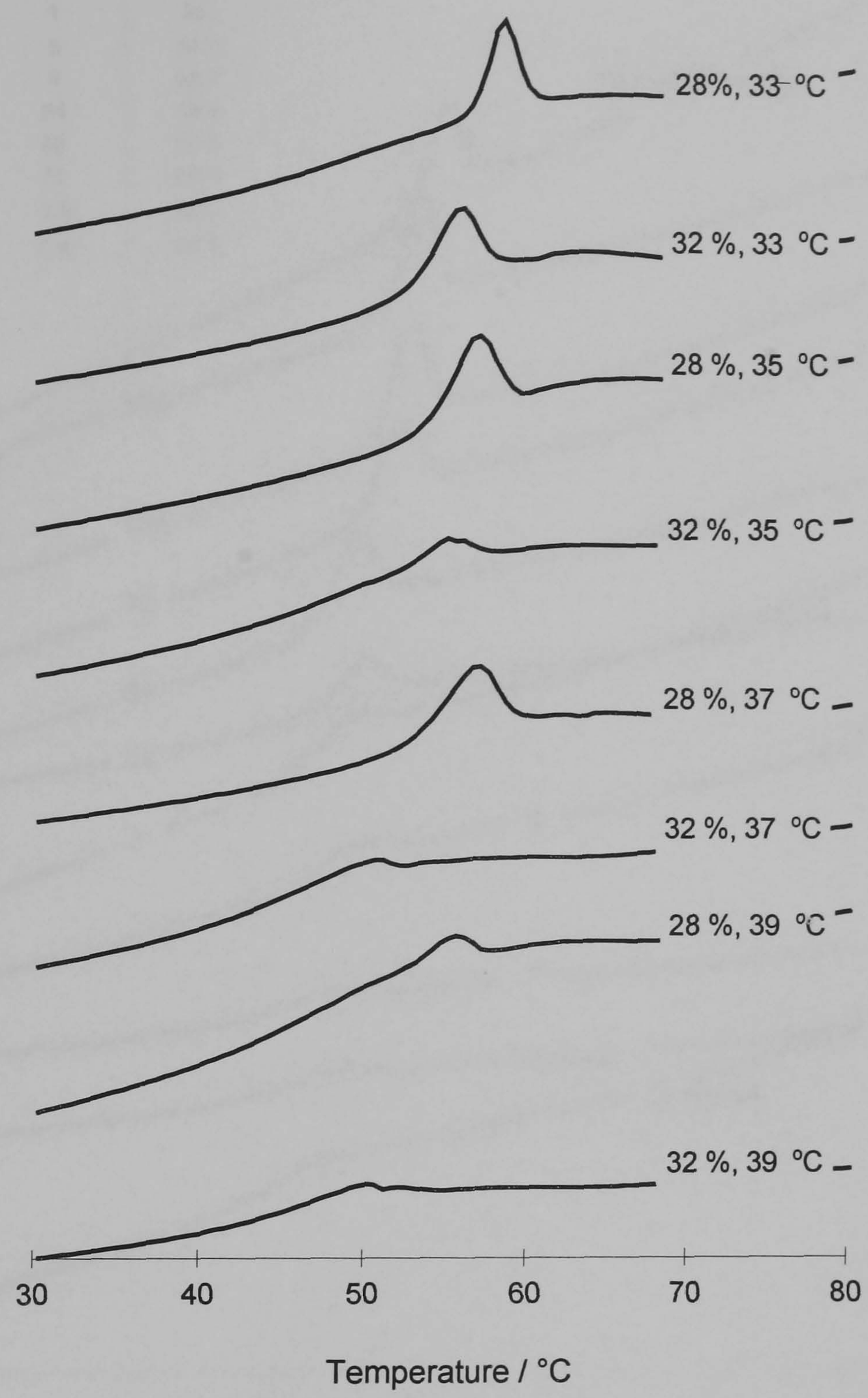

Figure 6.12 *DSC thermograms of recovered and desiccated residue of batch #29 (32 %w/w R104) and of batch #34 (28 %w/w R104) during dissolution using method B. Labels indicate the proportion of R104, and the temperature of the medium, respectively.*

Time / d	Peak / °C
1	53.
3	55.6
5	55.7
24	56.9
48	57.5
72	58.6
336	59.9
CW	63.8

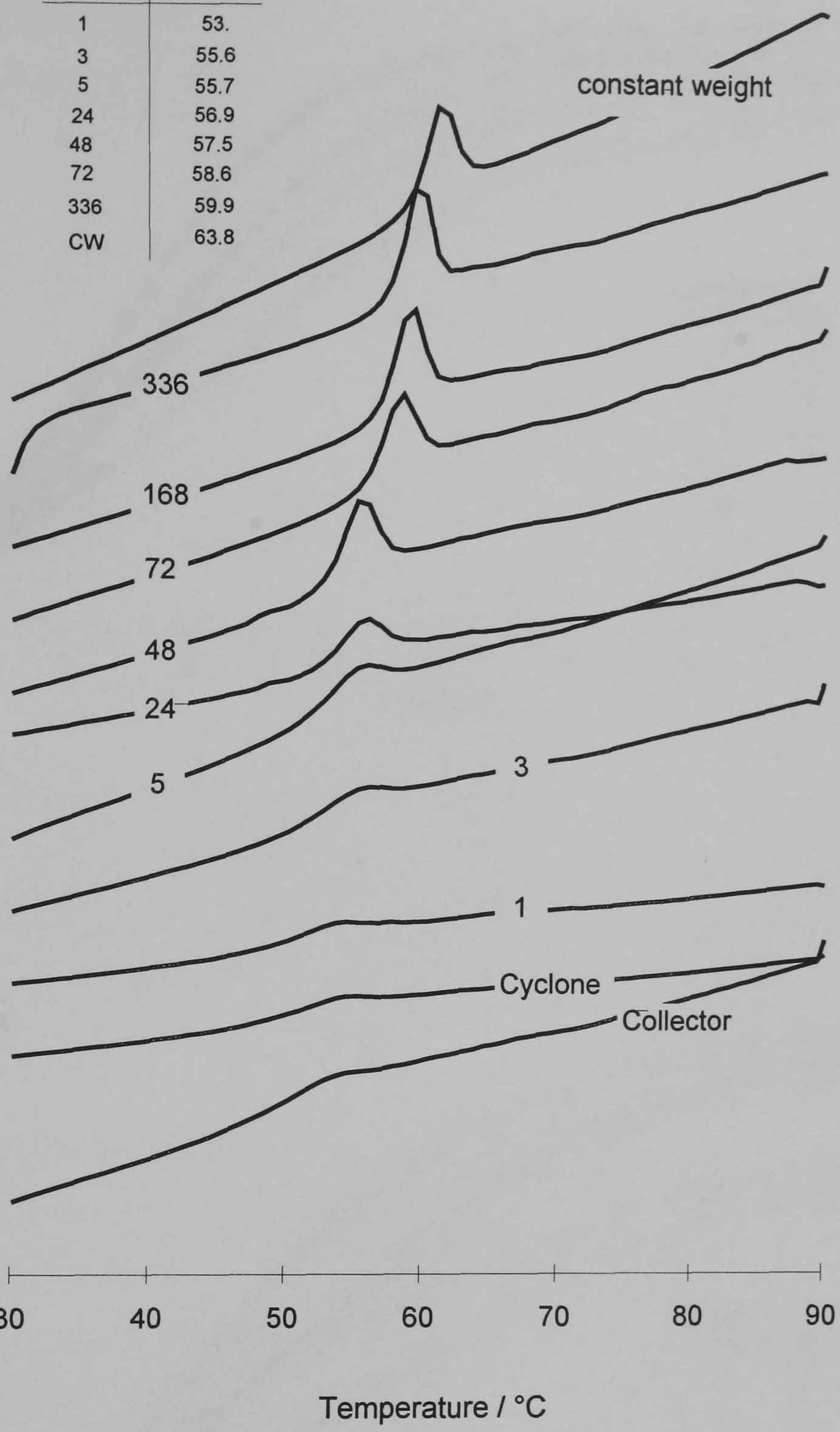

Figure 6.13 *DSC thermograms of batch #33 (30 %w/w R104) after various storage times in vacuo at 24 ± 2.0 °C. Labels indicate the storage period in hours, or location of collection at t = 0. Annotated table indicates the evolution of peak position.*

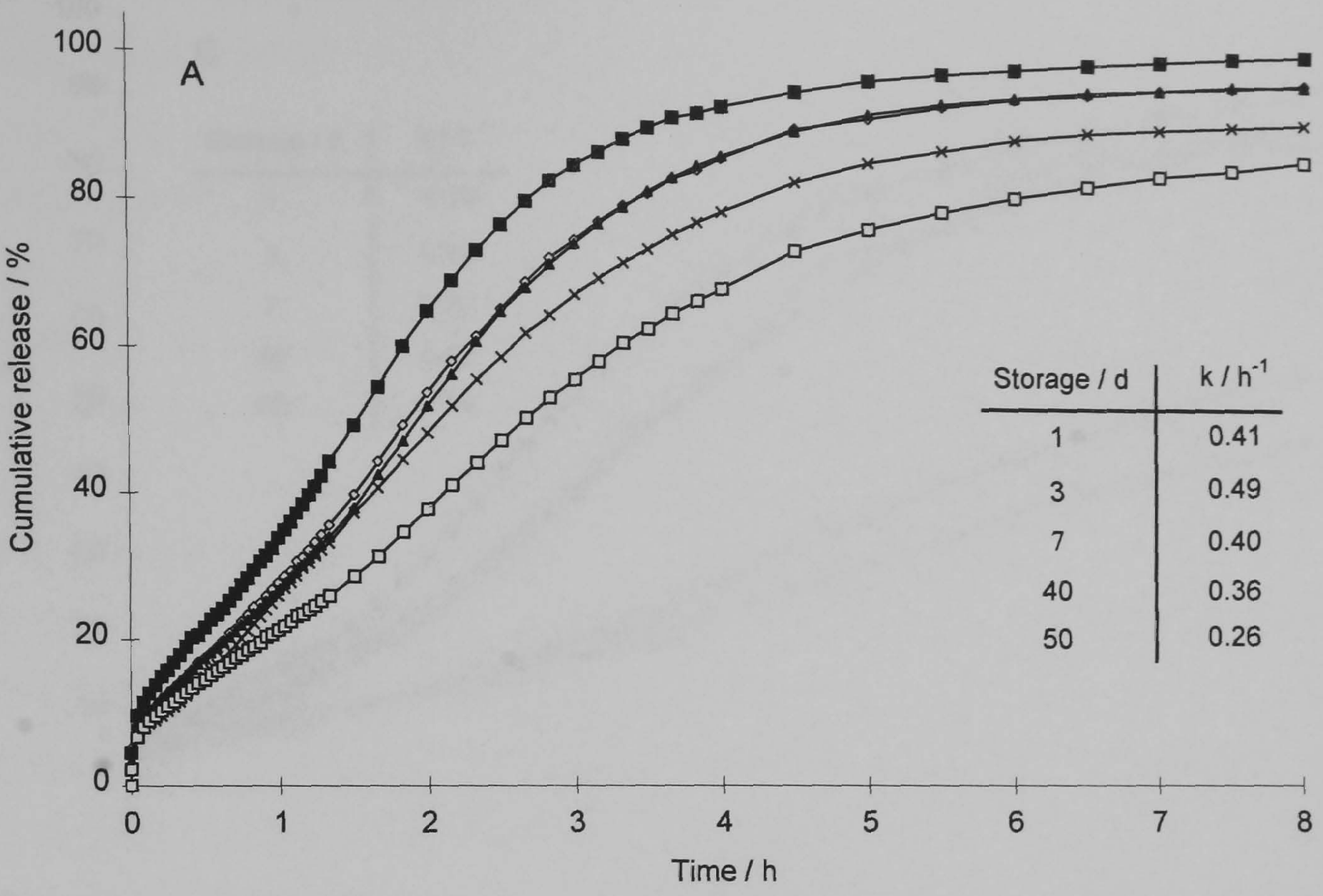

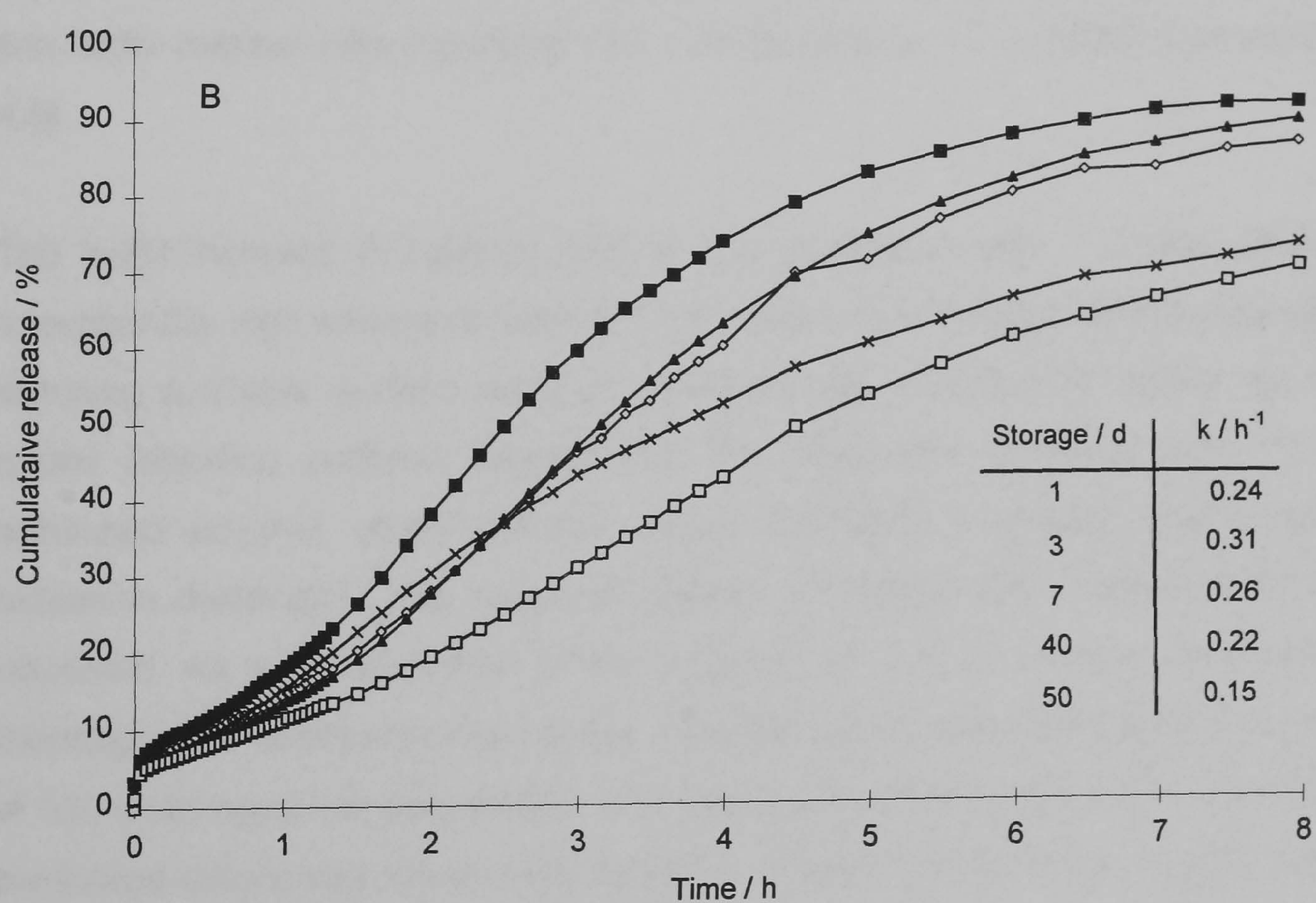

Figure 6.14 *[contd. overleaf]*

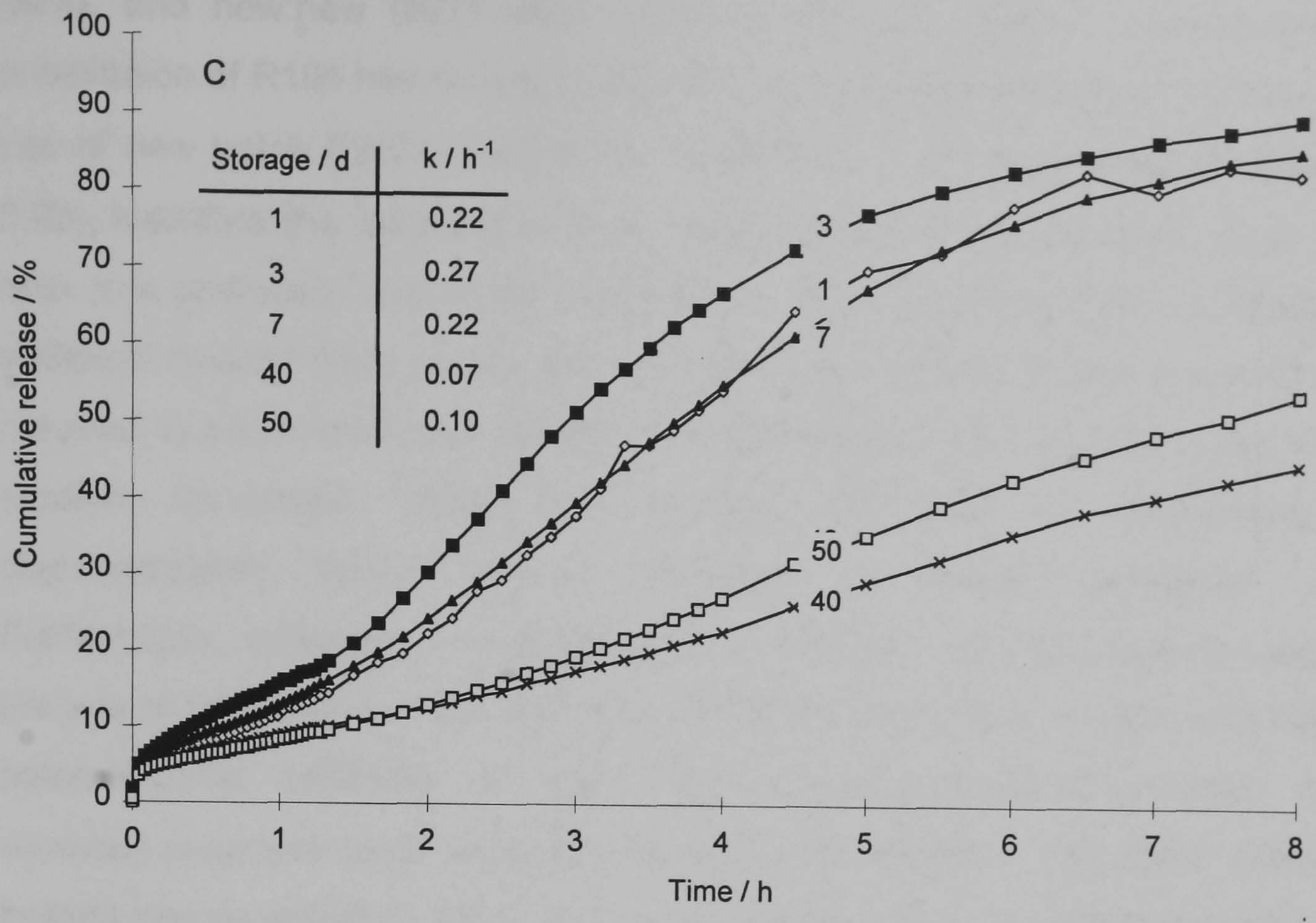

Figure 6.14 *Effect of storage on the release profiles of RIF at a stirring rate of 100 ± 1 rpm and 37 ± 0.1 °C from microspheres prepared from: A, 31 %w/w R104 (#32); B, 30 %w/w R104 (#33); and, C, 29 %w/w R104 (#34), n = 3. Tabulated data represents the first order release rate constants (10 ≤ 80 % release, r^2 ≥ 0.980) (standard deviation ≤ 4.8)*

The initial increase in release rate at 3 d compared with 1 d was attributed to the exceptionally high solvent residue at t = 0, which: 1) promoted particle aggregation hence reducing available surface area; 2) preferentially retained RIF within the microsphere matrix retarding partition thereof into the dissolution medium; and, 3) resulted in enhanced polymer chain stiffness which transiently increased matrix stability. After extensive desiccation, the expected pattern of release with respect R104 content was observed. As a consequence of the influence of solvent residue on drug release and thermographic characteristics, further characterization was performed only after a period of 100 d storage post preparation. Standardization of characterization conditions ensured measured differences arose from variation in matrix composition, largely independent of the influence of any remaining solvent residue.

The first order release constants of microspheres after exhaustive storage *in vacuo* prepared from polymer blends R104:R202H (40:60) original:original (#9), original:new

(#28), and new:new (#27) were 0.304, 1.469 and 1.843 h^{-1}, respectively. That the substitution of R104 had no significant effect on drug release rate ($P > 0.05$), whereas the use of new batch R202H resulted in a significant 5-6 fold increase in release rate ($P < 0.05$), identified this latter material as being responsible for the wide variability in release rate. It is postulated that slight reductions in MW of the new batch of R202H conferred sufficient hydrophilicity on the microspheres such that much less modulating R104 was required to attain controlled hydration as the temperatures of the T_g and the dissolution medium converged. These data highlight the need for comprehensive polymer characterization before device fabrication to ensure predictable performance. Furthermore, variations in polymer physicochemistry are consequently accentuated by the use of relatively low MW polymers. Whereas Deasy et al. (1989) drew attention to the batch-to-batch variability of poly-α-hydroxy acids prepared in-house, commercially available polymers have however received scant attention. Therefore, although residual solvent has an overlying affect on drug release from the hydrophilic particles, the inherent difficulties in the consistent preparation of relatively low MW PDLLA (Dr Liedtke, 1997, personal communication) — prepared by ring-opening polymerization — accounted for the variability in polymer performance.

6.3.3 Studies of release mechanism

6.3.3.1 Hydration

In Figure 6.15, the time-dependent destruction of the ordered microsphere structure, as evidenced from the progressive decrease in endotherm height and increase in endotherm breadth (see Appendix 7), was indicative of progressive hydration during release studies. Partial preservation of matrix integrity was again evident at slight increases in R202H level beyond the critical composition under the conditions of these investigations. These data are corroborated by the hydration data shown in Figure 6.16. The lack of direct correlation between drug release and hydration profiles was attributed to entrapped interstitial water between the microspheres during gravimetric determination which resulted in erroneously high levels of calculated water content, particularly in the earlier stages when the relative error is magnified.

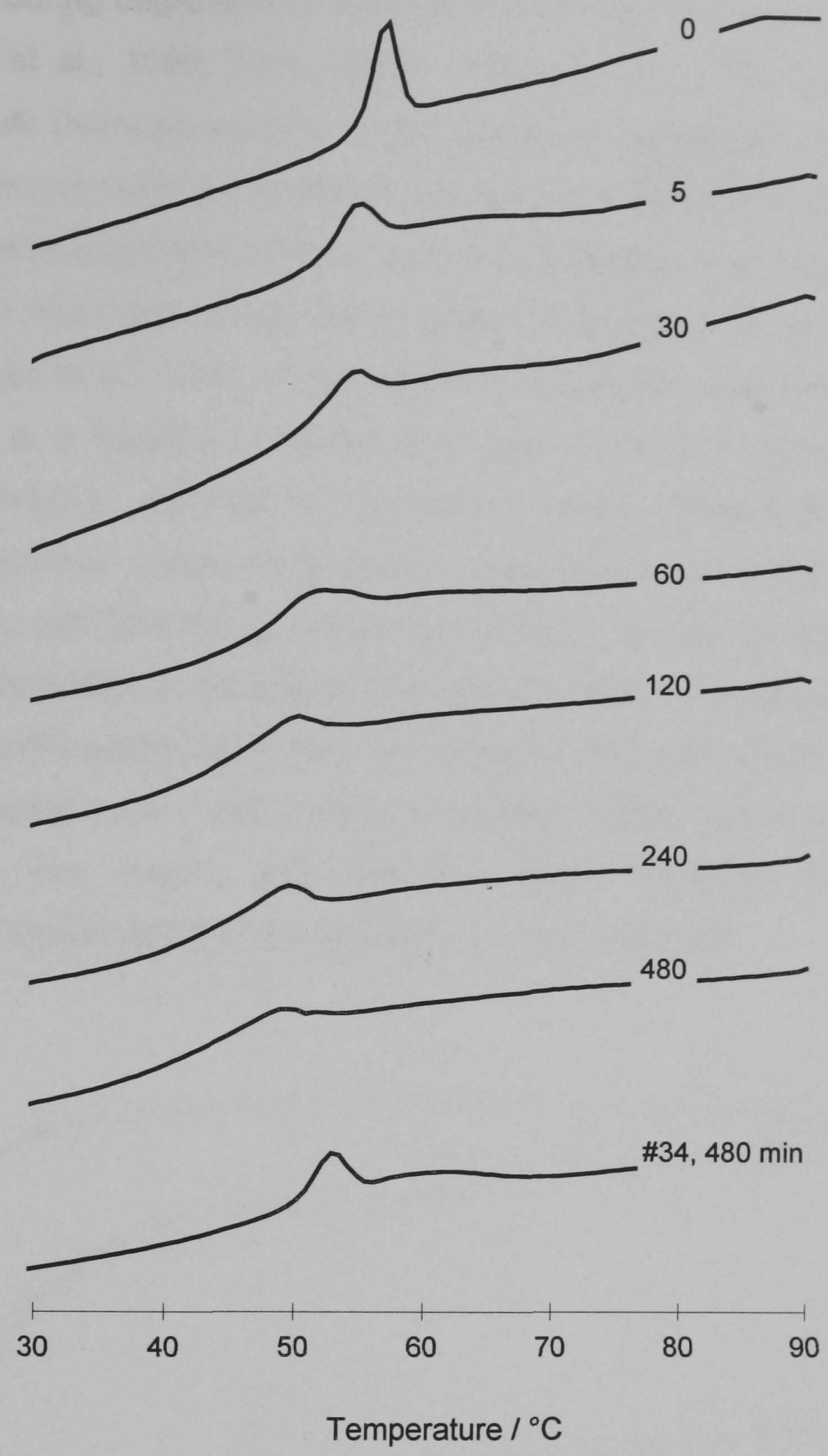

Figure 6.15 *DSC thermograms of recovered and desiccated residue of batch #29 (32 %w/w R104) during dissolution using method B. Labels indicate the dissolution period in minutes. Batch #34 (28 %w/w R104) is included for comparison purposes.*

6.3.3.2 Erosion

Preferential diffusion and loss of oligomers have been cited as a contributing factor to the release of drugs from matrices to which a proportion of low MW polymer has been incorporated (Bodmeier et al., 1989; Le Corre et al., 1994b). Corroborating evidence has included reductions in release medium pH — due to release of oligomers terminating in deprotonated COOH groups — and the emergence of oligomeric peaks during the initial

'burst' phase during degradation investigations (Witschi & Doelker, 1998) using aqueous SEC (Mehta et al., 1996; Park, 1994). Poly-α-hydroxy acids hydrolyse by geometry-dependent bulk (homogeneous) or heterogeneous degradation. Microspheres prepared from individual polymers are generally considered to degrade homogeneously, although drug dependent autocatalytic effects, ordinarily associated with larger devices, have been observed with microspheres containing basic drugs (Maulding et al., 1986; Cha & Pitt, 1989; Ramtoola et al., 1992). In the absence of drug induced catalysis, the intensity of autocatalysis is a function of the relative rates of polymer hydrolysis and associated oligomer generation, and that of oligomeric leaching. Interpretation is confounded by oligomeric extraction during initial polymer degradation which can result in a transient increase in T_g and MW (Park, 1994). Nonetheless, where low MW material has been purposely incorporated in the design of a delivery system, leaching of oligomeric fractions accelerates as the proportion of low MW ingredient increases (Shah et al., 1992, Mehta et al., 1996; Mauduit et al., 1996; Witschi & Doelker, 1998); due to reduced T_g, enhanced hydrophilicity, free volume, and ultimately, matrix diffusivity. Furthermore, elevated temperatures should serve only to accelerate these processes.

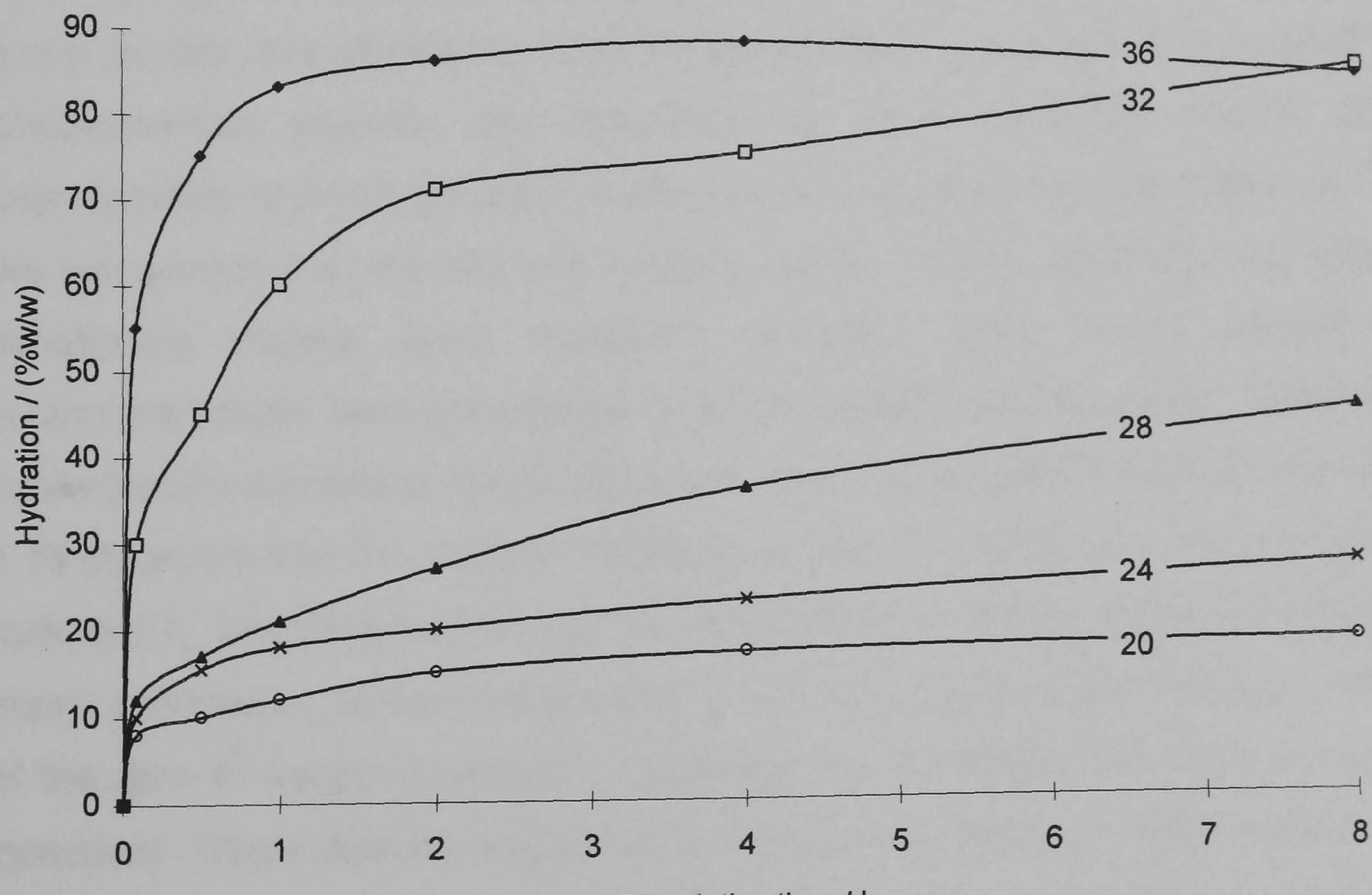

Figure 6.16 *Hydration profiles during release studies at 37 ± 0.1 °C and 100 ± 1 rpm using method B. Labels indicate the weight proportion of R104 (%w/w), n = 3. (standard deviation ≤ 15.8)*

Table 6.3 *Gravimetric determination of erosion of microspheres at various temperatures using method B*

		Polymer weight differential / % (original)			
		Medium / °C			
Batch	**R104 / %w/w**	**33**	**35**	**37**	**39**
31	32	+10.04	+7.13	+2.02	+0.32
32	31	+14.52	+0.43	+10.99	+5.47
33	30	+16.56	+7.33	+21.52	+2.33
34	29	+16.91	+18.03	+9.10	+8.29
35	28	+17.01	+8.31	+21.51	+1.79
36	24	+14.31	+10.16	+16.83	-12.54

The gravimetric determination of microsphere erosion — taking account of released drug — yielded the results in Table 6.3. These data are at odds with the anticipated pattern of erosion, whereby, with the exception of #36, at 39 °C, all other matrices showed a net weight gain.

The number of carboxylic end-groups (acid number) is inversely proportional to MW of the chains of the fabricating matrix. Thus for low MW species the COOH group density is relatively high. Notwithstanding ongoing polymer deesterification which increases COOH group density, this situation is further supplemented by the use of H-series PDLLA as the complementary polymer, the end-groups of which have free COOH moieties. The deprotonation of these groups in contact with aqueous phosphate buffer, pH 7.4, renders the loci around the end-chain hydrophilic, which, in turn, facilitates the advance of the penetrating solvent front. However, *di*-sodium salts which interact to restore environmental pH, were considered to persist despite washing steps. These imbibed salts subsequently precipitate during desiccation. As the proportion of R104 increased, Figure 6.16 illustrates that the level of hydration increased. Additionally, that the anhydrous and hydrated T_g' converge as the medium temperature increases, further enhances hydration, matrix protonation, and hence sorption of salt from the medium. However, the magnitude of the gain in weight appeared to decrease as the factors promoting matrix hydration increased. These data are suggestive of erosion of accessible oligomers from the rubbery superficial areas of the matrix. Therefore, two competing processes confound interpretation of the gravimetric results. On the one hand, hydration promotes sorption of salts which increases matrix mass; on the other, oligomer depletion causes a direct reduction in weight and a concomitant reduction in the ionic density, with a consequent reduction in the binding capacity of the matrix for salt ions. As an aside, neutralization of

deprotonated COOH by specific cation-induced salting out effects have been shown to inhibit polymer degradation (Reich & Bernickel, 1998). However, the influence of this process is considered minimal in the context of the diffusion mechanism which is considered to predominate here. In order to elucidate the significance of matrix erosion, morphological observation of microsphere residue and size analyses were performed on SEM photomicrographs. The population and volume granulometric statistics are shown in Table 6.4 and 6.5 respectively. The large variation between population and volume statistics was attributed to the existence of a few very large particles which resulted in a substantial positive skew for the latter statistic.

Table 6.4 *Effect of polymer composition and medium temperature on the population granulometric statistics of microsphere residue recovered after release studies using method B*

Batch	***R104 / (%w/w)***	***Medium / °C***											
		33			***35***			***37***			***39***		
	Diameter / μm	d_{25}	d_{50}	d_{75}	d_{25}	d_{50}	d_{75}	d_{25}	d_{50}	d_{75}	d_{25}	d_{50}	d_{75}
31	32	0.91	1.32	1.96	0.66	0.99	1.48	0.86	1.24	1.83	0.82	1.24	1.91
32	31	0.89	1.28	1.90	0.69	0.95	1.36	0.78	1.17	1.81	0.94	1.36	2.03
33	30	0.99	1.38	1.98	0.89	1.28	1.90	0.73	1.09	1.68	0.91	1.38	2.14
34	29	0.89	1.28	1.90	0.96	1.46	2.28	0.76	1.07	1.56	0.76	1.07	1.56
35	28	0.87	1.25	1.86	0.75	1.11	1.17	0.83	1.26	1.94	1.03	1.58	2.48
36	24	0.85	1.22	1.80	0.68	1.01	1.54	0.82	1.17	1.73	1.06	1.56	2.36

Table 6.5 *Effect of polymer composition and medium temperature on the volume granulometric statistics of microsphere residue recovered after release studies using method B*

Batch	***R104 / (%w/w)***	***Medium / °C***											
		33			***35***			***37***			***39***		
	Diameter / μm	d_{25}	d_{50}	d_{75}	d_{25}	d_{50}	d_{75}	d_{25}	d_{50}	d_{75}	d_{25}	d_{50}	d_{75}
31	32	2.77	3.40	4.87	2.16	3.16	4.05	2.53	3.39	4.33	2.59	3.88	5.54
32	31	2.08	3.75	5.41	1.65	3.02	3.87	5.02	5.88	6.27	3.57	5.29	6.08
33	30	2.11	3.12	4.69	2.58	3.89	5.08	2.35	3.53	4.70	3.00	4.49	6.06
34	29	3.21	4.74	5.60	3.17	4.94	6.67	2.60	3.48	4.11	2.69	3.63	4.26
35	28	2.30	3.30	4.59	2.13	3.24	5.29	2.13	3.24	5.29	2.40	4.08	6.32
36	24	3.07	4.18	5.03	2.17	3.36	4.33	2.61	3.50	4.37	4.12	5.88	6.95

That no obvious temperature or composition dependent trends were apparent, except perhaps for a slight general increase in volume statistics at 39 °C, was accepted as evidence that neither erosion, nor swelling made a significant contribution to the controlled release of RIF by predominantly diffusion. The porous nature of the particles was considered to accommodate the plasticizing water, which also accounted for maintenance of sphericity after residue recovery and drying (micrographs not shown). Attempts to perform these analyses by laser diffractometry were hindered by partial fusion of hydrated samples which resulted in misleading positive skew of the size distribution.

6.3.3.3 Models of release

Drug release data were fitted to three models of release, namely, first order, zero order and the generalized power law, the statistics of which feature in Appendices 8 a-c. The latter model demonstrated best correlation overall. However, that both the coefficient and exponent varied as the mechanism and kinetics thereof varied with change in release conditions and matrix composition, made batch-to-batch comparison difficult. Whereas the coefficient increased with temperature irrespective of polymer composition indicative of generally a more rapid diffusive mechanism, the exponent decreased at relatively high R104 levels, although this trend was reversed at/around the critical composition. These variations were considered to reflect the change in the diffusion character of the polymer as the hydration and thermal character of the matrix varied under the conditions of the release studies. That the data seldom fitted to the Higuchian $t^{0.5}$ relationship was attributed to the lack of matrix inertness whereby matrix hydration and softening provided mechanistic control (see Appendix 8a). Linear regression demonstrated the anticipated pattern of increased release rate and 'burst' as temperature and %w/w R104 increased as evidenced by the coefficients denoted by *b* (gradient) and *a* (intercept), respectively (Appendix 8b). Similarly, first order profiles provided a single index of release rate, denoted by the fractional rate constant, *b*. The fraction of drug released per unit time again increased with proportion of R104 and temperature as seen in Appendix 8c.

Notional activation energies of drug release were computed by plotting the logarithm of the first order release rate constant on the reciprocal of release medium temperature (K) (Jalil, 1989). These data and associated regression statistics are presented in Table 6.6. The activation analogue for the release process was considered to represent the

resistance to mass transfer of drug through the matrices. Thus, as %w/w of R104 increases, matrix free volume increases and the energy barrier to drug diffusion decreases; resulting in a continuum of release rate. However, the overshadowing influence of matrix hydrophilicity and the associated role of matrix T_g account for the substantial variation in Arrhenius derived statistics around the critical matrix composition. Indeed, Schellhorn & Buchholz (1996) concluded prediction of degradation rate of PDLGA and PDLLA was not possible based on E_a values due to extensive hydration, and hence change in the degradation mechanism of the matrix in the rubbery state. The poor correlation observed at 52 %w/w is attributable to the large variations in first order rate constants as the level of hydration, and hence drug diffusivity / release mechanism change under the influence of ingressing water. Above this weight composition, hydration is ostensibly instantaneous, regardless of temperature (within the studied range). On the other hand, controlled temperature-dependent hydration is responsible for constancy of E_a below this critical composition range. Comparable statistics were calculated for the second batches of studied polymer. Additionally, based on the correspondence of E_a values, neither residual solvent nor polymer batch affected the mechanism of drug diffusion, although the rates did increase under its influence as shown in Figure 6.14. It was therefore concluded that 320 and 630 J mol^{-1} represented the activation energies for RIF diffusion through PDLLA of a rubbery hydrated and glassy anhydrous character, respectively.

Table 6.6 *Arrhenius computed activation energies of rifampicin release for selected batches before and after exhaustive in vacuo drying at 24 ± 2.0 °C*

		Before in vacuo storage			***After in vacuo storage***		
Batch	***R104 / %w/w***	***E_a / kJ mol^{-1}***	***ln A***	***r^2***	***E_a / kJ mol^{-1}***	***ln A***	***r^2***
4	*60*	*324.1*	*55.21*	*0.963*			
5	*56*	*324.2*	*55.27*	*0.987*			
6	*52*	*520.3*	*88.03*	*0.886*			
7	*48*	*590.4*	*99.40*	*0.957*			
8	*44*	*631.2*	*106.0*	*0.997*			
9	*40*	*630.7*	*105.9*	*0.964*			
30	36	373.2	61.09	0.952	349.6	59.23	0.957
31	32	626.2	105.0	0.998	643.4	107.8	0.999
32	31	656.5	110.0	0.997	636.0	106.6	0.997
33	30	702.2	117.6	0.994	667.0	111.8	0.993
34	29	619.1	103.5	0.984	666.9	111.7	0.945
35	28	605.7	101.3	0.997	618.0	103.3	0.988
36	24	581.5	100.0	0.983	523.8	87.12	0.972

data in italics represents the batches prepared from the original PDLLA batches

6.3.3.4 Thermal analysis

In order to confirm the mutual interaction of plasticizing water, matrix thermal character and hydrophilicity with that of the dissolution medium temperature, DSC analyses were performed on hydrated samples during release studies, the results of which are presented in Table 6.7. The transitions reported are those after 15 min air drying, after which time a proportion of the total original plasticizing water had been lost; shifting the T_g temperature slightly up-scale.

Table 6.7 *DSC analyses of hydrated residue 15 min after recovery during release studies at 37 °C using method B*

	T_g (½C_p) / °C			
	Batch #, R104 / (%w/w total polymer)			
Time / min	**#29, 40**	**#31, 32**	**#33, 30**	**#37, 20**
0	52.39	55.42	55.50	56.18
5	42.14	39.23	42.31	46.23
15	39.84			
30	37.02	38.58	40.66	40.38
45	37.00			
60	38.42	39.15	39.32	44.62
120	36.11	39.52	42.75	40.02
240	37.02	38.79	40.23	
480	35.86	37.74	41.23	

DSC of samples immediately after filtration yielded only a broad endotherm, which overwhelmed the observed T_g as shown in Figure 6.17. This broad endotherm was considered due to interstitial water and the high heat capacity of same. Owing to these operational difficulties, 15 min air drying was considered an acceptable compromise in terms of data accuracy and event detection. Overall, the different blends showed a rapid initial reduction in the T_g as water was absorbed, behaviour typified by amorphous and partially amorphous pharmaceutical solids (Hancock & Zografi, 1994). Thereafter, a general and progressive reduction in T_g occurred as the degree of plasticization increased with more extensive hydration. Moreover, in accordance with the proposed mechanism of release, the T_g and medium temperatures showed remarkable correspondence. Generally, as %w/w R104 increased, associated inaccuracies in sample handling and preparation did not allow the subtle thermal differences — thought to be so instrumental in the control of drug release — to be discerned around the critical composition at which drug release showed marked changes in release rate. Nonetheless, batch #29, (40 %w/w

R104) from which RIF was rapidly released, attained a T_g of ≤ 37 °C within 30 min, whereas T_g suppression of #37 (20 %w/w R104) was insufficient to achieve medium temperature correspondence; consistent with matrix resistance to hydration and the consequent low and slow release from the latter blend.

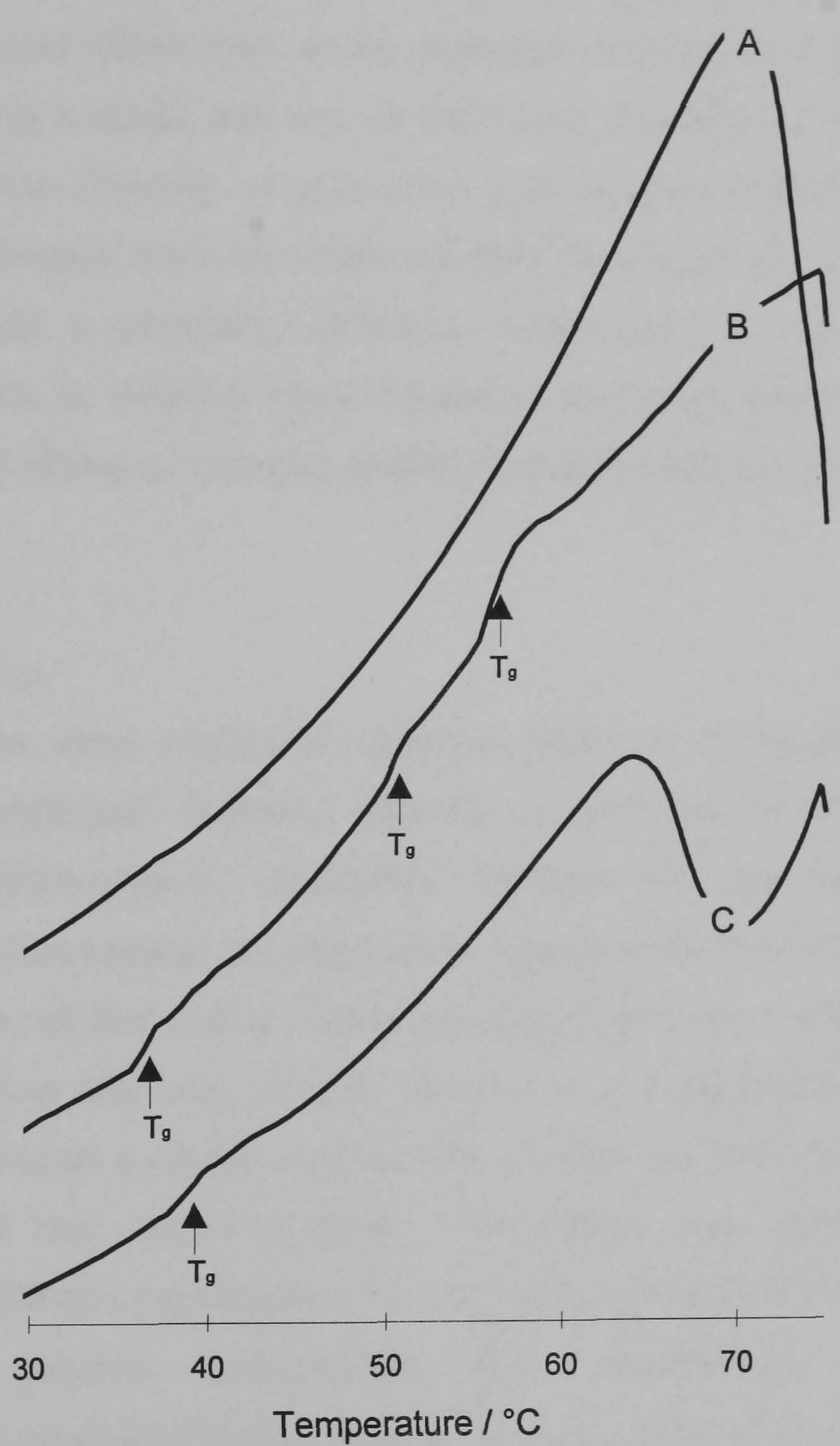

Figure 6.17 *DSC thermograms of hydrated microsphere residue during dissolution at 37 ± 0.1 °C using method B of: A, batch #30 , 60 min dissolution time, immediately after filtration; B, as per A, but after 15 min air drying; and, C, batch #33, 480 min dissolution time, 15 min air drying.*

Multiple T_g represented the formation of several polymer domains in the microsphere population. Park (1994) assigned the existence of two T_g' to heterogeneous degradation,

whereby entrapped oligomers exerted an autocatalytic influence in the PDLLA microsphere core, whereas slower degradation in the microsphere shell represented a second polymer domain. This postulation fails to account for the three apparent T_g' observed with batch #30 (36 %w/w R104) at 60 min annotated on Figure 6.17. The presence of a range of particle sizes with different diffusional paths dictates that volumetric proportion of the microsphere which exists in the hydrated rubbery state will increase as diameter decreases. Therefore, thermal heterogeneity is considered to arise due to particle size differences which determine the overall hydrated state of individual populations within a range, and not via differential degradation mechanisms (Park, 1994). It follows that the diversity of population granulometry contributes significantly to the control of drug release from low:moderate MW PDLLA blends, where drug release occurs by the described autohydration-diffusion mechanism, i.e., as solvent penetrates the microsphere core at different rates, hydration and drug liberation by diffusion occur at different rates, yielding a controlled profile of drug release (see section 7.3.7).

6.3.4 Conclusion

In general terms, drug release accelerated when an increased proportion of low MW polymer was employed. Dramatic variation in both release rate and mechanism were attributed to hydrodynamic differences between the two release methods studied. Hydration, and thus release characteristics, appear to be inextricably linked to the thermal character of the polymer blend. There would appear to be a critical polymer composition at which hydration and drug release proceed in a controlled fashion, below and above which, release shows a pattern reminiscent of either polymer used alone. The high batch-dependency of this critical polymer composition was attributed to batch-to-batch differences in MW and polydispersity of the moderate MW PDLLA, which, in the absence of definitive polymer specification and microsphere pre-fabrication polymer characterization may limit the robustness, if not the utility of this approach to drug release modulation.

Whereas low molecular impurities and oligomers are putatively inflammatory triggers (Vert et al., 1992; Bittner et al., 1998), it has been counter suggested that increased particle hydrophilicity might improve microparticle tolerability (Wang, 1990) and that the extent and severity of immunogenic reactions are accentuated by polymers of low degradation rates (Bittner et al., 1998). Accordingly, it is postulated that the hydrophilic

character of these particles may afford greater biocompatibility, particularly to immunologically sensitive epithelia, such as those in the lung. Indeed, when administered intra-pulmonary, microspheres prepared from moderately high MW PDLLA, 16 kD, have been demonstrated to illicit a significant and limiting immune response (Armstrong et al., 1992; 1994). That 90% of particles were < 10 μm, and a substantial volumetric proportion coincided with the target range of 0.5 - 3.0 μm for alveolar deposition, highlights the prepared particles potential for drug delivery via this route. Furthermore, the auto-hydration mechanism linked to the T_g of the hydrophilic microspheres should facilitate and provide controlled drug release in the low volume of liquid which prevails in the lung.

Finally, temperature dependent release may have application in the delivery of drugs from biodegradable systems where elevated local biochemical activity promotes release of drug in response to an increased pharmacological need, e.g., delivery of steroids to arthritic joints, post-operative antibiotic prophylaxis to joint prostheses. Indeed, recent reports specifically indicate RIF-containing regimens to treat staphylococcal infections associated with orthopaedic implants (Editorial, Pharmaceutical Journal 1998).

7. Investigations of solvent influence on the characteristics of spray-dried microspheres

7.1 Introduction

Preparative techniques for biodegradable poly-α-hydroxy acid microspheres, with few exceptions, employ potentially toxic, halogenated solvents to prepare polymeric solutions as a prerequisite for most procedures. However, reports of residual solvent content are few in number and have considered only the bio- or ecotoxicological consequences thereof, frequently making use of USP limits as markers of acceptability: 50 ppm for CFM; and, 500 ppm for DCM (Benoît et al., 1986; Splenlehauer et al., 1986, 1989; Gangrade & Price., 1992; Ruchatz et al., 1995, 1996; Thoma & Schlütermann, 1992; Bitz & Doelker, 1995). Microparticle architecture and granulometry are principal determinants of the magnitude of entrapped solvent; which themselves are a complex interplay between the solvent(s) employed, the process and its parameters and the polymer and drug used. Additionally, external factors such as drying conditions, i.e., temperature and pressure (Mabuchi et al., 1995; Bitz & Doelker, 1995) and duration (Mabuchi et al., 1995) have been shown to dramatically alter residual solvent content. Based on the multitude of factors which affect residual solvent content, it is little surprise a wide variety of determined loads have been reported.

Splenlehauer et al. (1989) reported a 3 %w/w DCM residue in cisplatin-loaded microspheres prepared by an aqueous-ESE procedure. Previously, these workers identified particle size, drug loading and the addition of non-solvent as being influential factors on residual solvent load (Splenlehauer et al., 1988). Benoît et al. (1986) found 1.8 - 4.7 %w/w DCM residue in progesterone-bearing microspheres, whereas dramatically lower values of 0.036 - 0.68 %w/w were determined for preparatively and compositionally similar particles after drying *in vacuo* (Courteille et al., 1994). Norethisterone-loaded microspheres prepared by Lewis et al. (1988) harboured 0.25 %w/w organic residue. In contrast, prodigiously low values of < 59 ppm have also been recorded for microparticles prepared by solvent evaporation (Gangrade & Price, 1992).

As a result of regulatory restrictions and apparent bioincompatibilities, the substitution of DCM and CFM with less toxic acetone (ACT) (Rafler & Jobmann, 1994) and halothane (HAL) (Guiziou et al., 1996) has been proposed for the preparation of biodegradable microspheres by spray-drying and ESE respectively. Other workers have examined the

potential of alternative microparticle preparative techniques in reducing toxic residue. These latter studies have however yielded conflicting results. Thoma & Schlütermann (1992) reported a reduced organic residue in cinchocain-bearing microspheres prepared by spray-drying (0.3 %w/w) when compared with those from a solvent-evaporation procedure (2.1 %w/w). On the contrary, Bitz & Doelker (1995) observed considerably greater organo-burdens in tetracosactide-loaded particles prepared by spray-drying than the corresponding product of a w/o/w process. Differential CFM and DCM loads of 934 - 5998 ppm and 281 - 705 ppm respectively were presumably a result of the use of a reduced inlet temperature during spray-drying with less volatile CFM. Storage *in vacuo* for 72 h effectively reduced the DCM load within USP limits, whereas CFM failed to conform after such treatment. More recently, aerosol solvent extraction system (ASES) (Ruchatz et al., 1995, 1996), a technique which relies on the extraction properties of supercritical CO_2, has emerged as a process yielding microparticles with consistently low organic residue in the range 87 - 450 ppm. Bitz & Doelker (1996) demonstrated during a comparison of three preparative methods, including w/o/w, methanolic residue complied with an arbitrary limit of 1000 ppm immediately after preparation, whereas ASES prepared material required storage under vacuum to conform regards DCM. In spite of a higher inlet temperature, non-compliant CFM residue persisted in particles spray-dried from CFM:DCM, whereas DCM was satisfactorily removed after 72 h storage. To eliminate toxicological considerations, microparticles have been prepared without the use of organics. Wichert & Rohdewald (1990) developed a novel preparative technique which obviated the use of organic solvent, whereby solid microspheres were formed by quench cooling subsequent to emulsification of a molten mixture of drug and polymer. Others have described the grinding of cooled mixtures in which drug was incorporated to molten PDLLA (Smith & Hunneyball, 1986).

Despite the growing number of publications concerned with the toxicological implications, no specific reports on the influence of residual solvent on the physicochemical characteristics of PDLLA microspheres exist. Indeed, some workers have discounted the influence of residues as high as 1.8 - 4.7 %w/w as being insignificant (Benoît et al., 1986). This chapter demonstrates the influence of solvent choice on microsphere characteristics prepared by spray-drying from CFM, DCM, ACT, halothane (HAL) and mixtures thereof. A single fixed matrix composition was selected from Chapter 6 to allow detailed evaluation of the effects of solvent and correlation of microsphere properties in relation to solvent

physicochemistry and the interaction of polymer with solvent in the context of the spray-drying process.

7.2 Experimental procedures

7.2.1 Microsphere preparation

Microspheres of fixed composition were prepared from (co)solutions (3 %w/w total solid) containing poly(D,L-lactide) Resomer® R104 (24 %w/w), R202H (56 %w/w) and RIF (20 %w/w). Solutions were spray-dried at a constant air flow and feed rates of 600 Nlh^{-1} and 3.5 $mLmin^{-1}$ respectively, according to the parameters in Table 7.1. Microspheres were harvested and characterized at predetermined intervals during storage under vacuum desiccation. Selected physicochemical data of the organic solvents used are presented in Table 7.2

Table 7.1 *Preparative conditions for microspheres prepared with various organic solvents, n=1*

Batch	***Solvent (s)***		***Spray parameters***		
	Nature	***Ratio***	***Inlet / °C***	***Outlet / °C***	***Aspiration / %***
1	DCM	100 %	40	35	100
2	DCM:ACT	2:1	40	35	100
3	DCM:ACT	2:1	40	35	50
4	ACT	100 %	40	35	100
5	DCM:CFM	1:1	40	35	100
6	DCM:CFM	1:1	50	39	100
7	CFM:ACT	2:1	40	35	100
*8	DCM	100 %	40	35	100
9	HAL	100 %	50	40	100
10	HAL	100 %	40	40	100

Key: DCM, dichloromethane; ACT, acetone; CFM, chloroform; HAL, halothane

* blank microspheres

Table 7.2 *Physicochemical properties of solvents used to prepare microspheres*

Property	***Solvent***	***DCM***	***CFM***	***ACT***	***HAL***
Mol. formula		CH_2Cl_2	$CHCl_3$	C_3H_6O	$C_2HBrClF_3$
Mol. weight / RMU		84.94	119.39	58.08	197.39
Boiling point / °C		39.9	61.7	56.5	50.2
d_{25}^{25} *$/ (g\ cm^{-3})$*		1.325	1.480	0.788	1.825
Heat capacity$_{25\ °C}$ $/ (J\ K^{-1}\ mol^{-1})$		100.88	116.90	74.52	100.01
ΔH_{vap} $/ (kJ\ mol^{-1})$		27.98	29.37	29.08	29.07
Molar volume / $cm^3\ mol^{-1}$		64.11	80.67	73.52	105.44
Aqueous sol. / (% v/v) °C		2.500 $_{25\ °C}$	0.792 $_{25\ °C}$	miscible$_{25\ °C}$	0.345 $_{25\ °C}$
		0.880 $_{45\ °C}$	0.712 $_{41\ °C}$	miscible$_{25\ °C}$	0.800 $_{37\ °C}$

data obtained from the Handbook of Chemistry and Physics (1967-68), Rathburn Chemicals and Zeneca pharmaceuticals

7.2.2 Solubility studies

7.2.2.1 Viscosity

Viscosities of the polymer blend-RIF cosolution (3 %w/w total solid) in each individual solvent were determined in triplicate with a U-tube viscometer (size A) at 25 ± 0.1 °C in a thermostated bath. Prepared solutions were allowed to stand for 24 h prior to measurement to ensure complete polymer solution. Flow times were measured again after 168 h to ensure the solvents studied did not promote solvolysis of the polymer chains during this equilibration time. Flow times exceeded 150 s for all measurements. Water (1.000 $Cp_{25\ °C}$) , ACT (0.316 $Cp_{25\ °C}$) and CFM (0.542 $Cp_{25\ °C}$) were used as flow time-viscosity calibrants (Handbook of Chemistry and Physics, 1966-67). Viscosities in centipoise were determined by substitution of the experimental values in Equation 7.1:

$$\eta_1 = \frac{\eta_2 \rho_1 t_1}{\rho_2 t_2} \qquad \textit{(Equation 7.1)}$$

where η_1 and η_2 are the respective viscosities of the unknown and standard liquid, ρ_1 and ρ_2 are the corresponding densities, and, t_1 and t_2 are the flow times, respectively. Densities for dilute polymer solutions were assumed to be equal to the density of the pure solvent used to prepare these solutions, thus eliminating density terms from equation 7.1. Relative viscosities were determined according to equation 7.2:

$$\eta_{rel} = \frac{\eta}{\eta_0} \qquad \textit{(Equation 7.2)}$$

where η and η_0 are the viscosities of the polymer solution and solvent, respectively. Kinematic viscosity was additionally calculated by equation 7.3:

$$\eta_{kin} = \frac{\eta}{\rho} \qquad \textit{(Equation 7.3)}$$

where ρ was assumed to be equal to the density of the solvent.

7.2.2.2 Cloud-point titration

The cloud-point of R202H was determined as described in section 5.2.2 in the individual solvents used to prepare microspheres. Triplicate measurements were made.

7.2.3 Product attributes

Drug loading and yield were determined as described previously. Where yields were extremely low, additional material was retrieved from the cyclone wall to allow comprehensive characterization. Morphological examination and particle size analyses were performed as described in section 6.2.2.

7.2.4 Residual solvent

7.2.4.1 Gravimetric analysis

The loss of solvent residue from microspheres stored *in vacuo* at 24 ± 2.0 °C was followed gravimetrically from a sample of each batch (≥ 300 mg) until the samples attained constant weight. Constant weight was considered attained where three successive weekly measurements varied by less than ± 0.05 mg total sample.

7.2.4.2 Head-space analysis

A Perkin-Elmer Autosystem gas chromatograph (Connecticut, USA) fitted with a flame ionization detector was employed, to which was interfaced a Perkin-Elmer HS 40 headspace injector. The data was processed using Turbochrom® version 4.1 software. Standard solutions of DCM, CFM, ACT and HAL were prepared in phenoxyethanol at five levels in the concentration range 0.01- 0.20 $\mu L mL^{-1}$. Approximately 25 mg samples were accurately weighed into individual headspace vials, to which 1 mL of phenoxyethanol was added to disperse samples. The standards and samples were loaded into the headspace injector and after a predefined time in a heated compartment a constant volume of the headspace was admitted to the gas chromatograph. Calibration graphs for each solvent studied were constructed by linear regression of the peak areas obtained from standards on concentration prepared. The residual solvents present in the samples were then determined after correction for solvent densities from peak areas obtained by reading off the calibration graphs.

7.2.5 Particle architecture

The surface areas of selected samples were analysed by BET adsorption using a Micromeritics® 2360 Gemini (Micromeritics, Dunstable, UK). Analyses were performed with N_2 as adsorbate. Free space of sample was measured using He gas. True densities of drug-bearing and drug-free microspheres, batch #1 and #8 respectively, were determined by He gas as 1.311 and 1.276 gcm^{-3}.

7.2.6 Thermal analysis

The effect of *in vacuo* storage at 24 ± 2.0 °C on the thermal characteristics of microspheres prepared with different solvents was examined by DSC as described in section 5.2.3.6. Onset, mid-point, heat capacity change, ΔCp, and corresponding indices of the anomalous endotherm associated with the T_g were determined. In addition, the thermal behaviour of microsphere residue after dissolution was examined as described in section 6.2.2. The activation energies of the T_g for each batch at constant weight were calculated by linear regression of the logarithm of the scanning rate, ϕ, on the reciprocal of T_g (K^{-1}) according to Equation 7.4 (Fukuoka et al., 1986):

$$ln\,\phi = C^{1} - \frac{E_a}{RT} \qquad \textit{(Equation 7.4)}$$

where C^1 is a constant for a given polymer, and T is the apparent T_g corresponding to the linear heating rate, ϕ. Equation 7.4 therefore represents a heating rate analogue of the Arrhenius activation energy equation for the T_g.

7.2.7 *In vitro* release studies

Drug release was investigated by the USP paddle (method II) described as method B in section 5.2.3.6 at a stirring speed of 100 ± 1 rpm and temperature of 37 ± 0.5 °C immediately after microsphere preparation and at 5, 10 and 100 d storage under vacuum at 24 ± 2.0 °C. The first order release rate constant at each time interval was determined based on the data for 10 - ≤ 80 % cumulative drug release using CurveExpert 1.3.

7.3 Results and Discussion

In technological terms, the criteria for solvent selection for the preparation of biodegradable poly-α-hydroxy acids by ESE is based on factors such as the solubility constraints of polymer and solvent mass transfer considerations, e.g., partial water miscibility of DCM allowed controlled phase separation whereas use of water miscible ACT produced distorted agglomerates due to rapid solvent exchange (Bodmeier & McGinity, 1988b). The same selection criterion for solvent use for spray-drying have been arbitrarily applied, with little justification for their selection on technological grounds. Thus, DCM (Bodmeier & Chen, 1988; Mathiowitz et al., 1992; Gupta et al., 1993; Wagenaar & Müller, 1994), CFM, and mixtures thereof (Pavenetto et al., 1993; Conti et al., 1994; Conte et al., 1994a; Giunchedi et al., 1998) are invariably used; the work of Rafler & Jobmann (1994) who utilized acetonic systems on toxicological grounds excepted.

Under the conditions of rapid microdroplet desolvation which prevail during spray-drying, the more rapid the polymer deposition rate the greater the overall porosity of the particles formed. Thus, the use of solvents in which the polymer has low solubility, or those which require low absolute quantities of thermal energy to effect vapourization, should provide more rapid polymer phase separation — and hence greater void volume — by comparison to solvents of high solvency and heats of vapourization. The total heat requirements — taking account of specific heat capacities, boiling points, latent heats of vaporization and molar volumes — to vaporize 100 mL of each individual solvent were in ascending order: HAL, 29.96 kJ; CFM, 41.73 kJ; ACT, 42.76 kJ; and, DCM, 46.17 kJ. Therefore, microsphere porosity should be inversely related to these values, HAL-based products being of greatest porosity whereas other solvents should generate particles of approximately equal porosity. This postulation assumes no differences in the solubility of the polymer between solvents, which, on the contrary, was found to increase in approximately the opposite order to that given above.

7.3.1 Solubility studies

Theoretically, both the heat required to vaporize that solvent and polymer solubility therein should determine microdroplet solidification point. Variation in drug release described later, considered as a reliable indirect indicator of matrix structure, was apparently more influenced by differences in the magnitude of the polymer-solvent interaction as discussed below, than the heat requirements.

7.3.1.1 Cloud-point titration

End-point volumes for R202H were in ascending order 12.50, 13.85, 14.94 and 17.09 mL for HAL, ACT, CFM and DCM, respectively. Microsphere porosity and hence drug release was considered to decrease in the same trend, contrary to the results observed. It was reasoned that cloud-point is useful for comparison of the relative solubilities of different polymers in the same solvent system, However, due to potential cosolvency effects, cloud-point provides a relatively unreliable index where the quality of different solvents for identical polymer systems is being considered. Consequently, viscosity determinations were performed, which are believed to provide a more accurate indication of the intensity of association between polymer and solvent.

7.3.1.2 Viscosity studies

Polymer chains conform differently depending on the quality of the solvent in which they are dissolved (Bodmeier & McGinity, 1988b). Thus, in dilute solutions greater solvency is marked by an increased viscosity due to enhanced chain stiffness as a result of the chains existing in a more expanded state — with a commensurate increase in hydrodynamic volume (Stevens, 1990) — than in a poor solvent. Bodmeier & McGinity (1988b) observed relative viscosities in ascending order: ACT < benzene < DCM < CFM. Armstrong et al. (1994) found an exponential increase in viscosity with polymer concentration for DCM and HAL over the range 1 - 8 %w/v, whereby the exponent for HAL was notably greater than that for DCM. Based on these data, which substantiate the results in Table 7.3 for relative viscosity, the solvation power — and thus polymer solubility therein — of the four studied solvents in ascending order was concluded to be ACT < DCM < CFM < HAL.

Table 7.3 *Viscosity data for rifampicin-polymer solutions in selected organic solvents at 25 ± 0.1 °C, n=3*

	Solvent			
Viscosity	***DCM***	***CFM***	***ACT***	***HAL***
Absolute / cp	0.778	1.080	0.414	1.252
Kinematic / cs	0.584	0.730	0.524	0.668
Relative	1.495	1.636	1.310	1.616

7.2.1.3 Theoretical considerations

An alternative approach to the quantification of solvation power of a solvent is that of solubility parameters (Barton, 1975). The basic premise of the solubility parameter concept is a correlation between cohesive energy density (potential energy per unit volume) and mutual solubility. The one-component solubility parameter of Hildebrand, which approximates to equation 7.5 is considered useful for regular solutions, i.e. those without specific interaction or molecular polarity:

$$\delta_o = \left(\frac{-E}{V}\right)^{0.5} \qquad \textbf{(Equation 7.5)}$$

where E is the molar cohesive energy and V is the molar volume. Generally, a good solvent for a certain (nonelectrolyte) solute such as a polymer has a solubility parameter value close to that of the solute.

Shively et al. (1995) measured the solubility of PDLLA in solvents having total solubility parameters ranging from 8.9 - 14.8 $cal^{1/2}\,cm^{-3/2}$ to empirically determine a Hildebrand total solubility parameter for PDLLA of 9.8 $cal^{1/2}\,cm^{-3/2}$. A second slightly smaller solubility maxima at 13.0 $cal^{1/2}\,cm^{-3/2}$ was also observed with a distinct trough between these two values. Assuming a true density for the PDLLA composite studied of 1.276 gcm^{-3}, a total theoretical solubility parameter can be calculated based on molar attraction constants by equation 7.6 (Martin, 1993):

$$\delta = \frac{\rho \sum F}{M} \qquad \textit{(Equation 7.6)}$$

where M and ρ are the MW of the repeat unit and polymer density respectively. Such a calculation yields a value in accord with that determined by Shively et al. (1995) of 9.68 $cal^{1/2}\,cm^{-3/2}$.

Table 7.4 *Solubility parameters of (co)solvent(s) used to prepare spray-dried microspheres calculated by Equation 7.9*

		Solubility parameter /($cal^{1/2}\,cm^{-3/2}$)						
Solvent(s)	***Ratio***	δ_d	F_d	δ_p	F_p	δ_h	F_h	δ_0
ACT	100 %	7.6	47.2	5.1	27.9	31.7	21.1	9.8
DCM	100 %	10.0	45.5	8.9	34.6	40.5	14.1	13.7
CFM	100 %	8.7	66.9	1.5	11.0	11.5	21.5	9.3
DCM:CFM	1:1	9.35	53.4	5.2	26.5	29.7	16.9	11.5
CFM:ACT	2:1	8.33	59.4	2.69	17.9	19.2	21.4	9.3
DCM:ACT	2:1	9.2	46	7.6	32.8	38	16	12.4
TCTF	reference	7.2		0.8				7.2
TCE	reference	9.2		2.5				10.6
HAL	100 %							15.9

TCTF (1,1,2-trichlorotrifluorethane) and TCE (1,1,2,-trichloroethane) as reference solvents from Barton (1975).

Based on the data in Table 7.4 and theoretical determination of solubility parameter, both DCM and CFM were predicted to be excellent solvents for PDLLA. However, the correspondence of parameters for ACT and PDLLA (Shively et al., 1995) should render it a superior solvent. This is in contrast to viscosity determinations where it was concluded the poorest of those studied. In the absence of literature vales, the total solubility parameter of HAL, δ_0, was theoretically determined from ΔH_{vap} as 15.9 $cal^{1/2}\,cm^{-3/2}$ from Equation 7.7:

$$\delta_o = \left(\frac{H_{vap} - RT}{V} \right)^{0.5} \qquad \textbf{(Equation 7.7)}$$

where R is the gas constant, and T is the absolute temperature. For a liquid to dissolve a polymer, the differential between their δ_o should be less than 2 (Martin, 1993). Contrary therefore to viscosity determinations, HAL would be expected to behave as a polymer non-solvent. Indeed, the calculated value for HAL appears too large when compared with related molecules TCTF and TCE. Additionally, the intermolecular forces of attraction of fluorinated hydrocarbons are relatively small: they are non-polar liquids with low solubility parameters (Horvath, 1982); and, whilst miscible with aliphatic hydrocarbons ($\delta_o \cong 7.0$), partial miscibility prevails with solvents of $\delta_o \geq 8.5$. These data highlight the limitations of the single solubility parameter to predict solvent performance. The Hildebrand hypothesis has been largely superseded by the multicomponent solubility parameter approach of (Hansen, 1967). The total solubility parameter, δ, is the square root of the sum of the contributions from dispersive forces , δ_d^2, polar interactions, δ_p^2, and hydrogen bonding, δ_h^2, according to Equation 7.8.

$$\delta^2 = \delta_d^2 + \delta_p^2 + \delta_h^2 \qquad \textbf{(Equation 7.8)}$$

Where cosolvents are used the individual parameters contributions are additive, defined by Equation 7.9:

$$\delta_{x,c} = \phi_1 \delta_{x,1} + \phi_2 \delta_{x,2} \qquad \textbf{(Equation 7.9)}$$

where x= d, p, h and ø is the corresponding volume fraction of each component. The partial solubility parameters of the (co)solvent(s) studied here are presented in Table 7.4. Bodmeier & McGinity (1988b) used a ternary diagram with fractional partial Hansen parameters — calculated according to Equation 7.10 — constituting the axes to define the solubility envelope of PDLLA.

$$F_x = \frac{100.\delta_x}{\left(\delta_d + \delta_p + \delta_h\right)} \qquad \textbf{(Equation 7.10)}$$

Where F_x is the fractional contribution from dispersive, polar and hydrogen bonding forces. Overall, from the position of the phase boundary, relatively high fractional dispersive forces appeared to be the most significant factor for polymer solubility. Polar forces were of secondary importance, whereas solvents with relatively strong hydrogen bonding components had poor solvent power. Therefore, from these collective observations, good solvency for PDLLA should prevail for solvents which possess a δ_o

value of 9.8 ± 2.0 $cal^{1/2}$ $cm^{-3/2}$, a considerable contribution to which is from dispersive forces. These considerations place DCM, ACT and CFM in order of solvent power ascendancy. The mixture of DCM:ACT was anticipated to be the poorest cosolvent with the lowest dispersive contribution and a total solubility parameter corresponding to the solubility trough determined by Shively et al. (1995). Similarly, DCM:CFM was also anticipated to occupy this trough, whereas CFM:ACT better matched the criteria of a good solvent. Few of these data however correlated with the factors considered to be critical to microsphere deposition kinetics, and, in turn, release kinetics. Viscosity was therefore considered a more reliable marker of solvent power; solubility parameters, whilst being a useful predictive tool of gross polymer solubility, could not differentiate between the subtle differences apparently so critical to matrix structure under the aggressive desolvation conditions of microsphere preparation.

7.3.2 Product attributes

The chemical inertness of the studied solvents was established by the fact that drug loading corresponded to the nominal 20 %w/w ($P > 0.05$) for all batches. The low levels of RQU detected during analyses were consistent with limited oxidative degradation inherent to the associated extraction procedure. Polymer stability was indirectly confirmed by the constancy of viscosity determinations after 168 h storage.

Microsphere yields and site of product deposition are listed in Table 7.5. The polymer and processing factors which affect yield of production were discussed in sections 5.3.1 and 6.3.1.2. Variation in microsphere yield is ultimately attributable to variable solvent-polymer interactions between the solvents used, which, in turn, affects: microsphere architecture through its influence on the deposition kinetics of the microsphere matrix; solvent residue; and, the T_g of the microsphere matrix, as does drying temperature. Indirect studies of polymer solubility in the four solvents based on viscosity measurements (section 7.3.1.2) indicated solvency power increased in the following order: ACT < DCM < CFM < HAL. The concentration at which the polymer blend achieved saturation should therefore show an identical trend. Additionally, in the absence of confounding factors, the propensity of the polymer to retain solvent as unwanted residue should increase in parallel with medium solvency power. Thus, rapid solvent evaporation of volatile ACT yielded a low density porous product with low solvent load which was readily exhausted from the apparatus. In an effort to increase product yield, the aspiration was reduced to 50 % for batch #3

compared with batch #2. The reduced vacuum in the area of the cyclone at this setting was expected to assist the deposition of particles of low specific weight in the collector. On the contrary, a 10 fold reduction in product yield was observed, whereby a considerable proportion of material deposited on the cyclone walls and in the region of the vacuum connector at the top of the cyclone. Furthermore, little material impacted with the drying chamber suggesting desiccation occurred in this area although the air flow pattern was significantly disrupted to promote material impaction on the cyclone walls and ultimately reduce product yield. Process generalizations do exist (Büchi, 1993). However, these data highlight the complex interplay of drying parameters which operates during spray-drying, each of which require specific optimization for individual products.

Table 7.5 *Yields of production of microspheres prepared from various organic (co)solutions. (n = 1)*

	Solvent		***Yield / % total solid***		
Batch	***Nature***	***Ratio***	***Cyclone***	***Collector***	***Total***
1	DCM	100 %	19.3	42.7	62.0
2	DCM:ACT	2:1	17.3	4.0	21.3
3	DCM:ACT*	2:1	0.33	0.01	2.0
4	ACT	100 %	0.33	0.66	2.0
5	DCM:CFM	1:1	46.0	10.0	56.0
6	DCM:CFM	1:1	28.6	12.7	41.3
7	CFM:ACT	2:1	31.0	5.0	36.0
8	DCM	100 %	16.0	39.3	55.3
9	HAL	100 %	4.0	2.7	6.7
10	HAL	100 %	28.0	8.0	36.0

*Aspiration = 50%

High solvent residue lowers the T_g. This promotes adherence of product to pre-collector glassware elements where the T_g temperature is below that of the drying air, thus reducing product yield. Scanning electron micrographs in section 7.3.3 did not reveal any discernible differences between batches, even at high magnification. These features were typical of the formation of a porous pliable crust during microsphere formation which permitted the transfer of solvent, without distortion, according to the model of Kawashima et al. (1972). In contrast to this overall pattern with ACT based solvents, reduced microsphere formation rate associated with the use of DCM, CFM and HAL, particularly at lower temperatures, resulted in a more coherent matrix. High solvent residue reported in section 7.3.5 is associated with the formation of a more coherent matrix with a greater density which reduces the proportion of particles exhausted from the apparatus, whilst promoting particle deposition in the apparatus collector. Considerable residue of relatively

dense solvents presented in Table 7.5 such as DCM, CFM and HAL contributes to individual particle density and further promotes high microsphere yields.

7.3.3 Scanning electron microscopy

Irrespective of the solvent system used to prepare these products, photomicrographs revealed discrete microspheres with seemingly smooth morphology absent of blow-holes and other surface discontinuities, morphological flaws associated with spray-drying of volatile solvents (Masters, 1992). Particle granulometry was typically characterized by a unimodal, narrow size distribution. The high halothanic residue in batch #9 accounted for the apparent partial fusion of microspheres shown in Figure 7.1 (B) which was considered to occur after formation in the collection vessel.

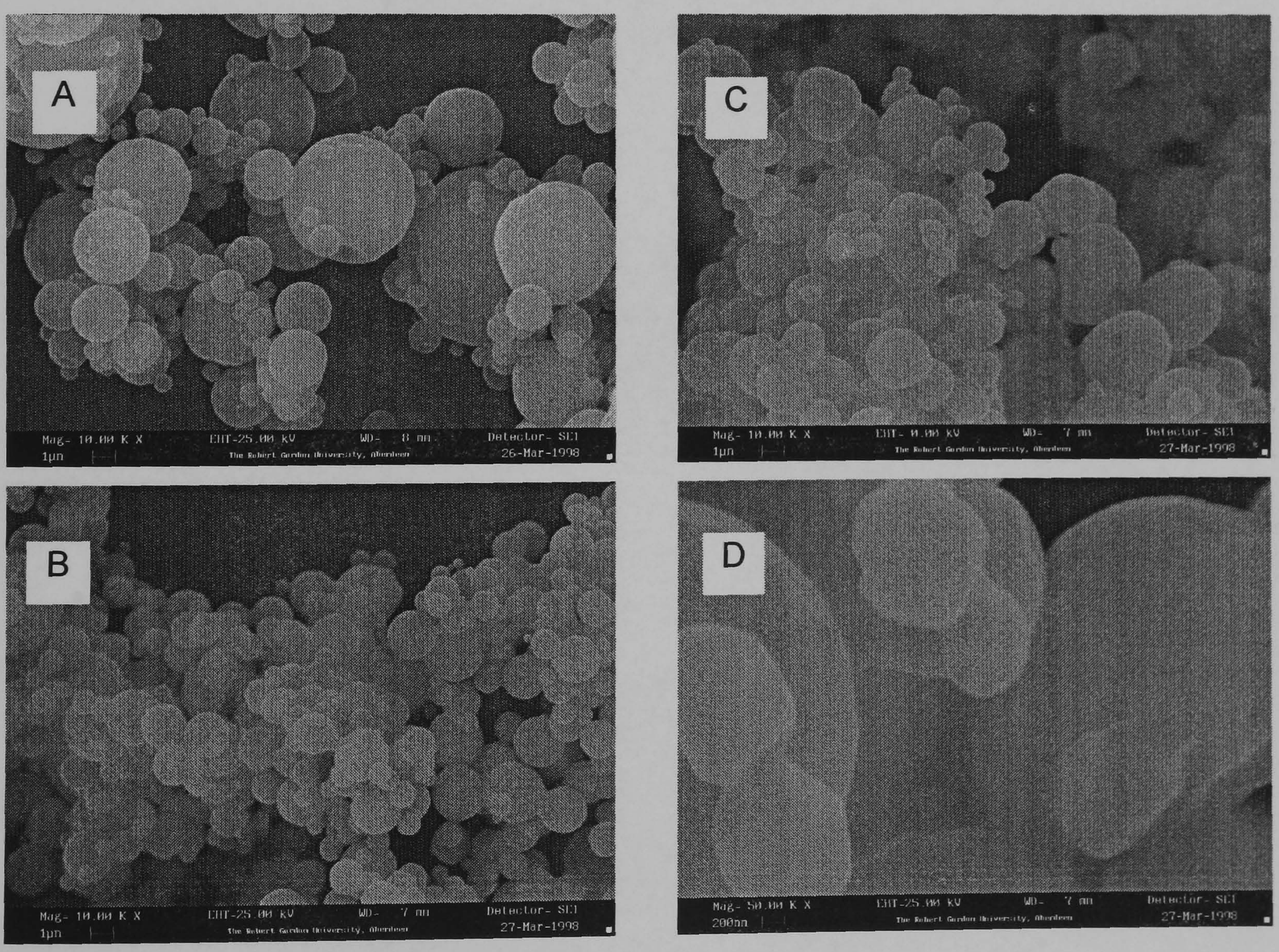

Figure 7.1 *Photomicrographs of: A, batch #1 (mag^n, 10 k); B, batch #9 (mag^n, 10 k); C, batch #4 (mag^n, 10 k); and, D, batch #4, (mag^n ,50 k). Batch # according to Table 7.1.*

Histographic variation in mean diameter shown in Figure 7.2 was explained in the context of the generalized pattern of particle formation based on solvent power. Under otherwise constant processing parameters, variation in microdroplet size is a function of the intermolecular forces between chains, or, more simply, solution viscosity. Therefore, microdroplet diameter at the point of generation would be expected to increase in the order: ACT < DCM < CFM < HAL. That the particles had no surface distortion, e.g., collapsed / shrivelled surface, it follows that microsphere mean diameter should exhibit a similar trend. However, with the exception of DCM, with which the volume distribution was positively skewed by a few particularly large particles, microsphere diameter increased as solvent strength decreased, supportive evidence of more rapid polymer deposition and the generation of a more open porous matrix. In contrast, solvents of greater solvent power and heat requirements preserved particle fluidity for longer periods during drying, e.g., HAL and CFM:DCM respectively. This allowed for more controlled polymer deposition and solvent transfer to the surface from where evaporation occurred, with a resultant increase in matrix density and a reduced mean diameter.

7.3.4 Residual solvent

Polymer-solvent affinity and drying conditions were influential factors on microsphere architecture, which, in turn, affected the level of residual organic adulterant. Despite the interplay of these factors, two generalizations based on the data could be made: 1) retention of solvent was in parallel to solvency power of individual solvents; and, 2) high matrix porosity promoted solvent loss.

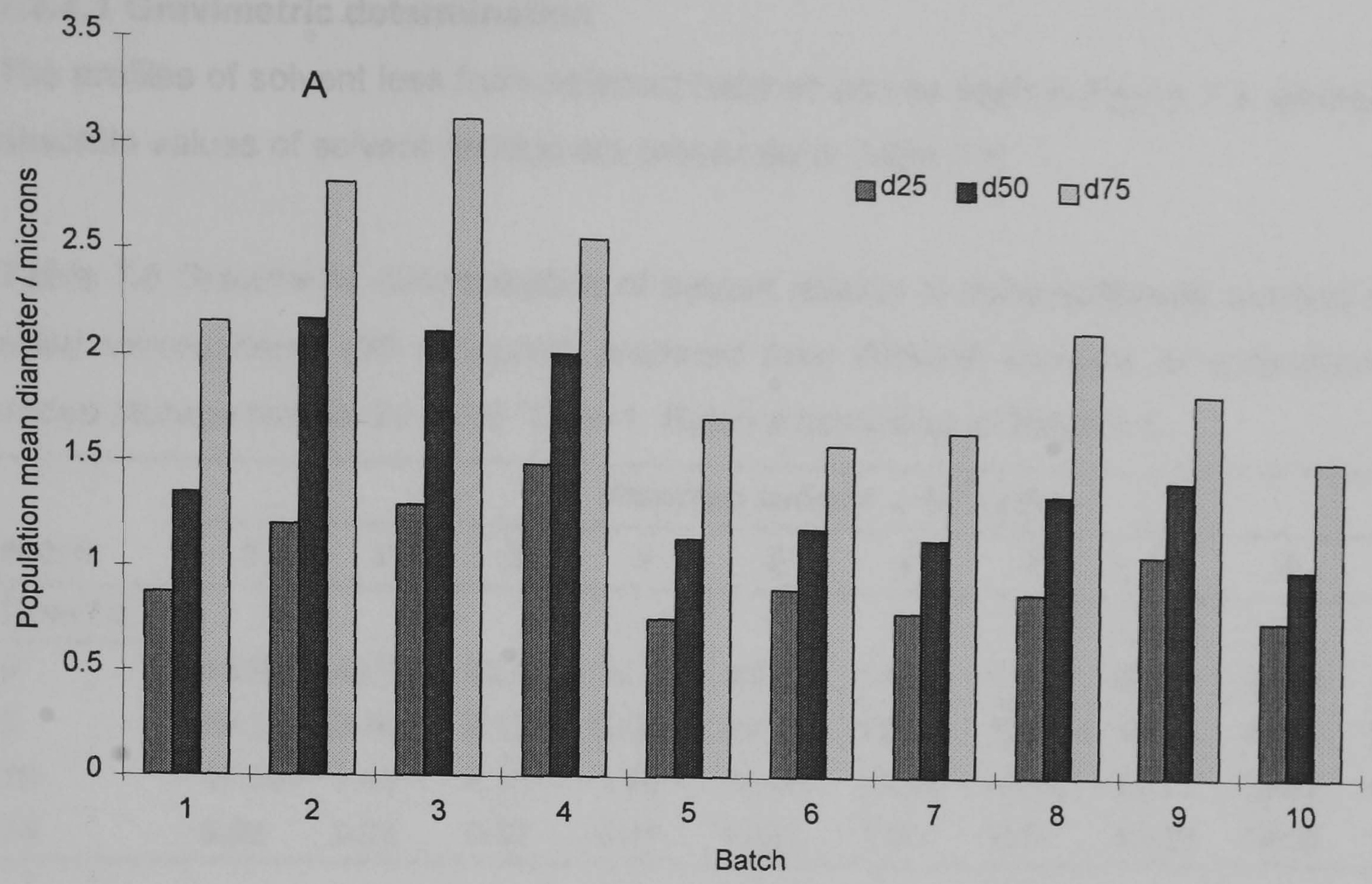

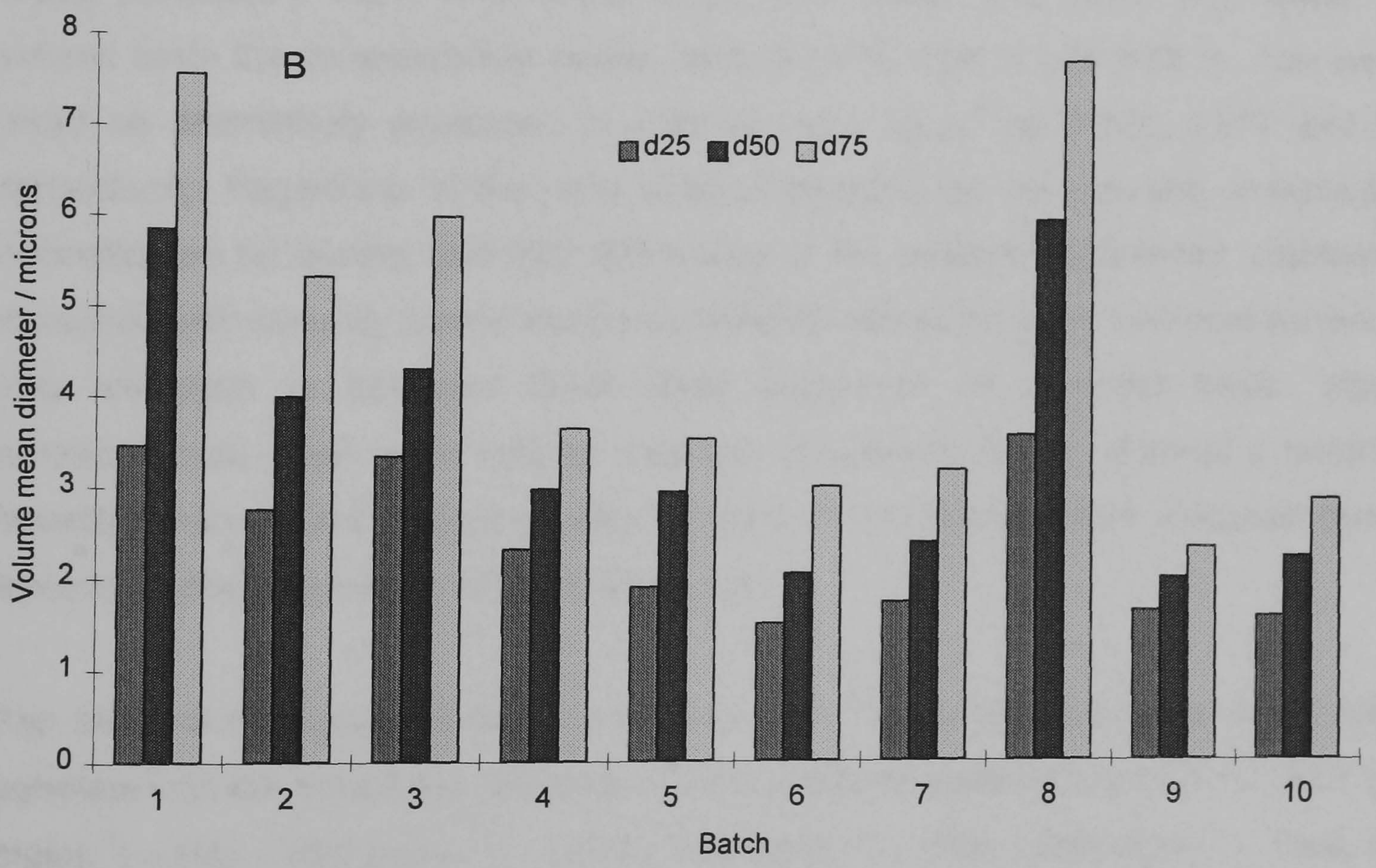

Figure 7.2 *Histograms of population (A) and volume (B) granulometric statistics for compositionally identical microspheres. Legend represents 25% (d25), 50% (d50) and 75% (d75) undersize quartiles. Processing parameters according to Table 7.1.*

7.3.4.1 Gravimetric determination

The profiles of solvent loss from selected batches can be seen in Figure 7.3, whereas the absolute values of solvent residue are presented in Table 7.6.

Table 7.6 *Gravimetric determination of solvent residue in compositionally identical spray-dried microspheres (#8 excepted) prepared from different solvents as a function of in vacuo storage time at 24 ± 2.0 °C, n=1. Batch # according to Table 7.1.*

	Residual solvent x 10^{-3} / ppm									
Batch	***1***	***2***	***3***	***4***	***5***	***6***	***7***	***8***	***9***	***10***
Time / d										
0	60.69	40.52	42.30	24.73	93.52	68.06	106.3	86.23	90.56	125.5
5	29.26	8.16	9.12	6.09	62.56	48.25	70.25	40.31	40.23	75.23
10	17.53	1.41	2.15	1.59	18.25	10.26	22.12	26.01	23.22	45.21
15	9.03	0.28	0.32	0.45	4.56	1.85	7.27	11.06	12.36	15.1

Substantial loads of residual solvent were recorded irrespective of the solvent system and drying parameters: ACT, 2.48 %w/w; DCM, 6.07 %w/w; and, HAL, 12.6 %w/w. On a volume basis the corresponding values were 3.14 %, 4.56 % and 6.85 %. The residues might be alternatively expressed in units of $mol_{sol}\ kg_{mat}^{-1}$ as 0.043, 0.072 and 0.064 respectively. Regardless of the units used to describe the residue and, irrespective of normalization for density and MW differences of the solvents determined, residual load increased with solvency power and hence polymer affinity for each individual solvent. The only exception to this was DCM when expressed on a molar basis. Viscosity measurements, used as an indirect measure of solvency power, showed a remarkable linearity when plotted against residual solvent of the microspheres prepared from the three individual solvents as seen in Figure 7.4.

The effect of encapsulated drug on residue level, in analogy to polymer blend, did not correlate with the solubilities determined during preformulation at 24 ± 2.0 °C: ACT (41.7 $mgmL^{-1}$) < HAL (76.9 $mgmL^{-1}$) < DCM (216 $mgmL^{-1}$) < CFM (349 $mgmL^{-1}$). Thus, it was concluded that the polymer had the overriding influence on residual solvent as it comprised the predominant component of the matrix.

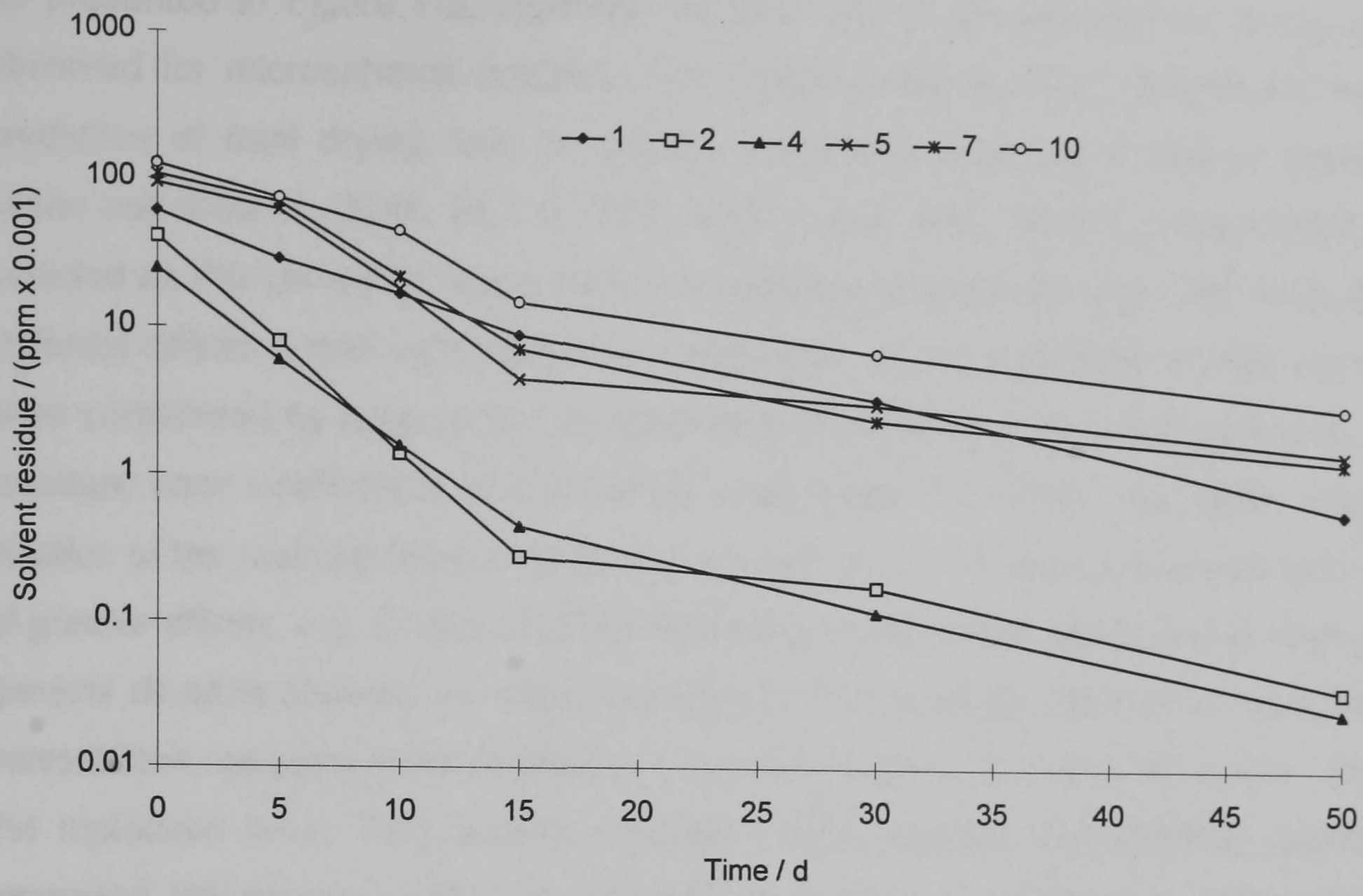

Figure 7.3 *Semi-logarithmic profiles of solvent loss from compositionally identical spray-dried microspheres prepared from different solvents during in vacuo storage at 24 ± 2.0 °C. Legend indicates batch according to Table 7.1.*

In processing terms, an increased inlet temperature, i.e., 50 compared with 40 °C resulted in a reduced solvent load for DCM:CFM (#6 and #5) and HAL (#9 and #10) as a result of greater drying efficiency at elevated temperatures. Elevated inlet temperatures were anticipated to produce greater matrix porosity associated with more rapid polymer deposition and hence more rapid residue depletion. On the contrary, decreased kinetic constants for solvent loss in Table 7.7 for comparable batches prepared at 50 °C when compared with those at 40 °C were at apparent odds with this hypothesis. The initial rates of solvent loss were consistent with the anticipated pattern however, loss of linearity with the onset of a secondary slower phase of solvent loss accounted for this disparity.

Table 7.7 *First order regression statistics for gravimetrically determined solvent loss from compositionally identical spray-dried microspheres prepared from different solvents during in vacuo storage at 24 ± 2.0 °C, n=1. Batch # according to Table 7.1.*

	Batch									
	1	***2***	***3***	***4***	***5***	***6***	***7***	***8***	***9***	***10***
Statistics										
k / d^{-1}	0.088	0.126	0.126	0.130	0.081	0.068	0.089	0.087	0.052	0.073
$t_{0.5}$ / d	7.875	5.500	5.500	5.331	8.556	10.19	7.787	7.966	13.33	9.493
r^2	0.985	0.824	0.831	0.909	0.809	0.839	0.876	0.977	0.739	0.919

As presented in Figure 7.3, log-linear dependence of solvent load on drying time was observed for microspheres prepared from single solvents. This allowed the theoretical prediction of total drying time to achieve essentially equilibrium organic residue after seven half-lives of: DCM, 55.1 d; ACT, 37.3 d; and, HAL, 66.5 d. Seven half-lives was selected as this period corresponded to compliance of batch #1 with USP limits for DCM. Different diffusion and vaporization characteristics of the individual solvent components were considered to account for the deviations from linearity for mixed solvents and the resultant poor coefficients of correlation seen Table 7.7. Thus, the faster evaporation kinetics of the residual fraction of poorer solvent, e.g., ACT when compared with solvents of greater affinity, e.g., CFM and DCM resulted in an apparent biexponential drying plot. In general all plots showed an 'elbow' at around 15 d storage. During the early stages of solvent loss, ongoing 'stress-relaxation' processes result in matrix structural changes at the molecular level. This feature, coupled to the reduced concentration gradient and increased diffusional pathlength might account for the approximate first-order drying kinetics.

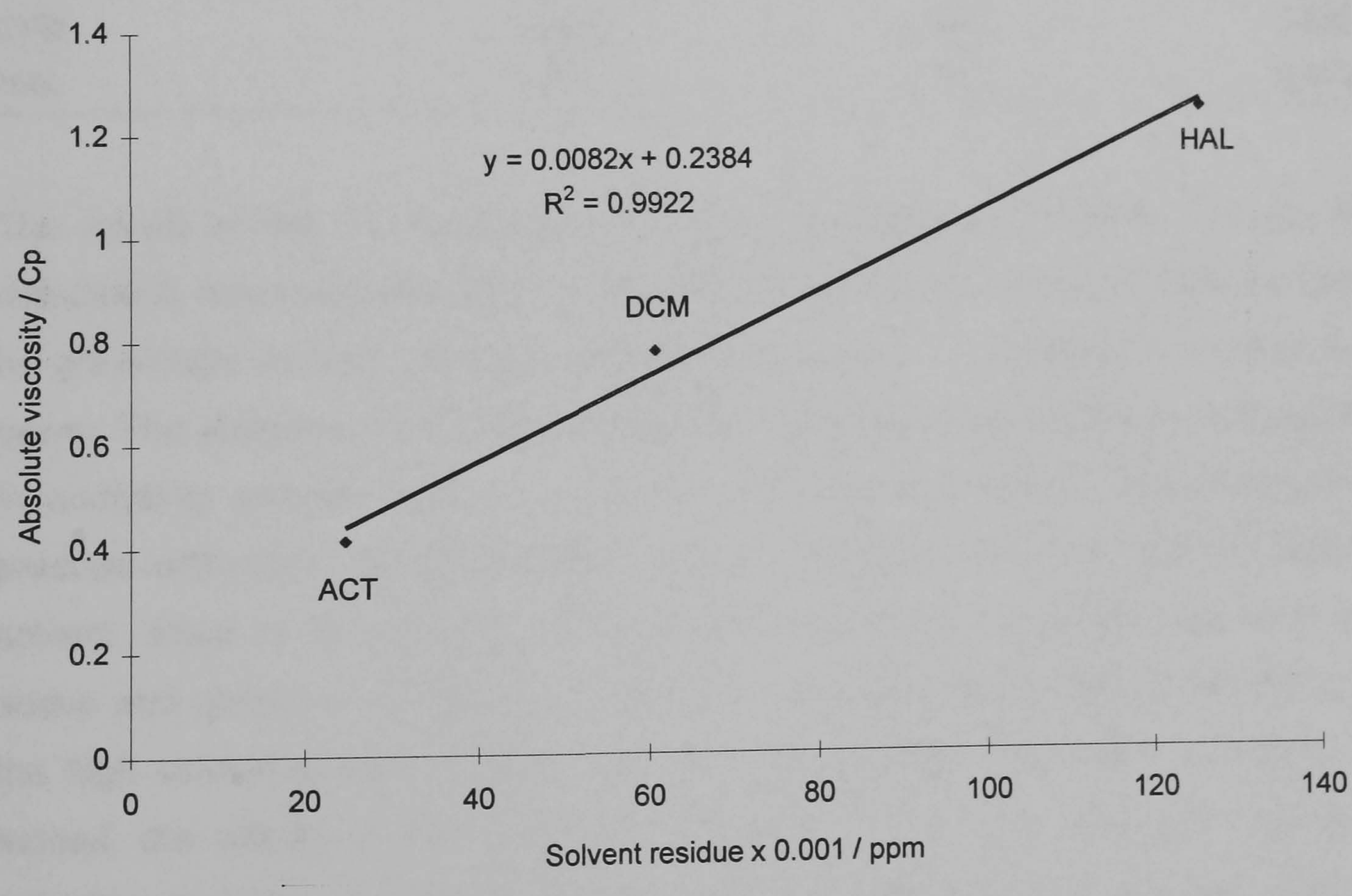

Figure 7.4 *Plot showing the apparent relationship between absolute viscosity (3 %w/v) of rifampicin-polymer blend in individual solvents versus the residual solvent content of microspheres prepared with same*

7.3.4.2 Head-space analysis

Headspace gas chromatographic analysis has largely superseded both thermogravimetric and chlorine analysis (Benoît et al., 1986) for organic residue determinations due to the high mass sensitivity and selectivity afforded by the technique (Gangrade & Price, 1992). Owing to these attributes, headspace analysis was therefore employed to confirm the preferential loss of solvents during storage. Linearity of detector was established for each individual solvent as seen in Table 7.8. Absence of interference was established as the mean intercepts for all calibration lines were not greater than ± 0.95 % of the values for detector response at the 100 % analyte level.

Table 7.8 *Regression statistics for detector response on concentration of individual solvents for head-space analysis, n=5.*

	Regression statistic		
	slope x 10^{-5}	***intercept x 10^{-3}***	***r^2***
Solvent			
ACT	5.634	1.749	1.000
DCM	4.382	2.092	0.999
CFM	2.606	0.899	1.000
HAL	6.964	2.200	0.999

The results of the GC headspace analysis are presented in Table 7.9. No ACT was detected in these analysis and the results did not correlate with the residues determined by gravimetric means, although general trends were still evident in relation to solvent power. The absence of ACT and largely DCM was attributed to solvent loss and the delay in analysing samples sent to a remote site for investigation. Notwithstanding these practical difficulties, omnipresence of CFM in samples prepared with a fraction of this solvent, allied to the absence of cosolvent, confirmed the preferential loss described above and observed in Figure 7.3. Likewise, considerable halothanic residue confirmed the high solvent powers of these two solvents and the intransigent retention of same. Indeed, the affinity of both drug and polymer for CFM was strikingly apparent by its detection in batch #1 where it was not used. This apparent anomaly was perhaps attributable to the use of CFM to prime and clean the feed tubing and the drier nozzle prior to spraying the feed solution.

Table 7.9 *Head-space gas chromatographic determination of solvent residue in compositionally identical spray-dried microspheres prepared from different solvents as a function of in vacuo storage time at 24 ± 2.0 °C, n=1. Batch # according to Table 7.1.*

			Residual solvent x 10^{-3} / ppm		
Batch	***Solvent(s)***	***Storage time / d***	***0***	***5***	***10***
1	CFM		0.122	0.0210	0.00968
2	DCM		0.0126	–	–
5	CFM		17.55	3.559	2.112
6	CFM		13.31	2.006	2.232
7	CFM		34.57	0.735	0.804
9	HAL		41.96	40.35	44.29
10	HAL		53.16	43.74	37.24

7.3.5 Particle architecture

Density determination of drug-bearing and drug-free microspheres, batch #1 and #8 respectively, were 1.311 and 1.276 gcm^{-3}. Using the volume size distributions described above and assuming zero porosity, these values were used as a reference for the determination of theoretical surface areas for selected batches. The experimental results are compared with theoretical values in Table 7.10.

Table 7.10 *Theoretical and determined specific surface areas for selected batches of compositionally identical spray-dried microspheres (batch #8 excepted), n=1. Process parameters as per Table 7.2.*

	Specific surface area / (m^2 g^{-1})		
Batch	***Theoretical (T)***	***Experimental (E)***	***Factor of Deviation (E/T)***
1	0.186	1.43	7.68
2	0.270	2.28	8.44
3	0.154	-	-
4	0.208	2.30	11.06
5	0.242	2.99	12.36
6	0.292	-	-
7	0.265	-	-
8	0.132	3.05	23.12
9	0.300	-	-
10	0.290	2.78	9.59

The considerable deviation between theoretical and determined surface areas was attributed to the use of true density, whereas apparent density would provide a more accurate index of the actual number of particles which constituted one gram of microspheres. Notwithstanding the limitations of these determinations and, despite the apparent pore-free nature of all batches from SEM, substantial N_2 accessible pores were evident from these measurements; typically a feature of spray-dried PDLLA particles (Conti et al., 1991; Pavanetto et al. 1992). These workers calculated a three-fold increase in specific surface area for spray-dried particles when compared with non-porous particles of equivalent diameter. Correlation between porosity and anticipated polymer deposition kinetics based on solvency power was generally poor, although batch 1,2 and 4 did follow the expected pattern.

The absence of drug in the formulation had the most remarkable effect on overall porosity. During drying it is postulated that drug precipitates before the polymer thus behaving as nuclei around which polymer can deposit. Shively et al. (1995) determined an approximate solubility of PDLLA in 'good' solvents of 750 - 1000 mg. It is postulated that the greater the differential between drug and polymer solubility then the greater the phase separation between the components. Thus, in ACT (RIF solubility = 41.7 $mgmL^{-1}$), drug precipitates before the polymer concentration, and therefore viscosity, can reach a critical value which impedes further crystal growth around formed nuclei. This feature should result in larger precipitates embedded within the matrix when compared with solutions sprayed from CFM (RIF solubility = 349 $mgmL^{-1}$) where drug dispersion within the matrix should approximate to the molecular state. Relative drug and polymer deposition kinetics also might have implications for the thermal character of the matrix. Drug might otherwise have a 'salting-in' effect as was apparent with progesterone (Benoît et al., 1986). Delayed polymer precipitation under these circumstances would be considered to produce a less porous matrix. There are particular limitations to the reliability of these results, however they do act to illustrate the considerable influence of solvent choice on matrix architecture, which, in turn, is a principal determinant of drug release kinetics as discussed in section 7.3.7.

7.3.6 Thermal analysis

It is well established that the thermal history of the polymer can greatly affect the observed T_g. Influential factors include, preparation temperature, cooling rates and subsequent annealing conditions (Ford & Timmins, 1989). The area and position of the

anomalous peak associated with the T_g have been found to increase with decreasing cooling rate of melt during glass formation (Serajuddin et al., 1986; Fukuoka et al., 1986). These observations reflected the dynamics of freezing of molecular motion and the quantity of glass relaxation occurring during same. Consequently, matrices thus formed can be considered to possess an excess of enthalpy when compared to their equilibrium state which is released slowly under ambient conditions, whereupon the polymer molecules attain a more favourable thermodynamic arrangement. This latter process is referred to as enthalpy relaxation (Kerc & Srcic, 1995).

The endotherm for spray-dried products is, by analogy, also a function of the rate at which large scale molecular motion is frozen during polymer deposition. Therefore, deposition rate dictates both matrix coherence and the amount of strain or excess enthalpy in the system. Increased matrix density restricts polymer chain motion due to reduced free volume both at a macroscopic and microscopic level. This factor was considered to account for the suppression of T_g with ACT derived products, whereas increased density, molecular association and bonding of those prepared from DCM or HAL elevated the ultimate T_g for compositionally identical products. Thus, T_g was accepted as a useful index of matrix compactness. The extent of division of RIF should also affect the position of the T_g. At low states of division, e.g., exclusively embedded crystals, polymer and drug behave as two phases and the position of the T_g should correlate to that in the absence of drug. As the state of division increases there is a parallel elevation of T_g with the introduction of interposing drug particles between polymer chains, the effect of which is maximal when the drug is molecularly dispersed. In this latter state however, the T_g may fall dramatically with the onset of solid solution where the polymer and drug interact significantly. Thus, as described in section 7.3.5, larger drug crystallites / precipitates formed with ACT, compared with CFM, would result in a reduced 'filler-effect' and a lesser elevation of T_g. This postulation is largely consistent with the position of the determined T_g in relation to drug solubility in the various solvents.

This simplification when comparing melt quenching and spray-drying is however complicated by the facilitative action of solvent residue on isothermal enthalpy relaxation, although from Table 7.11 peak position, if not area, followed this trend. The comparative data for quench cooling rates was however based on the measurement of T_g temperature immediately after preparation rather than upon storage. Therefore, the endothermic areas

at 100 d were a reflection of the total strain conferred during drying, which was accordingly inversely related to solvency power. Furthermore, the final endothermic area (which represents the residual strain in the system), whilst being inversely related to overall matrix stability, showed a remarkable correlation with drug release rate.

Table 7.11 *Thermal analysis of the ageing effects of compositionally identical spray-dried microspheres upon storage at 24 ± 2.0 °C in vacuo. Process parameters as per Table 7.1*

	Peak / °C				Transition $^1/_2$Cp / °C				Endotherm / (Jg^{-1})			
Time / d	0	5	10	100	0	5	10	100	0	5	10	100
Batch												
1	53.6	56.8	57.1	61.5	52.6	54.5	53.9	56.2	*	2.45	2.62	4.15
2	47.1	51.4	52.3	56.3	43.3	45.7	47.0	49.1	*	4.23	4.21	5.40
3	45.1	50.9	51.6	54.6	41.3	44.9	45.3	45.9	*	4.35	4.66	6.21
4	40.4	44.7	45.9	48.6	38.9	37.6	37.7	40.3	*	2.79	3.65	5.69
5	*	57.5	57.0	59.0	39.8	50.6	51.6	55.0	*	2.60	3.40	5.60
6	*	58.0	59.3	62.9	46.4	52.2	53.3	55.6	*	2.68	3.25	5.20
7	*	52.9	53.0	58.2	39.0	46.3	46.8	48.0	*	4.07	4.12	6.74
8	43.2	48.6	48.5	51.3	39.4	42.1	42.0	42.1	*	5.64	6.51	8.12
9	*	48.9	51.1	59.0	42.9	47.0	47.3	50.7	*	2.06	4.17	4.79
10	*	48.1	52.1	59.8	37.3	43.2	43.8	49.5	*	*	6.86	5.57

* large diffuse peak between 30 - 70 °C

****data based on 2nd scan**

In relation to solvent residue, thermograms revealed diffuse, in some cases indiscernible thermal events for freshly prepared products, whereupon desiccation an endotherm (heat capacity maximum) rapidly developed, the magnitude of which was time- and solvent-dependent as seen in Figure 7.5. Moreover, the position of the endotherm and the underlying T_g shifted up-scale as the plasticizing action of the residual solvent diminished with increased storage time. Residual solvent load determined the magnitude of this shift, which increased as the solvency of the solvent system increased and, in contrast, the drying temperature decreased. This ageing process, traced by the up-scale shift of the T_g and the development of an endotherm, represented loss of 'stored' energy generated by rapid microsphere formation during spray-drying as discussed above. Whereas with ACT prepared products, high matrix porosity allows rapid residue evaporation, reduced microsphere formation rate with other solvents studied, particularly at lower inlet temperatures, results in a more coherent matrix. High matrix tortuosity associated with the use of good solvents contributed to the tenacious retention of organic solvent.

Additionally, high and persistent solvent residue permitted significant polymer relaxation upon storage due to its plasticizing action.

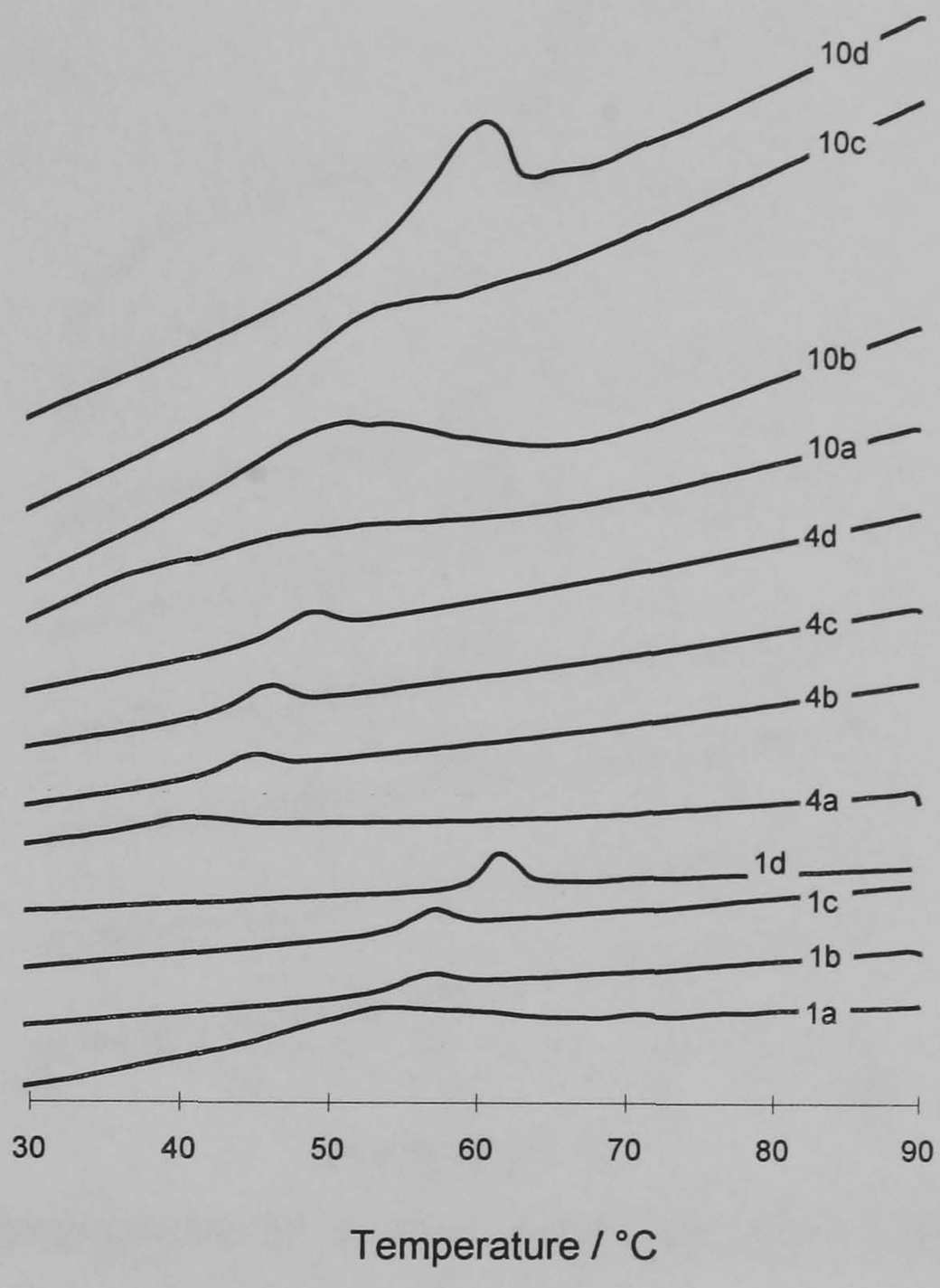

Figure 7.5 *DSC thermograms of microspheres after various storage times in vacuo at 24 ± 2.0 °C. Key: a) immediately after preparation; b) 5 d; c) 10 d; and, d) 100 d. Number indicates batch according to Table 7.1.*

After exhaustive *in vacuo* drying, apparent activation energies in Table 7.12 of T_g were determined. The effect of heating rate on the position of T_g temperature is shown in Figure 7.6. Three indices of glass transition were considered in these calculations: onset temperature, T_f ; maximum temperature of the anomalous endotherm, T_m ; and, post-transition baseline-endotherm intersept, T_i . The regression statistics demonstrated excellent correlation for T_f and T_m whereas comparatively poor linearity using the T_i. Nonetheless, the computed statistics associated with the latter index, the general convention for such calculations (Ford & Timmins, 1989), were used for assessment.

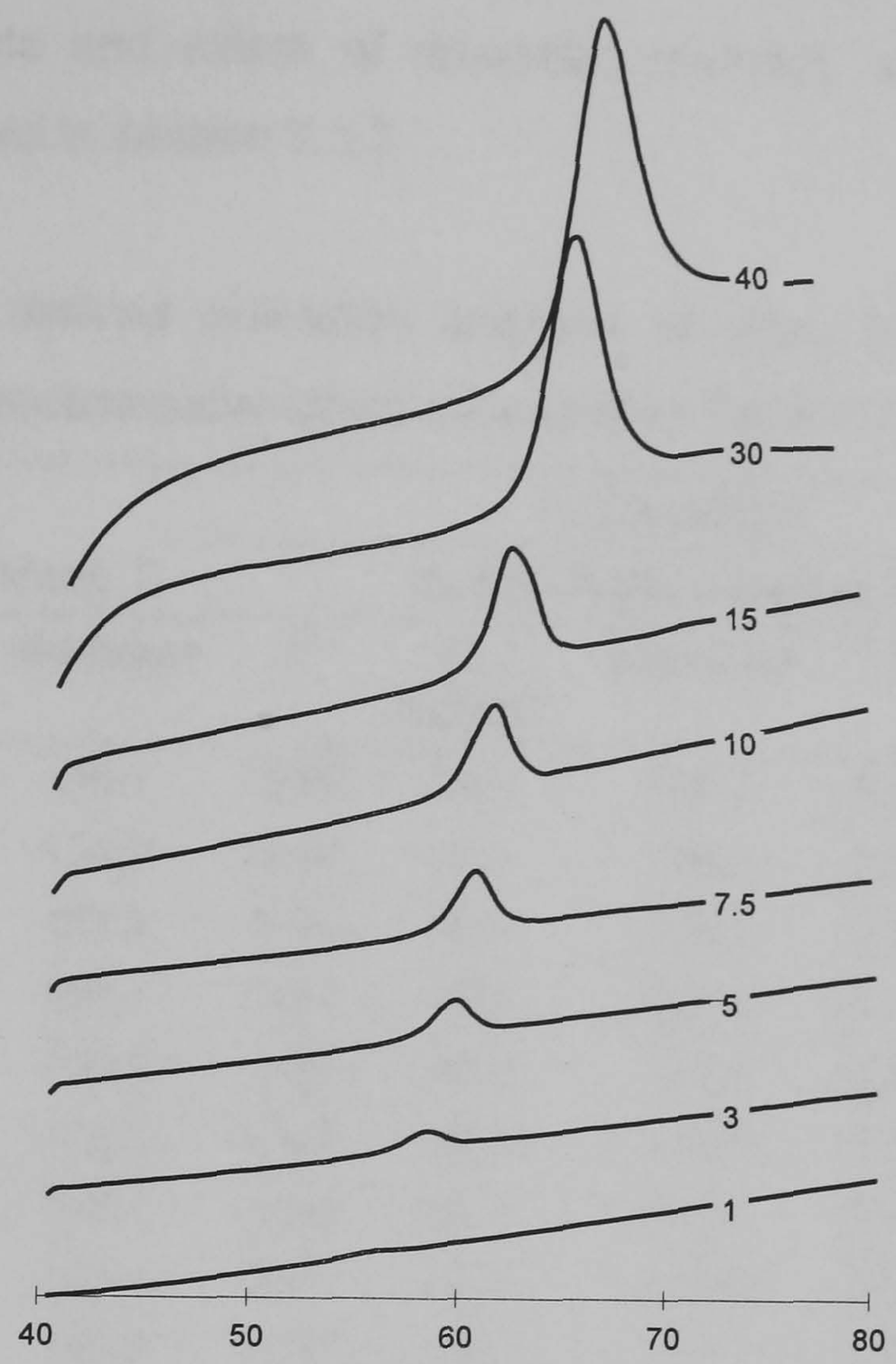

Figure 7.6 *DSC thermograms at various scanning rates of batch #1 at constant weight (plot labels indicate scanning rates in °Cmin^{-1})*

Apparent activation energies in Table 7.12 for the T_g were inversely related to the enthalpy of the endotherm for the associated recovery process. The latter parameter was however directly related to the level of solvent residue which facilitates molecular movement associated with relaxation. Structural relaxation is associated with the formation of a more stable microsphere matrix and has been described in terms of the 'Hole Theory' of bulk viscosity. In simple terms, during relaxation, hole disappearance and genesis occur concurrently, however, an equilibrium is thought to exist between the 'liquid' lattice and the number and volume of holes during relaxation. Consequently, the volume and the energy of holes decrease through an activated state, the potential barrier to which can be considered proportional to the apparent E_a. Thus, based on this factor, microspheres prepared from DCM:ACT (#2 & 3) and HAL (#9 & #10) were expected to result in slowest drug release (section 7.3.7). However, these indices are relative and give no indication of the initial or final energy state of the matrices. Additionally, related to relaxation, the T_g of the matrices formed proved a more reliable indicator of microsphere

stability, release rate decreasing as the T_g increased. Clearly, other factors influenced by the drying process, such as matrix density, have a role in determining the magnitude of the T_g and the rate and extent of relaxation recovery, which, in turn, modulate drug release as described in section 7.3.7.

Table 7.12 *DSC derived activation energies of glass transition for microspheres at constant weight. Process parameters according to Table 7.1.*

	T_g Transition								
	Onset, T_f			Extrapolated baseline, T_i			Endothermic peak, T_m		
Batch	E_a / kJmol^{-1}	intercept	r^2	E_a / kJmol^{-1}	intercept	r^2	E_a / kJmol^{-1}	intercept	r^2
1	58.5	178.1	0.95	54.7	167.1	0.99	39.5	120.4	1.00
2	43.2	134.7	0.95	37.1	128.3	0.92	38.4	119.1	0.98
3	38.9	121.8	0.99	36.1	113.8	0.91	37.2	115.7	0.98
4	70.8	225.4	0.97	75.9	241.9	0.91	50.0	158.2	1.00
5	45.7	139.2	0.98	46.0	140.6	0.92	43.1	130.8	1.00
6	45.3	138.0	0.98	46.2	140.9	0.90	43.6	132.0	1.00
7	42.8	132.7	0.98	38.4	119.6	0.90	37.8	116.5	0.99
8	48.7	153.1	0.97	40.1	126.8	0.99	44.1	138.0	0.99
9	38.1	155.3	0.97	32.0	107.2	0.94	34.9	107.1	0.99
10	39.7	159.7	0.98	35.0	108.8	0.95	35.3	108.2	1.00

7.3.7. Drug release studies

In the previous chapter the thermal behaviour of blends of low and moderate MW PDLLA was identified as a critical determinant of RIF release. Other important factors include matrix hydrophilicity and structure. For compositionally identical microspheres, intrinsic hydrophilicity should remain ostensibly constant. Thus, the remarkable differences in release of RIF with change in process conditions as seen in Figure 7.7 can be attributed to a resultant variation in matrix architecture and thermal character as discussed throughout this chapter.

Upon incubation, microspheres slowly hydrate. Water ingresses slowly causing matrix softening until the matrix T_g temperature corresponds to that of the dissolution medium, when water uptake accelerates promoting drug release by predominantly diffusion. This mechanism accounts for the sigmoidal pattern seen in Figure 7.7 for microspheres prepared from DCM and DCM:CFM blends. These comprised induction, accelerated and slow terminal phases. For drug release in Figure 7.7, however, from microspheres

immediately after preparation with high residual solvent, the T_g was close, if not below that of the dissolution medium, resulting in a rapid 'burst' with a short induction period. As residual solvent is lost under vacuum, the 'burst' reduces and the induction period lengthens as polymer chain stress-relaxation occurs, elevating the T_g, which retards RIF release.

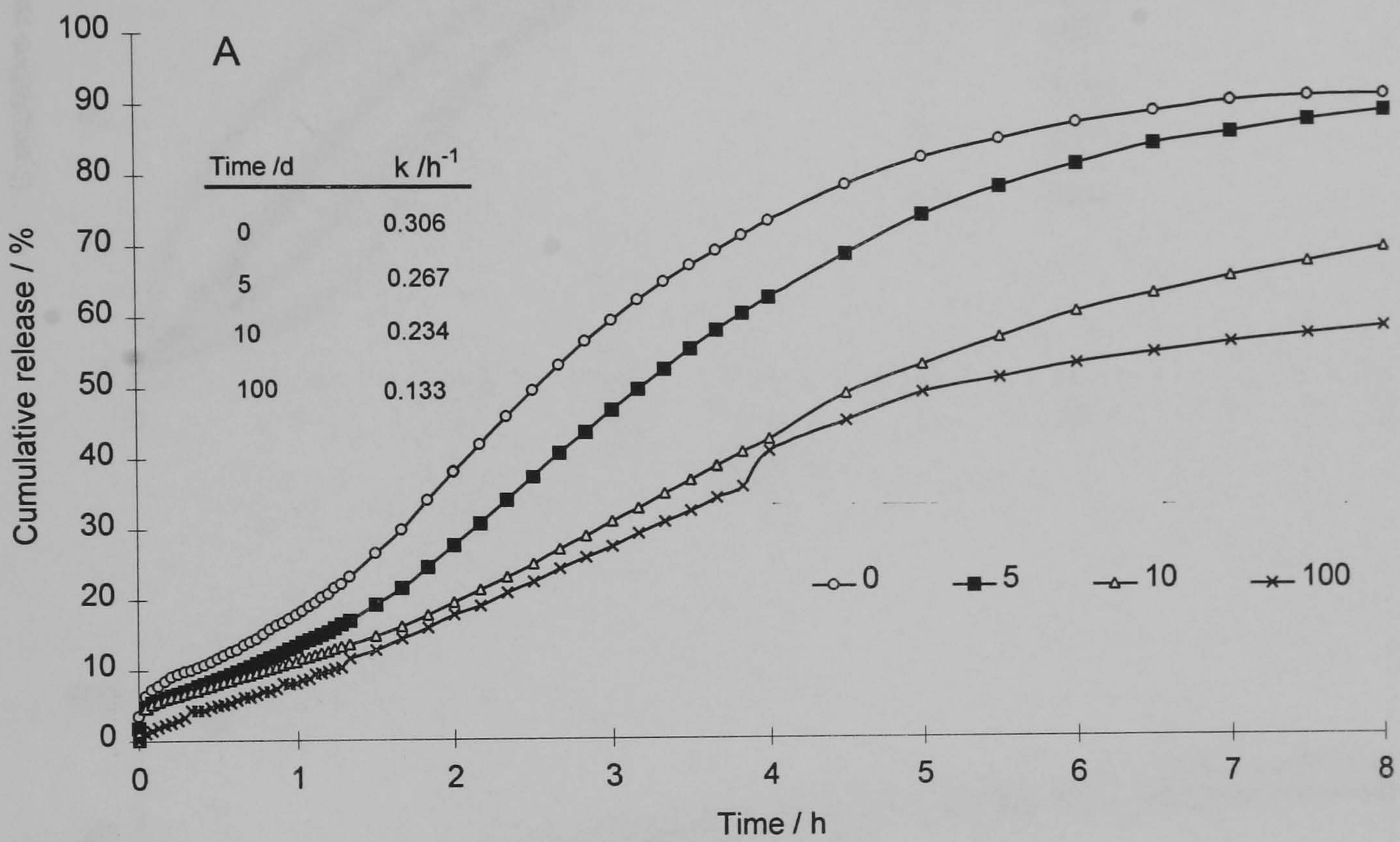

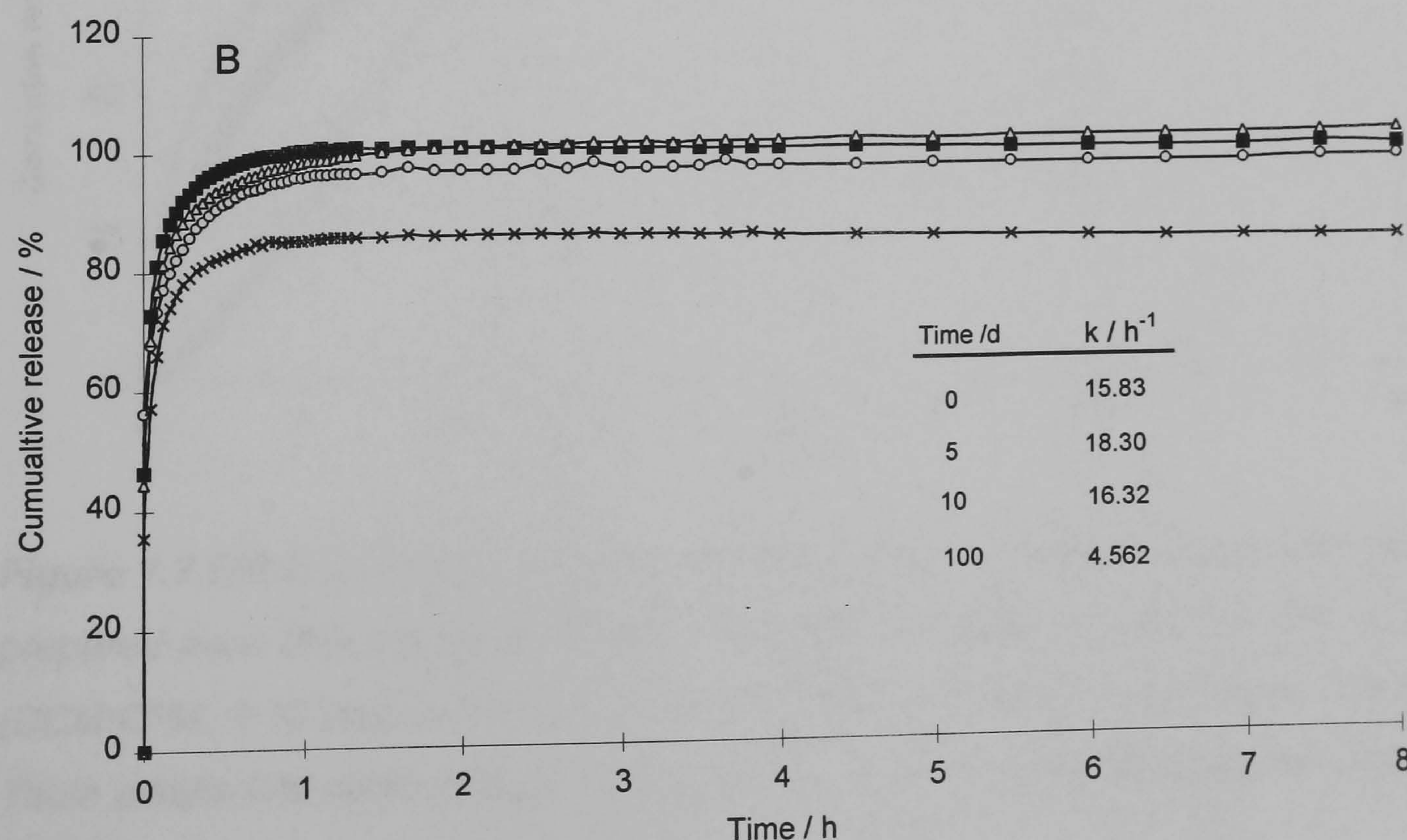

Figure 7.7 *[contd. overleaf]*

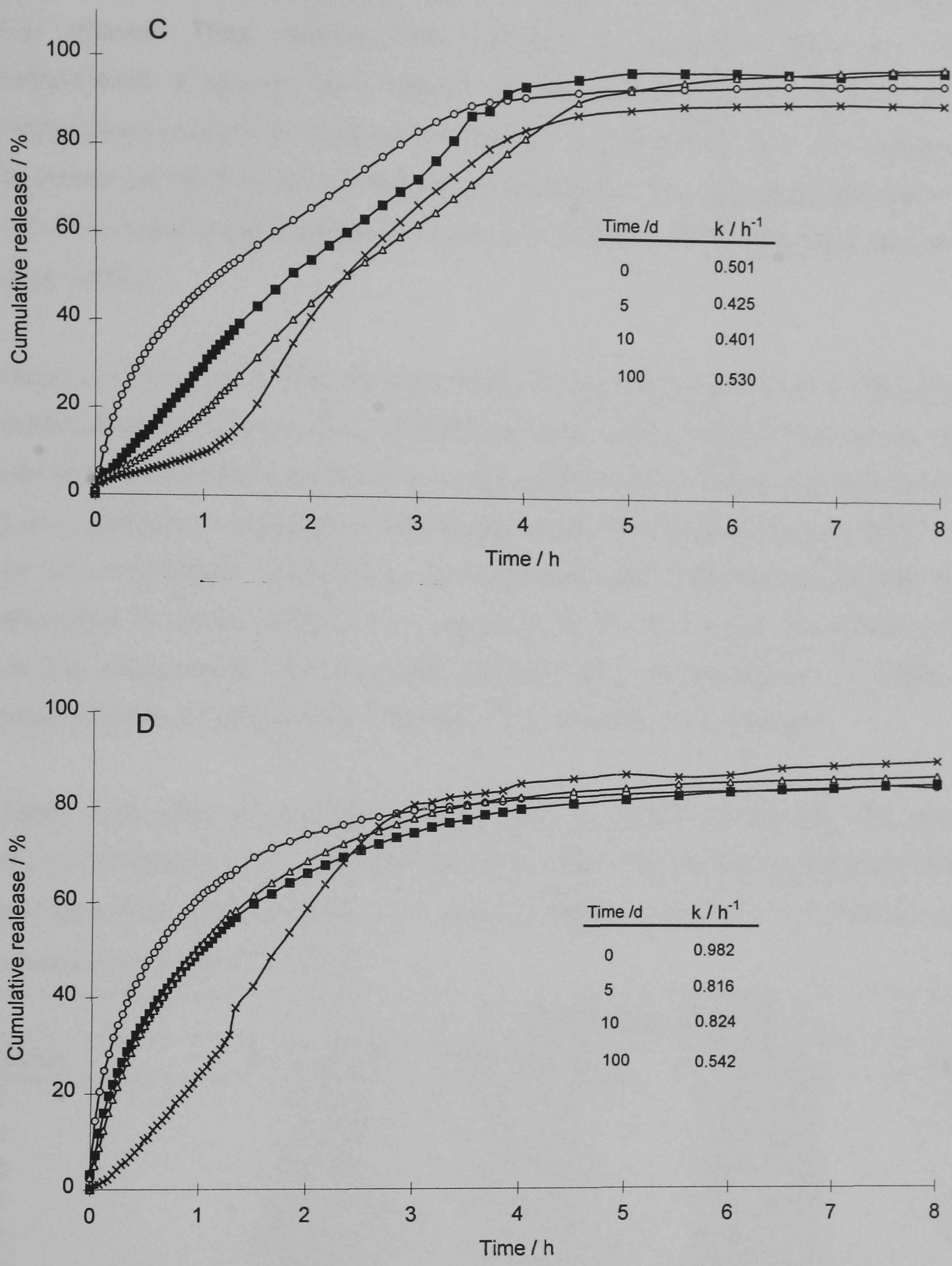

Figure 7.7 *Effect of storage in vacuo at 24 ± 2.0 °C on release profiles for microspheres prepared from different (co)solvent(s): A, batch 1 (DCM); B, batch 4 (ACT); C, batch 5 (DCM:CFM, 1:1); and, D, batch 9 (HAL) Process parameters according to Table 7.1. Inset Table details first order release constant (10 - ≤ 80 %) (Key indicates the storage time in days).*

At high matrix porosity, thermal behaviour is largely inconsequential, release being characterized by a single rapid phase, the rate of which increases as a function of matrix free volume. Thus, release from microspheres prepared from ACT was largely independent of storage time, release accelerating as the proportion of ACT used in microsphere preparation increased in line with the production of a more porous matrix as illustrated by the first order release rate constants of drug release annotated on Figure 7.7. Furthermore, the substitution in acetonic mixtures of CFM for DCM had little effect on drug release.

Reports of the use of HAL for microsphere preparation are limited to the preparation of microsphere by aqueous ESE (Armstrong et al. 1994, 1995; Guiziou et al., 1996). HAL was proposed on the grounds of its comparable physicochemistry to DCM and its inferred biocompatibility — assigned to the stability of the C-F bond (Horvath, 1982) — in its use as an inhalational anaesthetic. Comparisons with DCM demonstrated a manifest difference in matrix stability, the magnitude of the burst and, the overall rate of drug release being greater for HAL-based products. This was ascribed to T_g depression, as a result of solvent residue in corroboration of the results presented here.

Table 7.13 *Effect of processing parameters on first order release rate constants for rifampicin release (10 - ≤ 80 %) from spray-dried microspheres prepared from different (co)solvent(s) after exhaustive in vacuo drying at 24 ± 2.0 °C. Process parameters according to Table 7.1. (n = 3)*

	Regression statistics			
Batch	***k / h^{-1} (RSD)***	***intercept (RSD)***	***r^2 (RSD)***	***k$_{norm}$ / h^{-1}***
1	0.13 (3.19)	106.7 (1.34)	0.993 (0.28)	0.21
2	1.41 (5.38)	88.4 (0.13)	0.975 (0.44)	1.51
3	2.69 (16.8)	107.7 (3.49)	0.999 (0.07)	-
4	4.56 (1.70)	57.5 (5.20)	0.954 (0.59)	6.36
5	0.53 (18.41)	167.5 (17.5)	0.995 (0.14)	0.64
6	0.96 (5.46)	273.0 (12.9)	0.995 (0.21)	-
7	1.85 (5.00)	117.4 (5.12)	0.992 (0.07)	-
9	0.54 (0.26)	125.9 (0.39)	0.987 (0.29)	-
10	0.54 (0.91)	99.5 (0.95)	0.999 (0.05)	0.54

Jalil & Nixon (1990d,e,g,h) normalized fractional rate constants for phenobarbitone release in respect of specific surface area. Such corrections do not, however, take account of the distribution skew and, more importantly, the effect of diffusional pathlength as a consequence of such deviations from distribution normality. Particle size

distributions were comparable in the current work with the exception of batch #1 (#2 & #3). Nonetheless, rate constants after normalization against batch #10 with respect surface area (according to data in Table 7.10) are included in Table 7.13. Irrespective of such treatment, release from batch #1 remained the most sustained despite the fact that the T_g for batch #5, at 62.8 °C, was anticipated to confer the slowest release of drug. This disparity was attributed to the existence of a limited number of relatively large particles which comprised approximately 33 % of the total volume of the sample. Therefore, regardless of the correction for surface area, a meaningful proportion of drug had to diffuse through a significantly greater pathlength to be liberated from batch #1 when compared with batch #5. Overall, these observations account for the greater induction period with batch #5, consistent with T_g, but the more rapid release thereafter due to reduced diffusion pathlength from these particles, when compared with batch #1. In general, however, due to the otherwise similar granulometric characteristics of other batches, the corrected rate constants showed good correlation with T_g as shown in Figure 7.8.

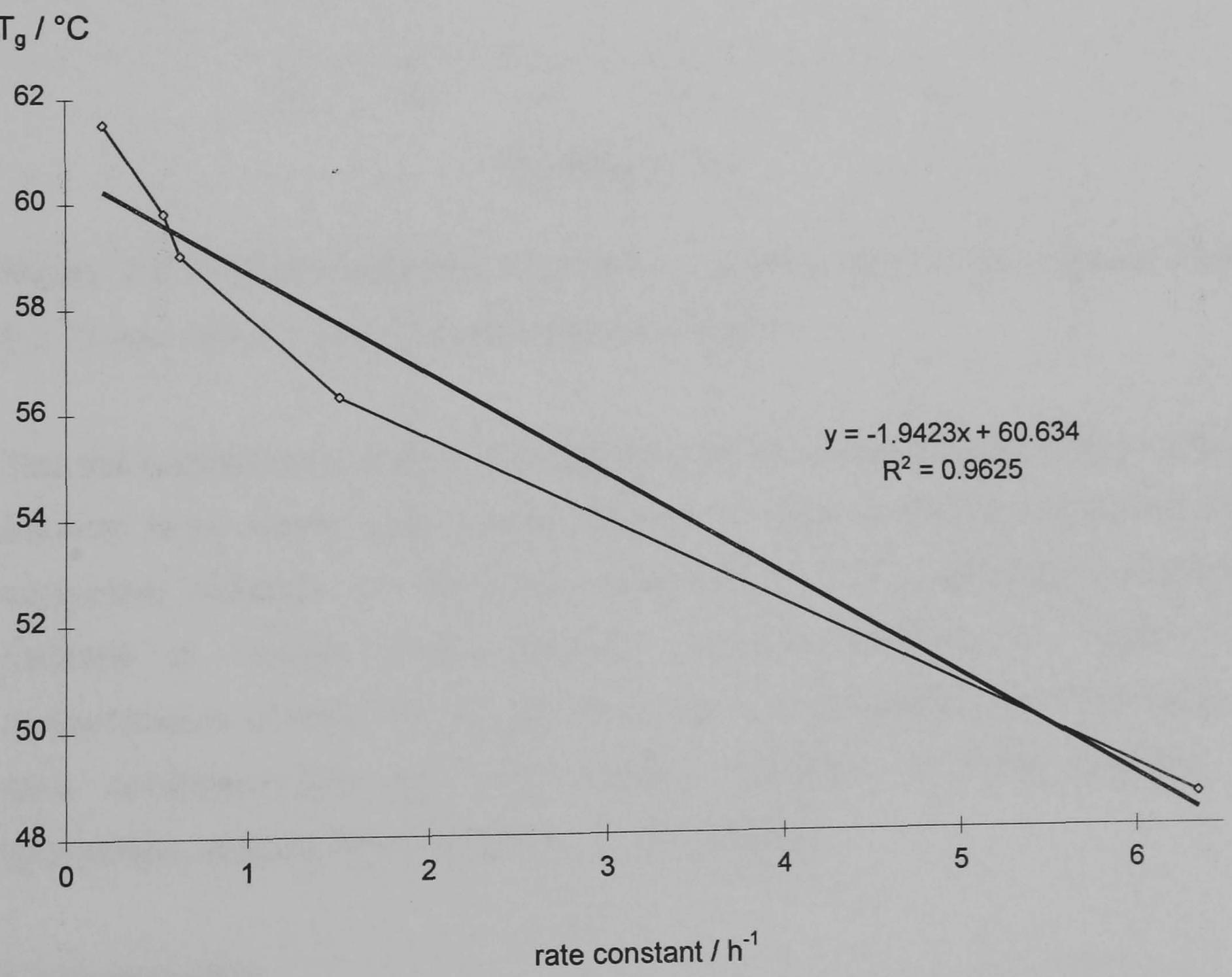

Figure 7.8 *Apparent correlation of glass transition temperature of spray-dried microspheres and first order release rate constant (0 - ≤ 80 % release).*

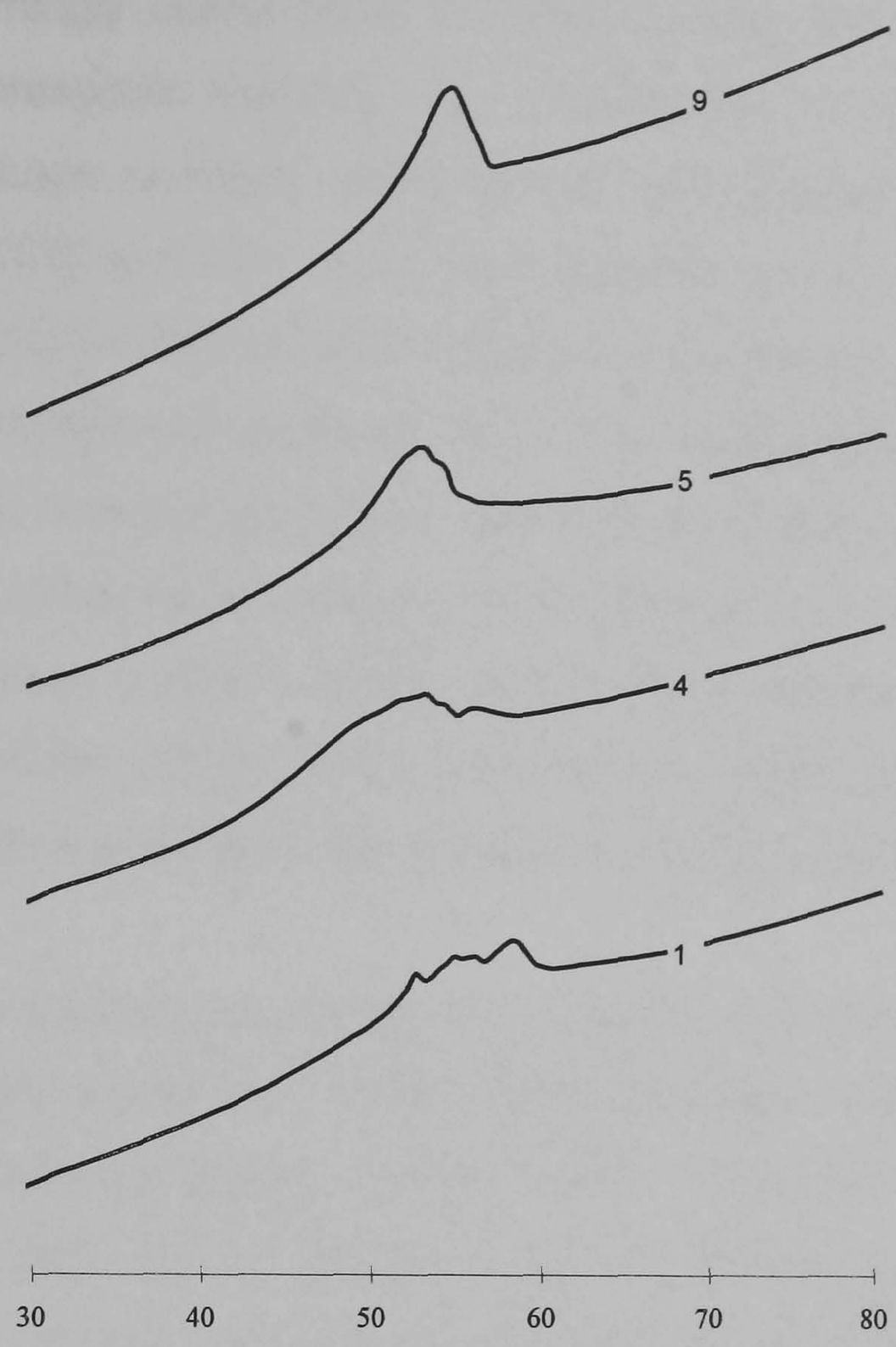

Figure 7.9 *DSC thermograms of recovered residue from in vitro release studies at 37 ± 0.1 °C and 100 ± 1 rpm. Legend indicates batch #.*

That the endothermic peak of thermograms for recovered sample residue after dissolution became more erratic and broader as particle size distribution increased in breadth is supportive evidence for differential hydration, and thus diffusion characteristics, from particles of variable mean diameter between batches. In Figure 7.9, thermal characteristics of batch #1 represent a disperse population, whereas batch #5 and #9 were consistent with the monodisperse character of these products. Batch #4, accordingly, showed intermediate thermal behaviour.

7.4 Conclusion

Under the conditions of these studies, solvent choice has a profound influence on the characteristics of biodegradable microspheres prepared by spray-drying. The influence of solvent power on microdroplet drying kinetics, within extremely narrow limits, accounts for

this remarkable sensitivity of microsphere properties to solvent choice. Viscosity studies provided a seemingly useful index of solvent power. Drug release was determined by exclusively macroscopic features, e.g., architecture for relatively poor solvents, ACT, whereas microscopic changes, which altered thermal character were also influential with good solvents, DCM and HAL. Moderate evaporation rates associated with good solvents appear to promote the formation of coherent microspheres whilst providing high product yield. This latter feature accounts for the ultimately slower release from microspheres and the high original residual solvent of products thus prepared. On the one hand, high solvent residue accelerates release initially through a matrix plasticizing action, on the other, it facilitates molecular mobility, associated stress-relaxation, which manifests as a progressive elevation of the softening temperature which was paralleled by an increase in the induction period and a general retardation of drug release.

Of the solvents studied, microspheres prepared from DCM were considered superior. Indeed, a recent report has hailed DCM an ideal choice of solvent, rejecting its carcinogenicity and ecotoxicity (Jones, 1996). The rapid drug release from acetonic products precluded use of this solvent. Microspheres properties from HAL were considered intermediate; however, protracted storage times were required to ensure satisfactory solvent removal. Architectural improvements might be achieved by the use of reduced drying temperatures with both ACT and HAL.

On a precautionary note, the effect of high solvent residue on microsphere release character might result in erroneous conclusions being drawn where adequate desiccation has not been performed. Overall, solvent choice for spray-drying has a considerable influence on the final microsphere characteristics and should accordingly be carefully considered from both a technological in addition to a traditional toxicological viewpoint.

8. Modulation of rifampicin release from spray-dried microspheres: combinations of poly(DL-lactide) and poly(DL-lactide-co-glycolide)

8.1 Introduction

Biodegradable poly-α-hydroxy acids drug-loaded microspheres have recently been investigated to target chemotherapeutics to the lung whilst providing a sustained release and thus therapeutic action (Armstrong et al., 1994, 1995; Giunchedi et al., 1995, 1998; Guiziou et al., 1996; El-Baseir et al., 1997). Pathologically, asthma has hitherto been the focus of these studies. Microencapsulated hydrocortisone (Giunchedi et al., 1995, 1998), beclomethasone and nedocromil sodium (El-Baseir et al., 1997), and, more speculatively, NSAIDs (Armstrong et al., 1994, 1995; Guiziou et al., 1996) have been suggested as having potential in the control of chronic inflammatory conditions when delivered directly to the lung.

Despite inherent disadvantages when compared with spray-drying, preparation of inhalational microspheres has largely relied upon various modifications of the ESE principle. El-Baseir et al. (1997) reported adjustment of stirring rate and emulsifier concentration was required to achieve a suitable size for aerolization. Preparation times of 5 and 7.5 h were required for batches of nedocromil sodium and beclomethasone prepared by w/o/w and o/w ESE, respectively. Guiziou et al. (1996) included a 24 h post-preparation *in situ* incubation step, prior to microsphere recovery, to presumably extract residual solvent. Further modifications involved substitution with the anaesthetic, halothane (HAL), as an alternative solvent in response to the suspicion that DCM residual was the cause of the pro-inflammatory activity of PDLLA microspheres delivered to the lung (Armstrong et al., 1992; 1994). Both solvents resulted in a significant respirable fraction of the overall microsphere population, the authors quoting a range of 2.0 - 6.0 μm (Guiziou et al., 1996). In contrast, Giunchedi et al. (1995; 1998) concluded advantageous loading and the overall convenience of spray-drying outweighed the lower yields when compared with granulometrically similar particles prepared by single and double emulsion methodologies. Notwithstanding these advantages, the rapidity with which equivalent quantities of microspheres can be produced by spray-drying further underlines its outstanding utility for the preparation of microspheres with inhalational application.

As TB affects an extensive area of the lung tissue (not only the area adjacent to the bronchial wall), inhalation therapy alone might not be able to penetrate deeply enough to achieve effective concentrations. However, certain medical opinion believe that inhaled sustained release microspheres may have application as an adjunct to oral therapy to deliver high concentrations of antimycobacterials to the luminal aspect of tuberculosis cavities (P Chapman, 1998, personal communication). Conventional therapy does not penetrate well into this area from the pulmonary capillaries. Such an approach, may, therefore, have a particular role in retractable infection or to effect an earlier cure than conventional oral regimes alone. Furthermore, resultingly shorter treatment schedules might alleviate the drug resistance problems associated with patient non-compliance which complicates protracted therapy. Finally, targeting of a fraction of the overall therapy may reduce the incidence of dose-limiting hepatotoxicity associated with systemically administered RIF (Mandell & Sande, 1985).

In chapters 6 and 7, microspheres of high and predictable loading and the required granulometry for deep alveolar penetration, 0.3 - 3.0 μm, were readily prepared by spray-drying. Moreover, the incorporation to ostensibly hydrophobic materials of a fraction of PDLLA oligomers should provide more sustained release of drug when compared to the typically asymptotic behaviour of piroxicam and hydrocortisone in PDLLA of 16 - 330 kD (Armstrong et al., 1994,1995; Guiziou et al., 1996) and 28 kD (Giunchedi et al., 1995), respectively. It is anticipated that the low volume of liquid which lines the pulmonary epithelium would serve only to accentuate this latter pattern of release.

The purpose of the work in this chapter was therefore to investigate the comparative utility of blending low MW PDLLA (Resomer® R104) with a MW and compositional range of lactide-glycolide copolymers of greater MW than the complementary PDLLA examined in chapters 6 and 7. Higher MW materials were selected to obviate the batch-to-batch variation in polymer behaviour considered attributable to small changes in MW demonstrated in chapter 6. Additionally, given the critical balance of matrix hydrophilicity and the associated role of T_g to the provision of controlled drug release, use of more hydrophilic copolymers was intended to offset MW dependent hydrophobicity as chain length of the copolymer increased.

8.2 Experimental procedures

8.2.1 Microsphere preparation

Microspheres were prepared from Resomer® R104 combined with each of RG502 (15.5 kD); RG503 (39 kD); RG503H (33.5 kD); RG504 (56.5 kD); RG752 (20 kD) and RG755 (63 kD) at polymer weight proportions: 44:56; 40:60; 36.6:63.3; 33.3:66.6; (30:70, RG752 and RG755 only); 25:75; 20:80; 10:90, (RG502; RG503; RG503H; and, RG504 only). Solutions (3 %w/v) of RIF (20 %w/w total solid) and polymer blends were prepared in DCM. Processing parameters were: inlet = 40 °C; outlet = 35 °C; flow rate, 600 NLh^{-1} ; aspiration, 100 %; and feed, 3.5 $mLmin^{-1}$. Batch # was assigned according to Table 8.1.

Table 8.1 *Polymeric composition and batch index of spray-dried microspheres prepared from blends of Resomer® R104 and various Resomer® lactide-glycolide copolymers containing 20 %w/w rifampicin (n = 1)*

Complementary polymer	***R104 / (%w/w)***	***Batch***							
		44	***40***	***36.6***	***33.3***	***30***	***25***	***20***	***10***
RG502		1	7	13	19		31	37	25
RG503		2	8	14	20		32	38	26
RG503H		3	9	15	21		33	39	27
RG504		4	10	16	22		34	40	28
RG752		5	11	17	23	29	35	41	
RG755		6	12	18	24	30	36	42	

8.2.2 Microsphere characterization

Microsphere yield was calculated as described in section 5.2.3.1, whereas solvent residue was determined as described in section 7.2.4.1 for microspheres prepared from each polymer blended with 25 %w/w R104 (Batch #31 - 36). Drug release was monitored by method B as described in sections 5.2.3.4. Drug release profiles were assessed by the fitting of these data to the reciprocal biexponential function shown below as Equation 8.1:

$$\% \text{ released} = 100 - (A*exp^{-\alpha t} + B*exp^{-\beta t}) \qquad \textbf{(Equation 8.1)}$$

where A and B are coefficients for the two concurrent first order processes, the rates of which are defined by the rate constants, exponents α and β, respectively. The rates of

release were examined again at 33, 35, 37 and 39 ± 0.1 °C to examine the temperature dependence of drug release. Activation energies of the initial phase of drug release were calculated as per section 6.2.2.

8.3 Results and Discussion

8.3.1 Microsphere yield

Corresponding microsphere yields for products of the compositions detailed in Table 8.1 feature below in Table 8.2. Using the optimized conditions described in section 5.3.7, with few exceptions, yields were greater than 50 %, which compares favourably with previous reports (Pavanetto et al., 1992; 1994a). Yields were generally 10 % lower than those for PDLLA combinations of comparable R104 content. These data approximate to the differential behaviour observed for PDLLA and PDLGA spray-dried by Wagenaar & Müller (1994) and are assigned to the influence of deposition kinetics and subsequent density-dependent yields discussed for individual polymers and combinations of PDLLA in sections 5.3.1 and 6.3.1.2, respectively. Summation of the yields for each composition of R104 and, for each group of batches based on polymer type, revealed no apparent trends with regard to these variables. Accordingly, variation was attributed to small, yet apparently significant between-batch differences in spray-drier performance.

Table 8.2 *Total yields of spray-dried microspheres prepared from blends of Resomer® R104 and various Resomer® lactide-glycolide copolymers containing 20 %w/w rifampicin (total solid)*

Complementary polymer	***R104 / (%w/w)***	***Yield / %***							
		44	***40***	***36.6***	***33.3***	***30***	***25***	***20***	***10***
RG502		68.0	66.0	54.6	57.3		65.3	64.0	67.3
RG503		61.3	66.0	56.3	59.3		62.6	66.6	66.6
RG503H		62.0	55.3	53.3	58.0		78.6	64.0	55.3
RG504		64.0	74.6	60.6	60.6		78.0	64.6	47.3
RG752		68.6	72.6	59.3	59.3	49.3	65.3	64.0	
RG755		64.6	65.3	57.0	54.6	58.6	67.3	60.6	

8.3.2 Effect of polymer type

Inherent polymer properties, i.e., polymer hydrophobicity and T_g temperature, and resultant matrix architecture were identified in chapters 6 and 7, respectively, as the two principle factors which affected drug release from spray-dried microspheres prepared from combinations of low and moderate MW PDLLA (of equivalent drug loading and granulometry). According to the data in chapter 7, under standard processing conditions, the microporosity of the resultant microspheres (and hence drug release rate) is inversely related to polymer solubility in the feed solvent.

Of the other factors, hydrophilicity increases as: lactide:glycolide ratio decreases, being maximal at 15:85 (Gilding & Reed, 1979); as MW decreases; and, as the density of free terminal carboxylic acid groups increases. Moreover, polymer T_g is reduced as the glycolide contribution increases whereby fewer CH_3 sidechains permits greater axial chain rotation. Accordingly, these factors culminate in PDLGA being substantially more hydrophilic and diffusive than PDLLA racemate of equivalent chain length.

8.3.2.1 *In vitro* drug release

The profiles of drug release were governed by matrix architecture and polymer hydrophobicity. These influenced the relative magnitude of both the extent (denoted by A and B) and the rates (denoted by α and β) of the two concurrent first order processes as defined by equation 8.1. The overall excellent fit of the experimental data as shown in Appendix 9 a-f to the reciprocal biexponential function provided reliable indices for the comparison of the effect of material, and the variables of processing and characterization on drug release of the combination matrices prepared.

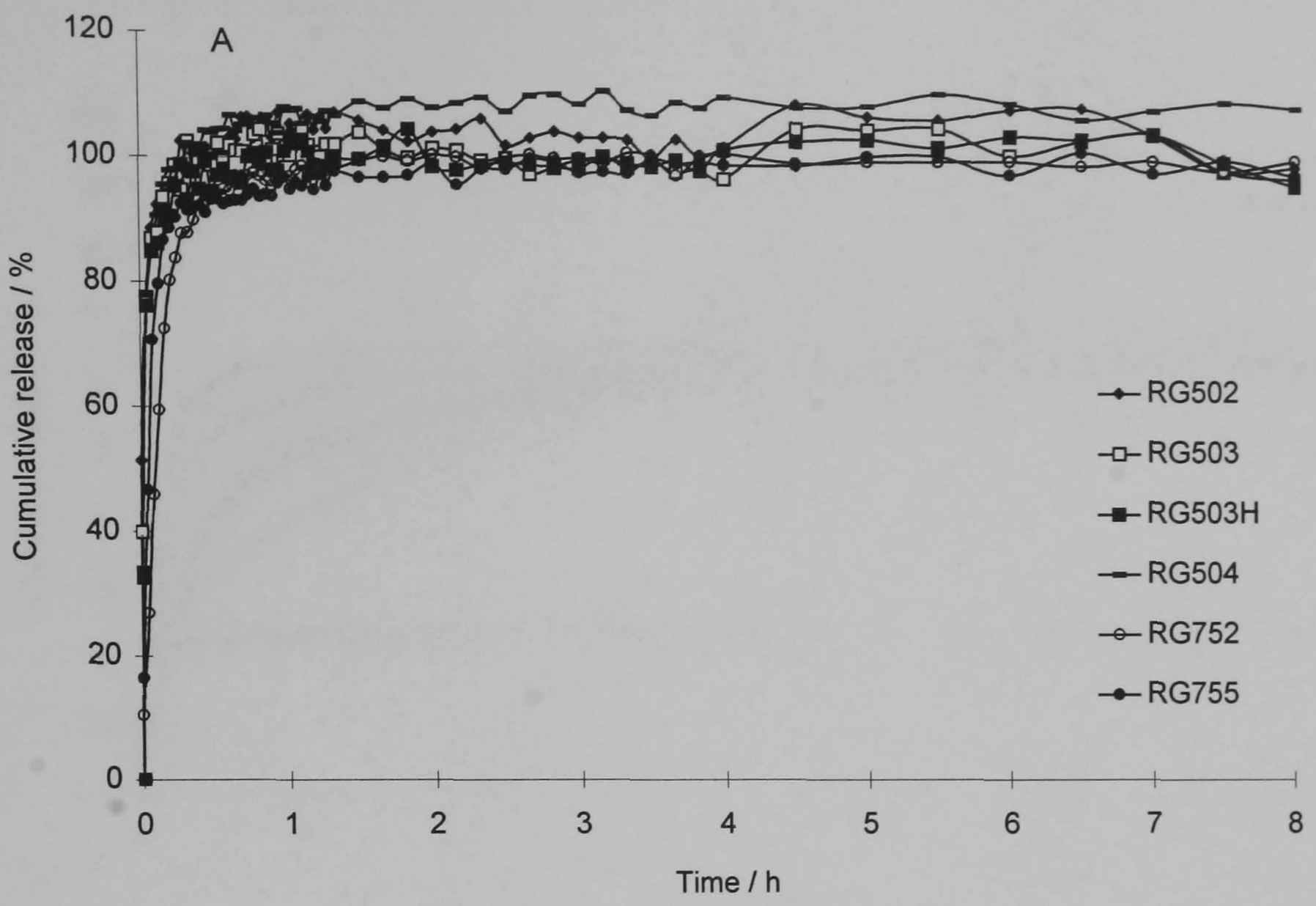

Figure 8.1 *[contd. overleaf]*

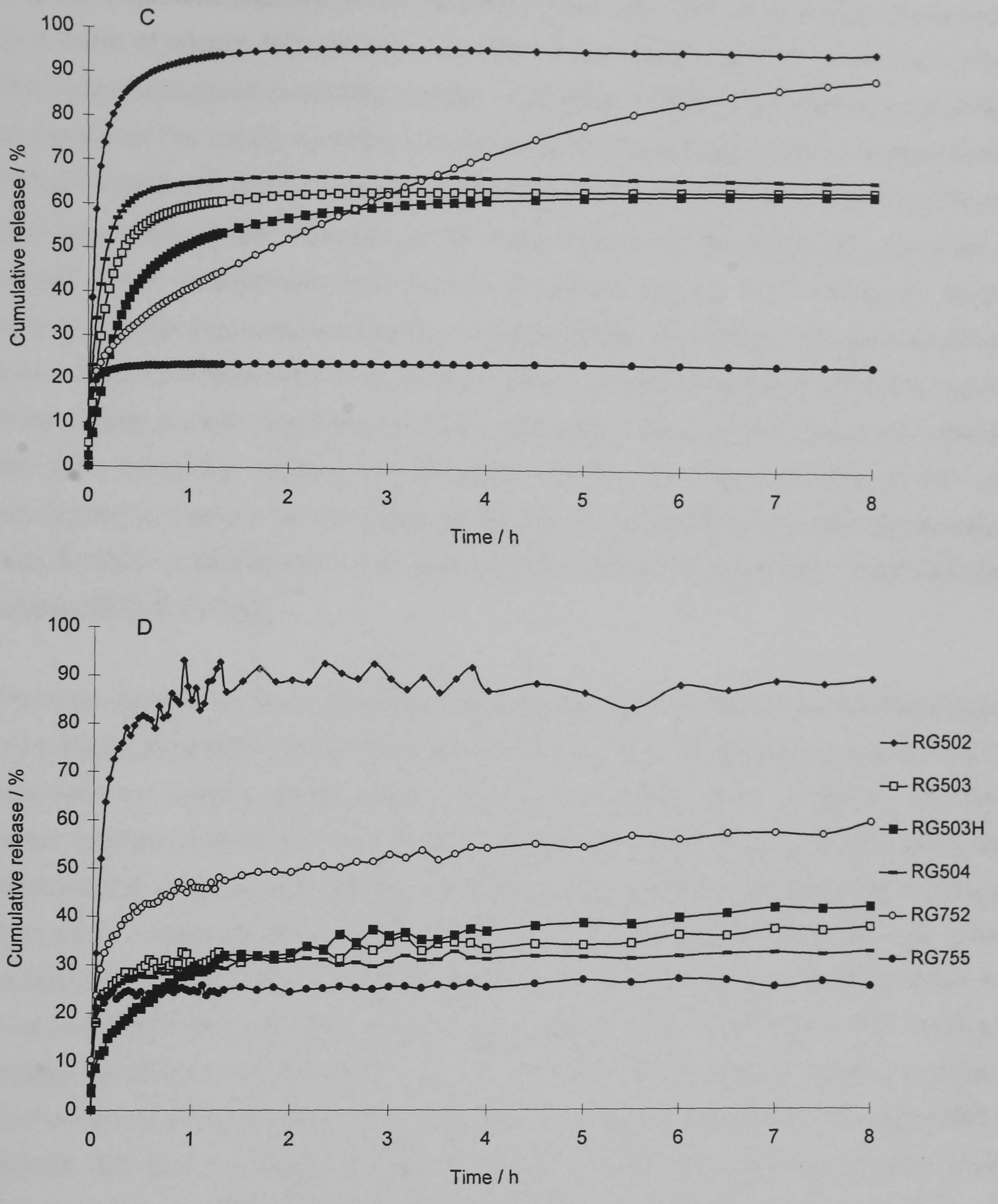

Figure 8.1 *Effect of matrix composition on release profiles of rifampicin from microspheres prepared from a range of Resomer® materials blended with R104, weight proportion : A, 44; B, 33.3; C, 25; and, D, 20 %w/w (total polymer) at a stirring rate of 100 ± 1 rpm and 37 ± 0.1 °C. Labels indicate the material used. (n = 3, standard deviation ≤ 5.7)*

In Figure 8.1, the effect of polymer type on the release profile of RIF is shown at selected levels of oligomeric adjuvant, R104. Release profiles were almost invariably characterized by a 'burst' of release followed by a slow diffusion of inaccessible RIF. At 44 %w/w R104, the profiles comprised essentially a single rapid phase whereby the inherent hydrophilicity conferred on the matrix by R104 overwhelmed the sustaining action of complementary PDLGA Resomer®. With the exception of RG755, this was also true of matrices prepared with 33.3 %w/w R104. However, at 25 %w/w, differential behaviour was observed as overall matrix hydrophilicity and thermal properties became more influential. Further reduction in the oligomeric contribution, resulted in release profiles which approximated to those shown in Figure 5.5. On the contrary, the intrinsic hydrophilicity of RG502 resulted in essentially a single rapid release phase, irrespective of the blend studied. The potential for ionic interaction between deprotonated COOH and basic moieties of RIF was considered to account for the unexpectedly slower release from microspheres prepared with RG503H (33.5 kD) when compared with that of more hydrophobic, higher MW, end-capped RG503 (39 kD).

The magnitude of the 'burst' effect is dependent on the proportion of overall drug which is immediately accessible to the release medium. Therefore, the specific surface area of the microspheres, matrix hydrophobicity, and, microporosity, are all influential. The latter factor describes the volume, and hence the depth of, porous interconnection, which was anticipated to increase with polymer MW in accordance with the general rules of polymer deposition. However, the contact angle will simultaneously increase with matrix hydrophobicity, therefore restricting the ability of the medium to wet the surface and penetrate the core by capillary action. Thus, faster deposition of RG504 from DCM and greater associated microsporosity during microdroplet drying was considered to account for the enhanced 'burst' when compared with that from RG503. Despite the higher MW of RG755 (63 kD), its overall greater solubility in DCM and resultingly greater matrix densification — allied to its greater hydrophobicity — accounted for the reduced 'burst' with this material when compared with PDLGA of equivalent MW, RG504 (56.5 kD). By analogy, more sustained release from RG752 (20 kD) containing microspheres, when compared with RG502 (15.5 kD) at identical levels of R104 was also observed.

8.3.2.2 Thermal analysis

The thermal behaviour of the matrix was instrumental in the modulation of drug release from microspheres prepared from blends of low and moderate MW PDLLA. In Table 8.3 the peak position of the anomalous endotherm for each batch is presented. Other associated thermal indices feature in Appendix 10. In chapter 7, the position of the anomalous peak was considered a useful index of microsphere stability for matrices of identical composition. In contrast, the position of the endotherm for different materials is affected by more fundamental factors such as MW and monomeric composition (Kerc & Srcic, 1995). Furthermore, these factors affect the degree of stress conferred on the matrix during drying and also its ability to undergo relaxation which is itself influenced by the level of solvent residue within the matrix. The complex interplay of these factors dictates the final peak position of the anomalous endotherm and therefore confounds comparison based solely on this index. Nevertheless, a generalized pattern of T_g elevation was observed as the R104 level decreased, the complementary polymer MW increased, and, the density of chain stiffening CH_3 sidechains increased. These data are presented in Table 8.3 and shown in Figure 8.2.

Table 8.3 *Peak position of the anomalous endotherm of microspheres prepared from blends of Resomer® R104 and various Resomer® lactide-glycolide copolymers containing 20 %w/w rifampicin (total solid)*

Complementary polymer	***R104 / (%w/w)***	***Anomalous endotherm / °C***					
		44	***40***	***36.6***	***33.3***	***25***	***20***
RG502		48.2	48.2	47.3	49.3	52.1	49.7
RG503		52.3	55.8	51.5	54.3	56.3	55.3
RG503H		57.0	56.4	53.1	57.4	57.0	54.5
RG504		56.7	55.6	54.3	57.1	56.7	56.5
RG752		56.4	58.1	57.1	56.8	57.0	55.8
RG755		53.6	59.3	59.3	60.2	59.2	60.1

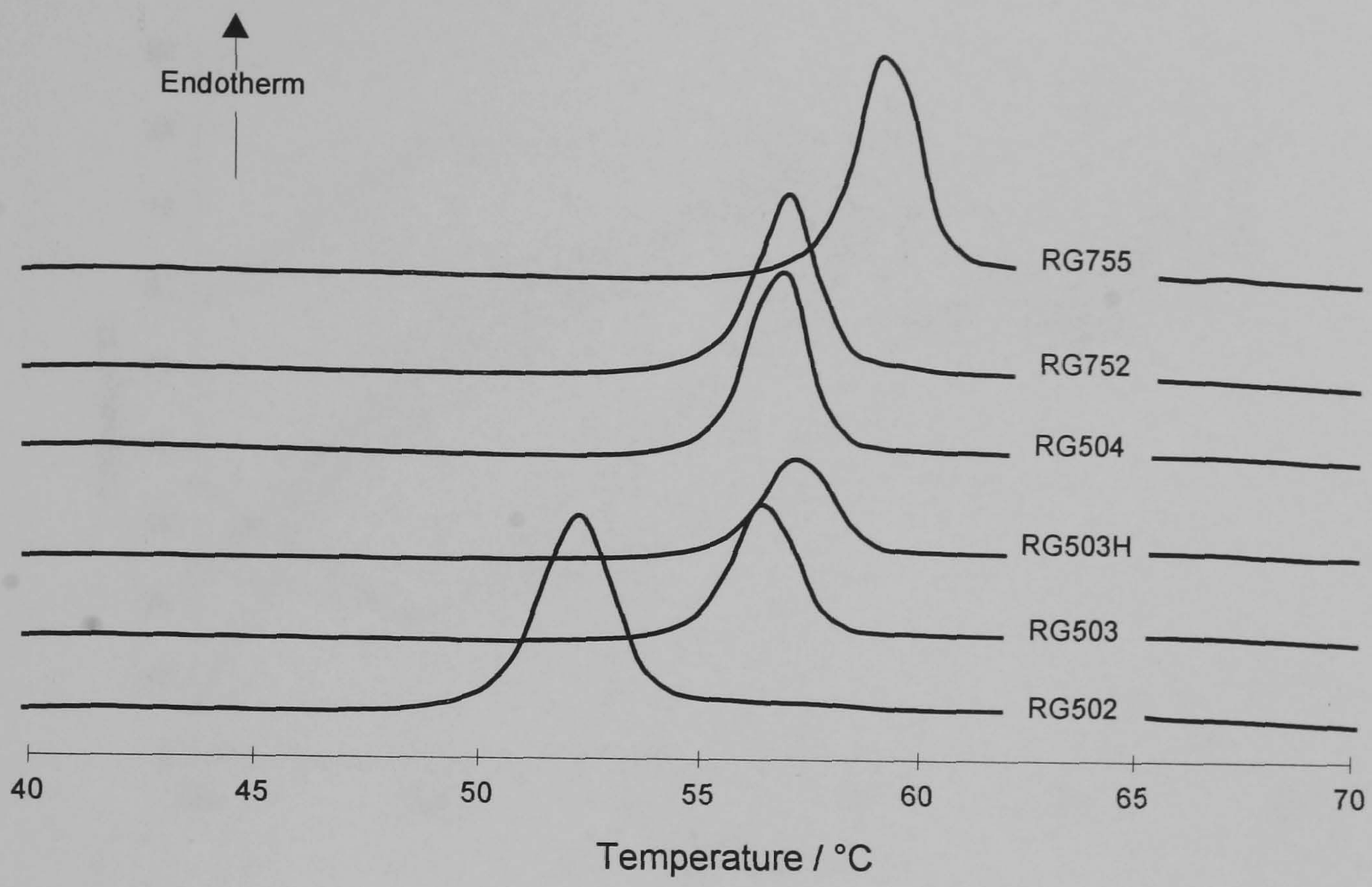

Figure 8.2 *First heat DSC thermograms of microspheres containing 20 %w/w rifampicin prepared with 25 %w/w R104 in a range of Resomer® lactide-glycolide copolymers (batch #31 - 36 as per Table 8.1). Labels indicate the complementary material used.*

8.3.3 Effect of oligomer proportion

8.3.3.1 *In vitro* drug release

The effect of R104 content on the coefficients and exponents of release data fitted to equation 8.1 is shown in Figure 8.3. The data presented were considered in general terms, deviations from these generalities are selectively discussed. Theoretically, the A and B coefficient terms of equation 8.1 represent the percentage contributions of the initial rapid and the slow terminal phases of drug release. Accordingly, as shown in Figures 8.5 (1) and (2) respectively, as the 'burst' of drug release increases there is an approximate reciprocal decrease in the magnitude of B, the latter representing the percentage of inaccessible drug. Mechanistically, A and B represent the fractions of drug released by diffusion through a hydrated network and anhydrous glassy matrix, respectively. The initial process is the product of diffusion through either aqueous filled channels or through a hydrated matrix, both of which afford minimal resistance to drug

liberation. It follows that, the constants, α and β, define the rates of these respective diffusive processes during the time course of the release studies.

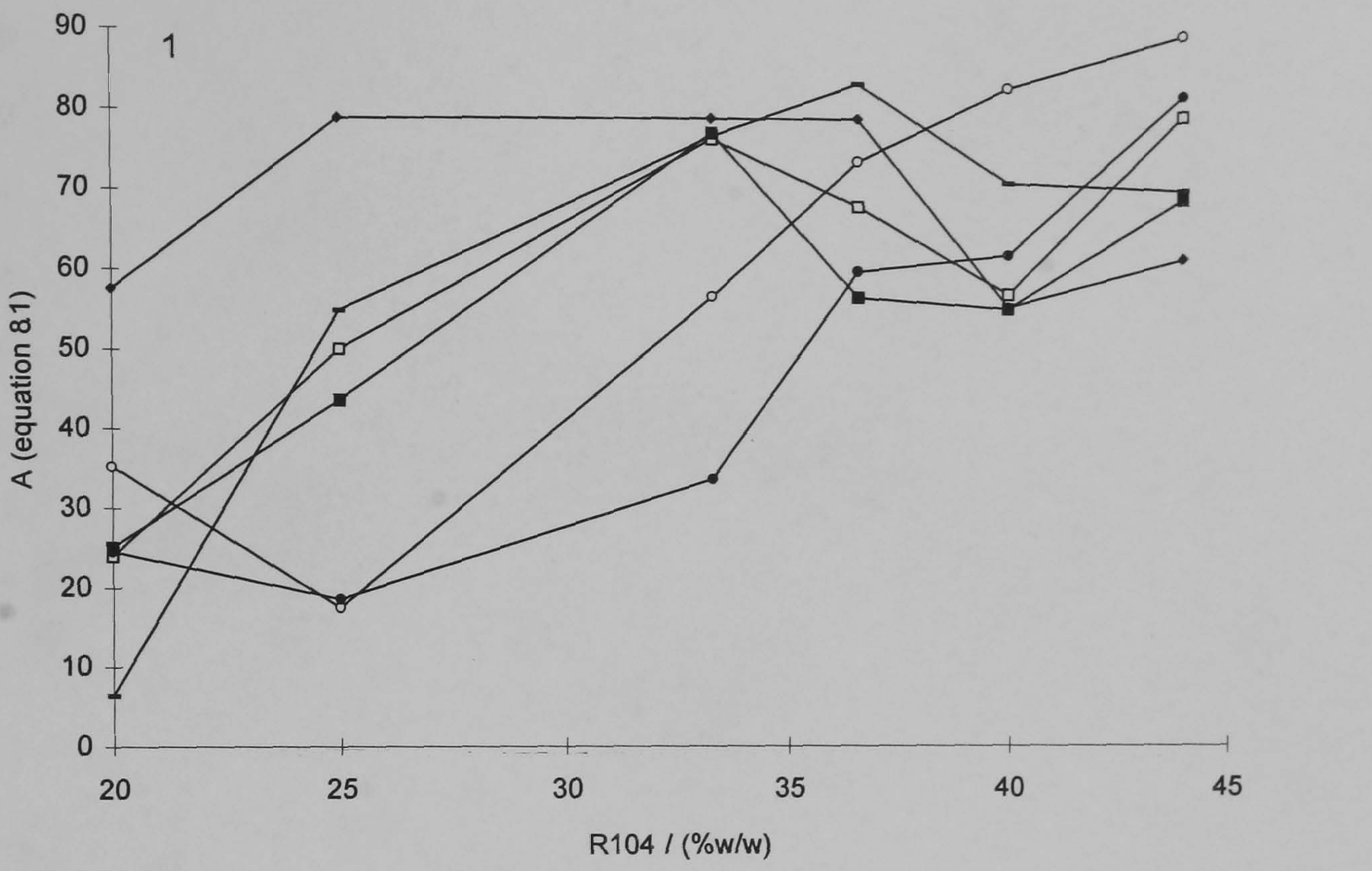

Figure 8.3 *[contd. overleaf]*

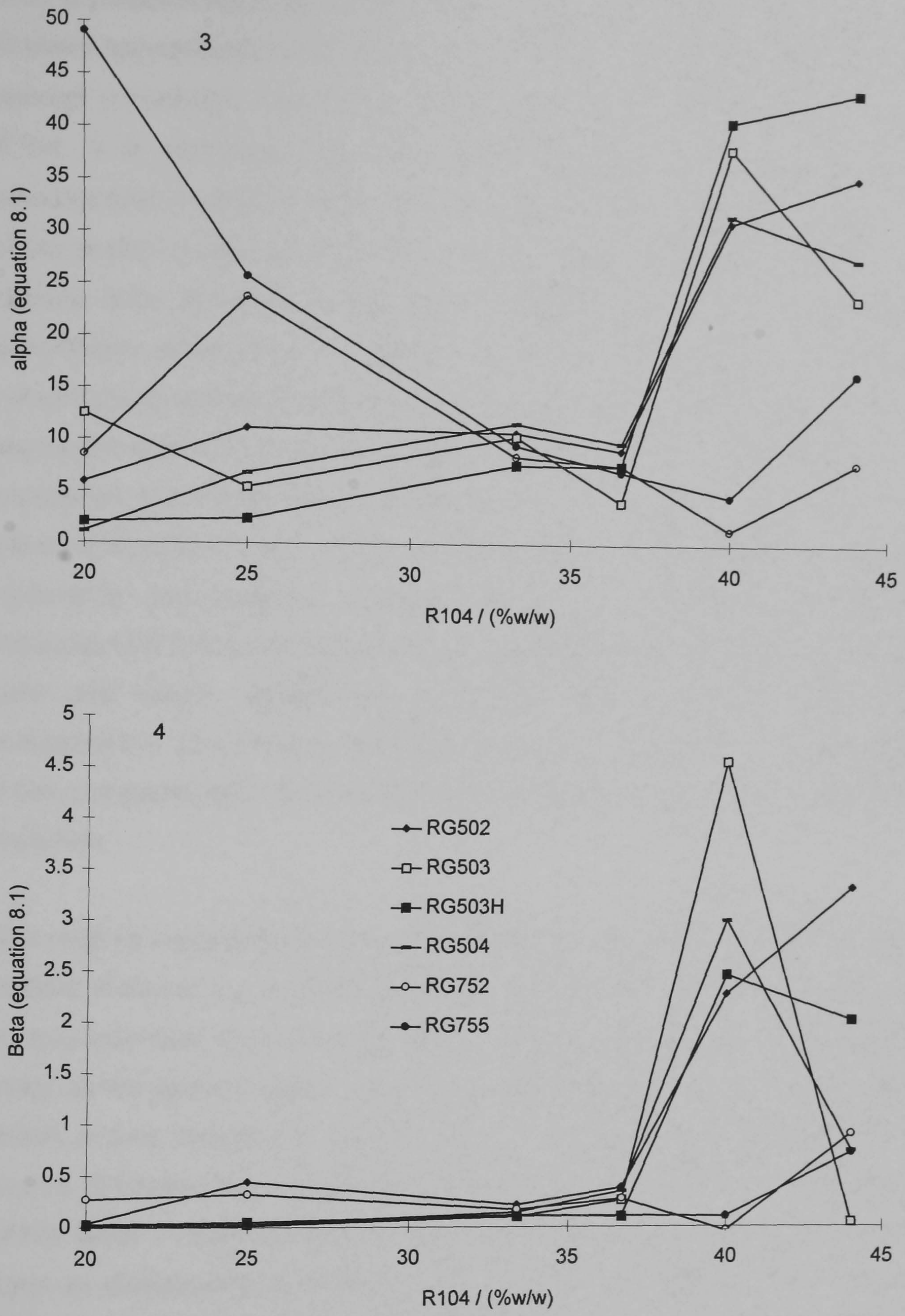

Figure 8.3 *Profiles of the effect of oligomeric contribution, R104, on the coefficients (1, A; 2, B) and exponents (3, alpha; 4, beta) of rifampicin (20 %w/w) release data fitted to equation 8.1 using method B at 37 ± 0.1 °C and 100 ± 1 rpm from spray-dried microspheres prepared from a range of lactide-glycolide copolymers. Legend indicates the complementary material used.*

That A predominated over B for RG502, irrespective of the blend, is consistent with the inherent hydrophilicity of this material and the rapid diffusion of the large majority of drug through a hydrated matrix. The 'burst' progressively increased with the proportion of R104. It is postulated that R104 level dependent leaching at the surface of the microspheres increased the fraction of accessible RIF; the number, depth and dimension of the pores conceivably all increasing with levels of oligomer. However, gravimetrically derived data failed to convincingly substantiate this erosive contribution and was accordingly disregarded for reasons outlined in section 6.3.3.2. Nonetheless, it was reasoned that approximately linear increases in the magnitude of A with %w/w R104, was supportive evidence for the propagation of drug release by pore diffusion. Considerable parallelism and correspondence of values of A and B were observed for PDLGA (50:50) blends below 33.3 %w/w. Within this range, hydrophobic effects overwhelm thermal and hydrophilic characteristics, whereby variation in the 'burst' were attributable to the influence of R104 leaching and other structural effects. Above this level, matrix hydration, over and above architectural differences was influential, confounding differential interpretation. This linearity extended over a broader range with blends of PDLGA (75:25) when compared with PDLGA (50:50) in keeping with the greater hydrophobicity of these materials.

The relative magnitude of the two first order processes are additionally influenced by the extents of same, e.g., a small 'burst' may yield an exceptionally high value for α, whereas a more extensive, and hence significant rapid phase, might give lower values of the same index as the depth of inward water penetration determines the extent of the initial phase, which, in turn, dictates the thickness of the diffusion barrier through which mass transfer occurs. It follows, that the extent of the initial phase has obvious implications for the rate of this 'burst' — the mechanistic origin of the initial phase dictating the observed parabolic trend as discussed later in this chapter. The influence of polymer physicochemistry is none so more evident than with RG755, whereby α increased with RG755 contribution, contrary to the trend observed with PDLGA (50:50). Lower MW RG752 generally showed comparable behaviour. Accordingly, the relative significance of the two release phases cannot be equated with their corresponding rate constants, with the exception perhaps where the initial phase comprises the predominant release mechanism.

On the basis of the autohydration mechanism discussed in Chapters 6 and 7, these data suggest that the criticality of matrix composition is accentuated by the use of less hydrophobic materials. The inherent hydrophilicity of complementary PDLGA (50:50) polymers results in poorly controlled hydration at the critical level which proved exceptionally sensitive to polymer composition. The acuteness of this sensitivity is evident from the considerable acceleration — in the presence of comparable A values — of the initial phase between 36.6 and 40 %w/w R104, where α values increased from 10 to 40 h^{-1} with PDLGA (50:50) based products. In contrast, the use of more hydrophobic PDLLA described in Chapter 6, R202H, behaved to regulate the autohydration process thereby conferring a greater degree of control on the release of RIF by diffusion. The greater the correspondence of α and β, the greater the overall acceptability of the release profile in terms of providing constant release. In this respect, few blends afforded satisfactory release profiles. Exceptions included batches prepared with 60 % (#11) and 70 %w/w RG752 (#29). It is postulated that use of this material of intermediate hydrophobicity had a partially analogous effect to that of PDLLA R202H.

Overall, empirical studies suggest PDLLA represents a more valuable material to explore its modulating capacity when combined with oligomers of the same nature. The between batch non-reproducibility alludes to the ability to modify release kinetics by modulating the MW and hence the hydrophobicity of the complementary material. Hydrophilic plasticizing oligomeric fractions behave as 'initiator' for the hydration process, itself triggered by the correspondence of the medium and T_g temperatures. On the other hand, complementary PDLLA served to modify release rate and is referred to as 'modulator'. Furthermore, the more coherent matrices formed with PDLLA by virtue of their enhanced solubility in DCM further supports their use in preference to PDLGA. However, in the event that a suitable solvent with greater solvency for PDLGA can be identified, improvements in matrix coherence are conceivably possible with copolymer.

8.3.3.2 Thermal analysis

During thermal analysis, a second peak shown in Figure 8.4 was recorded after the anomalous T_g - associated endotherm in PDLGA (50:50) blends of $\geq$ 25 %w/w R104 during the first scan, the relative magnitude of which was a direct function of the proportion of oligomer incorporated as shown in Figure 8.5. At 20 %w/w the second

endotherm became poorly discerned and was largely absent at 10 %w/w. Solubilization of undissolved RIF was the putative origin of this second peak as evidenced from cursory hot stage microscopy observations described in section 6.3.1.5. Summation of the total area for both peaks revealed an approximately constant energy requirement for both processes of 5.0 Jg^{-1}. Therefore, as the proportion of R104 decreases, a greater fraction of the dispersed RIF simultaneously dissolves as molecular motion is freed at the T_g. The relative magnitude of the secondary peak is hence a marker of overall RIF solubility within the matrix blend, higher temperatures and additional energy being required to solubilize the undissolved remainder.

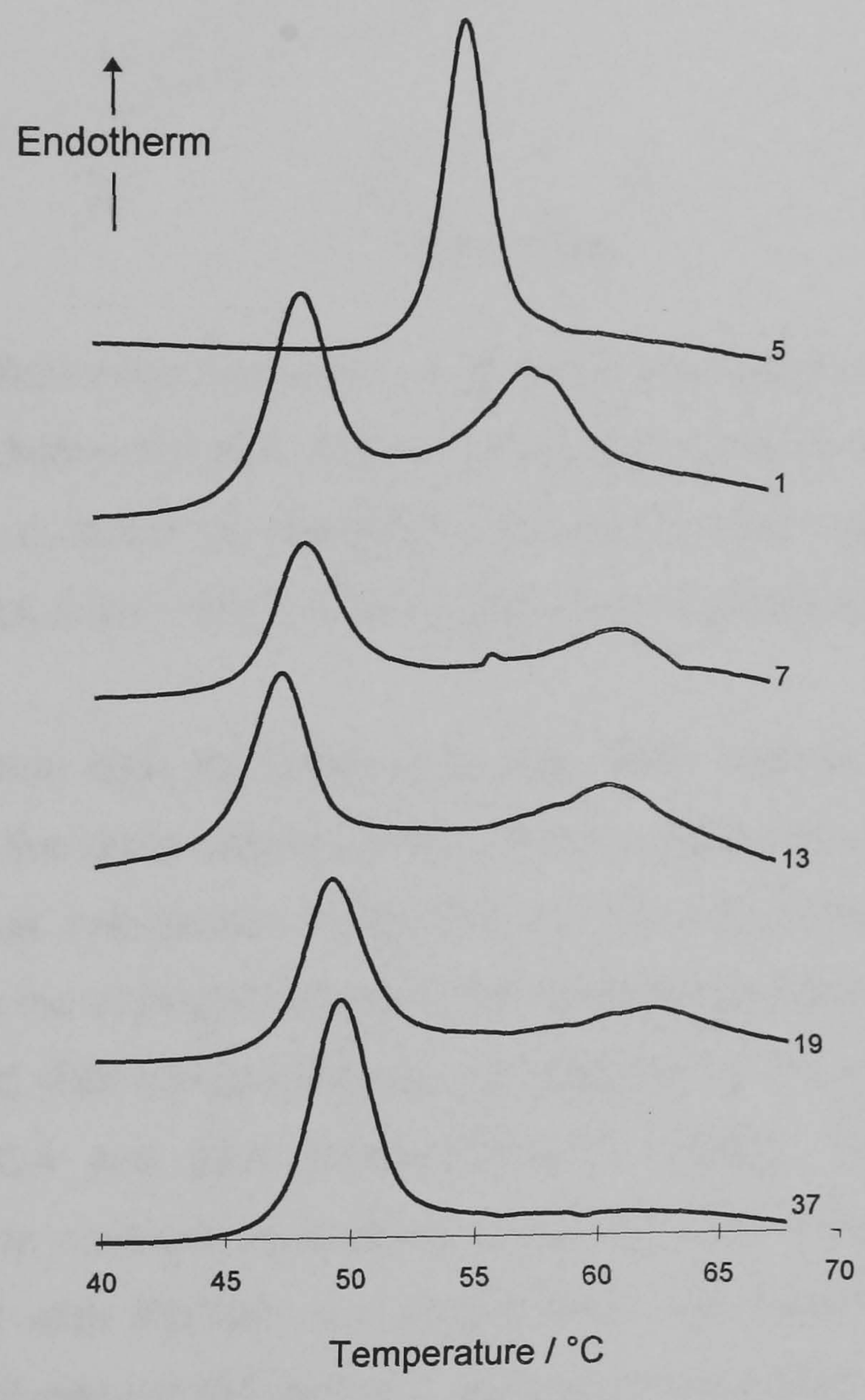

Figure 8.4 *Effect of the proportion of R104 on the first heat DSC thermograms of microspheres containing 20 %w/w rifampicin prepared with 56 %w/w RG752, (#5), and #1, #7, #13, #19, #37 with 56, 60, 63.3, 66.6, and 80 %w/w RG502, respectively. Labels indicate the batch # according to Table 8.1.*

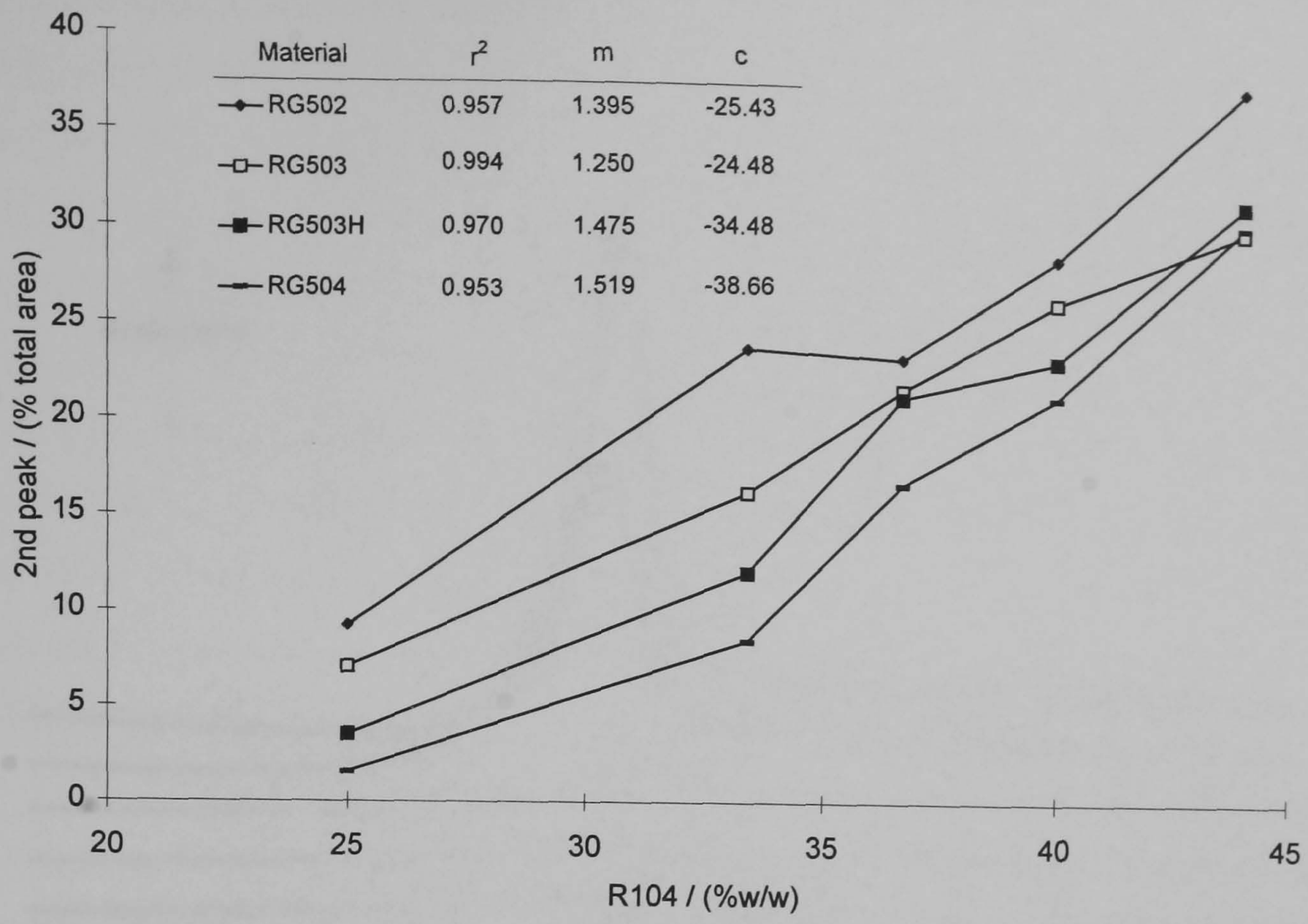

Figure 8.5 *Effect of the proportion of R104 incorporated on the relative magnitude of the second peak during the first DSC scan of microspheres containing 20 %w/w rifampicin prepared with a range of Resomer® lactide-glycolide copolymers. Labels indicate the copolymer used. Inset Table indicates the linear regression statistics of each plot.*

Linear regression data for these plots has been inset to Figure 8.5. The approximate parallelism of the plots indicated the solubility dependence of RIF on %w/w R104 was essentially equal irrespective of the PDLGA (50:50) studied. However, the displacement of the plots up the ordinate indicated RIF solubility decreased as complementary polymer MW decreased. Plot extrapolation to the intercept on the abscissa gave solubility limits of 18.2, 19.6, 23.4 and 24.5 %w/w R104 for RG502, RG503, RG503H and RG504, respectively. In contrast, regardless of the oligomer concentration, no secondary peak was observed with RG752, nor with RG755. Increased lactide content appeared to improve the solubility of RIF at the T_g as was corroborated by the data in chapter 6 where racemate PDLLA demonstrated similar behaviour. However, the MW dependence of RIF solubility is also evident with racemate PDLLA from the 'salting-out' influence of R104 combined with RG50X materials. The significance of these data is not known; however, diffusion is considered to accelerate as mutual drug-polymer solubility improves. On the contrary, these subtle solubility differences are probably overshadowed by the reduced free volume within the matrix and increased hydrophobic effects as MW increases, which serve to impede diffusion.

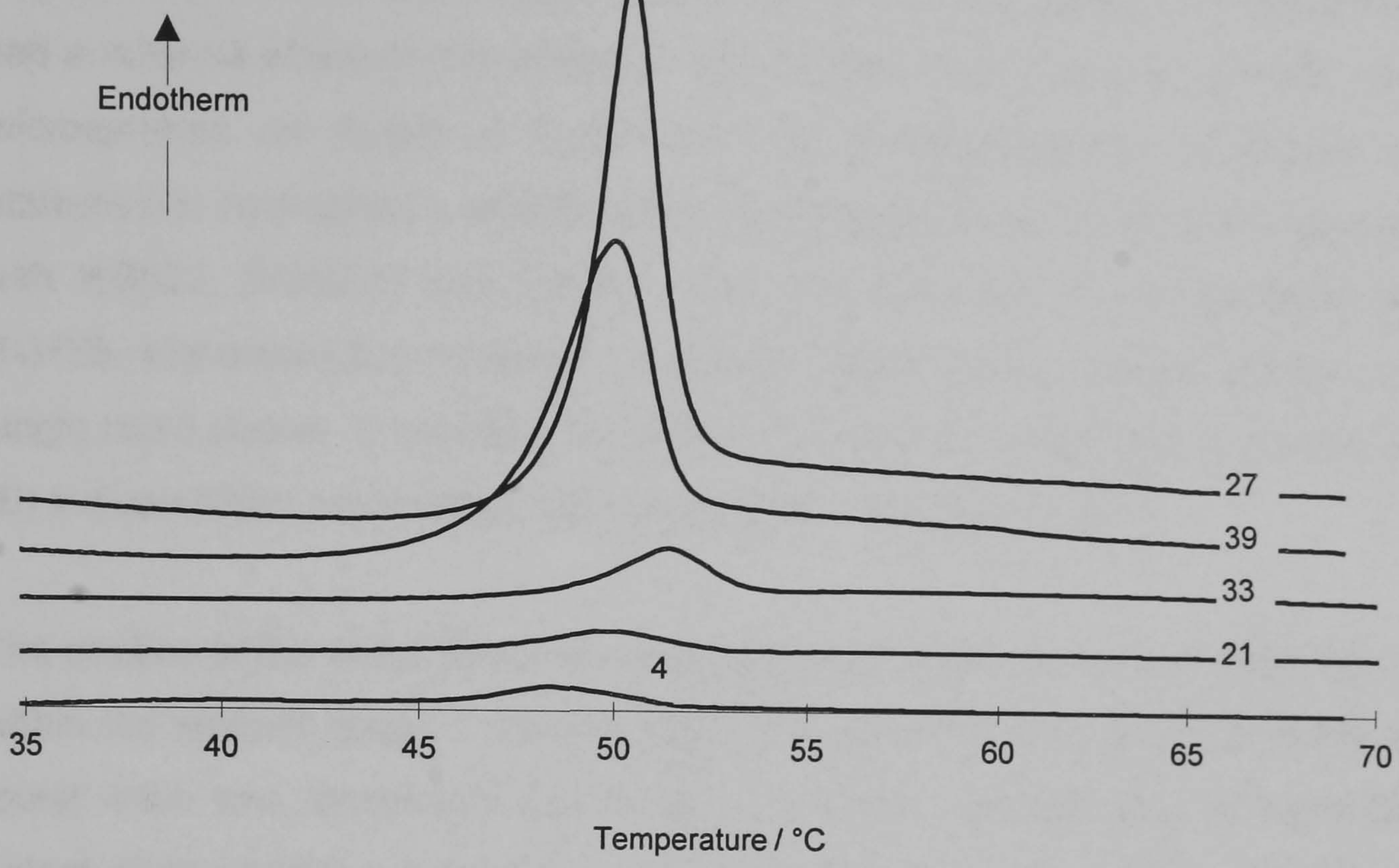

Figure 8.6 *Effect of the proportion of R104 on the first heat DSC thermograms of microsphere residue from release studies using method B at 37 ± 0.1 °C and 100 ± 1 rpm containing 20 %w/w rifampicin prepared with RG503H. Labels indicate the batch # according to Table 8.1.*

The effect of oligomer content on the thermograms of microsphere residue from selected batches prepared with RG503H after 8 h drug release study is shown in Figure 8.6, whereas data for all other batches appear in Appendix 11 a-g. Enhanced hydration and more extensive drug release resulted in a progressive decrease in the amplitude of the endotherm as %w/w R104 increased. However, microspheres with relatively high levels of RG503H largely retained their pre-dissolution thermographic features. The minimal endothermic fronting observed was attributed to modest surface hydration. Furthermore, as RIF was released and the overall residual loading fell within the solubility limits of the blend at the T_g, the second endotherm disappeared.

8.3.4 Effect of medium temperature

Figures 8.7 and 8.8 show the effect of medium temperature on the release profiles at 25 %w/w R104 and profiles of the initial release phase on R104 %w/w for selected blends, respectively. In contrast to matrices derived from blends of PDLLA, temperature generally had a minimal effect on the profile of RIF release at 25 %w/w for PDLGA (50:50) based microspheres as shown in Figure 8.7 (A). Correspondence of release profiles was attributed to hydrophobic effects which impeded hydration and consequent plasticization with RG503, RG503H and RG504. This was also true of microspheres derived from RG755. Instantaneous hydration of RG502 based blends yielded profiles comprising a single rapid phase. In contrast, the differential behaviour with RG752 shown in Figure 8.7 (B) indicated this composition approximated to the critical level.

The profiles of the initial phase were generally parabolic where the critical composition fell within the studied range. Parabolic behaviour was attributed to the evolution of the initial 'burst' from one dependent exclusively on matrix microporosity, whereas the rate and extent of microsphere hydration augmented this phase beyond the critical level of %w/w R104. Thus, on the one hand, α increases as the %w/w R104 at the surface and therefore rate of hydration increases, while on the other, limited solvent penetration at lower levels of oligomer result in an extremely rapid short-lived 'burst' phase. Examination of Figure 8.5 showed that exceptions included RG502 and RG755, where increases in the rate of hydration (RG502) or extent (RG755) resulted in a progressive increase and decrease respectively in the values of α as %w/w R104.

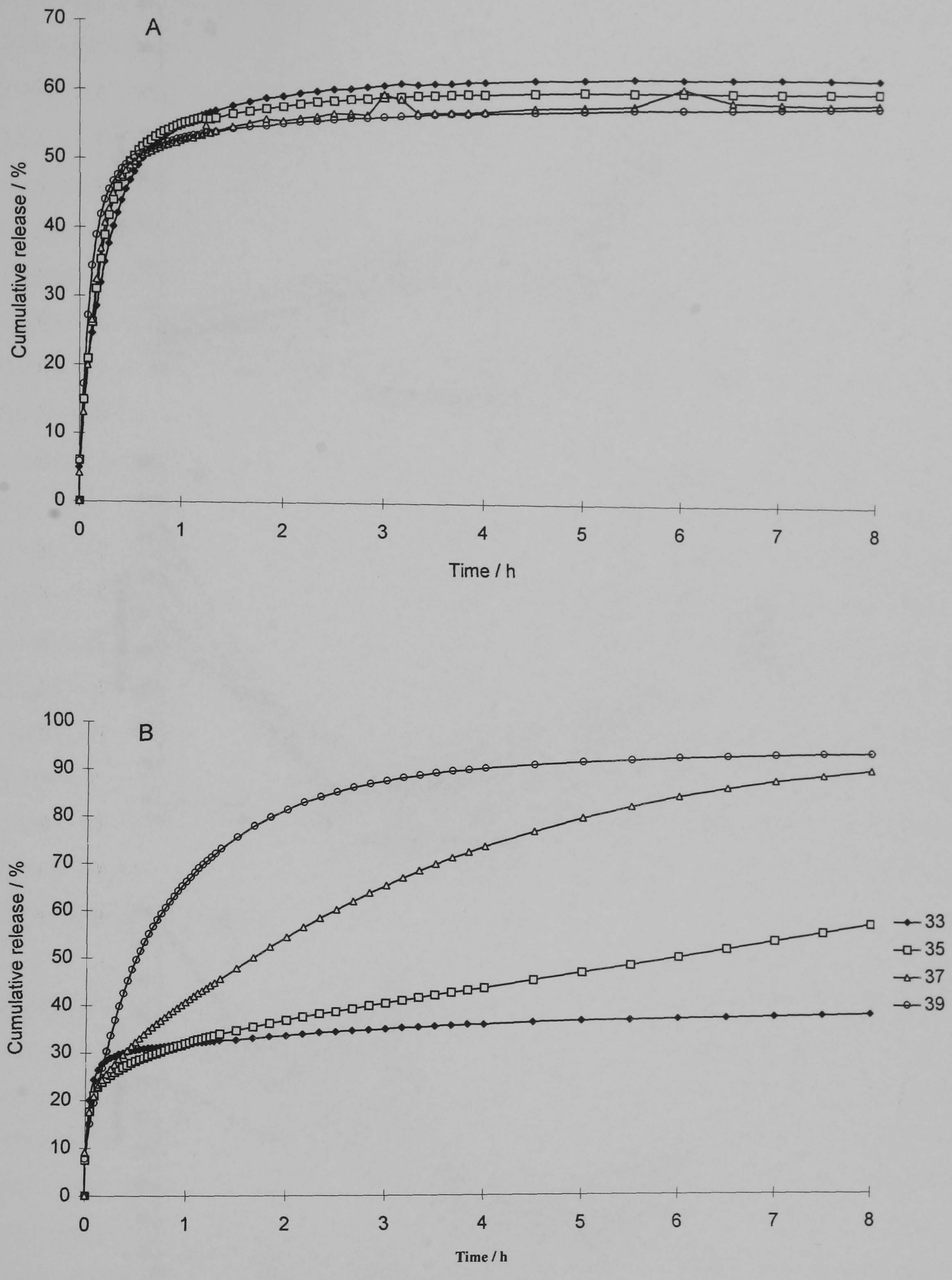

Figure 8.7 *Effect of temperature on the release of rifampicin from microspheres prepared from 25 %w/w Resomer® R104 and: A, RG503; and, B, RG752 using method B at 100 ± 1 rpm. Labels indicate the temperature ± 0.1 °C of the release medium. (n =3, RSD ≤ 3.8)*

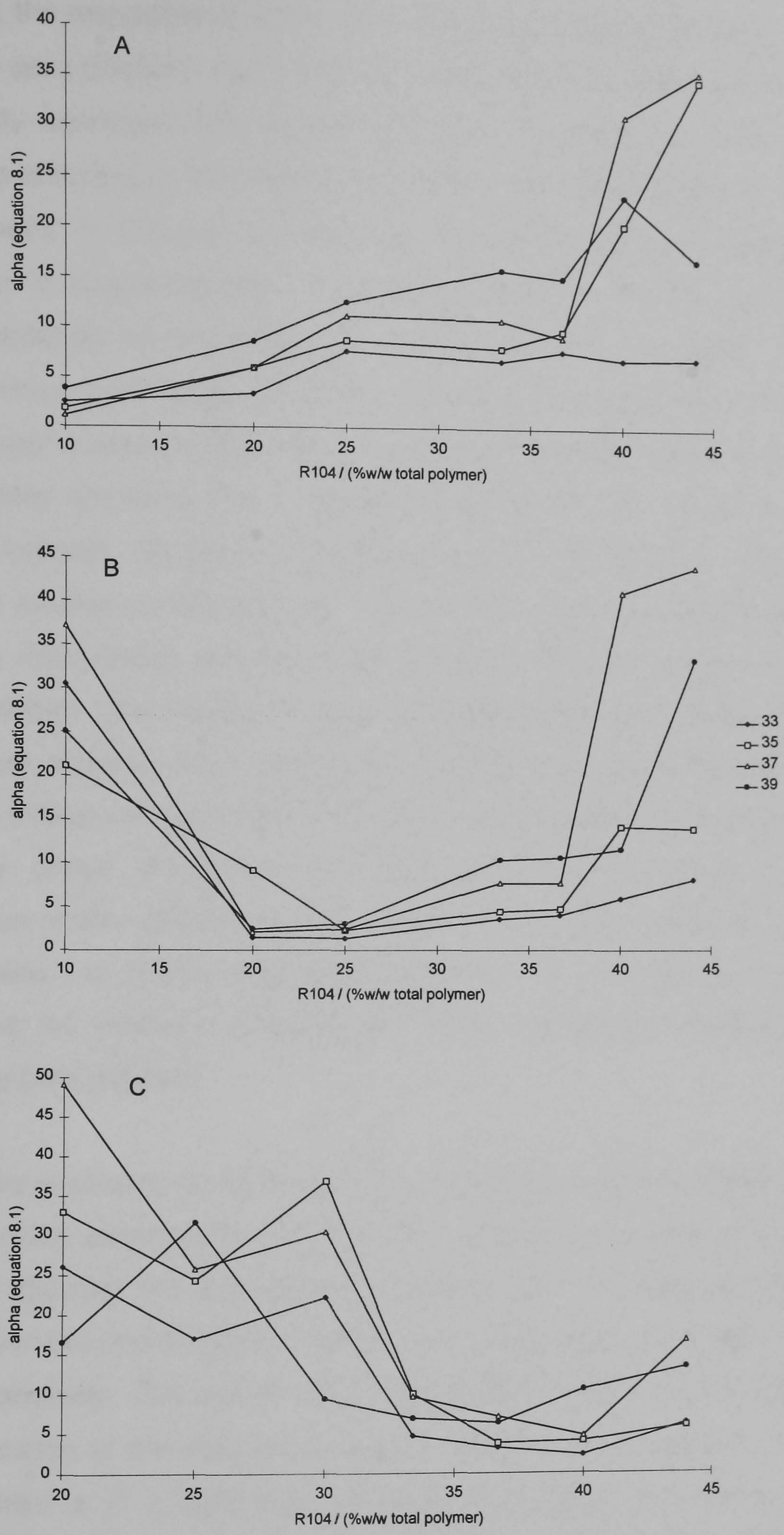

Figure 8.8 *Profiles of the effect of oligomeric contribution on the rate of the initial release phase of rifampicin as defined by equation 8.1 from microspheres prepared from blends of Resomer® R104 and: A, RG502; B, RG503H; and, C, RG755 using method B at 37 ± 0.1 °C and 100 ± 1 rpm.*

Generally, the respective α values converge at the parabolic trough, indicative of release by largely pore diffusion due to the low temperature dependent solubilization of surface and weakly associated RIF. Modest increases in release rate with temperature at this point were attributed to the endothermic nature of RIF dissolution in aqueous medium as demonstrated in Chapter 3. Attempts to define the temperature dependence of dissolution of spray-dried RIF were hampered by its rapidity due to the high surface energy conferred on the drug in its amorphous form (Corrigan, 1995). Studies at a reduced temperature range (23-29 °C) with intended extrapolation to that of the release studies failed to improve this situation. The rapidity of RIF dissolution also contributed to the variability of values for α, where initial release was often complete after a few sampling intervals. Above the critical composition, temperature dependent hydration of the matrix resulted in an enhanced contribution of the initial phase to overall release as previously inaccessible domains not contiguous with the porous surface are freed by water imbibition. The profiles in Figure 8.7 (B) illustrate an enhanced 'burst' with medium temperature, whereas the A indices in Appendix 9 a-f would suggest an opposite trend above the critical composition. This is due to a concomitant and interfering increase in the secondary phase of release with temperature which results in a compensatory suppression of the computed extent of the 'burst'. Nonetheless, the constancy of the A values below the critical composition indicates a set fraction of drug was released irrespective of medium temperature; further supportive evidence for release by exclusively pore diffusion.

Quantitative evaluation of the temperature dependence of RIF release for the initial phase was performed according to the Arrhenius equation as described in section 6.3.4. The computed statistics are presented in Appendix 12. The activation energies of diffusion through hydrated and anhydrous PDLLA were determined in chapter 6 as 320 and 630 J mol^{-1}, respectively. The erratic nature of the determined α values generally resulted in poor correlation of the data when fitted to the Arrhenius function. Therefore, only data which yielded a $r^2 \geq 0.85$ were considered. Significantly, matrix microporosity and enhanced free volume with the use of copolymers resulted in markedly lower values for E_a compared with PDLLA. Values of 110 ± 30 J mol^{-1} at 33.3, 25, 25, 40 for RG502, RG503, RG503H and RG755, respectively, were considered to represent the temperature dependent dissolution of accessible RIF domains due to their general correspondence to the respective minima in Figure 8.8. Despite their greater porosity, moderately higher values for RG504 based microspheres, 170 ± 40 J mol^{-1} (33.3 - 36.6 %w/w) were

attributed to the more extensive initial phase which necessitated diffusion of RIF through an overall more tortuous matrix. Corresponding values for RG752 of > 200 J mol^{-1} above 33.3 %w/w were considered due to enhanced matrix coherence by virtue of its greater solubility in the organic solvent used for microsphere preparation. It is acknowledged the relatively low values of E_a for the initial phase were due to the significant contribution of pore diffusion, which occurs more readily than that through a hydrated matrix as was the case with PDLLA.

8.3.5 Effect of residual solvent on microsphere characteristics

Comparable residual solvent loads of 2.03 %w/w (RG502), 2.47 %w/w (RG503), 2.36 %w/w (RG503H), 2.04 %w/w (RG504), 2.61 %w/w (RG752), and 1.83 %w/w (RG755) were gravimetrically determined from microspheres prepared with 25 %w/w R104. In analogy to PDLLA blends examined in chapters 6 and 7, thermal indices detailed in Appendix 13 progressively increased with an approximate logarithmic dependence of time. Therefore, these stress-relaxation data mirrored the first order kinetics of residual solvent loss determined for PDLLA blends in section 7.3.4. The statistics of release data determined after 14, 40 and 120 d storage fitted to Equation 8.1 are presented in Appendix 13. General, albeit small, reductions in A, α, and β and simultaneous increases in B were observed as stress-relaxation stabilization of the matrix proceeded under the influence of residual solvent load. The minor variation in these indices was consistent with the predominant influence of matrix architecture on release data of the matrices at 25 %w/w R104, in contrast to their thermal behaviour as was the case with PDLLA blends. Indeed, relatively high microporosity of copolymer derived microspheres aided rapid solvent loss. It follows, molecular rearrangement was restricted, yielding release profiles reminiscent of those seen with acetonic based microspheres in chapter 7.

8.4 Conclusion

Owing to high matrix porosity associated with the use of DCM as solvent for the spray-drying of PDLGA, release profiles of RIF from microspheres based on blends of R104 and PDLGA were typically characterized by a substantial 'burst', matrix hydrophobicity accounting for the slow terminal diffusion of residual RIF thereafter. These data contrast with that in chapter 6, where coherent microspheres prepared from comparable blends of PDLLA released RIF by a controlled hydration mechanism based on microsphere hydrophilicity and thermal behaviour. Overall, the sensitivity of RIF release to small changes in matrix composition was accentuated with the use of PDLGA as complementary polymer. The data for RG502H blends for instance, suggested that bulk hydration, once triggered, occurs in an uncontrolled fashion with PDLGA, whereas the inclusion of hydrophobic lactic acid units served to moderate this process with PDLLA. Thus, in the absence of suitable, superior solvents for PDLGA, it is PDLLA that remains the most promising excipient for the preparation of inhalational microspheres which will adequately release their payload in a controlled fashion once impacted in the surrounding small volume of liquid in the lung.

9. Preparation and characterization of biodegradable microspheres containing isoniazid

9.1 Introduction

Despite substantial *in vitro* and *in vivo* assessment of biodegradable INH implantable systems (Gangadharam et al., 1989, 1991; 1993; 1994; Gangadharam & Kailasam, 1993; Hsu et al., 1994, 1996; Kailasam et al. 1994a,b), no reports of the drug's delivery by biodegradable microspheres have been described. This is undoubtedly attributable to the unfavourable physicochemistry of INH, particularly its hydrophilicity, which has discouraged investigation when formulated as biodegradable microspheres.

As an alternative to poly-α-hydroxy acids, more hydrophilic polymers have been spray-dried: chitosan (Genta et al., 1994), polycaprolactone (Giunchedi et al., 1994b) hydroxypropyl cellulose (HPC) (Lee at al., 1997) casein (CAS) (Foster & Leatherman, 1995) and albumin (ALB) (Conte et al., 1994b; Giunchedi et al., 1994a). The latter material has been used to both accelerate (Giunchedi et al., 1994a) and sustain drug release (Pavanetto et al., 1994b) when spray-dried. Carbamazepine showed a remarkable acceleration in dissolution rate when encapsulated in ALB (Giunchedi et al., 1994b). In contrast, thermal denaturation of ALB conferred sustained release on dexamethasone by exposure to dry-heat for 6 - 24 h at both 100 and 150 °C. Additionally, ALB has itself been encapsulated in PDLLA (Gander et al., 1996) and PDLGA (Bittner et al., 1998) by spray-drying. Double-walled microparticles have also been prepared by a 2-step spray-drying procedure (Lee et al., 1997). To minimize the deleterious effects of organic solvent on activity, antibody HBsAg was first embedded in a spray-dried hydroxypropylcellulose (HPC) matrix. The cores thus formed were subsequently suspended in an ethylacetate solution of PDLGA which, when spray-dried, produced antibody microcapsules. HBsAg retained 92 % of its original activity and gave comparable antibody titres to conventional two shot alum formulation. Elsewhere, dispersions of preformed spray-dried acid orange and somatostatin have been coated with polyanhydride by spray-drying (Mathiowitz et al., 1992).

Transmission of *M. tuberculosis* is primarily via the pulmonary route. Thus, droplets expelled during coughing, sneezing or talking represent a significant risk to those sharing air-space with the infected individual. Even with treatment of INH to sensitive organisms, individuals generally remain sputum-positive for 14 d during which time they can infect

many others (Lemke, 1995). In terms of disease control and public health, much is therefore to be gained by expedient attainment of sputum negativity, for which intra-pulmonary delivery of bactericidal INH directly to the lesions might have great potential (Crofton, personal communication, 1996).

Therefore, the potential of effective encapsulation of INH at high drug loadings for localized delivery of high concentrations of INH to tuberculosis lesions was investigated. In this respect, the formidable potential of spray-drying as a preparative technique has been investigated as part of recently popularized two-stage techniques, whereby preformed cores are coated with a rate limiting element in the form of a biodegradable polymer (Mathiowitz et al., 1992; Lee et al., 1997).

9.2 Experimental procedures

9.2.1 Microsphere preparation

9.2.1.1 Production of small cores

Aqueous isoniazid 12.5 %w/v solution (100 mL) was spray-dried in the preparation of drug cores for subsequent coating with poly-α-hydroxy acid according to Table 9.1.

9.2.1.2 Microencapulation of small cores

Selected drug cores were coated with RG755 at core:polymer ratios 0.5:1.0; 0.5:2.0 and 0.5:3.0. Solvent, DCM, was used to separately prepare a dispersion (50 mL) and solution (50 mL) of INH (500 mg) and polymer, respectively. Cores were dispersed with ultrasonification (Sonicator XL, Heat Systems, N.Y., USA) and polymer solution added under constant stirring. This suspension was then spray-dried at inlet = 40 °C; flow = 600 NLh^{-1}; aspiration = 100 %; and feed = 4 $mLmin^{-1}$.

9.2.1.3 Microencapulation with proteinaceous polymers

Solutions of INH and protein, albumin (ALB) and casein (CAS), were prepared in HPLC water (3 %w/v total solid) at D:P ratios of 0.1:0.9, 0.2:0.8, 0.3:0.7, 0.4:0.6 and 0.5:0.5 according to Table 9.2. Processing parameters were: inlet = 110 °C; outlet = 75 - 77 °C; flow = 800 NLh^{-1}; aspiration = 100 %; and feed = 4 $mLmin^{-1}$. Each batch was prepared in duplicate. Heat denatured (125 ± 5 °C, 24 h) microspheres (500 mg) with D:P ratio 0.1:0.9 (#27) 0.3:0.7 (#29) and 0.5:0.5 (#31) were dispersed and spray-coated with RG755 (2.5 %w/v, 100 mL) in DCM as described in section 9.2.1.2.

Table 9.1 *Spray-drying conditions for the preparation of isoniazid spheres for microencapsulation*

Batch	Inlet / °C	Outlet / °C	Flow / NLh^{-1}	Pump / %	Yield / %
1	155	116	800	5	25
2	145	111	800	5	22
3	135	107	800	5	19
4	125	100	800	5	15
5	165	123	800	5	25
6	165	120	600	5	< 1
7	155	116	600	5	< 1
8	145	114	600	5	7
9	135	98	600	5	5
10	125	96	600	5	18
11	165	132	400	5	< 1
12	155	125	400	5	< 1
13	145	115	400	5	< 1
14	135	103	400	5	< 1
15	125	95	400	5	< 1
16	145	117	800	10	25
17	145	99	800	15	22
18	145	89	800	20	23.5
19	145	86	800	25	21
20	165	115	800	10	20
21	165	113	800	15	10
22	165	111	800	20	22
23	165	100	800	25	27
24	155	110	800	10	30
25	155	105	800	15	17
26	155	99	800	20	18

Aspiration = 100 %

Table 9.2 *Spray-drying parameters and production attributes of isoniazid-protein microspheres (n = 2)*

Batch		Dissolved solid / 200 mL		Yield / %	
albumin	casein	INH / g	protein / g	albumin	casein
27	32	0.6	5.4	52.9	51.4
28	33	1.2	4.8	52.7	48.8
29	34	1.8	4.2	55.5	47.2
30	35	2.4	3.6	53.7	32.7
31	36	3.0	3.0	45.1	31.0

9.2.2 Microsphere characterization

Drug loading was assessed by extraction of INH from microspheres (10 mg) in a mixture of HCl (0.01 mol L^{-1}, 20 mL) and DCM (20 mL). Each layer was separated and drug extracted quantified by HPLC as described in section 2.3.2. Morphological assessment of spray-dried microparticles was performed by SEM. Particle size analysis were performed on Mastersizer S (Malvern Instruments Ltd., Malvern). Image analysis to further assess the aggregative state of selected batches was also performed (Coulter Electronics Ltd., Luton). Drug release studies were performed according to method A with quantification of released drug by HPLC (section 2.3.2). Spray-dried INH and encapsulated products thereof were examined by DSC as described in section 5.2.3.6. To quantify the degree of disorder conferred on crystalline INH by spray-drying, the entropy analogue was determined for each batch based on thermal indices according to equation 9.1.

$$\Delta S^f = \frac{\Delta H^f}{T_m} \qquad \textit{(Equation 9.1)}$$

Residual moisture for selected batches was also determined (CA-20, Mitsubishi Kasei Corporation, Japan). XRD was also performed on selected batches of ALB microspheres before and after heat denaturation in dried air at 125 ± 5.0 °C for 3, 6, 10 and 24 h.

9.3 Results and Discussion

9.3.1. Characterization of INH cores

Although the effect of flow rate, pump speed and aspiration were all systematically examined, it was apparent that spray conditions below 600 NLh^{-1} and 100 % aspiration gave inadequate yields, i.e., < 5 %. This was considered due to the dense character of the ostensibly crystalline particles produced. The high specific weight of these products required a considerable vacuum to effectively draw the particles through the apparatus. In addition, high flow rates were required to sufficiently divide the stream of solution, producing particles below the critical mass which thus remained airborne in the glassware. Due to the rapidity of the process, spray-drying is known to generate disorder in the crystal lattice (Corrigan, 1995), not uncommonly destroying crystallinity completely (Broadhead et al., 1992; Masters, 1992); as was shown in chapter 6 for RIF. On the contrary, the crystalline character of the cores produced was verified by DSC as shown in Figure 9.1 and by the calculation of the entropy analogues for each product.

Characteristic melting endotherms were present in all spray-dried products with only small reductions in both heat of melting, i.e., 206 ± 5.60 Jg^{-1} and entropy analogue 0.451 ± 0.03 Jg^{-1} K^{-1} when compared with stock reference for which corresponding values were 211 Jg^{-1} and 0.473 Jg^{-1} K^{-1}, respectively. Furthermore, SEM revealed geometrical regularity, some products appearing distinctly cuboidal as shown in Figure 9.2 (B). The small particle size and associated high surface energy accounted for considerable aggregation evident both in optical and SEM micrographs in Figure 9.2 (A) and (D) respectively. Particle fusion was further facilitated by residual moisture, which ranged between 0.55 - 3.25 %w/w, with no clear dependence on drying parameters. Collision of partially dried microdroplets in the area of the drying chamber further contributed to particle fusion seen in Figure 9.2 (C & D).

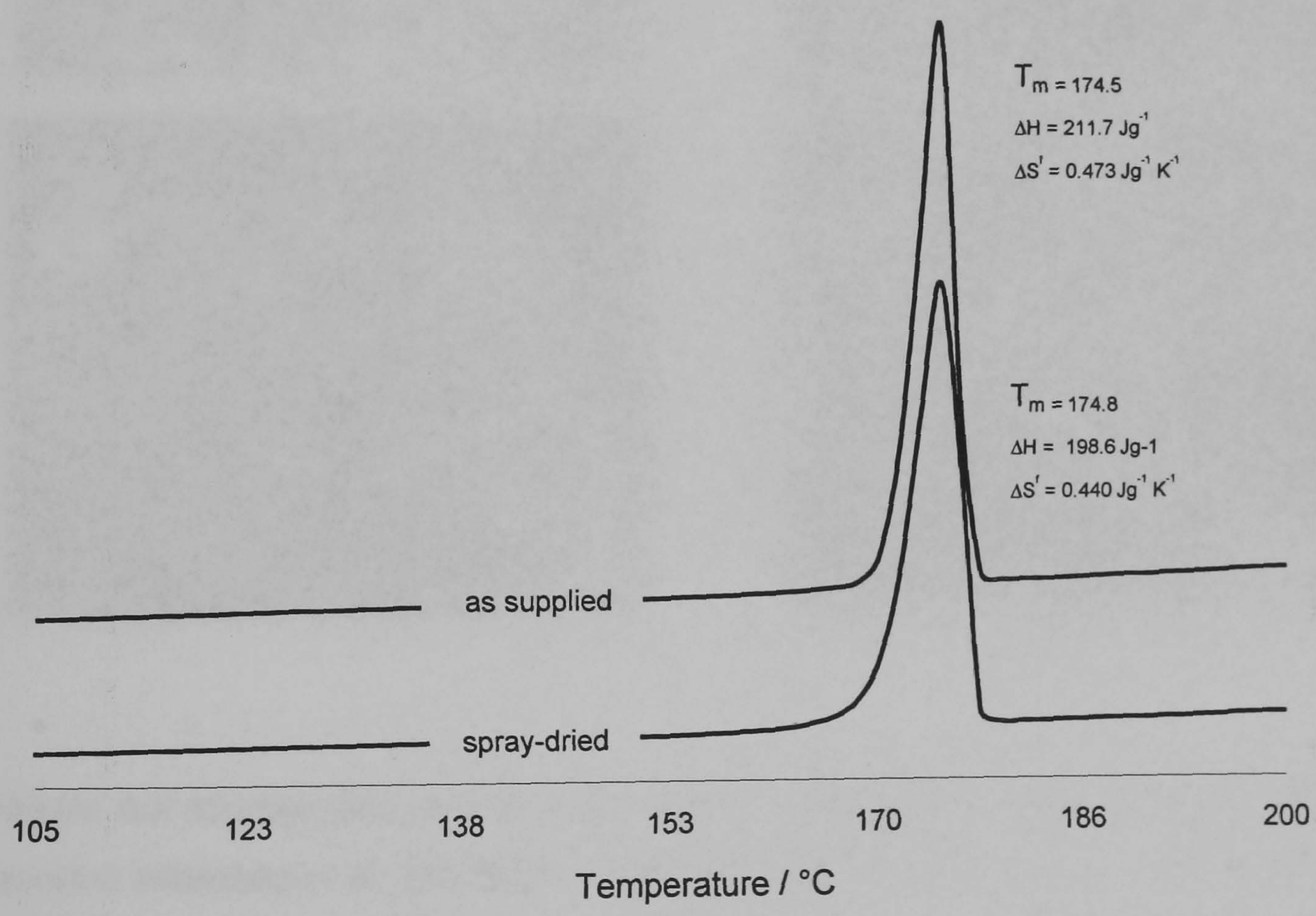

Figure 9.1 *Representative DSC scans of spray-dried and crystalline isoniazid.*

Owusu-Ababio & Rogers (1996) prepared cephalexin PLLA microparticles, precipitating polymer around preformed spray-dried particles. By suspending spray-dried cores in a polymer solution, spray-dried polyanhydride microcapsules thus obtained had diameters approximating to those of the drug particles. The authors concluded that a single drug particle was contained within each microparticle (Mathiowitz et al., 1992). On this basis, it

was reasoned that a suitable product for subsequent coating should possess a mean diameter smaller than that normally generated by spray-drying of the coating, be deaggregated and of uniform diameter. No product actually satisfied these criteria. Morphologically, #11 appeared to yield the highest proportion of small uniform and individualized particles, however, yields were particularly low; the drying parameters appeared to fraction suitable particles. Accordingly, #5 was selected in terms of particle appearance, shape and fusion of those batches yielding > 15 % of that attempted.

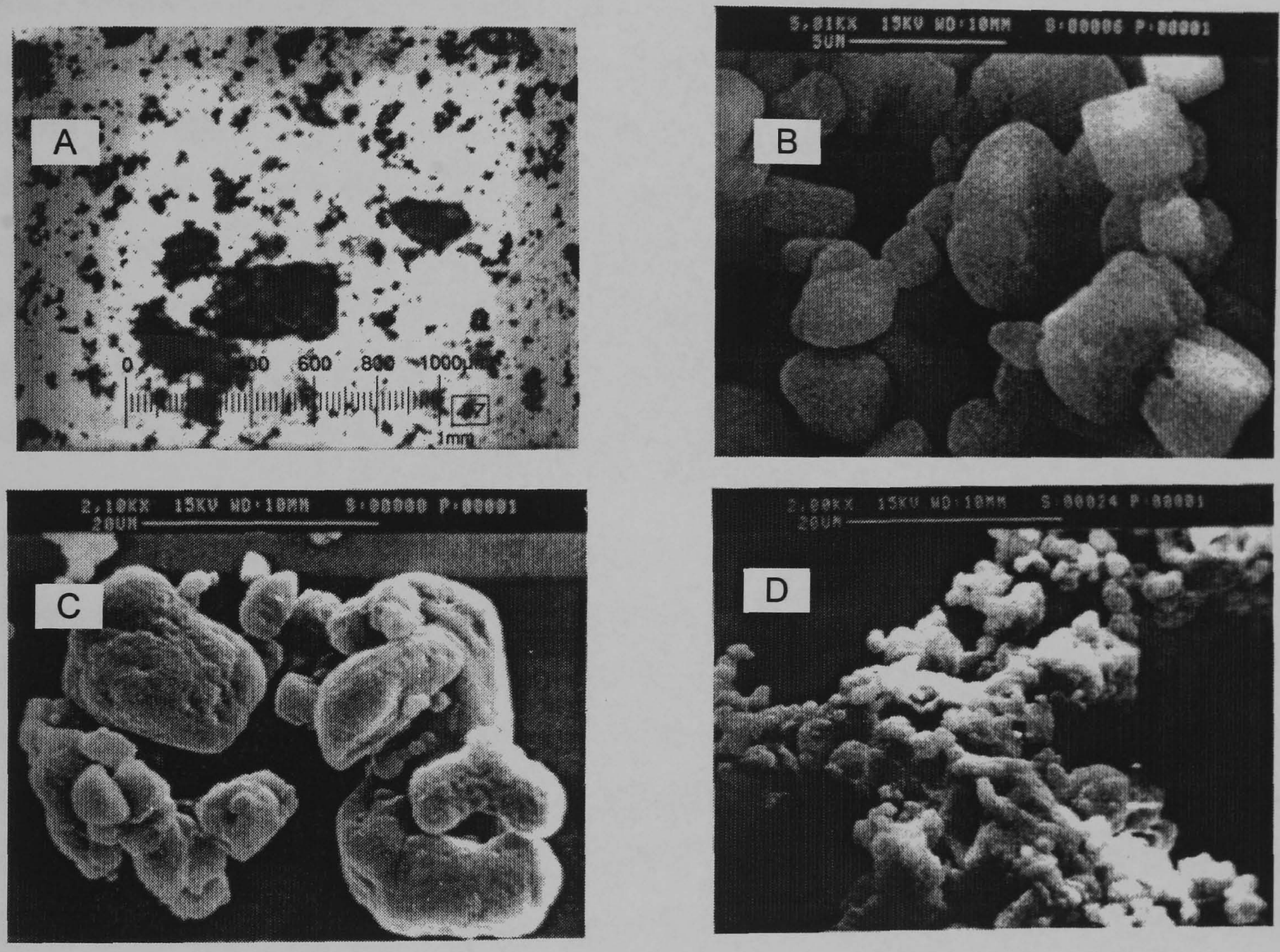

Figure 9.2 *Micrographs of INH cores captured by optical microscopy (A), and scanning electron microscopy: B, #6 (Mag^n = 5.01 k); C, #8 (Mag^n = 2.10 k); and, D, #24 (Mag^n = 2.00 k).*

Irrespective of the D:P ratio, release profiles were characterized by a rapid release of drug, i.e., 100 % in < 5 min. This was attributed to the poor coating efficiency of the slowly degrading polymer RG755 and the partial solubility of INH in the suspending solvent, DCM (1.95 mgmL^{-1}). The former effect was exacerbated by the aggregative nature of the suspended cores which required probe sonification to facilitate dispersion, which, in turn, aided solubilization of approximately 30-50 % of added INH. The inclusion of surfactant to

aid particle wetting, and judicious choice of dispersion solvent in which INH and poly-α-hydroxy acid have minimal and maximal solubility, respectively, should conceivably improve the sustained release character of such particles. The substitution for other polymers, e.g., polyanhydrides with which the coating utility of spray-drying has been demonstrated (Mathiowitz et al., 1992), represents another parameter which requires further investigation.

9.3.2 Characterization of isoniazid-protein microspheres

In order to prepare deaggregated particles of uniform diameter and of improved sphericity, highly loaded INH spheres were prepared with proteins, ALB and CAS (Magee et al., 1993). These materials were selected on the basis of their sprayability (Foster & Leatherman, 1995) and putative biocompatible (Magee et al., 1993). In addition, these proteins can be denatured by heat and/or chemical modification (Chen et al., 1987; Gupta et al., 1989) during (Przyborowski et al., 1982) or subsequent to spray-drying (Pavanetto et al., 1994b) to confer an additional level of sustained release on entrapped drug.

9.3.2.1 Morphology and granulometry

Yields of production in Table 9.2 showed a remarkable dependence on particle size distribution presented in Figure 9.3 (A). The relative invariability of granulometry for ALB microspheres corresponded well with their yield, whereas yield decreased in direct relation to particle diameter with CAS. These data support the fact that a critical range of microsphere mass exists, below and above which, product is either exhausted or impacts before the region of the cyclone. Both phenomena result in dramatic reductions in yield.

Scanning electron micrographs revealed typical surface disparities (Pavanetto et al., 1994b; Foster & Leatherman, 1995), including blow-holes, surface folds, shrivelling and sphere fracture. These arise due to the non-equilibrium drying conditions which prevail during drying of multi-phase microspheres which creates internal pressurization and regional stresses at the evaporating surface (Masters, 1992). Accordingly, the surface characteristics deteriorated as the phase ratio approached unity, i.e., as drug loading increased as shown in Figure 9.4. This deterioration was traced by an increased tendency to aggregate and by deviation from microparticle sphericity; reminiscent of drug cores shown in Figure 9.2. For comparable compositions, ALB based spheres demonstrated greater individualization and sphericity. The faster drying of ALB compared with CAS was reflected in the preponderance of the former to 'blow-holes' (internal

pressure) and the latter to folding. These morphologies reflect the position of the product in the drier as surface precipitation occurred. Folding is suggestive of the surface solidification arising at a point below the boiling point of the solvent, whereas blow-holes indicate precipitation at a region closer to the nozzle where the air is hotter (Masters, 1992).

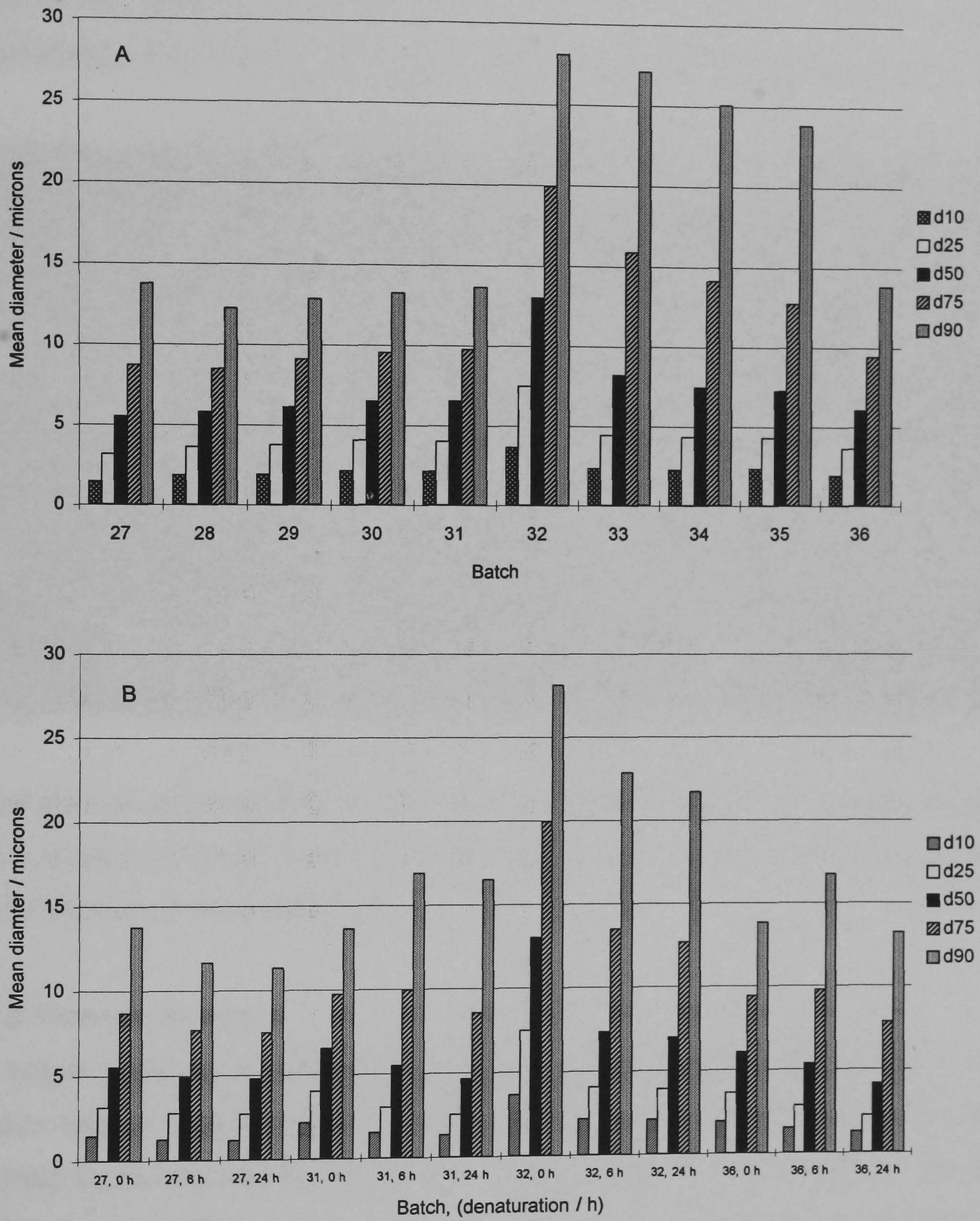

Figure 9.3 *Granulometric statistics (volume) of isoniazid-protein based microspheres before (A) and after (B) heat denaturation (125 ± 5.0 °C). Legend represents 10 % (d10) 25 % (d25), 50 % (d50) 75 % (d75) and 90 % (d90) undersize fractions. Processing parameters according to Table 9.2*

Morphological results observed with ALB microspheres are in contrast to those previously observed with nicardipine-bearing spray-dried particles (Conte et al., 1994b). Upon introduction of nicardipine to the spray solution, smooth microspheres resulted in comparison to the shrivelled appearance of the corresponding blank ALB product. This was presumably due to amorphous nature of the drug under the conditions of preparation (Conte et al., 1994b). However, crumpled surfaces have also been observed with carbamazepine (Giunchedi et al., 1994) and dexamethasone (Pavanetto et al., 1994b).

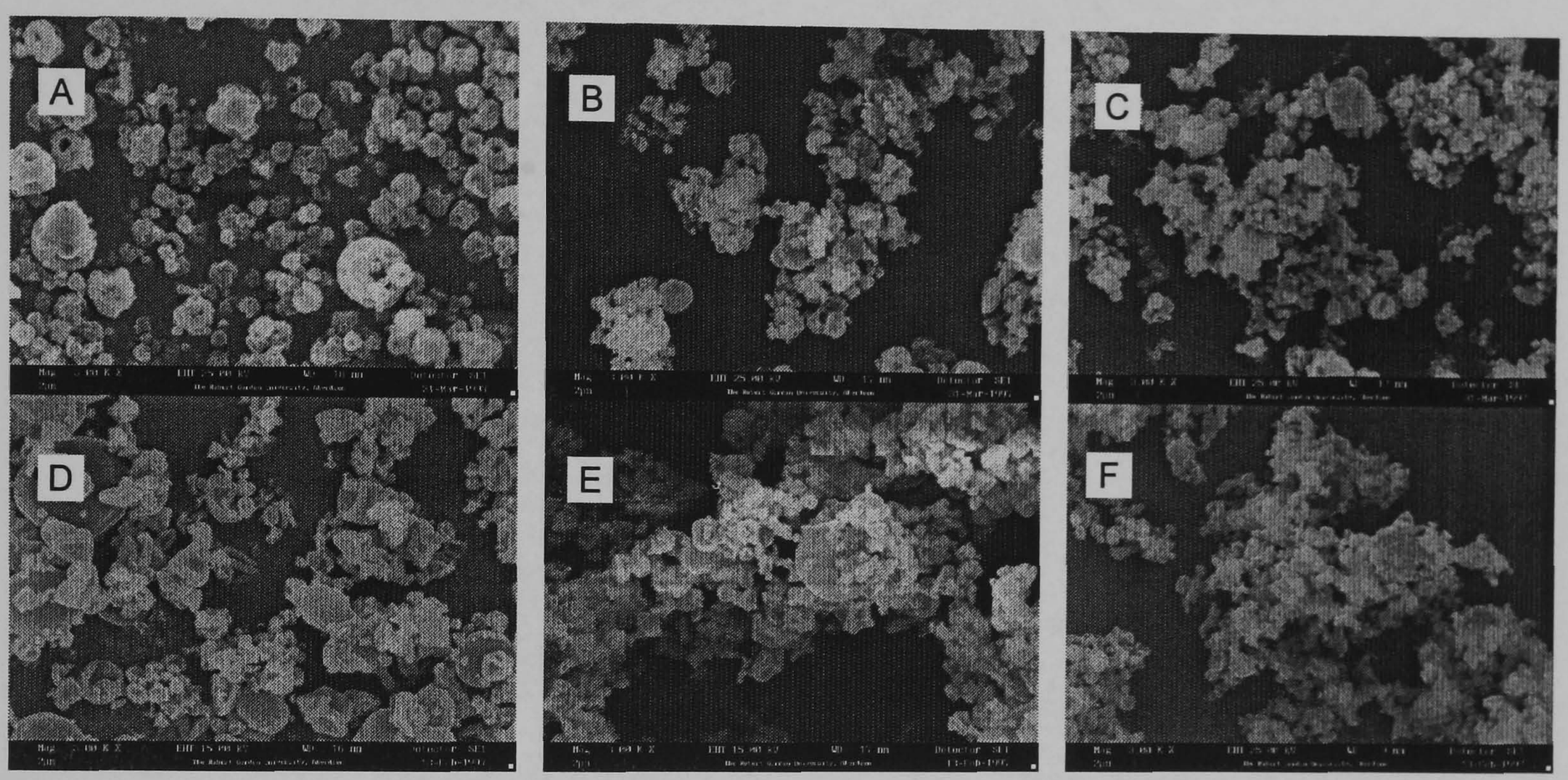

Figure 9.4 *Scanning electron micrographs showing the effect of isoniazid:protein ratio at 0.1:0.9, 0.3:0.7 and 0.5:0.5 on the morphology of spray-dried albumin (A,B,C) and casein (D,E,F) microspheres respectively.*

9.3.2.2 Thermal analysis

DSC scans presented in Figure 9.5 showed a characteristic event around 100 °C as aqueous residue was driven off under the heating cycle. The origin of this event was confirmed by its absence in DSC scans of heat denatured microspheres. The propensity for INH to recrystallize even under the rapid drying conditions was evident from the presence of sharp endotherms at all INH:ALB ratios although their position did not always correspond to that expected for INH. In contrast, only at the highest studied D:P ratio did a melting event for INH appear in CAS based systems. The origin of the broad endotherm at 125 - 135 °C and 140 - 170 °C for ALB and CAS microspheres respectively was considered due to the interaction of INH with protein as its area increased as the D:P ratio approached unity.

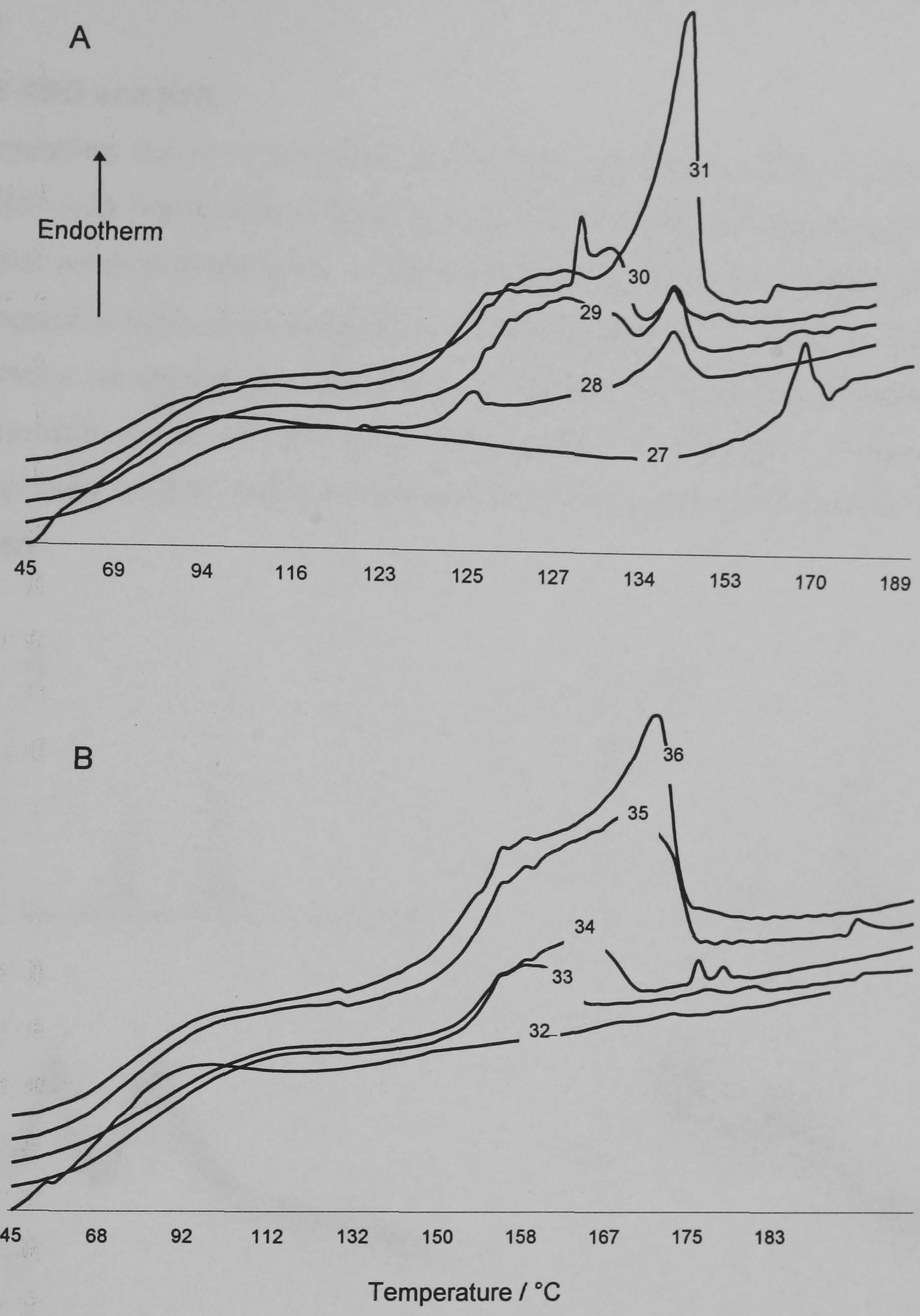

Figure 9.5 *Differential scanning calorimetric analysis of isoniazid loaded microspheres prepared with: A, albumin; and, B, casein. Labels indicate batch according to Table 9.2.*

During denaturation, endotherms corresponding to crystalline drug reduced in area in a time dependent fashion such that no peak was evident for #27 after 6 h and the peak for #31 was reduced to half its original area in 24 h. This was considered due to solubilization of hydrophilic INH in the hydrophilic ALB matrix. Considerable solubilization of INH in CAS was evident from the fact no melting endotherm corresponding to INH was apparent after 24 h heat treatment. In addition, the broad ill-defined endotherm between 150 - 175 °C also disappeared irrespective of the encapsulant. Recoveries of drug were 95 - 100 %

during HPLC assessment of denatured samples which ruled-out drug degradation as the cause.

9.3.2.3 XRD analysis

The crystalline nature of spray-dried INH was confirmed by XRD. Comparison of spray-dried INH was made with crystalline drug and a theoretical output based on a previous structural solution (Bhat et al., 1974) as shown in Figure 9.6. Despite the presence of a thermographic peak corresponding to crystalline INH at D:P ratios of 0.1:0.9, low signal-noise ratios for diffraction intensities as a result of the presence of protein obscured the characteristic peaks for the drug. Examination of diffraction patterns of denatured microspheres at D:P (0.5:0.5) verified the persistence of crystalline drug after heat treatment.

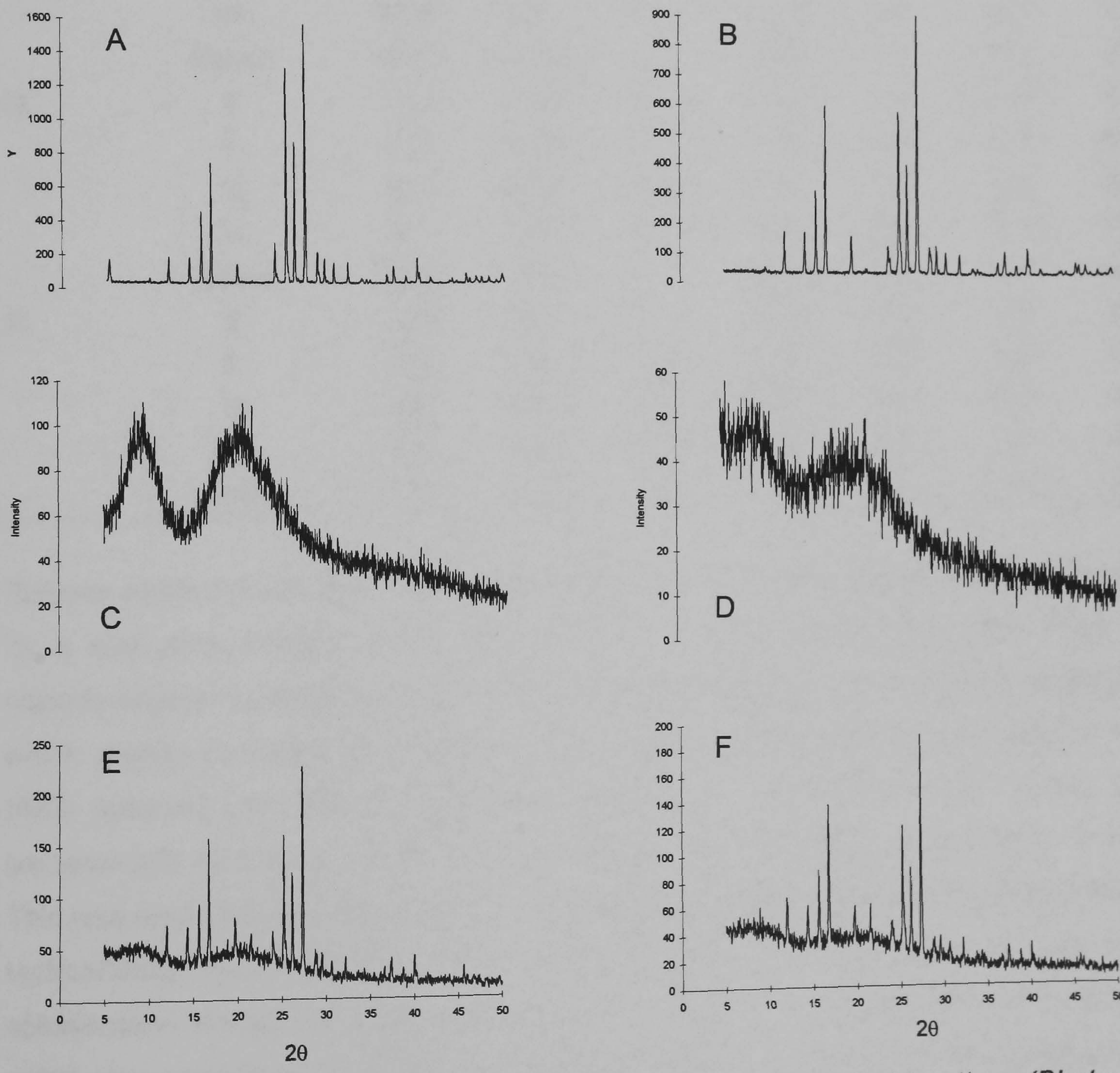

Figure 9.6 *X-ray powder diffractograms of: A, theoretical isoniazid pattern (Bhat et al., 1974); B, spray-dried isoniazid; C, native albumin; D, spray-dried isoniazid-albumin microsphere (D:P), 0.1;0.9; and, 0.5:0.5 before (E) and after (F) heat denaturation at 125 ± 5 °C for 24 h.*

9.3.2.4 *In vitro* drug release

Due to the biphasic pattern of drug release, *in vitro* profiles of denatured ALB microspheres were fitted to equation 8.1 to yield the data shown in Table 9.3.

Table 9.3 *Statistics of drug release data fitted to equation 8.1 of heat denatured spray-dried isoniazid microspheres using method A at 37 ± 0.1 °C. Batch according to Table 9.2. (r^2 = > 0.997, n = 3, SD ≤ 10.2).*

Batch	Denaturation / h	Biexponential coefficients				Quartile release / min		
		A / %	α / min^{-1}	B / %	β / min^{-1}	25	50	75
27	3	99.6	0.235	-0.04	0.001	1.01	2.01	4.23
	6	100.6	0.153	-0.07	0.01	1.91	4.55	9.06
	10	90.3	0.091	9.62	< 0.001	3.55	8.84	19.42
	24	99.36	0.081	0.92	< 0.001	3.61	8.67	17.43
	coated	93.19	0.033	7.84	< 0.001	10.0	24.2	51.3
29	3	85.8	0.305	14.18	0.002	1.12	2.85	6.71
	6	87.2	0.225	12.77	< 0.001	1.50	3.77	8.68
	10	84.5	0.185	15.45	0.001	1.79	5.21	12.23
	24	84.1	0.089	15.95	< 0.001	4.60	12.57	17.12
	coated	88.25	0.037	11.75	0.002	7.91	19.17	38.92
31	3	89.6	0.518	10.39	0.005	0.63	1.57	3.48
	6	90.2	0.517	9.82	0.003	0.63	1.56	3.43
	10	88.2	0.360	12.03	0.001	0.98	2.45	4.63
	24	88.3	0.321	11.36	0.004	1.34	2.78	5.98
	coated	89.59	0.058	10.07	0.002	5.44	13.61	29.7

Release profiles were again all characterized by a predominant 'burst' of release followed by a very slow release of the small fraction of INH residue. The latter effect was considered due to gelation of the protein matrix and subsequent microsphere aggregation which greatly increased the diffusional pathlength. Microspheres loaded with 10 %w/w (#27) released their total INH payload in the 'burst' phase. The extent of the 'burst' paradoxically decreased for 30 %w/w (#29) and 50 %w/w (#31) microspheres to 90 %. This was attributed to more rapid and enhanced aggregation of the microspheres as their hydrophilicity increased with greater drug loading. On the one hand, the partial solubilization of drug within the matrix during denaturation observed with thermal analysis might also account for the apparent increased affinity of the drug for the protein matrix. On the other hand, plasticization of the matrix by INH as observed in section 3.3.3.2 would be expected to accelerate release as drug loading increased.

Coating of dispersed denatured microspheres with RG755 resulted in a 2.6, 2.1 and 5.5 fold reduction in the rate of initial release for batch #27, #29 and #31 respectively. However, despite the apparent improvement in coating efficiency, effective drug loading fell more than six-fold to 1.55, 4.61 and 7.92 %w/w due to the presence of spray-dried coating / microspheres which were not separated from microcapsules. Calculated loadings were approximately 90 - 95 % of that anticipated due to adherence of some dispersed microspheres, to the vessel in which they were suspended. Indeed, approximate correspondence of batch #27 after 24 h denaturation (10 %w/w loading) with the release rate statistics of #31 (7.92 %w/w effective loading) would indicate that little was to be gained in terms of sustaining drug release by the additional coating step. However, by increasing the size of the microsphere cores to be coated, this might allow individual populations of microspheres and microcapsules to be separated and hence a partial restoration of drug loading. In addition, as suggested above, judicious choice of solvent which dissolves the polymer but has little capacity to dissolve entrapped drug might allow further improvements to be made to the preliminary data presented from the two-stage encapsulation process.

9.4 Conclusion

The highly water soluble and crystalline structure of INH precluded the effective encapsulation of spray-dried cores under the spray-drying conditions examined. However, encapsulation within spray-dried ALB matrices conferred measurable sustained release despite the persistence of crystalline drug. Drug release was further sustained by spray-coating of an additional rate-limiting membrane of biodegradable Resomer® but at the expense of a several fold reduction in effective loading. It is postulated that establishment of an organic solvent in which Resomer® (or other suitable biodegradable polymer) is soluble but INH is not, would allow improved coating efficiency and hence a further retardation of drug release. Furthermore, work is required to examine the potential separation of unwanted microspherical coating from coated microcapsules by a suitable technique, e.g., microsieving. If improvements in these two attributes can be made, it is believed that the early intra-pulmonary delivery of such a product might significantly reduce the potential infectivity of the growing population of TB victims.

General Conclusions

These studies have affirmed spray-drying as an excellent technique to rapidly and reproducibly obtain large quantities of biodegradable microspheres of high loading and predictable character. Its industrial applicability is further underlined by its capacity to be a continuous process in which microspheres can be prepared aseptically. Moreover, with judicious choice of process conditions, spray-drying can efficiently incorporate drugs of different hydrophilicities. In addition, although seldom reported, the technique offers attractive opportunities for the coformulation of drugs in poly-α-hydroxy acids and other biodegradable polymers.

In previous reports of spray-dried poly-α-hydroxy acids, scant consideration has been paid to solvent selection, whereby strategies to modulate microparticle properties being based solely on incipient and excipient physicochemistry. DCM has often being arbitrarily selected based presumably on its historical use in other microencapsulation techniques. These investigations have provided sound justification for its previous, serendipitous selection with PDLLA, whereas optimal solvents for PDLGA are still to be identified.

Empirical studies suggest PDLLA represents a more valuable material to explore its modulating capacity when combined with oligomers of the same nature. The between batch non-reproducibility alludes to the ability to modify release kinetics by modulating the MW and hence the hydrophobicity of the complementary material. On the one hand, hydrophilic plasticizing oligomeric fractions behave as 'initiator' for the hydration process, itself triggered by the correspondence of the medium and T_g temperatures. On the other hand, complementary PDLLA served to modify release rate and is referred to as 'modulator'. Furthermore, the more coherent matrices formed with PDLLA by virtue of their enhanced solubility in DCM further supports their use in preference to PDLGA. However, in the event that a suitable solvent with greater solvency for PDLGA can be identified, improvements in matrix coherence are conceivably possible with copolymer. Overall, this strategy offers a generic approach by which the release of a variety of drugs of comparable solubility character might be modulated. It is recognized, however, that the critical weight proportions of each polymer providing controlled release will vary depending on the influence of each individual drug on the thermal and hydrophilic character of the encapsulating composite.

Where convenient administration devices can be developed, or existing ones utilized,e.g., MDIs, intra-pulmonary delivery of spray-dried biodegradable microspheres might alleviate some of the problems currently associated with protracted therapy of tuberculosis and other chronic diseases of the broncho-pulmonary system.

References

Alex, R., and Bodmeier, R., 1990, Encapsulation of water-soluble drugs by a modified solvent evaporation method. I. Effect of process and formulation variables on drug entrapment. *J. Microencap.*, **7** (3), 347-355.

Armstrong, D.J., Elliot, P.N.C., Ford, J.L., Gadson, D., McCarthy, G.P., Overend, T., Rostron, C., and Worsley, M.D., 1991, The acute effects of inhaled polylactic acid microspheres upon the lungs of rabbits. *Proceed. 11th Pharm. Tech. Confer.*, **3**, 39-52.

Armstrong D.J., Elliot P.N.C., Ford J.L., Gadson D., Matzen J., McCarthy G.P., Rostron, C., and Worsley, M.D., 1992, Poly-(D,L)-lactic acid microspheres incorporating histological dyes for intra-pulmonary histopathological investigations. *Proceed. 12th Pharm. Tech. Confer.*, **2**, 494-505.

Armstrong, D.J., Elliot, P.N.C.E., Ford, J.L., Guiziou, B., and Rostron, C., 1994, A comparison of the use of halothane and dichloromethane in the preparation of PLA microspheres by a solvent evaporation technique. *Proceed. 13th Pharm. Tech. Confer.*, **1**, 51-64.

Armstrong, D.J., Elliot, P.N.C.E., Ford, J.L., Guiziou, B., McCarthy, G.P., and Rostron, C., 1995, Investigations of in vitro release of NSAIDs from PLA microspheres. *Proceed.14th Pharm. Tech. Confer.*, **1**, 43-51.

Armstrong, D.J., Elliot, P.N.C.E., Ford, J.L., Gadson, D., McCarthy, G.P., Rostron, C., and Worsley, M.D., 1996, Poly-(D,L)-lactic acid microspheres incorporating histological dyes for intra-pulmonary histopathological investigations. *J. Pharm. Pharmacol.*, **48**, 258-262.

Arshady, R., 1991, Preparation of biodegradable microspheres and microcapsules: 2. Polylactides and related polyesters. *J. Control. Rel.*, **17**, 1-22.

Asano, M., Fukuzaki, H., Yoshida, M., Mashimo, T., Yuasa, H., Imai, K., Yamanaka, H., and Suzuki, K., 1989, *In vivo* characteristics of low molecular weight copoly(L-lactic acid/glycolic acid) formulation with controlled release of luteinizing hormone-releasing hormone agonist. *J. Control. Rel.*, **9**, 111-122.

Asano, M., Fukuzaki, H., Yoshida, M., Kumakura, M., Mashimo, T., Yuasa, H., Imai, K., Yamanaka, H., 1990, Application of poly D,L-lactic acids of varying molecular weight in drug delivery systems. *Drug Design Deliv.*, **5**, 301-320.

Asano, M., Fukuzaki, H., Yoshida, M., Kumakura, M., Mashimo, T., Yuasa, H., Imai, K., Yamanaka, H., Kawaharada, U., and Suzuki, K., 1991, In vivo controlled release of a luteinizing hormone-releasing hormone agonist from poly(DL-lactic acid) formulations of varying degradation pattern. *Int. J. Pharm.*, **67**, 67-77.

Aso, Y., Yoshioka, S., and Terao, T., 1992, Release characteristics stability of poly(l-lactide) microspheres and chemical stability of drugs in the microspheres. *Proceed. Intern. Symp. Control. Rel. Bioact. Mater.*, **19**, 310-311.

Atkins, T.W., Peacock, S.J., and Yates, D.J., 1998, Incorporation and release of vancomycin from poly(D,L-lactide-co-glycolide) microspheres. *J. Microencap.*, **15** (1), 31-44.

Avgoustakis, K., and Nixon, J.R., 1991, Biodegradable controlled release tablets: I. Preparative variables affecting the properties of poly(lactide-co-glycolide) copolymers as matrix forming materials. *Int. J. Pharm.*, **70**, 77-85.

Avgoustakis, K., and Nixon, J.R., 1993a, Biodegradable controlled release tablets: II. Preparation and properties of poly(lactide-co-glycolide) powders. *Int. J. Pharm.*, **99**, 239-246.

Avgoustakis, K., and Nixon, J.R., 1993b, Biodegradable controlled release tablets: II. Preparation and properties of poly(lactide-co-glycolide) powders. *Int. J. Pharm.*, **99**, 239-246.

Barton, A.F.M., 1975, Solubility parameters. *Chem. Rev.*, **75**, 731-753

Bayer, R., and Wilkinson, D., 1995, Directly observed therapy for tuberculosis: history of an idea. *Lancet,* **345**, 1545-1548.

Bazile, D.V., Ropert, C., Huve, P., Verrecchia, T., Marlard, M., Frydman, A., Veillard, M., and Splenlehauer, G., 1992, Body distributiion of fully biodegradable [^{14}C]-poly(lactic acid) nanoparticles coated with albumin after parenteral administration to rats. *Biomaterials*, **13** (15), 1093-1102.

Beck, L.R., Cowsar, D.R., Lewis, D.H., Cosgrove, R.J., Riddel, C.T., Lowry, S.L., and Epperly, T., 1979, A new long-acting injectable microcapsule system for administration of progesterone. *Fert. Steril.*, 31 (5), 545-551.

Beck, L.R., Pope, V.Z., Tice, T.R., and Gilley, R.M., 1985, Long-acting injectable microsphere formulation for the parenteral administration of levonorgesterol. *Adv. Contracept.*, 1, 119-129.

Bell, C., and IP, D.P., 1993, Utility of column switching to analyse low dose dissolution samples for pharmaceutical formulations. *J. Pharm. Biomed. Anal.*, **11**, 171-181.

Bellbella, A., Vauthier, C., Fessi, H., Devissaguet, J.-P., and Puisieux, F., 1996, *In vitro* degradation of nanospheres from poly(D,L-lactides) of different molecular weights and polydispersities. *Int. J. Pharm.*, **129**, 95-102.

Bendix, D., 1990, Analytical studies of the solubility problem of poly(D,L-lactide-co-glycolide) 50:50. *Proceed. Intern, Symp. Control. Rel. Bioact. Mater.*, **17**, 244-245.

Benelli, P., Conti, B., Genta, I., Constantini, M., and Montanari, L., 1998, Clonazepam microencapsulation in poly-D,L-lactide-co-glycolide microspheres. *J. Microencap.*, **15** (4), 431-443.

Benita, S., Benoît, J.P., Puisieux, F., and Thies, C., 1984, Characterization of drug-loaded poly(*d,l* -lactide) microspheres. *J. Pharm. Sci.*, **73** (12), 1721-1724.

Benita, S., 1996, Microencapsulation: Methods and Industrial Applications. (New York, Marcel Dekker).

Benoît, J.P., Courteille, F., and Thies, C., 1986, A physicochemical study of the morphology of progesterone-loaded poly(D,L-lactide) microspheres., *Int. J. Pharm.*, **29**, 95-102.

Bhat, T.N., Singh, T.P. and Vijayan, M., 1974, Isonicotinic acid hydrazide – a reinvestigation. *Acta Cryst.*, **B30**, 2921-2922.

Bissery, M., Valeroite, F., and Thies, C., 1984, In vitro and in vivo evaluation of CCNU-loaded microspheres prepared from poly((±)-lactide) and poly(β-hydroxybutyrate)., in *Microspheres and Drug Therapy. Pharmaceutical, Immunological and Medical Aspects.* (Eds.) Davis, S.S., Illum, L., McVie, J.G., and Tomlinson, E., Elsevier Science Publishers B.V., 217-227.

Bittner, B., Ronneberger, B., Zange, R., Volland, C., Anderson, J.M., and Kissel, T., 1998, Bovine serum albumin loaded poly(lactide-co-glycolide) microspheres: the influence of polymer purity on particle characteristics. *J. Microencap.*, **15** (4), 495-514.

Bitz, C., and Doelker, E., 1995, Influence of the preparation method on residual solvents in biodegradable microspheres. *1st World Meeting APGI / APV*, 409-410.

Bodmeier, R., and McGinity, J.W., 1986, Preparation variables of d,l-polylactic acid microspheres. *Proceed. 4th Intern. Conf. Pharm. Tech.*, **II**, 168-172.

Bodmeier, R., and McGinity, J.W., 1987a, Polylactic acid microspheres containing quinidine sulphate prepared by the solvent evaporation technique: I. Methods and morphology. *J. Microencap.*, **4**, 279-288.

Bodmeier, R., and McGinity, J.W., 1987b, Polylactic acid microspheres containing quinidine base and quinidine sulphate prepared by the solvent evaporation technique. II. Some process parameters influencing the preparation and properties of microspheres. *J. Microencap.*, **4**, 289-297.

Bodmeier, R., and McGinity, J.W., 1987c, The preparation and evaluation of drug-containing poly(d,l-lactide) microspheres formed by the solvent evaporation method. *Pharm. Res.*, **4**, 465-471.

Bodmeier, R., and McGinity, J.W., 1988a, Polylactic acid microspheres containing quinidine base and quinidine sulphate prepared by the solvent evaporation technique. III. Morphology of the microspheres during dissolution studies. *J. Microencap.*, **5**, 325-330.

Bodmeier, R., and McGinity, J.W., 1988b, Solvent selection in the preparation of poly(D,L-lactide) microspheres prepared by the solvent evaporation method. *Int. J. Pharm.*, **43**, 179-186.

Bodmeier, R., and Chen, H., 1988, Preparation of biodegradable poly (±) lactide microparticles using a spray-drying technique. *J. Pharm. Pharmacol.*, **40**, 754-757.

Bodmeier, R., & Chen, H., 1989, Evaluation of biodegradable poly(lactide) pellets prepared by direct compression. *J. Pharm Sci.*, **78** (10), 819-822.

Bodmeier, R., Oh, K.H., and Chen, H., 1989, The effect of the addition of low molecular weight poly(DL-lactide) on drug release from biodegradable poly(DL-lactide) drug delivery systems. *Int. J.Pharm.*, **51**, 1-8.

Boehringer Ingelheim, 1992, Product catalogue. Boehringer Ingelheim KG, D-55216, Ingelheim am Rhein.

Boisdron-Celle, M., Menei, Ph., and Benoît, J.P., 1995, Preparation and characterization of 5-fluorouracil microparticles as biodegradable anticancer drug carriers. *J. Pharm. Pharmacol.*, **47**, 108-114.

Bosla,A.A., El Sayed,M.M., and Mahmoud,M., 1998, Preparation of targeted isoniazid microspheres. *Boll. Chem. Farm.*, **137** (3), 77-81.

Boury,F., Marchais,H., Proust,J.E., and Benoît,J.P., 1997, Bovine serum albumin release from poly(α-hydroxy acid) microspheres: effect of polymer molecular weight and surface properties. *J. Control. Rel.*, **45**, 75-86.

Brady,J.M., Cutright,D.E., Miller,R.A., and Battistone,G.C., 1973, Resorption rate, route of elimination and ultrastructure of the implant site of polylactic acid in the abdominal wall of the rat. *J. Biomed Mater. Res.*, **7**, 155-166.

Braggio,S., Barnaby,R.J., Grossi,P., and Cugola,M., 1996, A strategy for validation of bioanalytical methods. *J. Pharm. Biomed. Anal.*, **14**, 375.

Brannon-Peppas,L., 1995, Recent advances on the use of biodegradable microparticles and nanoparticles in controlled drug delivery. *Int. J. Pharm.*, **116**, 1-9.

British National Formulary, 1995, 30th edition, The General Medical Association and The Royal Pharmaceutical Society of Great Britain.

Broadhead, J., Edmond, Rouan, S.K., and Rhodes, C.T., 1992, The spray drying of pharmaceuticals. *Drug. Dev. Ind. Pharm.*, **18**, 1169-1206.

Bruhn, B.W., and Müller, B.W., 1991, Preparation and characterization of spray-dried poly(DL-lactide) micro-spheres. *Proceed. Intern. Symp. Control. Rel. Bioact. Mater.*, **18**, 667-668.

Büchi Minispray information no. 1: 1993, Principles, copyright by Büchi Laboratory-Techniques Ltd., CH-9230, Flawil, Switzerland.

Butterfield, A.G., Curran, N.M., Lovering, E.G., Matsui, F.F., Robertson, D.L., and Sears, R.W., 1981, Determination of hydrazine in Pharmaceuticals I: isoniazid. *Canadian J. Pharm Sci.*, **16** (1), 15-19.

Castelli, F., Conti, B., Puglisi, G., Conte, U., Mazzone, G., 1994, Calorimetric studies on tolmetin release from poly-D,L-lactide microspheres to lipid model membrane. *Int. J. Pharm.*, **103**, 217-223.

Cavalier, M., Benoît, J.P., and Thies, C., 1986, The formation and characterization of hydrocortisone-loaded poly((±)-lactide) microspheres. *J. Pharm. Pharmacol.*, **38**, 249-253.

Celebi, N., Erden, N., and Türkyilmaz, A., 1996, The preparation and evaluation of salbutamol sulphate containing poly(lactic acid-co-glycolic acid) microspheres with factorial design-based studies. *Int. J. Pharm.*, **136**, 89-100.

Cha, Y., and Pitt, C.G., 1989, The acceleration of degradation-controlled drug delivery from polyester microspheres. *J. Control. Rel.*, **8**, 259-265.

Chapman, P., personal communication, 1998. Pulmonologist, Cape Town, South Africa, Reg # 971163321.

Chaulet, P., 1987, Compliance with anti-tuberculosis chemotherapy in developing countries. Suppl. *Tubercle*, **68**, 19-24.

Chen, Y., Willmott, N., Anderson, J., and Florence, A.T., 1987, Comparisons of albumin and casein microspheres as a carrier for doxorubicin. *J. Pharm. Pharmacol.*, **39**, 978-985.

Chern, R.T., Wilson, R.A., Tang, J., and Zhao, Z., 1996, Some observations on the solvent extraction and drying characteristics of PLGA microspheres. *Proceed. Inter. Symp. Control. Rel. Bioact. Mater.*, **23**, 363-364.

Chu, C.C., 1981a, The *in vitro* degradation of poly(glycolic acid) sutures – effect of pH. *J. Biomed. Mater. Res.*, **15**, 795-804.

Chu, C.C., 1981b, An *in vitro* study of the effect of buffer on the degradation of poly(glycolic acid) sutures. *J. Biomed. Mater. Res.*, **15**, 19-27.

Chu, C.C., and Campbell N.D., 1982, Scanning electron microscopic study of the hydrolytic degradation of poly(glycolic) suture. *J. Biomed. Mater. Res.*, **16**, 417-430.

Chu, C.C., 1985, Degradation phenomena of two linear aliphatic polyester fibres used in medicine and surgery. *Polymer*, **26**, 591-594.

Clarke, N., O'Connor, K., and Ramtoola, Z., 1998, Influence of formulation variables on the morphology of biodegradable microspheres prepared by spray-drying. *Drug. Dev. Ind. Pharm.*, **24** (2), 169-174.

Conte, U., Conti, B., Giunchedi, P., and Maggi, L., 1994a, Spray dried polylactide microsphere preparation: influence of the technological parameters. *Drug Dev. Ind. Pharm.*, **20** (3), 235-258.

Conte, U., Giunchedi, P., Maggi, L., and Torre, M.L., 1994b, Spray-dried microspheres containing nicardipine. *Eur. J. Pharm. Biopharm.*, **40**, 203-208.

Conti, B., Pavanetto, F., Genta, I., and Giunchedi, P., 1991, Solvent evaporation, solvent extraction and spray drying for polylactide microsphere preparation. *Proceed. 10th Pharm. Tech. Confer.*, **1**, 16-29.

Conti, B., Puglisi, G., Ventura, C.A., Giunchedi, P., Conte, U., Caruso, A., and Cutuli, V., 1994, Tolmetin poly-D,L-lactide microspheres: *in vitro/in vivo* evaluation. *S.T.P. Pharma Sci.*, **4** (4), 269-274.

Conti, B., Genta, I., Modena, T., and Pavanetto, F., 1995a, Investigations on process parameters involved in polylactide-co-glycolide microspheres preparation. *Drug Dev. Ind. Pharm.*, **21** (3), 615-622.

Conti, B., Genta, I., Giunchedi, P., and Modena, T., 1995b, Testing of "in vitro" dissolution behaviour of microparticulate drug delivery systems. *Drug Dev. Ind. Pharm.*, **21** (10), 1223-1233.

Conti, B., Bucolo, C., Giannavola, C., Puglisi, G., Giunchedi, P., and Conte, U., 1997, Biodegradable microspheres for the intravitreal administration of acyclovir: *in vitro I in vivo* evaluation. *Eur. J. Pharm. Sci.*, **5**, 287-293.

Coombes, A.G.A., Scholes, P.D., Davies, M.C., Illum, L., and Davis, S.S., 1994, Resorbable polymeric microspheres for drug delivery – production and simultaneous surface modification using PEO-PPO surfactants. *Biomaterials*, **15** (9), 673-680.

Corrigan, O.I., 1995, Thermal analysis of spray dried products. *Thermochim. Acta*, **248**, 245-258.

Courteille, F., Benoît, J.P., and Thies, C., 1994, The morphology of progesterone-loaded polystyrene microspheres. *J. Control. Rel.*, **30**, 17-26.

Cowsar, D.R., Tice, T.R., Gilley, R.M., and English, J.P., 1985, [8] Poly(lactide-co-glycolide) microcapsules for controlled release of steroids. *Methods. Enzymol.*, **112**, 101-116.

Crofton, Sir J., 1996, personal communication at The 133rd British Pharmaceutical Conference Symposium entitled Tuberculosis. Glasgow, 10 - 11 September.

Crossan, I.M., and Whateley, T.L., 1994, Microspheres of dexamethasone as a biodegradable controlled release drug delivery system, *Proc. Intern. Symp. Control. Rel. Bioact. Mater.*, **21**, 184-185.

Dawson, R.M.C., Elliot, D.C., Elliot, W.H., and Jones, K.M., 1962, in *Data for Biochemical Research*. Oxford University Press, London.

Deasy, P.B., Finan, M.P., and Meegan, M.J., 1989, Preparation and characterization of lactic/glycolic acid polymers and copolymers. *J. Microencap.*, **6** (3), 369-378.

Deasy P.B., Finan, M.P., Klatt, P.R., Hornykiewytsch, T., 1993, Design and evaluation of a biodegradable implant for improved delivery of oestradiol - 17β to steers. *Int. J. Pharm.*, **89**, 251-259.

Deol, P., Khuller, G.K., and Joshi, K., 1997, Therapeutic efficacies of isoniazid and rifampin in lung-specific liposomes against Mycobacterium tuberculosis infection induced in mice. *Antimicrob. Agents Chemother.*, **41** (6), 1211-1214.

Dubernet, C., 1995, Thermoanalysis of microspheres.*Thermochimica Acta*, **248**, 259-269.

Editorial, 1998, Rifampicin combination effective in orthopaedic implant infections. *Pharm. J.*, May 30, 773.

Eenink, M.J.D., Feijen, J., Olijslager, J., Albers, J.H.M., Rieke, J.C., and Greidanus, P.J., 1987, Biodegradable hollow fibres for the controlled release of hormones. *J. Control. Rel.*, **6**, 225-247.

El-Baseir, M.M., Phipps, M.A., and Kellaway, I.W., 1997, Preparation and subsequent degradation of poly(L-lactic acid) microspheres suitable for aerolisation: a physicochemical study. *Int. J. Pharm.*, **151**, 145-53.

Elkheshen, S., 1996, Simplex lattice design for the optimization of the microencapsulation of a water soluble drug using poly(lactic acid) and poly(lactide-co-glycolide) copolymer. *J. Microencap.*, **13** (4), 447-462.

Esposito, E., Cortesi, R., Cervellati, F., Menegatti, E., and Nastruzzi, C., 1997, Biodegradable microparticles for sustained delivery of tetracycline to the periodontal pocket: formulatory and drug release studies. *J. Microencap.*, **14** (2), 175-187.

Fieser, L.F., Fieser, M., 1957, Introduction to organic chemistry, D.C. Heath and Company, Boston USA, 448-49

Flandroy, P., Grandfils, Ch., Daenen, B., Snaps, F., Dondelinger, R.F., Jérôme, R., Bassleer, R., and Heinen, E., 1997, In vivo behavior of poly(D,L)-lactide microspheres designed for chemoembolization. *J. Control. Rel.*, **44**, 153-170.

Florence, A., and Attwood, D., 1988, in *Physicochemical Principles of Pharmacy*, 2nd Edition, The Macmillan Press Ltd, London.

Fong, J.W., Maulding, H.V., Visscher, G.E., Nazareno, J.P., and Pearson, J.E., 1986, Evaluation of biodegradabe microcapsules prepared by solvent evaporation process using sodium oleate as emulsifier. *J. Contol. Rel.*, **3**, 119-130.

Ford, J.L., and Timmins, P., 1989, Pharmaceutical thermal analysis: techniques and applications. Ellis Horwood Ltd., Chichester, England.

Foster, T.P., and Leatherman, M.W., 1995, Powder characteristics of proteins spray-dried from different spray-driers. *Drug Dev. Ind. Pharm.*, **21** (15), 1705-1723.

Fox, W., 1958, The problem of self-administration of drugs; with particular reference to pulmonary tuberculosis. *Tubercle*, **39**, 269-274.

Fox, W., 1983, Compliance of patients and physicians: experience and lessons from tuberculosis – I. *B. M. J.*, **287**, 33-35.

Fox, W., 1983, Compliance of patients and physicians: experience and lessons from tuberculosis – II. *B. M. J.*, **287**, 101-105.

Fukuoka, E., Makita, M., and Yamamura, S., 1986, Some Physicochemical properties of glassy indomethacin. *Chem. Pharm. Bull.*, **34**, 4314-4321.

Fukuzaki, H., Yoshida, M., Asano, M., and Kumakura, M., 1989, Synthesis of copoly(D,L-lactic acid) with relatively low molecular weight and *in vitro* degradation. *Eur. Polym. J.*, **25**, 1019-1026.

Gadret, P.M., Goursolle, M., Leger, J.M., and Colleter, J.C., 1975, Structure de la rifampicine $C_{43}N_4O_{12}H_{58}.5H_2O$. *Acta. Cryst.*, **B31**, 1454-1462.

Gaitonde, C.D., and Pathak, P.V., 1990, Rapid liquid chromatographic method for the estimation of isoniazid and pyrazinamide in plasma and urine. *J. Chromatogr.*, **532**, 418-423.

Gallo, G.G., and Radaelli, P., 1968, Rifampin, in: *Analytical profiles of drug substances*. Ed. Florey K. Academic Press, New York, 467-513.

Gander, B., Johansen, P., Nam-Trân, H., and Merkle, H.P., 1996, Thermodynamic approach to protein microencapsulation into poly(D,L-lactide) by spray-drying. *Int. J. Pharm.*, **129**, 51-61.

Gangadharam, P.R.J., Hill, M., Kesavalu, L., Ashteker, D.R., Parikh, K., and Wise, D.L., 1989, Sustained release of isoniazid *in vivo* from a biodegradable polymer implant. *Tubercle*, 70, 54-58.

Gangadharam, P.R.J., Ashteker, D.R., Farhi, D.C., and Wise, D.L., 1991, Sustained release of isoniazid *in vivo* from a single implant of a biodegradable polymer. *Tubercle*, **72**, 115-22.

Gangadharam, P.R.J., and Kailasam, S., 1993, Sustained release of pyrazinamide in mice from a single implant of a biodegradable polymer. *Proceed. 18th Int. Cong. Chemother.*, Stockholm, 488-489.

Gangadharam, P.R.J., Kailasam, S., Ashteker, D.R., and Wise, D.L., 1993, Release of isoniazid for prolonged periods from a biodegradable polymer under several in vitro and simulated in vivo conditions and in animals. *J. Control. Rel.*, **26**, 87-98.

Gangadharam, P.R.J., Kailsam, S., Srinivasan, S., Wise, D.L., 1994, Experimental chemotherapy of tuberculosis using a single dose treatment with isoniazid in biodegradable polymers. *J. Antimicrob. Chemother.*, **33**, 265-271.

Gangrade, N., and Price, J.C., 1992, Simple gas chromatographic headspace analysis of residual organic solvent in microspheres. *J. Pharm Sci.*, **81** (2), 201-202.

Genta, I., Pavanetto, F., Conti, B., and Giunchedi, P., 1991, *In vitro* dissolution of vitamin D_3 loaded polylactide microspheres. *Proceed. Intern. Symp. Control. Rel. Bioact. Mater.*, **18**, 676-677.

Genta, I., Pavanetto, F., Conti, B., Giunchedi, P., and Conte, U., 1994, Spray-drying for the preparation of chitosan microspheres. *Proceed. Intern. Symp. Control. Rel. Bioact. Mater.*, **21**, 616-617.

Gharbo, S.A., Cognion, M.M., and Williamson, M.J., 1989, Modified dissolution method for rifampicin. *Drug. Dev. Ind. Pharm.*, **15**, 331-335.

Gilding, D.K., and Reed, A.M., 1979, Biodegradable polymers for use in surgery – poly(glycolic) / poly(lactic acid) homo- and co-polymers. *Polymer*, **20**, 1459 - 1464.

Giunchedi, P., Maggi, L., Torre, M.L., and Conte, U., 1994a, Spray-dried albumin microspheres containing carbamazepine. *Proceed. Intern. Symp. Control. Rel. Bioact. Mater.*, **21**, 622-623.

Giunchedi, P., Conti, B., Maggi, L., and Conte, U., 1994b, Cellulose acetate butyrate and polycaprolactone for ketoprofen spray-dried microsphere preparation. *J. Microencap.*, **11** (4), 381-393.

Giunchedi, P., and Conte, U., 1995, Spray-drying as a preparation method of microparticulate drug delivery systems: an overview. *S.T.P. Pharma Sciences*, **5** (4), 276-290.

Giunchedi, P., Benvenga, A., Alpar, H.O., and Conte, U., 1995, PDLLA microspheres containing steroids: Spray-drying and w/o/w emulsification as preparation methods. *Proceed. 1st Wld. Meet. Pharm.*, **1**, 389-390.

Giunchedi, P., Alpar, H.O., and Conte, U., 1998, PDLLA microspheres containing steroids: spray-drying, o/w and w/o/w emulsification as preparation methods. *J. Microencap.*, **15**, 185-195.

Gohel, M.C., Patel, M.M., Kaul, J.S., Patel, R.B., Patel, S.R., and Jani, T.R., 1996, An investigation of the synthesis of poly(D,L-lactic acid) and preparation of microspheres containing indomethacin. *Drug. Dev. Ind. Pharm.*, **22** (7), 637-643.

Graham, K.C., 1979, High performance liquid chromatographic analysis of rifampicin and related impurities in pharmaceutical impurities. *J. Liq. Chromatogr.*, **2**, 365-371.

Grandfils, C., Flandroy, P., Nihant, N., Barbette, S., Jérome, R., Teyssié, Ph., and Thibaut, A., 1992, Preparation of poly(D,L)lactide microspheres by emulsion-solvent evaporation, and their clinical applications as a convenient embolic material. *J. Biomed. Mat. Res.*, **26**, 467-479.

Guillaumont, M., Leclercq, M., Frobert, Y., Guise, B., 1982, Determination of rifampicin, desacetylrifampicin, isoniazid and acetylisoniazid by high-performance liquid chromatography: application to human serum extracts, polymorphonucleocytes and alveolar macrophages. *J. Chromatogr.*, **232**, 369-376.

Guiziou, B., Armstrong, D.J., Elliot, P.N.C.E., Ford, J.L., and Rostron C., 1996, Investigations of *in-vitro* release characteristics of NSAID-loaded polylactic microspheres. *J. Microencap.*, **13** (6), 701-708.

Gupta, P.K., and Hung, C.T., 1989, Albumin microspheres I: physico-chemical characteristics. *J. Microencap.*, **6** (4), 427-462.

Gupta, P.K., Johnson, H., and Allexon, C., 1993, In vitro and in vivo evaluation of clarithromycin / poly(lactic acid) microspheres for intramuscular delivery. *J. Control. Rel.*, **26**, 229-238.

Gürkan, H., Yalabik, H.S., Hincal, A.A., and Ercan, M.T., Streptomycin sulphate microspheres: formulation and *in vivo* distribution. *J. Microencap.*, **3** (2), 101-108.

Hald, J.G., 1969, The stability of isoniazid in aqueous solutions containing sucrose or sorbitol. *Dansk. Tidsskr. Farm.*, **43**, 156-59.

Hancock, B.C., and Zografi, G., 1994, The relationship between the glass transition temperature and the water content of amorphous pharmaceutical solids. *Pharm. Res.*, **11** (4), 471-477.

Handbook of Chemistry and Physics, 1966-1967, Weast R.C., and Selby S.M. (Eds) 47th Edition, , The Chemical Rubber Co., Ohio, USA.

Hansch, C., Leo, A., and Hoekman, D., 1995, Exploring QSAR, hydrophobic, electronic and steric constants. American Chemical Society, USA.

Hansen, C.M., 1967, The three dimensional solubility parameter - key to paint component affinities. *J. Paint Technol.*, **39**, 505-514.

Hausberger, A. and DeLuca, P., 1995, Characterization of biodegradable poly(D,L-lactide-co-glycolide) polymers and microspheres. *J. Pharm. Biomed. Anal.*, **13** (6), 747-760.

Hausberger, A.G., Kenley, R.A., and DeLuca, P.P., 1995, Gamma irradiation effects on molecular weight and *in vitro* degradation of poly(D,L-lactide-co-glycolide) microparticles. *Pharm. Res.*, **12** (6), 851-856.

Heller, J., 1980, Controlled release of biologically active compounds from bioerodible polymers. *Biomaterials*, **1**, 51-57.

Herrman, J.B., Kelly, R.J., and Higgins, G.A., 1970, Polyglycolic acid sutures. *Arch. Surg.*, **100**, 486-490.

Heya, T., Okada, H., Tanigawara, Y., Ogawa, Y., and Toguchi, H., 1991, Effects of counteranion of TRH and loading amount on control of TRH release from copoly(d,l-lactic / glycolic) microspheres prepared by an in-water drying method. *Int. J. Pharm.*, **69**, 69-75.

Hora, M.S., Rana, R.K., Nunberg, J.H., Tice, T.R., Gilley, R.M., Hudson, M.E., 1990, Release of human serum albumin from poly(lactide-co-glycolide) microspheres. *Pharm. Res.*, **7** (11), 1190-1194.

Horvath, A.L., 1982, Halogenated hydrocarbons, solubility - miscibility with water. Marcel Dekker Inc., New York

Hsu, Y-Y., Gresser, J., Trantolo, D.J., Lyons, C.M., Gangadharam, P.R.J., and Wise, D.L., 1994, In vitro controlled release of isoniazid from poly(lactide-co-glycolide) matrices. *J. Control. Rel.*, **31**, 223-28.

Hsu, Y-Y., Gresser, J., Stewart, R.R., Trantolo, D.J., Lyons, C.M., Simons, G.A., Gangadharam, P.R.J., and Wise, D.L., 1996, Mechanisms of isoniazid release from poly(*d,l*-lactide-*co*-glycolide) matrices prepared by dry-mixing and low density polymeric foam methods. *J. Pharm. Sci.*, **85** (7), 706-13.

Huebner, R.E., and Castro, K.G., 1995, The changing face of tuberculosis. *Annu. Rev. Med.*, **46**, 47-55.

Hutchings, A., Monie, R.D., Spragg, B., and Routledge, P.A., 1983a, A method to prevent the loss of isoniazid and acetylisoniazid in human plasma. *Br. J. Clin. Pharmacol.*, **15**, 263-66.

Hutchings, A., Monie, R.D., Spragg, B., and Routledge, P.A., 1983b, High-performance liquid chromatographic analysis of isoniazid and acetylisoniazid in biological fluids. *J.Chromatogr.*, **277**, 385-390.

Hutchings, A., Monie, R.D., and Routledge, P.A., 1988, Stability of isoniazid and acetylisoniazid in saliva. *Therapeutic Drug Monitoring*, **10**, 234-36.

Hutchinson, F.G., and Furr, B.J.A., 1990, Biodegradable polymer systems for the sustained release of polypeptides. *J. Control. Rel.*, **13**, 279-294.

Ike, O., Shimizu, Y., Wada, R., Hyon, S.-H., and Ikada, Y, 1992, Controlled cisplatin delivery system using poly(D,L-lactic acid). *Biomaterials.*, **13** (4), 230-234.

Iseri, E., Kas, S., and Hincal, A.A., 1989, Rifampicin microspheres: formulation and in vitro release characteristics. *Chimicaoggi*, **7**, 15-16.

Iseri, E., Ercan, M.T., Kas, H.S., and Hincal, A.A., 1991, The *in vivo* distribution of the ^{99m}Tc-labelled albumin and gelatin microspheres of a tuberculostatic agent, rifampicin.*Boll. Chim. Farm.*, **130**, 66-70.

Iwata, M., and McGinity, J.W., 1992, Preparation of multi-phase microspheres of poly(D,L-lactic acid) and poly(D,L-lactic-co-glycolic acid) containing a W/O emulsion by a multiple emulsion solvent evaporation technique. *J. Microencap.*, **9** (2), 201-214.

Izumikawa, S., Yoshioka, S., Aso, Y., and Takeda, Y., 1991, Preparation of poly(*l*-lactide) microspheres of different crystalline morphology and the effect of crystalline morphology on drug release rate. *J. Control. Rel.*, **15**, 133-140.

Jain, S.R., and Madan, A.K., 1974, Stability of isoniazid in syrupy malt extract. *Indian J. Pharm.*, **36** (5), 113-15.

Jain, C.P., and Vyas, S.P., 1995, Preparation and characterization of niosomes containing rifampicin for lung targeting. *J. Microencap.*, **12** (4), 401-407.

Jalil, R., Nixon, J.R., 1989a, Microencapsulation using poly(L-lactic acid) I: Microcapsule properties affected by the preparative technique. *J. Microencap.*, **6** (4), 473-484.

Jalil, R., 1989b, Ph.D thesis, Kings College, London.

Jalil, R., Nixon, J.R., 1990a, Microencapsulation using poly(L-lactic acid) II: Preparative variables affecting microcapsule properties. *J. Microencap.*, **7** (1), 25-39.

Jalil, R., Nixon, J.R., 1990b, Microencapsulation using poly(L-lactic acid) III: Effect of polymer molecular weight on the microcapsule properties. *J. Microencap.*, **7** (1), 41-52.

Jalil, R., Nixon, J.R., 1990c, Microencapsulation using poly(L-lactic acid) IV: Release properties of microcapsules containing phenobarbitone. *J. Microencap.*, **7** (1), 53-66.

Jalil, R., Nixon, J.R., 1990d, Microencapsulation using poly(DL-lactic acid) I: Effect of preparative variables on the microcapsule characteristics and release kinetics. *J. Microencap.*, **7** (2), 229-244.

Jalil, R., Nixon, J.R., 1990e, Microencapsulation using poly(DL-lactic acid) II: Effect of polymer molecular weight on the microcapsule properties. *J. Microencap.*, **7** (2), 245-252.

Jalil, R., Nixon, J.R., 1990f, Biodegradable poly(lactic acid) and poly(lactide-co-glycolide) microcapsules: problems associated with the preparative techniques and release properties. *J. Microencap.*, **7** (3), 297-325.

Jalil, R., Nixon, J.R., 1990g, Microencapsulation using poly(DL-lactic acid) III: Effect of polymer molecular weight on the release kinetics. *J. Microencap.*, **7** (3), 357-374.

Jalil, R., Nixon, J.R., 1990h, Microencapsulation using poly(DL-lactic acid) IV: Effect of storage on microcapsule characteristics. *J. Microencap.*, **7** (3), 375-383.

Jamshidi, K., Hyon, S.-H., and Ikada, Y., 1988, Thermal charcterization of polylactides. *Polymer*, **29**, 2229-2234.

Jindal, K.C et al, 1994, Dissolution test method for rifampicin-isoniazid fixed dose formulations. *J. Pharm. Biomed. Anal.*, **12** (4), 493-497.

Jindal, K.C., Chaudary, R.S., Singla, A.K., Gangwal, S.S., and Khanna, S. 1995, Effects of buffers and pH on rifampicin stability. *Pharm. Ind.* 57, 420-422.

Joly, V., Encina, G.G., Cohen, M.S., and Thies, C., 1994, Effect of salts on the formation of lactide-glycolide microparticles in aqueous media. *Proceed. Intern. Symp. Control. Rel. Bioact. Mater.*, **21**, 282-283.

Jones, E., Methylene Chloride — An overview of human and environmental effects. *Pharm. Tech. Eur.*, **8** (10), 1996, 30-32.

Juni, K., Ogata, J., Matsui, M., Kubota, M., and Nakano, M., 1985a, Control of release rate of bleomycin from polylactic acid microspheres. *Chem. Pharm. Bull.*, **33**, 1609-1614.

Juni, K., Ogata, J., Matsui, M., Kubota, M., and Nakano, M., 1985b, Modification of the release rate of aclarubicin from polylactic acid microspheres by using additives. *Chem. Pharm. Bull.*, **33**, 1734-1738.

Kader, A., and Jalil, R., 1998a, In vitro release of theophylline from poly(lactic acid) sustained release pellets prepared by direct compression. *Drug Dev. Ind. Pharm.*, **24** (6), 527-534.

Kader, A., and Jalil, R., 1998b, Effect of physicochemical factors on the release kinetics of hydrophilic drugs from poly(L-lactic acid) (L-PLA) pellets. *Drug Dev. Ind. Pharm.*, **24** (6), 535-539.

Kailasam, S., Daneluzzi, D., and Gangadharam, P.R.J., 1994a, Maintenace of therapeutically active levels of isoniazid for prolonged periods in rabbits after a single implant of biodegradable polymer. *Tubercle and Lung Dis.*, **75**, 361-65.

Kailasam, S., Wise, D.L., and Gangadharam, P.R.J., 1994b, Bioavailability of clofazimine *in vivo* for prolonged period following a single implant of a biodegradable polymer. *J. Antimicrob. Chemother.*, **33**, 273-279.

Kalb, B., and Pennings, A.J., 1980, General crystallization behaviour of poly(L-lactic acid). *Polymer*, **21**, 607-611.

Karlson, A.G., and Ulrich, J.A., 1969, Stability of rifampicin in dimethylsulfoxide. *Appl. Microbiol.*, **18**, 692-693.

Kawashima, Y., Matsuda, K., and Takenaka, H., 1972, Physicochemical properties of spray-dried agglomerated particles of salicylic acid and sodium salicylate. *J. Pharm. Pharmacol.*, **24**, 505-512.

Kerc, J., and Srcic, S., 1995, Thermal analysis of glassy pharmaceuticals. *Thermochimica Acta*, **248**, 81-95.

Kilpatrick, G.S., 1987, Compliance in relation to tuberculosis. Suppl. *Tubercle*, **68**, 31-32.

Kissel, T., Brich, Z., Bantle, S., Lancranjan, I., Nimmerfall, F., and Vit, P., 1991, Parenteral depot systems on the basis of biodegradable polyesters. *J. Control. Rel.*, **16**, 27-42.

Krukenberg, C.C., Mischler, P.G., Massad, E.N., Moore, L.A. and Chandler, A.D., 1996, Stability of 1% rifampin suspensions prepared in five syrups. *Am. J. Hosp. Pharm.*, **43**, 2225-2228.

Kulkarni, R.K., Pani, K.C., Neuman, C., and Leonard, F., 1966, Polylactic acid for surgical implants. *Arch. Surg.*, **93**, 839-843.

Kulkarni, R.K., Moore, E.G., Heyelli, A.F., and Leonard, F., 1971, Biodegradable poly(lactic acid) polymers. *J. Biomed. Mater. Res.*, **5**, 169-181.

Lalla, J.K., and Sapna, K., 1993, Biodegradable microspheres of poly(DL-lactic acid) containing piroxicam as a model drug for controlled release via the parenteral route. *J. Microencap.*, **10** (4), 449-460.

Landry, F.B., Bazile, D.V., Splenlehauer, G., Veillard, M., and Kreuter, J., 1997, Release of the fluorescent marker Prodan® from poly(D,L-lactic acid) nanoparticles coated with albumin or polyvinyl alcohol in model digestive fluids (USP XXII). *J. Control. Rel.*, **44**, 227-236.

Langer, R., 1991, Polymer implants for drug delivery to the brain. *J. Control. Rel.*, **16**, 53-60.

Lau, Y.Y., Hanson, G.D., and Carel, B.J., 1996, Determination of rifampin in human plasma by high-performance liquid chromatography with ultraviolet detection. *J. Chromatogr. B*, **676**, 147-152.

Le Corre, P., Estèbe, J.P., Chevanne, F., Mallédant, Y., and Le Verge, R., 1994a, Spinal controlled delivery of bupivicaine from DL-lactic acid oligomers microspheres. *J. Pharm. Sci.*, **84** (1), 75-78.

Le Corre, P., Le Guevello, P., Gajan, V., Chevanne, F., and Le Verge, R., 1994b, Preparation and characterization of bupivicaine-loaded polylactide and polylactide-co-glycolide microspheres. *Int. J. Pharm.*, **107**, 41-49.

Le Corre, P., Rytting, J.H., Gajan, V., Chevanne, F., and Le Verge, R., 1997, *In vitro* controlled release kinetics of local anaesthetics from poly(D,L-lactide) and poly(lactide-co-glycolide) mivrospheres. *J. Microencap.*, **14** (2), 243-255.

Le Ray, A.M., Vert, M., Gautier, J.C., and Benoît, J.P., 1994, Fate of [^{14}C]poly(D,L-lactide-co-glycolide) nanoparticles after intravenous and oral administration to mice. *Int. J. Pharm.*, **106**, 201-211.

Lecaillon, J.B., Febvre, N., Metayer, J.P., and Souppart, C., 1978, Quantitative assay of rifampicin and three metabolites in human plasma, urine and saliva by high-performance liquid chromatography. *J. Chromatogr.*, **145**, 319-324.

Lee, H. K., Park, J.H., and Kwon, K.C., 1997, Double-walled microparticles for single shot vaccine. *J. Control. Rel.*, **44**, 283-293.

Leelarasamee, N., Howard, S.A., Malanga, C.J., Luzzi, L.A., Hogan, T.F., Kandzari, S.J., and Ma, J.K.H., 1986, Kinetics of drug release from polylactic acid-hydrocortisone microcapsules. *J. Microencap.*, **3** (3), 171-179.

Leelarasamee, N., Howard, S.A., and Ma, J.K.H., 1988a, Effect of surface active agents on drug release from polylactic acid-hydrocortisone microcapsules. *J. Microencap.*, **5** (1), 37-46.

Leelarasamee, N., Howard, S.A., Malanga, C.J., and Ma, J.K.H., 1988b, A method for the preparation of polylactic acid microcapsules of controlled particle size and drug loading. *J. Microencap.*, **5** (2), 147-157.

Lemke, T.L., 1995, in Principles of medicinal chemistry (4th edition). Foye W.O., Lemke, T.L., and Williams, D.A. (Eds.), Williams and Wilkins, PA, USA.

Lewin, E., and Hirsch, J.G., 1954, Studies on the stability of isoniazid. *Am. Rev. Tuberc. Pulmon. Dis.*, **71**, 732-742.

Lewis, D.H., Beck, L.R., Forman, T.D., Manek, T.A., and Pope, V., 1988, Reproducibility studies on microencapsulation of steroids in biodegradable polymers. *Proceed. Intern. Symp. Control. Rel. Bioact. Mater.*, **15**, 266-267.

Lewis, D.H., 1990, Controlled release of bioactive agents from lactide/glycolide polymers in *Biodegradable polymers as drug delivery systems*, Chasin M., and Langer R., (eds.), Marcel Dekker, Inc., New York and Basel, 1-42.

Li, S.M., Garreau, H., and Vert, M., 1990, Structure-property relationships in the case of the degradation of massive poly(α-hydroxy acids) in aqueous media. *J. Mater. Sci.*, **1**, 131-139.

Li, Wen-I., Anderson, K.W., Mehta, R.C., and DeLuca, P.P., 1995, Prediction of solvent removal profile and effect on properties for peptide-loaded PLGA microspheres prepared by solvent extraction / evaporation method. *J. Control. Rel.*, **37**, 199-214.

Liedtke, H., 1997, personal communication. Boehringer Ingelheim KG, D-55216, Ingelheim am Rhein.

Lovering, E.G., Matsui, F.F., Curran, N.M., Robertson, D.L., and Sears, R.W., 1983, Hydrazine levels in formulations of hydralazine, isoniazid, and phenelzine over a 2-year period. *J. Pharm Sci.*, **72** (8), 965-67.

Mabuchi, K., Nakayama, A., Hirano, H., and Iwamoto, K., 1995, Study on residual organic solvent and physicochemical characteristics of polylactic acid microspheres containing carmofur. *Jpn. J. Hosp. Pharm.*, **21** (4), 310-318.

Mäder, K., Bacic, G., Domb, A., Langer, R., and Swartz, H.M., 1995, Non-invasive *in vivo* characterization of biodegradable polymers by EPR spectroscopy and NMR imaging. *Proceed. Intern. Symp. Control. Rel. Bioact. Mater.*, **22**, 77-78.

Magee, G.A., Willmott, N., and Halbert, G.W., 1993, Development of a reproduceable *in vitro* method for assessing the biodegradation of protein microspheres. *J. Contol. Rel.*, **25**, 241-248.

Maggi, N., Pasqualucci, C.R., Ballotta, R., and Sensi, P., 1966, Rifampicin: a new orally active rifamycin. *Chemotherapia*, **11**, 285-292.

Maggi, N., Vigevani, A., Gallo, G.G., and Pasqualucci, C.R., 1968, Acetyl migration in rifampicin. *Experementia.*, **11**, 936-939.

Mahato, R.I., Halbert, G.W., Willmott, N., and Whateley, T.L., 1992, Preparation of microspheres for intra-articular administration. *Proceed. Intern. Symp. Control. Rel. Bioact. Mater.*, **19**, 341-342.

Makino, K., Arakawa, M., and Kondo, T., 1985, Preparation and *in vitro* properties of polylactide microcapsules. *Chem. Pharm. Bull.*, **33** (3), 1195-1201.

Makino, K., Ohshima, H., and Kondo, T., 1986a, Transfer of protons from bulk solution to the surface of poly(L-lactide) microcapsules. *J. Microencap.*, **3** (3), 195-202.

Makino, K., Ohshima, H., and Kondo, T., 1986b, Mechanism of hydrolytic degradation of poly(L-lactide) microcapsules: effects of pH, ionic strength and buffer concentration. *J. Microencap.*, **3** (3), 203-212.

Mandal, T.K., Lopez-Anaya, A., Onyebueke, E., and Shekleton, M., 1996, Preparation of biodegradable microcapsules containing zidovudine (AZT) using solvent evaporation technique. *J. Microencap.*, **13** (3), 257-267.

Mandell, G.L., and Sande, M.A., 1985, Antimicrobial agents in *The Pharmacological Basis of Therapeutics*. Gillman G.A., and Goodman L.S. (eds), Macmillan, New York, 1202-1205.

Martin, A., 1993, in *Physical Pharmacy*, Lea & Febiger, Philadelphia, London. 567-568.

Martinez, B., Lairion, F., Pena, M.B., Di Rocco, P., and Nacucchio, M.C., 1997, *In vitro* ciprofloxacin release from poly(lactide-co-glycolide) microspheres. *J. Microencap.*, **14** (2), 155-161.

Masters, K., 1992, Spray drying handbook. 5th Ed. Longman Scientific & Technical, New York.

Mathiowitz, E., Bernstein, H., Giannos, S., Dor, P., Turek, T., and Langer, R., 1992, Polyanhydride microspheres. IV. Morphology and characterization of systems made by spray-drying. *J. Appl. Polym. Sci.*, **45**, 125-134.

Matsui, F.F., McErlane, K.M., Lovering, E.G., and Robertson, D.L., 1978, Thin-later chromatographic procedures for the detection, identification and estimation of hydrazine in isoniazid preparations. *Canadian J. Pharm. Sci.*, **13**, 71-72.

Matsui, F.F., Robertson, D.L., and Lovering, E.G., 1983, Determination of hydrazine in pharmaceuticals III: hydralazine and isoniazid using GLC. *J. Pharm. Sci.*, **72** (8), 948-951.

Mauduit, J., Bukh, N., and Vert, M., 1993a, Gentamycin / poly (lactic acid) blends aimed at sustained release local antibiotic therapy administered per-operatively. I. The case of gentamycin base and gentamycin sulfate in poly(DL-lactic acid) oligomers. *J. Control. Rel.*, **23**, 209-220.

Mauduit, J., Bukh, N., and Vert, M., 1993b, Gentamycin / poly (lactic acid) blends aimed at sustained release local antibiotic therapy administered per-operatively. II. The case of gentamycin sulfate in high molecular weight poly(DL-lactic acid) and poly(L-lactic acid). *J. Control. Rel.*, **23**, 221-230.

Mauduit, J., Bukh, N., and Vert, M., 1993c, Gentamycin / poly (lactic acid) blends aimed at sustained release local antibiotic therapy administered per-operatively. II. The case of gentamycin sulfate in films prepared from high and low molecular weight poly(DL-lactic acids). *J. Control. Rel.*, **25**, 43-49.

Maulding, H.V., Tice, T.R., Cowsar, D.R., Fong, J.W., Pearson, J.E., and Nazareno, J.P., 1986, Biodegradable microcapsules: Acceleration of polymeric excipient hydrolytic rate by incorporation of a basic medicament. *J. Control. Rel.*, **3**, 103-117.

Maulding, H.V., 1987, Prolonged delivery of peptides by microcapsules. *J. Control. Rel.*, **6**, 167-176.

Medfile, 1993, Drug-resistant tuberculosis. **7** (11), 85-88.

Mehta, R.C., Thanoo, B.C., and DeLuca, P.P., 1996, Peptide containing microspheres from low molecular weight and hydrophilic poly(*d,l* -lactide-co-glycolide). *J. Control. Rel.*, **41**, 249-257.

Menegatti, E., Esposito, E., Cortesi, R., and Nastruzzi, C., 1995, Production of biodegradabel microspheres for sustained delivery of tetracyclines to the periodontal pocket: formulatory and drug release studies. *Proceed. Intem. Symp. Control. Rel. Bioact. Mater.*, **22**, 794-795.

Merck Index, 1976, Ed. M Windholz, Merck & Co., Inc., USA, 1047.

Miller, R.A., Brady, J.M., and Cutright, D.E., 1977, Degradation rates of oral resorbable implants (polylactates and polyglycolates): rate modification with changes in PLA/PGA copolymer ratios. *J. Biomed. Mater. Res.*, **11**, 711-719.

Moore, J.W., and Pearson, R.G., 1981, in *Kinetics and mechanisms*, 3rd Edn, Wiley, New York, 304-307.

Nahata, M.C., Morosco, R.S., and Hipple, T.F., 1994, Effect of preparation method and storage on rifampicin concentration in suspensions. *J. Clin. Pharm. Therap.*, **28**, 182-184.

Nakhare, S., and Vyas, S.P., 1995a, Prolonged release multiple emulsion based system bearing rifampicin: *in vitro* characterization. *Drug Dev. Ind. Pharm.*, **21** (7), 869-878.

Nakhare, S., and Vyas, S.P., 1995b, Prolonged release of rifampicin from multiple w/o/w emulsion systems. *J. Microencap.*, **12** (4), 409-415.

Nozawa, I., Suzuki, Y., Sato, S., Juni, K., Sugibayashi K., and Morimoto, Y., 1991, Preparation and evaluation of biodegradable thermoresponsive microspheres. *J. Control. Rel.*, **17**, 33-40.

Oldfield, S., Berg, J.D., Stiles, H.J., and Buckley, B.M., 1986, Measurement of rifampicin and desacetylrifampicin in biological fluids using high-performance liquid chromatography with direct sample injection. *J. Chromatog.*, **377**, 423-429.

Omelczuk, M.O., and McGinity, J.W., 1992, The influence of polymer glass transition temperature and molecular weight on drug release from tablets containing poly(D,L-lactic acid). *Pharm. Res.*, **9** (1), 26-32.

Owusu-Ababio, G., and Rogers, J.A., 1996, Formulation and release kinetics of cephalexin monohydrate from biodegradable polymeric microspheres. *J. Microencap.*, **13** (2), 195-205.

Pande, S., Vyas, S.P., and Dixit, V.K., 1991, Localized rifampicin albumin microspheres. *J. Microencap.*, **8** (1), 87-93.

Park, T.G., Cohen, S., and Langer, R., 1991, Protein release from poly(L-lactic acid)/Pluronic™ blends. *Proceed. Intem. Symp. Control. Rel. Bioact. Mater.*, **18**, 674-675.

Park, T.G., 1994, Degradation of poly(D,L-lactic acid) microspheres: effect of molecular weight. *J. Control. Rel.*, **30**, 161-173.

Pavanetto, F., Conti, B., Genta, I., and Giunchedi, P., 1992, Solvent evaporation, solvent extraction and spray drying for polylactide microsphere preparation. *Int. J. Pharm.*, **84**, 151-159.

Pavanetto, F., Genta, I., Giunchedi, P., and Conti, B., 1993, Evaluation of spray drying as a method for polylactide and polylactide-co-glycolide microsphere preparation. *J. Microencap.*, **10** (4), 487-497.

Pavanetto, F., Conti, B., Giunchedi, P., Genta, I., and Conte, U., 1994a, Polylactide microspheres for the controlled release of diazepam. *Eur. J. Pharm. Biopharm.*, **40** (1), 27-31.

Pavanetto, F., Genta, I., Giunchedi, P., Conti, B., and Conte, U., 1994b, Spray-dried albumin microspheres for the intra-articular delivery of dexamethasone. *J. Microencap.*, **11**, 445-454.

Pawelczyk, E., Hermann, T., and Sukowski, R., 1969, Kinetics of drug decomposition. Part V. Kinetics of acid-catalysed solvolysis of isoniazid. *Dissert. Pharm. Pharmacol.*, **21**, 481-488.

Peterlin, A., 1972, Morphology and properties of crystalline polymers with fiber structure. *Text. Res. J.*, **42**, 20-30.

Phillips, M., and Gresser, J.D., 1984, Sustained-release characteristics of a new implantable formulation of disulfiram. *J. Pharm. Sci.*, **73** (12), 1718-1720.

Pistner, H., Gutwald, R., Ordung, R., and Reuther, J., 1993, Poly(L-lactide): a long-term degradation study *in vivo*. *Biomaterials*, **14** (9), 671-677.

Pitt, C.G., Jeffcoat, A.R., Zweidinger, R.A., and Schindler, A., 1979, Sustained drug delivery systems. I. The permeability of poly(ε-caprolactone), poly(D,L-lactic acid), and their copolymers. *J. Biomed. Mater. Res.*, **13**, 497-507.

Polard, E., Le Corre, P., Chevanne, F., and Le Verge, R., 1996, *In vitro* and *in vivo* evaluation of polylactide-co-glycolide microspheres of morphine and site-specific delivery. *Int. J. Pharm.*, **134**, 37-46.

Prankerd, R.J., and Stella, V.J., 1989, Equilibria and kinetics of hydrolysis of Ebifuramin(NSC-201047), an azomethine containing structure exhibiting a reversible degradation step in acidic solutions. *Int. J. Pharm.*, **52**, 71-78.

Prankerd, R.J., Walters, J.M., and Parnes, J.H., 1992, Kinetics for degradation of rifampicin, an azomethine-containing drug which exhibits reversible hydrolysis in acidic solution. *Int. J. Pharm.*, **78**, 56-67.

Przyborowski, M., Lachnik, E., Wiza, J., and Licinska, I., 1982, Preparation of HSA microspheres in a one-step thermal denaturation of protein aerosol carried in gas-medium. *Eur. J. Nucl. Med.*, **7**, 71-72

Rafler, G., and Jobmann, M., 1994, Controlled release systems of biodegradable polymers, 2nd communication: Microparticle preparation by spray drying. *Drugs made in Germany*, **37** (4), 115-119.

Rak, J., Ford, J.L., Rostron, C., and Walters, V., 1985, The preparation and characterization of poly(D,L-lactic acid) for use as a biodegradable drug carrier. *Pharm. Acta. Helv.*, **60**, 162-169.

Ramtoola, Z., Corrigan, O.I., and Bourke, E., 1991, Characterization of biodegradable microspheres containing dehydro-iso-androsterone. *Drug Dev. Ind. Pharm.*, **17** (13), 1857-1873.

Ramtoola, Z., Corrigan, O.I., and Barrett, C.J., 1992, Release kinetics of fluphenazine from biodegradable microspheres. *J. Microencap.*, **9** (4), 415-423.

Rao, K.V.N., Kailasam, S., Menon, N.K., and Radhakrishna, S., 1971, Inactivation of isoniazid by condensation in a syrup preparation. *Wld. Hlth. Org.*, **45**, 625-632.

Ratcliffe, J.H., Hunneyball, I.M., Smith, A., Wison, C.G., and Davis, S.S., 1984, Preparation and evaluation of biodegradable polymeric systems for the intra-articular delivery of drugs. *J. Pharm. Pharmacol.*, **36**, 431-436.

Ratti, B., Rosina Parenti, R., Toselli, A., Zerilli, L.F., 1981, Quantitative assay of rifampicin and its main metabolite 25-desacetylrifampicin in human plasma by reversed-phase high-performance liquid chromatography. *J. Chromatogr.*, **225**, 526-531.

Reed, A.M., and Gilding, D.K., 1981, Biodegradable polymers for use in surgery – poly(glycolic)/poly(lactic acid) homo and copolymers: 2. *In vitro* degradation. *Polymer*, **22**, 494-498.

Reich, G., and Bernickel, E., 1998, Investigation of mechanisms governing the degradation kinetics of films prepared from blends of high and low molecular weight PLA/PLGA. *Proc. 2nd World Meeting APGI / APV*, Paris, 373-374.

Rekker & Nauta, 1964, protonation constants of INH (p22, chap3)

Richey, T., and Harris, F.W., 1995, Characterization of indomethacin-loaded microspheres. *Proceed. Intern. Symp. Control. Rel. Bioact. Mater.*, **22**, 416-417.

Rothen-Weinhold, A., Besseghir, K., and Gurny, R., 1997, Analysis of the influence of polymer characteristics and core loading on the in vivo release of a somatostatin anologue. *Eur. J. Pharm. Sci.*, **5**, 303-313.

Ruchatz, F., Thies, J., and Müller, B.W., 1995, Investigation of residual methylene chloride in microparticles produced by means of the ASES process. *1st World Meeting APGI / APV*, 447-448.

Ruchatz, F., Kleinebudde, P., and Müller, B.W. 1996, Residual solvents in biodegradable microparticles. Influence of process parameters on the residual solvent in microparticles produced by the aerosol solvent extraction system (ASES) process. *J. Pharm. Sci.*, **86** (1), 101-105.

Ruiz, J.M., Tissier, B., and Benoît, J.P., 1989, Microencapsulation of peptide: a study of the phase separation of poly(D,L-lactic acid-co-glycolic acid) copolymers 50/50 by silicone oil. *Int. J. Pharm.*, **49**, 69-77.

Sah, H., Smith, M.S., and Chern, R.T., 1995, The use of methyl ethyl ketone as a solvent for the preparation of PLGA microcapsules. *Proceed. Intern. Symp. Control. Rel. Bioact. Mater.*, **22**, 408-409.

Sam, A.P., de Haan, F., and Dirix, C., 1994, A novel process for manufacturing PLG microparticles by spray desolvation avoiding the use of toxic solvents. *Proceed. Intern. Symp. Contol. Rel. Bioact. Mater.*, **21**, 198-199.

Sánchez, A., Vila-Jato, J.L., Alonso, M.J., 1993, Development of biodegradable microspheres and nanospheres for the controlled release of cyclosporin A. *Int. J. Pharm.*, **99**, 263-273.

Sanders, L.M., McRae, G.I., Vitale, K.M., and Kell, B.A., 1985, Controlled delivery of an LHRH analogue from biodegradable injectable microspheres. *J. Control. Rel.*, **2**, 187-195.

Sansdrap, P., and Moës, A.J., 1993, Influence of manufacturing parameters on the size characteristics and the release profiles of nifedipine from poly(D,L-lactide-co-glycolide) microspheres. *Int. J. Pharm.*, **98**, 157-164.

Sansdrap, P., and Moës, A.J., 1997, In vitro evaluation of the hydrolytic degradation of dispersed and aggregated poly(D,L-lactide-co-glycolide) microspheres. *J. Control. Rel.*, **43**, 47-58.

Sansdrap, P., and Moës, A.J., 1998, Influence of additives on the release profiles of nifedipine from poly(D,L-lactide-co-glycolide) microspheres. *J. Microencap.*, **15** (5), 545-553.

Sato, T., Kanke, M., Schroeder, H.G., and DeLuca, P., 1988, Porous biodegradable microspheres for controlled drug delivery. I: Assessment of processing conditions and solvent removal technique. *Pharm. Res.*, **5**, 21-30.

Sawert, H., 1996, The re-emergence of tuberculosis and its economic implications. *Pharmacoeconomics*, **9** (5), 379-381.

Schellhorn, M., and Buchholz, B., 1996, Hydrolytic degradation of amorphous resorbable polymers. A study of the temperature dependency. *Proceed. Intern. Symp. Control. Rel. Bioact. Mater.*, **23**, 226-227.

Schindler, A., Jeffcoat, R., Kimmel, G.L., Pitt, C.G., Wall, M.E., and Zweidinger, R., 1977, Biodegradable polymers for sustained drug delivery in *Contemporary Topics in Polymer Science*, Pearce E.M., and Schaefgen J.R. (Eds.), Plenum Press, New York, 251-286.

Schwope, A.D., Wise, D.L., and Howes, J.F., 1975, Lactic/glycolic acid polymers as narcotic antagonist delivery system. *Life Sci.*, **17**, 1877-1886.

Scmitt, E.A., Flanagan, D.R., and Lindhardt, R.J., 1993, Degradation and release properties of pellets fabricated from three commercial poly(D,L-lactide-co-glycolide) biodegradable polymers. *J. Pharm. Sci.*, **82** (3), 326-329.

Seimann, U., 1985, The influence of water on the glass transition of poly(d,l-lactic acid). *Thermochim. Acta*, **85**, 513-516.

Sepkowitz, K.A., 1995, AIDS, tuberculosis, and the health care worker. *Clin. Infect. Dis.*, **20**, 232-242.

Serajuddin, T.M., Rosoff, M., and Mufson, D., 1986, Effect of thermal history on the glassy state of indapamide. *J. Pharm. Pharmacol.*, **38**, 219-220.

Seydel, J.K., 1970, Physico-chemical studies of rifampicin. *Antibiot. Chemotherapia*, **16**, 380-391.

Shah, S.S., Cha, Y., and Pitt, C.G., 1992, Poly(glycolic acid-co-D,L-lactic acid): diffusion or degradation controlled drug delivery. *J. Control. Rel.*, **18**, 261-270.

Shah, Y., Khanna, S., Jindal, K.C., and Dighe, V.S., 1992, Determination of rifampicin and isoniazid in pharmaceutical formulations by HPLC. *Drug Dev. Ind. Pharm.*, **18** (14), 1589-1596.

Shearer, B.G., 1994, MDR-TB, another challenge from the microbial world. *JADA*, **125**, 43-49.

Shimao, T., 1987, Drug resistance in tuberculosis control. Suppl. *Tubercle*, **68**, 31-32.

Shively, M.L., Coonts, B.A., Renner, W.D., Southard, J.L., and Bennet, A.T., 1995, Physico-chemical characterization of a polymeric injectable implant delivery system. *Int. J. Pharm.*, **33**, 237-243.

Singh, M., Li, X.-M., Qiu, H., Zamb, T., Wang, C.Y., and O'Hagan, D., 1996, Residual polyvinyl alcohol content in polylactide-co-glycolide microparticles prepared by the solvent evaporation process. *Proceed. Intern. Symp. Control. Rel. Bioact. Mater.*, **23**, 367-368.

Smith, A., and Hunneyball, I.M., 1986, Evaluation of poly(lactic acid) as a biodegradable drug delivery system for parenteral administration. *Int. J. Pharm.*, **30**, 215-220.

Speiser, P., and Hijnsbroek, R., 1979, Micropellets in a biodegradable carrier. German patent. 2 824 112. 6 Dec., *Chem. Abst.*, **92** : 135447w.

Splenlehauer, G., Veillard, M., and Benoît, J.P., 1986a, Formation and characterization of cisplatin loaded poly(*d,l*-lactide) microspheres for chemoembolization. *J. Pharm. Sci.*, **75** (8), 750-755.

Splenlehauer, G., Vert, M., Benoît, J.-P., Chabot, F., and Veillard, M., 1988, Biodegradable cisplatin microspheres prepared by the solvent evaporation method: morphology and release characteristics. *J. Control. Rel.*, **7**, 217-229.

Splenlehauer, G., Vert, M., Benoît, J.P., and Boddaert, A., 1989, *In vitro* and *in vivo* degradation of poly(D,L)lactide/glycolide type microspheres made by solvent evaporation method. *Biomaterials*, **10**, 557-563.

Suzuki, K., and Price, K.C., 1985, Microencapsulation and dissolution properties of neuroleptic in a biodegradable polymer, poly(d,l-lactide). *J. Pharm. Sci.*, **74** (1), 21-24.

Stevens, M.P., 1990, in *Polymer chemistry: an introduction*. 2nd edition, Oxford University Press, New York, 46.

Tabata, Y., and Ikada, Y., 1988, Macrophage phagocytosis of biodegradable microspheres composed of L-lactic acid/glycolic acid homo- and copolymers. *J. Biomed. Mater. Res.*, **22**, 837-858.

Takada, S., Uda, Y., Toguchi, H., and Ogawa, Y., 1995, Preparation and characterization of copoly(d,l-lactic/glycolic acid) microparticles for sustained release of thyrotrophin releasing hormone by double nozzle spray-drying method. *J. Contol. Rel.*, **32**, 79-85.

Takada, S., Kurokawa, T., Miyazaki, K., Iwasa, S., and Ogawa, Y., 1997, Sustained release of a water-soluble GP IIb/IIIa antagonist from copoly(D,L-lactic/glycolic)acid microspheres. *Int. J. Pharm.*, **146**, 147-157.

Taylor, R.B., Reid, R., and Hung, C.T., 1984, Selectivity effects between ionic and neutral solutes using hydrophobic pairing ions.*J. Chromatogr.*, **316**, 279-285.

Taylor, R.B., Richards, R.M.E., Low, A.S., and Hardie, L., 1994, Chemical stability of polymyxin in aqueous solution. *Int. J. Pharm.*, **102**, 201-206.

Taylor, R.B., personal communication, 1995, School of Pharmacy, The Robert Gordon University, Aberdeen, AB10 1FR.

Theeuwes et al., 1974

Thoma, K., and Schlütermann, B., 1992, Beziehungen zwischen herstellungsparametern und pharmazeutisch-technologischen anforderungen an biodegradierbare mikoropartiken. *Die Pharmazie*, **47**, 115-119.

Tice, T.R., and Cowsar, D.R., 1984, Biodegradable controlled-release parenteral systems. *Pharm Tech.*, November, 26-36.

Tsai, D.C., Howard, S.A., Hogan, S.A., Malanga, C.J., Klandzari, C.J., and Ma, J.K.H., 1986, Preparation and *in vitro* evaluation of of poly(lactic acid)/mitomycin-C microcapsules. *J. Microencap.*, **3** (3), 181-193.

Tuberculosis Chemotherapy Centre, Madras, 1970, A controlled comparison of twice-weekly and three once-weekly regimens in the initial treatment of pulmonary tuberculosis. *Bull. Wld. Hlth. Org.*, **43**, 143-206.

Vaughen, W.M., Duong, H.N., Blackman, K.P., Wood, B.A., Setterstrom, J.A., and van Hamont, J.E., 1996, Formulation of lidocaine-PLGA microspheres for the treatment of dental pain. *Proceed. Inter. Symp. Control. Rel. Bioact. Mater.*, **23**, 375-376.

Verrecchia, T., Huve, P., Bazile, D., Veillard, M., Splenlehauer, G., and Couvreur, P., 1993, Adsorption / desorption of human serum albumin at the surface of poly(lactic acid) nanoparticles prepared by a solvent evaporation process. *J. Biomed. Mater. Res.*, **27**, 1019-1028.

Vert, M., Li, S., and Garreau, H., 1991, More about the degradation of LA/GA-derived matrices in aqueous media. *J. Control. Rel.*, **16**, 305-311.

Vert, M., Li, S.M., Splenlehauer, G., Guerin, P., 1992, Bioresorbability and biocompatability of aliphatic polyesters. *J. Mat. Sci. Med.*, **3**, 432-446.

Vidmar, V., Smolcic-Bubalo, A., and Jalsenjak, I., 1984, Poly(lactic acid) microencapsulated oxytetracycline: *in vitro* and *in vivo* evaluation. *J. Microencap.*, **1** (2), 131-136.

Vidmar, V., Pepeljnjak, S., and Jalsenjak, I., 1985, The *in vivo* evaluation of poly(lactic acid) microcapsules of pilocarpine hydrochloride. *J. Microencap.*, **2** (4), 289-292.

Visscher, G.E., Pearson, J.E., Fong, J.W., Argentieri, G.J., Robison, R.L., and Maulding, H.V., 1988, Effect of particle size on the *in vitro* and *in vivo* degradation rates of poly(D,L-lactide-co-glycolide) microcapsules. *J. Biomed. Mater. Res.*, **22**, 733-746.

Volland, C., Wolff, M., and Kissel, T., 1994, The influence of gamma-sterilization on captopril containing poly(D,L-lactide-co-glycolide) microspheres. *J. Control. Rel.*, **31**, 293-305.

Wada, R., Tabata, Y., Hyon, S.-H., and Ikada, Y., 1988, Preparation of poly(lactic acid) microspheres containing anti-cancer drugs. *Bull. Inst. Chem. Res.*, **66** (3), 241-250.

Wagenaar, B.W., and Müller, B.W., 1994, Piroxicam release from spray-dried biodegradable microspheres. *Biomaterials*, **15** (1), 49-54.

Wakiyama, N., Juni, K., and Nakano, M., 1981, Preparation and in vitro evaluation of polylactic acid microspheres containing local anesthetics. *Chem. Pharm. Bull.*, **29** (11), 3363-3368.

Wakiyama, N., Juni, K., and Nakano, M., 1982a, Influence of physicochemical properties of polylactic acid on the characteristics and *in vitro* release patterns of polylactic acid microspheres containing local anesthetics. *Chem. Pharm. Bull.*, **30** (7), 2621-2628.

Wakiyama, N., Juni, K., and Nakano, M., 1982b, Preparation and evaluation *in vitro* and *in vivo* of polylactic acid microspheres containing dibucaine. *Chem. Pharm. Bull.*, **30** (10), 3719-3727.

Wang, H.T., Palmer, H., Linhardt, R.J., Flanagan, D.R., and Schmitt, E., 1990, Degradation of poly(ester) microspheres. *Biomaterials*, **11**, 679-685.

Watts, P.J., Davies, M.C., and Melia, C.D., 1990, Microencapsulation using emulsification/solvent evaporation: an overview of techniques and applications. *Crit. Rev. Ther. Drug Carrier Syst.*, **7** (3), 235-259.

Waxman, S., Gang, M., and Goldfrank, L., 1995, Tuberculosis in the HIV-infected patient. *Emerg. Med. Clin. North. America.*, **13** (1), 179-198.

Weis, S.E., Slocum, P.C., Blais, F.X., King, B., Nunn, M., Matney, B., Gomez, E., and Foresman, B.H., 1994, The effect of directly-observed therapy on the rates of drug resistance and relapse in tuberculosis. *New Eng. J. Med.*, **330** (17), 1179-1184.

Wells, J.I., 1988, in *Preformulation: the physicochemical properties of drug substances.* Ellis Horwood, Chichester, England.

Whateley, T.L., 1992, Biodegradable Microspheres for Controlled Drug Delivery in *Encapsulation and Controlled Release*, Karsa D.R., and Stephenson R.A. (eds.), Royal Society of Chemistry, Cambridge, 52-65.

Wichert, B., and Rohdewald, P., 1990, A new method for the preparation of drug containing polylactic acid microparticles without using organic solvents. *J. Control. Rel.*, **14**, 269-283.

Williams, D.F., and Mort, E., 1977, Enzyme-accelerated hydrolysis of polyglycolic acid. *J. Bioeng.*, **1**, 231-238.

Wise, D.L., McGormick, G.J., Willet, G.P., and Anderson, L.C., 1976, Sustained release of an antimalarial drug using a copolymer of glycolic/lactic acid. *Life Sci.*, **19**, 867-874.

Wise, D.L., McCormick, G.J., Willet, G.P., Anderson, L.C., and Howes, J.F., 1978, Sustained release of sulphadiazine. *J. Pharm. Pharmacol.*, **30**, 686-689.

Witschi, C., and Doelker, E., 1998, Influence of microencapsulation method and peptide loading on poly(lactic-co-glycolic acid) degradation during in vitro testing. *J. Control. Rel.*, **51**, 327-341.

Woo, J., Wong, C.L., Teoh, R., and Chan, K., 1987, Liquid chromatographic assay for the simultaneous determination of pyrazinamide and rifampicin in serum samples from patients with tuberculosis meningitis. *J. Chromatogr.*, **420**, 73-80.

Wood, D.A., 1980, Biodegradable drug delivery systems. *Int. J. Pharm.*, **7**, 1-18.

World Health Organization (WHO), 1995, WHO urges making directly-observed treatment the priority in global tuberculosis control, press report (WHO/22), March 20.

World Health Organization (WHO), 1996, TB deaths reach historic levels, press report (WHO/23), March 21.

Wu, X.S., 1995, in *Encyclopaedic Handbook of Biomaterials and Bioengineering* (Ed.) Wise, D.L., Marcel Dekker, Inc., New York, 1015-1054.

Yamaguchi, K., and Anderson, J.M., 1993, In vivo biocompatibility studies of medisorb 65/35 D,L-lactide/glycolide copolymer microspheres. *J. Control. Rel.*, **24**, 81-93.

Yolles, S., Leafe, T., Woodland, J.H.R., and Meyer, F.J., 1975, Long acting delivery systems for narcotic antagonists. II. Release rates of naltrexone from poly(lactic acid) composites. *J. Pharm. Sci.*, **64** (2), 348-349.

Yu, W.P., Wong, J.P., and Chang, T.M.S., 1998, Preparation of polylactic acid microcapsules containing ciprofloxacin. *J. Microencap.*, **15** (4), 515-523.

Zhifang, Z., Mingxing, Z., Shenghao, W., Fang, L., and Wenzhao, S., 1993, Preparation and evaluation in vitro and in vivo of copoly(lactic/glycolic) acid microspheres containing norethisterone. *Biomat. Art. Cells Immob. Biotech.*, **21** (1), 71-84.

Zhou, M., and Chang, T.M.S., 1988, Control release of prostaglandin E_2 from polylactic acid microcapsules, microparticles and modified microparticles. *J. Microencap.*, **5** (1), 27-36.

Appendix 1. *Details of materials used in experimental procedures*

Material	*Supplier*	*Grade*	*Comment*
rifampicin (RIF)	Lepetit, Milan, Italy	ethical	*syn.* 3-(4-methylpiperazin-1-ylimino-methyl)rifamycin
3-formyl rifamycin SV (RSV)	Ciba-Geigy, Basel, Switzerland	analytical	degradate of rifampicin
rifampicin quinone (RQU)	Merrel Dow, Middlesex, UK	analytical	degradate of rifampicin
25-desacetylrifampicin (DAR)		analytical	degradate of rifampicin
25-desacetyl-23-acetyl rifampicin (25-23)		analytical	degradate of rifampicin
25-desacety-21-acetyl lrifampicin (25-21)		analytical	degradate of rifampicin
isoniazid (INH)	Sigma, St Louis, USA	> 99 %	*syn.* isonicotinic acid hydrazide
iso-nicotinic acid N-oxide (INN)		> 99 %	degradate of isoniazid
iso-nicotinic acid (INA)		> 99 %	degradate of isoniazid
iso-nicotinamide (IAD)		> 99 %	degradate of isoniazid
sodium dihydrogen orthophosphate	Fisher Scientific UK Ltd., Loughborough, UK	S.L.R.	buffer salt
disodium hydrogen phosphate		S.L.R.	buffer salt
sodium acetate	Sigma	S.L.R.	buffer salt
sodium chloride	Fisher Scientific	S.L.R.	tonicity modifier
citric acid	Sigma	S.L.R.	buffer salt
potassium chloride	FSA Laboratory Supplies, Loughborough, UK	Analar	
acetic acid	Sigma	S.L.R.	buffer salt
sodium metabisulphite	Sigma	S.L.R	antioxidant
sodium sulphite		S.L.R.	antioxidant
iso-ascorbic acid (IAA)		S.L.R	antioxidant
methanol	Rathburn, Walkerburn, Scotland	HPLC	
dichloromethane		HPLC	
acetonitrile		HPLC	
chloroform		HPLC	
orthophosphoric acid	Sigma	S.L.R	buffering acid
double distilled water	in-house	HPLC	further purified by a Millipore Milli-Q system (Milford, MA, USA)

Material	*Supplier*	*Grade*	*Comment*
halothane	Sigma		stabilized by 0.01% thymol (*syn.* 2-bromo-2-chloro-1,1,1-trifluorethane)
methanol	Fisher Scientific		
ethanol			
butanol			
acetone			
n-hexane			
ethyl acetate			
Polyvinylalcohol	Sigma		cold-water soluble, 30 - 70 kD
albumin			minimum 98 % (fraction V)
casein sodium			water-soluble
Resomer®			
L204	Boehringer Ingelheim, Ingelheim, Germany		poly-L-lactide, 78 kD
R104			poly-D,L-lactic acid, 2 kD
R202H			poly-D,L-lactide, 11 kD
RG502			poly-D,L-lactide-co-glycolide (50:50) , 15.5 kD
RG502H			poly-D,L-lactide-co-glycolide (50:50) , 8 kD
RG503			poly-D,L-lactide-co-glycolide (50:50) , 39 kD
RG503H			poly-D,L-lactide-co-glycolide (50:50) , 33.5 kD
RG504			poly-D,L-lactide-co-glycolide (50:50) , 56.5 kD
RG506			poly-D,L-lactide-co-glycolide (50:50) , 68 kD
RG752			poly-D,L-lactide-co-glycolide (75:25) , 20 kD
RG755			poly-D,L-lactide-co-glycolide (75:25) , 63 kD

Appendix 2. *DSC data of selected samples prepared with R104:R202H, 44:66[*] (#16-21) and 40:60 (#22-27) at various drug loadings*

		Transition					
Batch	**RIF / %w/w**	**Tg(on) / °C**	**$^1/_2$ Cp / °C**	**ΔCp / Jg^{-1} * °C**	**Onset / °C**	**Peak / °C**	**ΔH / Jg^{-1}**
16[*]	1	35.17	37.78	0.28	39.56	43.17	7.23
17[*]	3	37.69	41.07	0.41	42.77	45.56	7.24
18[*]	5	37.45	42.05	0.52	43.68	46.23	7.08
19[*]	10	38.10	42.82	0.42	43.76	47.50	3.47
20[*]	20	42.28	45.25	0.32	47.98	50.59	3.93
21[*]	50	47.28	49.32	0.16	50.09	53.38	0.68
22	1	36.92	39.78	0.39	40.78	43.95	6.42
23	3	39.46	41.08	0.18	43.46	46.32	6.30
24	5	40.10	42.30	0.26	45.25	47.94	6.06
25	10	42.22	44.76	0.35	47.89	50.34	4.91
26	20	43.72	47.97	0.43	50.14	52.94	3.56
27	50	46.08	50.38	0.23	49.80	53.29	0.44

onset, peak and area refer to the anomalous endotherm recorded during the first run

T_g(on) - glass transition temperature onset

Appendix 3. *DSC data of microsphere annealed at 37 °C for various times*

Batch	RIF / %w/w total	R104 / %w/w	Transition						
			Tg(the) / °C	Tg(on) / °C	$^1/_2$ Cp / °C	ΔCp / Jg^{-1} •°C	Onset / °C	Peak / °C	ΔH / Jg^{-1}
16	1	1	37.25	37.63	38.26	0.16	35.88	40.38	1.63
		2					36.32	40.57	1.59
		4					26.59	40.82	1.67
17	3	1					37.60	42.13	1.82
		2					37.72	42.45	1.80
		4					39.22	43.65	2.23
18	5	1					39.47	44.35	2.68
		2					40.18	44.53	2.37
		4					40.08	44.51	2.38
19	10	1	42.74	42.11	44.54	0.32	46.47	49.96	4.84
		2	42.92	41.99	44.42	0.28	46.06	49.63	4.46
		4	42.37	41.46	43.37	0.32	45.23	48.95	3.92
20	20	1	44.53	43.08	46.83	0.41	50.57	53.32	4.64
		2	44.49	48.42	46.65	0.36	50.56	53.31	4.58
		4	44.61	42.80	46.93	0.39	50.48	53.31	4.53
21	50	1	47.51	44.24	49.25	0.16	52.05	54.72	1.23
		2	47.52	44.32	50.89	0.18	52.59	54.96	1.30
		4	47.99	44.83	51.28	0.17	55.89	56.25	1.48
22	1	1					36.25	40.90	1.62
		2					36.19	40.57	1.51
		4					37.02	41.02	1.70
23	3	1					39.01	43.66	2.15
		2					37.90	42.63	1.96
		4					38.91	43.32	1.97
24	5	1	40.29	39.99	41.95	0.24	41.30	45.89	2.90
		2	40.48	40.18	41.92	0.21	40.41	45.73	2.74
		4	40.71	40.21	42.22	0.23	41.46	45.76	2.70
25	10	1	43.11	41.43	44.70	0.36	47.11	50.28	4.64
		2	43.77	42.34	45.07	0.35	47.01	50.45	4.59
		4	43.63	42.57	45.29	0.33	47.08	50.64	4.58
26	20	1	45.94	43.50	48.34	0.43	51.36	54.17	4.28
		2	46.46	45.03	48.73	0.38	51.63	54.35	4.51
		4	46.43	44.14	48.53	0.41	51.87	54.67	4.79
27	50	1	48.94	45.68	51.20	0.19	53.23	56.19	1.10
		2	48.98	44.34	50.59	0.19	53.73	56.53	1.20
		4	49.49	46.07	51.35	0.17	55.23	57.88	1.54

T_g(the) - glass transition temperature theoretical onset where thermal curve leaves the pre-transition baseline

Appendix 4. *DSC data of recovered microsphere residue from release studies performed at various temperatures*

Batch	Medium / °C	Transition						ΔH / Jg^{-1}
		Tg(the) / °C	Tg(on) / °C	$^1/_2$ Cp / °C	ΔCp / $Jg^{-1} * °C$	Onset / °C	Peak / °C	
32	33	46.23	48.94	51.72	0.40	53.13	55.79	2.71
	35	41.69	44.36	48.14	0.44	51.55	55.53	1.61
	37	38.08	40.76	43.43	0.38	45.27	50.08	1.13
	39	39.00	36.27	42.03	0.39	43.99	49.75	0.50
31	33	44.69	47.91	51.09	0.44	53.38	56.63	2.99
	35	40.13	42.21	46.59	0.48	51.06	53.86	1.32
	37	36.92	39.04	41.56	0.33	45.44	49.32	1.18
	39	36.71	34.64	39.84	0.37	41.99	47.81	1.02
30	33	44.93	48.68	51.81	0.45	53.53	56.31	3.50
	35	42.55	44.64	50.29	0.46	51.76	54.44	1.45
	37	36.36	39.13	42.01	0.39	45.38	49.57	1.27
	39	37.34	36.34	41.10	0.39	43.07	47.56	1.11
29	33	45.35	48.91	51.90	0.45	53.37	56.71	3.80
	35	44.48	46.97	50.54	0.44	52.28	55.45	2.39
	37	37.32	40.51	43.59	0.43	45.10	49.75	1.20
	39	39.52	36.60	42.48	0.41	44.78	50.08	2.02
28	33	45.24	48.80	51.71	0.43	53.88	56.54	3.56
	35	45.40	47.62	50.65	0.36	52.79	56.37	2.77
	37	40.79	37.86	42.86	0.34	45.41	49.92	1.10
	39	40.10	38.99	42.95	0.50	44.82	49.75	1.80
24	33	44.20	49.40	52.16	0.45	54.23	57.12	3.46
	35	48.284	51.29	54.64	0.51	53.06	56.79	2.62
	37	43.34	46.14	49.82	0.44	51.69	54.87	1.60
	39	43.14	41.47	46.23	0.38	50.97	55.04	1.88

Appendix 5. *DSC data of selected samples during in vacuo storage at 24 ± 2.0 °C*

Batch	R104 / %w/w	Storage / h	Transition						
			Tg(the) / °C	Tg(on) / °C	$^1/_2$ Cp / °C	ΔCp / / $Jg^{-1} * °C$	Onset / °C	Peak / °C	ΔH / Jg^{-1}
32	31	Coll	47.51	44.29	51.53	0.52	48.31	52.92	0.85
		Cycl	49.71	46.66	52.20	0.36	48.63	53.45	2.52
		1	50.04	46.15	52.87	0.45	51.52	54.45	0.04
		3	49.49	42.47	53.19	0.59	50.98	55.28	1.90
		5	51.72	47.98	53.41	0.35	52.45	56.30	2.49
		24	50.66	45.09	52.59	0.40	53.70	56.80	3.50
		48	51.28	45.58	54.21	0.51	55.56	58.15	3.83
		72	51.64	44.62	52.90	0.45	56.57	58.78	3.86
		168	51.00	44.65	53.69	0.52	57.28	59.47	4.56
		336	50.80	45.66	52.38	0.48	57.80	59.80	4.91
		(100 d)	50.11	53.20	55.42	0.42	59.00	61.41	4.20
33	30	Coll	48.96	42.81	51.09	0.40	47.91	53.61	0.86
		Cycl	49.07	44.70	52.35	0.45	49.03	54.28	1.86
		1	47.75	40.59	50.02	0.41	48.89	53.94	2.27
		3	50.56	44.59	53.68	0.49	51.02	55.62	2.13
		5	50.68	47.40	52.95	0.40	51.52	55.63	2.25
		24	50.56	43.48	53.25	0.50	53.84	56.97	3.22
		48	50.36	41.95	52.68	0.49	55.02	57.47	3.69
		72	50.86	45.73	53.69	0.52	56.17	58.63	3.79
		168	51.046	44.81	54.09	0.53	57.28	59.47	4.57
		336	50.89	45.27	53.50	0.53	58.02	59.92	4.25
		(100 d)	50.32	53.60	55.75	0.46	59.55	61.49	4.10
34	29	Coll	45.73	41.16	49.62	0.46	47.10	53.27	2.28
		Cycl	48.66	41.34	53.12	0.52	49.36	54.79	2.46
		1	49.81	45.88	53.26	0.50	50.19	55.45	2.88
		3	50.23	46.12	53.51	0.51	51.02	55.68	3.02
		5	50.45	46.35	53.46	0.51	51.91	55.94	2.90
		24	51.74	48.94	53.81	0.41	54.05	57.14	2.80
		48	50.99	45.00	53.98	0.53	55.38	57.96	3.26
		72	50.61	42.26	53.57	0.55	55.76	58.29	4.27
		168	51.72	45.81	54.68	0.52	57.29	59.48	4.81
		336	51.04	45.92	53.21	0.46	57.71	59.63	4.54
		(100 d)	51.49	53.72	55.81	0.47	59.60	61.62	4.40

Appendix 6. *Effect of storage time on the first order release statistics at 37 ± 0.1 °C and 100 ± 1 rpm using method B. (amount released$_t$ = a_o e^{-bt})*

Batch	R104 / %w/w	Storage / d	a	b	r^2	se	Release / h		
							25 %	50 %	75 %
32	31	1	102.4	0.408	0.98	4.07	0.76	1.75	3.46
		3	99.5	0.487	0.98	4.68	0.58	1.41	2.83
		7	102.0	0.396	0.98	4.63	0.77	1.79	3.54
		40	103.3	0.361	0.99	2.14	0.88	2.01	3.93
		50	99.1	0.257	0.99	2.54	1.08	2.64	5.34
33	30	1	108.7	0.243	0.99	3.51	1.52	3.19	6.05
		3	107.8	0.312	0.98	4.17	1.16	2.46	4.68
		7	113.7	0.263	0.98	3.48	1.59	3.13	5.78
		40	105.3	0.221	0.99	1.80	2.01	4.67	9.19
		50	105.7	0.154	0.99	2.19	2.24	4.89	9.43
34	29	1	111.2	0.218	0.98	4.72	1.78	3.64	6.81
		3	108.9	0.271	0.98	4.27	1.37	2.87	5.43
		7	110.8	0.223	0.98	3.87	1.73	3.55	6.67
		40	101.8	0.074	0.99	1.38	4.10	9.59	18.98
		50	107.3	0.102	0.99	1.58	3.49	7.47	14.25

Appendix 7. *DSC data of microsphere residue during release studies at 37 ± 0.1 °C and 100 ± 1 rpm using method B.*

			Transition									
Batch	**R104 / %w/w**	**Time /min**	**Tg(the) / °C**	**Tg(on) / °C**	**$^1/_2$ Cp / °C**	**ΔCp/ Jg^{-1}*°C**	**Onset / °C**	**Peak / °C**	**Area / Jg^{-1}**	**Onset / °C**	**Peak / °C**	**Area / Jg^{-1}**
30	36	5	46.11	43.55	49.58	0.44	50.70	53.48	3.59	58.48	62.52	0.68
		30	43.61	38.29	47.28	0.48	49.39	52.37	1.84	56.44	61.68	1.14
		60	40.85	38.33	43.81	0.35	43.62	48.42	2.45	50.24	61.02	1.16
		120	39.26	36.15	41.80	0.36	41.24	47.20	3.13	52.41	59.72	2.94
		240	41.91	37.22	45.08	0.43	39.85	46.74	2.58	51.99	58.86	1.77
		480	41.95	36.01	44.90	0.41	41.63	47.16	2.94	25.44	29.89	1.27
31	32	5	46.88	42.20	49.93	0.45	51.61	54.20	3.18	59.11	62.99	3.04
		30	46.05	40.89	48.98	0.47	50.43	53.80	2.79	58.24	62.59	0.99
		60	43.07	37.72	46.12	0.50	46.53	50.28	2.88	57.62	61.93	0.43
		120	41.98	37.81	44.75	0.46	43.56	49.12	2.94	55.00	61.72	0.47
		240	40.94	37.39	43.76	0.41	43.40	49.03	3.15	54.23	64.36	1.86
		480	41.67	37.67	44.76	0.46	44.69	48.20	2.15			
35	28	5	43.83	37.49	47.43	0.56	50.38	52.76	4.47	58.33	61.70	0.72
		30	46.05	40.56	49.13	0.48	50.86	53.38	3.93	58.15	63.21	0.74
		60	45.08	39.48	47.83	0.44	50.80	53.33	3.96	57.94	61.82	0.79
		120	44.60	39.29	48.39	0.51	50.94	53.33	3.75	57.22	62.19	1.27
		240	43.11	37.36	46.47	0.50	50.17	52.91	3.81	56.94	61.51	1.04
		480	43.31	38.07	46.99	0.51	50.54	52.94	2.99	56.34	61.33	1.33
36	24	5	48.76	44.44	51.23	0.40	53.32	56.00	3.45	59.12	63.72	0.71
		30	48.09	42.30	51.79	0.54	52.85	55.58	3.34	58.95	63.95	0.98
		60	47.48	41.15	50.69	0.52	52.39	54.91	2.74	58.58	63.37	0.86
		120	47.29	40.98	50.97	0.54	52.27	54.9	2.95	58.25	64.19	0.98
		240	46.48	40.51	50.65	0.53	51.65	54.31	2.62	57.53	63.35	1.25
		480	46.43	38.31	49.39	0.49	51.34	54.31	2.35	57.01	62.14	0.56
37	20	5	48.13	42.13	51.31	0.49	52.92	55.65	3.23	60.78	64.10	0.42
		30	46.80	41.76	49.99	0.47	51.64	54.36	3.53	58.58	63.16	0.81
		60	46.32	42.43	49.73	0.47	53.13	54.03	2.81	58.16	65.43	0.73
		120	45.61	38.52	48.92	0.55	51.41	53.96	2.75	57.61	62.93	1.27
		240	45.73	40.33	48.96	0.47	50.97	53.47	2.52	57.80	62.68	1.08
		480	44.24	37.98	47.77	0.48	50.43	53.22	1.91	56.83	62.68	1.33

Appendix 8a. *Effect of medium temperature on the regression statistics of release profiles fitted to the power law using method B. amount released* $_t = a^* t^b$

Batch	R104 / %w/w	Medium / °C	a	b	r^2	SE	% released / h		
							25	50	75
4	60	33	29.78	1.647	0.998	1.24	0.899	1.37	1.75
		35	120.77	0.829	0.985	3.87	0.150	0.345	0.563
		37	238.40	0.858	0.992	3.44	0.072	0.162	0.260
		39	124.06	0.321	0.973	3.63	0.006	0.059	0.209
5	56	33	36.16	1.440	0.999	1.00	0.768	1.24	1.64
		35	120.53	0.818	0.987	3.79	0.146	0.341	0.560
		37	183.06	0.741	0.991	3.29	0.006	0.162	0.286
		39	156.66	0.409	0.982	3.50	0.012	0.061	0.165
6	52	33	156.66	0.409	0.932	3.50	0.011	0.061	0.165
		35	12.34	0.661	0.987	1.93	2.90	8.28	15.29
		37	75.58	0.624	0.990	2.75	0.170	0.516	0.988
		39	142.03	0.39	0.985	3.032	0.011	0.068	0.194
7	48	33	10.29	0.377	0.965	0.952	10.47	65.69	192.25
		35	16.35	1.011	0.988	3.23	1.52	3.02	4.51
		37	104.56	1.093	0.995	2.28	0.270	0.502	0.738
		39	185.60	1.296	0.995	2.41	0.213	0.363	0.497
8	44	33	8.74	0.296	0.973	0.803	34.74	361.47	1422
		35	13.05	0.917	0.990	3.26	2.03	4.32	6.72
		37	30.39	0.516	0.949	6.59	0.685	2.62	5.74
		39	127.55	1.105	0.990	3.64	0.229	0.429	0.618
9	40	33	5.22	0.360	0.956	0.777	77.40	530.79	1637
		35	6.82	1.104	0.998	1.12	3.23	6.06	8.75
		37	31.84	1.098	0.989	3.06	0.802	1.50	2.18
		39	109.43	0.810	0.995	2.22	0.162	0.380	0.627
31	32	33	no fit						
		35	7.81	0.702	0.981	1.60	5.23	14.06	25.07
		37	23.04	0.733	0.973	6.64	1.11	2.87	5.00
		39	60.21	0.900	0.987	3.80	0.377	0.815	1.27
32	31	33	9.92	0.196	0.988	0.344	119.35	4317	35452
		35	14.97	0.561	0.972	2.73	2.49	8.580	17.69
		37	25.44	0.795	0.991	3.24	0.978	2.33	3.89
		39	74.62	0.603	0.991	3.06	0.163	0.514	1.01
33	30	33	8.01	0.171	0.988	0.191	938.58		
		35	7.94	0.705	0.978	1.65	5.54	15.17	27.93
		37	15.07	0.902	0.993	3.56	1.75	3.77	5.914
		39	55.99	0.738	0.988	3.58	0.335	0.858	1.48
34	29	33	6.40	0.232	0.996	0.179	360.09	3036	44265
		35	6.83	0.425	0.979	0.803	21.67	110.03	284.84
		37	11.81	0.958	0.994	2.37	2.19	4.51	6.88
		39	47.02	0.782	0.991	3.23	0.445	1.08	1.81
35	28	33	7.53	0.176	0.998	0.129	4837	44150	436552
		35	9.32	0.414	0.972	1.22	10.81	57.64	153.41
		37	15.87	0.861	0.978	3.93	1.69	3.79	6.07
		39	45.09	0.875	0.992	2.94	0.509	1.12	1.79
36	24	33	5.25	0.191	0.995	0.154	3456		
		35	6.74	0.275	0.981	0.487	1117	4164	6401
		37	6.97	0.543	0.978	1.10	10.68	39.12	83.89
		39	11.15	0.853	0.994	1.91	2.57	6.07	9.33

Appendix 8b. *Effect of medium temperature on the linear regression statistics of release profiles using method B. amount released$_t$ = a + bt*

Batch	R104 / %w/w	Medium / °C	a	b	r^2	SE	% released / h		
							25	50	75
4	60	33	-21.15	52.82	0.992	2.56	0.874	1.34	1.82
		35	3.54	125.94	0.985	5.11	0.170	0.369	0.567
		37	4.28	263.06	0.988	5.20	0.078	0.174	0.269
		39	21.96	228.09	0.882	15.20			
5	56	33	-7.64	48.40	0.989	4.24	0.674	1.191	1.70
		35	4.78	124.25	0.984	5.17	0.163	0.364	0.565
		37	8.20	227.01	0.978	6.66	0.074	0.184	0.294
		39	15.91	326.98	0.920	13.92			
6	52	33	5.48	6.03	0.972	3.06	3.23	7.37	11.51
		35	8.02	109.14	0.976	6.21	0.156	0.385	0.614
		37	11.66	64.81	0.970	6.32	0.206	0.591	0.977
		39	14.52	317.83	0.928	12.84			
7	48	33	7.08	2.37	0.942	1.77	7.53	18.04	25.55
		35	2.94	13.57	0.976	6.27	1.62	3.46	5.309
		37	-1.83	102.18	0.995	2.79	0.263	0.507	0.752
		39	-4.75	154.55	0.991	3.81	0.193	0.354	0.516
8	44	33	6.59	1.51	0.879	1.70			
		35	1.12	11.05	0.986	3.84	2.16	4.42	6.68
		37	17.06	10.20	0.894	10.61			
		39	-2.95	125.10	0.994	3.30	0.223	0.423	0.623
9	40	33	3.76	1.06	0.834	1.46			
		35	-1.27	8.32	0.997	1.29	3.15	6.15	9.15
		37	-0.088	32.77	0.989	3.62	0.765	1.52	2.29
		39	4.55	113.14	0.991	3.78	0.181	0.402	0.622
31	32	33	4.97	0.827	0.891	0.877	24.23	54.48	84.74
		35	3.76	4.01	0.999	0.766	5.28	11.48	17.72
		37	9.32	13.56	0.961	8.06	1.15	3.001	4.86
		39	2.25	57.46	0.987	4.09	0.397	0.833	1.26
32	31	33	8.13	1.11	0.905	1.04	15.11	37.52	59.92
		35	8.58	5.61	0.992	1.46	2.92	7.37	11.82
		37	7.22	17.47	0.990	3.53	1.01	2.44	3.87
		39	17.87	56.33	0.974	5.35	0.126	0.570	1.01
33	30	33	6.73	0.77	0.877	0.894	21.74	50.35	78.95
		35	7.55	4.81	0.991	1.36	3.74	9.06	14.37
		37	2.80	12.41	0.987	4.19	1.78	3.80	5.81
		39	10.81	43.29	0.975	5.27	0.327	0.905	1.48
34	29	33	4.91	0.883	0.847	1.14	22.75	51.09	79.43
		35	4.35	1.84	0.974	0.881	11.27	24.90	38.53
		37	2.28	10.51	0.994	2.40	2.16	4.54	6.93
		39	8.55	36.65	0.982	4.57	0.448	1.131	1.81
35	28	33	6.08	0.801	0.812	1.19			
		35	6.04	2.4415	0.978	1.11	9.26	38.09	92.22
		37	3.68	11.85	0.983	4.60	1.79	3.90	6.01
		39	4.26	39.78	0.989	3.54	0.521	1.15	1.77
36	24	33	4.38	0.617	0.828	0.8695	33.40	73.91	114.41
		35	4.96	1.13	0.934	0.899	17.72	39.85	61.97
		37	4.04	2.51	0.991	0.719	8.37	18.38	28.38
		39	3.10	8.07	0.992	2.13	2.71	5.81	8.90

Appendix 8c. *Effect of medium temperature on the first order release statistics using method B. amount released$_t$ = ae^{-bt}*

Batch	R104 / %w/w	Medium / °C	a	b	r^2	SE	% released / h		
							25	50	75
4	60	33	112.52	0.587	0.938	8.89			
		35	105.05	2.34	0.991	3.98	0.144	0.317	0.613
		37	101.97	4.87	0.992	4.11	0.063	0.146	0.289
		39	91.97	7.04	0.974	7.39	0.029	0.086	0.185
5	56	33	112.80	0.713	0.947	9.32			
		35	103.93	2.35	0.993	3.58	0.139	0.311	0.605
		37	99.62	4.58	0.997	2.29	0.061	0.150	0.302
		39	95.13	8.75	0.989	5.19	0.027	0.735	0.150
6	52	33	96.39	0.084	0.982	2.45	2.974	7.78	15.99
		35	102.17	2.22	0.996	2.64	0.139	0.321	0.632
		37	99.70	1.39	0.999	1.35	0.204	0.495	0.993
		39	95.22	7.84	0.988	5.21	0.030	0.082	0.171
7	48	33	93.15	0.028	0.947	1.68	7.62	21.84	46.16
		35	108.17	0.270	0.987	4.61	1.35	2.858	5.42
		37	107.77	1.64	0.976	6.29	0.220	0.467	0.888
		39	107.74	2.21	0.961	8.00	0.164	0.350	0.660
8	44	33	93.52	0.017	0.884	1.66	12.73	36.11	76.09
		35	105.24	0.184	0.993	2.76	1.83	4.03	7.79
		37	96.15	0.273	0.973	5.50	0.909	2.39	4.92
		39	108.09	1.95	0.973	6.80	0.187	0.394	0.749
9	40	33	96.30	0.011	0.839	1.44	21.42	56.15	115.53
		35	103.63	0.112	0.986	2.90	2.88	6.50	12.69
		37	106.84	0.527	0.987	5.19	0.672	1.44	2.75
		39	103.28	2.06	0.996	2.59	0.155	0.351	0.686
31	32	33	95.05	0.009	0.894	12.69	49.66	113.23	118.60
		35	96.69	0.048	0.993	1.02	5.262	13.66	28.01
		37	95.08	0.012	0.937	0.879	19.02	51.53	107.11
		39	121.02	1.19	0.990	3.33	0.403	0.744	1.327
32	31	33	91.61	0.011	0.971	0.536	16.87	51.01	109.40
		35	92.45	0.076	0.988	1.76	2.72	7.99	17.24
		37	112.63	0.334	0.994	3.03	1.22	2.43	4.51
		39	99.99	1.42	0.999	1.25	0.202	0.485	0.970
33	30	33	93.06	0.007	0.934	0.559	27.21	78.44	166.02
		35	96.40	0.045	0.988	1.26	5.65	14.70	30.16
		37	101.87	0.331	0.983	4.49	0.924	2.14	4.24
		39	109.33	0.988	0.996	2.12	0.381	0.792	1.49
34	29	33	95.12	0.009	0.851	1.13	24.63	66.56	138.31
		35	95.75	0.020	0.977	0.855	11.91	31.61	65.32
		37	51.59	0.598	0.989	3.25	2.46	5.07	9.89
		39	109.71	0.795	0.992	3.01	0.478	0.989	1.85
35	28	33	93.94	0.008	0.8165	1.18	25.42	71.21	149.46
		35	94.15	0.028	0.9795	1.04	7.96	22.15	46.41
		37	104.26	0.170	0.981	4.37	1.93	4.32	8.40
		39	113.96	0.797	0.989	3.68	0.524	1.16	1.90
36	24	33	95.63	0.006	0.831	0.861	36.60	97.66	202.03
		35	95.08	0.012	0.937	0.879	19.02	51.53	107.11
		37	99.43	0.117	0.995	1.52	2.41	5.89	11.84
		39	109.35	0.231	0.992	3.19	1.63	3.38	6.37

Appendix 9a. *Effect of oligomer, R104 level on the biexponential coefficients of drug release using method B from microsphere prepared from RG502 (data fitted to equation 8.1)*

			Biexponential coefficients					Quartile release / h		
Medium / °C	**Batch**	**R104 / %w/w**	**A / %**	**α/ h^{-1}**	**B / %**	**β/ h^{-1}**	**r^2**	**25 %**	**50 %**	**75 %**
33	1	56	86.51	7.108	7.904	0.116	0.956	0.043	0.126	0.284
33	7	60	66.61	7.031	5.542	0.006	0.916	-0.006	0.057	0.096
33	13	63.3	79.99	7.791	17.19	0.060	0.997	0.041	0.114	0.302
33	19	66.6	82.01	6.774	15.13	0.090	0.998	0.046	0.125	0.307
33	31	75	81.29	7.651	14.16	0.261	0.998	0.037	0.542	0.255
33	37	80	54.47	3.330	20.73	0.026	0.917	0.0008	0.180	0.719
33	25	90	31.09	2.463	58.91	0.021	0.976	2.299	0.260	7.984
35	1	56	71.04	35.00	22.73	3.034	0.991	0.009	0.028	0.077
35	7	60	75.11	20.51	18.44	1.013	0.993	0.013	0.042	0.114
35	13	63.3	83.73	9.809	12.37	0.140	0.996	0.029	0.081	0.191
35	19	66.6	78.25	8.047	16.54	0.209	0.993	0.037	0.109	0.276
35	31	75	78.15	8.736	17.64	0.283	0.996	0.035	0.100	0.258
35	37	80	75.42	5.920	20.49	0.069	0.994	0.054	0.156	0.454
35	25	90	41.12	1.808	52.72	0.029	0.992	1.741	0.329	2.584
37	1	56	61.63	35.80	13.66	3.334	0.921	0.0004	0.018	0.053
37	7	60	55.49	31.42	13.07	2.281	0.949	0.004	0.025	0.069
37	13	63.3	78.94	9.195	13.55	0.382	0.997	0.027	0.083	0.208
37	19	66.6	78.87	10.84	16.71	0.212	0.995	0.027	0.076	0.200
37	31	75	78.76	11.17	15.83	0.439	0.997	0.025	0.073	0.181
37	37	80	57.46	5.913	13.26	0.037	0.895	-0.013	0.077	0.274
37	25	90	45.80	1.118	35.65	0.020	0.918	6.767	0.139	1.013
39	1	56	57.69	16.98	28.04	1.738	0.987	0.011	0.051	0.168
39	7	60	63.73	23.33	27.03	2.037	0.994	0.011	0.040	0.1205
39	13	63.3	79.90	15.11	12.65	0.386	0.994	0.016	0.050	0.124
39	19	66.6	76.00	15.89	16.44	0.498	0.992	0.016	0.050	0.130
39	31	75	73.64	12.53	19.55	0.374	0.992	0.023	0.073	0.206
39	37	80	88.74	8.554	15.37	0.181	0.995	0.046	0.109	0.252
39	25	90	69.17	3.799	31.88	0.180	0.997	1.024	0.124	0.366

Appendix 9b. *Effect of oligomer, R104 level on the biexponential coefficients of drug release using method B from microsphere prepared from RG503 (data fitted to equation 8.1)*

			Biexponential coefficients					Quartile release / h		
Medium / °C	**Batch**	**R104 / %w/w**	**A / %**	**α / h^{-1}**	**B / %**	**β / h^{-1}**	**r^2**	**25 %**	**50 %**	**75 %**
33	2	56	81.97	11.05	16.17	1.581	0.981	0.028	0.075	0.169
33	8	60	91.40	6.280	4.222	-0.060	0.971	0.040	0.110	0.236
33	14	63.3	68.93	8.045	25.45	0.582	0.998	0.042	0.144	18.66
33	20	66.6	75.94	7.048	15.95	0.067	0.996	0.035	0.113	0.297
33	32	75	52.44	3.385	42.04	0.031	0.997	0.135	0.533	16.52
33	38	80	27.22	20.09	70.19	0.008	0.980	0.085		
33	26	90	13.97	9.842	85.55	0.009	0.956	1.198	13.87	
35	2	56	73.83	28.83	20.82	2.742	0.993	0.010	0.030	0.076
35	8	60	61.61	23.79	30.52	4.156	0.983	0.012	0.039	0.104
35	14	63.3	86.34	5.700	13.35	0.068	0.992	0.061	0.158	0.408
35	20	66.6	77.43	5.279	16.85	0.062	0.996	0.053	0.159	0.417
35	32	75	52.34	4.456	43.24	0.026	0.997	0.111	0.444	20.62
35	38	80	27.57	16.70	66.71	0.011	0.969	0.071	26.00	
35	26	90	9.743	22.51	88.12	0.002	0.886	1.095		
37	2	56	79.56	24.10	5.536	0.039	0.952	0.002	0.019	0.048
37	8	60	57.14	38.55	33.01	4.573	0.976	0.0007	0.030	0.093
37	14	63.3	68.02	4.137	24.20	0.256	0.996	0.069	0.224	0.663
37	20	66.6	76.32	10.44	16.45	0.097	0.995	0.025	0.078	0.207
37	32	75	50.00	5.458	47.75	0.027	0.996	0.111	0.577	23.34
37	38	80	23.97	12.53	70.76	0.018	0.964	0.136	19.17	
37	26	90	10.29	33.06	87.14	0.004	0.887	1.158		
39	2	56	52.26	36.90	39.36	4.383	0.992	0.010	0.036	0.115
39	8	60	25.60	31.26	69.96	4.629	0.989	0.024	0.084	0.224
39	14	63.3	71.72	16.93	21.88	0.271	0.993	0.019	0.061	4.136
39	20	66.6	78.29	14.29	13.28	0.228	0.993	0.016	0.052	0.131
39	32	75	49.43	7.433	46.75	0.029	0.996	0.074	0.365	21.28
39	38	80	32.84	10.32	67.51	0.022	0.997	0.140	13.23	
39	26	90	11.95	17.50	87.94	0.006	0.990	0.292		

Appendix 9c. *Effect of oligomer, R104 level on the biexponential coefficients of drug release using method B from microsphere prepared from RG503H (data fitted to equation 8.1)*

			Biexponential coefficients					Quartile release / h		
Medium / °C	**Batch**	**R104 / %w/w**	**A / %**	**α / h^{-1}**	**B / %**	**β / h^{-1}**	**r^2**	**25**	**50**	**75**
33	3	56	90.99	8.137	11.14	0.116	0.989	0.043	0.104	0.229
33	9	60	89.25	5.944	9.940	0.030	0.99	0.053	0.134	0.299
33	15	63.3	68.29	4.009	30.39	0.018	0.999	0.106	0.313	11.47
33	21	66.6	76.90	3.567	21.19	0.039	0.999	0.099	0.273	0.798
33	33	75	46.20	1.346	51.52	0.027	0.999	0.419	2.269	26.35
33	39	80	11.78	1.425	82.97	0.013	0.974	7.714		
33	27	90	5.392	30.45	94.00	0.005	0.849	1.021		
35	3	56	81.66	13.99	14.33	0.569	0.991	0.021	0.058	0.138
35	9	60	77.56	14.24	17.61	1.028	0.995	0.023	0.059	0.015
35	15	63.3	86.59	4.725	16.35	0.061	0.993	0.082	0.200	0.504
35	21	66.6	79.31	4.409	17.96	0.063	0.997	0.076	0.209	0.549
35	33	75	41.35	2.291	53.67	0.038	0.999	0.330	3.050	20.77
35	39	80	24.16	9.152	69.66	0.015	0.977	0.589	25.64	
35	27	90	15.21	21.53	82.32	0.012	0.997	0.456		
37	3	56	69.16	44.08	15.30	2.029	0.967	0.003	0.016	0.270
37	9	60	55.31	41.18	37.24	2.472	0.980	0.009	0.032	0.165
37	15	63.3	56.62	7.719	39.71	0.096	0.992	0.077	1.623	6.284
37	21	66.6	77.07	7.706	20.75	0.114	0.998	0.045	0.124	0.354
37	33	75	43.58	2.399	54.15	0.046	0.998	0.293	1.981	16.35
37	39	80	25.06	2.052	68.36	0.026	0.991	0.732	13.60	
37	27	90	5.632	37.10	93.34	0.003	0.867	0.774		
39	3	56	51.56	33.44	42.95	2.821	0.995	0.013	0.045	0.199
39	9	60	55.84	11.60	42.73	1.620	0.997	0.044	0.127	0.329
39	15	63.3	67.05	10.64	30.42	0.081	0.997	0.276	0.140	8.203
39	21	66.6	76.66	10.38	18.51	0.217	0.995	0.029	0.084	0.226
39	33	75	49.47	2.988	48.73	0.035	0.996	0.195	0.872	18.18
39	39	80	33.81	2.404	64.00	0.015	0.997	0.452	15.55	

Appendix 9d. *Effect of oligomer, R104 level on the biexponential coefficients of drug release using method B from microsphere prepared from RG504 (data fitted to equation 8.1)*

			Biexponential coefficients					Quartile release / h		
Medium / °C	**Batch**	**R104 / %w/w**	**A / %**	**α / h^{-1}**	**B / %**	**β / h^{-1}**	**r^2**	**25 %**	**50 %**	**75 %**
33	4	56	85.28	11.69	9.894	0.55	0.990	0.022	0.063	0.144
33	10	60	64.27	9.309	8.090	2.167	0.924	-0.004	0.044	0.133
33	16	63.3	83.02	12.31	11.23	0.382	0.956	0.036		
33	22	66.6	75.21	13.25	14.23	0.187	0.992	0.087		
33	34	75	49.97	3.749	45.07	0.029	0.997	0.231	1.165	20.51
33	40	80	12.10	2.628	58.30	0.004	0.524	-0.066		
33	28	90	19.67	26.69	73.83	0.015	0.900	1.798	0.243	6.118
35	4	56	74.08	11.36	21.10	0.686	0.997	0.040	0.459	0.199
35	10	60	78.10	27.12	10.02	2.191	0.986	0.006	0.024	0.058
35	16	63.3	86.80	5.266	10.71	0.124	0.997	0.060	0.155	0.349
35	22	66.6	77.99	8.227	12.96	0.015	0.996	0.165	0.524	0.238
35	34	75	53.71	6.684	38.91	0.026	0.993	0.059	0.233	16.95
35	40	80	24.19	8.446	68.37	0.008	0.959	0.152	36.87	
35	28	90	6.568	30.52	91.33	0.001	0.791	1.043		
37	4	56	70.29	27.98	12.95	0.743	0.972	0.005	0.024	0.064
37	10	60	71.04	32.12	17.43	3.010	1.258	0.006	0.023	0.450
37	16	63.3	83.32	9.919	11.00	0.345	0.997	0.026	0.076	0.176
37	22	66.6	76.67	11.73	15.44	0.140	0.994	0.023	0.384	0.174
37	34	75	54.82	6.848	38.91	0.025	0.995	0.050	0.190	18.194
37	40	80	6.412	1.128	69.08	0.003	0.960	0.039		
37	28	90	4.125	0.952	71.23	0.001	0.941	0.041		
39	4	56	42.53	42.54	54.10	4.823	0.980	0.0098	0.037	0.141
39	10	60	61.90	33.92	27.37	4.942	0.987	0.008	0.029	0.078
39	16	63.3	80.95	16.01	10.65	0.782	0.996	0.014	0.044	0.105
39	22	66.6	78.24	17.37	11.41	0.185	0.991	0.011	0.040	0.099
39	34	75	53.29	13.25	39.73	0.027	0.994	0.031	0.124	16.90
39	40	80	25.78	10.13	74.34	0.010	0.996	1.044	33.72	
39	28	90	7.323	13.22	92.39	0.003	0.990	0.176		

Appendix 9e. *Effect of oligomer, R104 level on the biexponential coefficients of drug release using method B from microsphere prepared from RG752 (data fitted to equation 8.1)*

Medium / °C	Batch	R104 / %w/w	Biexponential coefficients				r^2	Quartile release / h		
			A / %	α / h^{-1}	B / %	β / h^{-1}		25 %	50 %	75 %
33	5	56	83.07	1.735	15.69	0.060	0.997	0.193	0.506	1.256
33	11	60	80.23	1.234	16.24	0.042	0.995	0.265	0.605	1.356
33	17	63.3	50.25	2.356	43.58	0.039	0.976	0.150	3.211	
33	23	66.6	43.12	9.231	52.35	0.038	0.983	0.752	5.321	
33	29	70	32.63	15.25	65.45	0.025	0.984	1.034	7.359	10.898
33	35	75	28.07	17.85	68.86	0.021	0.987	0.083	14.89	
33	41	80	35.71	13.10	58.17	0.020	0.974	0.060	8.152	
35	5	56	80.60	5.416	17.45	0.958	0.998	0.059	0.153	0.339
35	11	60	73.49	1.018	14.58	0.114	0.994	0.199	0.680	1.674
35	17	63.3	71.09	3.237	28:09	0.138	0.973	0.126	0.347	1.239
35	23	66.6	59.08	4.535	34.56	0.003	0.996	0.083	0.296	
35	29	70	26.59	29.42	70.87	0.009	0.977	1.146	0.076	
35	35	75	22.76	14.95	72.72	0.072	0.994	0.137	5.193	14.80
35	41	80	34.30	11.42	58.28	0.023	0.969	0.006	7.118	
37	5	56	89.63	7.988	6.288	0.907	0.996	0.033	0.893	0.191
37	11	60	82.93	1.430	7.591	-0.044	0.995	0.145	0.472	1.107
37	17	63.3	73.62	7.688	21.25	0.272	0.997	0.040	0.119	0.336
37	23	66.6	56.62	8.531	38.26	0.166	0.995	0.055	0.271	2.559
37	29	70	34.91	3.869	57.06	0.319	0.993	2.577	0.143	0.635
37	35	75	17.46	23.78	77.93	0.2715	0.999	0.162	1.640	4.201
37	41	80	35.20	8.558	57.26	0.292	0.981	0.425	2.793	17.46
39	5	56	72.56	11.91	23.59	2.024	0.998	0.028	0.497	0.189
39	11	60	79.96	9.005	14.58	0.150	0.997	0.030	0.089	0.221
39	17	63.3	66.44	10.08	28.11	0.445	0.991	0.033	0.105	0.437
39	23	66.6	76.00	7.980	19.32	0.309	0.996	0.037	0.110	0.292
39	29	70	72.05	3.279	23.60	0.276	0.997	1.423	0.524	0.287
39	35	75	50.88	2.395	42.13	0.469	0.998	0.148	0.477	1.311
39	41	80	29.69	6.745	69.01	0.055	0.994	0.219	5.880	22.49

Appendix 9f. *Effect of oligomer, R104 level on the biexponential coefficients of drug release using method B from microsphere prepared from RG755 (data fitted to equation 8.1)*

			Biexponential coefficients					Quartile release / h		
Medium / °C	**Batch**	**R104 / %w/w**	**A / %**	**α / h^{-1}**	**B / %**	**β / h^{-1}**	**r^2**	**25 %**	**50 %**	**75 %**
33	6	56	77.43	6.272	19.83	0.119	0.993	0.053	0.149	0.409
33	12	60	57.13	2.291	32.89	0.045	0.993	0.132	0.516	6.106
33	18	63.3	47.21	2.841	43.84	0.024	0.965	0.145		
33	24	66.6	35.27	2.541	58.35	0.009	0.989	0.541		
33	30	70	27.92	22.16	70.53	0.008	0.975	1.285	0.082	
33	36	75	20.10	17.00	76.52	0.007	0.981	2.646		
33	42	80	28.29	26.05	68.34	0.007	0.983	0.055		
35	6	56	83.90	5.944	13.44	0.321	0.998	0.051	0.137	0.316
35	12	60	62.73	4.061	30.97	0.060	0.994	0.079	0.266	2.620
35	18	63.3	58.01	3.808	39.50	0.068	0.998	0.129	0.426	6.646
35	24	66.6	29.18	9.979	65.51	0.003	0.980	0.112		
35	30	70	26.57	36.86	68.67	0.011	0.977	1.195	0.038	
35	36	75	19.14	24.32	77.81	0.005	0.984	7.090		
35	42	80	24.38	32.99	72.42	0.009	0.972	0.068		
37	6	56	82.07	16.72	10.31	0.723	0.993	0.014	0.043	0.100
37	12	60	62.04	4.685	31.65	0.097	0.991	0.439	0.256	3.348
37	18	63.3	59.86	7.110	34.55	0.105	0.995	0.300	0.185	3.069
37	24	66.6	33.70	9.622	62.02	0.102	0.991	0.140	4.432	4.575
37	30	70	14.50	30.42	83.31	0.012	0.912	1.060	0.138	19.48
37	36	75	18.54	25.75	77.52	0.004	0.976	7.986		
37	42	80	24.48	49.06	76.00	0.005	0.973	2.480		
39	6	56	81.09	13.33	16.33	1.698	0.993	0.022	0.060	0.137
39	12	60	72.84	10.53	24.15	0.151	0.997	0.183	0.097	0.339
39	18	63.3	60.12	6.351	32.72	0.150	0.991	0.055	0.204	1.798
39	24	66.6	36.17	6.906	56.66	0.107	0.986	0.095	1.168	7.625
39	30	70	29.00	9.354	70.34	0.035	0.993	0.828		
39	36	75	15.77	31.63	80.10	0.006	0.969	10.20		
39	42	80	19.78	16.55	80.78	0.005	0.989	13.90		

Appendix 10. *DSC statistics for spray-dried microspheres containing 20 %w/w rifampicin prepared from blends of Resomer® R104 and various lactide-glycolide copolymers*

							1st peak			2nd peak		
			Transition / °C				Transition / °C			Transition / °C		
Compl. polymer	Batch	Polymer / %w/w	Tg(on)	Tg(the)	$^1/_2$ Cp	ΔCp / Jg^{-1} •°C	Onset	Peak	Area / Jg^{-1}	Onset	Peak	Area / Jg^{-1}
RG502	1	56	39.68	37.63	40.82	0.15	46.13	48.21	2.67	54.74	57.41	1.61
	7	60	40.42	38.08	41.20	0.17	46.26	48.22	3.09	57.71	60.99	1.24
	13	63.3	41.72	39.59	41.60	0.05	45.22	47.27	2.83	57.52	60.51	0.86
	19	66.6	40.85	39.85	41.38	0.15	47.27	49.25	4.18	58.64	62.34	1.30
	31	75	40.88	39.26	41.71	0.26	50.68	52.31	5.17	61.38	63.71	0.52
	37	80	39.20	36.85	40.40	0.41	47.44	49.72	9.70			
RG503	2	56	43.67	41.86	44.71	0.14	50.81	52.297	3.55	57.09	59.95	1.53
	8	60	45.09	42.74	46.06	0.20	54.00	55.80	4.33	62.73	65.68	1.55
	14	63.3	44.90	41.92	45.66	0.22	49.95	51.52	3.21	61.26	64.45	0.89
	20	66.6	44.57	43.05	44.82	0.15	52.52	54.29	4.95	61.90	64.56	0.96
	32	75	46.05	42.71	46.70	0.28	54.87	56.34	5.28	63.12	65.88	0.40
	38	80	44.47	42.13	45.64	0.31	53.82	55.28	5.58			
RG503H	3	56	45.15	42.40	46.56	0.22	51.98	53.49	3.16	56.84	59.61	1.46
	9	60	45.85	43.84	47.94	0.32	54.82	56.45	4.11	60.52	63.34	1.25
	15	63.3	46.84	46.71	48.70	0.26	50.98	53.07	3.47	61.28	64.32	0.94
	21	66.6	46.01	41.77	47.02	0.30	55.83	57.42	4.81	61.70	64.29	0.66
	33	75	47.16	44.26	47.56	0.22	55.47	57.00	5.22	62.88	65.55	0.19
	39	80	46.95	44.79	48.11	0.31	53.41	54.50	5.89			
RG504	4	56	44.28	42.38	45.59	0.18	51.26	52.80	3.59	57.49	60.30	1.57
	10	60	44.67	40.22	44.63	0.33	54.03	55.64	4.44	62.14	64.85	1.20
	16	63.3	45.30	43.59	45.72	0.19	52.84	54.29	4.52	61.11	64.04	0.91
	22	66.6	45.52	42.81	45.44	0.22	55.78	57.13	4.21	63.26	64.67	0.39
	34	75	46.24	43.35	47.68	0.35	55.32	56.67	5.09	64.54	66.72	0.08
	40	80	46.00	44.47	46.53	0.20	55.07	56.45	6.54			
RG752	5	56	44.31	42.98	46.41	0.35	55.32	56.49	7.21			
	11	60	46.24	45.04	48.04	0.30	56.60	58.14	7.24			
	17	63.3	44.98	40.49	46.61	0.35	55.61	57.07	7.46			
	23	66.6	44.72	41.50	46.56	0.40	54.93	56.79	6.60			
	35	75	46.17	45.04	47.42	0.25	55.61	57.00	5.62			
	41	80	44.55	40.11	45.85	0.40	53.92	55.78	7.07			
RG755	6	56										
	12	60	49.46	46.75	50.04	0.27	58.16	59.26	5.86			
	18	63.3	49.05	43.80	49.80	0.51	57.90	59.28	5.64			
	24	66.6	49.57	43.05	50.44	0.34	58.80	60.15	5.71			
	36	75	49.95	46.59	50.20	0.28	57.88	59.18	4.56			
	42	80	50.05	48.32	50.92	0.29	58.85	60.13	6.26			

Appendix 11a. *DSC data of recovered residue from release studies performed at various temperatures. Microspheres prepared with Resomer® various lactide-glycolide copolymers at R104 levels of 44 %w/w total polymer containing 20 %w/w rifampicin*

Polymer	Medium / °C	Transition / °C			ΔCp / Jg^{-1} •°C	Transition / °C		ΔH / Jg^{-1}
		Tg(the)	Tg(on)	$^1/_2$ Cp		Onset	Peak	
RG502	33	36.12	34.46	38.37	0.26	45.23	47.00	3.11
	35	35.54	33.72	37.20	0.25	43.93	46.14	3.21
	37	36.23	34.21	37.11	0.31	44.37	45.98	3.26
	39	37.34	35.53	39.00	0.34	44.47	46.87	4.28
RG503	33	38.56	36.56	40.85	0.34	45.77	50.69	3.57
	35	38.25	36.12	40.35	0.38	47.99	47.99	1.73
	37	37.18	36.00	39.23	0.23	47.00	49.51	2.54
	39	39.35	36.78	41.53	0.41	48.01	50.74	2.67
RG503H	33	37.09	35.67	39.91	0.41	44.08	47.17	2.42
	35	40.21	37.48	43.08	0.45	48.57	52.03	2.48
	37	42.22	39.23	44.20	0.39	46.19	48.34	1.88
	39	40.83	38.74	42.39	0.29	47.75	50.57	2.80
RG504	33	38.63	35.91	38.63	0.30	45.38	50.86	3.74
	35	40.55	38.00	43.15	0.41	48.27	50.24	1.47
	37	39.83	37.11	41.99	0.39	47.00	49.52	2.44
	39	40.02	35.66	41.31	0.38	46.73	49.05	2.26
RG752	33	37.37	34.73	39.82	0.34	44.52	50.36	2.50
	35	40.41	38.01	42.65	0.44	47.14	50.07	2.68
	37	39.23	36.23	40.23	0.41	44.81	48.13	2.74
	39	38.47	36.83	40.70	0.43	44.57	48.21	3.28
RG755	33	42.71	39.68	44.65	0.40	50.31	53.20	4.17
	35	41.07	39.13	44.10	0.38	48.57	51.76	1.13
	37	41.82	39.88	43.98	0.32	47.42	50.70	1.72
	39	39.29	36.71	42.01	0.36	47.39	50.07	0.94

Appendix 11b. *DSC data of recovered residue from release studies performed at various temperatures. Microspheres prepared with various Resomer® lactide-glycolide copolymers at R104 levels of 40 %w/w total polymer containing 20 %w/w rifampicin*

Polymer	Medium / °C	Transition / °C			ΔCp / Jg^{-1} •°C	Transition / °C		ΔH / Jg^{-1}
		Tg(the)	Tg(on)	$^1/_2$ Cp		Onset	Peak	
RG502	33	37.05	34.51	38.80	0.40	43.06	45.96	4.53
	35	38.95	36.59	40.53	0.34	44.16	46.99	3.82
	37	35.84	33.45	36.99	0.31	45.79	48.35	2.23
	39	35.30	32.97	37.28	0.34	41.73	43.85	2.94
RG503	33	33.20	34.51	36.06	0.24	48.19	51.36	4.44
	35	40.62	36.10	42.45	0.44	46.75	51.19	3.10
	37	38.16	36.29	40.09	0.41	46.23	49.19	2.82
	39	37.93	32.80	39.95	0.43	43.80	46.20	1.68
RG503H	33	37.77	34.87	40.22	0.35	45.03	49.00	3.24
	35	40.67	37.41	43.44	0.38	46.05	49.36	2.49
	37	35.87	33.87	42.41	0.34	44.20	45.99	2.75
	39	38.71	32.86	41.43	0.32	43.16	44.85	0.60
RG504	33	40.91	37.98	41.86	0.33	47.09	51.53	4.04
	35	40.52	36.39	41.75	0.30	46.87	51.36	2.57
	37	39.54	34.87	40.76	0.24	46.60	49.33	2.22
	39	38.36	33.00	39.90	0.23	42.65	45.36	1.10
RG752	33	42.24	37.17	43.73	0.48	43.85	47.83	5.45
	35	39.83	37.82	41.92	0.37	45.17	47.17	1.58
	37	37.24	35.89	39.35	0.38	44.47	47.69	2.77
	39	36.32	33.28	38.69	0.39	40.95	44.34	0.84
RG755	33	46.09	41.32	48.04	0.56	51.70	55.40	4.08
	35	47.60	45.55	49.43	0.37	50.10	55.73	2.87
	37	41.12	38.99	45.98	0.40	48.00	51.77	1.93
	39	40.27	34.19	42.57	0.40	46.61	48.89	0.35

Appendix 11c. *DSC data of recovered residue from release studies performed at various temperatures. Microspheres prepared with various Resomer® lactide-glycolide copolymers at R104 levels of 36.6 %w/w total polymer containing 20 %w/w rifampicin*

Polymer	Medium / °C	Transition / °C			ΔCp / Jg^{-1} •°C	Transition / °C		ΔH / Jg^{-1}
		Tg(the)	Tg(on)	$^1/_2$ Cp		Onset	Peak	
RG502	33	31.16	30.98	31.37	26.45	32.02	32.32	2.99
	35	30.25	31.25	31.51	21.21	32.01	32.51	2.21
	37	32.46	32.14	32.75	27.26	32.89	33.15	2.38
	39	31.43	30.95	31.52	26.57	32.25	32.47	2.95
RG503	33	33.90	33.38	33.86	28.46	34.44	34.85	2.81
	35	32.54	30.11	31.25	26.21	32.14	32.12	2.12
	37	31.27	30.75	31.25	26.32	31.75	31.76	2.18
	39	33.09	32.45	33.00	27.70	33.76	34.06	2.01
RG503H	33	33.99	33.48	34.30	28.74	34.75	35.29	2.06
	35	33.10	32.57	33.07	27.54	33.28	33.59	2.57
	37	32.99	32.61	33.61	28.10	33.75	34.40	2.58
	39	33.09	32.38	33.16	27.79	33.72	33.98	2.93
RG504	33	33.82	33.32	33.82	28.42	34.44	34.77	2.63
	35	32.49	32.19	33.07	27.93	33.92	34.24	2.21
	37	32.21	31.81	32.41	27.38	34.03	33.26	2.62
	39	32.89	32.39	33.26	28.23	34.25	34.67	2.60
RG752	33	34.27	34.12	35.04	29.50	35.59	35.98	3.08
	35	31.10	31.10	31.10	31.10	31.10	31.10	3.10
	37	30.45	29.97	30.50	25.706	31.18	31.55	2.99
	39	31.53	31.00	31.58	26.50	32.06	32.51	2.97
RG755	33	37.50	36.98	37.60	31.54	38.02	38.48	3.82
	35	35.24	44.13	44.87	33.76	37.07	39.85	3.39
	37	35.19	34.79	35.40	29.67	35.78	36.26	2.88
	39	34.71	34.39	35.13	29.46	35.34	35.76	2.49

Appendix 11d. *DSC data of recovered residue from release studies performed at various temperatures. Microspheres prepared with various Resomer® lactide-glycolide copolymers at R104 levels of 33.3 %w/w total polymer containing 20 %w/w rifampicin*

Polymer	Medium / °C	Transition / °C			ΔCp / Jg^{-1} •°C	Transition / °C		ΔH / Jg^{-1}
		Tg(the)	Tg(on)	$^1/_2$ Cp		Onset	Peak	
RG502	33	37.57	35.30	39.22	0.39	44.72	46.64	4.28
	35	37.31	34.60	38.83	0.37	44.13	46.16	4.13
	37	35.64	32.61	37.64	0.38	41.92	43.76	3.97
	39	38.13	35.04	39.65	0.41	45.48	47.33	4.36
RG503	33	42.81	19.09	44.02	0.44	49.27	51.86	3.66
	35	40.77	38.04	40.93	0.28	46.30	48.64	2.44
	37	42.14	37.88	44.16	0.47	47.34	49.66	3.13
	39	40.56	37.21	42.76	0.36	47.27	49.64	2.60
RG503H	33	44.60	39.65	45.95	0.46	49.98	52.95	3.67
	35	40.83	37.33	42.62	0.41	46.16	48.98	1.91
	37	44.38	39.04	46.26	0.48	46.68	49.87	3.40
	39	43.89	39.59	44.19	0.31	46.84	49.57	2.53
RG504	33	41.14	38.25	42.42	0.34	46.97	49.39	2.26
	35	41.12	38.24	42.36	0.37	46.51	49.06	2.29
	37	40.51	36.05	42.35	0.43	46.26	49.0	2.26
	39	42.41	38.70	43.98	0.36	47.51	50.24	2.23
RG752	33	42.85	39.496	44.38	0.45	47.54	50.33	3.60
	35	39.45	36.27	41.28	0.44	44.47	46.95	1.66
	37	39.70	36.71	40.72	0.39	44.61	47.45	2.13
	39	40.63	36.93	42.32	0.43	45.14	48.99	3.10
RG755	33	48.50	43.30	49.66	0.41	51.71	54.45	3.31
	35	44.42	40.33	46.28	0.39	49.38	51.57	1.84
	37	47.17	43.51	48.81	0.46	50.23	52.49	1.88
	39	45.87	41.55	47.26	0.39	48.79	52.84	2.23

Appendix 11e. *DSC data of recovered residue from release studies performed at various temperatures. Microspheres prepared with various Resomer® lactide-glycolide copolymers at R104 levels of 25 %w/w total polymer containing 20 %w/w rifampicin*

Polymer	Medium / °C	Transition / °C			ΔCp / Jg^{-1} •°C	Transition / °C		ΔH / Jg^{-1}
		Tg(the)	Tg(on)	$^1/_2$ Cp		Onset	Peak	
RG502	33	38.05	36.22	39.55	0.37	43.28	45.36	4.31
	35	38.60	36.53	39.96	0.36	44.69	46.61	4.50
	37	38.82	36.41	40.23	0.41	44.62	46.61	4.65
	39	39.62	36.67	41.01	0.44	44.72	46.78	4.60
RG503	33	45.54	41.67	46.19	0.36	47.79	50.16	3.09
	35	44.22	41.09	45.65	0.40	47.91	50.16	3.16
	37	45.14	42.84	45.97	0.316	48.71	50.92	3.83
	39	44.56	41.12	46.12	0.44	48.41	50.49	3.02
RG503H	33	44.90	42.43	46.49	0.41	47.86	50.59	3.43
	35	45.27	42.88	46.90	0.40	48.32	50.82	3.29
	37	45.40	42.45	47.19	0.46	49.05	51.51	3.20
	39	45.32	41.42	46.59	0.43	48.22	50.58	2.72
RG504	33	44.63	41.59	45.71	0.37	47.30	49.64	2.88
	35	44.59	42.00	46.04	0.40	47.89	50.16	2.82
	37	46.11	42.80	46.57	0.35	48.38	50.50	2.54
	39	45.84	43.74	46.69	0.33	47.98	50.07	2.73
RG752	33	40.67	38.52	42.90	0.41	47.44	49.74	3.93
	35	43.63	40.94	45.45	0.44	47.06	49.91	1541
	37	42.46	39.80	43.84	0.40	47.01	49.41	2.74
	39	41.51	38.22	41.90	0.33	46.31	48.90	2.53
RG755	33	44.57	41.55	46.92	0.41	49.44	47.25	1642
	35	47.66	44.76	49.08	0.34	50.94	53.34	3.15
	37	48.60	45.50	50.32	0.39	51.72	53.77	3.18
	39	48.43	43.26	48.81	0.38	51.40	53.35	3.09

Appendix 11f. *DSC data of recovered residue from release studies performed at various temperatures. Microspheres prepared with various Resomer® lactide-glycolide copolymers at R104 levels of 20 %w/w total polymer containing 20 %w/w rifampicin*

Polymer	Medium / °C	Transition / °C			ΔCp / Jg^{-1} •°C	Transition / °C		ΔH / Jg^{-1}
		Tg(the)	Tg(on)	$^1/_2$ Cp		Onset	Peak	
RG502	33	39.26	35.76	40.51	0.45	44.38	47.32	6.29
	35	39.51	38.83	42.23	0.38	45.79	48.35	2.23
	37	38.71	34.23	40.89	0.41	44.22	45.98	6.24
	39	39.14	35.02	39.97	0.35	43.32	45.54	4.91
RG503	33	44.96	41.78	45.61	0.35	51.34	53.05	5.29
	35	44.32	42.41	46.62	0.39	46.23	49.19	2.82
	37	40.70	39.81	41.70	0.30	48.11	49.70	4.24
	39	43.26	35.43	44.57	0.44	46.70	48.75	4.81
RG503H	33	46.04	39.90	47.59	0.46	50.83	53.83	4.91
	35	41.99	39.21	43.11	0.34	44.20	45.99	2.75
	37	40.31	38.40	42.26	0.31	47.48	50.02	3.54
	39	41.94	37.53	43.93	0.40	46.10	48.91	2.89
RG504	33	45.42	41.04	45.89	0.35	52.01	53.71	5.37
	35	45.49	42.88	47.20	0.31	46.60	49.33	2.22
	37	44.63	42.11	46.61	0.29	48.89	50.37	4.13
	39	44.51	40.49	46.12	0.43	46.03	47.69	2.43
RG752	33	48.45	45.04	49.25	0.37	55.65	57.24	4.98
	35	40.92	39.32	43.20	0.32	44.47	47.69	2.77
	37	41.23	39.00	43.10	0.30	46.70	49.70	4.17
	39	40.90	37.55	42.42	0.42	44.74	47.38	2.05
RG755	33	42.42	38.03	44.24	0.47	51.70	53.70	5.98
	35	48.11	45.23	49.23	0.38	48.40	51.77	1.93
	37	47.97	44.23	48.97	0.34	51.51	53.07	4.04
	39	47.26	43.18	48.76	0.30	49.80	51.59	2.89

Appendix 11g. *DSC data of recovered residue from release studies performed at various temperatures. Microspheres prepared with various Resomer® lactide-glycolide copolymers at R104 levels of 10 %w/w (batch #25 - 28) and 30 %w/w (batch #29 & 30) total polymer containing 20 %w/w rifampicin*

Polymer	Medium / °C	Transition / °C			ΔCp / Jg^{-1} •°C	Transition / °C		ΔH / Jg^{-1}
		Tg(the)	Tg(on)	$^1/_2$ Cp		Onset	Peak	
RG502	33	39.80	35.80	41.12	0.47	44.28	46.99	6.93
	35	40.58	36.25	41.81	0.46	42.00	44.80	1.67
	37	37.93	36.10	39.83	0.41	44.02	45.99	6.44
	39	42.47	39.80	44.39	0.34	47.82	49.57	3.07
RG503	33	45.18	40.79	46.51	0.43	52.41	53.88	6.44
	35	47.53	45.31	48.43	0.27	52.13	53.70	4.79
	37	44.72	43.82	46.34	0.26	48.35	49.68	4.87
	39	44.86	41.74	45.20	0.22	47.18	48.73	4.10
RG503H	33	47.32	44.56	48.39	0.34	53.04	54.38	5.85
	35	45.40	43.12	46.43	0.31	51.40	52.86	5.83
	37	40.12	39.23	44.21	0.34	48.90	50.37	4.71
	39	35.22	35.29	39.08	0.37	42.78	44.85	5.57
RG504	33	45.70	41.90	46.44	0.33	52.02	53.53	6.03
	35	46.40	43.55	47.66	0.32	52.38	53.70	5.34
	37	43.72	42.80	47.03	0.32	48.46	49.85	4.63
	39	45.84	42.33	46.74	0.30	46.99	48.73	4.10
RG752	33	42.66	39.87	44.25	0.40	51.00	53.19	4.94
	35	42.98	39.82	44.37	0.40	48.43	50.36	2.81
	37	40.17	37.82	42.11	0.39	48.45	47.23	2.10
	39	38.02	35.99	40.14	0.37	43.31	45.36	1.53
RG755	33	48.01	43.68	49.40	0.40	54.73	56.40	4.41
	35	49.20	46.91	50.26	0.27	55.50	56.90	3.35
	37	46.13	44.23	49.11	0.42	50.72	52.39	3.12
	39	44.68	41.58	47.06	0.41	48.85	50.57	1.62

Appendix 12. *Effect of polymer composition on the Arrhenius derived activation energies of initial drug release using method B from microsphere prepared from various blends of Resomer® R104 and lactide-glycolide copolymers*

			Mean			RSD		
Compl. polymer	**Batch**	**R104 / (%w/w)**	**E_a / kJ**	**r^2**	**ln A**	**E_a**	**r2**	**ln A**
RG502	1	44	113.1	0.236	46.99	34.5	63.1	31.5
	7	40	155.9	0.586	63.57	18.6	8.04	18.0
	13	36.6	75.92	0.764	31.87	17.1	0.94	16.0
	19	33.3	113.9	0.932	46.63	6.74	7.06	6.24
	31	25	66.94	0.847	28.34	23.5	18.4	21.8
	37	20	111.9	0.846	43.62	5.46	9.45	3.65
RG503	2	44	131.3	0.632	54.2	32.2	28.5	30.4
	8	40	206.5	0.672	83.4	16.8	28.2	16.3
	14	36.6	74.46	0.156	31.0	5.42	12.3	5.19
	20	33.3	110.9	0.684	45.3	4.13	10.3	3.96
	33	25	101.6	0.985	41.1	1.61	1.68	1.52
	39	20	90.83	0.971	32.6	5.82	2.58	6.38
RG503H	3	44	211.3	0.811	85.27	15.15	5.65	14.80
	9	40	119.4	0.270	48.94	25.5	69.8	24.8
	15	36.6	135.4	0.962	54.55	2.25	0.57	2.30
	21	33.3	149.4	0.961	59.94	1.48	4.43	1.40
	33	25	97.85	0.866	38.86	22.2	0.34	21.6
	39	20	71.27	0.986	28.33	2.01	0.30	2.03
RG504	4	44	188.4	0.863	76.33	2.10	2.54	1.97
	10	40	154.4	0.668	63.23	25.4	32.6	24.4
	16	36.6	224.8	0.994	89.49	14.4	0.20	13.9
	22	33.3	149.3	0.990	60.41	1.53	1.10	1.49
	34	25	167.3	0.751	67.04	56.9	31.9	55.2
	40	20	81.31	0.06	33.03	17.9	9.52	16.8
RG752	5	44	243.8	0.920	79.14	9.04	1.16	29.6
	11	40	289.9	0.859	169.1	86.4	0.40	0.36
	17	36.6	227.3	0.918	90.07	1.82	0.38	1.73
	23	33.3	113.0	0.654	45.77	0.49	47.8	0.32
	29	25	219.5	0.471	83.06	1.92	7.42	1.92
	41	20	99.84	0.988	36.71	14.1	1.00	14.4
RG755	6	44	130.9	0.781	53.09	0.98	17.6	0.96
	12	40	127.8	0.932	74.35	85.4	3.39	3.98
	18	36.6	101.7	0.525	41.18	56.6	63.8	54.2
	24	33.3	49.64	0.770	26.50	94.5	21.7	29.5
	36	25	76.19	0.902	32.84	3.96	2.78	3.48
	42	20	38.62	0.095	-11.67	64.9	107	-84.4

Appendix 13. *Effect of storage time on the biexponential coefficients of drug release using method B from microsphere prepared with 25 %w/w R104 and a range of Resomer® lactide-glycolide copolymers (data fitted to equation 8.1)*

			Biexponential coefficients					**Quartile release / h**		
Batch	**Polymer**	**Time**	**A / %**	**α / h^{-1}**	**B / %**	**β / h^{-1}**	**r^2**	**25 %**	**50 %**	**75 %**
31	RG502	14	78.76	11.16	15.83	0.439	0.997	0.024	0.073	0.181
		40	80.04	11.55	14.27	0.539	0.995	0.023	0.069	0.166
		120	76.44	7.785	14.96	0.330	0.992	0.030	0.102	0.259
32	RG503	14	49.97	5.469	47.78	0.027	0.996	0.111	0.581	23.30
		40	55.85	4.940	40.69	0.028	0.997	0.099	0.358	19.73
		120	63.61	4.882	35.20	0.027	0.998	0.096	0.298	13.90
33	RG503H	14	43.58	2.399	54.15	0.047	0.997	0.293	1.980	16.35
		40	53.61	3.587	43.61	0.033	0.997	0.159	0.627	16.66
		120	62.53	2.117	35.49	0.045	0.989	0.215	0.667	7.781
34	RG504	14	54.83	8.337	38.91	0.024	0.995	0.050	0.190	18.56
		40	58.81	7.332	35.78	0.017	0.996	0.055	0.192	20.74
		120	62.64	7.077	33.50	0.017	0.998	0.059	0.190	17.87
35	RG752	14	17.46	23.76	77.93	0.271	0.999	0.162	1.640	4.2015
		40	18.78	23.43	76.65	0.251	0.998	0.134	1.704	4.467
		120	22.53	8.803	72.31	0.342	0.997	0.171	1.086	3.096
36	RG755	14	18.54	25.75	77.52	0.004	0.976	7.956		
		40	18.37	23.24	77.10	0.004	0.969	7.207		
		120	18.95	16.71	78.01	0.007	0.984	6.472		

Supporting studies

The following activities were undertaken in association with the program of research in partial fulfilment of the requirements for the degree of Doctor of Philosophy.

1. Participation in various 'Research Methods' courses at The Robert Gordon University, session 1995-96.

2. Participation in 'Using Microsoft Word' course. The Robert Gordon University, June, 1995.

3. Participation in 'Using Microsoft Excel' course. The Robert Gordon University, August, 1995.

4. Participation in 'SPSS for Windows' course. The Robert Gordon University, January, 1996.

5. Visit to Knoll Pharmaceuticals, November 1995 and December 1996 to discuss project progress with external advisor, Dr A. Smith.

6. Visit to Knoll Pharmaceuticals, September 1998 to review and discuss thesis progress with Dr A. Smith.

7. Visit to St Andrews University for X-ray studies, October, 1997.

8. Attendance, poster and oral presentation, both entitled *Preparation of rifampicin-loaded biodegradable microspheres*, at The Third European Congress of Pharmaceutical Sciences, Edinburgh, 15 - 17 September, 1996

9. Attendance at The 133rd British Pharmaceutical Conference Symposium entitled Tuberculosis, Glasgow, 10 - 11 September, 1996.

10. Attendance and oral presentation entitled *Spray-dried blends of biodegradable polymers to modulate drug release* at The 134th British Pharmaceutical Conference. Scarborough, 15 - 18 September, 1997.

11. Attendance and poster presentation entitled *Effect of residual solvent on the characteristics of biodegradable microspheres prepared by spray-drying* at The Fifth European Symposium on Controlled Drug Delivery, Leiden, April 1998.

12. Attendance and poster presentation entitled *Thermal studies on spray-dried biodegradable microspheres prepared from various solvents* at The 135th British Pharmaceutical Conference, Eastbourne, 8 - 11 September, 1998.

Communications associated with this thesis

D.F. Bain, D.L.Munday and P.J. Cox. Preparation of rifampicin-loaded biodegradable microspheres. *Eur. J. Pharm. Sci.*, 1996, **4**, S158.

D.F. Bain, D.L.Munday, P.J. Cox and A. Smith. Spray-dried blends of biodegradable polymers to modulate drug release. *J. Pharm. Pharmacol.*, 1997, **49**, Suppl 4, 75.

D.F. Bain, D.L.Munday and A. Smith. Mechanisms of rifampicin release from spray-dried blends of biodegradable poly(D,L-lactide) for intra-pulmonary administration. *Second World Congress of Pharmaceutics, Biopharmaceutics and Pharmacokinetics*, Paris, May 1998.

D.F. Bain, D.L.Munday and A. Smith. Effect of residual solvent on the characteristics of biodegradable microspheres prepared by spray-drying. *Proceedings of the Fifth European Symposium on Controlled Drug Delivery*, Leiden, April 1998.

D.F. Bain, D.L.Munday and P.J. Cox. Evaluation of biodegradable rifampicin-bearing microsphere formulations using a stability-indicating high-performance liquid chromatographic assay. *Eur. J. Pharm. Sci.*, 1998, **7**, 57-65.

D.F. Bain, D.L.Munday and A. Smith. Modulation of rifampicin release from spray-dried microspheres using combinations of poly(D,L-lactide). *J. Microencap.* in press.

D.F. Bain, D.L.Munday and A. Smith. Solvent influence on spray-dried biodegradable microspheres. *J. Microencap.* in press.

D.F. Bain, D.L.Munday and A. Smith. Thermal studies on spray-dried biodegradable microspheres prepared from various solvents. *J. Pharm. Pharmacol.*, **50**, 161.

P2.001 **PREPARATION OF RIFAMPICIN-LOADED BIODEGRADABLE MICROSPHERES**

D F Bain*, D L Munday, P J Cox

School of Pharmacy, The Robert Gordon University, Schoolhill, Aberdeen, AB9 1FR, UK

Rifampicin is often taken orally over prolonged periods for the treatment of mycobacterial infections. However compliance is poor, resulting in treatment failure and drug resistance. To overcome this problem, biodegradable polylactide(PLA) and polylactide-co-glycolide(PLGA) may be useful in the development of controlled release parenterals containing antimycobacterial drugs. Rifampicin-loaded microspheres were produced utilising a solvent evaporation technique. This work examines the effect of process variables on microsphere characteristics and *in vitro* release. Efforts to maximise rifampicin loading included presaturation of continuum, optimisation of pH and adjustments to phase volumes and drug:polymer(D:P) ratios. A continuum of unbuffered 1% polyvinyl alcohol at pH 5.0 minimised partitioning of dispersed rifampicin into the continuum. By adjustment of continous:disperse phase volume ratio to 3:1, loadings of 35%w/w were achieved at a D:P ratio of 1:1. When comparing microspheres prepared with drug free continuum, presaturation had a significant effect on loading depending on D:P ratio. At D:P 0.2:1, loading increased threefold, whereas at D:P 1:1 loading paradoxically decreased. This was due to dissolution of crystals formed at the surface during evaporation at the stage of microsphere washing. With increasing D:P ratio there was an associated sharp increase in both initial 'burst' and overall release rate. Scanning electron micrographs show a porous microsphere surface accounting for these observations. After a modest 'burst' of ≅ 15% loaded rifampicin (D:P ratio 0.2:1) release was sustained for about 30 days. These profiles were observed for both PLA and PLGA, release being faster from the latter. Microsphere size was largely independent of process variable (30-100µm), PLGA prepared microspheres being consistently smaller than PLA for comparable conditions. In conclusion, PLGA/PLA microspheres with suitable surface characteristics and release profiles were prepared using low D:P ratios. Efforts to maximise loading in order to minimise dose volume have resulted in predominantly 'burst' with little sustained release.

45 SPRAY-DRIED COMBINATIONS OF BIODEGRADABLE POLYMERS TO MODULATE DRUG RELEASE

DF Bain, DL Munday, PJ Cox and A Smith* School of Pharmacy, The Robert Gordon University, Schoolhill, Aberdeen, AB10 1FR.

*Knoll Pharmaceuticals, Pharmaceutical Development R4, Pennyfoot Street, Nottingham, NG1 1GF.

Spray-dried biodegradable poly(DL-lactide) (PDLA) microspheres frequently exhibit considerable 'burst' release, particularly at high drug loadings. Use of slowly degrading polymers results in a reduced 'burst' but with a protracted terminal release phase. The permeability of these polymers can be increased by incorporating channelling agents (Latha and Sapna, 1993). An alternative approach whereby the release of rifampicin, as a model drug, has been modulated by varying the proportions of low and moderate molecular weight PDLA was examined. This technique, which avoids the use of potentially toxic release-controlling excipients, has previously been applied to films and solvent-evaporated microspheres (Bodmeier et al., 1989) with a PDLA of MW 120,000. However, this approach has hitherto not been examined using spray-drying.

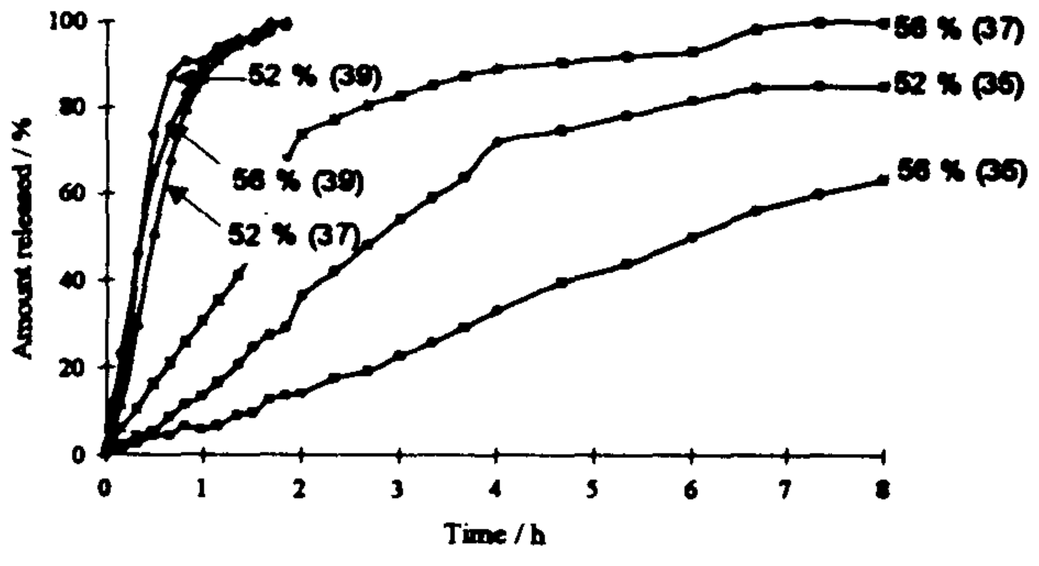

Figure 1. Release profiles using method B at two levels of R202H (temperatures in °C in parentheses)

Microspheres containing 20% w/w rifampicin were prepared by spray-drying a solution (3% w/v total solid) of combinations of Resomer® R104 (MW 2000) and R202H (MW 9000) in the % ratios 90:10, 80:20, 60:40, 56:44, 52:48, 48:52, 44:56, 40:60, 20:80 and 10:90 through the nozzle of a spray-drier (Buchi model B191): inlet temp. 40°C; flow rate 600 NL/h. Dissolution studies in pH 7.4 phosphate buffer were performed at different temperatures comparing two methods: shaking bath (method A) and USP paddle (method B). Surface morphology and thermal behaviour before and after dissolution (method A) were examined using SEM and DSC respectively.

Method B achieved similiar but dramatically faster dissolution profiles compared with method A. This was attributed to the considerably greater agitation afforded by the former. Dissolution studies showed a dramatic change in drug release particularly between 52 and 56 w/w R202H (Figure 1). Furthermore, drug release rate showed a remarkable dependence on temperature (Figure 1) as illustrated by the microspheres containing 56% R202H which approximated to zero order (r^2=0.969), first order (r^2=0.981) and biexponential release (r^2=0.991) at 35, 37 and 39°C respectively. DSC gave slight, but progressive increases in melting onsets between 10 and 90 % R202H of 55.3-58.7°C before dissolution However the corresponding values, most notably for 52 and 56% R202H, were 34 and 51°C after dissolution (7 days) respectively. The reduced onset of melting when 52% R202H was used was attributed to the hydrolysis of R104, indicated by a broad endotherm corresponding to oligomeric fractions of this polymer. With 56% R202H, a secondary peak superimposed on the R104 oligomeric peak corresponding to higher MW R202H, indicated preservation of matrix integrity. The proposed mechanism of polymer hydrolysis, and softening of the microsphere matrix was supported by SEM after dissolution. From SEM, the absence of surface roughening or reduction in microsphere size ruled out erosion as a significant contribution to the release. These data highlight the criticality of matrix composition and the role of temperature to the release mechanism. Moreover, the utility of low MW PDLA fractions to modulate release i.e. reduce 'burst' whilst maintaining acceptable release from spray-dried biodegradable particles is highlighted.

Latha L. and Sapna K. (1993) J. Microencap. 10(1), 466-80
Bodmeier R., Oh K.H. and Chen H. (1989) Int. J. Pharm., 51, 1-8

Fifth European Symposium on Controlled Drug Delivery

EFFECT OF RESIDUAL SOLVENT ON THE CHARACTERISTICS OF BIODEGRADABLE MICROSPHERES PREPARED BY SPRAY-DRYING

D.F. Bain[1], D.L. Munday[1] and A. Smith[2]

[1] *School of Pharmacy, The Robert Gordon University, Aberdeen, AB10 1FR, United Kingdom*

[2] *Knoll Pharmaceuticals, Pennyfoot Street, Nottingham, NG1 1GF, United Kingdom*

Introduction

Spray-drying has emerged in recent years as a convenient one-step procedure for producing microspheres of predictable drug loading and release characteristics[1]. Typically, however, this procedure results in reduced product yields when compared with traditional emulsification-solvent-evaporation as a preparative technique[2]. We have demonstrated that with judicious choice of organic solvent and processing conditions, yields in excess of 66% w/w theoretical can be consistently achieved at the expense of high residual solvent loads. Reports of residual solvent have considered only the toxicological consequences[3, 4], using USP limits as markers of acceptability[4]. No reports exist of the influence of residual solvent on the physicochemical characteristics of biodegradable microspheres.

The purpose of this work is to demonstrate the influence of the solvent choice on the microsphere characteristics prepared by spray-drying blends of biodegradable poly-(D,L-lactide). Blends of polymer have been previously shown to readily modulate rifampicin (RIF) release from microspheres thus prepared[1].

Experimental Methods

Materials, poly(D,L-lactide) Resomer® R104 (MW=2000) and R202H (MW=9000) were purchased from Boehringer Ingelheim (Ingelheim, Germany). Rifampicin was gifted by Lepetit (Milan, Italy). All other chemicals were of reagent grade or better. Microspheres were prepared from co-solutions (3 % w/v total solid) comprising 24 % w/w R104, 56% w/w R202H and 20% w/w RIF, which were sprayed through the nozzle of a Buchi® Minispray-drier (Flawil, Switzerland) according to Table 1 at a constant flow rate of 600 $NL.h^{-1}$. Microspheres were vacuum dessicated and characterized at predetermined intervals as follows. Thermal characteristics of the microspheres and residual solvent were examined by DSC (Pyris 1, Perkin Elmer, Connecticut, USA) at a scanning rate of 10 °C min^{-1} and gravimetrically respectively. Release of RIF was studied using the USP paddle method (Sotax AT7, Basel, Sweden) in 500 cm^3 Sørensens buffer (pH 7.4) (modified) containing 0.1% w/v 'Tween' 80 at 37 °C at 100 rpm with UV detection at 330 nm (the isobestic point of RIF and its major quinone degradation product).

Table 1. Preparation conditions for spray-drying

Batch	Solvents		Spray parameters		Yield/ g
	Type	Ratio	Inlet temp / °C	Aspiration / %	(1.5g total)
1	DCM	100%	40	100	0.93
2	DCM:ACT	2:1	40	100	0.32
3	DCM:ACT	2:1	40	50	0.03
4	ACT	100%	40	100	0.03
5	DCM:CFM	1:1	40	100	0.84
6	DCM:CFM	1:1	50	100	0.62
7	CFM:ACT	2:1	40	100	0.54

Key: DCM. dichloromethane; ACT. acetone; CFM. chloroform

Results and Discussion

The release profiles in Figure 1 and Figure 2 of microspheres prepared with compositionally identical polymer blends highlight the dramatic influence of solvent and storage period respectively on their release characteristics. The results are explained below in terms of the mechanism of microsphere formation and the plasticizing action of residual solvent, amounts of which are listed in Table 2. Thermograms in Figure 3 revealed no discernable thermal events for freshly prepared products, whereas upon dessication an endotherm rapidly developed, the magnitude of which was time-dependent. Moreover, the position of this endotherm and the underlying glass transition, Tg, shifted upscale as the plasticizing action of residual solvent diminished with increased storage time. Residual solvent load, determined the magnitude of this shift, which in parallel increased as the boiling point of the solvent system increased and, in contrast, the drying temperature decreased.

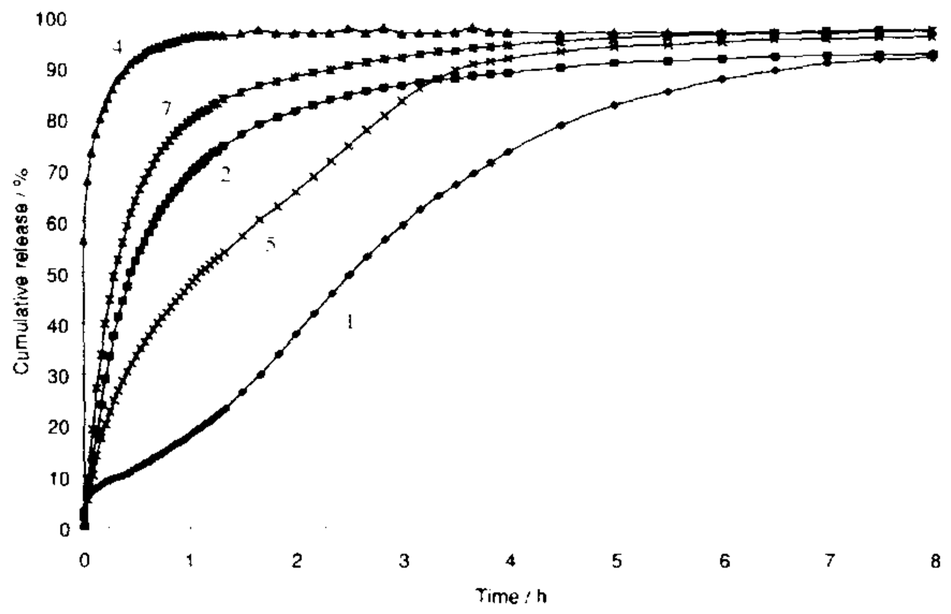

Figure 1. Release profiles of RIF from microspheres freshly prepared from different solvents (adjacent legend indicates batch reference)

The thermal behaviour of blends of low and moderate MW PDLA has been identified as a critical determinant of drug release[1]. Other important factors include matrix hydrophilicity and structure. For compositionally identical microspheres, intrinsic hydrophilicity should however remain ostensibly constant. Thus, the differences in release of RIF with change in process conditions can be attributed to variation in matrix architecture and thermal characteristics. Upon incubation, microspheres slowly hydrate. Water ingresses slowly, causing matrix softening until the softening temperature corresponds to that of the dissolution medium, when water uptake accelerates promoting drug release. This mechanism accounts for the sigmoidal release pattern in Figure 2 from microspheres stored for 10 days prepared with DCM and DCM:CFM blends. These comprised induction, accelerated and slow terminal phases. For drug release in Figure 1, however, from microspheres immediately after preparation with high residual solvent (Batch 1 & 5), the softening temperature was close, if not below that of the dissolution medium, resulting in a rapid burst with a short induction period. However, as residual solvent is lost under vacuum, the burst reduces and the induction period lengthens as polymer chain rearrangement creates an ordered structure, elevating the Tg, which retards RIF release. In contrast, release from microspheres prepared from ACT was independent of storage time, release accelerating as the proportion of the ACT used in the microsphere preparation increased (batch 2 c.f 4).

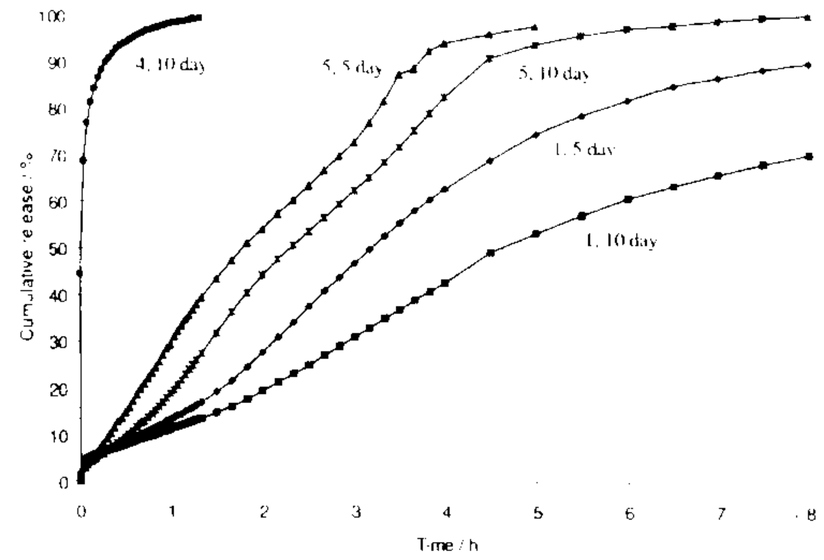

Figure 2. Effect of storage time on RIF release
(legend indicates batch reference and period of storage)

Solvent choice and drying temperature affects the microsphere structure through their influence on solvent evaporation rate, which, in turn, affects matrix deposition rate. In general terms, highly volatile ACT rapidly evaporates to yield microspheres with a highly porous structure which also explains the low solvent residue measurements and the rapid release from these formulations irrespective of storage time. In contrast, reduced microsphere formation rate with CFM or DCM, particularly at lower inlet temperatures, results in a more coherent matrix. High matrix tortuousity thus formed explains their tenacious retention of organic solvent and the correspondingly slower release of RIF therefrom. The high solvent residue does however facilitate molecular mobility within the matrix allowing greater order to be achieved during solvent removal. This feature further attributes for the slower release rate from microspheres with high original residual solvent, which accelerates release initially, before dessication, through a matrix plasticizing action. Progressive elevation of the softening temperature is paralleled by an increase in the induction period. This feature is consistent with the mechanism of drug release described above.

Table 2. Residual solvent analysis

Batch	Residual solvent / ppm x 10^{-3}		
Storage/day	0	5	10
1	39.43	19.47	1.022
2	2.460	1.406	0.626
3	2.457	1.307	0.507
4	1.219	0.719	0.456
5	36.91	8.017	2.697
6	26.14	7.019	2.180
7	34.26	9.012	1.483

Variation in yield of production can be attributed to microsphere architecture, solvent residue and the Tg of the microsphere matrix. Rapid solvent evaporation of ACT produces low density porous particles with low solvent load which are readily exhausted from the apparatus. High solvent residue lowers the Tg which would promote product adherence to the glassware were it below that of the drying air. In contrast, high solvent residue is associated with formation of a more coherent matrix with a greater density which reduces the proportion of particles exhausted from the glassware, whilst promoting particle deposition in the apparatus collector. Considerable residue of relatively dense solvents such as CFM and DCM, further contributes to individual particle density and promotes high microsphere yields.

The results in Table 1 and the release profiles noted in Figure 2 support this pattern of product formation and yield which collectively indicate high product yields are promoted at the expense of considerable solvent loads. However, prolonged drying can effectively lower these to acceptable levels[3].

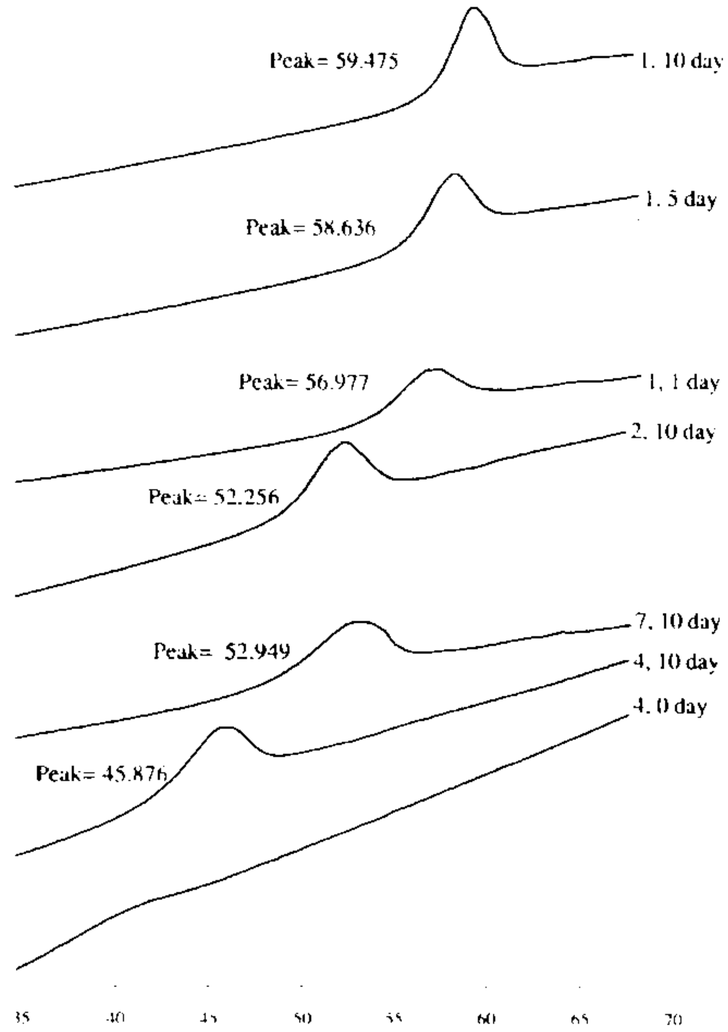

Figure 3. Thermograms after various storage times
(legend indicates batch, storage time) Peak temperature in ^0C

Conclusion

Moderate evaporation rates provided by DCM appear to promote the formation of coherent microspheres with relatively slow release rate whilst providing high product yield. The effect of high solvent residue on microsphere release character might however result in erroneous conclusions being drawn where adequate dessication has not been perfomed. Overall, solvent choice for spray-drying has a considerable influence on final microsphere characteristics and should be carefully considered from both a technological in addition to a traditional toxicological view point.

Acknowledgement

The financial support of Knoll Pharmaceuticals is gratefully acknowledged.

References

1. Bain D.F, Munday D.L., Cox P.J., and Smith A. J. Pharm. Pharmacol., 49, (S4), 29, 1997.
2. Pavanetto F., Conti B., Genta I, & Giunchedi P., Int J Pharm, 84, 151-159, 1992.
3. Bitz C. & Doelker E. Proc. 1st World Meeting APGI/APV, Budapest, 409-410, 1995.
4. Rafler G. & Jobmann M., Drugs made in Germany, 37(4), 115-119, 1994.

MECHANISMS OF RIFAMPICIN RELEASE FROM SPRAY-DRIED BLENDS OF BIODEGRADABLE POLY(D,L-LACTIDE) FOR INTRA-PULMONARY ADMINISTRATION

D.F. Bain[1], D.L. Munday[1] and A. Smith[2]

[1]School of Pharmacy, The Robert Gordon University, Aberdeen, United Kingdom
[2]Knoll Pharmaceuticals, Pennyfoot Street, Nottingham, United Kingdom

Introduction

Rifampicin (RIF), in combination with other anti-mycobacterials, represents the mainstay of effective tuberculosis therapy. However, hepatotoxicity can limit its application when administered systemically[1]. Biodegradable drug-loaded microspheres have been investigated as a technique to target chemotherapeutics to the lung whilst providing a sustained release and thus therapeutic action[2]. Spray-drying is emerging as a convenient one-step continuous procedure for reproducibly preparing large quanitiies of microspheres of predictable character and drug loading[3]. Moreover, the granulometry of these products renders them ameniable to alveolar penetration, allowing a reduction in dosage and fewer systemic side-effects[2]. Previously we demonstrated the utility of blends of poly(D,L-lactide) (PDLA) as a means to reduce the 'burst' of drug release, and accelerate the terminal phase characteristic of low and high molecular weight PDLA respectively, when used individually[3]. The mechanism of drug release from these hydrophilic matrix systems is considered here.

Experimental

Materials

Poly(D,L-lactide) Resomer® R104 and R202H were purchased from Boerhinger Ingelheim (Ingelheim, Germany). Rifampicin was gifted by Lepetit® (Milan, Italy). All other chemicals were of reagent grade or better.

Methods

Microsphere preparation

Co-solutions in dichloromethane (DCM) of R104 and R202H containing 20% w/w dissolved RIF were sprayed through the nozzle of a Buchi® Minispray-drier (Flawil, Switzerland) according to Table 1 under the conditions: Inlet temp., 40°C; Outlet, 35°C, Aspiration, 100%; flow rate, 600 NL h^{-1}. Microspheres were vacuum dessicated before characterization.

Microsphere characterization

Thermal behaviour of microspheres was examined by DSC at a scanning rate of 10°C min^{-1} (Pyris 1, Perkin Elmer, Connecticut, USA). Release of RIF was studied using the USP paddle method (Sotax AT7, Basel, Sweden) in 500 cm^{-3} Sorensens buffer (pH 7.4) (modified) containing 0.1% 'Tween' 80 between 33-39°C at 100 rpm. Residual microspheres post-dissolution were recovered by filtration and also thermally characterized. Hydration studies were performed gravimetrically on recovered microspheres. Microsphere granulometry was determined by Coulter Multisizer (Coulter Electronics Ltd., Luton, UK).

Table 1. Composition of 20% w/w RIF-loaded microspheres

Batch	Polymeric composition / (%w/w)	
	R104	R202H
1	36	64
2	32	68
3	31	69
4	30	70
5	29	71
6	28	72
7	24	76
8	20	80

Results and Discussion

Particle size distributions typical of the technique were relatively monodisperse, with mean diameter, d_{50}, increasing from 2.6-3.3 μm as the proportion of R202H increased. In addition, 90% of particles were <10 μm, independent of the encapsulating polymer blend. These coincided with the target range of 0.5-3.0 μm for alveolar deposition[2].

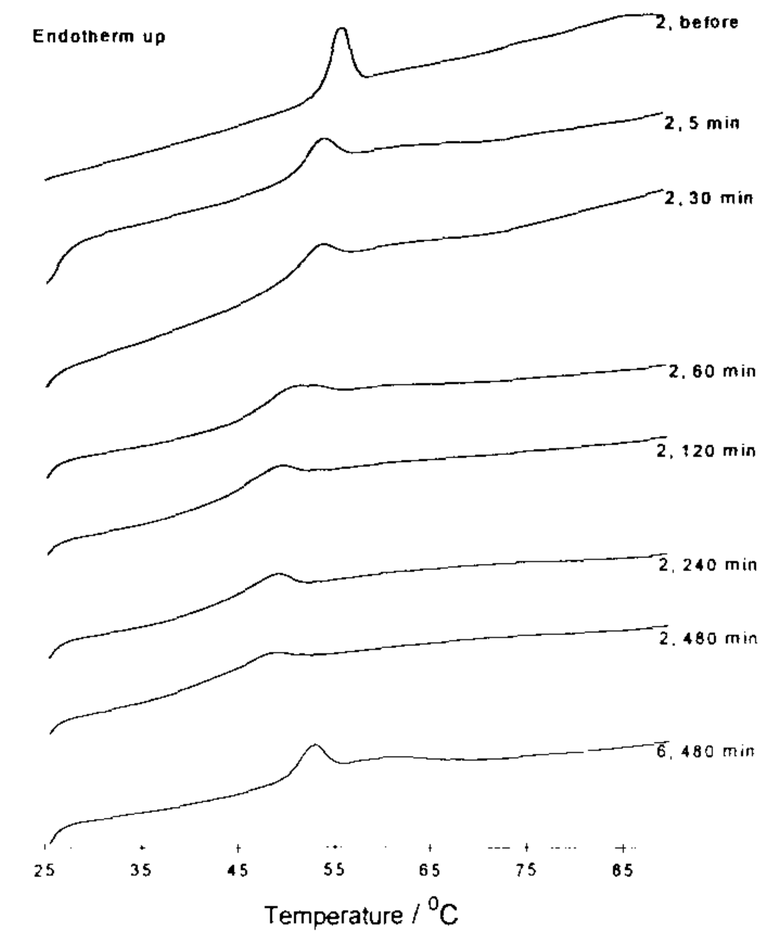

Figure 1. DSC thermograms of microspheres (legend indicates batch, time of dissolution)

Proc. 2nd World Meeting APGI/APV, Paris, 25/28 May 1998

The utility of combinations of low and moderate molecular weight PDLA to modulate release of RIF microspheres has been established[3]. The criticality of matrix composition and other experimental variables on drug release within a narrow range of polymer composition was, however, highlighted in that work. A number of factors have been cited as promoting drug release by diffusion including 1) depression of glass transition, (Tg), of the polymer network; 2) pore formation and; 3) polymer degradation which itself promotes 1) and 2) above. Matrix hydration associated with these changes accelerates the flux of entrapped drug molecules when compared with diffusion through an amorphous dehydrated network.

Figure 1 shows the thermograms of microspheres following 14 days vacuum dessication. Typical thermograms registered a glass transition underlying an endothermic peak representing formation of a structured order within the matrix which developed as residual DCM was removed.

Figure 2 shows the release profiles from microspheres at 37^{0}C. Minor changes in polymer composition showed a significant effect on drug release rate around a critical composition.

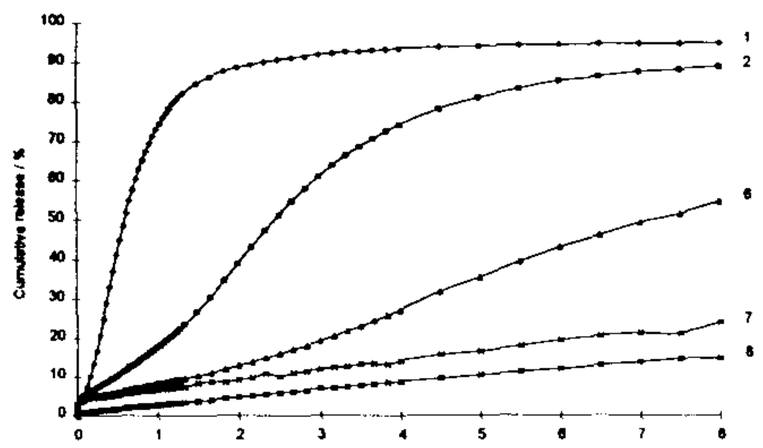

Figure 2. Release profiles for microspheres at 37^{0}C

The modulation of release rate by this technique was attributed to modification of the rate and delay in hydration of the matrix with minor variation in matrix composition. As water ingresses the thermal character of the polymer changes with the plasticizing action of water and the matrix softens. Once the softening temperature, Tg, of the matrix decreases below the temperature of the release medium, water uptake accelerates promoting release by diffusion. This proposed mechanism is supported by the sigmoidal release patterns, whereby after an initial induction period, further water uptake propogates water penetration deep into the microsphere matrix. In figure 1, the time-dependent destruction of the ordered matrix structure is indicative of increased hydration. However, with batch 6, the endothermic peak persisted indicating partial preservation of matrix integrity. These data are corroborated by the hydration data in Figure 3.

Acknowledgement
The financial support of Knoll Pharmaceuticals is gratefully acknowledged.

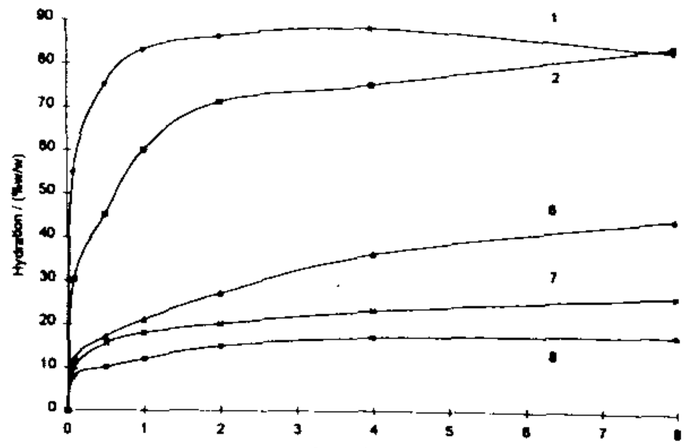

Figure 3. Hydration data for microspheres during dissolution at 37^{0}C (batch adjacent to each line)

The importance of matrix softening and hydration to the release mechanism was further supported by the first order release rate constants at different dissolution medium temperatures listed in Table 2. These data showed the anticipated pattern of increased release rate as temperature and proportion of low MW PDLA increased. The dramatic multi-fold increase in the fractional rate constant occurred at higher temperatures as the proportion of higher MW and hydrophobic R202H increased which is commensurate with increases in matrix Tg . However, the Tg of the samples assessed did not correspond with the temperature of the dissolution medium. During dessication, the Tg partially recovered upon removal of aqueous plasticizer. Further thermal studies of hydrated samples are therefore required to confirm the correspondence of accelerated drug release with matrix softening.

Table 2. First order release data for selected microsphere blends

	1st order rate constant* (x10^2) / h^{-1}			
Temp / ^{0}C	33	35	37	39
Batch				
1	1.35	11.05	122	505.5
2	1.19	7.69	32.80	142.8
3	0.903	4.83	33.40	119.1
4	0.461	4.55	23.25	98.80
5	0.942	2.075	21.25	79.55
6	0.880	2.855	17.00	79.55
7	0.605	2.19	2.64	11.70
8	0.237	0.995	1.995	7.87

$r^2 \geq 0.980$, (10 - ≤ 80% release)

Conclusion

Microspheres of the required granulometry for intra-pulmonary delivery were readily prepared by spray-drying. The auto-hydration mechanism linked to the Tg of the hydrophilic microspheres should facilitate and provide controlled drug release in the low volume of liquid which prevails in the lung.

References

1. Girling D.J. *J. Antimicrob Chemother*, 3, 115-32, 1977.
2. El-Baseir M.M., Phipps M.A. and Kellaway I.W. *Int. J. Pharm.*, 151, 145-153, 1997.
3. Bain D.F, Munday D.L., Cox P.J and Smith A. *J. Pharm. Pharmacol.*, 49, (S4), 29, 1997.

J. Pharm. Pharmacol. 1998, 50 (Supplement): 161

Thermal studies on spray-dried biodegradable microspheres from various organic solvents

D. F. BAIN, D. L. MUNDAY AND A. SMITH*

*School of Pharmacy, The Robert Gordon University, Schoolhill, Aberdeen AB10 1FR, and *Knoll Pharmaceuticals, Pennyfoot Street, Nottingham NG1 1GF*

The substitution of dichloromethane and chloroform with less toxic acetone (Rafler & Jobmann, 1994) and halothane (Guiziou et al, 1996) has been proposed for the preparation of biodegradable microspheres. However, little consideration has been paid to the technological consequences of such substitution on drug release. This report describes thermal characterization of compositionally identical microspheres prepared from different organic solvents and its correlation with other determined characteristics.

Microspheres were prepared from solutions of the (co)solvents listed in Table 1 (3 % w/v total solid) comprising 24, 56 and 20 % w/v poly(D,L-lactide) Resomer® R104, R202H (Boehringer Ingelheim) and rifampicin (Lepetit) respectively. DSC (Pyris 1, Perkin Elmer, USA) was performed at various scanning rates to compute Arrhenius derived activation energies (E_a) of glass transition (Tg). Other thermal data in Table 1 was gathered at a rate of 10 °C min^{-1}. Solvent residue and drug release were determined as described previously (Bain et al., 1998).

Table 1. Preparative conditions, thermal and residual solvent data

Batch	Solvent(s)		Tg / °C	enthalpy / kJ g^{-1}	E_a / J g^{-1}	residue / ppm x10^{-3}
	nature	ratio				
1	DCM	100%	58.3	4.15	5.47	60.69
2	HAL	100%	49.9	5.57	3.50	125.51
3	ACT	100%	42.3	3.69	7.59	24.73
4	DCM:CFM	1:1	58.1	5.60	4.61	93.52
5	DCM:ACT	2:1	51.7	5.40	4.11	40.50
6	CFM:ACT	2:1	53.5	6.74	3.84	106.29

Key: DCM, dichloromethane; ACT, acetone; CFM, chloroform; HAL, halothane

Solvent change led to variation in thermal behaviour and release character (see Figure 1) which can be related to the microsphere formation mechanism (Bain et al, 1998). In general, rapid polymer deposition associated with highly volatile solvents e.g. ACT produced a porous matrix and rapid drug release, whereas other solvents resulted in a slower release. However, high and persistent solvent residue permitted significant polymer enthalpy relaxation upon storage due to its plasticizing action. This ageing process can be followed by the up-scale shift of the Tg and the progressive development of an anomalous endotherm. These changes marked the loss of excess enthalpy generated by rapid microsphere formation during spray-drying. After exhaustive *in vacuo* drying, activation energies in Table 1 for the Tg were inversely related to the enthalpy of the endotherm. The latter parameter was, in contrast, directly related to the level of solvent residue which facilitates molecular movement associated with relaxation and Tg elevation.

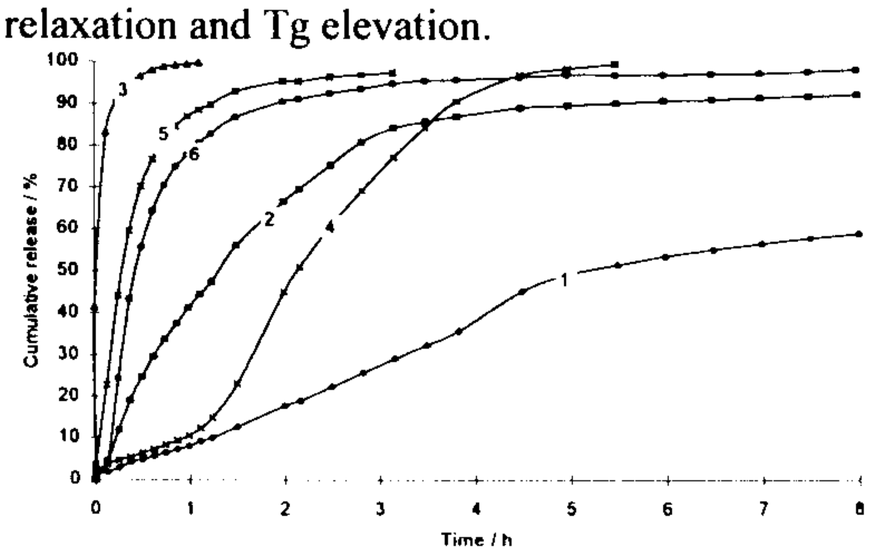

Figure 1. Release profiles of microspheres

Relaxation corresponds to the formation of a more stable microsphere matrix. Thus, based on this factor, those prepared from HAL (2) and CFM:ACT (6) should result in slowest drug release. However, related to relaxation, the Tg of the matrices formed proved a more reliable indicator of microsphere stability, release rate decreasing as Tg increased. Clearly, other factors influenced by the drying process, such as matrix density, have a role in determining the magnitude of the Tg and relaxation recovery, which in turn modulate drug release. In conclusion, solvent selection for spray-drying has significant technological implications in addition to toxicological considerations.

Bain DF, Munday DL & Smith A, 1998, *Fifth European Symposium on Controlled Drug Delivery*, Noordwijk aan Zee, 92-4.

Rafler G. & Jobmann M., 1994, *Drugs made in Germany*, 37(4), 37, 115-19.

Guiziou B, Armstrong D, Elliot E, Ford J and Rostron C, 1996, *J. Microencap*, 10, 466-80.